

STRUCTURE-, STEREOCHEMISTRY-, AND METAL-
REGULATED DNA BINDING/CLEAVING MOLECULES

Thesis by

John Hampton Griffin

In Partial Fulfillment of the Requirements
for the Degree of Doctor of Philosophy

California Institute of Technology

Pasadena, California

1990

(Submitted July 11, 1989)

© 1990

John Hampton Griffin

All Rights Reserved

To my Parents and Linda

Acknowledgements

I would like to thank my advisor, Peter Dervan, for contributions far beyond the physical and intellectual space provided in support of the research described in this dissertation. I have appreciated his guidance, and look with enthusiasm to a new era in our relationship. I would also like to thank the National Science Foundation, the ACS Organic Division, Merck Sharp & Dohme, and the Department of Education for graduate fellowships. I profess my indebtedness to members of the Dervan group, past and present, for collegiality, friendship, criticism, and help. Last but not least, I wish to thank my wife and colleague, Linda, for her love and empathetic support during graduate school. It has been my great privilege and pleasure to have shared this adventure with her.

Overview

In the cell, the binding of proteins to specific sequences of double helical DNA is essential for controlling the processes of protein synthesis (at the level of DNA transcription) and cell proliferation (at the level of DNA replication). In the laboratory, the sequence-specific DNA binding/cleaving properties of restriction endonuclease enzymes (secreted by microorganisms to protect them from foreign DNA molecules) have helped to fuel a revolution in molecular biology. The strength and specificity of a protein:DNA interaction depend upon structural features inherent to the protein and DNA sequences, but it is now appreciated that these features (and therefore protein:DNA complexation) may be altered (regulated) by other protein:DNA complexes, or by environmental factors such as temperature or the presence of specific organic molecules or inorganic ions. It is also now appreciated that molecules much smaller than proteins (including antibiotics of molecular weight < 2000 and oligonucleotides) can bind to double-helical DNA in sequence-specific fashion. Elucidation of structural motifs and microscopic interactions responsible for the specific molecular recognition of DNA leads to greater understanding of natural processes and provides a basis for the design of novel sequence-specific DNA binding molecules. This thesis describes the synthesis and DNA binding/cleaving characteristics of molecules designed to probe structural, stereochemical, and environmental factors that regulate sequence-specific DNA recognition.

Chapter One introduces the DNA minor groove binding antibiotics Netropsin and Distamycin A, which are di- and tri(*N*-methylpyrrolecarboxamide) peptides, respectively. The method of DNA affinity cleaving, which has been employed to determine DNA binding properties of designed synthetic molecules is described. The design and synthesis of a series of Netropsin dimers linked in tail-to-tail fashion (by oxalic, malonic, succinic, or fumaric acid), or in head-to-tail fashion (by glycine, β -alanine, and γ -aminobutyric acid (GABA)) are presented. These Bis(Netropsin)s were appended with the iron-chelating functionality EDTA in order to make use of the technique of DNA affinity cleaving.

Bis(Netropsin)-EDTA compounds are analogs of penta(*N*-methylpyrrolecarboxamide)-EDTA (P5E), which may be considered a head-to-tail Netropsin dimer linked by *N*-methylpyrrolecarboxamide. Low- and high-resolution analysis of pBR322 DNA affinity cleaving by the iron complexes of these molecules indicated that small changes in the length and nature of the linker had significant effects on DNA binding/cleaving efficiency (a measure of DNA binding affinity). DNA binding/cleaving efficiency was found to decrease with changes in the linker in the order β -alanine > succinamide > fumaramide > *N*-methylpyrrolecarboxamide > malonamide > glycine, γ -aminobutanamide > oxalamide. In general, the Bis(Netropsin)-EDTA:Fe compounds retained the specificity for seven contiguous A:T base pairs characteristic of P5E:Fe binding. However, Bis(Netropsin)-Oxalamide-EDTA:Fe exhibited decreased specificity for A:T base pairs, and Bis(Netropsin)-Gaba-EDTA:Fe exhibited some DNA binding sites of less than seven base pairs. Bis(Netropsin)s linked with diacids have C_2 -symmetrical DNA binding subunits and exhibited little DNA binding orientation preference. Bis(Netropsin)s linked with amino acids lack C_2 -symmetrical DNA binding subunits and exhibited higher orientation preferences. A model for the high DNA binding orientation preferences observed with head-to-tail DNA minor groove binding molecules is presented.

Chapter Two describes the design, synthesis, and DNA binding properties of a series of chiral molecules: Bis(Netropsin)-EDTA compounds with linkers derived from (*R,R*)-, (*S,S*)-, and (*RS,SR*)-tartaric acids, (*R,R*)-, (*S,S*)-, and (*RS,SR*)-tartaric acid acetonides, (*R*)- and (*S*)-malic acids, *N,N*-dimethylaminoaspartic acid, and (*R*)- and (*S*)-alanine, as well as three constitutional isomers in which an *N*-methylpyrrolecarboxamide (P1) subunit and a tri(*N*-methylpyrrolecarboxamide)-EDTA (P3-EDTA) subunit were linked by succinic acid, (*R,R*)-, and (*S,S*)-tartaric acids. DNA binding/cleaving efficiencies among this series of molecules and the Bis(Netropsin)s described in Chapter One were found to decrease with changes in the linker in the order β -alanine > succinamide > P1-succinamide-P3 > fumaramide > (*S*)-malicamide > *N*-methylpyrrolecarboxamide >

(*R*)-malicamide > malonamide > *N,N*-dimethylaminoaspartamide > glycine = Gaba = (*S,S*)-tartaramide = P1-(*S,S*)-tartaramide-P3 > oxalamide > (*RS,SR*)-tartaramide = P1-(*R,R*)-tartaramide-P3 > (*R,R*)-tartaramide (no sequence-specific DNA binding was detected for Bis(Netropsin)s linked by (*R*)- or (*S*)-alanine or by tartaric acid acetonides). The chiral molecules retained DNA binding specificity for seven contiguous A:T base pairs. From the DNA affinity cleaving data it could be determined that: 1) Addition of one or two substituents to the linker of Bis(Netropsin)-Succinamide resulted in stepwise decreases in DNA binding affinity; 2) molecules with single hydroxyl substituents bound DNA more strongly than molecules with single dimethylamino substituents; 3) hydroxyl-substituted molecules of (*S*) configuration bound more strongly to DNA than molecules of (*R*) configuration. This stereochemical regulation of DNA binding is proposed to arise from the inherent right-handed twist of (*S*)-enantiomeric Bis(Netropsin)s versus the inherent left-handed twist of (*R*)-enantiomeric Bis(Netropsin)s, which makes the (*S*)-enantiomers more complementary to the right-handed twist of B form DNA.

Chapter Three describes the design and synthesis of molecules for the study of metalloregulated DNA binding phenomena. Among a series of Bis(Netropsin)-EDTA compounds linked by homologous tethers bearing four, five, or six oxygen atoms, the Bis(Netropsin) linked by a pentaether tether exhibited strongly enhanced DNA binding/cleaving in the presence of strontium or barium cations. The observed metallospecificity was consistent with the known affinities of metal cations for the cyclic hexaether 18-crown-6 in water. High-resolution DNA affinity cleaving analysis indicated that DNA binding by this molecule in the presence of strontium or barium was not only stronger but of different sequence-specificity than the (weak) binding observed in the absence of metal cations. The metalloregulated binding sites were consistent with A:T binding by the Netropsin subunits and G:C binding by a strontium or barium:pentaether complex. A model for the observed positive metalloregulation and novel sequence-specificity is presented. The effects of 44 different cations on DNA affinity cleaving by

P5E:Fe were examined. A series of Bis(Netropsin)-EDTA compounds linked by tethers bearing two, three, four, or five amino groups was also synthesized. These molecules exhibited strong and specific binding to A:T rich regions of DNA. It was found that the iron complexes of these molecules bound and cleaved DNA most efficiently at pH 6.0-6.5, while P5E:Fe bound and cleaved most efficiently at pH 7.5-8.0. Incubating the Bis(Netropsin) Polyamine-EDTA:Fe molecules with K_2PdCl_4 abolished their DNA binding/cleaving activity. It is proposed that the observed negative metalloregulation arises from kinetically inert Bis(Netropsin) Polyamine:Pd(II) complexes or aggregates, which are sterically unsuitable for DNA complexation. Finally, attempts to produce a synthetic metalloregulated DNA binding protein are described. For this study, five derivatives of a synthetic 52 amino acid residue DNA binding/cleaving protein were produced. The synthetic mutant proteins carried a novel pentaether ionophoric amino acid residue at different positions within the primary sequence. The proteins did not exhibit significant DNA binding/cleaving activity, but they served to illustrate the potential for introducing novel amino acid residues within DNA binding protein sequences, and for the development of the tricyclohexyl ester of EDTA as a superior reagent for the introduction of EDTA into synthetic proteins.

Chapter Four describes the discovery and characterization of a new DNA binding/cleaving agent, [SalenMn(III)]OAc. This metal complex produces single- and double-strand cleavage of DNA, with specificity for A:T rich regions, in the presence of oxygen atom donors such as iodosyl benzene, hydrogen peroxide, or peracids. Maximal cleavage by [SalenMn(III)]OAc was produced at pH 6-7. A comparison of DNA single- and double-strand cleavage by $[SalenMn(III)]^+$ and other small molecules (Methidiumpropyl-EDTA:Fe, Distamycin-EDTA:Fe, Neocarzinostatin, Bleomycin:Fe) is presented. It was found that DNA cleavage by $[SalenMn(III)]^+$ did not require the presence of dioxygen, and that base treatment of DNA subsequent to cleavage by $[SalenMn(III)]^+$ afforded greater cleavage and alterations in the cleavage patterns. Analysis

of DNA products formed upon DNA cleavage by [SalenMn(III)] indicated that cleavage was due to oxidation of the sugar-phosphate backbone of DNA. Several mechanisms consistent with the observed products and reaction requirements are discussed.

Chapter Five describes progress on some additional studies. In one study, the DNA binding/cleaving specificities of Distamycin-EDTA derivatives bearing pyrrole *N*-isopropyl substituents were found to be the same as those of derivatives bearing pyrrole *N*-methyl substituents. In a second study, the design of and synthetic progress towards a series of nucleopeptide activators of transcription are presented. Five synthetic plasmids designed to test for activation of *in vitro* run-off transcription by DNA triple helix-forming oligonucleotides or nucleopeptides are described.

Chapter Six contains the experimental documentation of the thesis work.

Table of Contents

Acknowledgements	iv
Overview	v
CHAPTER ONE: STRUCTURAL REGULATION OF SEQUENCE-SPECIFIC DNA BINDING/CLEAVING BY BIS(NETROPSIN)S	
Introduction	1
Results	
Design	15
Synthesis	19
DNA Affinity Cleaving	22
Discussion	43
References	50
CHAPTER TWO: STEREOCHEMICAL REGULATION OF SEQUENCE-SPECIFIC DNA BINDING/CLEAVING BY CHIRAL BIS(NETROPSIN)S	
Introduction	53
Results	
Design	60
Synthesis	68
DNA Affinity Cleaving	73
Discussion	104
References	111
CHAPTER THREE: METAL-REGULATED DNA BINDING/ CLEAVING MOLECULES	
Introduction	114
Part 1: Positive Metalloregulation in the Sequence-specific Binding of a Synthetic Small Molecule to DNA.	

Results	
Design	115
Synthesis	118
DNA Affinity Cleaving	128
Discussion	157
Part 2: Negative Metalloregulation in the Sequence-specific Binding of Synthetic Small Molecules to DNA.	
Results	
Design	162
Synthesis	162
DNA Affinity Cleaving	165
Discussion	180
Part 3: Design and Synthesis of Metalloregulated DNA Binding/Cleaving Proteins.	
Results and Discussion	
Design	186
Synthesis	186
DNA Affinity Cleaving	195
Part 4: Additional Studies	
Results and Discussion	
Design	196
Synthesis	196
DNA Affinity Cleaving	196
References	200
CHAPTER FOUR: DNA CLEAVAGE MEDIATED BY [SalenMn(III)] ⁺	
Introduction	203

Results	
Synthesis	203
DNA Cleavage	203
Discussion	240
References	255
CHAPTER FIVE: ADDITIONAL STUDIES	
Results and Discussion	257
References	263
CHAPTER SIX: EXPERIMENTAL	
Synthesis	265
DNA Manipulations	342
References	364

List of Figures and Tables

CHAPTER ONE

Figure 1.1	Right-Handed Double Helical B Form DNA	3
Figure 1.2	A:T and G:C DNA Base Pairs	4
Figure 1.3	Ethidium, Netropsin, Distamycin A	5
Figure 1.4	Bleomycin A2	8
Figure 1.5	DNA Affinity Cleaving	10,11
Figure 1.6	MPE:Fe, DE:Fe, P5E:Fe	12
Figure 1.7	Head-to-Head, Head-to-Tail, and Tail-to-Tail Netropsin Dimers	14
Figure 1.8	BED, BEDF, BEDP, BENP	16
Figure 1.9	Bis(Netropsin) Diacid-EDTA:Fe Compounds	17
Figure 1.10	Bis(Netropsin) Amino Acid-EDTA:Fe Compounds	18

Figure 1.11	Bifurcated Hydrogen Bonding Models	20
Figure 1.12	Scheme for the Synthesis of BNSE	21
Figure 1.13	Scheme for the Synthesis of BNGabaE	23
Figure 1.14	Scheme for the Synthesis of BN- β -AE	24
Figure 1.15	BNDiacid-EDTA:Fe ds Cleavage	26
Figure 1.16	BNAmido Acid-EDTA:Fe ds Cleavage	29
Figure 1.17	BNDiacid-EDTA:Fe ds Cleavage Histogram	30
Figure 1.18	BNAmido Acid-EDTA:Fe ds Cleavage Histogram	31
Figure 1.19	BNDiacid-EDTA:Fe 517 Fragment Cleavage	34
Figure 1.20	BNOE:Fe, P5E:Fe 517 Fragment Cleavage	36
Figure 1.21	BNAmido Acid-EDTA:Fe 517 Fragment Cleavage	38
Figure 1.22	BNDiacid-EDTA:Fe 517 Fragment Cleavage Histogram	40
Figure 1.23	BNAmido Acid-EDTA:Fe 517 Fragment Cleavage Histogram	41
Figure 1.24	Orientation Preference Model	47
Figure 1.25	(P4) ₃ -(β -A) _{2-E:Fe}	49

CHAPTER TWO

Figure 2.1	Δ - and Λ -Tris(Phenanthroline)Metal Complexes, CC-1065, Dihydrodiol Epoxides	56
Figure 2.2	Daunomycin, Chromomycin A3	57
Figure 2.3	Triostin A, Actinomycin D	58
Figure 2.4	Calichemicin γ_1^I , Esperamicin A ₁ , NCZS Chromophore	59
Figure 2.5	Chiral Bis(Netropsin)-EDTA:Fe Compounds	61
Figure 2.6	Bis(Netropsin)-Tartaramide-EDTA:Fe Compounds	62
Figure 2.7	Bis(Netropsin)-Tartaramide Acetonide-EDTA:Fe Compounds	63
Figure 2.8	Bis(Netropsin)-Malicamide-EDTA:Fe Compounds	64

Figure 2.9	Bis(Netropsin)-DMAAspartamide-EDTA:Fe Compounds	65
Figure 2.10	P1-Linker-P3-EDTA:Fe Compounds	66
Figure 2.11	Bis(Netropsin)-Alanine-EDTA:Fe Compounds	67
Figure 2.12	Scheme for the Synthesis of BN-(<i>R,R</i>)-Tar-E	69
Figure 2.13	Synthons for the Synthesis of Chiral Bis(Netropsin)s	70
Figure 2.14	Scheme for the Synthesis of P1-S-P3-E	71
Figure 2.15	BNTartaramides-EDTA:Fe ds Cleavage	75
Figure 2.16	BNMalicamides-EDTA:Fe ds Cleavage	78
Figure 2.17	BNDMAAspartamides-EDTA:Fe ds Cleavage	80
Figure 2.18	P1-Linker-P3-EDTA:Fe ds Cleavage	82
Figure 2.19	BNTartaramides-EDTA:Fe ds Cleavage Histogram	84
Figure 2.20	BNMalicamides-EDTA:Fe ds Cleavage Histogram	85
Figure 2.21	BNDMAAspartamides-EDTA:Fe ds Cleavage Histogram	86
Figure 2.22	P1-Linker-P3-EDTA:Fe ds Cleavage Histogram	87
Figure 2.23	BNTartaramides-EDTA:Fe 517 Fragment Cleavage	91
Figure 2.24	BNMalicamides-EDTA:Fe 517 Fragment Cleavage	93
Figure 2.25	BNDMAAspartamides-EDTA:Fe 517 Fragment Cleavage	95
Figure 2.26	P1-Linker-P3-EDTA:Fe 517 Fragment Cleavage	97
Figure 2.27	BNTartaramides-EDTA:Fe 517 Fragment Cleavage Histogram	98
Figure 2.28	BNMalicamides-EDTA:Fe 517 Fragment Cleavage Histogram	99
Figure 2.29	BNDMAAspartamides-EDTA:Fe 517 Fragment Cleavage Histogram	100
Figure 2.30	P1-Linker-P3-EDTA:Fe 517 Fragment Cleavage Histogram	101
Figure 2.31	CPK Models of (<i>R,R</i>)- and (<i>S,S</i>)-Tartaramides	109

CHAPTER THREE

Figure 3.1	Equilibria Associated with Metalloregulated DNA Binding	116
Figure 3.2	Design of Bis(Netropsin)Polyether-EDTA:Fe Compounds	117

Figure 3.3	Scheme for the Synthesis of BNTetraEGE	119
Figure 3.4	BNPolyethers-EDTA:Fe ds Cleavage: Concentration Study	121
Figure 3.5	BNPolyethers-EDTA:Fe ds Cleavage: Metal Study	124
Figure 3.6	Periodic Table	126
Figures 3.7-3.15	P5E:Fe ds Cleavage with Metals Control Study	128-136
Table 3.1	Effects of Metals (1.0 mM) on DNA Affinity Cleaving by P5E:Fe	139
Table 3.2	Effects of Metals (0.1 mM) on DNA Affinity Cleaving by P5E:Fe	141
Figure 3.16	BNTetraEGE:Fe ds Cleavage Histogram	143
Figure 3.17	BNTetraEGE:Fe 517 Fragment Cleavage with Metals	146
Figure 3.18	Graph of Cleavage by BNTetraEGE:Fe Versus Barium Concentration	147
Figure 3.19	BNPolyethers-EDTA:Fe 517 Fragment Cleavage with Barium	149
Figure 3.20	BNTetraEGE:Fe 517 Fragment Cleavage \pm Barium Histogram	150
Figure 3.21	BNPolyethers-EDTA:Fe 169 Fragment Cleavage with Barium	153
Figure 3.22	BNTetraEGE:Fe 169 Fragment Cleavage \pm Barium Histogram	154
Figure 3.23	Netropsin and P5 TetraEG Monomers	155
Figure 3.24	TetraEG Monomer Synthon and Potential "Barium Binding Finger"	156
Figure 3.25	Model for Barium-Mediated DNA Binding by BNTetraEGE:Fe	160
Figure 3.26	Bis(Netropsin)Polyamine-EDTA Compounds	163
Figure 3.27	Scheme for the Synthesis of BNN3E	164
Figure 3.28	BNPolyamines-EDTA:Fe ds Cleavage	167
Figure 3.29	BNPolyamines-EDTA:Fe ds Cleavage pH Study	169
Figure 3.30	pH Profile of ds Cleavage by BNPolyamines-EDTA:Fe and P5E:Fe	170
Figure 3.31	BNPolyamines-EDTA:Fe ds Cleavage Histogram	171
Figure 3.32	BNPolyamines-EDTA:Fe 517 Fragment Cleavage	174
Figure 3.33	BNPolyamines-EDTA:Fe 517 Fragment Cleavage Histogram	175
Figure 3.34	BNPolyamines-EDTA:Fe 169 Fragment Cleavage	178
Figure 3.35	BNPolyamines-EDTA:Fe 169 Fragment Cleavage Histogram	179

Figure 3.36	BNPolyamines-EDTA:Fe ds Cleavage Palladium(II) Study	182
Figure 3.37	Pd(II) Dependence Graph	183
Figure 3.38	Design and Synthesis of an Ionophoric Peptide β -Turn Mimic	187
Figure 3.39	SPPS Summary of Hin(139-190) Ionomutant Proteins	189
Figure 3.40	Syntheis of TriCyE	190
Figure 3.41	HPLC Purification of Hin(139-190) Ionomutant Protein	192
Figure 3.42	400 MHz ^1H NMR Spectrum of Purified Ionomutant Protein	194
Figure 3.43	Design and Synthesis of BN2O2SE:Fe	197
Figure 3.44	Design and Synthesis of BNDBPE:Fe	198

CHAPTER FOUR

Figure 4.1	Synthesis of [SalenMn(III)]OAc	204
Figure 4.2	Additional SalenMetal Complexes	205
Figure 4.3	MnS ds Cleavage: Concentration Study	208
Figure 4.4	MnS ds Cleavage: Oxidant Study	210
Figure 4.5	MnS ds Cleavage: pH Study	212
Figure 4.6	Graph of pH Dependence of ds Cleavage by MnS	214
Figure 4.7	MnS, MPE:Fe, NCZS, Blm:Fe ds Cleavage	216
Figure 4.8	MnS, BNSE ds Cleavage	218
Figure 4.9	Densitometric Analysis of ds Cleavage by Small Molecules	220,221
Figure 4.10	DE:Fe, MnS, NCZS, MPE:Fe, Blm:Fe 517 Fragment Cleavage	224
Figure 4.11	DE:Fe, MnS, NCZS, MPE:Fe, Blm:Fe 167 Fragment Cleavage	226
Figure 4.12	DE:Fe, MnS, NCZS, MPE:Fe, Blm:Fe 169 Fragment Cleavage	228
Figure 4.13	Dioxygen, Base Workup Dependence of MnS Cleavage	231
Figure 4.14	Analysis of 3' DNA End Products Produced by MnS Cleavage	233
Figure 4.15	Analysis of 5' DNA End Products Produced by MnS Cleavage	236
Figure 4.16	HPLC Analysis of Base Products Produced by MnS Cleavage	239

Figure 4.17	MnS + Base Workup Cleavage 167 and 517 Fragments	242
Figure 4.18	MnS + Base Workup Cleavage 169 Fragment	244
Figure 4.19	MnS Cleavage 517, 167, 169 Fragments Histograms	246
Figure 4.20	DNA Binding/Cleaving Metalloporphyrins	250
Figure 4.21	Plausible Mechanisms for DNA Cleavage by MnS	252

CHAPTER FIVE

Figure 5.1	Design and Synthesis of <i>N</i> -Isopropyl Distamycin Analogs	258
Figure 5.2	Design of Synthetic Transcriptional Activators	260
Figure 5.3	Plasmids Constructed for In Vitro Transcription Studies	261

CHAPTER ONE: STRUCTURAL REGULATION OF SEQUENCE-SPECIFIC DNA BINDING/CLEAVING BY BIS(NETROPSIN)S

Introduction

In the cell, the binding of proteins to specific sequences of double-helical DNA is essential for controlling the processes of protein synthesis (at the level of DNA transcription) and cell proliferation (at the level of DNA replication). The strength and specificity of protein:DNA interactions depend upon structural features inherent to the protein and DNA sequences, but it is now appreciated that these features (and therefore protein:DNA complexation) may be altered (regulated) by interactions with other protein:DNA complexes or environmental factors such as temperature, specific organic molecules, or inorganic ions. It is also now appreciated that molecules much smaller than proteins (including antibiotics of molecular weight < 2000 and oligonucleotides) can bind to double-helical DNA in sequence-specific fashion. Elucidation of structural motifs and microscopic interactions responsible for the specific molecular recognition of DNA will lead to greater understanding of natural processes and provide a basis for the design of novel sequence-specific DNA binding molecules. In the simplest case imaginable, a molecule that binds to a specific DNA sequence would possess structural and ground-state conformational features complementary to the structural and ground-state conformational features of the DNA sequence (lock and key model). On the other hand, it can also be envisioned that the DNA and/or the DNA binding molecule could undergo subtle to extensive conformational reorganization in order to produce the most stable complex (induced fit model). Therefore, a knowledge of the structures and conformational properties of DNA, DNA binding molecules, and DNA:ligand complexes is essential for a detailed understanding of specific complexation processes.

From the point of view of sequence-specific recognition, right-handed double-helical B form DNA is considered to be the DNA conformation of greatest interest, as it constitutes the dominant solution conformation of DNA under physiological conditions. The first glimpse of the structural and conformational details of B form DNA was provided by Dickerson and coworkers when they solved the structure of the self-complementary DNA dodecamer d(CGCGAATTCGCG)₂ by x-ray diffraction (Figure 1.1).^{1,2} This structure showed the pronounced major and minor grooves of B DNA, which have walls formed by the phosphate-sugar backbone and floors formed by the edges of adenine:thymine (A:T) and guanine:cytosine (G:C) base pairs (Figure 1.2). This structure also showed that local DNA conformational properties such as base propeller twist, roll, slide, tilt, and groove width vary with the local DNA sequence. Another feature that varies with the DNA sequence is the pattern of hydrogen-bond donor and acceptor groups found on the floors of the DNA major and minor grooves. The most striking variations are found in the minor groove, where A:T base pairs present lone pairs of electrons from adenine N3 and thymine O2 atoms, while G:C base pairs present the protruding exocyclic N2 amino group from guanine. More recently, the x-ray structure of the B form duplex oligonucleotide d(CGCAAAAAAGCG):d(CGCTTTTGTGCG) has been described,³ as have the structures of several protein:B DNA cocrystals including Eco RI:d(TCGCGAATTCGCG)₂,⁴ 434 repressor (R1-69):d(ACAATATATATTGT)₂,⁵ 434 repressor(R1-69):d(TATACAAGAAAGTTGTACT):d(AAGTACAAACTTCTTGTAT),⁶ λ repressor:d(TATATCACCGCCAGTGGTAT):d(AATACCACTGGCGGTGATAT),⁷ and Trp repressor:d(TGTACTAGTTAACTAGTAC)₂.⁸

Figure 1.3 depicts the structures of three DNA binding small molecules. Ethidium binds DNA with little sequence-specificity by intercalation of its planar heteroaromatic chromophore between adjacent DNA base pairs.⁹ Intercalation increases the fluorescence lifetime of the chromophore, and ethidium is used routinely as a stain to detect DNA. The oligo(*N*-methylpyrrolecarboxamide) antibiotics Netropsin and Distamycin A (isolated from

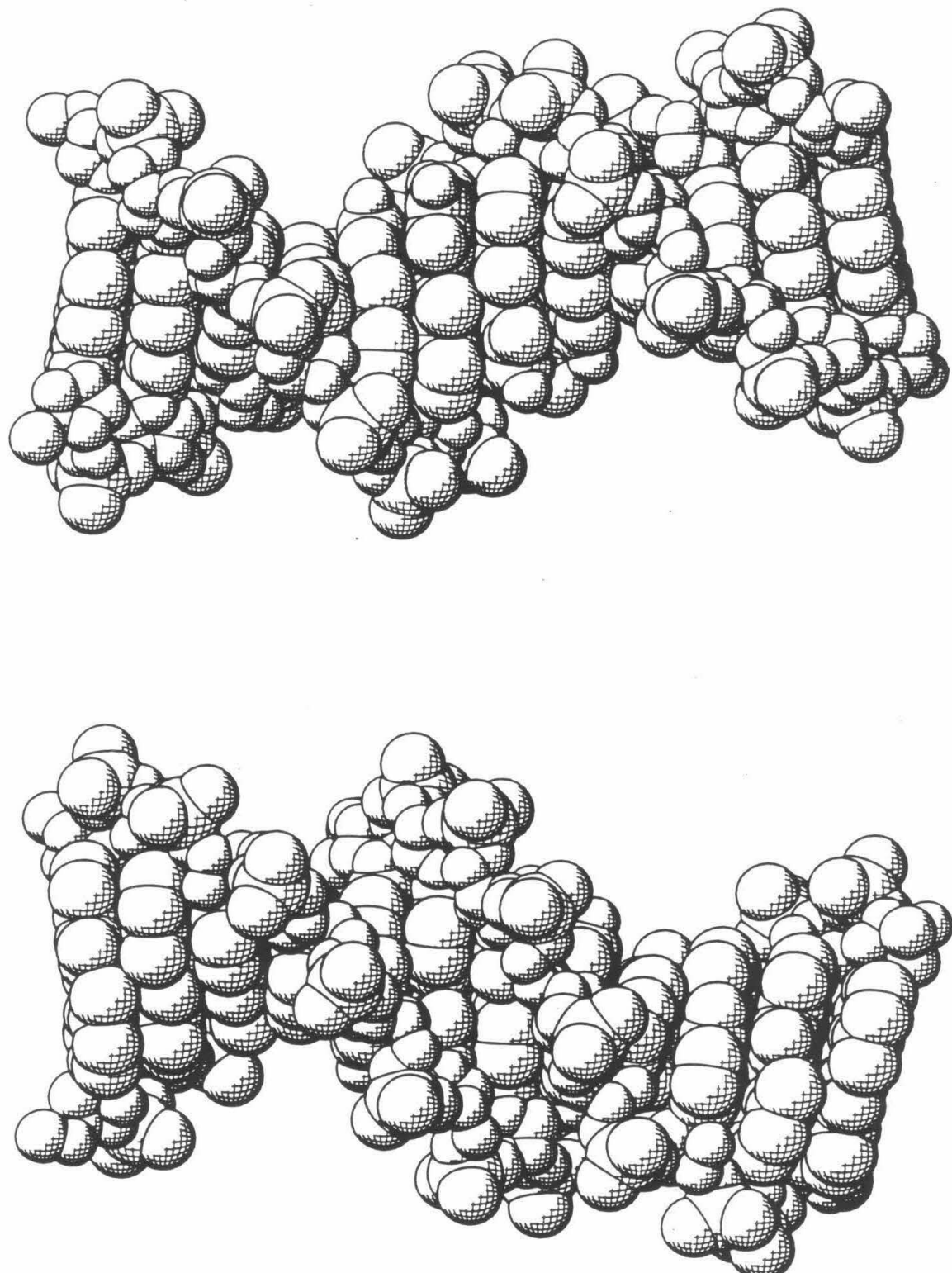


Figure 1.1. Right-handed double-helical B form DNA: $d(CGCGAATTCTCGG)_2$.

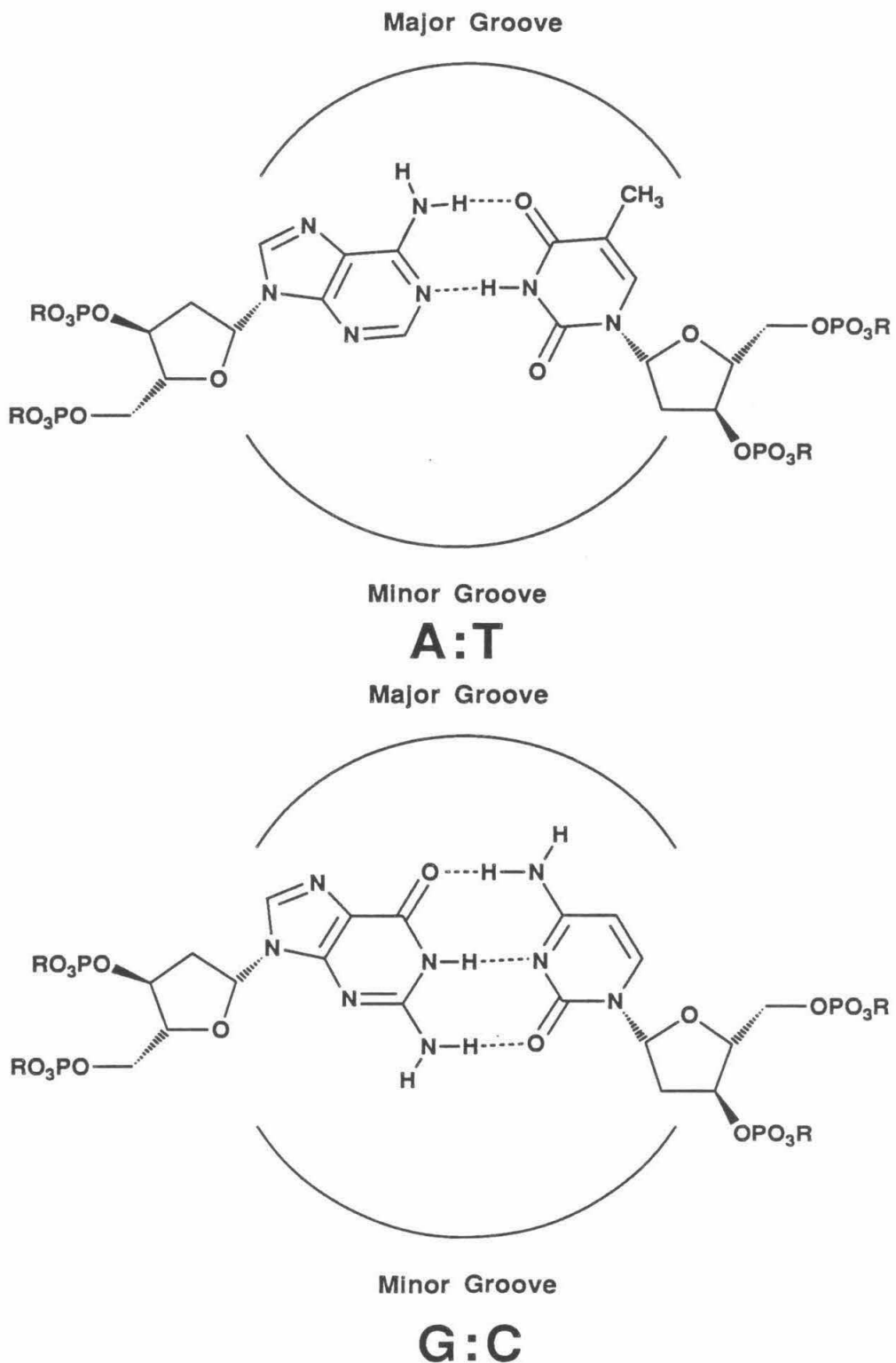


Figure 1.2. DNA Adenine:Thymine (A:T) and Guanine:Cytosine (G:C) Base Pairs.

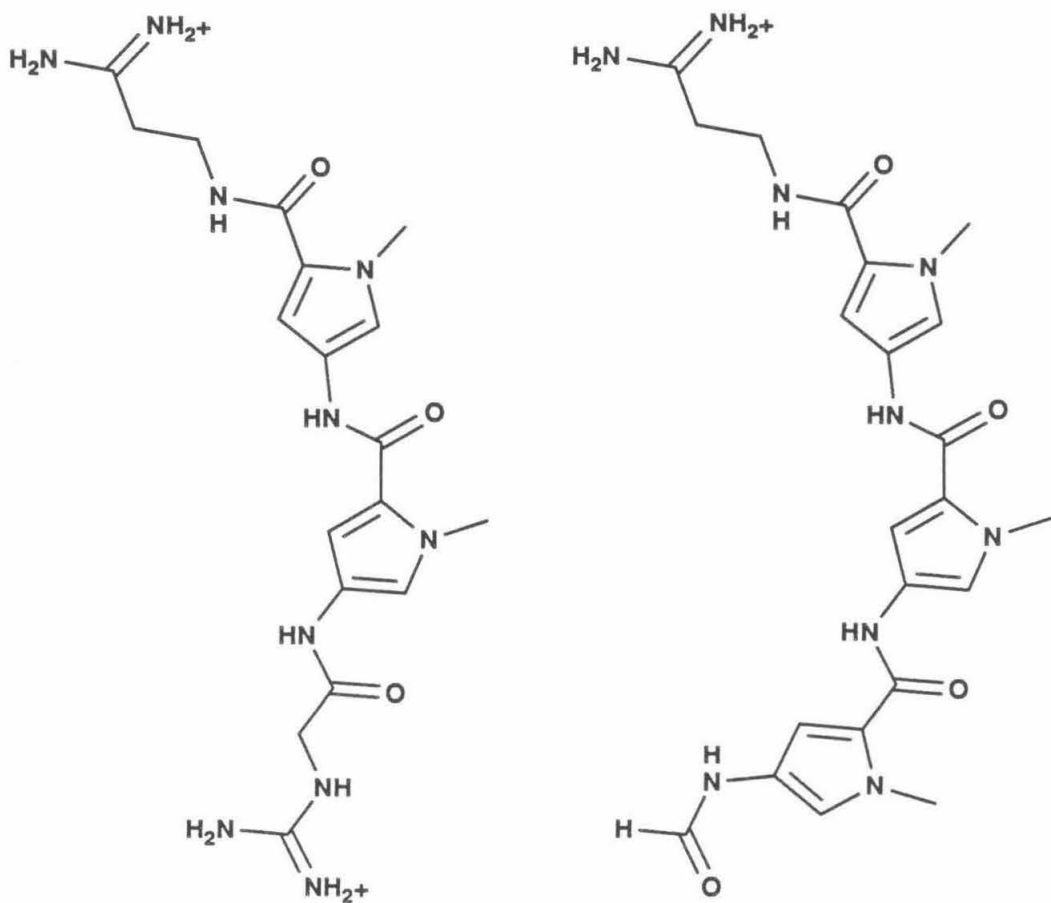
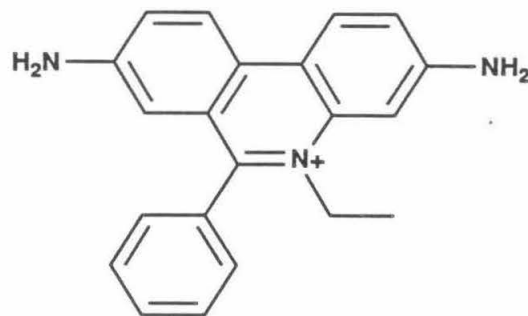


Figure 1.3. Top: The DNA intercalating molecule Ethidium. Bottom: The DNA minor groove binding molecules Netropsin (Left) and Distamycin A (Right).

Streptomyces cultures) are prototypical minor groove binding molecules specific for A:T rich regions of B DNA.¹⁰ The crystal structure of Netropsin reveals its crescent shape (in which amide NH and pyrrole C2H atoms form the concave edge) as well as the right-handed twist of one *N*-methylpyrrolecarboxamide (**MPC**) residue relative to the other.¹¹ The crystal and molecular structures of Netropsin complexed to the dodecamer d(CGCGAATT^{Br}CGCG)₂^{12,13} and Distamycin A complexed to the dodecamer (CGCAAATTGCG)₂¹⁴ have also been determined. In these structures, Netropsin and Distamycin A were found to be sandwiched within narrow minor grooves at the A:T tracts of these B form oligonucleotides. Considering these structures, it appears that A:T binding specificity for Netropsin and Distamycin A arises from 1) favorable van der Waals contacts between the antibiotics and deoxyribose residues of the DNA sugar-phosphate backbone, 2) a series of consecutive bifurcated hydrogen-bonds between **MPC** NHs and lone pair electrons from adenine N3 and thymine O2 atoms located on adjacent (to the 3' side) base pairs on opposite strands of the DNA double helix, and 3) favorable van der Waals contacts between pyrrole C3H atoms and adenine C2H atoms. Dickerson and coworkers also proposed that steric clashes between pyrrole C3H atoms and guanine N2 amino groups prevent oligo(*N*-methylpyrrolecarboxamide)s from penetrating into the minor groove and forming strong van der Waals contacts and hydrogen-bonds at sites containing G:C base pairs. Interactions of Netropsin and Distamycin A with oligonucleotides have also been analyzed by NMR spectroscopy^{15,16} and thermodynamic studies.¹⁷

A technique for the study of DNA:DNA binding molecule interactions, which complements diffraction, spectroscopic, and calorimetric techniques, is known as DNA affinity cleaving. The power of this method derives from the coupling of a DNA binding event to a DNA cleaving event, since DNA cleavage may be conveniently determined to nucleotide resolution by gel electrophoresis. The most widely recognized and used DNA affinity cleaving agents are the Type II restriction endonuclease enzymes, which bind and cleave specific DNA sequences 4-8 base pairs in length. The antitumor antibiotic

Bleomycin A2 (**Blm**, Figure 1.4) is an example of a naturally occurring DNA affinity cleaving small molecule. In the presence of ferrous ions and dioxygen (or ferric ions, dioxygen, and a reducing agent), **Blm** mediates oxidative DNA cleavage at 5'-GC-3' and 5'-GT-3' sites.¹⁸ DNA affinity cleaving has been adapted to the study of synthetic DNA binding molecules in the Dervan laboratories.¹⁹⁻²¹ The approach taken has been to synthetically attach the iron-chelating functionality EDTA to the DNA binding molecule (small molecule, oligonucleotide, protein) of interest (Figure 1.5). In the presence of dioxygen and a reducing agent such as dithiothreitol or ascorbic acid, the EDTA:Fe moiety catalytically produces reactive species (perhaps hydroxyl radical) capable of oxidatively cleaving the sugar-phosphate backbone of DNA in regions proximal to the molecule's DNA binding sites. Double-strand cleavage of large DNAs (>1000 base pairs) affords fragments that may be separated by size on agarose gels. Analysis of the electrophoretic mobilities of the cleavage fragments relative to the mobilities of fragments of known molecular weight allows DNA binding/cleaving sites to be mapped within ± 20 base pairs. Densitometric analysis of band intensities allows determination of relative DNA binding/cleaving efficiencies by various molecules at their binding/cleaving sites. End-labeled DNA restriction fragments, which contain these cleavage loci, are then prepared and cleaved. Products of DNA restriction fragment cleavage are separated to nucleotide resolution by denaturing polyacrylamide gel electrophoresis and visualized by autoradiography. Densitometric analysis of band intensities and positions relative to chemical sequencing ladders affords quantitative information about DNA binding affinity, binding site sizes, sequence-specificity, groove location, binding orientations, and the effects that reaction conditions have on these DNA binding properties.

The first DNA binding/cleaving agents synthesized and studied in the Dervan laboratories are depicted in Figure 1.6. Methidiumpropyl-EDTA (**MPE**) is a useful reagent for footprinting DNA binding small molecules, oligonucleotides, and proteins because of the relatively nonspecific DNA cleavage it produces in the presence of iron, dioxygen, and

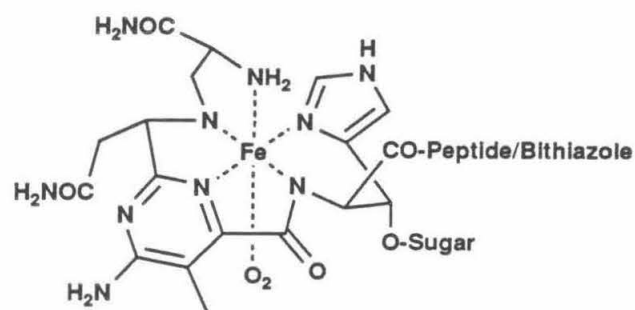
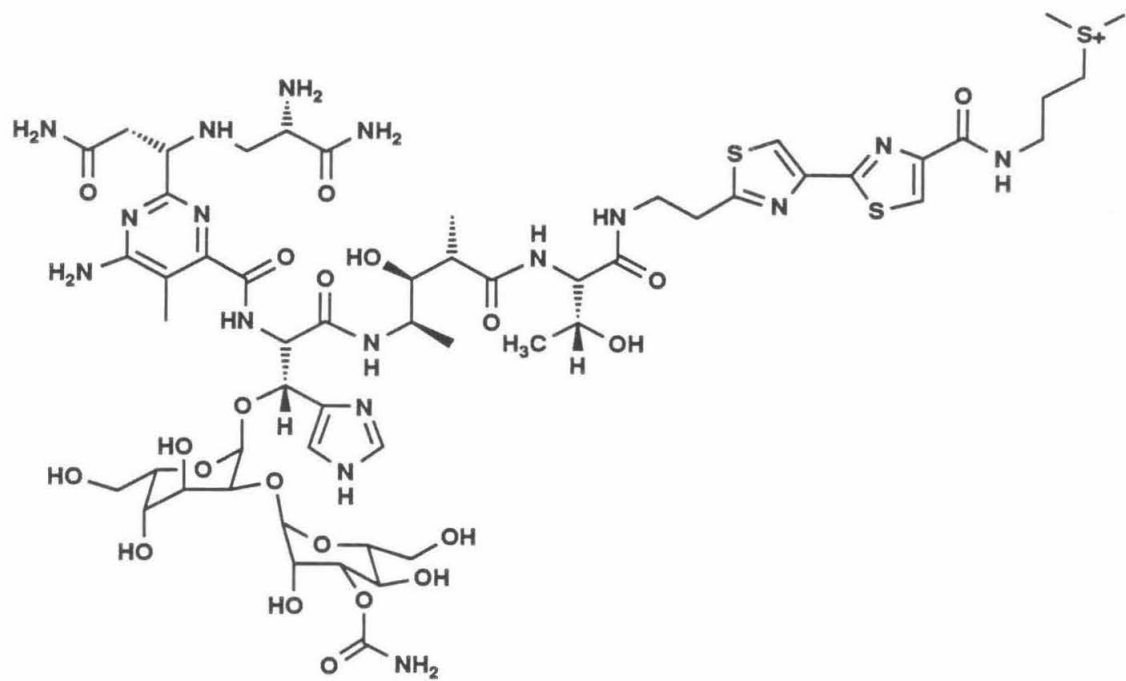
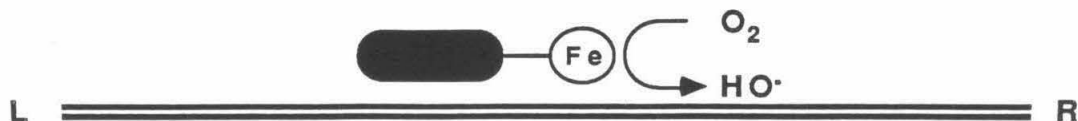


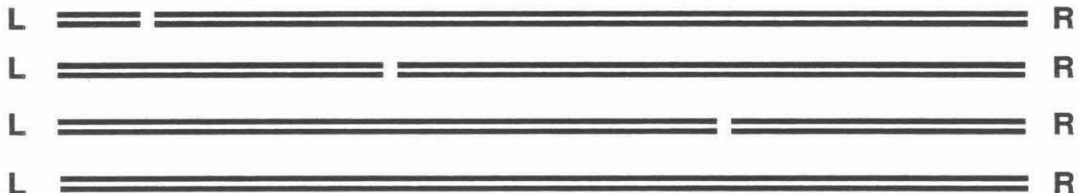
Figure 1.4. Top: Bleomycin A2 (Blm). Bottom: Proposed structure of the Blm:Fe:O₂ complex.¹⁸

Figure 1.5

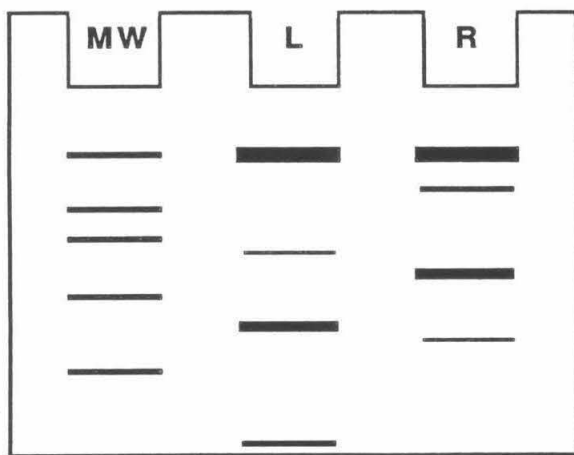
DNA Affinity Cleaving. First page: Low-resolution (± 20 bp) mapping of DNA binding sites by DNA double-strand cleavage / agarose gel electrophoresis. Second page: High-resolution (± 1 bp) analysis of DNA binding sites by DNA single-strand cleavage/ denaturing polyacrylamide gel electrophoresis.



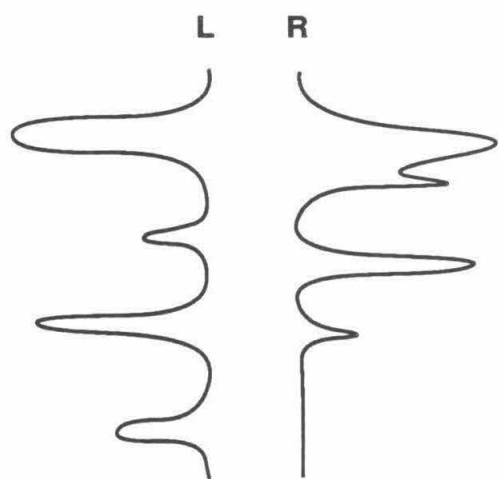
Affinity Cleaving Reaction



Double-Strand Cleavage Fragments



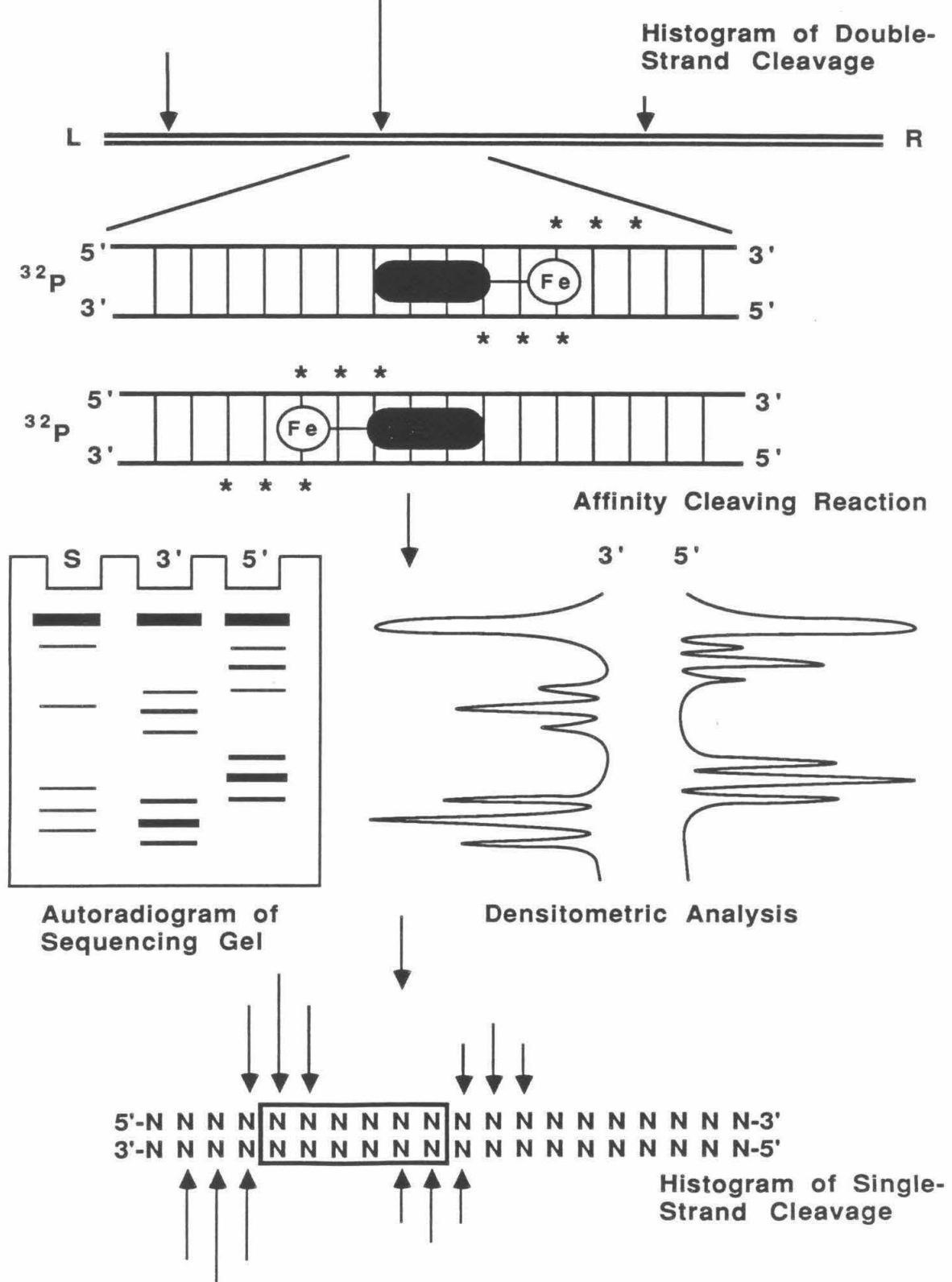
Autoradiogram of Agarose Gel



Densitometric Analysis

L _____ R

Histogram of Double-Strand Cleavage



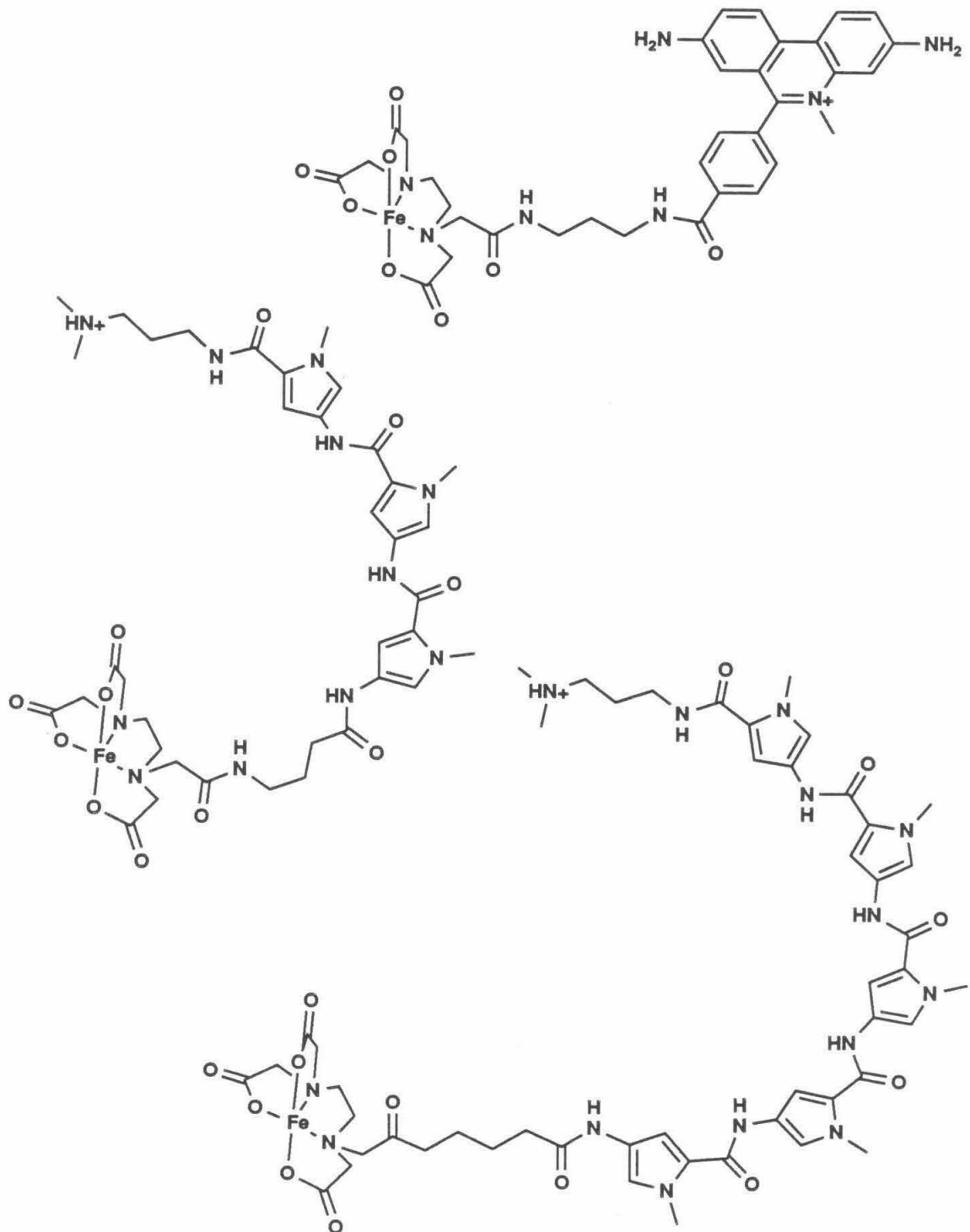


Figure 1.6. Top: Methidiumpropyl-EDTA:Fe (**MPE:Fe**). Middle: Distamycin-EDTA:Fe (**DE:Fe**). Bottom: Penta(*N*-methylpyrrolecarboxamide)-EDTA:Fe (**P5E:Fe**).

a reducing agent.²²⁻²⁶ "DNA affinity cleaving" was first used to describe the sequence-specific DNA binding/cleaving properties of Distamycin-EDTA (**DE**).^{27,28} In the presence of iron, dioxygen, and dithiothreitol, **DE** produces diffuse cleavage patterns that cover four to six base pairs flanking its DNA binding sites. The cleavage patterns are pseudo-*C*₂ symmetric and shifted to the 3' side on one DNA strand relative to the other strand. The 3' shift is consistent with **DE:Fe** being bound in the minor groove of B DNA, where the most proximal sugar residues on opposite strands of the DNA double helix are part of nucleotides shifted two to three positions in the 3' direction on one polynucleotide strand relative to the other. The pseudo-*C*₂ symmetrical cleavage patterns allow the average positions of the EDTA:Fe moiety to be determined. From the EDTA:Fe positions, Distamycin binding sites of five contiguous A:T base pairs have been assigned. Synthetic **DE** homologs having four through nine **MPC** units (bearing five through ten **MPC** NHs, respectively) were found to bind to specific sites of six through eleven contiguous A:T base pairs, respectively.^{29,30} Thus, *n* **MPC** NHs afford DNA binding sites of *n*+1 base pairs. This *n* + 1 rule is consistent with the consecutive bifurcated hydrogen-bonding patterns observed in the cocrystals of Netropsin and Distamycin A with B form oligonucleotides.

The synthesis of oligo(*N*-methylpyrrolecarboxamide) homologs represents one approach to achieving greater DNA binding specificity. A more flexible approach to highly specific DNA binding molecules could be to couple DNA binding subunits of similar or diverse sequence-specificities into larger, more specific DNA binding structures. Khorlin and coworkers were the first to synthesize dimers of Netropsin (Figure 1.7), and to point out that since Netropsin had distinct amino and carboxyl termini, it could be linked in head-to-head, head-to-tail, or tail-to-tail fashion (defining the carboxyl and amino termini of Netropsin as head and tail, respectively, in analogy to the depiction of peptide β -sheet structures).^{31,32} CD titration and DNase I footprinting studies of these molecules indicated that they bound specifically to A:T rich regions of DNA. In some instances the Bis(Netropsin)s exhibited larger binding sites than observed with Netropsin itself. A series

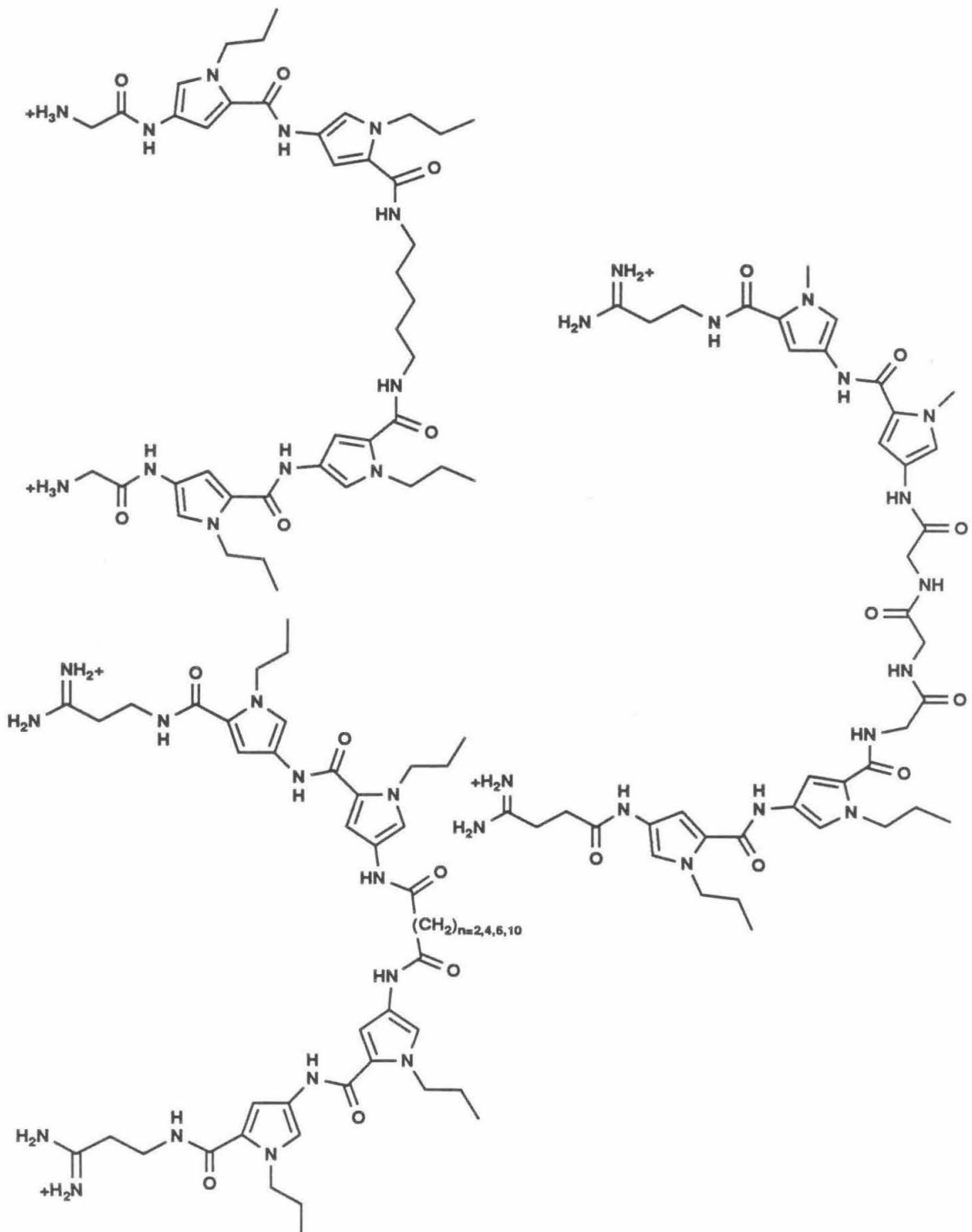


Figure 1.7. Bis(Netropsin)s prepared by Khorlin and coworkers. Top Left: Bis(Netropsin) Diamine compound. Center Right: Bis(Netropsin) Amino acid compound. Bottom: Bis(Netropsin) Diacid compounds.

of dimeric DNA binding/cleaving molecules designed and synthesized at Caltech are depicted in Figure 1.8. Schultz and Dervan prepared dimers of Distamycin that were linked by heptanedicarboxylic acid and equipped with one or two EDTA functions (**BED**).³³ DNA affinity cleaving experiments with **BED:Fe** revealed DNA binding sites of five and eight contiguous A:T base pairs, indicating that binding modes were possible in which one or both Distamycin subunits of **BED** contacted DNA. Youngquist and Dervan redesigned the dicarboxylic acid linker to mimic more closely the length and rigidity of **MPC**. The result was Bis(EDTA-Distamycin)-Fumaramide (**BEDF**), a crescent-shaped tail-to-tail dimer which was shown by affinity cleaving to bind sites of eight or nine contiguous A:T base pairs.³⁴ That five base pair binding sites were not observed was consistent with exclusive simultaneous binding by both Distamycin subunits of **BEDF**. At this point we undertook the synthesis and study of tail-to-tail and head-to-tail Netropsin dimers linked by a series of short chain diacids and amino acids in order to determine the effects that small, incremental changes in linker length and structure have on DNA binding properties among a series of structurally analogous molecules.

Results

Design. Figures 1.9 and 1.10 depict the Bis(Netropsin)s prepared for this study. Bis(Netropsin)s linked in tail-to-tail fashion by oxalic, malonic, succinic, and fumaric acids are shown in Figure 1.9. Bis(Netropsin)s linked in head-to-tail fashion by glycine, β -alanine, and γ -aminobutanoic acid (Gaba) are shown in Figure 1.10. Head-to-tail Netropsin dimers are analogs of penta(*N*-methylpyrrolecarboxamide-EDTA (**P5E**, Figure 1.6) in which the central **MPC** residue has been replaced by an amino acid. **P5E** has been found to bind specifically to minor groove sites of seven contiguous A:T base pairs with preference for homopolymeric (A)_n:(T)_n tracts.^{29,30} Tail-to-tail Netropsin dimers are constitutional analogs of **P5E** in which the central **MPC** residue has been replaced by a diacid, and the directionality of one Netropsin subunit has been reversed. Bis(Netropsin)s were appended with the iron-chelating functionality EDTA at one terminus in order to make

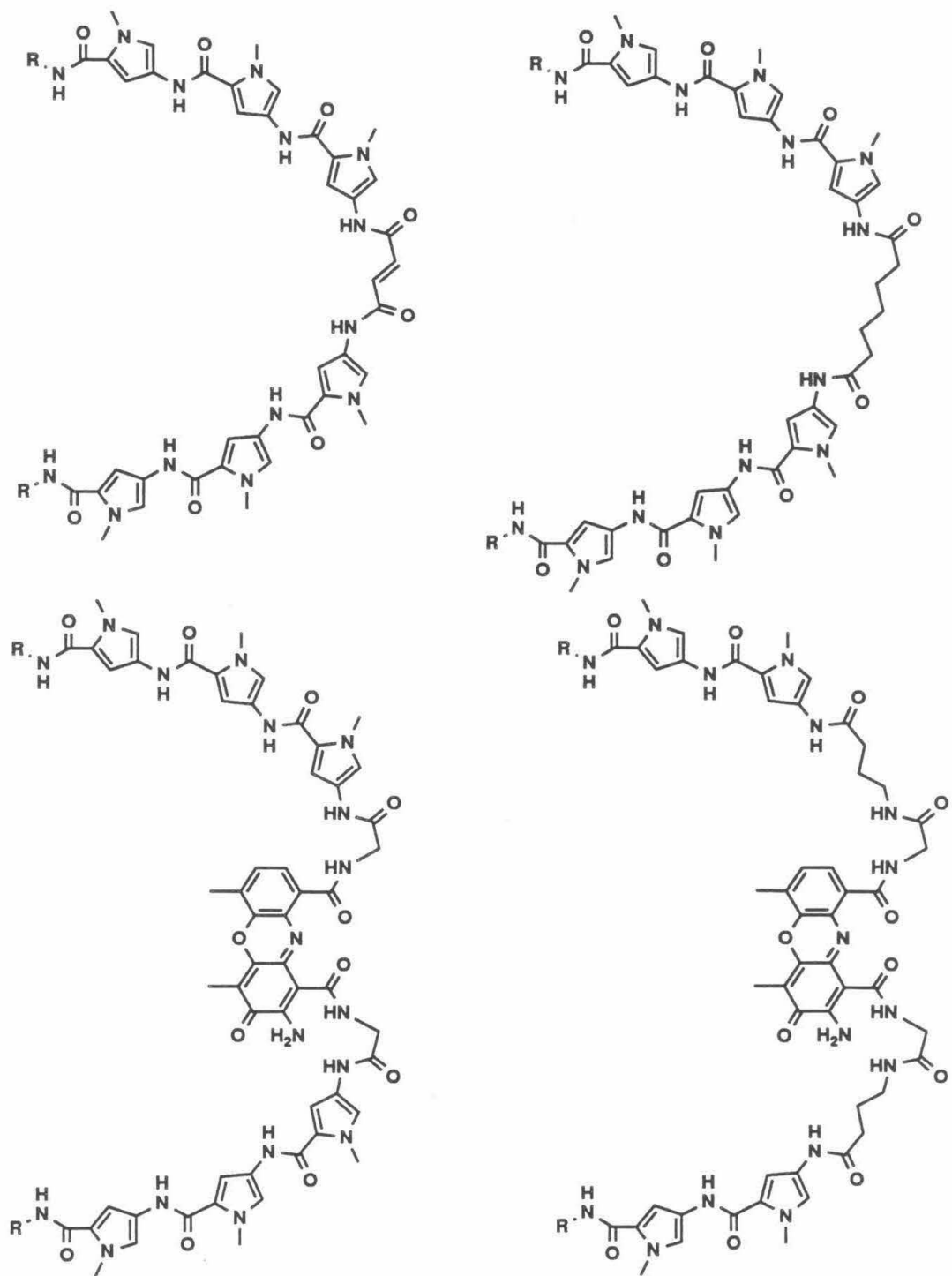


Figure 1.8. Top Left: Bis(EDTA-Distamycin)Fumaramide (**BEDF**). Top Right: Bis(EDTA-Distamycin) (**BED**). Bottom Left: Bis(EDTA-Distamycin)Phenoxazone (**BEDP**). Bottom Right: Bis(EDTA-Netropsin)Phenoxazone (**BENP**). R = propane-EDTA, or dimethylaminopropane.

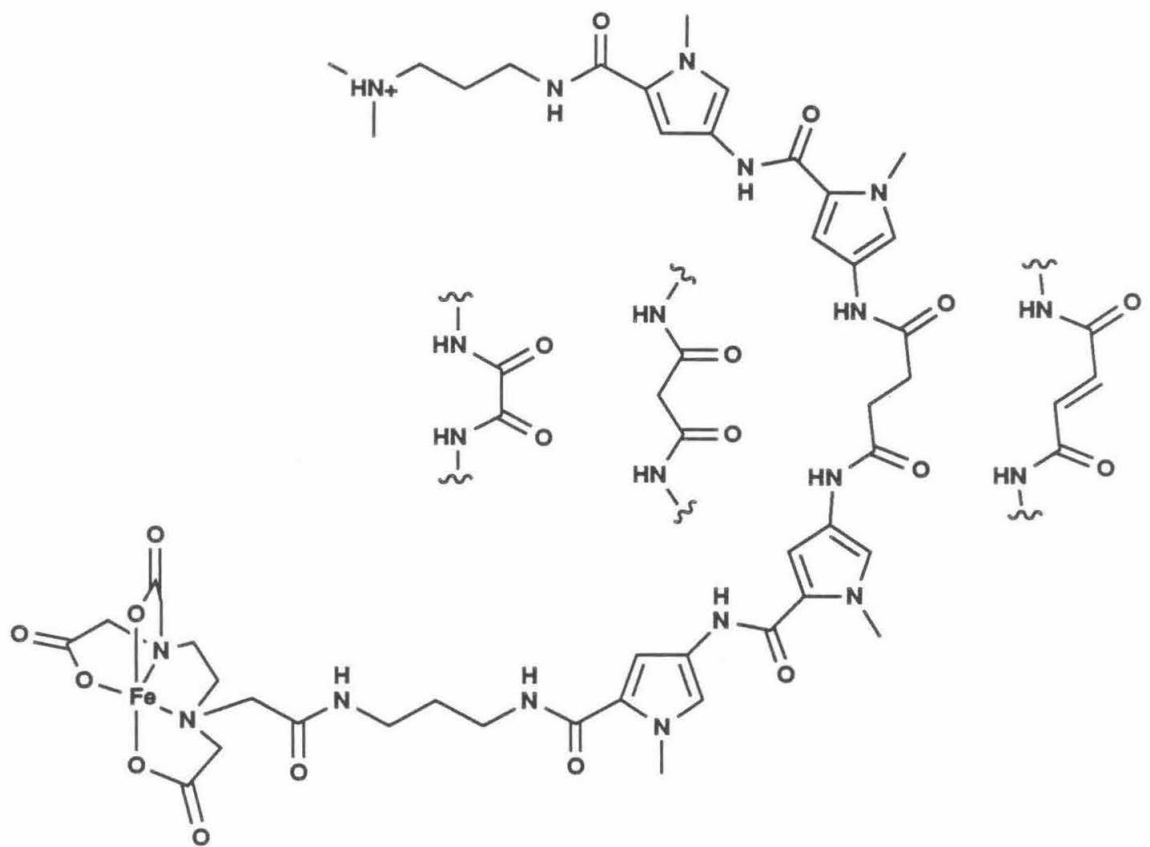


Figure 1.9. Bis(Netropsin) Diacid-EDTA:Fe compounds. Left: Bis(Netropsin)-Oxalamide-EDTA:Fe (**BNOE:Fe**). Center Left: Bis(Netropsin)-Malonamide-EDTA:Fe (**BNME:Fe**). Center Right: Bis(Netropsin)-Succinamide-EDTA:Fe (**BNSE:Fe**). Right: Bis(Netropsin)-Fumaramide-EDTA:Fe (**BNFE:Fe**).

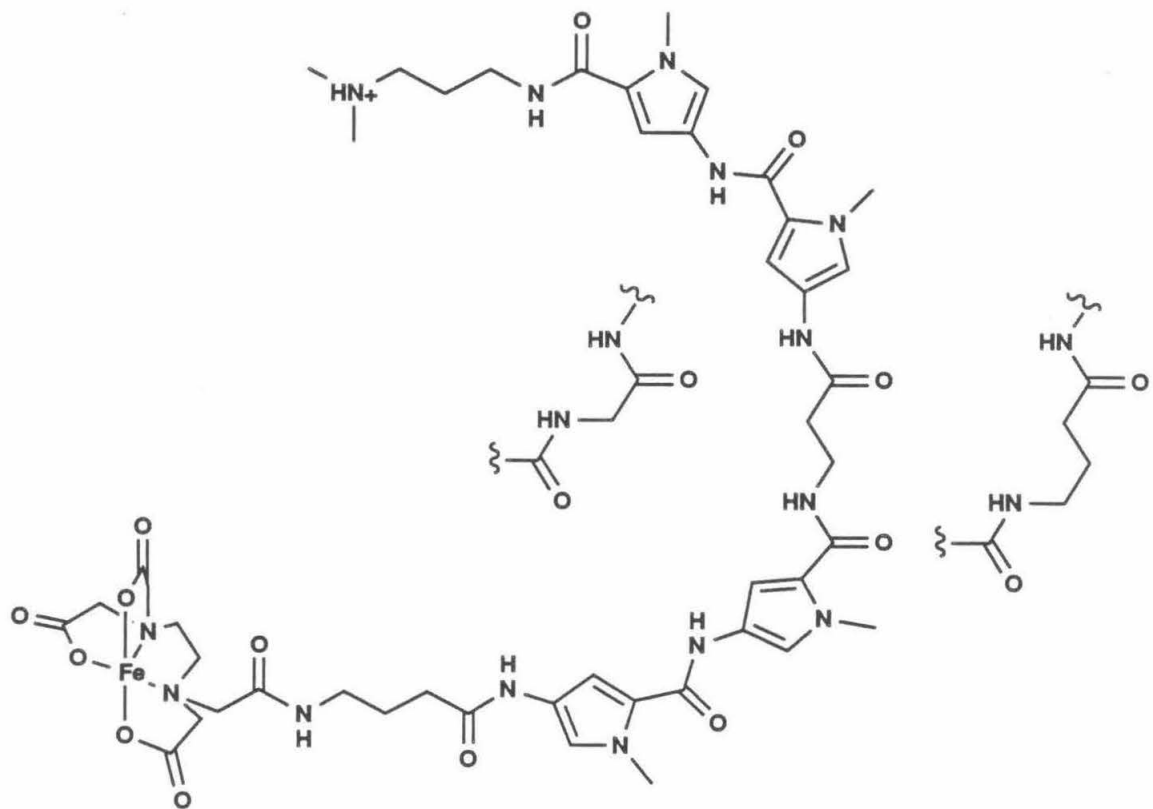


Figure 1.10. Bis(Netropsin) Amino Acid-EDTA:Fe compounds. Left: Bis(Netropsin)-Glycine-EDTA:Fe (BNGE:Fe). Center: Bis(Netropsin)- β -Alanine-EDTA:Fe (BN- β -AE:Fe). Right: Bis(Netropsin)-Gaba-EDTA:Fe (BNGabaE:Fe).

use of the technique of DNA affinity cleaving to determine their DNA binding properties. It was expected that the observed DNA binding properties would in part reflect the interactions of the linkers with the minor groove of DNA. As first approximations, consecutive bifurcated hydrogen-bonding models for the linkers are depicted in Figure 1.11. These hydrogen-bonding patterns are analogous to those observed in the cocrystals of Netropsin and Distamycin A with DNA dodecamers,¹²⁻¹⁴ and derived from DNA affinity cleaving experiments with **DE** and homologs.^{29,30}

Synthesis. *N*-methyl-4-(*N*-methyl-4-nitropyrrole-2-carboxamide)-2-carboxylic acid (O_2NP2CO_2H), available in six steps from commercially available *N*-methylpyrrole-2-carboxylic acid,³⁵ served as a common synthetic intermediate for all Bis(Netropsin)-EDTA compounds. Amide coupling reactions were carried out in dimethylformamide and were mediated by either *N,N'*-dicyclohexylcarbodiimide/1-hydroxybenzotriazole or by *N,N'*-carbonyldiimidazole.

The synthesis of tail-to-tail dimers is exemplified by the synthesis of Bis(Netropsin)-Succinamide-EDTA (**BNSE**, **I-54**, Figure 1.12). O_2NP2CO_2H was coupled with 3-dimethylaminopropylamine or mono Boc 1,3-diaminopropane (**IV-161**) to afford the terminally differentiated Netropsin analogs **I-22** and **IV-129**. Reduction of **I-22** and coupling with an excess of succinic acid (or with one equivalent of succinic acid, mono methyl ester followed by hydrolysis of the ester) produced Netropsin-Succinamic acid **II-78**. **IV-129** was reduced and coupled with **II-78** to afford Boc Bis(Netropsin)-Succinamide **II-62**. The terminal amine of **II-62** was deprotected and coupled with the triethyl ester of EDTA.³⁶ The EDTA ester groups were removed by hydrolysis to afford **BNSE**. Modifications were made in the synthesis of Bis(Netropsin)-Oxalamide-EDTA. Reduced **I-22** was coupled with ethyl oxalyl chloride in the presence of excess triethylamine. The resulting crude ester was hydrolyzed without purification to afford Netropsin-Oxalamic acid, which was elaborated to **BNOE** following the procedure described for the conversion of Netropsin-Succinamic acid to **BNSE**.

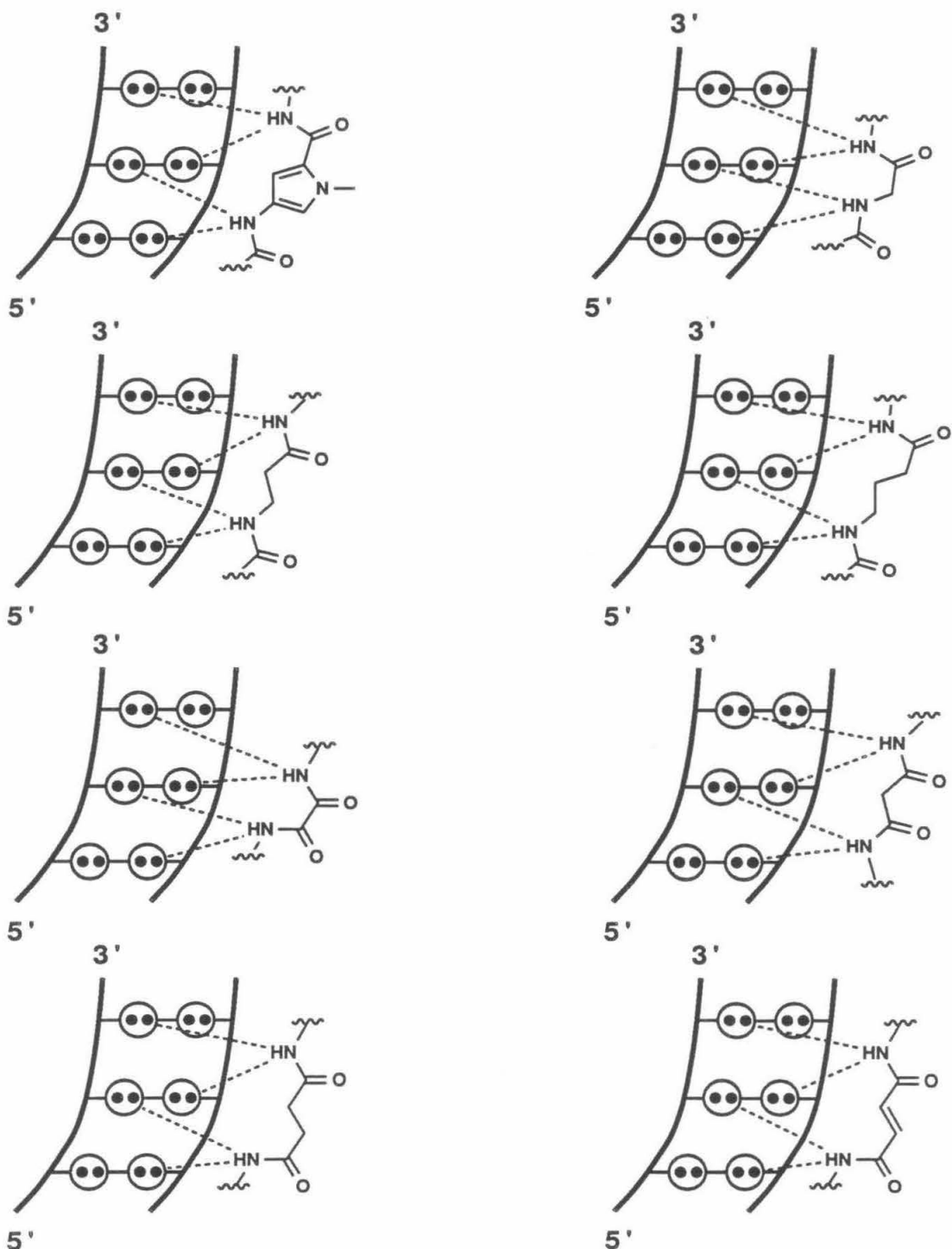


Figure 1.11. Bifurcated hydrogen-bonding models for minor groove recognition of A:T basepairs by (clockwise, from top left) MPC, glycine, Gaba, malonamide, fumaramide, succinamide, oxalamide, and β -alanine groups. Circles with two dots represent lone pairs of electrons on adenine N3 or thymine O2 atoms at the edges of the base pairs on the floor of the minor groove of the right-handed B DNA helix.

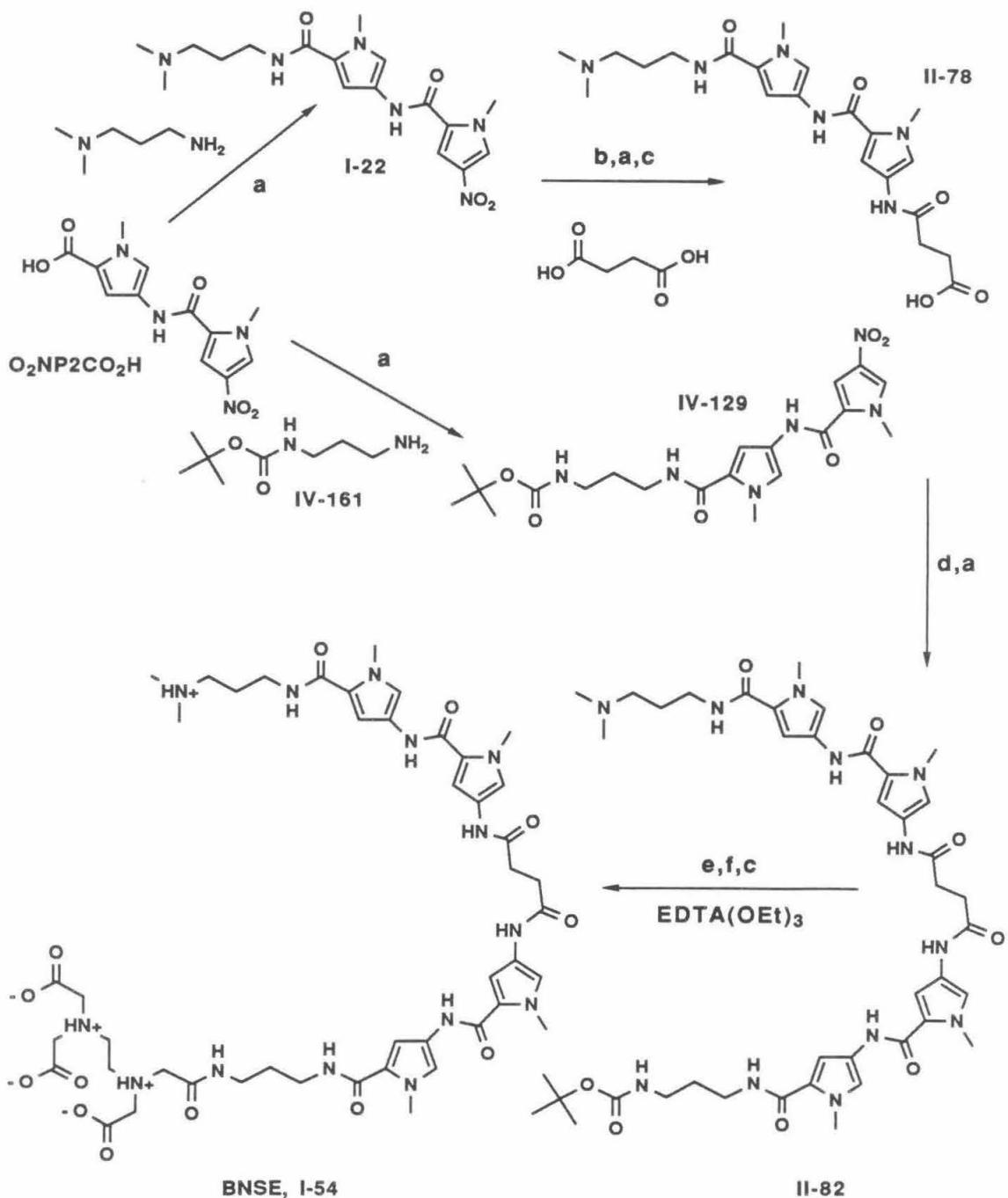


Figure 1.12. Scheme for the synthesis of BNSE. Reaction conditions: **a**, DCC, HOBT, DMF; **b**, H₂ (1 atm), Pd/C, DMF; **c**, LiOH, MeOH, H₂O; **d**, H₂ (3 atm), Pd/C, DMF; **e**, TFA, CH₂Cl₂; **f**, EDTA(OEt)₃, CDI, DMF.

The synthesis of head-to-tail dimers is exemplified by the synthesis of Bis(Netropsin)-Gaba-EDTA (**BNGabaE, I-230**, Figure 1.13). The terminally differentiated Netropsin subunits employed in these syntheses were **I-22** and **I-204**. **I-204** was prepared by coupling reduced **O₂NP2CO₂H** with Boc Gaba **I-203**. **I-22** was reduced and coupled with **I-203** to afford Boc Netropsin-Gaba **I-208**. The terminal amino group of **I-208** was deprotected and coupled with **I-204** to produce Boc Bis(Netropsin)-Gaba **I-218**. The terminal amino group of **I-218** was deprotected and coupled with the triethyl ester of EDTA. The ester groups were removed by hydrolysis to afford **BNGE**. Modifications were made in the synthesis of Bis(Netropsin)- β -Alanine-EDTA (**BN- β -AE, I-265**, Figure 1.14). Reduced **I-22** was coupled with cyanoacetic acid to afford a Netropsin nitrile intermediate. The nitrile group was reduced to produce Netropsin- β -Alanine (**I-257**), which was elaborated to **BN- β -AE** following the procedure described for the conversion of Netropsin-Gaba to **BNGE**.

DNA Affinity Cleaving. DNA affinity cleaving by **P5E** and Bis(Netropsin)-EDTA compounds was examined under conditions determined to be optimal for DNA binding/cleaving by oligo(*N*-methylpyrrolecarboxamide)-EDTA compounds.³⁷ 1:1 complexes of **P5E** or Bis(Netropsin)-EDTA compound and iron were allowed to equilibrate with the DNA substrate and calf thymus carrier DNA for one hour at 37°C in pH 7.9 Tris/sodium acetate buffer before DNA cleavage was initiated by the addition of dithiothreitol solution. DNA cleavage was allowed to proceed for two hours at 37°C before the DNA cleavage products were separated by gel electrophoresis and the DNA cleavage patterns visualized by autoradiography.

An autoradiograph of the double-strand cleavage patterns produced by **P5E:Fe** and Bis(Netropsin) Diacid-EDTA:Fe compounds on pBR322 plasmid DNA is shown in Figure 1.15. The DNA substrate (4367 base pairs in length) had been linearized with restriction endonuclease Sty I and labeled separately on each of its unique 3' ends with ³²P. The DNA cleavage patterns were separated by agarose gel electrophoresis. **P5E:Fe** produced

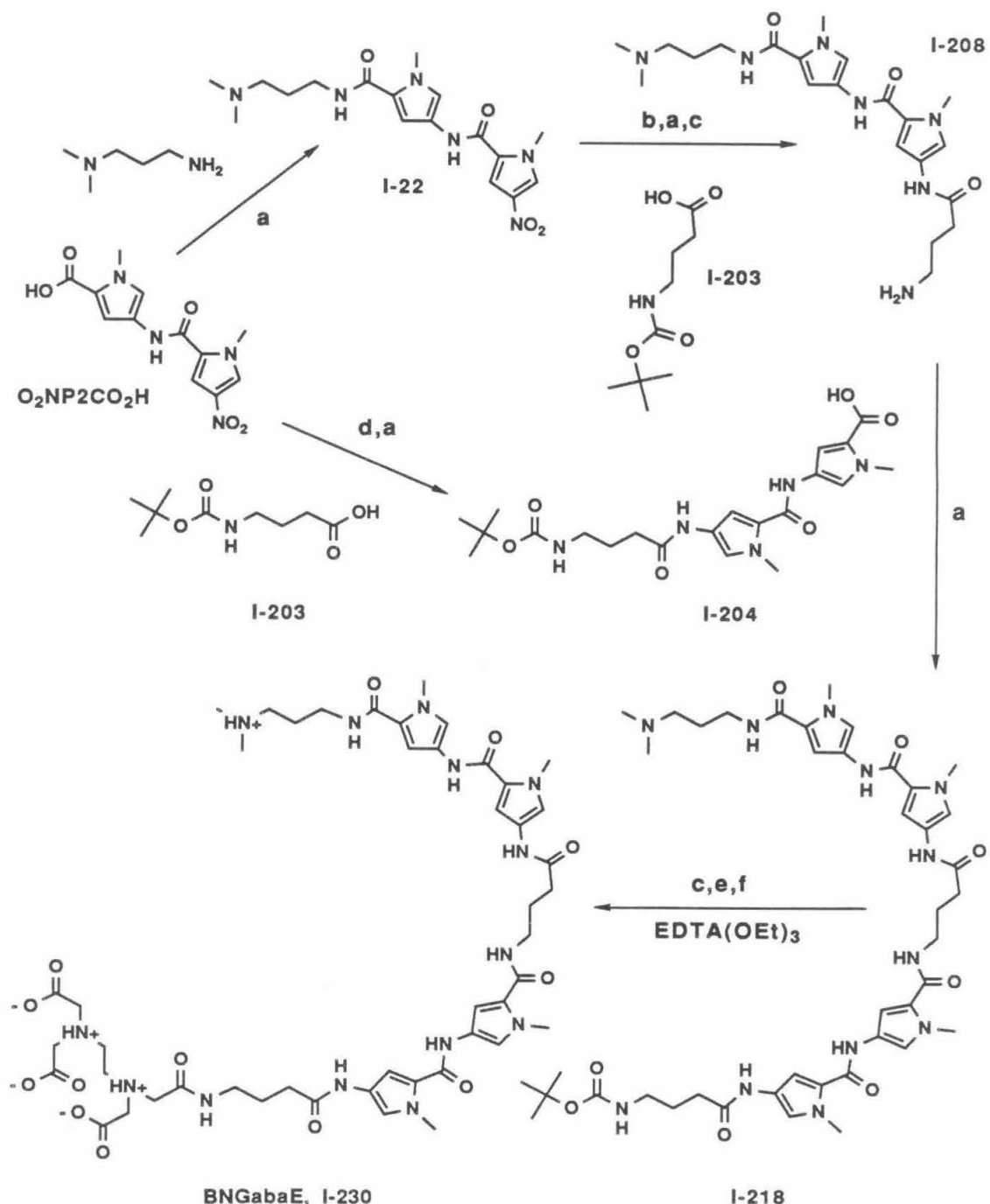


Figure 1.13. Scheme for the synthesis of BNGabaE. Reaction conditions: **a**, DCC, HOBT, DMF; **b**, H₂ (1 atm), Pd/C, DMF; **c**, TFA, CH₂Cl₂; **d**, H₂ (1 atm), Pd/C, Et₃N, DMF; **e**, EDTA(OEt)₃, CDI, DMF; **f**, LiOH, MeOH, H₂O.

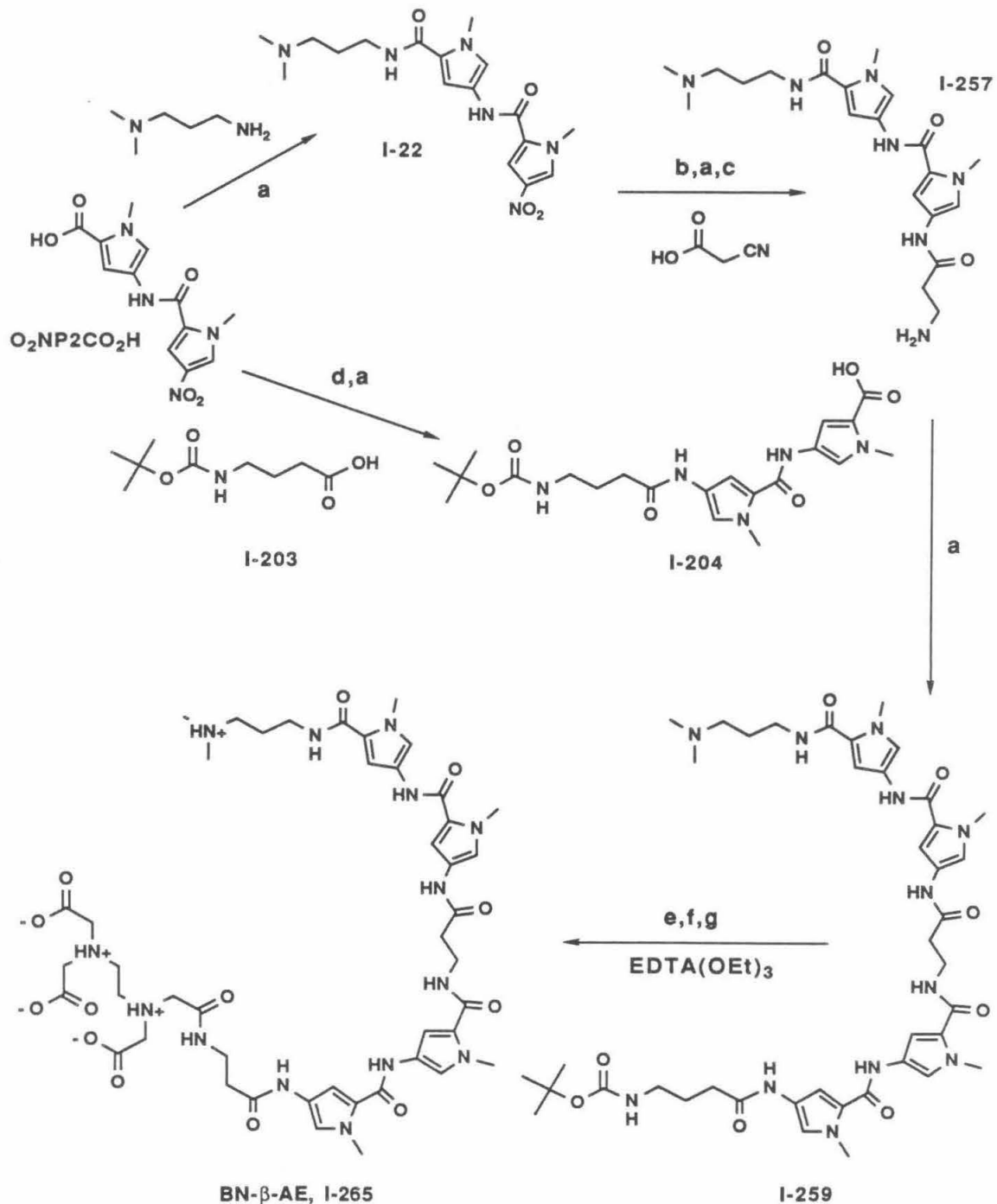
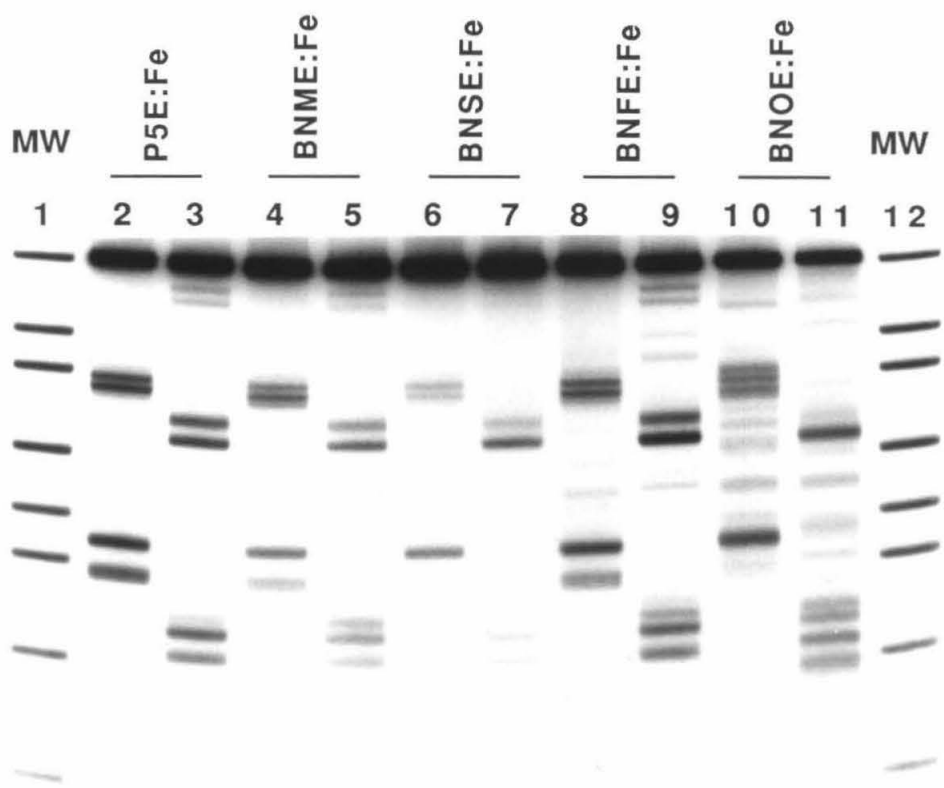


Figure 1.14. Scheme for the synthesis of BN- β -AE. Reaction conditions: **a**, DCC, HOBT, DMF; **b**, H_2 (1 atm), Pd/C, DMF; **c**, H_2 (3 atm) PtO_2 , HOAc; **d**, H_2 (3 atm), Pd/C, Et_3N , DMF; **e**, TFA, CH_2Cl_2 ; **f**, $\text{EDTA}(\text{OEt})_3$, CDI, DMF; **g**, LiOH , MeOH , H_2O .

Figure 1.15

Autoradiograph of DNA double-strand cleavage patterns produced by **P5E:Fe** and Bis(Netropsin) Diacid-EDTA:Fe compounds on Sty I linearized, 3'-³²P end-labeled pBR322 plasmid DNA in the presence of dioxygen and dithiothreitol. Cleavage patterns were resolved by electrophoresis on a 1% agarose gel. Lanes 2,4,6,8,10 contain DNA labeled at one end with α -³²P dATP, while lanes 3,5,7,9,11 contain DNA labeled at the other end with α -³²P TTP. Lanes 1 and 12, molecular weight markers consisting of pBR322 restriction fragments 4363, 3371, 2994, 2368, 1998, 1768, 1372, 995, and 666 bp in length; lanes 2 and 3, **P5E:Fe** at 1.0 μ M concentration; lanes 4 and 5, **BNME:Fe** at 1.0 μ M concentration; lanes 6 and 7, **BNSE:Fe** at 0.10 μ M concentration; lanes 8 and 9, **BNFE:Fe** at 0.50 μ M concentration; lanes 10 and 11, **BNOE:Fe** at 4.0 μ M concentration.



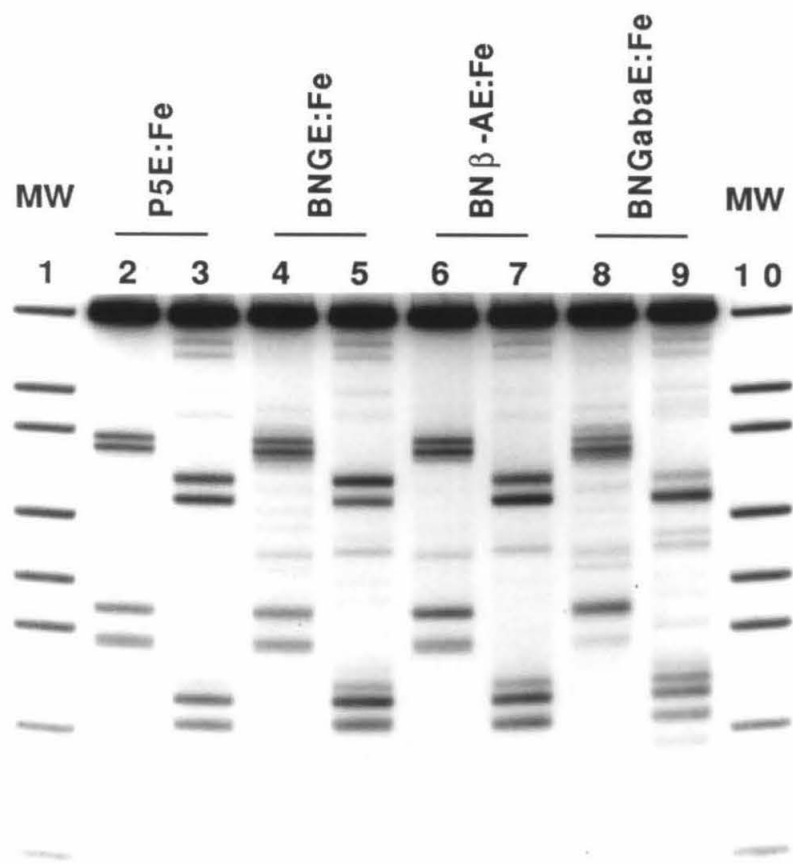
four intense cleavage loci. **BNME:Fe**, **BNSE:Fe**, and **BNFE:Fe** also produced these cleavage loci, but with these molecules the relative intensities of the four bands were more variable than with **P5E:Fe**. **BNOE:Fe** produced a significantly different cleavage pattern. One of the intense cleavage loci observed with **P5E:Fe**, **BNME:Fe**, **BNSE:Fe**, and **BNFE:Fe** was not observed with **BNOE:Fe**, and **BNOE:Fe** produced a number of significant unique cleavage bands. The unique cleavage pattern produced by **BNOE:Fe** indicates a reduction and change of its binding specificity relative to the other molecules.

An autoradiograph of double-strand cleavage patterns produced by **P5E:Fe** and Bis(Netropsin) Amino acid-EDTA:Fe compounds is shown in Figure 1.16. The four cleavage loci of approximately equal intensity produced by **P5E:Fe** were also produced by **BNGE:Fe** and **BN- β -AE:Fe**. **BNGabaE:Fe** also produced these cleavage loci, but with this compound the relative intensities of the cleavage bands were more variable.

Electrophoretic mobilities of DNA cleavage bands were determined by densitometric analysis of the autoradiographs shown in Figures 1.15 and 1.16. Positions of pBR322 plasmid DNA double-strand cleavage by these molecules were determined from the electrophoretic mobilities of the observed DNA cleavage bands and a linear control plot of electrophoretic mobilities of molecular weight marker bands versus the logarithm of the molecular weights (in base pairs) of the marker bands.³⁸ Histograms of DNA double-strand cleavage by **P5E:Fe** and the Bis(Netropsin)-EDTA:Fe compounds are shown in Figures 1.17 and 1.18. The cleavage loci observed with these compounds map to regions of pBR322 rich in A:T base pairs. The cleavage locus observed near pBR322 position 3100 is consistent with DNA binding/cleaving at two closely spaced seven base pair homopolymer A:T sequences, 5'-TTTTTTT-3' (centered at position 3079), and 5'-AAAAAAA-3' (centered at position 3111). On some gels, DNA cleavage at these two sites has been resolved. The cleavage locus near position 3250 maps to the longest contiguous stretch of A:T base pairs (15) found on pBR322, 5'-TTTTAAATTAAAAAT-3' (centered at position 3236). The cleavage locus near position 4250 maps to the nine base pair sequence

Figure 1.16

Autoradiograph of DNA double-strand cleavage patterns produced by **P5E:Fe** and Bis(Netropsin) Amino Acid-EDTA:Fe compounds on Sty I linearized, 3'-³²P end-labeled pBR322 plasmid DNA in the presence of dioxygen and dithiothreitol. Cleavage patterns were resolved by electrophoresis on a 1% agarose gel. Lanes 2,4,6,8 contain DNA labeled at one end with α -³²P dATP, while lanes 3,5,7,9 contain DNA labeled at the other end with α -³²P TTP. Lanes 1 and 10, molecular weight markers consisting of pBR322 restriction fragments 4363, 3371, 2994, 2368, 1998, 1768, 1372, 995, and 666 bp in length; lanes 2 and 3, **P5E:Fe** at 0.50 μ M concentration; lanes 4 and 5, **BNGE:Fe** at 4.0 μ M concentration; lanes 6 and 7, **BN β -AE:Fe** at 0.05 μ M concentration; lanes 8 and 9, **BNGabaE:Fe** at 4.0 μ M concentration.



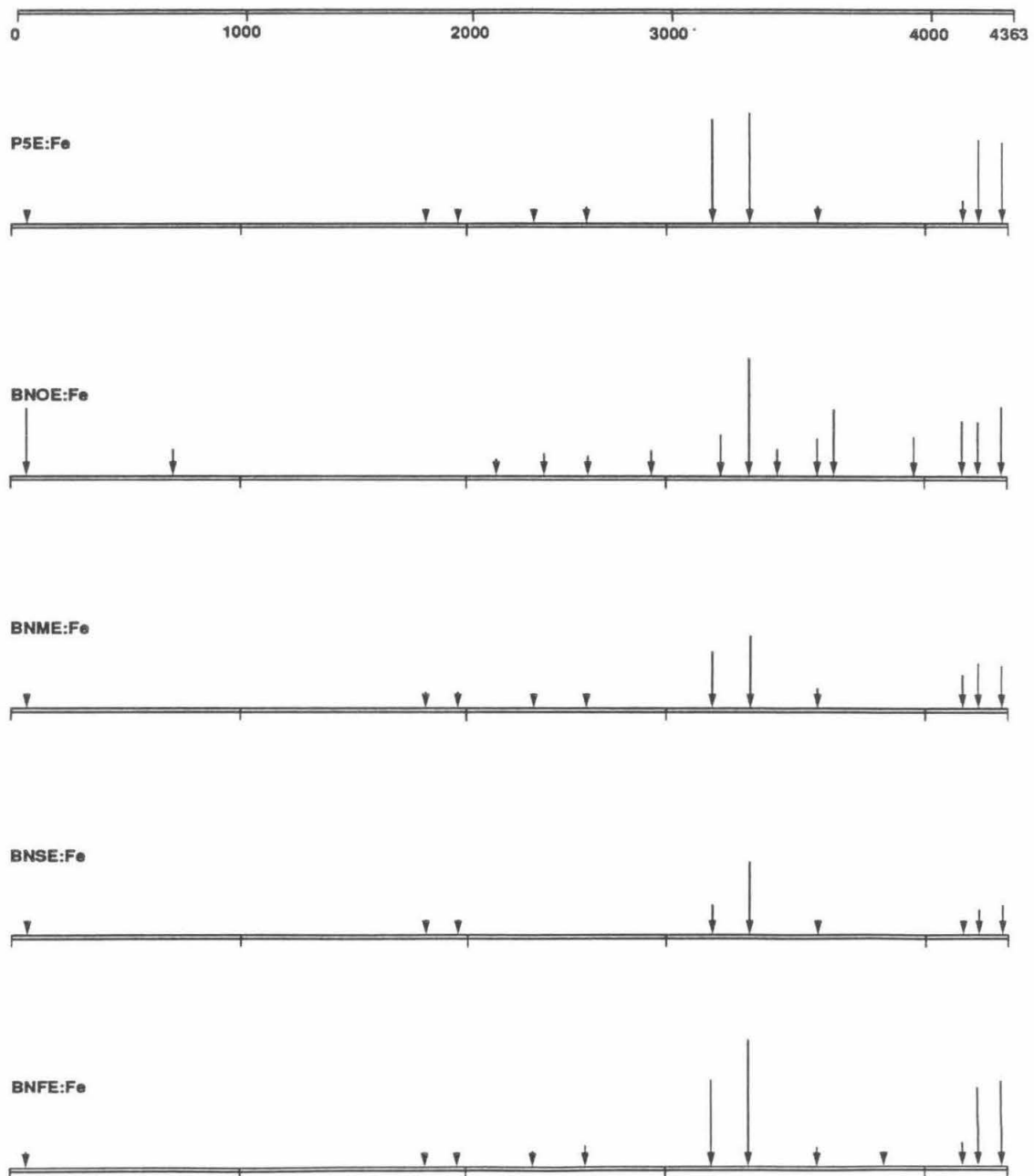


Figure 1.17. Histograms of DNA double-strand cleavage produced by PSE:Fe and Bis(Netropsin) Diacid-EDTA:Fe compounds on Sty I linearized pBR322 plasmid DNA in the presence of dioxygen and dithiothreitol. Lengths of arrows correspond to the relative amounts of cleavage, determined by optical densitometry, at the various cleavage loci. Positions of cleavage were determined by analyzing the measured electrophoretic mobilities of DNA cleavage fragments relative to a standard curve derived from the measured electrophoretic mobilities of marker fragments of known molecular weights.

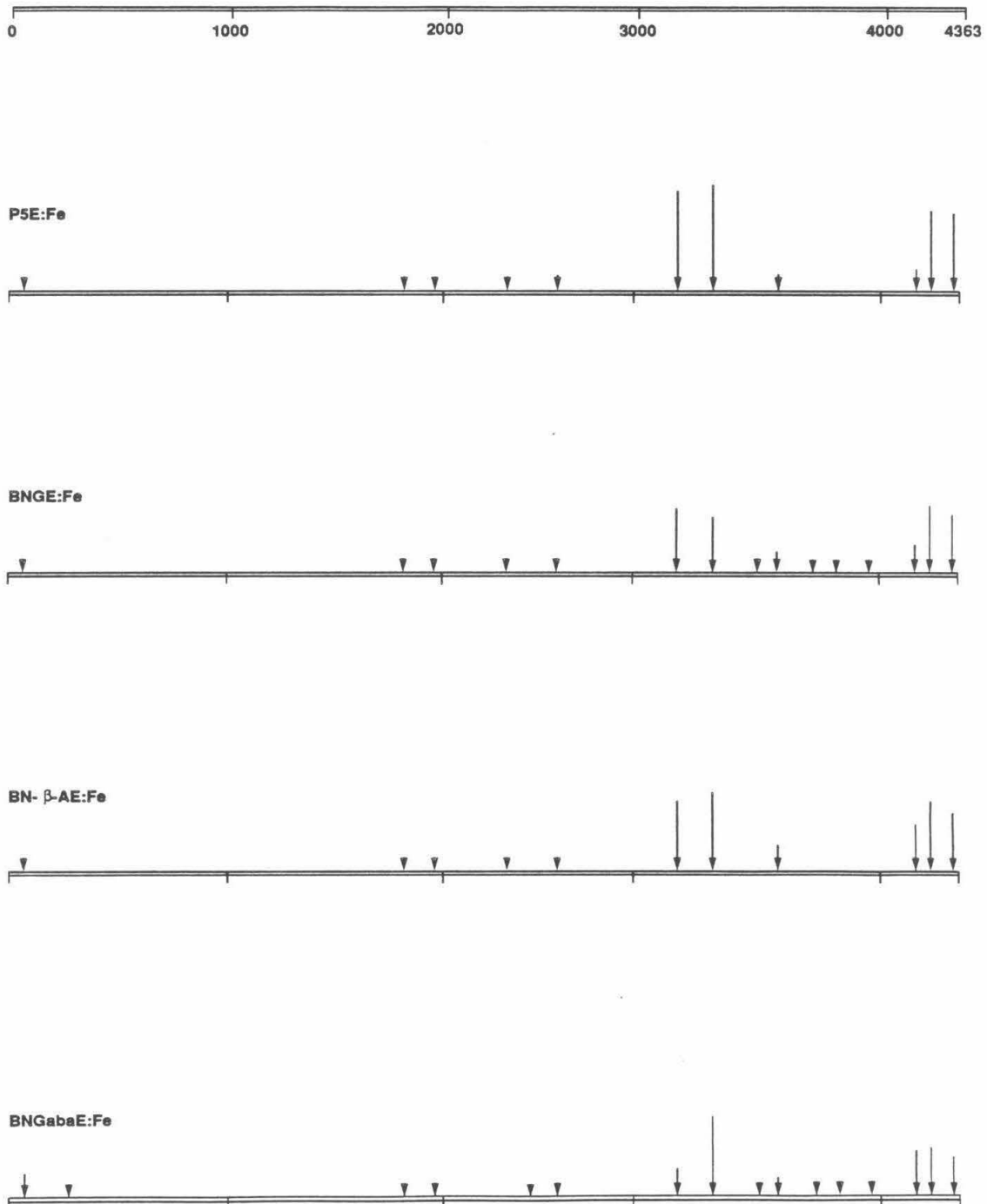


Figure 1.18. Histograms of DNA double-strand cleavage produced by P5E:Fe and Bis(Netropsin) Amino Acid-EDTA:Fe compounds on Sty I linearized pBR322 plasmid DNA in the presence of dioxygen and di-thiothreitol. Lengths of arrows correspond to the relative amounts of cleavage, determined by densitometry, at the various cleavage loci. Positions of cleavage were determined by analyzing the measured electrophoretic mobilities of DNA cleavage fragments relative to a standard curve derived from the measured electrophoretic mobilities of marker fragments of known molecular weights.

5'-TTTATTTT-3' (centered at position 4237). The cleavage locus near position 4300 maps to the ten base pair sequence 5'-TATTTTATA-3' (centered at position 4325), and may also reflect cleavage at the neighboring eight base pair sequence 5'-ATAATAAT-3' (centered at position 4303). Notable minor cleavage loci observed with these molecules map to the sequences 5'-AATAATATT-3' (centered at position 4173) and 5'-TTAAATT-3' (centered at position 59).

The amounts of DNA cleavage produced at each site by each compound were also determined by densitometry, and are depicted in the histograms. Given these data, the relative DNA binding/cleaving efficiencies (E) of these compounds may be considered as the ratio of DNA cleavage produced by one molecule (per unit concentration) to the cleavage produced by a second (control) molecule (per unit concentration). While the exact relationship between relative DNA binding/cleaving efficiencies and ratios of equilibrium binding constants is not known, it is assumed that E_{rel} values indicate trends in relative binding affinities. For overall cleavage of pBR322 by **P5E:Fe** and Bis(Netropsin)-EDTA:Fe compounds, E_{rel} decreases in the order **BN- β -AE:Fe** > **BNSE:Fe** > **BNFE:Fe** > **P5E:Fe** > **BNME:Fe** > **BNGE:Fe** = **BNGabaE:Fe** = **BNOE:Fe**.

Two of the major DNA binding/cleaving loci identified by double-strand cleavage analysis were examined at nucleotide resolution. For these experiments, 517 base pair Eco RI/Rsa I restriction fragments from pBR322 were prepared with ^{32}P at either the 3'- or 5' Eco RI end. These fragments contained the major cleavage loci centered at or near pBR322 positions 4237 and 4325. DNA cleavage products were separated by denaturing polyacrylamide gel electrophoresis. Autoradiographs of the DNA cleavage patterns produced by **P5E:Fe** and Bis(Netropsin) Diacid-EDTA:Fe compounds on these restriction fragments are shown in Figures 1.19 and 1.20. An autoradiograph of the DNA cleavage patterns produced by **P5E:Fe** and Bis(Netropsin) Amino acid-EDTA:Fe compounds is shown in Figure 1.21.

Figure 1.19

Autoradiograph of DNA cleavage patterns produced by **P5E:Fe** and Bis(Netropsin) Diacid-EDTA:Fe compounds on 3'- and 5'-³²P end-labeled 517 bp restriction fragments (Eco RI/Rsa I) from plasmid pBR322 DNA, in the presence of dioxygen and dithiothreitol. Cleavage patterns were resolved by electrophoresis on a 1:20 cross-linked 8% polyacrylamide, 50% urea denaturing gel. Lanes 1-14 were with 3' end-labeled DNA, while lanes 15-28 were with 5' end-labeled DNA. Lanes 1 and 28, uncleaved DNA; lanes 2 and 27, Maxam-Gilbert chemical sequencing G reactions; lanes 3-5 and 15-17, **P5E:Fe** at 0.50, 1.0, and 2.0 μ M concentrations; lanes 6-8 and 18-20, **BNME:Fe** at 1.0, 2.0, and 5.0 μ M concentrations; lanes 9-11 and 21-23, **BNSE:Fe** at 0.50, 1.0, and 2.0 μ M concentrations; lanes 12-14 and 24-26, **BNFE:Fe** at 0.50, 1.0, and 2.5 μ M concentrations.

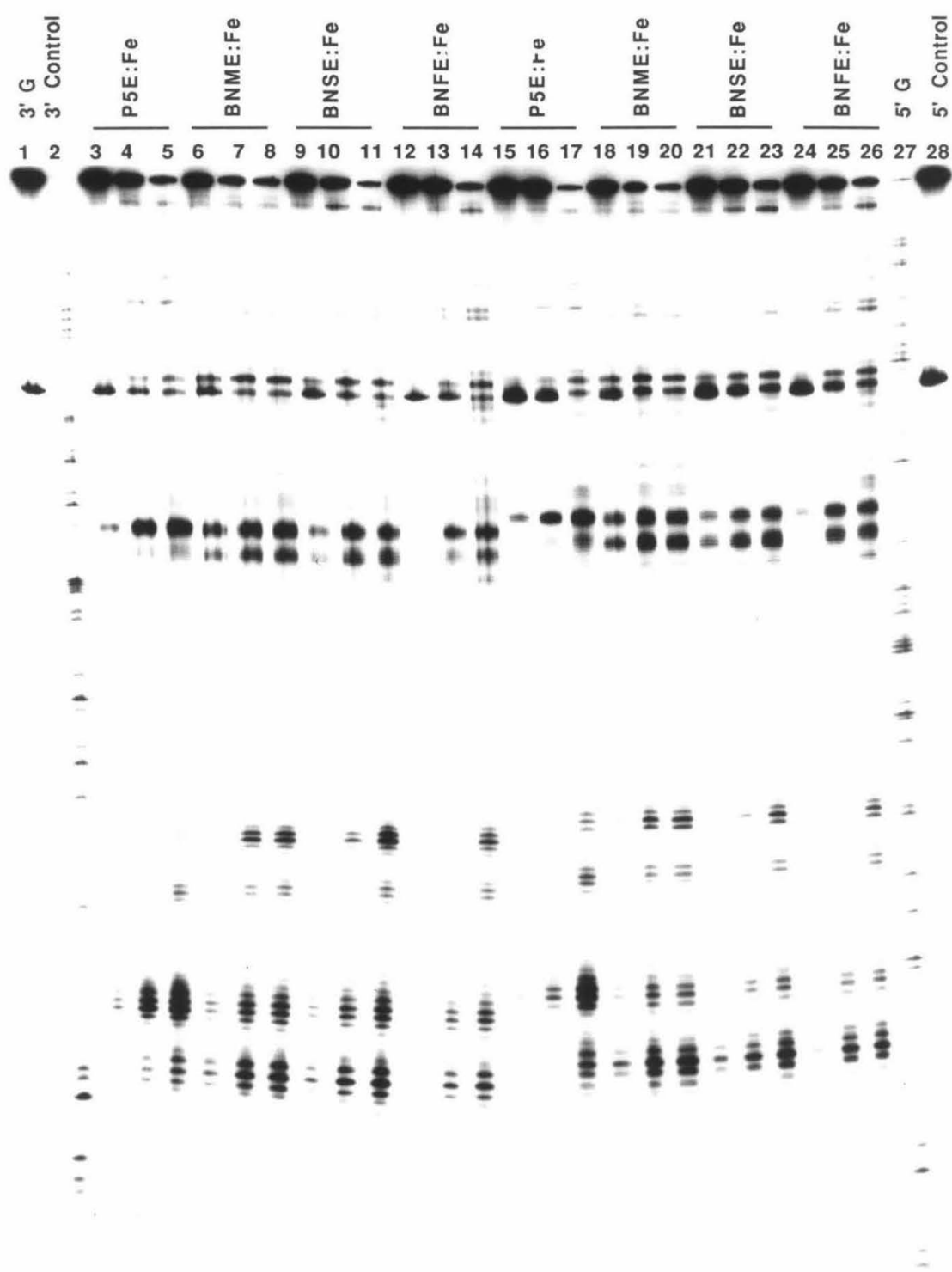


Figure 1.20

Autoradiograph of DNA cleavage patterns produced by **P5E:Fe** and **BNOE:Fe** on 3'- and 5'-³²P end-labeled 517 bp restriction fragments (Eco RI/Rsa I) from plasmid pBR322 DNA, in the presence of dioxygen and dithiothreitol. Cleavage patterns were resolved by electrophoresis on a 1:20 cross-linked 8% polyacrylamide, 50% urea denaturing gel. Lanes 1-8 were with 3' end-labeled DNA, while lanes 9-16 were with 5' end-labeled DNA. Lanes 1 and 16, uncleaved DNA; lanes 2 and 15, Maxam-Gilbert chemical sequencing G reactions; lanes 3-5 and 9-11, **P5E:Fe** at 0.50, 1.0, and 2.0 μ M concentrations; lanes 6-8 and 12-14, **BNOE:Fe** at 1.0, 20, and 50 μ M concentrations.

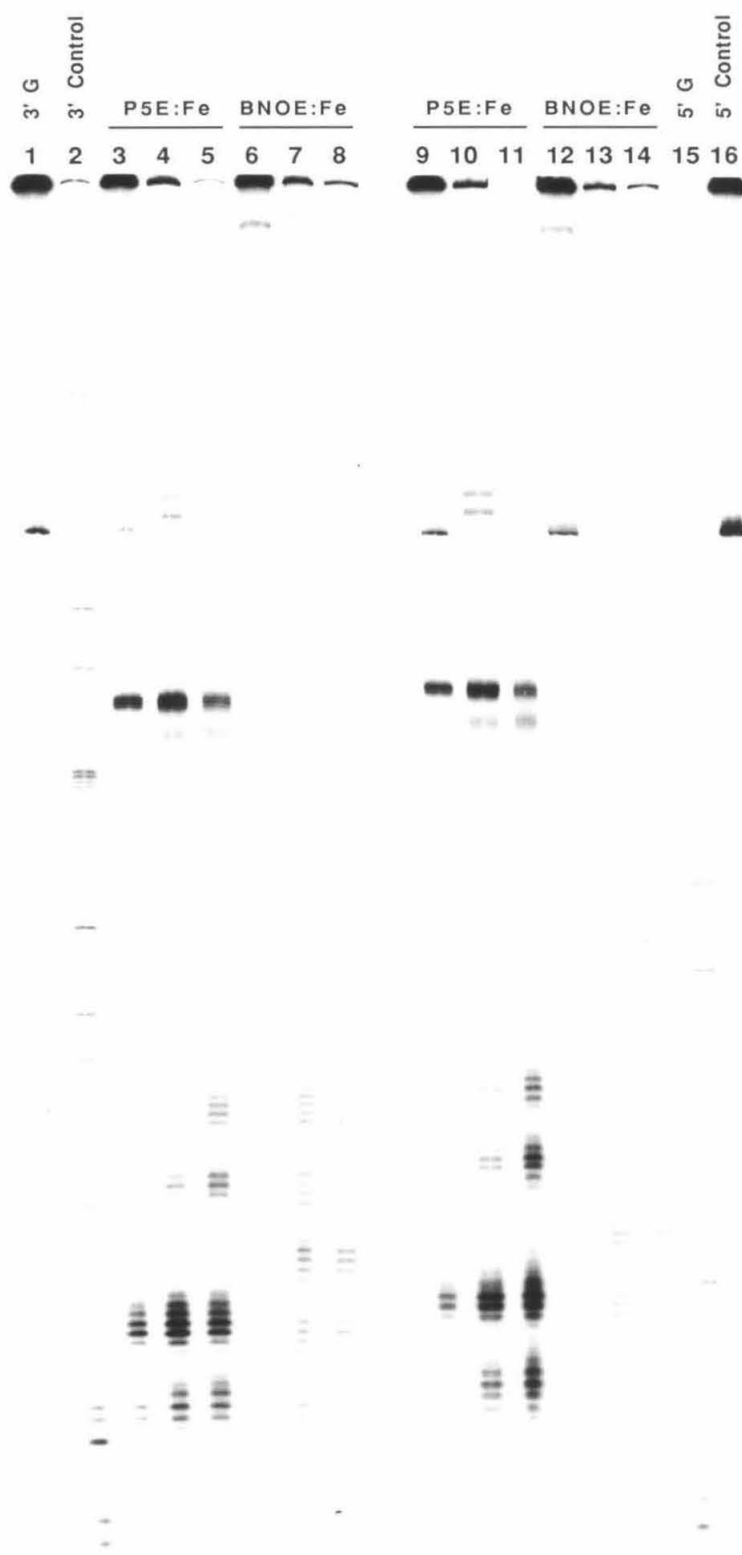
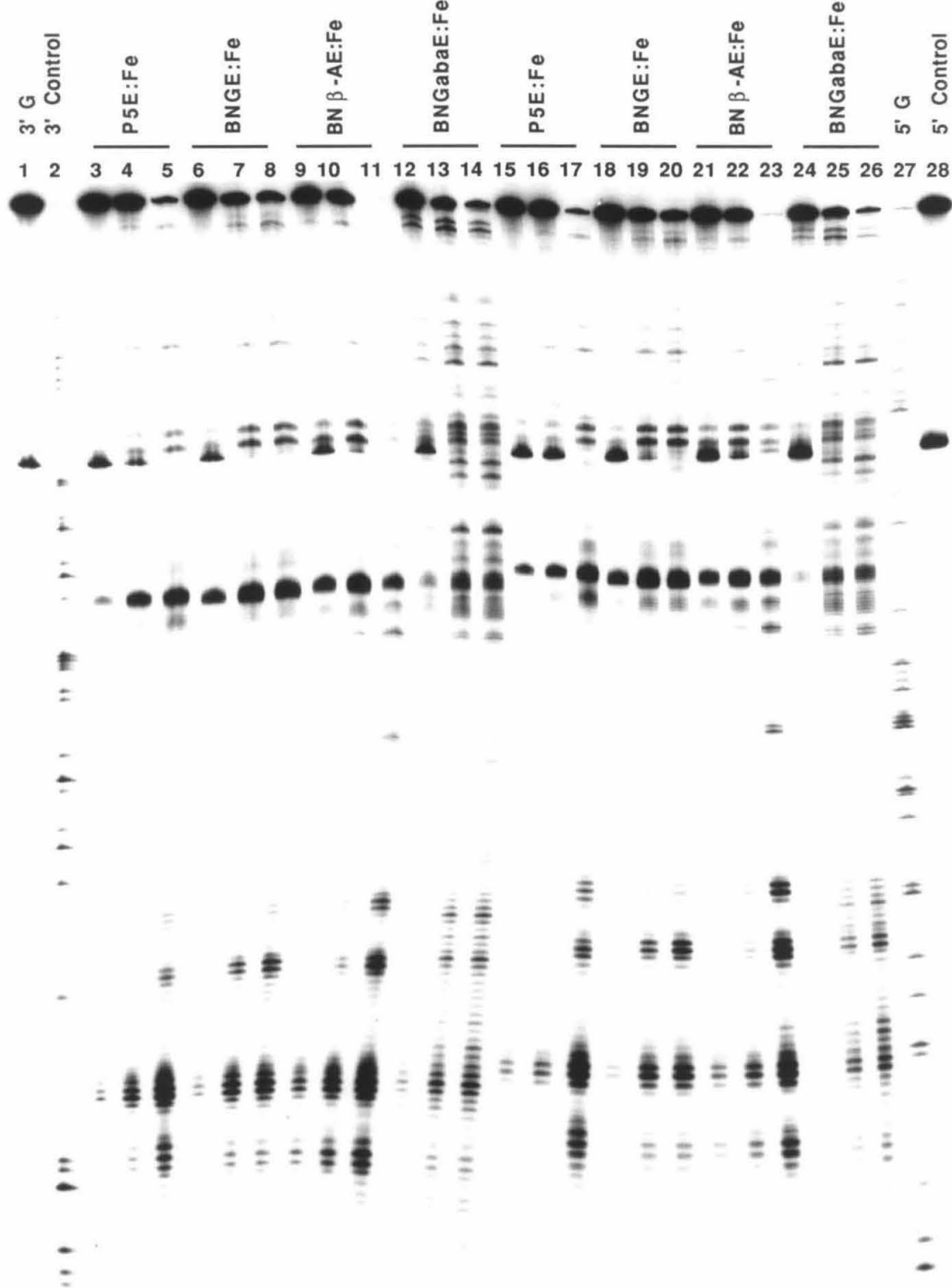


Figure 1.21

Autoradiograph of DNA cleavage patterns produced by **P5E:Fe** and Bis(Netropsin) Amino Acid-EDTA:Fe compounds on 3'- and 5'-³²P end-labeled 517 bp restriction fragments (Eco RI/Rsa I) from plasmid pBR322 DNA, in the presence of dioxygen and dithiothreitol. Cleavage patterns were resolved by electrophoresis on a 1:20 cross-linked 8% polyacrylamide, 50% urea denaturing gel. Lanes 1-14 were with 3' end-labeled DNA, while lanes 15-28 were with 5' end-labeled DNA. Lanes 1 and 28, uncleaved DNA; lanes 2 and 27, Maxam-Gilbert chemical sequencing G reactions; lanes 3-5 and 15-17, **P5E:Fe** at 0.50, 1.0, and 2.0 μ M concentrations; lanes 6-8 and 18-20, **BNGE:Fe** at 2.0, 10, and 20 μ M concentrations; lanes 9-11 and 21-23, **BN β -AE:Fe** at 0.25, 0.50, and 2.0 μ M concentrations; lanes 12-14 and 24-26, **BNGabaE:Fe** at 2.0, 10, and 20 μ M concentrations.



Several observations may be made from inspection of these autoradiographs. First, except for **BNOE:Fe**, the Bis(Netropsin)-EDTA:Fe compounds produced DNA cleavage in the same general regions as **P5E:Fe**. **BNOE:Fe** produced specific cleavage in these and other unique regions. In addition, **BNOE:Fe** produced a significant amount of nonspecific background cleavage. Second, except for **BNOE:Fe**, these molecules produced strong cleavage at two sites on the 517 base pair restriction fragment (at the bottom and in the upper middle parts of the autoradiographs), and weak or moderate cleavage at two additional sites (in the lower middle and in the upper parts of the autoradiographs). Third, **P5E:Fe**, **BNGE:Fe**, **BN- β -AE:Fe**, and **BNGabaE:Fe** (which have non- C_2 symmetrical DNA binding subunits) exhibit more pronounced DNA binding/cleaving orientation preferences than the Bis(Netropsin) Diacid-EDTA:Fe compounds (which have C_2 symmetrical DNA binding subunits). Fourth, the Bis(Netropsin)-EDTA:Fe compounds exhibit lower site selectivity than **P5E:Fe**: They produce significantly more cleavage at the lower middle and upper sites (relative to the cleavage they produce at the bottom and upper middle sites) than does **P5E:Fe**.

The DNA cleavage patterns on these and other autoradiographs were quantified by densitometry and converted to histogram form (Figures 1.22 and 1.23). Equilibrium minor groove binding sites for these molecules, assigned on the basis of their 3'-shifted, pseudo- C_2 symmetrical cleavage patterns,²⁸ are indicated as boxes in the histograms. For **P5E:Fe** and the Bis(Netropsin)-EDTA:Fe compounds except **BNOE:Fe**, the DNA binding site observed at the bottom of the autoradiographs (Site A) is 5'-ATTTTTA-3'. This sequence lies within the ten base pair A:T sequence centered at pBR322 position 4325 and was mapped by DNA double-strand affinity cleaving analysis. In the lower middle of the autoradiographs (Site B), **P5E:Fe** binds to the sequence 5'-ATAATAA-3', while **BNME:Fe**, **BNSE:Fe**, **BNFE:Fe**, and **BNGE:Fe** bind to the sequence 5'-TAATAAT-3'. In this region and in regions further up the autoradiograph shown in Figure 1.21, **BNGabaE:Fe** produced complex patterns of cleavage. These patterns are indicative of

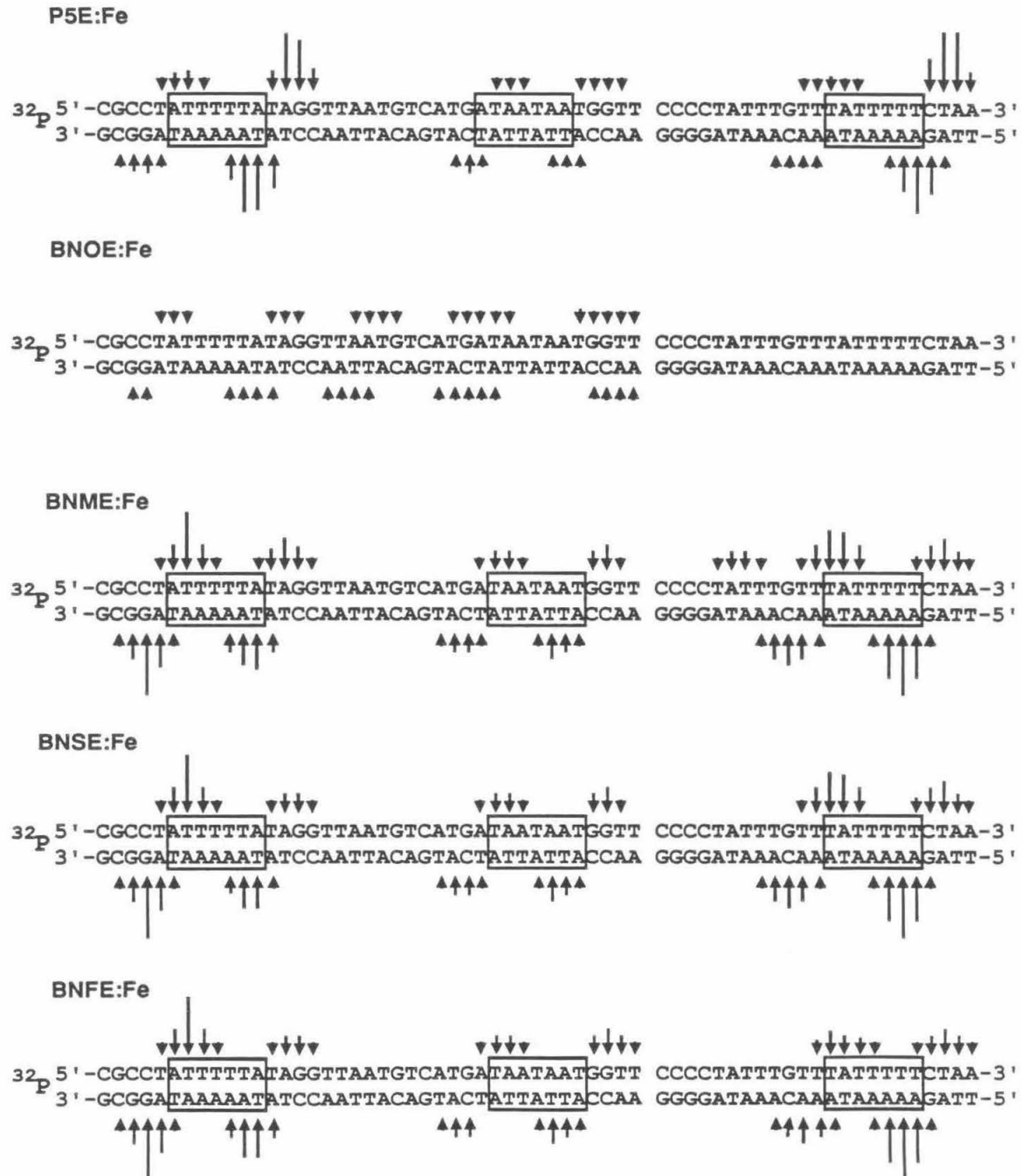


Figure 1.22. Histograms of DNA cleavage produced by P5E:Fe and Bis(Netropsin) Diacid-EDTA:Fe compounds on the 517 bp DNA restriction fragment (Eco RI/Rsa I) from plasmid pBR322 DNA. Lengths of arrows correspond to the relative amounts of cleavage that result in removal of the indicated base. DNA minor groove binding sites (boxed) were assigned from the observed cleavage patterns and the model described by Taylor, Schultz, and Dervan (Reference 28).

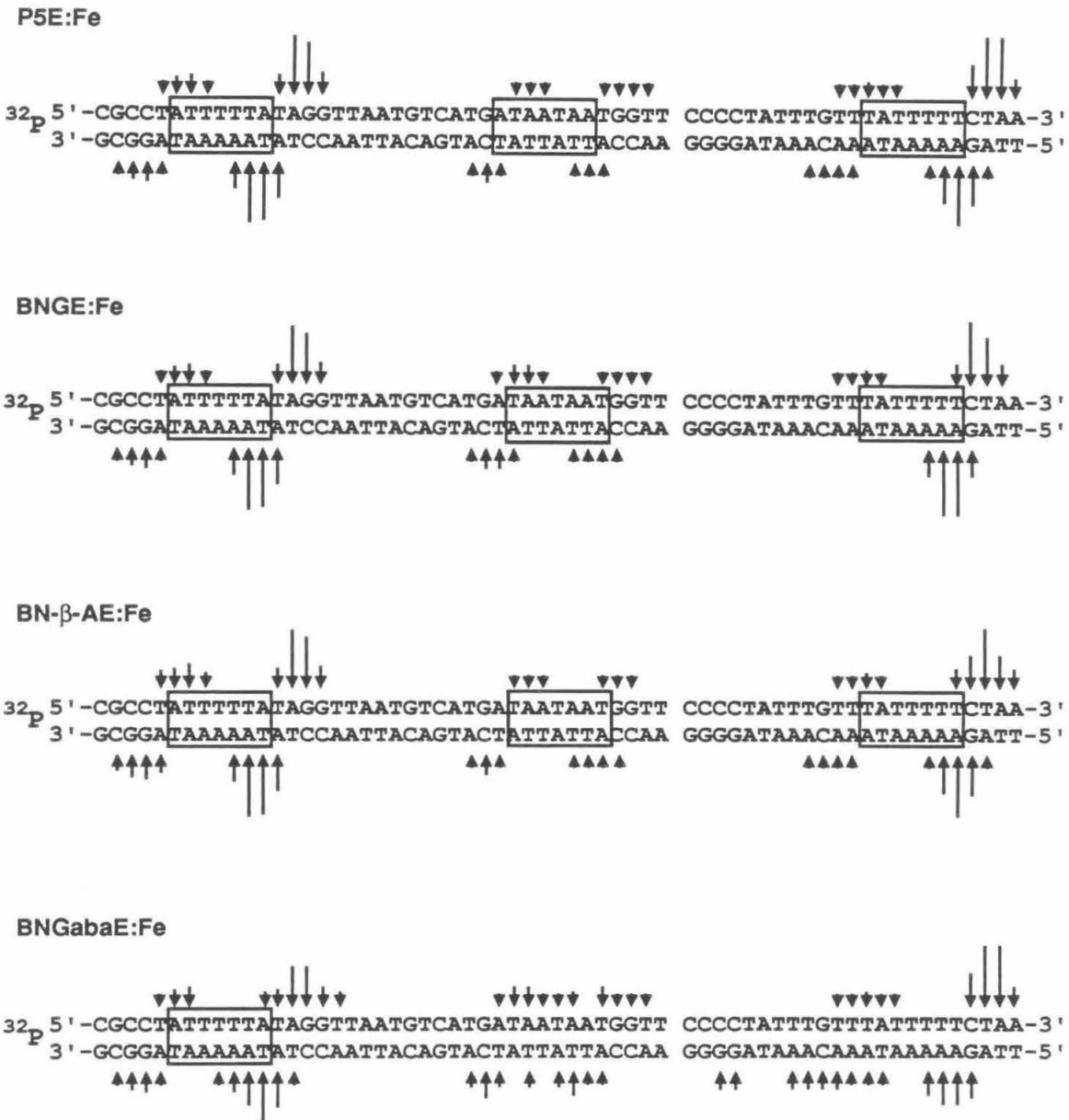


Figure 1.23. Histograms of DNA cleavage produced by P5E:Fe and Bis(Netropsin) Amino Acid-EDTA:Fe compounds on the 517 bp DNA restriction fragment (Eco RI/Rsa I) from plasmid pBR322 DNA. Lengths of arrows correspond to the relative amounts of cleavage that result in removal of the indicated base. DNA minor groove binding sites (boxed) were assigned from the observed cleavage patterns and the model described by Taylor, Schultz, and Dervan (Reference 28).

competitive monomeric and dimeric binding modes for **BNGabaE:Fe** in which one or both Netropsin subunits are in contact with DNA. Thus, Gaba does not *enforce* dimeric binding by flanking Netropsin subunits. At the strong binding site in the upper middle of the autoradiographs (Site C), **P5E:Fe**, **BNME:Fe**, **BNSE:Fe**, **BNFE:Fe**, **BNGE:Fe**, and **BN- β -AE:Fe** bind to the seven base pair sequence 5'-TATTTTT-3'. This binding site lies within the nine base pair A:T sequence centered at pBR322 position 4237 and was mapped by DNA double-strand affinity cleaving analysis.

Densitometric analysis of cleavage intensities produced by these molecules allowed values of binding orientation preferences and relative DNA binding/cleaving efficiencies to be calculated for these molecules at Sites A, B, and C. These data are collected in the following tables. The estimated error in the calculated values is $\pm 20\%$. Orientation preferences were calculated by dividing the total amount of cleavage observed on the lower side (towards the bottom of the autoradiograph) of a binding site by the total amount of cleavage observed on the higher side of that binding site. For the Bis(Netropsin) Diacid-EDTA compounds, orientation preferences ranged from 1.1 to 2.5. For the Bis(Netropsin) Amino acid-EDTA compounds, orientation preferences ranged from 2.2 to 6.3. E_{rel} values were calculated by dividing the total amount of cleavage produced by a given compound at Sites A, B, or C by the total amount of cleavage produced by **P5E:Fe** at Site

Orientation Preference

<u>Compound</u>	<u>Site A</u>	<u>Site B</u>	<u>Site C</u>
P5E:Fe	1:4.4	1.7:1	1:5.7
BNME:Fe	1.5:1	1:1.6	1:1.1
BNSE:Fe	1.7:1	1:2.1	1:1.1
BNFE:Fe	1.5:1	1:1.3	1:1.2
BNGE:Fe	1:4.0	5.8:1	1:6.3
BN-β-AE:Fe	1:2.2	1.9:1	1:4.2
BNGabaE:Fe	1:3.7	-----	-----

Relative DNA Binding/Cleaving Efficiency (E_{rel})

<u>Compound</u>	<u>Site A</u>	<u>Site B</u>	<u>Site C</u>
P5E:Fe	1.0	0.18	0.97
BNME:Fe	1.0	0.36	0.66
BNSE:Fe	1.51	0.70	1.52
BNFE:Fe	0.86	0.14	0.84
BNGE:Fe	0.15	0.07	0.22
BN-β-AE:Fe	3.3	0.70	3.9
BNGabaE:Fe	0.10	-----	-----

A, and then correcting for the differences in concentrations of compounds employed. At the strongest binding sites, Sites A and C, E_{rel} decreased in the order **BN- β -AE:Fe** > **P5E:Fe**, **BNME:Fe**, **BNSE:Fe**, **BNFE:Fe** > **BNGE:Fe**, **BNGabaE:Fe** > **BNOE:Fe**. The reduced site selectivity of Bis(Netropsin)-EDTA:Fe compounds relative to **P5E:Fe** is reflected in DNA binding/cleaving efficiencies at Site B, where E_{rel} decreases in the order **BN- β -AE:Fe** > **BNME:Fe**, **BNSE:Fe** > **BNFE:Fe**, **P5E:Fe** > **BNGE:Fe**.

Discussion

Straightforward procedures have been developed for the synthesis of Bis(Netropsin)-EDTA compounds linked in tail-to-tail fashion by diacids and in head-to-tail fashion by amino acids. Each synthesis required sixteen or seventeen convergent synthetic steps from commercially available starting materials. The use of the advanced intermediate $O_2NP_2CO_2H$ shortened the syntheses to ten or eleven steps. The limitations to these methods would seem to be the availability and chemical stability of the diacid or amino acid linker synthons (see Chapters Two and Three).

The major conclusion to be drawn from the DNA affinity cleaving data is that except for **BNOE:Fe**, the Bis(Netropsin)-EDTA:Fe compounds bind preferentially to the same A:T rich sites with significant homopolymer character preferred by **P5E:Fe**. However, these data also show that small differences in linker structure can have significant effects on DNA binding/cleaving properties. The lengths and natures of the linkers have significant effects on the relative DNA binding/cleaving efficiencies of Bis(Netropsin)-EDTA:Fe compounds. Given that the Netropsin:dodecamer and Distamycin A:dodecamer structures indicate that **MPC** is approximately 20% too large for B DNA (in terms of isohelical spacing of amide NHs and lone pair electrons from adenine N3 and thymine O2 atoms),^{12-14,39} Bis(Netropsin)s linked by residues that are somewhat smaller or more flexible than **MPC** might bind more strongly to DNA than **P5E** because of their ability to optimize hydrogen-bond donor-acceptor interactions. The data support this hypothesis. β -Alanine is more flexible and slightly smaller than **MPC** in terms of the distance between amide NHs at the ends of the linker. **BN- β -AE:Fe** produces specific DNA cleavage more efficiently than the other Bis(Netropsin)-EDTA:Fe compounds or **P5E:Fe**. Preliminary results from quantitative affinity cleaving (QAC) experiments⁴⁰ indicate that **BN- β -AE:Fe** binds to Sites A, B, and C with affinity constants in the range $1-5 \times 10^7 \text{ M}^{-1}$. The results with **BN- β -AE:Fe** are interesting in that they differ from results reported by Dasgupta, Parrack, and Sasisekharan.⁴¹ These workers found that analogs of Distamycin A in which the central or C-terminal *N*-methylpyrrolecarboxamide residue was replaced by β -alanine bound more weakly than Distamycin A to the alternating DNA copolymer (AT)_n:(AT)_n. The discrepancy between these findings and the results presented in this Chapter may be due to the context in which the β -alanine moiety was studied (P3 analogs versus P5 analogs). Malonamide is also slightly smaller and more flexible than **MPC**. **BNME:Fe** binds and cleaves DNA with efficiency comparable to **P5E:Fe**. Succinamide and fumaramide approximate **MPC** in size, and are more flexible. **BNSE:Fe** and **BNFE:Fe** produce specific DNA cleavage as efficiently as **P5E:Fe**.

The reduced DNA binding/cleaving efficiency of **BNGabaE:Fe** and its propensity to bind in monomeric fashion are understandable in terms of the properties of its linker. Gaba is slightly larger and much more flexible than **MPC**. The length of Gaba exacerbates hydrogen-bond donor:acceptor mis-registration in the DNA minor groove. The conformation of Gaba that most closely mimics the contour of **MPC** is severely distorted from the expected all-*trans* ground state conformation. The flexibility of Gaba may then allow one Netropsin subunit to swing away from the DNA into solution. This action would relieve distortion of the Gaba linker and allow water to form hydrogen-bonds with the amide NHs and the adenine N3 and thymine O2 lone pair electrons, which are stronger than the out-of-register hydrogen-bonds that would be formed between the amide NHs and the DNA bases.

Glycine and oxalamide are much smaller than **MPC**, and rather rigid. **BNGE:Fe** and **BNOE:Fe** are much less efficient than **PSE:Fe** at producing sequence-specific DNA cleavage. The reduced DNA binding/cleaving efficiency and specificity observed with **BNOE:Fe** may be interpreted in terms of the conformational properties of the linker. Oxalamide should prefer the s-*trans* conformation rather than the s-*cis* conformation shown in Figure 1.11. Models indicated that s-*trans* oxalamide disrupts the crescent shape of **BNOE** and directs one carboxamide oxygen atom towards the floor of the DNA minor groove. The lone pair electrons on this oxygen atom should interact with the N2 amino group of guanine in preference to the lone pair electrons from adenine N3 or thymine O2 atoms, thereby decreasing the affinity of **BNOE:Fe** for sites containing only A:T base pairs while increasing its affinity for sites containing G:C base pairs.⁴²

As the DNA binding subunits of Bis(Netropsin) Diacid compounds are *C*₂ symmetric, these subunits are not by themselves capable of binding with orientation preference at any DNA site. Thus, the orientation preferences observed with Bis(Netropsin) Diacid-EDTA:Fe compounds must reflect unequal interactions of their unsymmetrical ends with the DNA sequences that flank the DNA binding sites. Such

effects appear to be small, since binding orientation preferences for these molecules range from 1.1 to 2.5. Binding orientation preferences are more pronounced for **P5E:Fe** and the Bis(Netropsin) Amino acid-EDTA:Fe compounds, ranging from 2.2 to 6.3. These values reflect a combination of unequal end-group interactions as well as unsymmetrical interactions between non- C_2 symmetrical (nonpalindromic) DNA binding sequences and the non- C_2 symmetrical DNA binding subunits of **P5E:Fe** and the Bis(Netropsin) Amino acid-EDTA:Fe compounds. At Sites A and B, **P5E:Fe** and the head-to-tail dimers prefer an orientation *opposite* to that preferred by the tail-to-tail dimers. Thus, the unsymmetrical nature of the DNA binding subunits of **P5E:Fe** and Bis(Netropsin) Amino acid-EDTA:Fe compounds is a greater determinant of binding orientation preference than is the unsymmetrical nature of the ends of these molecules.

The greatest DNA binding orientation preferences are observed at sites of highest binding affinity--sites with significant homopolymer A:T content. A model for pronounced DNA binding orientation preference by oligo(*N*-methylpyrrolecarboxamide)s (and, by analogy, head-to-tail Netropsin dimers) is presented in Figure 1.24. The hallmark of this model is the optimization of hydrogen-bonding interactions between amide NHs and lone pair electrons on thymine O2 atoms. Models indicate that the amide NHs of oligo(*N*-methylpyrrolecarboxamide)s are skewed towards the amino terminus of these peptides. If the oligo(*N*-methylpyrrolecarboxamide) is oriented in the minor groove with its amino terminus at the 3' end of a run of Ts, the most colinear hydrogen-bonds between the amide NHs and thymine O2 atoms are formed, since this orientation juxtaposes the directionality of the amide NHs and the 5' propeller twist of the thymine bases.^{3,12-14} This orientation is the one observed experimentally and also favorably opposes the macrodipole of the oligo(*N*-methylpyrrolecarboxamide) with the macrodipole of the collection of O2 atoms on the propeller-twisted thymine bases.⁴³ Support for the notion that oligo(*N*-methylpyrrolecarboxamide)s prefer to interact with thymine O2 rather than adenine N3 atoms comes from the Netropsin:dodecamer and Distamycin A:dodecamer crystal structures

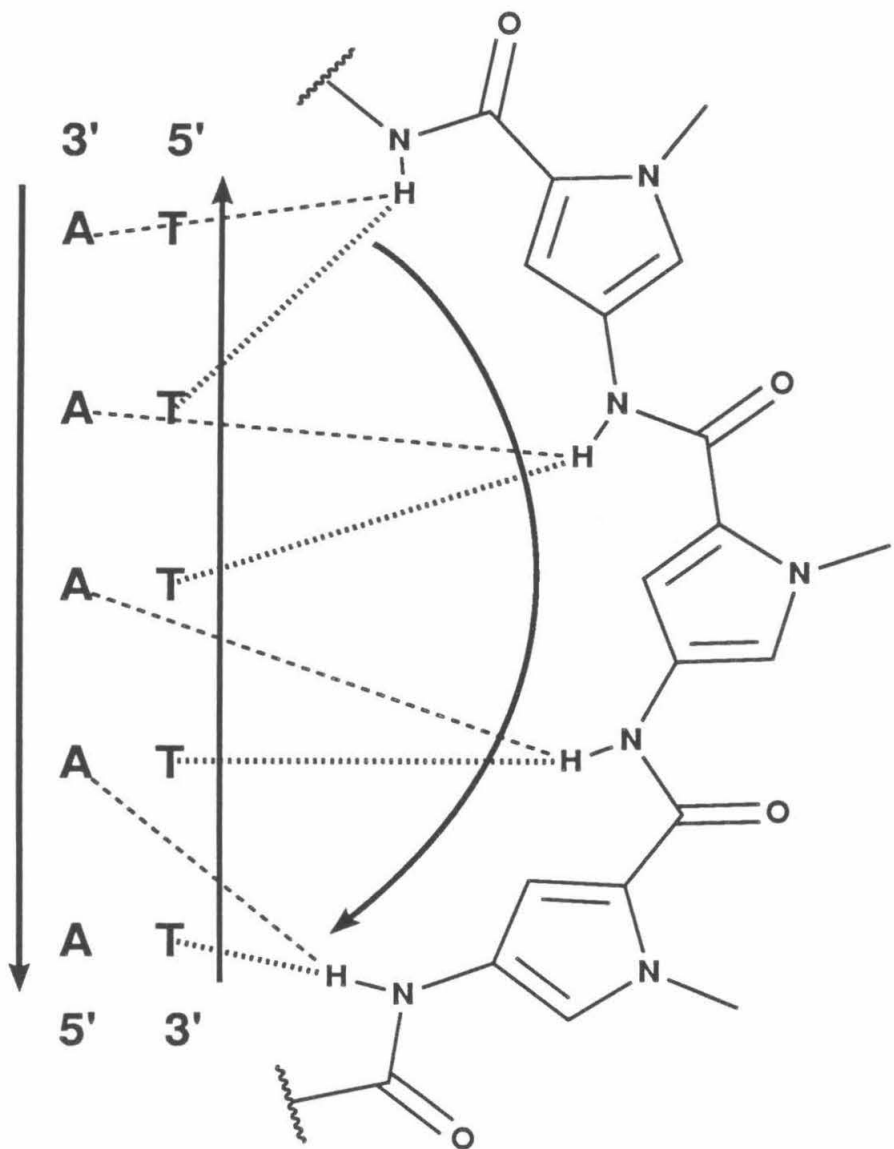


Figure 1.24. Proposed model for the pronounced binding orientation preferences observed with the minor groove complexation of oligo(*N*-methylpyrrolecarboxamide)s and Bis(Netropsin) Amino Acid compounds to homopolymeric (dA)_n:(dT)_n DNA sites. The straight arrows indicate the 3'-to-5' direction of base propeller twist in the minor groove. The curved arrow indicates the skew of oligo(*N*-methylpyrrolecarboxamide) NHs toward the amino terminus of the peptide. Dashed lines indicate hydrogen bonds between amide NHs and adenine N₃ atoms. Stippled lines indicate hydrogen bonds between amide NHs and thymine O₂ atoms.

In these structures, the carboxamide nitrogen to thymine oxygen distances are shorter than the carboxamide nitrogen to adenine nitrogen distances (2.68, 2.56, 3.2, 3.3, and 2.9 Å versus 3.28, 3.45, 3.3, 3.2, and 3.1 Å).¹²⁻¹⁴

At Sites A and C, **P5E:Fe**, **BNME:Fe**, **BNSE:Fe**, **BNFE:Fe**, **BNGE:Fe**, and **BN-β-AE:Fe** exhibit the same binding sequences of seven contiguous A:T base pairs. These results are consistent with the $n + 1$ rule for molecules with six amide NHs in their DNA binding subunits.^{33,34} At Site B, **P5E:Fe**, **BNME:Fe**, **BNSE:Fe**, **BNFE:Fe**, **BNGE:Fe**, and **BN-β-AE:Fe** also bind to seven base pair A:T sequences, but **P5E:Fe** binds to a sequence that is shifted by one base pair relative to the other molecules. The reasons for this shift are unclear, and might be attributable to the inherent precision limit associated with binding site assignment based on DNA affinity cleaving data. Alternatively, it might be that the more flexible Bis(Netropsin)-EDTA:Fe compounds are able to reorganize and engage in stronger interactions at the slightly different site.

The strong and specific cleavage observed with **BN-β-AE:Fe** suggested that β-alanine would be a good candidate for use in the preparation of larger and more specific DNA binding molecules. Accordingly, Youngquist and Dervan designed and synthesized a trimer of tetra(*N*-methylpyrrolecarboxamide) subunits linked by two β-alanine residues ((**P4**)₃-(β-A)₂-E, Figure 1.25).⁴⁴ **MPE:Fe** footprinting and DNA affinity cleaving analyses indicated that this molecule, which contains 15 amide NHs in the DNA binding domain, bound specifically to a sequence of sixteen contiguous A:T base pairs on a 205 base pair restriction fragment from SV-CAT plasmid DNA. However, this molecule produced double-strand cleavage of the linearized SV-CAT plasmid (5045 base pairs) with specificity no greater than **P4E:Fe**, indicating that DNA binding modes in addition to the trimeric interaction were possible. Perhaps a pentameric assembly of P2 Netropsin subunits linked by four β-alanine residues would exhibit greater specificity for pentameric binding, since the interaction of single Netropsin subunits with DNA is weaker than the interaction of single P4 subunits with DNA.

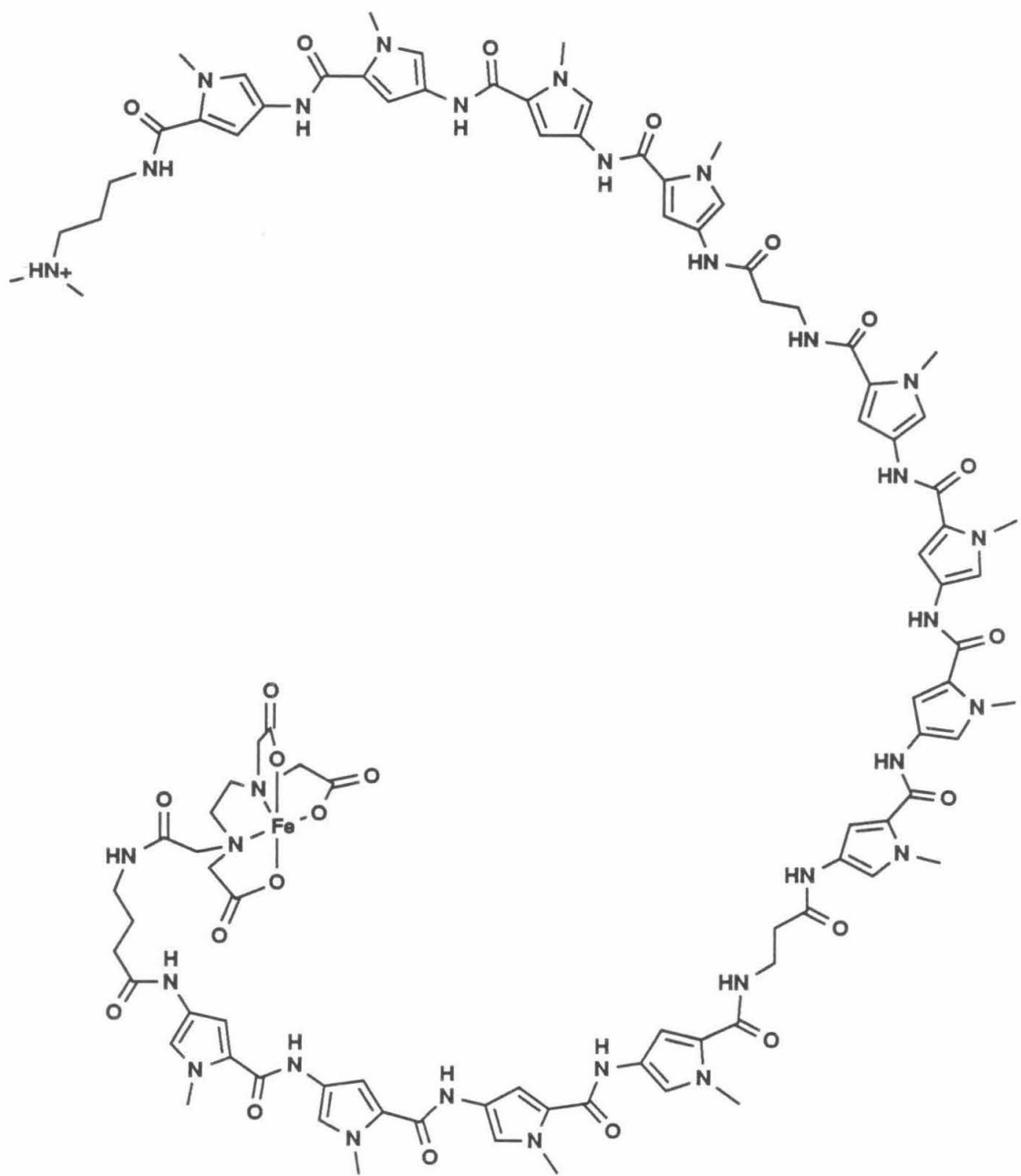


Figure 1.25. Tris[tetra(*N*-methylpyrrolecarboxamide)]-bis(β-Alanine)-EDTA:Fe, (P4)3-(β-A)2-E:Fe.

References

¹Drew, H.R.; Wing, R.M.; Tokano, T; Broka, C.; Tanaka, S.; Itakura, K.; Dickerson, R.E. *Proc. Natl. Acad. Sci. USA* **1981**, *78*, 2179-2183.

²Dickerson, R.E.; Drew, H.R. *J. Molec. Biol.* **1981**, *149*, 761-786.

³Nelson, H.C.M.; Finch, J.T.; Bonaventura, F.L.; Klug, A. *Nature*, **1987**, *330*, 221-226.

⁴McClarin, J.A.; Frederick, B.C.; Wang, P.; Greene, H.; Boyer, J.; Grable, J.; Rosenberg, J. *Science* **1986**, *234*, 1526-1541.

⁵Anderson, J.E.; Ptashne, M.; Harrison, S.C. *Nature* **1987**, *326*, 846-852.

⁶Aggarwal, A.K.; Rodgers, D.W.; Drott, M.; Ptashne, M.; Harrison, S.C. *Science* **1988**, *242*, 899-907.

⁷Jordan, S.R.; Pabo, C.O. *Science* **1988**, *242*, 893-899.

⁸Otwinowski, Z.; Schevitz, R.W.; Zhang, R.-G.; Lawson, C.L.; Joachimiak, A.; Marmorstein, R.Q.; Luisi, B.F.; Sigler, P.B. *Nature* **1988**, *335*, 321-329.

⁹Sobell, H.M.; Tsai, C.C.; Jain, S.C.; Gilbert, S.G. *J. Mol. Biol.* **1977**, *114*, 333-365, and references therein.

¹⁰Reviewed in Zimmer, C.; Wahnert, U. *Prog. Biophys. Mol. Biol.* **1986**, *47*, 31-112.

¹¹Berman, H.M.; Neidle, S.; Zimmer, C.; Thrum, H. *Biochim. Biophys. Acta* **1979**, *561*, 124-131.

¹²Kopka, M.L.; Yoon, C.; Goodsell, D.; Pjura, P.; Dickerson, R.E. *Proc. Natl. Acad. Sci. USA* **1985**, *82*, 1376-1380.

¹³Kopka, M.L.; Yoon, C.; Goodsell, D.; Pjura, P.; Dickerson, R.E. *J. Mol. Biol.* **1985**, *183*, 553-563.

¹⁴Coll, M.; Frederick, C.; Wang, A.H.-J.; Rich, A. *Proc. Natl. Acad. Sci. USA* **1987**, *84*, 8385-8389.

¹⁵Patel, D.J.; Shapiro, L. *J. Biol. Chem.* **1986**, *261*, 1230-1240, and references therein.

¹⁶Klevit, R.E.; Wemmer, D.E.; Reid, B.R. *Biochemistry* **1986**, *25*, 3296-3303.

¹⁷Breslauer, K.J.; Remeta, B.P.; Chou, W.-Y.; Ferrante, R.; Curry, J.; Zaunczkowski, D.; Snyder, J.G.; Marky, L.A. *Proc. Natl. Acad. Sci. USA* **1987**, *84*, 8922-8926.

¹⁸Stubbe, J.; Kozarich, J.W. *Chem. Rev.* **1987**, *87*, 1107-1136.

¹⁹Dervan, P.B. *Science* **1986**, *232*, 464-470.

²⁰Moser, H.E.; Dervan, P.B. *Science* **1987**, *238*, 645-650.

²¹Sluka, J.P.; Horvath, S.J.; Bruist, M.F.; Simon, M.I.; Dervan, P.B. *Science* **1987**, *238*, 1129-1132.

²²Hertzberg, R.P.; Dervan, P.B. *J. Am. Chem. Soc.* **1982**, *104*, 313-315.

²³Hertzberg, R.P.; Dervan, P.B. *Biochemistry* **1984**, *23*, 3934-3945.

²⁴Van Dyke, M.W.; Hertzberg, R.P.; Dervan, P.B. *Proc. Natl. Acad. Sci. USA* **1982**, *79*, 5470-5474.

²⁵Van Dyke, M.W.; Dervan, P.B. *Biochemistry* **1983**, *22*, 2373-2377.

²⁶Van Dyke, M.W.; Dervan, P.B. *Nucleic Acids Res.* **1983**, *11*, 5555-5567.

²⁷Schultz, P.G.; Taylor, J.S.; Dervan, P.B. *J. Am. Chem. Soc.* **1982**, *104*, 6861-6863.

²⁸Taylor, J.S.; Schultz, P.G.; Dervan, P.B. *Tetrahedron* **1984**, *40*, 457-465.

²⁹Schultz, P.G.; Dervan, P.B. *Proc. Natl. Acad. Sci. USA* **1983**, *80*, 6834-6837.

³⁰Youngquist, R.S.; Dervan, P.B. *Proc. Natl. Acad. Sci. USA* **1985**, *82*, 2565-2569.

³¹Khorlin, A.A.; Krylov, A.S.; Grokhovsky, S.L.; Zhuze, A.L.; Zasedatelev, A.S.; Gursky, G.V.; Gottikh, B.P. *FEBS Lett.* **1980**, *118*, 311-314.

³²Skamrov, A.V.; Rybalkin, I.N.; Bibilashvili, R.S.; Gottikh, B.P.; Grokhovski, S.L.; Gurskii, G.V.; Zhuze, A.L.; Zasedatelev, A.S.; Nechipurenko, Y.D.; Khorlin, A.A. *Molekulyarnaya Biologiya (Engl. Trans.)* **1985**, *19*, 153-167.

³³Schultz, P.G.; Dervan, P.B. *J. Am. Chem. Soc.* **1983**, *105*, 7748-7750.

³⁴Youngquist, R.S.; Dervan, P.B. *J. Am. Chem. Soc.* **1985**, *107*, 5528-5529.

³⁵Bialer, M.; Yagen, B.; Mechoulam, R. *Tetrahedron* **1978**, *34*, 2389-2391.

³⁶Hay, R.; Nolan, K. *J. Chem. Soc., Dalton Trans.* **1975**, 1348-1351.

³⁷Youngquist, R.S. Ph.D. Thesis, California Institute of Technology, Pasadena, California, 1988.

³⁸Maniatis, T.; Fritsch, E.F.; Sambrook, J. *Molecular Cloning: A Laboratory Manual*. Cold Spring Harbor Laboratory: Cold Spring Harbor, New York, 1982, pp. 150-152.

³⁹Goodsell, D.; Dickerson, R.E. *J. Med. Chem.* **1986**, *29*, 727-733.

⁴⁰Shin, J.A.; Wade, W.S.; Dervan, P.B., manuscript in preparation.

⁴¹Dasgupta, D.; Parrack, P.; Sasisekharan, V. *Biochemistry* **1987**, *26*, 6381-6386.

⁴²Wade, W.S.; Dervan, P.B. *J. Am. Chem. Soc.* **1987**, *109*, 1574-1575.

⁴³Hol, W.G.J. *Prog. Biophys. Mol. Biol.* **1985**, *45*, 149-195.

⁴⁴Youngquist, R.S.; Dervan, P.B. *J. Am. Chem. Soc.* **1987**, *109*, 7564-7566.

CHAPTER TWO: STEREOCHEMICAL REGULATION OF SEQUENCE SPECIFIC DNA BINDING/CLEAVING BY CHIRAL BIS(NETROPSIN)S

Introduction

Double-stranded DNA is a chiral polymer composed of interwound, antiparallel polynucleotide strands in which the nucleotide monomer subunits contain D-2'-deoxyribose residues. In addition to the chiral sugar residues, double-stranded DNA also possesses conformation-dependent helicity. To date, three distinct canonical conformations of double-helical DNA have been identified and characterized by x-ray diffraction.^{1,2} A DNA and B DNA are right-handed double-helical forms, while Z DNA is a left-handed double-helical form. Because of its chiral nature, double-helical DNA interacts with different stereoisomeric forms of a given chiral DNA binding molecule to produce diastereomeric complexes. Several chiral DNA binding small molecules are shown in Figures 1.4 and 2.1-2.4. These molecules range from having one stereogenic center (Tris(1,10-phenanthroline)metal complexes),³⁻⁸ two stereogenic centers (CC-1065),^{9,10} four stereogenic centers (Benzo[*a*]pyrene and Benzo[*c*]phenanthrene dihydrodiol epoxides),¹¹ six stereogenic centers (Daunomycin),¹²⁻¹⁴ eight stereogenic centers (Triostin A),¹⁵ ten stereogenic centers (Actinomycin D and Neocarzinostatin),^{16,17} to more than ten stereogenic centers (Chromomycin A3, Calicheamicin γ_1^I , Esperamicin A₁, and Bleomycin A2).¹⁸⁻²² The dependence of DNA binding properties on DNA binding molecule stereochemistry has been studied at various levels of detail for some molecules.

Barton and coworkers have studied the interactions of chiral octahedral metal complexes with double-helical DNA, and certain complexes have been developed as probes of DNA topology. For example, right-handed Δ enantiomers of tris(1,10-phenanthroline)- or tris(4,7-diphenyl-1,10-phenanthroline) complexes with metals bind more strongly to right-handed B DNA than the corresponding left-handed Λ enantiomers.³ Δ and Λ enantiomers bind equally well to left-handed Z DNA. The observed *enantiospecific binding* is consistent with a model, derived from photophysical^{4,5} and other studies, in

which one ligand from the metal complex intercalates between DNA base pairs from the DNA major groove. When bound to B DNA in this fashion, the nonintercalated phenanthroline ligands of right-handed Δ complexes are oriented favorably along the major groove, while the nonintercalated ligands of left-handed Λ complexes clash with the phosphate-sugar backbone. The major groove of Z DNA is wider and shallower than the major groove of B DNA, and does not interact strongly with the nonintercalated ligands from bound Δ or Λ enantiomers. Thus, enantiomeric tris(phenanthroline)metal complexes are not strongly discriminated upon intercalation into Z DNA.

In related studies, Barton and Mei have shown that both enantiomers of tris(3,4,7,8-tetramethyl-1,10-phenanthroline)ruthenium(II) bind to A DNA but not to B DNA or Z DNA, and that the left-handed Λ isomer binds more strongly than the right-handed Δ enantiomer.⁶ These complexes bind to the surface or grooves of A DNA rather than by intercalation. In light of the results for these complexes, and for the tris(1,10-phenanthroline)- and tris(4,7-diphenyl-1,10-phenanthroline) complexes, it has been proposed that intercalative DNA binding is favored for metal complexes of the same handedness as the DNA template, while groove or surface binding is favored for complexes of handedness opposite or complementary to the DNA template.³ Finally, Barton and coworkers have found that complexes of Ru(II), Co(III), and Rh(III) produce DNA photocleavage, and may be used to map metal complex binding sites by DNA affinity cleaving.^{7,8}

Hurley and coworkers used the DNA binding/alkylating specificity of CC-1065 to predict the absolute stereochemistry of the natural product.^{9,10} CC-1065 binds in the minor groove of B DNA with specificity for the five base pair sequences 5'-PuNTTA-3' and 5'-AAAAA-3' and alkylates the N3 atom of the C-terminal adenine in these sequences. By examining models, Hurley et al. concluded that only the C3b(*R*), C4a(*S*) configuration of CC-1065 could be accommodated in the minor groove in the observed binding/alkylating orientation.

Reardon et al. have studied the sequence specificity of DNA alkylation by stereoisomers of Benzo[*a*]pyrene and Benzo[*c*]phenanthrene dihydrodiol epoxides.¹¹ They found that enantiomers and diastereomers of these carcinogens produce subtly different patterns of DNA alkylation.

TANDEM (an analog of Triostin A) binds specifically to sequences of A:T base pairs with affinity constants of approximately 10^7 .²³ Fox, Olsen, and Waring showed that inversion at one or both D-serine residues of TANDEM has "disastrous" effects on DNA binding affinity.²⁴ Binding constants for D-Ser, L-Ser TANDEM or L-Ser, L-Ser TANDEM were lower by at least three orders of magnitude. Crystal structures of Triostin A and an analog, Echinomycin, complexed to oligonucleotides show that these antibiotics bind specifically to DNA through intercalation of both quinoxaline chromophores between DNA base pairs, and through contacts between cyclic depsipeptides and the DNA minor groove. Inversion at either or both D-serine residues would cause drastic disruptions of intercalation and depsipeptide:minor groove interactions.

The effects of epimerization at various stereogenic centers of Daunomycin or the related anthracycline antibiotic Adriamycin have been examined.¹²⁻¹⁴ Daunomycin and Adriamycin have the 1'(*R*), 3'(*S*), 4'(*S*), 5'(*S*), 7(*S*), 9(*S*) absolute configuration and bind to B DNA with affinity constants in the range $1-5 \times 10^6 \text{ M}^{-1}$.¹² Most notably, epimerization at C-7 (where the sugar residue joins the tetracyclic chromophore) or at the anomeric C-1' center drastically reduces DNA binding affinity, and appears to change the mode by which these molecules interact with DNA.^{12,13} The molecular structure of a Daunomycin:DNA cocrystal shows that the planar chromophore of the antibiotic intercalates lengthwise between DNA base pairs, while the amino sugar moiety is bound snugly in the DNA minor groove.¹⁴ Inverting the stereochemistry at the anomeric center of the sugar or at the center where the sugar joins the tetracyclic chromophore would change the manner in which the amino sugar residue could interact with the minor groove, consistent with the experimental results.

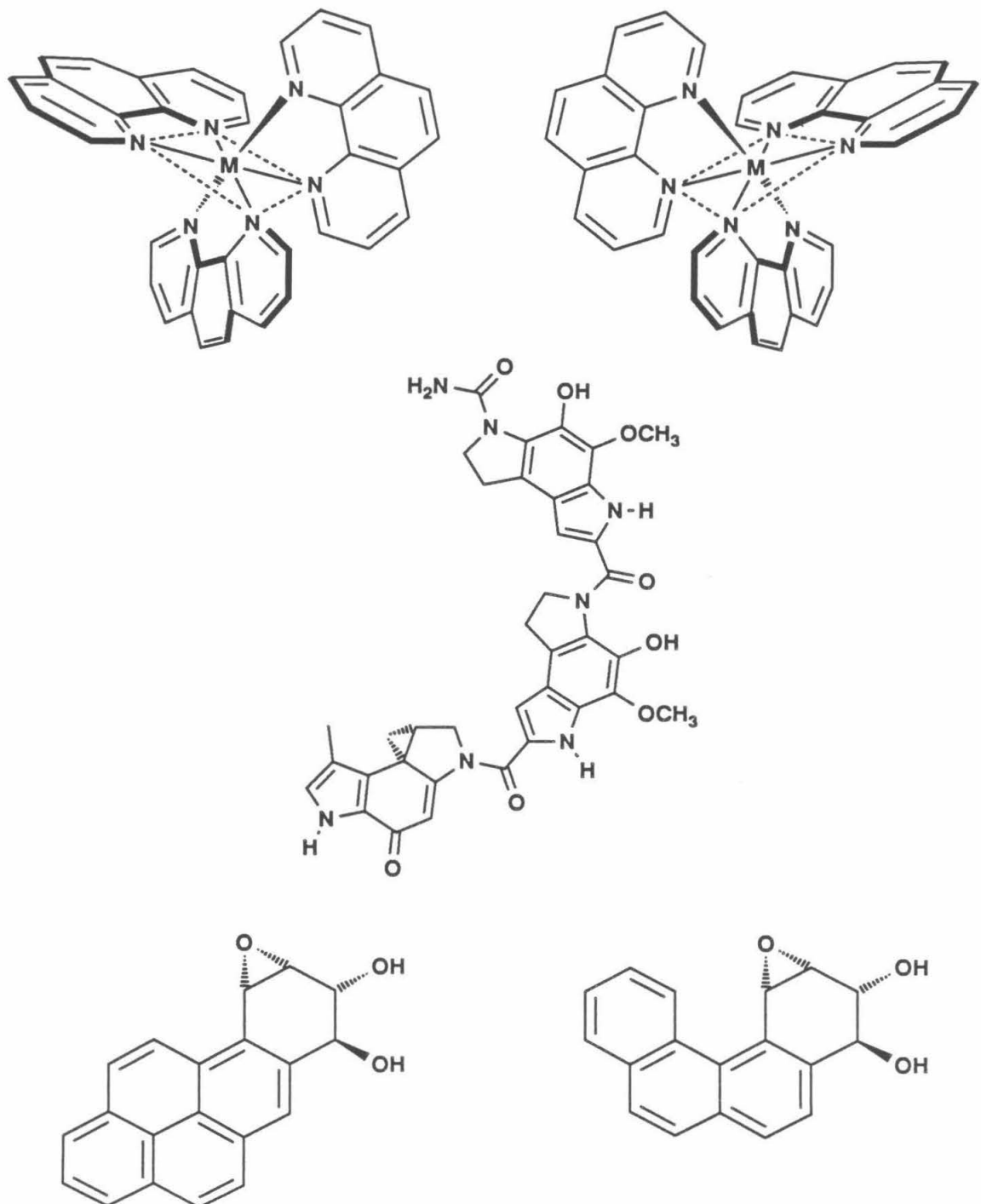


Figure 2.1. Chiral DNA binding molecules. Top Left: Δ -Tris(1,10-phenanthroline)-Metal complex. Top Right: Λ -Tris(1,10-phenanthroline)Metal complex. Center: CC-1065. Bottom Left: Benzo[a]pyrene dihydrodiol epoxide. Bottom Right: Benzo[c]phenanthrene dihydrodiol epoxide.

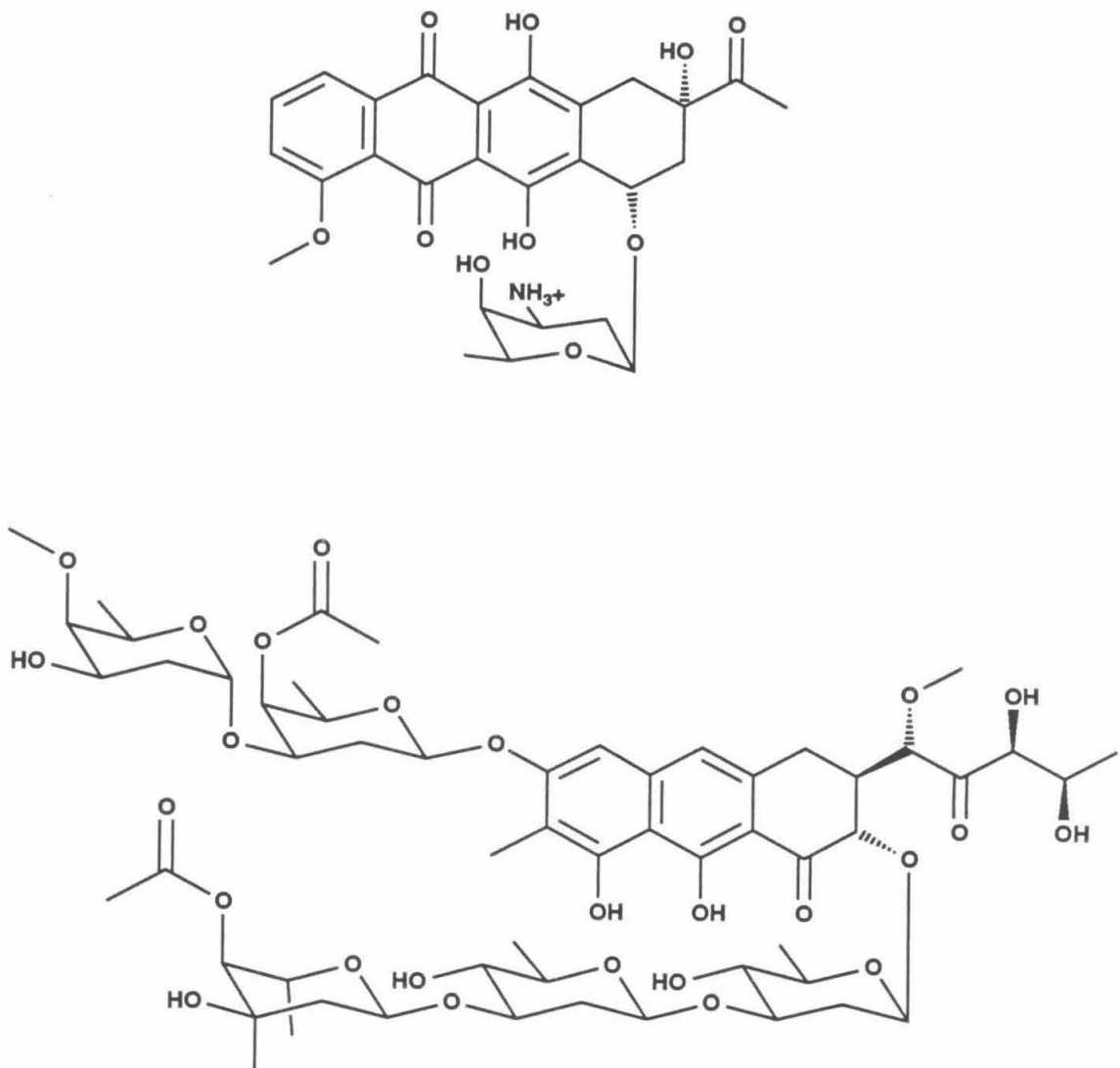


Figure 2.2. Chiral DNA binding molecules. Top: Daunomycin. Center: Chromomycin A3.

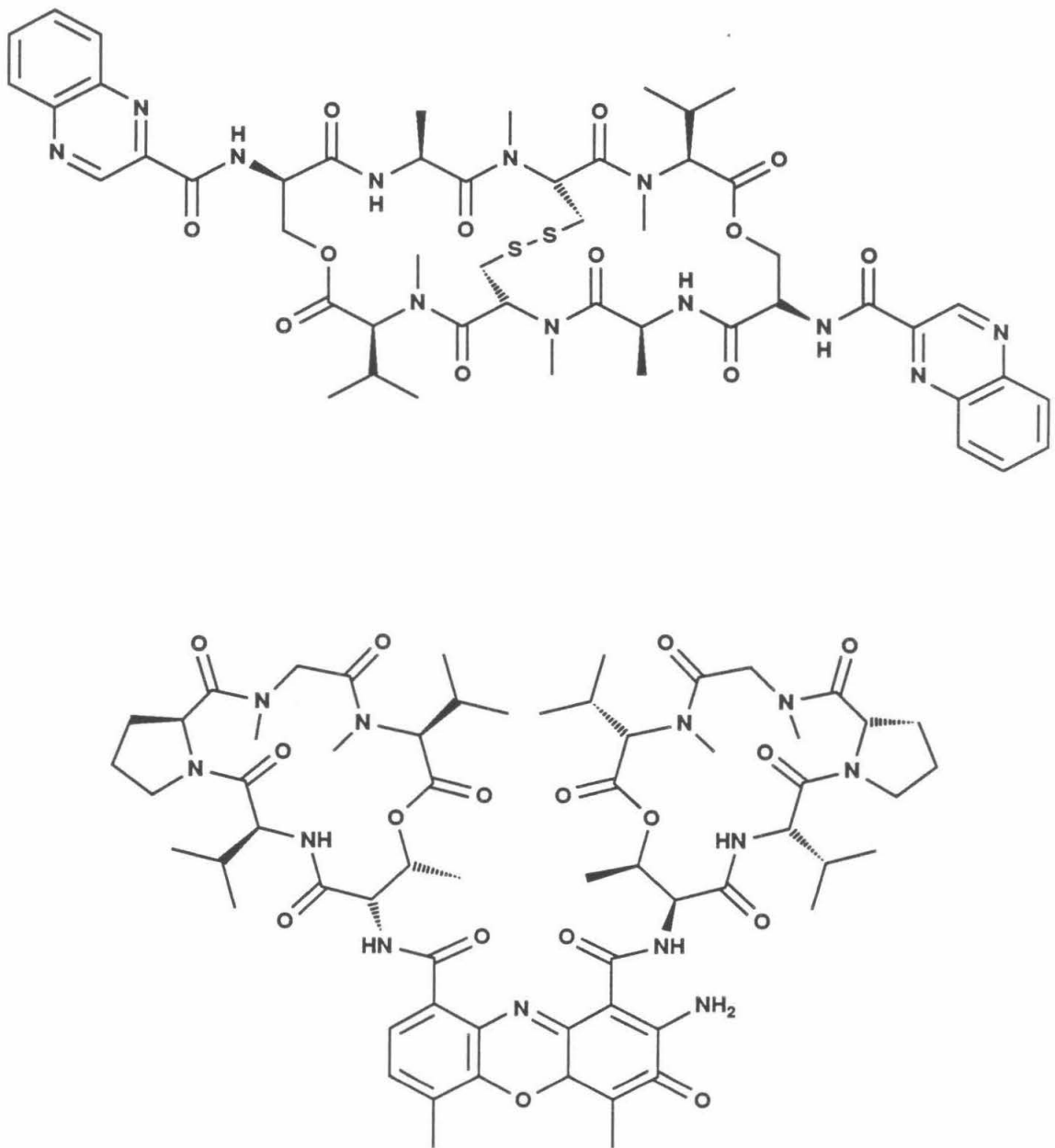


Figure 2.3. Chiral DNA binding molecules. Top: Triostin A. Center: Actinomycin D.

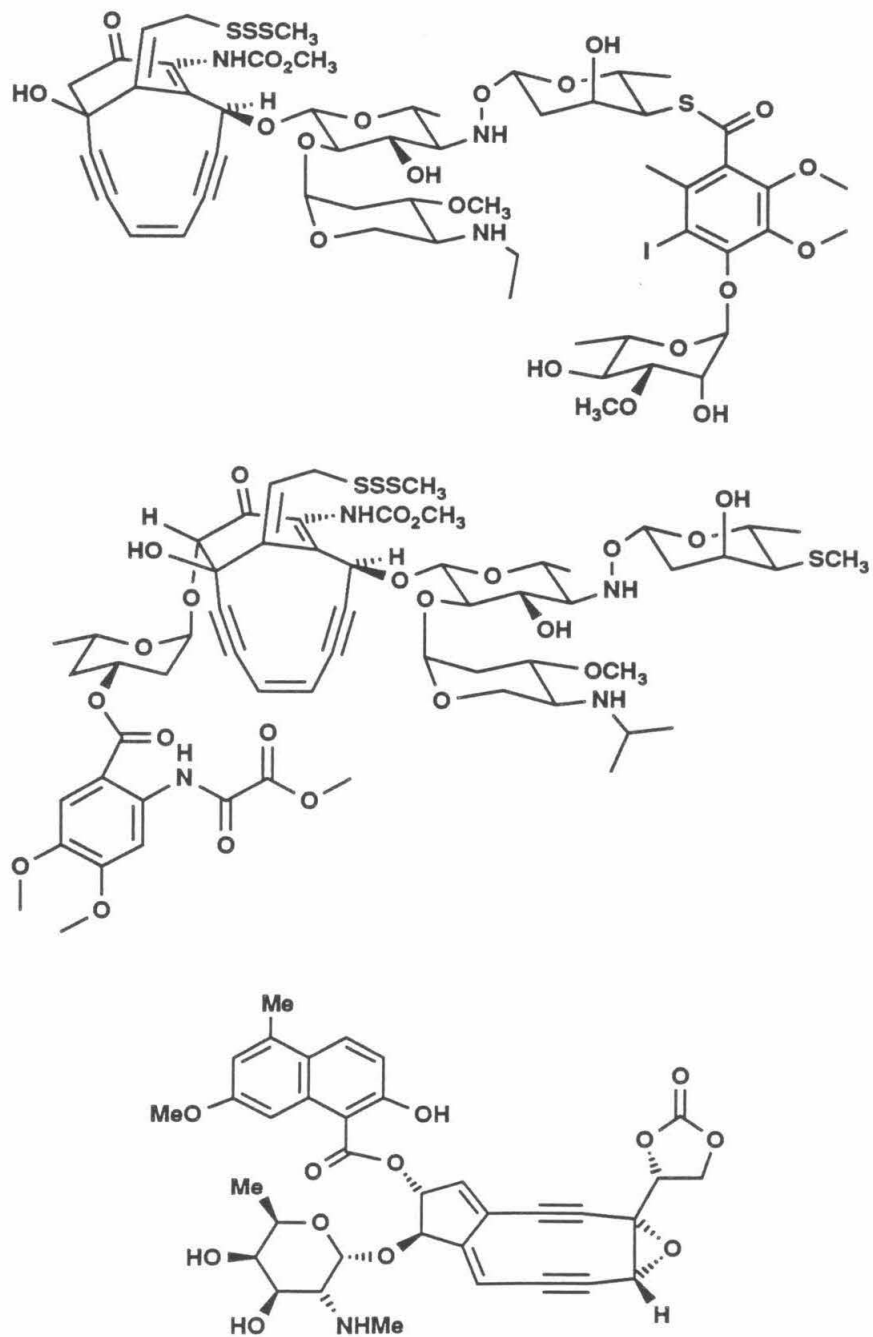


Figure 2.4. Chiral DNA binding molecules. Top: Calichemicin γ_1^I . Center: Esperamicin A1. Bottom: Neocarzinostatin chromophore.

Results

Design. In order to provide new insight into enantiospecific DNA complexation, we undertook the design, synthesis, and characterization of a series of related chiral DNA minor groove binding/cleaving small molecules. Figures 2.5-2.11 depict the molecules prepared for this study. The majority of these compounds are derivatives of Bis(Netropsin)-Succinamide-EDTA (BNSE, described in Chapter One) in which one dimethylamino substituent or one or two hydroxyl substituents have been added to the succinamide linker (Figure 2.5). Figures 2.6-2.9 show Netropsin dimers linked in tail-to-tail fashion by (*S,S*)-, (*R,R*)-, and (*RS,SR*)-tartaric acids (Figure 2.6), the acetonides of (*S,S*)-, (*R,R*)-, and (*RS,SR*)-tartaric acids (Figure 2.7), (*S*)- and (*R*)-malic acids (Figure 2.8), and (*S*)- and (*R*)-*N,N*-dimethylaminoaspartic acids (Figure 2.9). Figure 2.10 depicts the structures of three molecules in which an *N*-methylpyrrolecarboxamide (P1) subunit and a tri(*N*-methylpyrrolecarboxamide) (P3) subunit are linked in tail-to-tail fashion by succinic acid, (*S,S*)-tartaric acid, and (*R,R*)-tartaric acid. These molecules are constitutional isomers of **BNSE**, **BN-(*S,S*)-Tar-E**, and **BN-(*R,R*)-Tar-E**, respectively. While P1-Linker-P3-EDTA compounds bear C_2 symmetrical linkers, their DNA binding subunits are not, as a whole, C_2 symmetric. Figure 2.11 depicts the structures of head-to-tail Netropsin dimers linked by (*S*)-alanine and (*R*)-alanine. **BN-(*S*)-AE** and **BN-(*R*)-AE** are methyl-substituted analogs of Bis(Netropsin)-Glycine-EDTA (**BNGE**, described in Chapter One). The iron-chelating functionality EDTA was appended to one terminus of each molecule in this series in order to determine DNA binding properties by DNA affinity cleaving.²⁵ While the Fe:EDTA moieties of these molecules are themselves stereogenic, we anticipated that this feature would not mask enantiospecific binding effects arising from the chiral linkers because the Fe:EDTA subunit is the same for each molecule and is not believed to be intimately associated with the DNA.

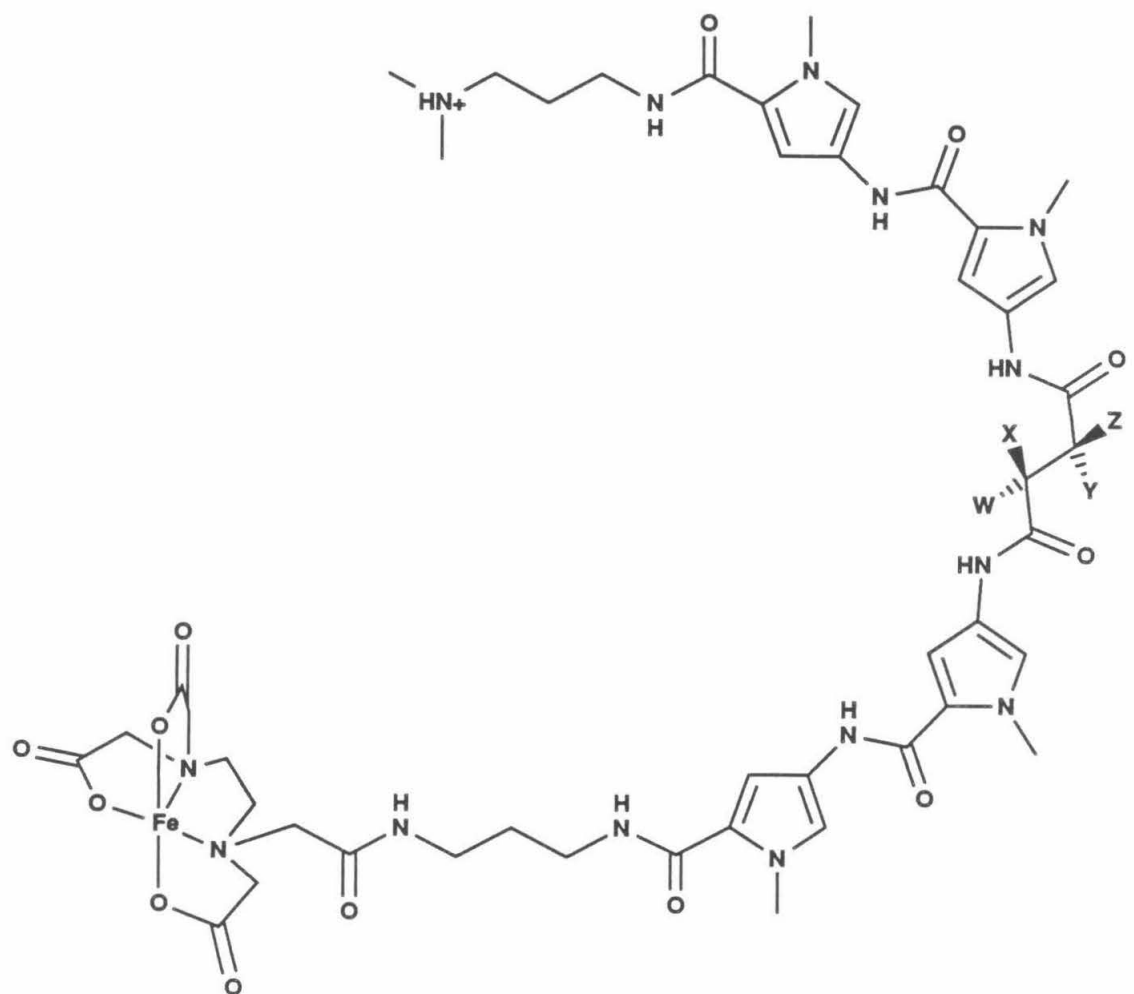


Figure 2.5. Design of chiral DNA binding/cleaving molecules: Substituted Bis(Netropsin)-Succinamide-EDTA:Fe compounds.

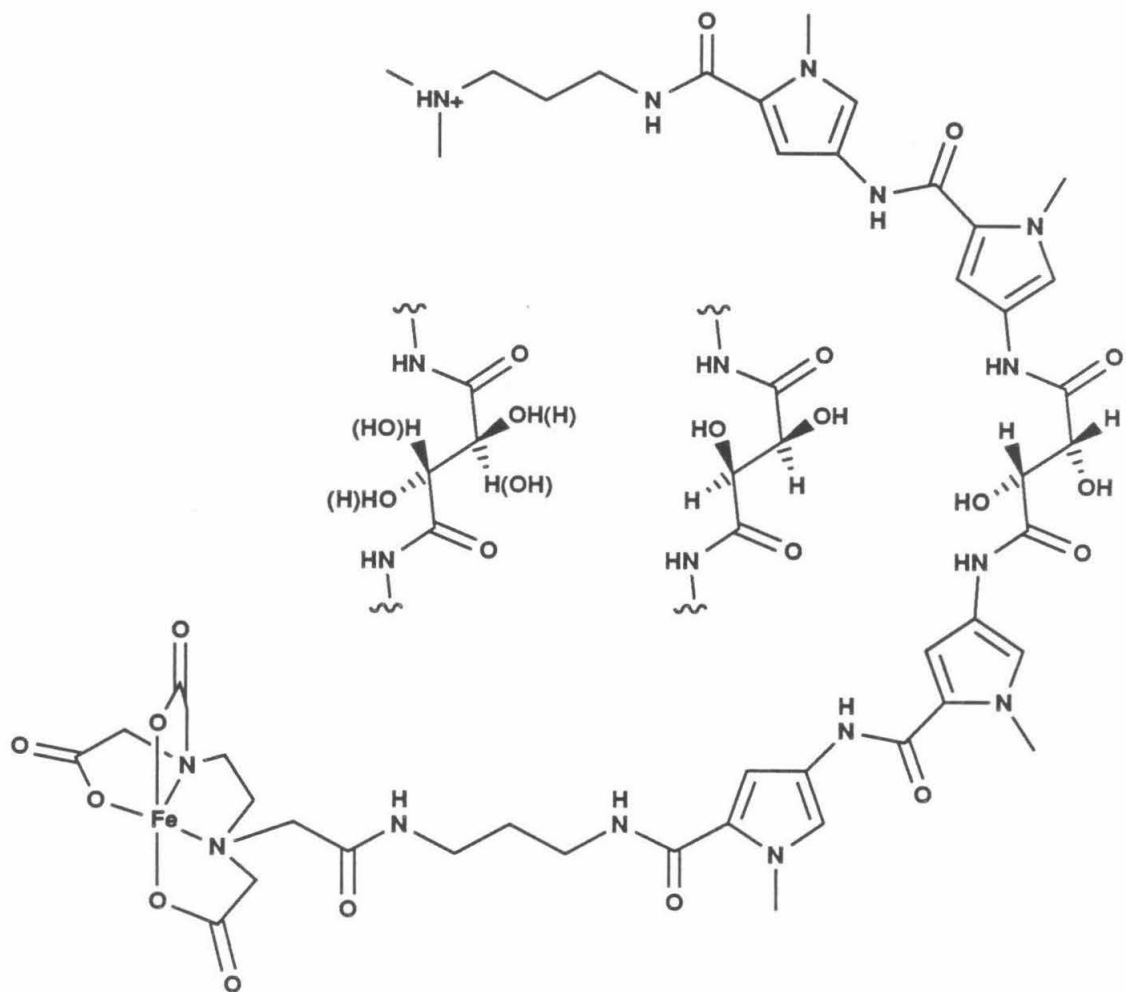


Figure 2.6. Bis(Netropsin)-Tartaramide-EDTA:Fe compounds. Left: Bis(Netropsin)-(RS,SR)-Tartaramide-EDTA:Fe (BN-(RS,SR)-Tar-E:Fe). Center: Bis(Netropsin)-(S,S)-Tartaramide-EDTA:Fe (BN-(S,S)-Tar-E:Fe). Right: Bis(Netropsin)-(R,R)-Tartaramide-EDTA:Fe (BN-(R,R)-Tar-E:Fe).

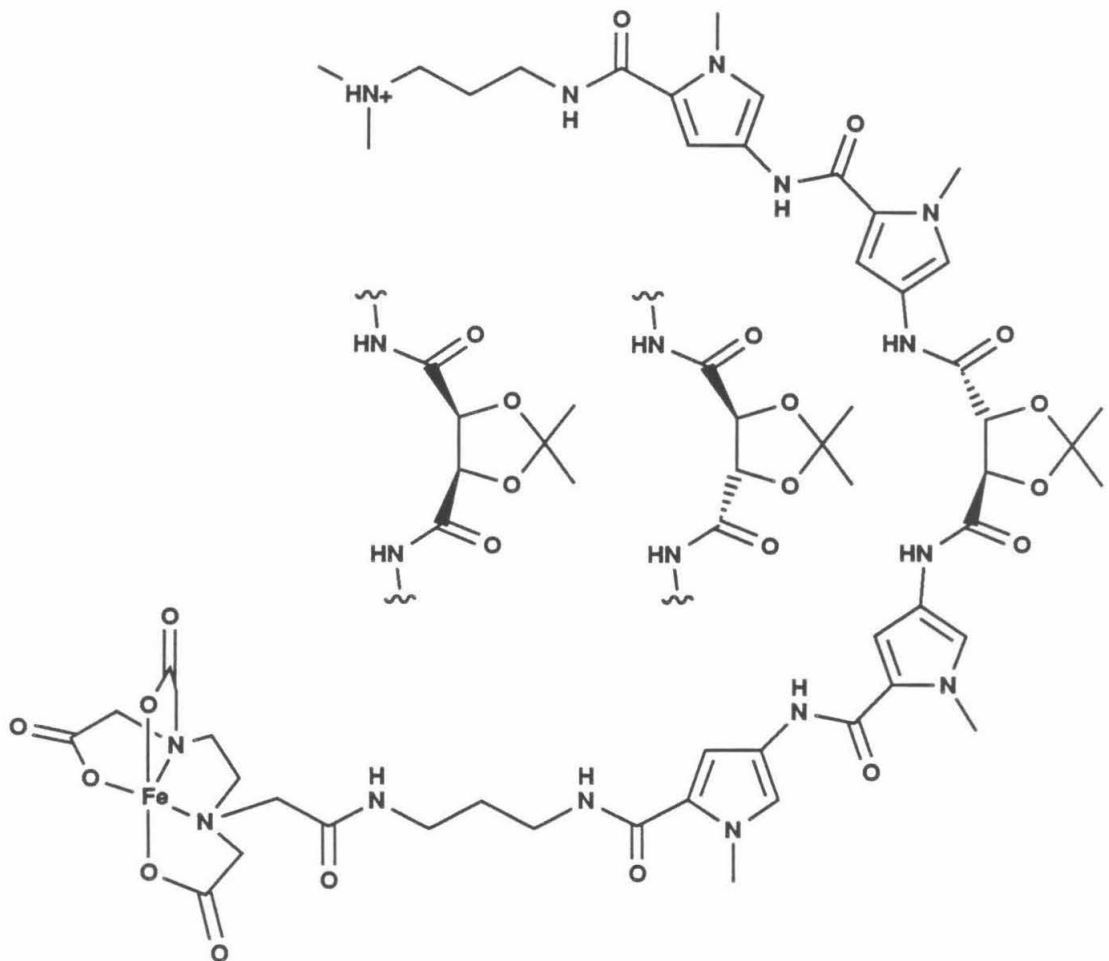


Figure 2.7. Bis(Netropsin)-Tartaramide Acetonide-EDTA:Fe compounds. Left: Bis(Netropsin)-(RS,SR)-Tartaramide Acetonide-EDTA:Fe (**BN-(RS,SR)-TarAc-E:Fe**). Center: Bis(Netropsin)-(S,S)-Tartaramide Acetonide-EDTA:Fe (**BN-(S,S)-TarAc-E:Fe**). Right: Bis(Netropsin)-(R,R)-Tartaramide Acetonide-EDTA:Fe (**BN-(R,R)-TarAc-E:Fe**).

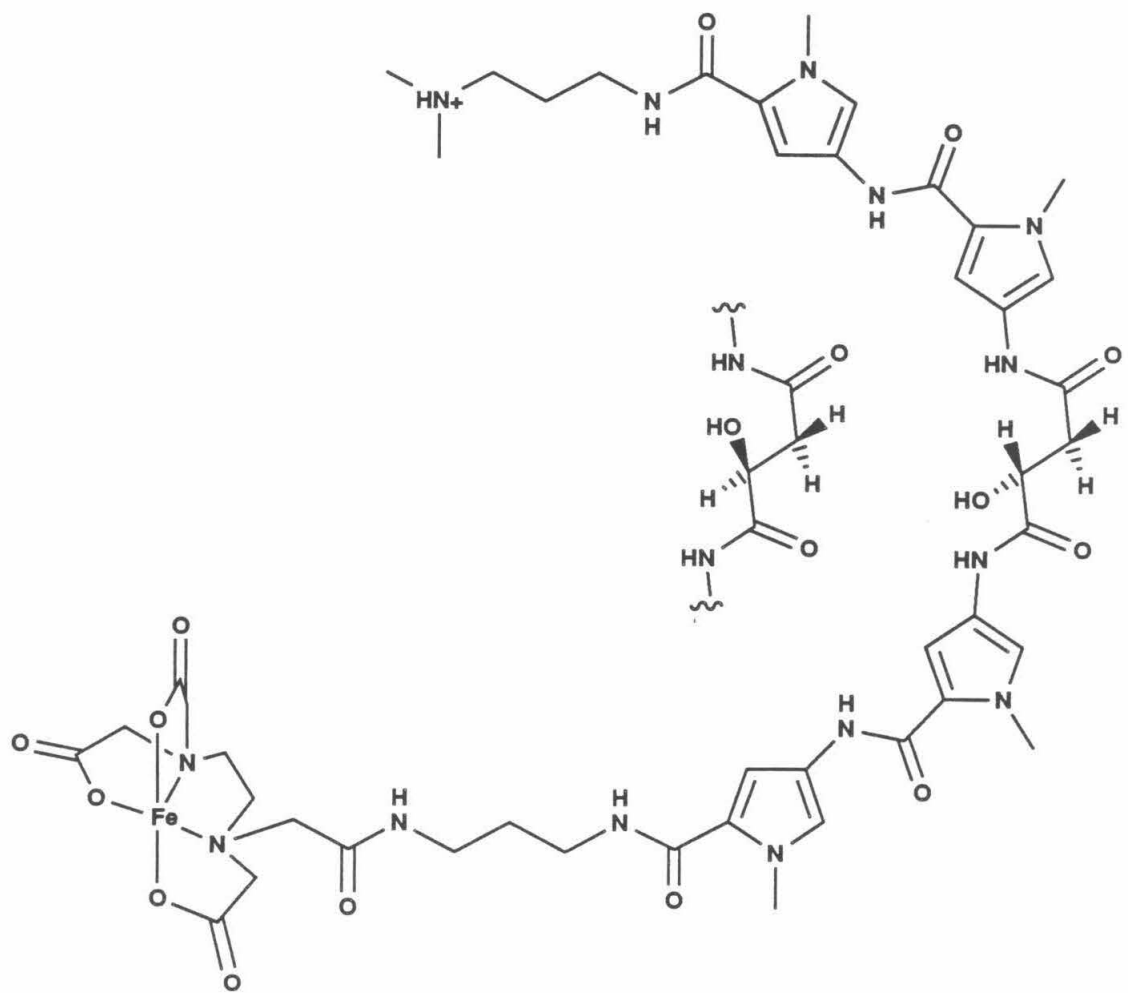


Figure 2.8. Bis(Netropsin)-Malicamide-EDTA:Fe compounds. Left: Bis(Netropsin)-2-(*S*)-Malicamide-EDTA:Fe (**BN-2-(*S*)-Mal-E:Fe**). Right: Bis(Netropsin)-2-(*R*)-Malicamide-EDTA:Fe (**BN-2-(*R*)-Mal-E:Fe**).

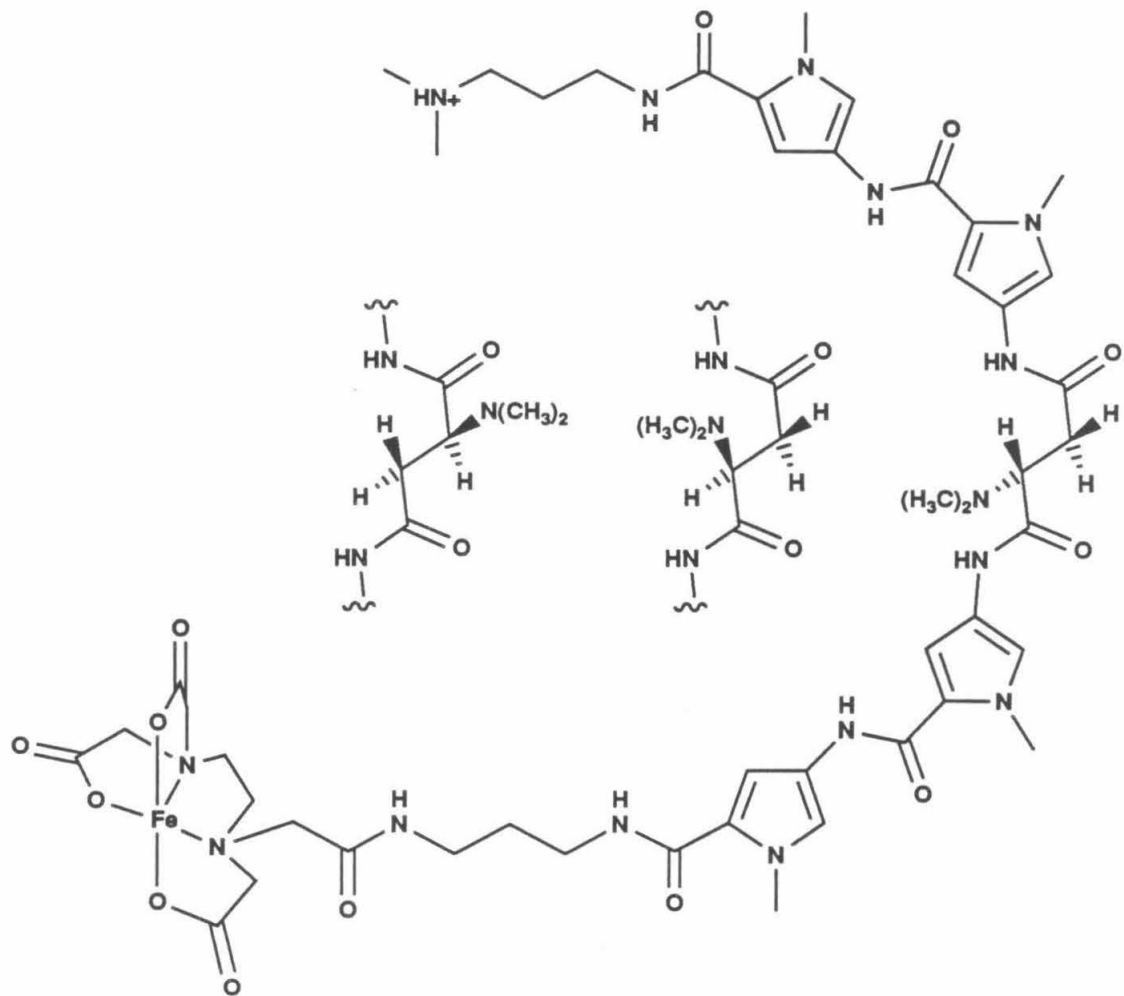


Figure 2.9. Bis(Netropsin)-Dimethylaminoaspartamide-EDTA:Fe compounds. Left: Bis(Netropsin)-3-(*S*)-Dimethylaminoaspartamide-EDTA:Fe (**BN-3-(*S*)-DMAsp-E:Fe**). Center: Bis(Netropsin)-2-(*S*)-Dimethylaminoaspartamide-EDTA:Fe (**BN-2-(*S*)-DMAsp-E:Fe**). Right: Bis(Netropsin)-2-(*R*)-Dimethylaminoaspartamide-EDTA:Fe (**BN-2-(*R*)-DMAsp-E:Fe**).

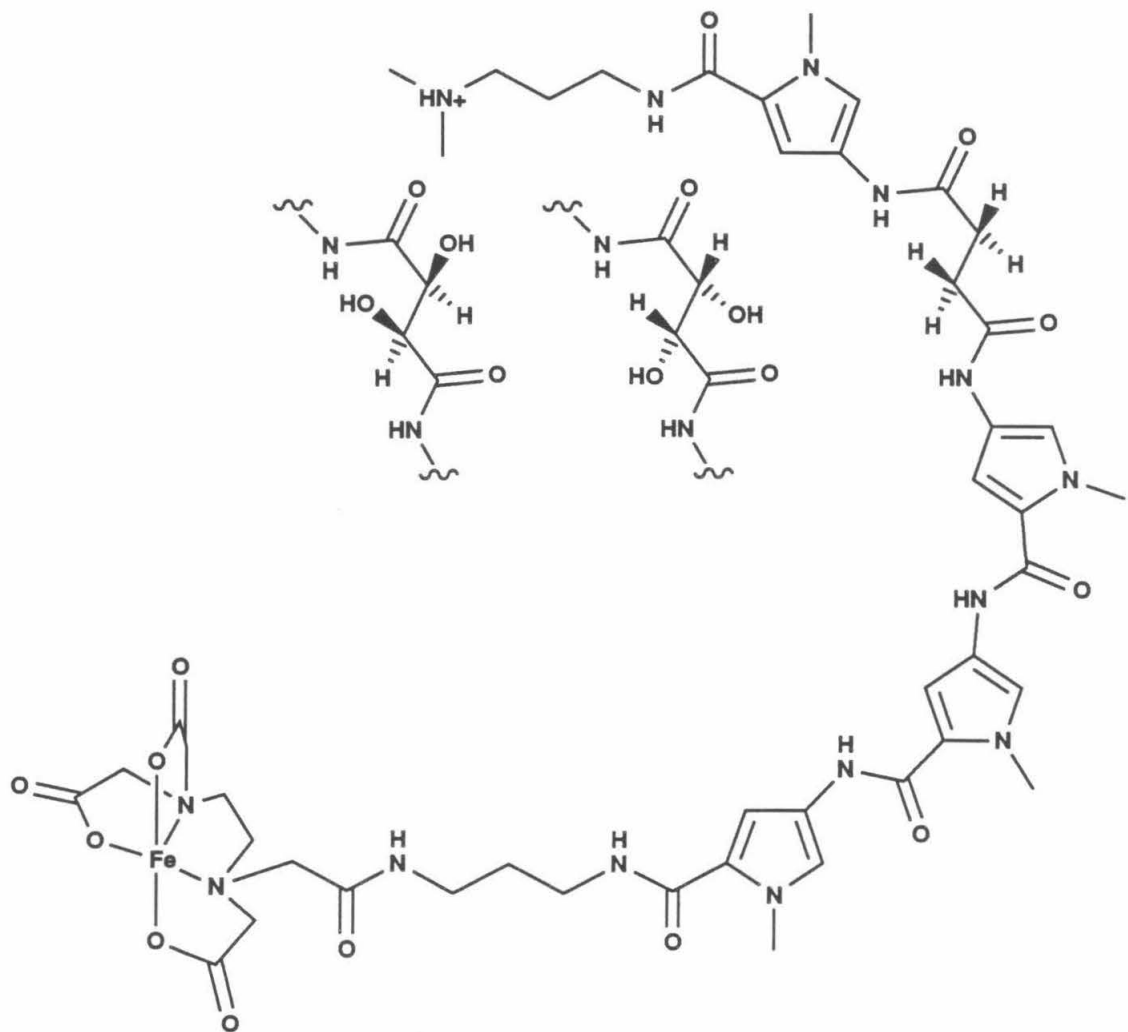


Figure 2.10. P1-Linker-P3-EDTA:Fe compounds. Left: P1-(S,S)-Tartaramide-P3-EDTA:Fe (P1-(S,S)-Tar-P3-E:Fe). Center: P1-(R,R)-Tartaramide-P3-EDTA:Fe (P1-(R,R)-Tar-P3-E:Fe). Right: P1-Succinamide-P3-EDTA:Fe (P1-S-Tar-P3-E:Fe).

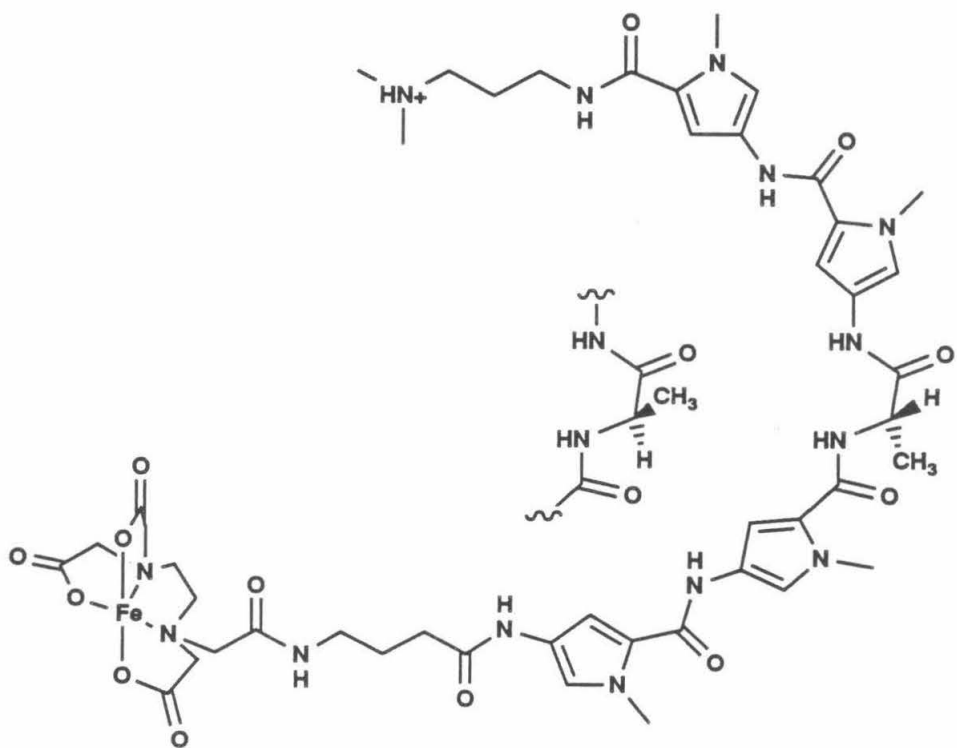


Figure 2.11. Left: Bis(Netropsin)-(R)-Alanine-EDTA:Fe (BN-(R)-AE:Fe). Right: Bis(Netropsin)-(S)-Alanine-EDTA:Fe (BN-(S)-AE:Fe).

Synthesis. The synthesis of Bis(Netropsin)s linked by chiral diacids is exemplified by the synthesis of Bis(Netropsin)-(R,R)-Tartaramide-EDTA (**BN-(R,R)-Tar-E, II-143**, Figure 2.12), which followed the general procedure developed for the synthesis of Bis(Netropsin) Diacid-EDTA compounds (Chapter One, Figure 1.12). **I-22** was reduced, coupled with an excess of (R,R)-tartaric acid to afford Netropsin-(R,R)-Tartaramic acid **I-108**. **IV-129** was reduced and coupled with **I-108** to afford Boc Bis(Netropsin)-(R,R)-Tartaramide **I-119**. The terminal amino group of **I-119** was deprotected and coupled with the triethyl ester of EDTA. The EDTA ester groups were removed by hydrolysis to afford **BN-(R,R)-Tar-E**. For the synthesis of BN-Tartaramide acetonide-EDTA compounds, **BN-2-(S)-DMAsp-E** and **BN-3-(S)-DMAsp-E**, reduced **I-22** was coupled with one equivalent of a mono ester linker synthon to afford Netropsin esters, which were hydrolyzed and elaborated following the procedure described for the conversion of Netropsin-(R,R)-Tartaramic acid to **BN-(R,R)-Tar-E**. The chiral linker synthons employed in these syntheses are shown in Figure 2.13.²⁶⁻²⁸

The synthesis of P1-Linker-P3-EDTA compounds is exemplified by the synthesis of P1-Succinamide-P3-EDTA (**P1-S-P3-E, I-264**, Figure 2.14). $O_2NP_1CO_2H$ was coupled with 3-dimethylaminopropylamine to afford **I-200**. $O_2NP_3CO_2H$ was coupled with **IV-161** to afford **I-209**. Reduction of **I-200** and coupling with an excess of succinic acid produced P1-Succinamic acid **I-254**. **I-209** was reduced and coupled with **I-254** to afford Boc P1-Succinamide-P3 **I-256**. The terminal amino group of **I-256** was deprotected and coupled with the triethyl ester of EDTA. The EDTA ester groups were removed by hydrolysis to afford **P1-S-P3-E**.

The head-to-tail dimers **BN-(S)-AE** and **BN-(R)-AE** were synthesized following the general procedure described for the synthesis of Bis(Netropsin) Amino acid-EDTA compounds (Chapter One, Figure 1.13).

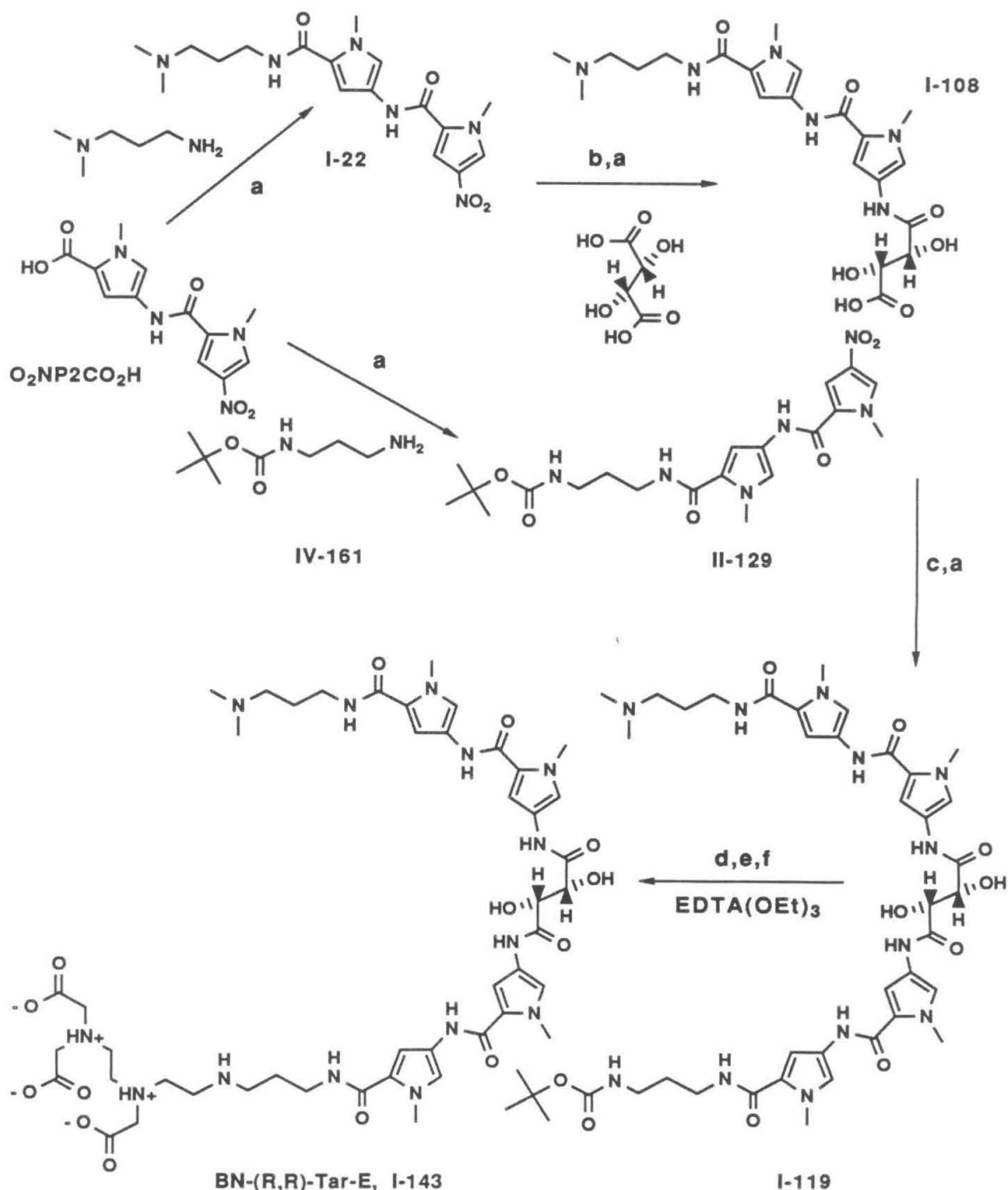


Figure 2.12. Scheme for the synthesis of BN-(R,R)-Tar-E. Reaction conditions: a, DCC, HOBT, DMF; b, H_2 (1 atm), Pd/C, DMF; c, H_2 (3 atm), Pd/C, DMF; d, TFA, CH_2Cl_2 ; e, $\text{EDTA}(\text{OEt})_3$, CDI, DMF; f, LiOH, MeOH, H_2O .

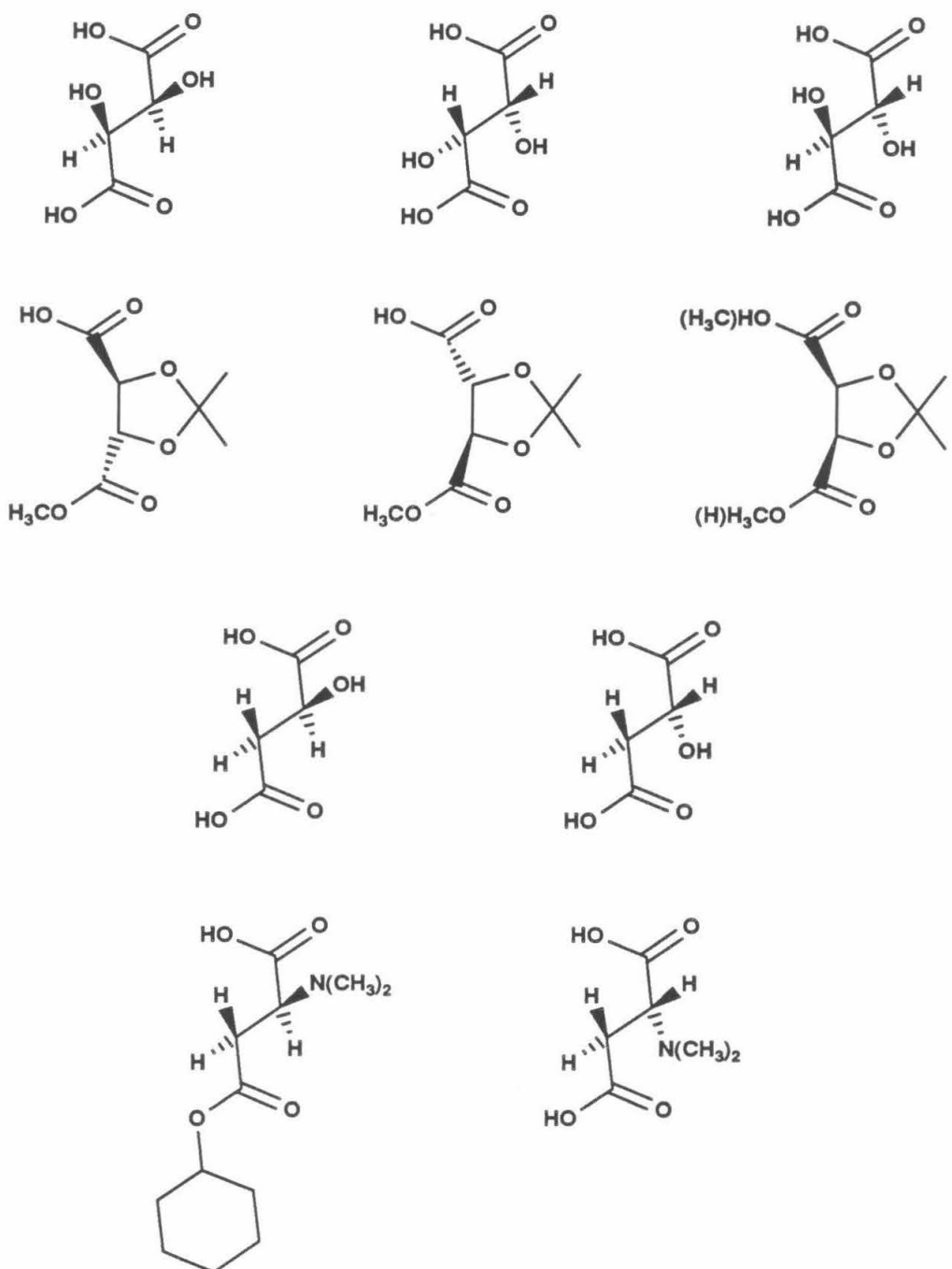


Figure 2.13. Linker synthons used to prepare chiral, substituted Bis(Netropsin)-Succinamide-EDTA compounds and P1-Linker-P3-EDTA compounds.

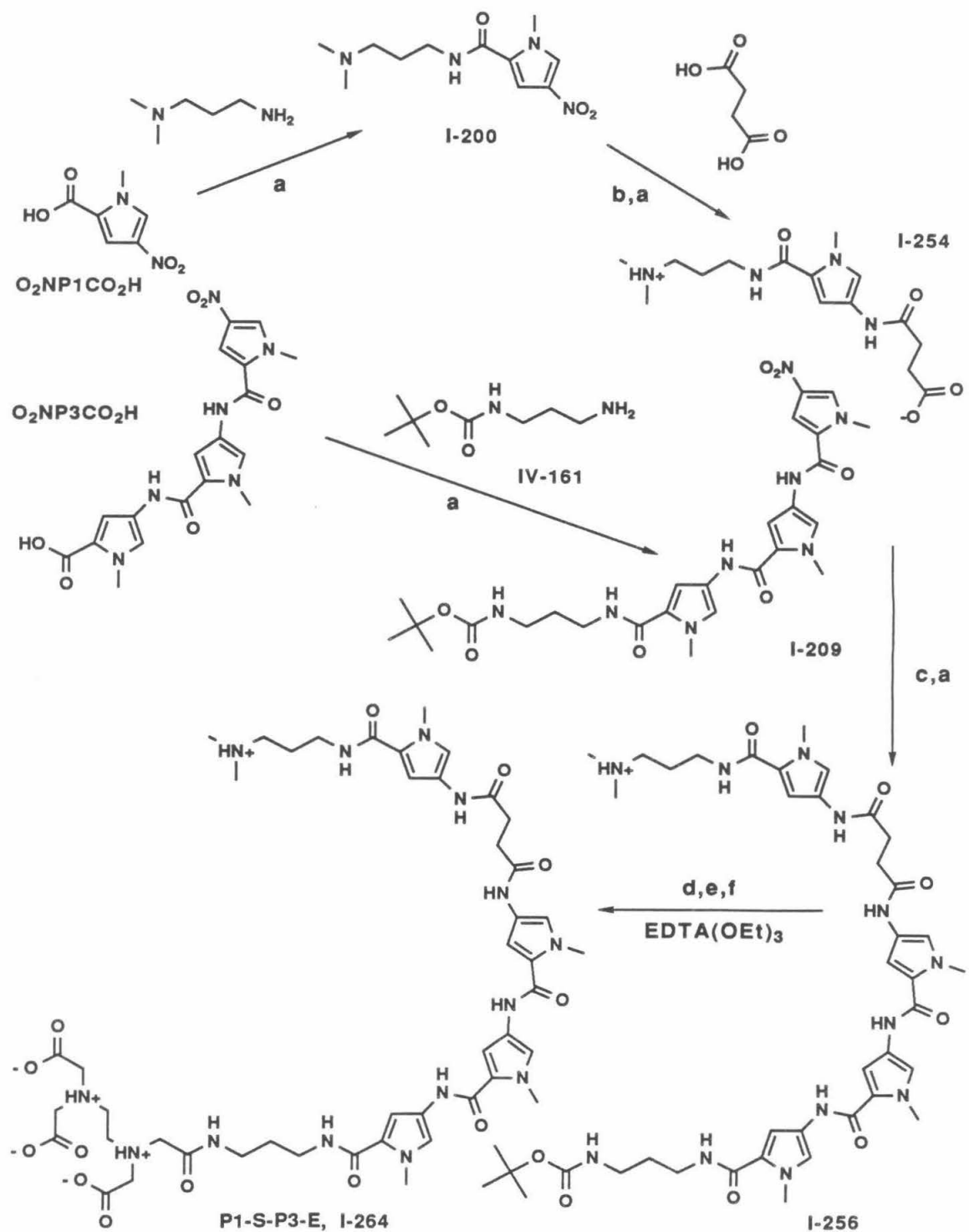


Figure 2.14. Scheme for the synthesis of **P1-S-P3-E**. Reaction conditions: **a**, DCC, HOBT, DMF; **b**, H₂ (1 atm), Pd/C, DMF; **c**, H₂ (3 atm), Pd/C, DMF; **d**, TFA, CH₂Cl₂; **e**, EDTA(OEt)₃, CDI, DMF; **f**, LiOH, MeOH, H₂O.

Polarimetry was used to assess the optical activity of the chiral molecules. Specific rotation values, measured at room temperature in 10% concentrated aqueous ammonia/ethanol solution, are collected in the following table.

<u>Compound</u>	$[\alpha]_D^{24}$	c
BN-(R,R)-Tar-E	+7.7	0.33
BN-(S,S)-Tar-E	-17.9	0.33
BN-(R,R)-TarAc-E	-19.7	0.36
BN-(S,S)-TarAc-E	+15.6	0.38
BN-2-(R)-Mal-E	+11.4	0.30
BN-2-(S)-Mal-E	-14.8	0.29
BN-2-(R)-DMAsp-E	-0.9	0.22
BN-2-(S)-DMAsp-E	-1.0	0.20
BN-3-(S)-DMAsp-E	0.0	0.22
P1-(R,R)-Tar-P3-E	+32.9	0.35
P1-(S,S)-Tar-P3-E	-31.1	0.31
BN-(R)-AE	+73.2	0.31
BN-(S)-AE	-72.3	0.29

Several observations may be made from this data. First, the Bis(Netropsin)-Dimethylaminoaspartamide-EDTA compounds exhibit little or no optical activity at the sodium D line (589 nm). These molecules do not exhibit optical activity at other wavelengths, and must therefore be considered as racemic mixtures **BN-2-DMAsp-E** and **BN-3-DMAsp-E**. Second, **BN-(R,R)-Tar-E** and **BN-(S,S)-Tar-E** exhibit optical activity of opposite sign but not of equal magnitude. Thus, some amount of racemization appears to have occurred during the synthesis and/or storage of these compounds. It was determined by optical rotation and NMR shift reagent studies that the starting (R,R)- and (S,S)-tartaric acids were of > 99% enantiomeric purity. In addition, the specific rotations of the penultimate EDTA triethyl ester intermediates to **BN-(R,R)-Tar-E** and **BN-**

(S,S)-Tar-E were found to be equal in magnitude and opposite in sign, indicating that racemization occurred during or after hydrolysis of the ester groups. Given the measured specific rotations, the enantiomeric purity of **BN-(R,R)-Tar-E** must not exceed 43% [(7.7/17.9)100]. Finally, enantiomers of Bis(Netropsin)-Tartaramide acetonide-EDTA compounds, Bis(Netropsin)-Malicamide-EDTA compounds, P1-Linker-P3-EDTA compounds, and Bis(Netropsin)-Alanine-EDTA compounds exhibit optical activities of opposite sign and approximately equal magnitude ($\pm 15\%$), suggesting that these pairs of enantiomers have undergone little or no racemization, or have been racemized to nearly the same extent.

DNA Affinity Cleaving. DNA affinity cleaving studies with **P5E**, **BNSE**, **P1-S-P3-E**, and the chiral molecules were carried out under conditions determined to be optimal for DNA binding/cleaving by oligo(*N*-methylpyrrolecarboxamide)-EDTA compounds.²⁹ DNA double-strand cleavage by these molecules was examined on Sty I-linearized, 3'-³²P end-labeled pBR322 plasmid DNA. DNA cleavage products were separated by agarose gel electrophoresis and visualized by autoradiography.

Figure 2.15 shows an autoradiograph of DNA double-strand cleavage patterns produced by **P5E:Fe**, **BNSE:Fe**, and the Bis(Netropsin)-Tartaramide-EDTA:Fe compounds. Here it can be seen that the Bis(Netropsin)-Tartaramide-EDTA:Fe compounds produce the same intense cleavage loci produced by **P5E:Fe** and **BNSE:Fe**. The relative cleavage intensities produced by **BN-(S,S)-Tar-E:Fe**, **BN-(R,R)-Tar-E:Fe**, and **BN-(RS,SR)-Tar-E:Fe** at these major cleavage loci match the relative intensities produced by **BNSE:Fe** more closely than the relative intensities produced by **P5E:Fe**. Bis(Netropsin)-Tartaramide-EDTA:Fe compounds also produce significant cleavage at additional sites observed only weakly or not at all with **P5E:Fe** or **BNSE:Fe**. Finally, the chiral molecules produced more nonspecific (background) cleavage than **P5E:Fe** or **BNSE:Fe**. Background cleavage is most apparent with **BN-(R,R)-Tar-E:Fe**.

Figure 2.15

Autoradiograph of DNA double-strand cleavage patterns produced by **P5E:Fe**, **BNSE:Fe**, and Bis(Netropsin)-Tartaramide-EDTA:Fe compounds on Sty I-linearized, 3'-³²P end-labeled pBR322 plasmid DNA in the presence of dioxygen and dithiothreitol. Cleavage patterns were resolved by electrophoresis on a 1% agarose gel. Lanes 2,4,6,8,10 contain DNA labeled at one end with α -³²P dATP, while lanes 3,5,7,9,11 contain DNA labeled at the other end with α -³²P TTP. Lanes 1 and 12, molecular weight markers consisting of pBR322 restriction fragments 4363, 3371, 2994, 2368, 1998, 1768, 1372, 995, and 666 bp in length; lanes 2 and 3, **P5E:Fe** at 0.50 μ M concentration; lanes 4 and 5, **BNSE:Fe** at 0.10 μ M concentration; lanes 6 and 7, **BN-(S,S)-Tar-E:Fe** at 4.0 μ M concentration; lanes 8 and 9, **BN-(R,R)-Tar-E:Fe** at 20 μ M concentration; lanes 10 and 11, **BN-(RS,SR)-Tar-E:Fe** at 8.0 μ M concentration.

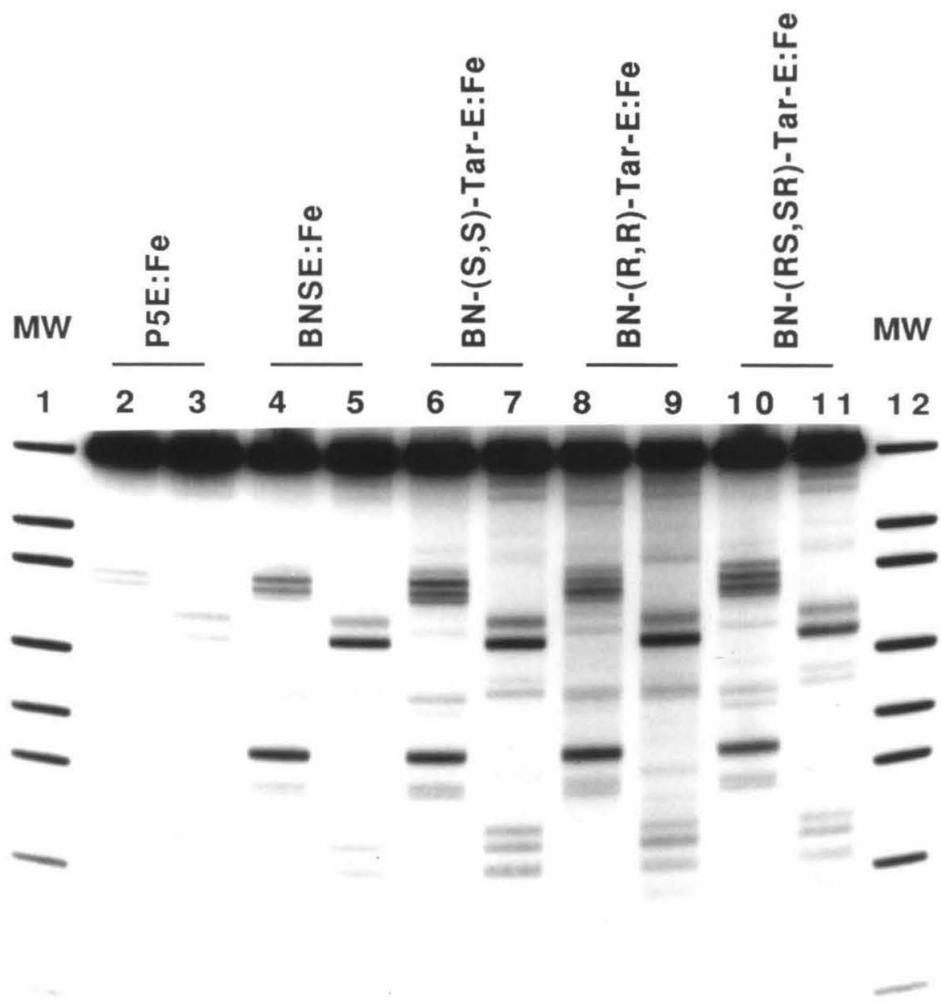


Figure 2.16 shows an autoradiograph of DNA double-strand cleavage patterns produced by **P5E:Fe**, **BNSE:Fe**, and the Bis(Netropsin)-Malcamide-EDTA:Fe compounds. Here it can be seen that the cleavage patterns produced by **BN-2-(S)-Mal-E:Fe** and **BN-2-(R)-Mal-E:Fe** are nearly identical to the cleavage patterns produced by **BNSE:Fe**.

Figure 2.17 shows an autoradiograph of DNA double-strand cleavage patterns produced by **P5E:Fe**, **BNSE:Fe**, and the Bis(Netropsin)-Dimethylaminoaspartamide-EDTA:Fe compounds. It is assumed that lanes 6, 7, 8, and 9 each contain a racemic mixture of **BN-2-(S)-DMAsp-E:Fe** and **BN-2-(R)-DMAsp-E:Fe** at 2.0 μ M total concentration, and that lanes 10 and 11 contain a racemic mixture of **BN-3-(S)-DMAsp-E:Fe** and **BN-3-(R)-DMAsp-E:Fe** at 2.0 μ M total concentration. The lane headings in Figure 2.17 indicate the stereochemistry that the Bis(Netropsin)-Dimethylamino-aspartamide-EDTA compounds would have had in the absence of racemization. The variations in cleavage intensity in lanes 6-9 indicate the extent to which DNA binding/cleaving is reproducible in these experiments. The cleavage intensities at the four major cleavage loci observed with the **BN-2-DMAsp-E:Fe** and **BN-3-DMAsp-E:Fe** are nearly equal, as observed with **P5E:Fe** rather than **BNSE:Fe**.

Figure 2.18 shows an autoradiograph of the DNA double-strand cleavage patterns produced by **P5E:Fe**, **BNSE:Fe**, and the P1-Linker-P3-EDTA:Fe compounds. Here it can be seen that **P1-S-P3-EDTA:Fe**, **P1-(S,S)-Tar-P3-EDTA:Fe**, and **P1-(R,R)-Tar-P3-EDTA:Fe** produce cleavage patterns similar to those produced by **BNSE:Fe**.

Bis(Netropsin)-Tartaramide Acetonide-EDTA:Fe compounds and Bis(Netropsin)-Alanine-EDTA:Fe compounds did not produce significant DNA double-strand cleavage, even at 100 μ M concentrations.

Figure 2.16

Autoradiograph of DNA double-strand cleavage patterns produced by **P5E:Fe**, **BNSE:Fe**, and Bis(Netropsin)-Malcamide-EDTA:Fe compounds on Sty I-linearized, 3'-³²P end-labeled pBR322 plasmid DNA in the presence of dioxygen and dithiothreitol. Cleavage patterns were resolved by electrophoresis on a 1% agarose gel. Lanes 2,4,6,8 contain DNA labeled at one end with α -³²P dATP, while lanes 3,5,7,9 contain DNA labeled at the other end with α -³²P TTP. Lanes 1 and 10, molecular weight markers consisting of pBR322 restriction fragments 4363, 3371, 2994, 2368, 1998, 1768, 1372, 995, and 666 bp in length; lanes 2 and 3, **P5E:Fe** at 0.50 μ M concentration; lanes 4 and 5, **BNSE:Fe** at 0.10 μ M concentration; lanes 6 and 7, **BN-2-(S)-Mal-E:Fe** at 0.50 μ M concentration; lanes 8 and 9, **BN-2-(R)-Mal-E:Fe** at 1.0 μ M concentration.

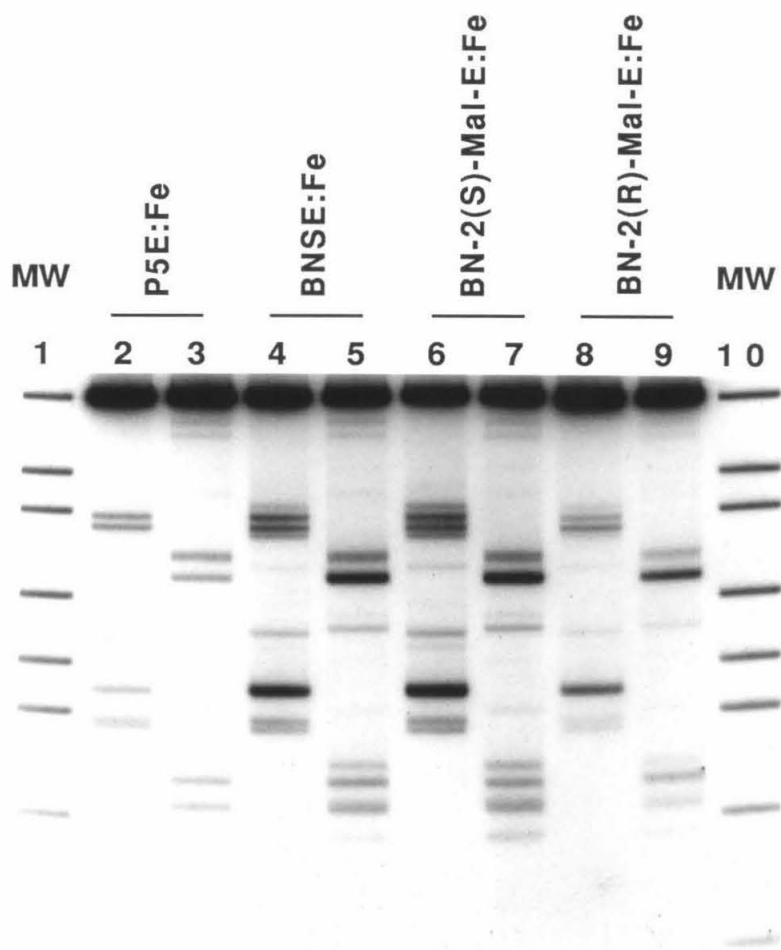


Figure 2.17

Autoradiograph of DNA double-strand cleavage patterns produced by **P5E:Fe**, **BNSE:Fe**, and Bis(Netropsin)-Dimethylaminoaspartamide-EDTA:Fe compounds on Sty I-linearized, 3'-³²P end-labeled pBR322 plasmid DNA in the presence of dioxygen and dithiothreitol. Cleavage patterns were resolved by electrophoresis on a 1% agarose gel. Lanes 2,4,6,8,10 contain DNA labeled at one end with α -³²P dATP, while lanes 3,5,7,9,11 contain DNA labeled at the other end with α -³²P TTP. Lanes 1 and 12, molecular weight markers consisting of pBR322 restriction fragments 4363, 3371, 2994, 2368, 1998, 1768, 1372, 995, and 666 bp in length; lanes 2 and 3, **P5E:Fe** at 0.50 μ M concentration; lanes 4 and 5, **BNSE:Fe** at 0.10 μ M concentration; lanes 6 and 7, racemic **BN-2-DMAsp-E:Fe** at 2.0 μ M concentration; lanes 8 and 9, racemic **BN-2-DMAsp-E:Fe** at 2.0 μ M concentration; lanes 10 and 11, racemic **BN-3-DMAsp-E:Fe** at 2.0 μ M concentration.

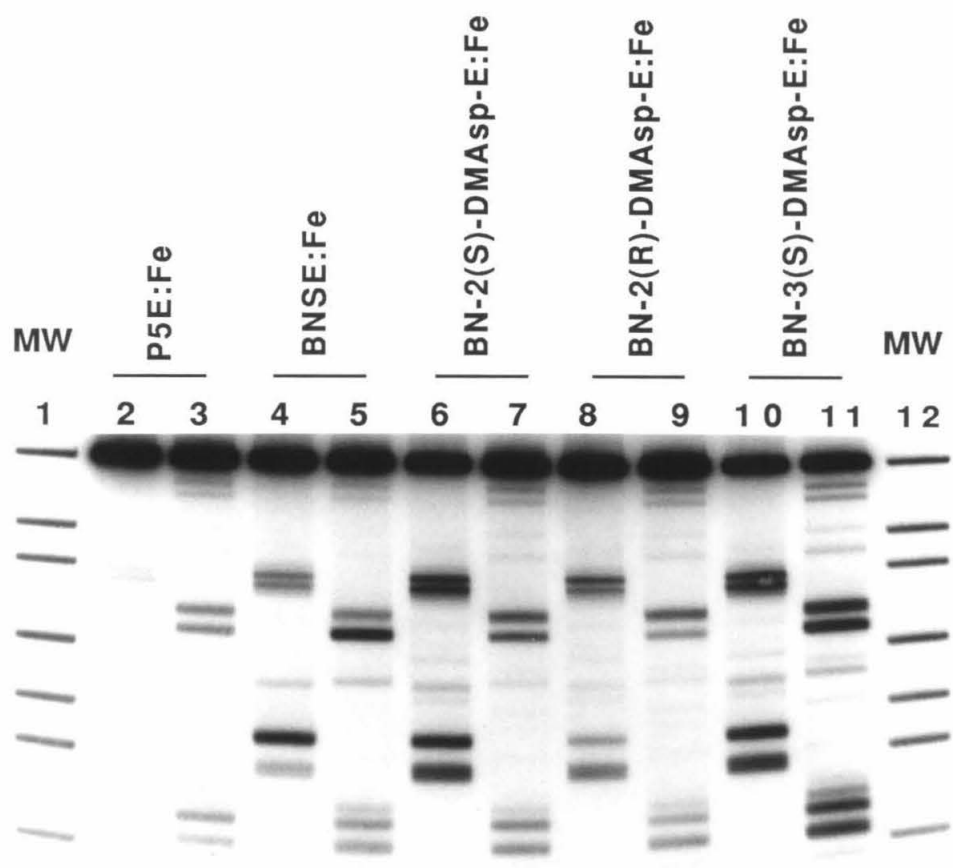
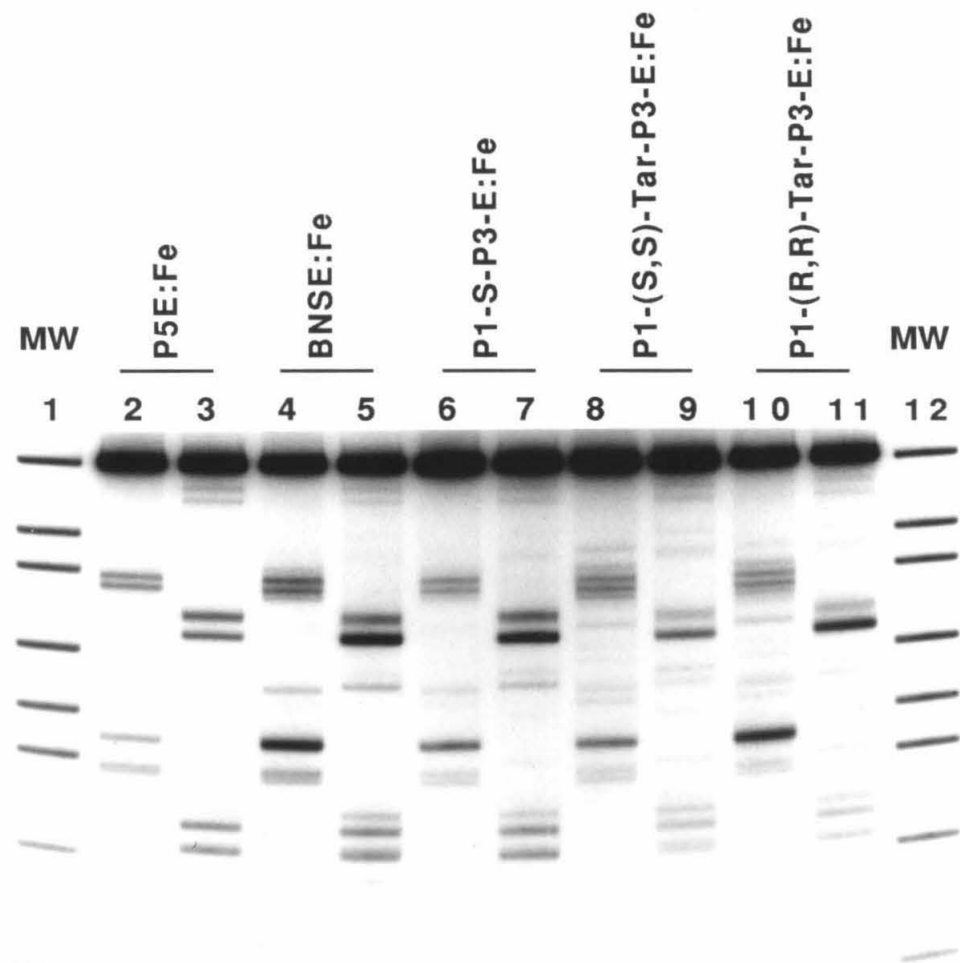


Figure 2.18

Autoradiograph of DNA double-strand cleavage patterns produced by **P5E:Fe**, **BNSE:Fe**, and **P1-Linker-P3-EDTA:Fe** compounds on Sty I-linearized, 3'-³²P end-labeled pBR322 plasmid DNA in the presence of dioxygen and dithiothreitol. Cleavage patterns were resolved by electrophoresis on a 1% agarose gel. Lanes 2,4,6,8,10 contain DNA labeled at one end with α -³²P dATP, while lanes 3,5,7,9,11 contain DNA labeled at the other end with α -³²P TTP. Lanes 1 and 12, molecular weight markers consisting of pBR322 restriction fragments 4363, 3371, 2994, 2368, 1998, 1768, 1372, 995, and 666 bp in length; lanes 2 and 3, **P5E:Fe** at 0.50 μ M concentration; lanes 4 and 5, **BNSE:Fe** at 0.10 μ M concentration; lanes 6 and 7, **P1-S-P3-E:Fe** at 0.10 μ M concentration; lanes 8 and 9, **P1-(S,S)-Tar-P3-E:Fe** at 4.0 μ M concentration; lanes 10 and 11, **P1-(R,R)-Tar-P3-E:Fe** at 8.0 μ M concentration.



Densitometric analysis of the autoradiographs shown in Figures 2.15-2.18 allowed formulation of the histograms shown in Figures 2.19-2.22. Positions of pBR322 DNA cleavage were determined from the electrophoretic mobilities of the cleavage bands produced by these molecules and the bands in the molecular weight marker lanes. The cleavage loci observed with these molecules map to A:T rich regions of pBR322. The two closely spaced cleavage loci near position 3100 map to two closely spaced seven base pair homopolymer A:T sequences, 5'-TTTTTTT-3' (centered at position 3079), and 5'-AAAAAAA-3' (centered at position 3111). The cleavage locus near position 3250 maps to the longest contiguous stretch of A:T base pairs (15) found on pBR322, 5'-TTTAAATTAAAAAT-3' (centered at position 3236). The cleavage locus near position 4250 maps to the nine base pair sequence 5'-TTTTTATT-3' (centered at position 4237). The cleavage locus near position 4300 maps to the ten base pair sequence 5'-ATATTTTAT-3' (centered at position 4325), and may also reflect cleavage at the neighboring eight base pair sequence 5'-ATAATAAT-3' (centered at position 4303). Minor cleavage loci map to the sequences 5'-TTAAATT-3' (centered at position 59), 5'-ATTTTTC-3' (centered at position 1752), 5'-AAAAAAC-3' (centered at position 1932), 5'-GTAAAAAA-3' (centered at position 2513), 5'-ATTATAGCAATAAA-3' (centered at position 3465), 5'-TATTAATT-3' (centered at position 3540), 5'-TTTAAAAA-3' (centered at position 3945), and 5'-AATATTATT-3' (centered at position 4173).

From the intensities of cleavage observed on the autoradiographs and the concentrations required to achieve these cleavage intensities, overall DNA binding/cleaving efficiencies (E_{rel} values) for these molecules decrease in the order **BNSE:Fe, P1-S-P3-E:Fe > BN-2-(S)-Mal-E:Fe > P5E:Fe > BN-2-(R)-Mal-E:Fe, BN-3-DMAsp-E:Fe > BN-2-DMAsp-E:Fe > BN-(S,S)-Tar-E:Fe > P1-(S,S)-Tar-E:Fe > BN-(RS,SR)-Tar-E:Fe, P1-(R,R)-P3-E:Fe > BN-(R,R)-Tar-E:Fe > BN-(R,R)-TarAc-E:Fe, BN-(S,S)-TarAc-E:Fe, BN-(RS,SR)-TarAc-E:Fe, BN-(S)-AE:Fe, BN-(R)-AE:Fe.**

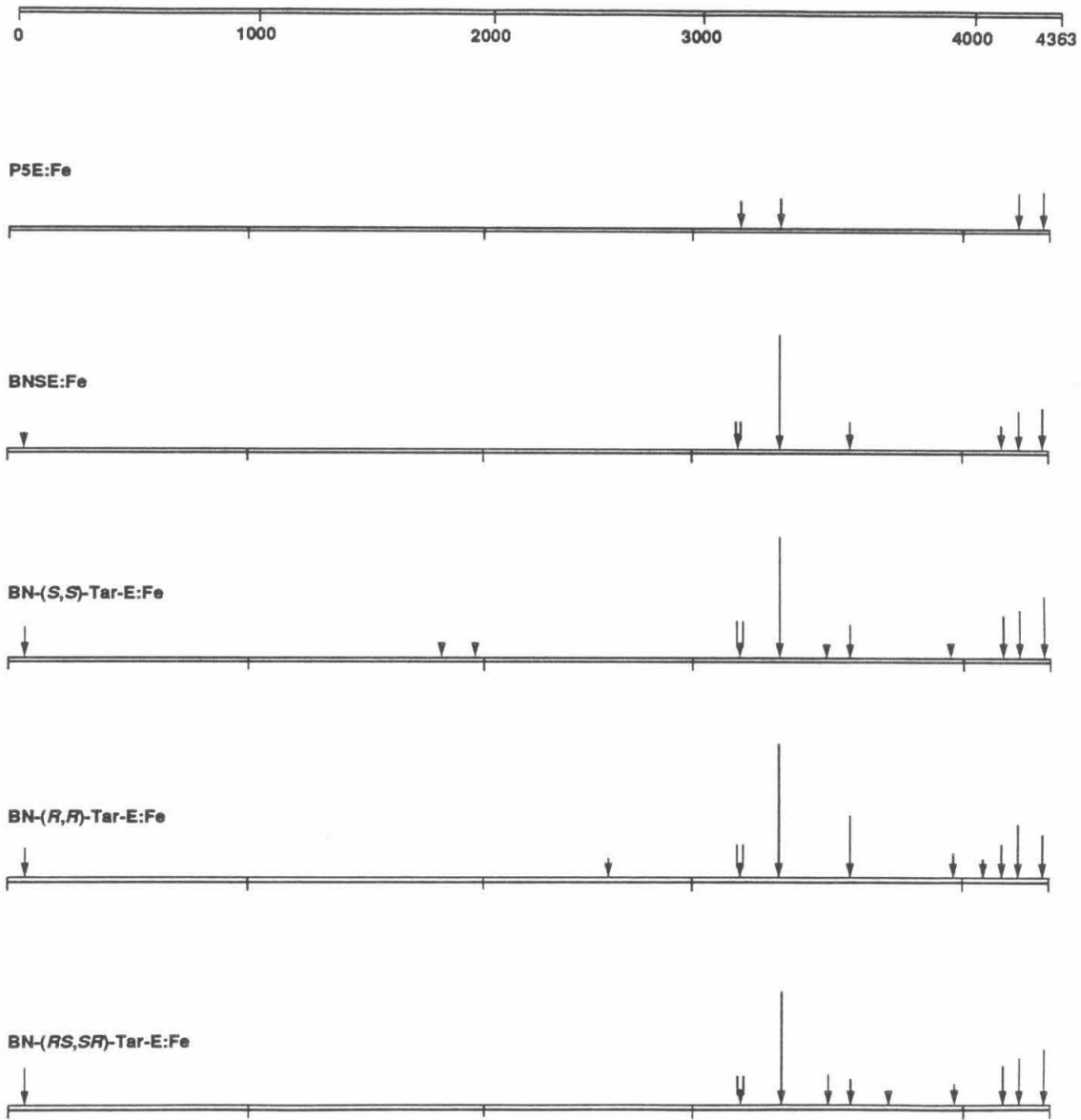


Figure 2.19. Histogram of DNA double-strand cleavage produced by PSE:Fe, BNSE:Fe, and Bis(Netropsin)-Tartaramide-EDTA:Fe compounds on Sty I-linearized pBR322 plasmid DNA in the presence of dioxygen and dithiothreitol. Lengths of arrows correspond to the relative amounts of cleavage, determined by optical densitometry, at the various cleavage loci. Positions of cleavage were determined by analyzing the measured electrophoretic mobilities of DNA cleavage fragments relative to a standard curve derived from the measured electrophoretic mobilities of marker fragments of known molecular weights.

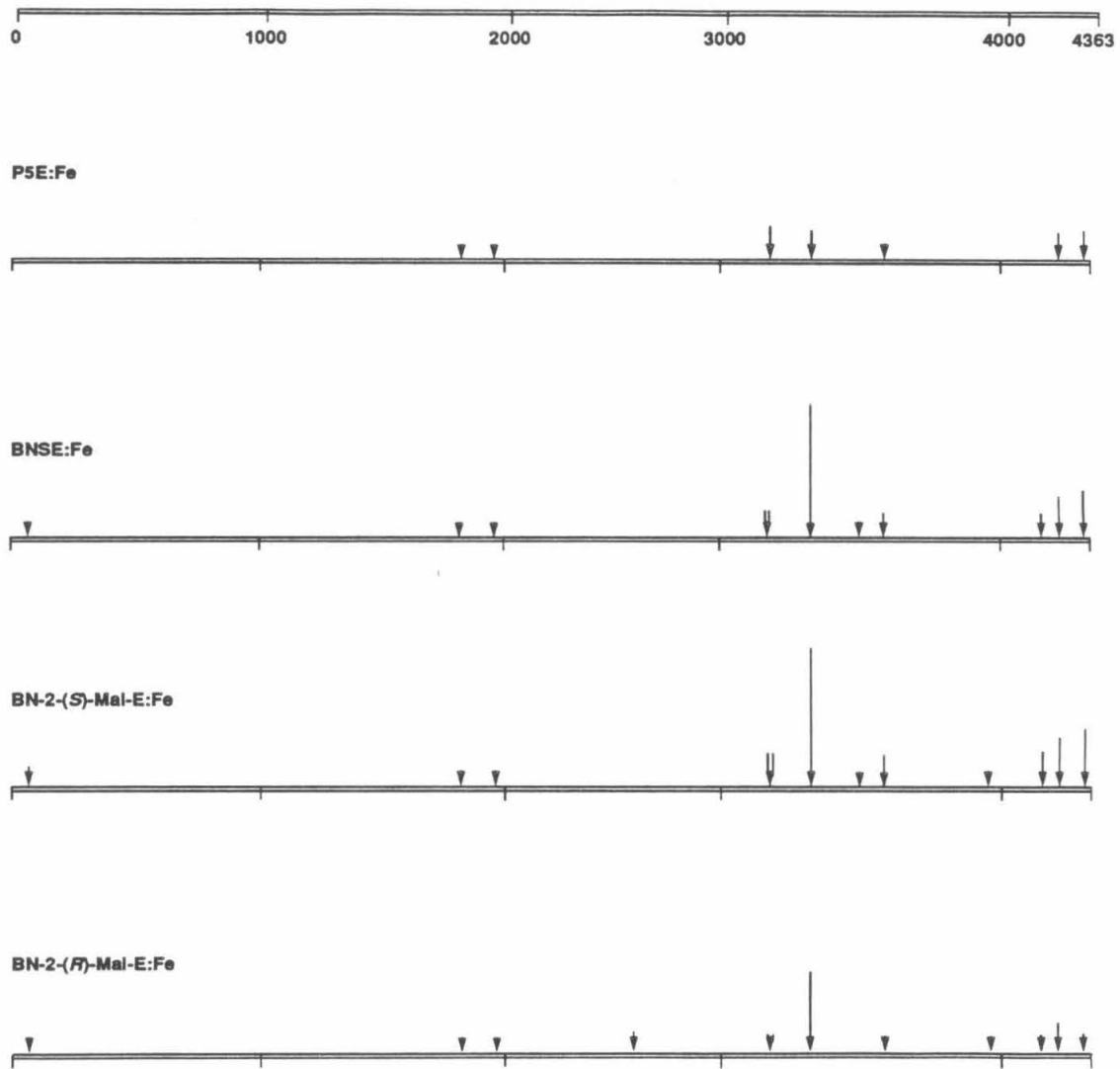


Figure 2.20. Histogram of DNA double-strand cleavage produced by P5E:Fe, BNSE:Fe, and Bis(Neropsin)-Malcamide-EDTA:Fe compounds on Sty I-linearized pBR322 plasmid DNA in the presence of dioxygen and dithiothreitol. Lengths of arrows correspond to the relative amounts of cleavage, determined by optical densitometry, at the various cleavage loci. Positions of cleavage were determined by analyzing the measured electrophoretic mobilities of DNA cleavage fragments relative to a standard curve derived from the measured electrophoretic mobilities of marker fragments of known molecular weights.

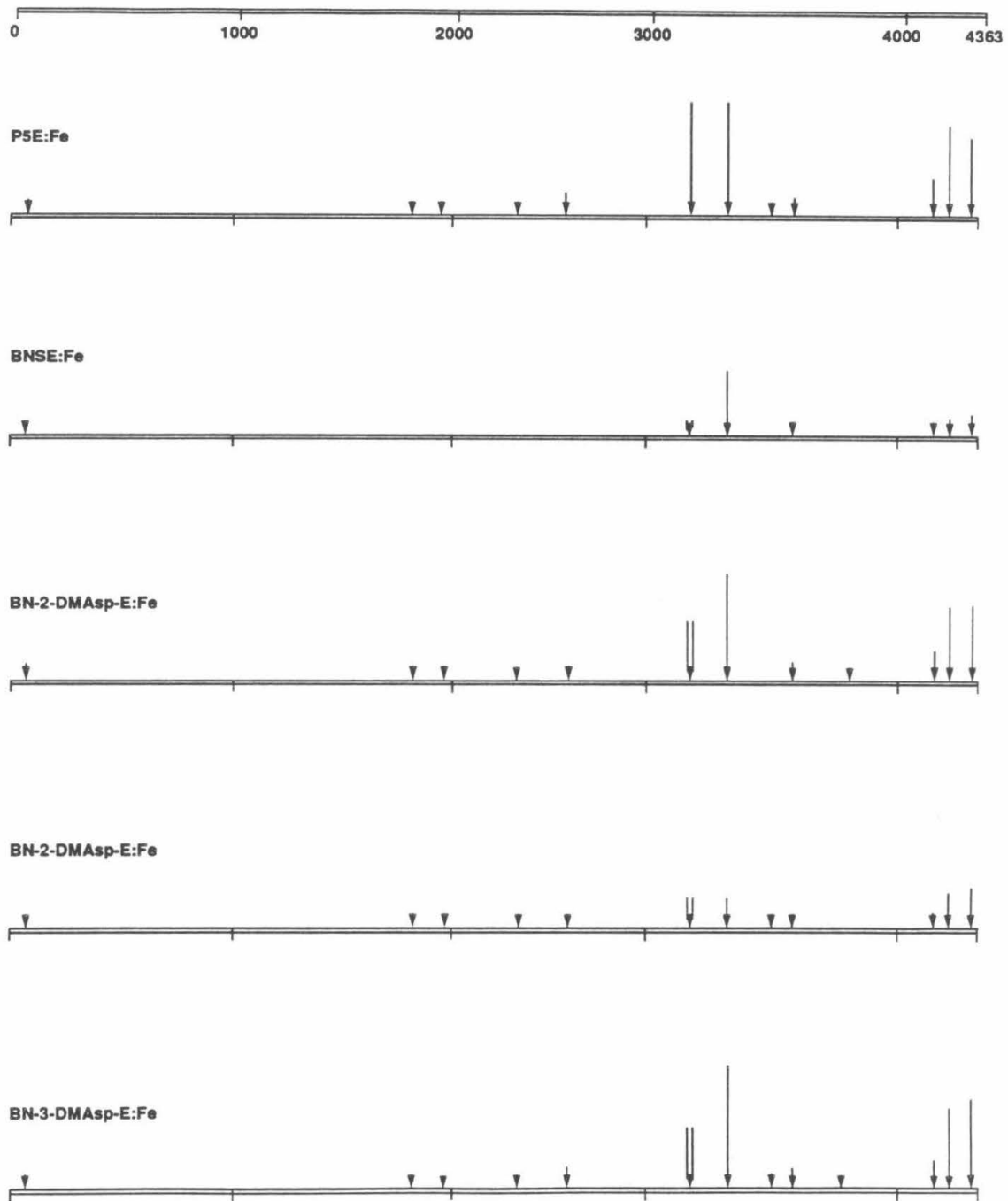


Figure 2.21. Histogram of DNA double-strand cleavage produced by P5E:Fe, BNSE:Fe, and Bis(Netropsin)-Dimethylaminoaspartamide-EDTA:Fe compounds on Sty I-linearized pBR322 plasmid DNA in the presence of dioxygen and dithiothreitol. Lengths of arrows correspond to the relative amounts of cleavage, determined by optical densitometry, at the various cleavage loci. Positions of cleavage were determined by analyzing the measured electrophoretic mobilities of DNA cleavage fragments relative to a standard curve derived from the measured electrophoretic mobilities of marker fragments of known molecular weights.

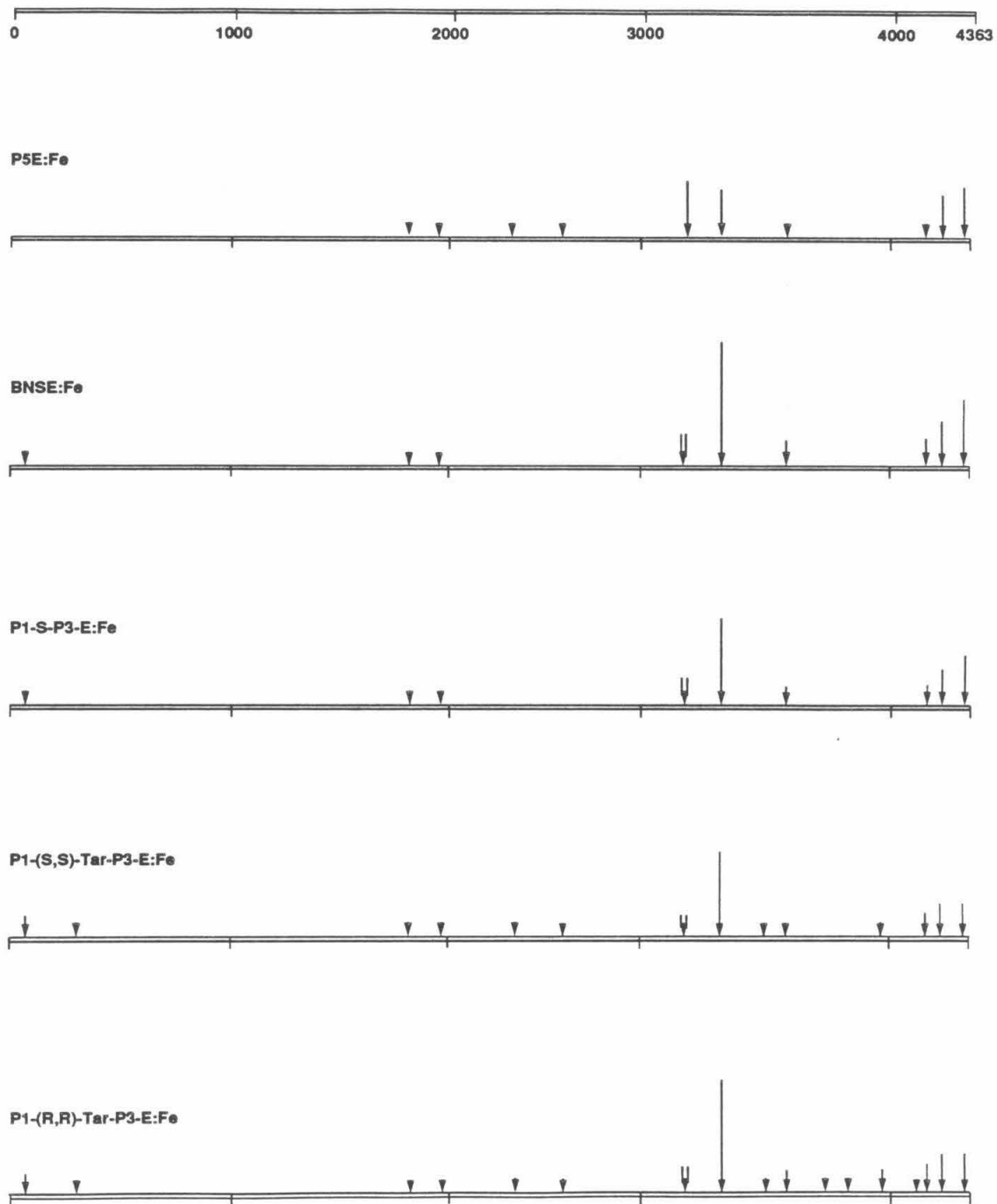


Figure 2.22. Histogram of DNA double-strand cleavage produced by P5E:Fe, BNSE:Fe, and P1-Linker-P3-EDTA:Fe compounds on Sty I-linearized pBR322 plasmid DNA in the presence of dioxygen and dithiothreitol. Lengths of arrows correspond to the relative amounts of cleavage, determined by optical densitometry, at the various cleavage loci. Positions of cleavage were determined by analyzing the measured electrophoretic mobilities of DNA cleavage fragments relative to a standard curve derived from the measured electrophoretic mobilities of marker fragments of known molecular weights.

Two of the major double-strand cleavage loci produced by these molecules were examined at nucleotide resolution. For these studies, 517 base pair Eco RI/Rsa I restriction fragments from pBR322 were prepared with ^{32}P at either the 3'- or 5' Eco RI end. DNA binding/cleaving of these fragments, which contain the major cleavage loci centered at or near pBR322 positions 4237 and 4325, was carried out under standard, optimal conditions.²⁹ DNA cleavage products were separated by denaturing polyacrylamide gel electrophoresis and visualized by autoradiography.

An autoradiograph of the cleavage patterns produced by **P5E:Fe**, **BNSE:Fe**, and the Bis(Netropsin)-Tartaramide-EDTA:Fe compounds on the 517 base pair restriction fragments is shown in Figure 2.23. Here it can be seen that the **BN-(S,S)-Tar-E:Fe**, **BN-(R,R)-Tar-E:Fe**, and **BN-(RS,SR)-Tar-E:Fe** produce specific cleavage in the same general regions as **P5E:Fe** and **BNSE:Fe**. However, the chiral Bis(Netropsin)-EDTA:Fe compounds exhibit lower site selectivities than **P5E:Fe** and **BNSE:Fe**. **P5E:Fe** and **BNSE:Fe** produce intense cleavage at sites near the bottom (Site A) and upper middle (Site C) parts of the autoradiograph, and weaker cleavage at sites in the lower middle (Site B) and upper (Site E) parts of the autoradiograph, **BN-(S,S)-Tar-E:Fe**, **BN-(R,R)-Tar-E:Fe**, and **BN-(RS,SR)-Tar-E:Fe** produce uniform intensities of cleavage at Sites A, B, C, and E. Bis(Netropsin)-Tartaramide-EDTA:Fe compounds produce significant background cleavage and complex cleavage patterns in the regions of Sites C and E. These patterns indicate multiple, overlapping binding sites for these molecules in these regions. The Bis(Netropsin)-Tartaramide-EDTA:Fe compounds exhibit small binding orientation preferences, similar to **BNSE:Fe**.

An autoradiograph of the cleavage patterns produced by **P5E:Fe**, **BNSE:Fe**, and the Bis(Netropsin)-Malcamide-EDTA:Fe compounds on the 517 base pair restriction fragments is shown in Figure 2.24. Here it can be seen that **BN-2-(S)-Mal-E:Fe** and **BN-2-(R)-Mal-E:Fe** produce specific cleavage at Sites A, B, C and E, and exhibit site selectivities and orientation preferences similar to **BNSE:Fe**. **BN-2-(R)-Mal-E:Fe**

produces a somewhat more complex cleavage pattern in the region of Site C, indicative of multiple overlapping binding sites in this region for this molecule.

An autoradiograph of the cleavage patterns produced by **P5E:Fe**, **BNSE:Fe**, and the Bis(Netropsin)-Dimethylaminoaspartamide-EDTA:Fe compounds on the 517 base pair restriction fragments is shown in Figure 2.25. The lane labels indicate the configurations that these materials would have had in the absence of racemization. Here it can be seen that **BN-2-DMAsp-E:Fe** and **BN-3-DMAsp-E:Fe** produce specific cleavage at Sites A, B, C, and E, and exhibit site selectivities and orientation preferences similar to **BNSE:Fe**.

An autoradiograph of the cleavage patterns produced by **P5E:Fe**, **BNSE:Fe**, and the P1-Linker-P3-EDTA:Fe compounds on the 517 base pair restriction fragments is shown in Figure 2.26. Here it can be seen that **P1-S-P3-EDTA:Fe**, **P1-(S,S)-Tar-P3-EDTA:Fe**, and **P1-(R,R)-Tar-P3-EDTA:Fe** produce specific DNA cleavage in the same general regions as **P5E:Fe** and **BNSE:Fe**, but with some significant differences in orientation preferences and site selectivities. The P1-Linker-P3-EDTA:Fe compounds exhibit very strong binding orientation preferences at Site A. **P1-S-P3-E:Fe** and **P1-(S,S)-Tar-P3-E:Fe** produce strong cleavage at a binding site (Site D) in the upper middle part of the autoradiograph, which is different from Site C preferred by **BNSE:Fe**. **P1-(R,R)-Tar-P3-E:Fe** produces significant background cleavage and complex patterns of cleavage in the regions of Sites B, C, and E, which are consistent with multiple overlapping binding sites in these regions for this molecule.

The DNA cleavage patterns on these autoradiographs were analyzed by densitometry and converted to histogram form (Figures 2.27-2.30). Equilibrium minor groove binding sites for these molecules, assigned on the basis of their 3'-shifted, pseudo- C_2 symmetrical cleavage patterns,²⁵ are indicated as boxes in the histograms. All of the molecules that exhibit sequence-specific DNA binding/cleaving behavior bind to the seven base pair sequence 5'-ATTTTTA-3' at Site A. This sequence lies within the ten base pair A:T sequence centered at pBR322 position 4325 and mapped by DNA double-strand

Figure 2.23

Autoradiograph of DNA cleavage patterns produced by **P5E:Fe**, **BNSE:Fe**, and Bis(Netropsin)-Tartaramide-EDTA:Fe compounds on 3'- and 5'-³²P end-labeled 517 bp restriction fragments (Eco RI/Rsa I) from plasmid pBR322 DNA, in the presence of dioxygen and dithiothreitol. Cleavage patterns were resolved by electrophoresis on a 1:20 cross-linked 8% polyacrylamide, 50% urea denaturing gel. Lanes 1-12 were with 3' end-labeled DNA, while lanes 13-24 were with 5' end-labeled DNA. Lanes 1 and 24, uncleaved DNA; lanes 2 and 23, Maxam-Gilbert chemical sequencing G reactions; lanes 3,4 and 13,14, **P5E:Fe** at 0.50 and 1.0 μ M concentrations; lanes 5,6 and 15,16, **BNSE:Fe** at 0.50 and 1.0 μ M concentrations; lanes 7,8 and 17,18, **BN-(S,S)-Tar-E:Fe** at 1.0, and 10 μ M concentrations; lanes 9,10 and 19,20, **BN-(R,R)-Tar-E:Fe** at 1.0 and 50 μ M concentrations; lanes 11,12 and 21,22, **BN-(RS,SR)-Tar-E:Fe** at 1.0 and 20 μ M concentrations.

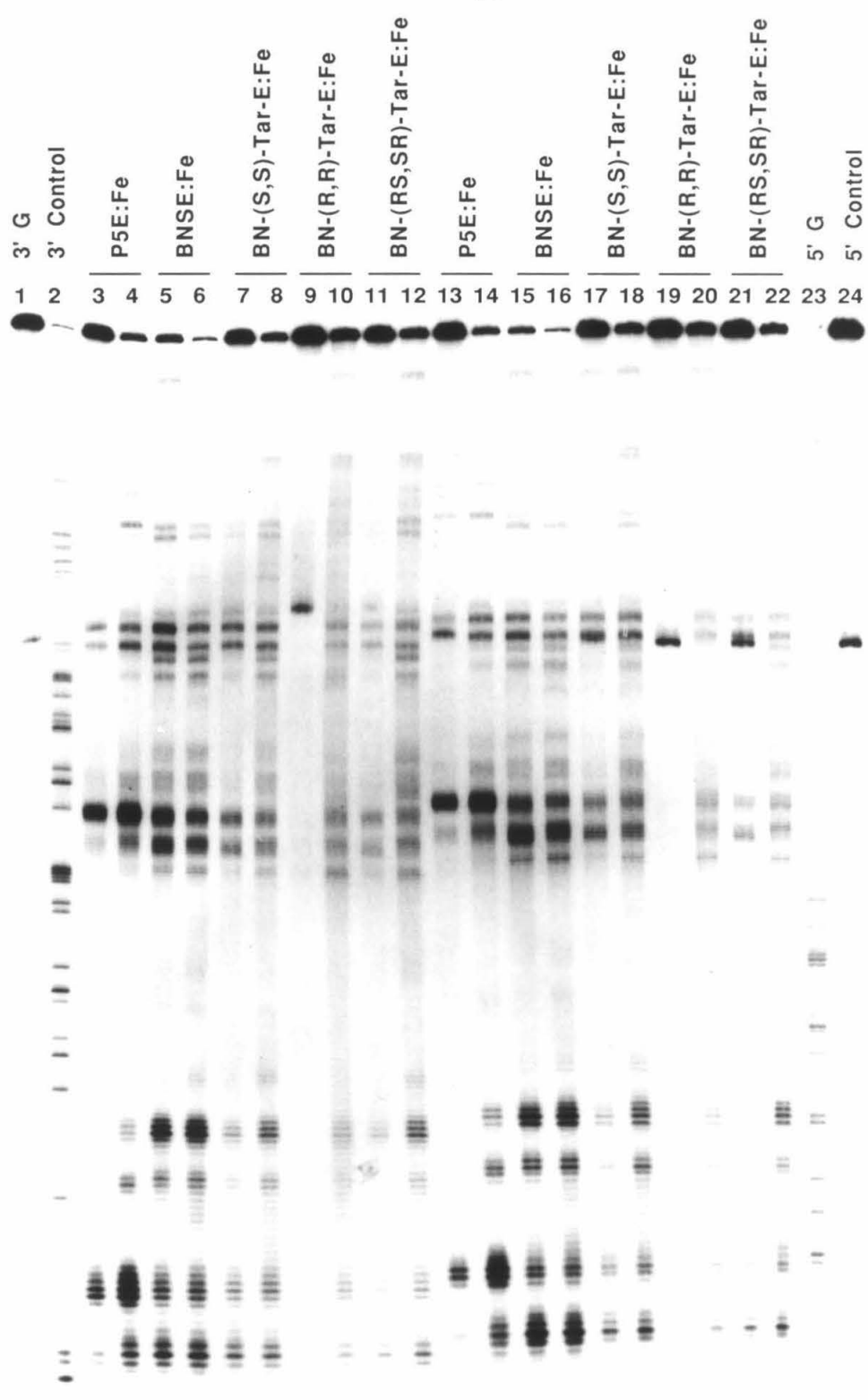


Figure 2.24

Autoradiograph of DNA cleavage patterns produced by **P5E:Fe**, **BNSE:Fe**, and Bis(Netropsin)-Malcamide-EDTA:Fe compounds on 3'- and 5'-³²P end-labeled 517 bp restriction fragments (Eco RI/Rsa I) from plasmid pBR322 DNA, in the presence of dioxygen and dithiothreitol. Cleavage patterns were resolved by electrophoresis on a 1:20 cross-linked 8% polyacrylamide, 50% urea denaturing gel. Lanes 1-10 were with 3' end-labeled DNA, while lanes 11-20 were with 5' end-labeled DNA. Lanes 1 and 20, uncleaved DNA; lanes 2 and 19, Maxam-Gilbert chemical sequencing G reactions; lanes 3,4 and 11,12, **P5E:Fe** at 0.50 and 1.0 μ M concentrations; lanes 5,6 and 13,14, **BNSE:Fe** at 0.50 and 1.0 μ M concentrations; lanes 7,8 and 15,16, **BN-2-(S)-Mal-E:Fe** at 0.50 and 1.0 μ M concentrations; lanes 9,10 and 17,18, **BN-2-(R)-Mal-E:Fe** at 1.0 and 2.0 μ M concentrations.

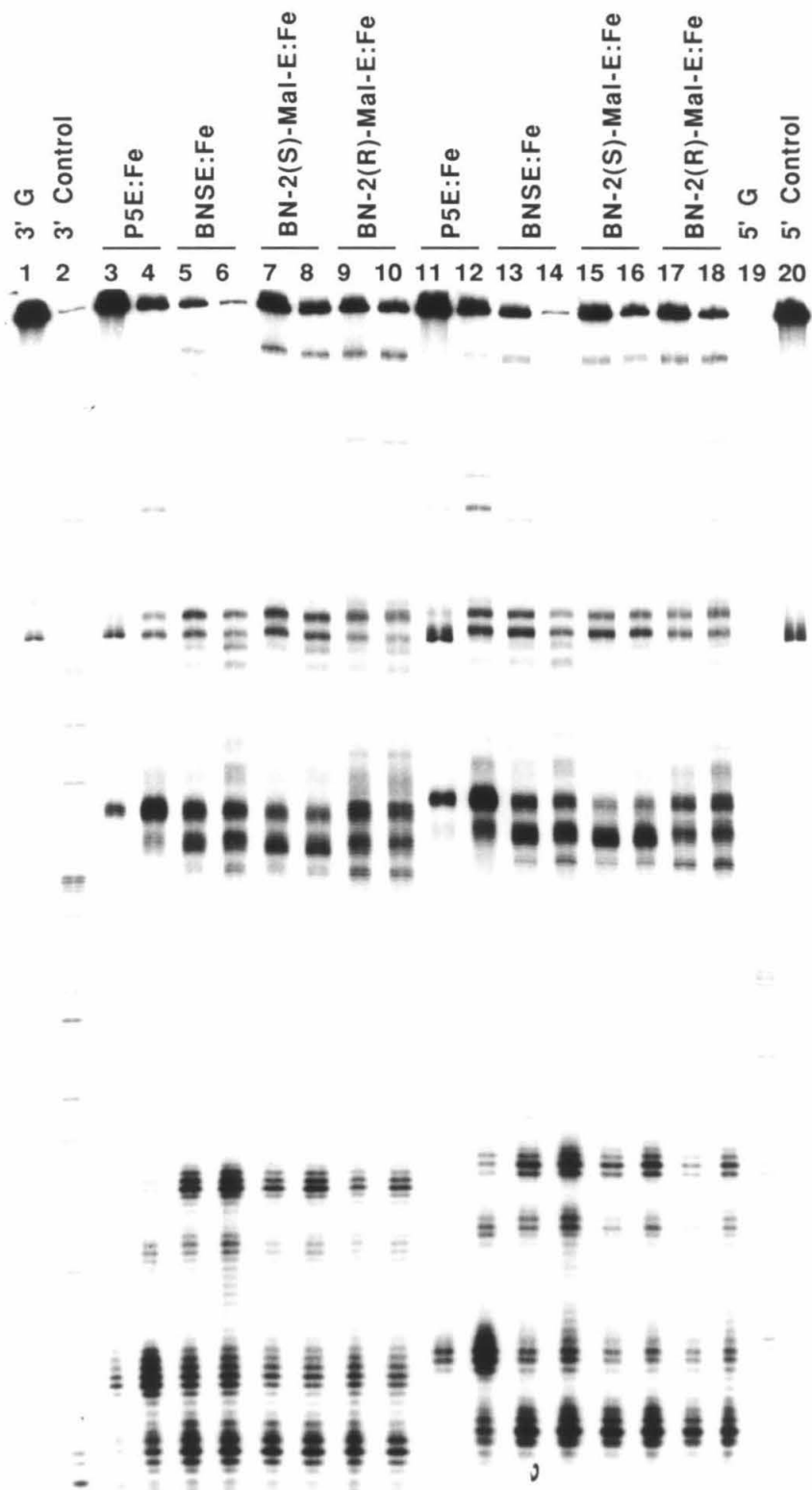


Figure 2.25

Autoradiograph of DNA cleavage patterns produced by **P5E:Fe**, **BNSE:Fe**, and Bis(Netropsin)-Dimethylaminoaspartamide-EDTA:Fe compounds on 3'- and 5'-³²P end-labeled 517 bp restriction fragments (Eco RI/Rsa I) from plasmid pBR322 DNA, in the presence of dioxygen and dithiothreitol. Cleavage patterns were resolved by electrophoresis on a 1:20 cross-linked 8% polyacrylamide, 50% urea denaturing gel. Lanes 1-12 were with 3' end-labeled DNA, while lanes 13-24 were with 5' end-labeled DNA. Lanes 1 and 24, uncleaved DNA; lanes 2 and 23, Maxam-Gilbert chemical sequencing G reactions; lanes 3,4 and 13,14, **P5E:Fe** at 0.50 and 1.0 μ M concentrations; lanes 5,6 and 15,16, **BNSE:Fe** at 0.50 and 1.0 μ M concentrations; lanes 7,8 and 17,18, **BN-2-DMAsp-E:Fe** at 1.0 and 15 μ M concentrations; lanes 9,10 and 19,20, **BN-2-DMAsp-E:Fe** at 1.0 and 20 μ M concentrations; lanes 11,12 and 21,22, **BN-3-DMAsp-E:Fe** at 1.0 and 10 μ M concentrations.

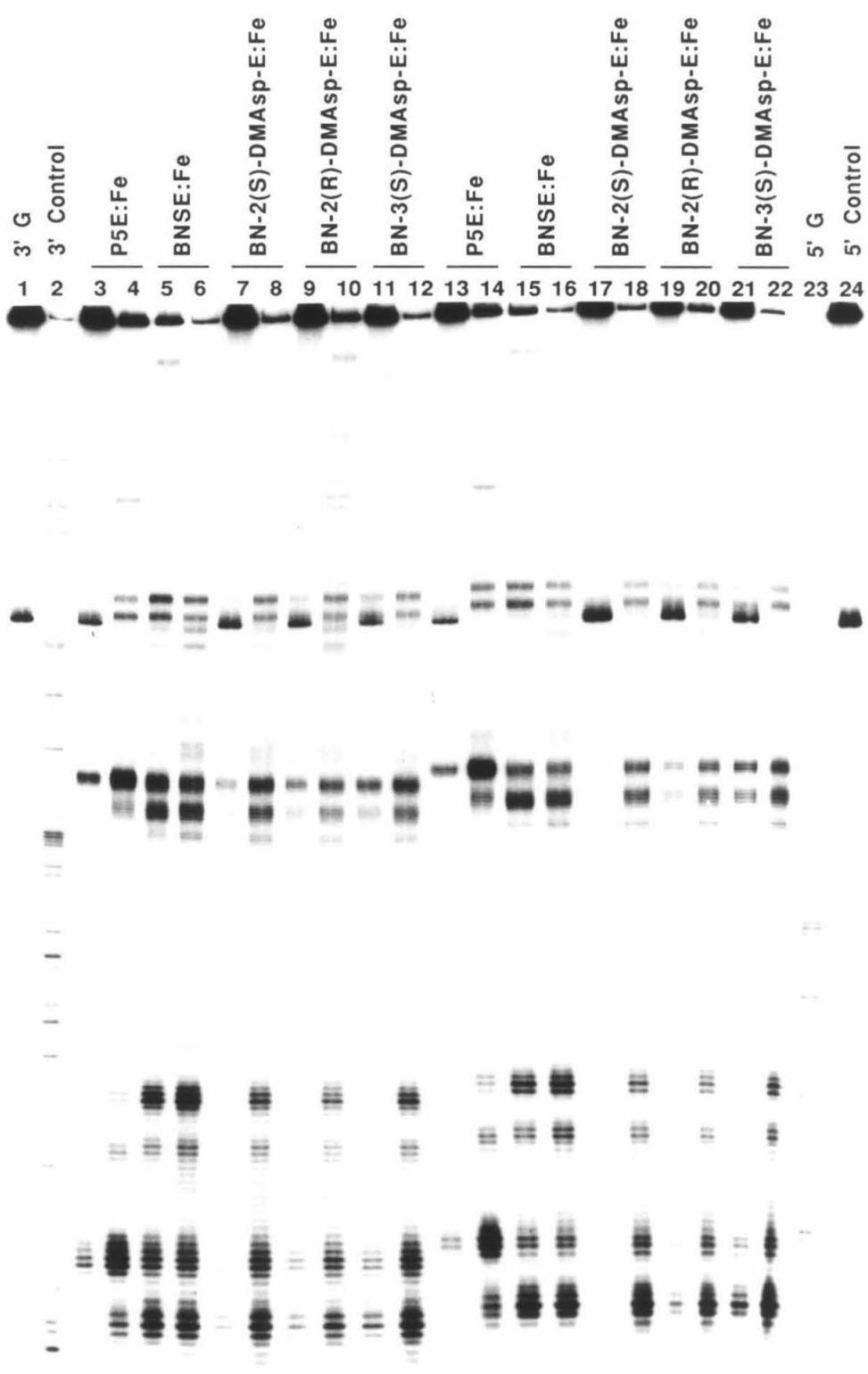
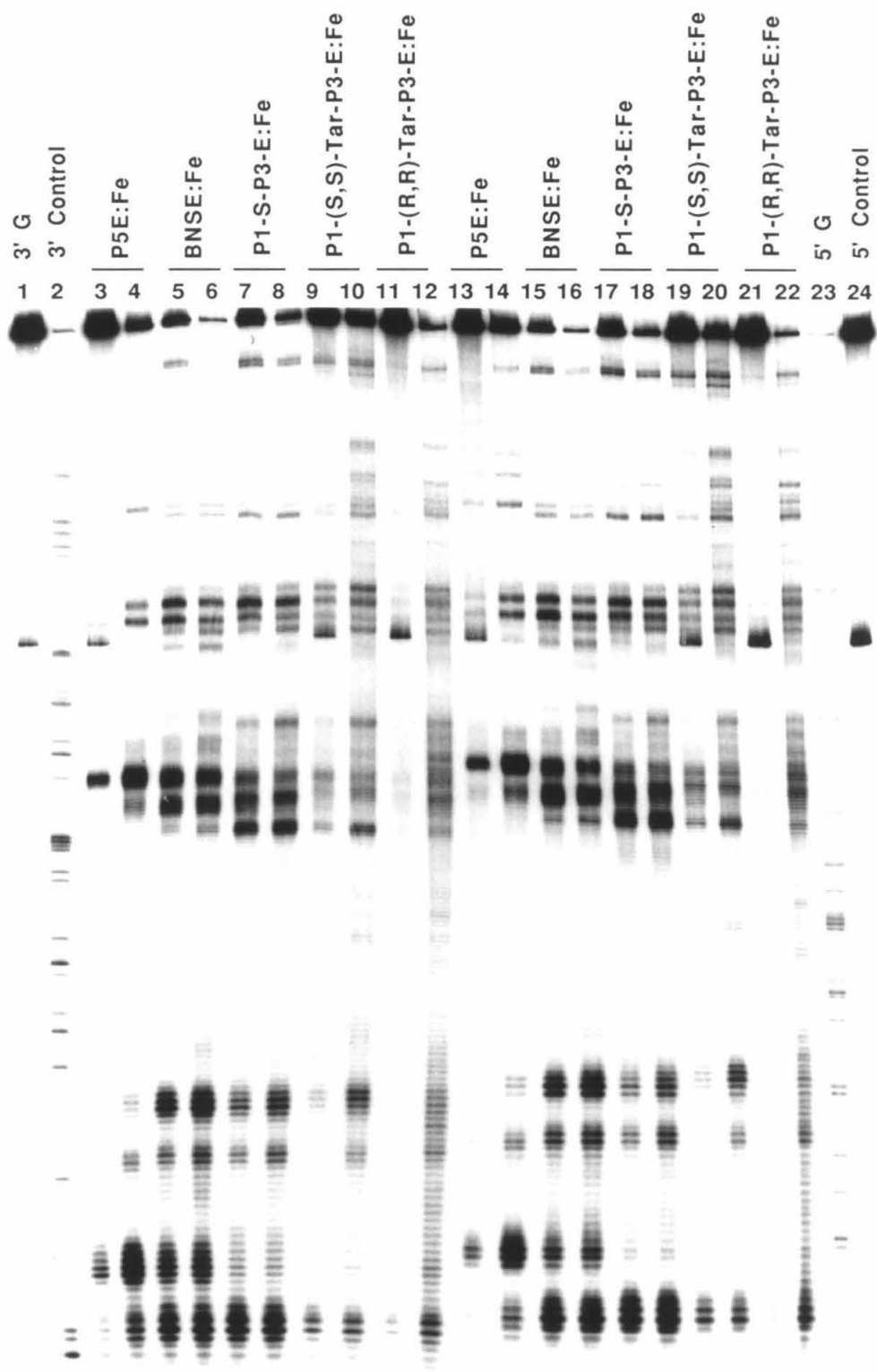


Figure 2.26

Autoradiograph of DNA cleavage patterns produced by **P5E:Fe**, **BNSE:Fe**, and **P1-Linker-P3-EDTA:Fe** compounds on 3'- and 5'-³²P end-labeled 517 bp restriction fragments (Eco RI/Rsa I) from plasmid pBR322 DNA, in the presence of dioxygen and dithiothreitol. Cleavage patterns were resolved by electrophoresis on a 1:20 cross-linked 8% polyacrylamide, 50% urea denaturing gel. Lanes 1-12 were with 3' end-labeled DNA, while lanes 13-24 were with 5' end-labeled DNA. Lanes 1 and 24, uncleaved DNA; lanes 2 and 23, Maxam-Gilbert chemical sequencing G reactions; lanes 3,4 and 13,14, **P5E:Fe** at 0.50 and 1.0 μ M concentrations; lanes 5,6 and 15,16, **BNSE:Fe** at 0.50 and 1.0 μ M concentrations; lanes 7,8 and 17,18, **P1-S-P3-E:Fe** at 0.5 and 1.0 μ M concentrations; lanes 9,10 and 19,20, **P1-(S,S)-Tar-P3-E:Fe** at 1.0 and 10 μ M concentrations; lanes 11,12 and 21,22, **P1-(R,R)-Tar-P3-E:Fe** at 1.0 and 20 μ M concentrations.



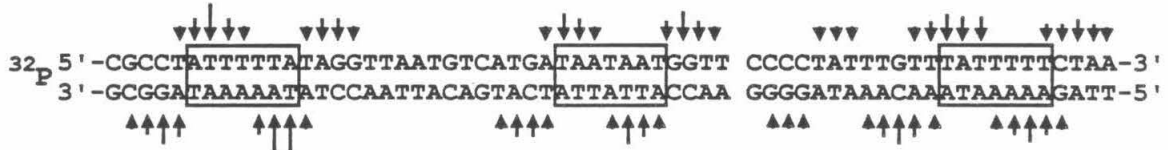
P5E:Fe



BNSE:Fe



BN-(S,S)-Tar-E:Fe



BN-(R,R)-Tar-E:Fe



BN-(RS,SR)-Tar-E:Fe

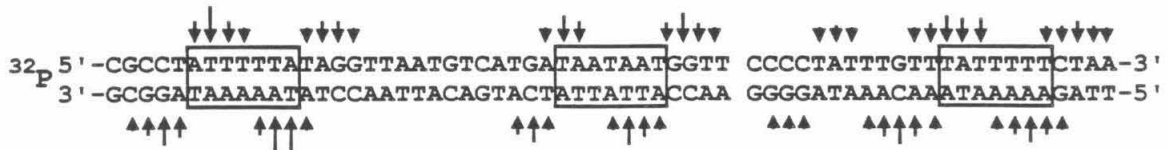


Figure 2.27. Histograms of DNA cleavage produced by P5E:Fe, BNSE:Fe, and Bis(Netropsin)-Tartaramide-EDTA:Fe compounds on the 517 bp DNA restriction fragment (Eco RI/Rsa I) from plasmid pBR322 DNA. Lengths of arrows correspond to the relative amounts of cleavage that result in removal of the indicated base. DNA minor groove binding sites (boxed) were assigned from the observed cleavage patterns and the model described by Taylor, Schultz, and Dervan (Reference 25).

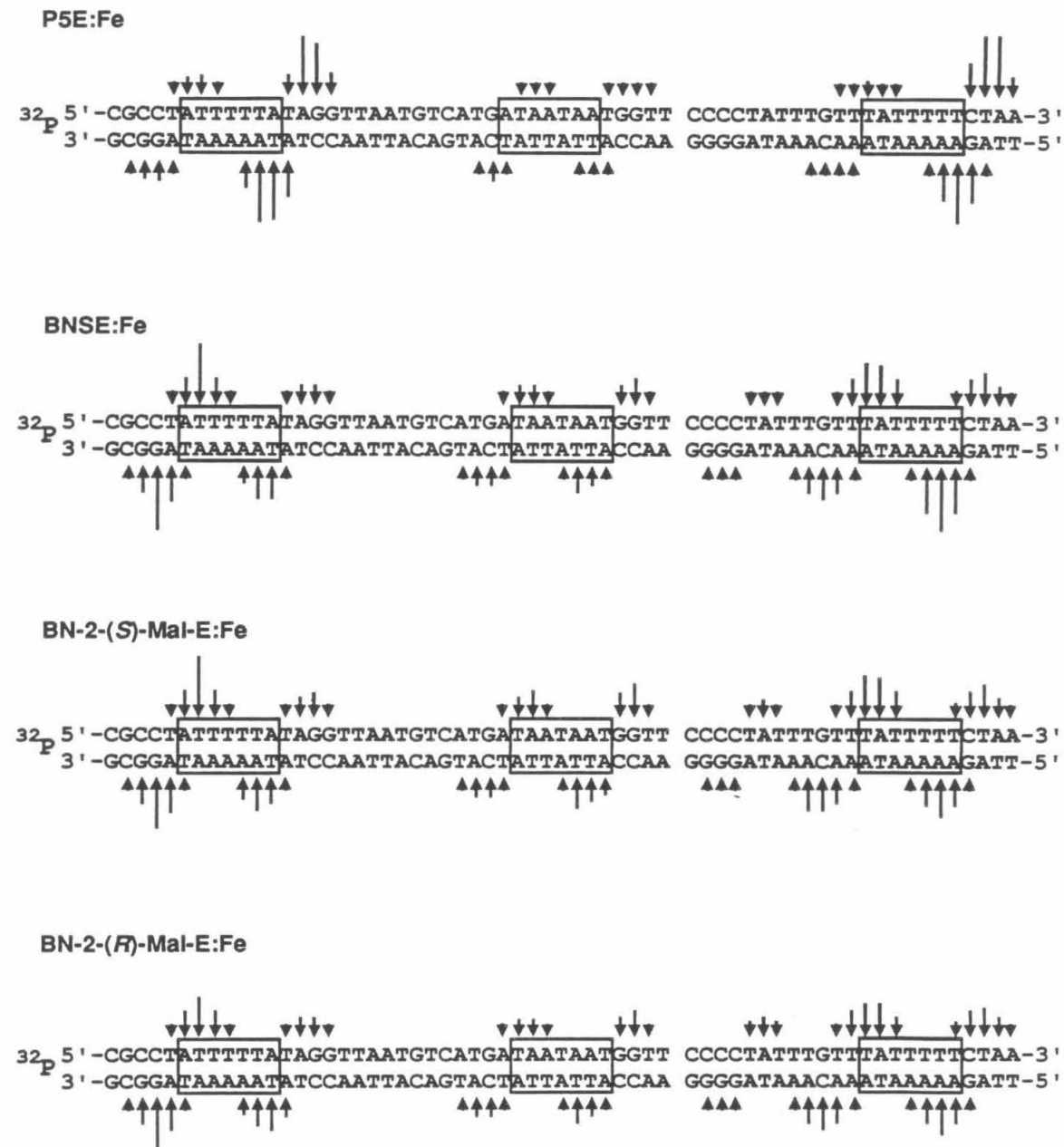
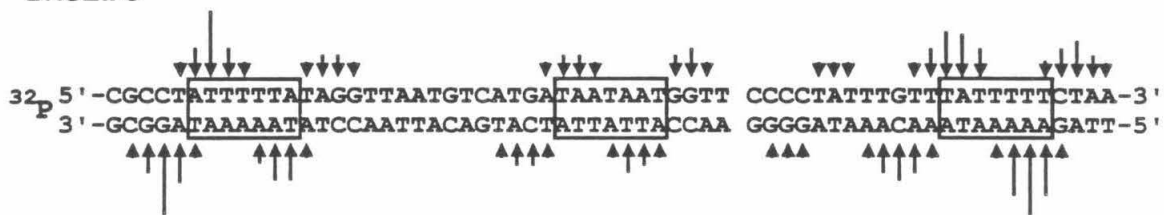


Figure 2.28. Histograms of DNA cleavage produced by **P5E:Fe**, **BNSE:Fe**, and Bis(Netropsin) Malicamide-EDTA:Fe compounds on the 517 bp DNA restriction fragment (Eco RI/Rsa I) from plasmid pBR322 DNA. Lengths of arrows correspond to the relative amounts of cleavage that result in removal of the indicated base. DNA minor groove binding sites (boxed) were assigned from the observed cleavage patterns and the model described by Taylor, Schultz, and Dervan (Reference 25).

P5E:Fe



BNSE:Fe



BN-2-DMAsp-E:Fe



BN-3-DMAsp-E:Fe

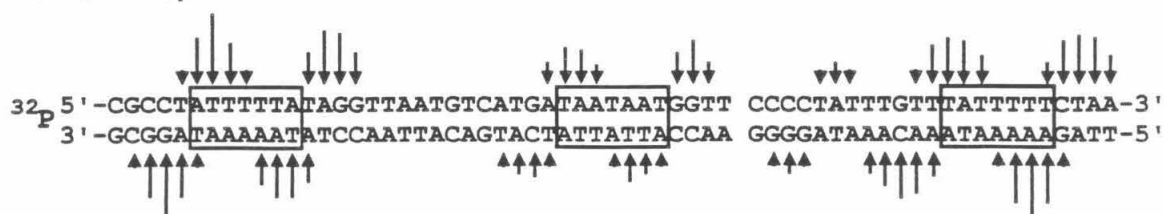


Figure 2.29. Histograms of DNA cleavage produced by P5E:Fe, BNSE:Fe, and Bis(Netropsin)-Dimethylaminoaspartamide-EDTA:Fe compounds on the 517 bp DNA restriction fragment (Eco RI/Rsa I) from plasmid pBR322 DNA. Lengths of arrows correspond to the relative amounts of cleavage that result in removal of the indicated base. DNA minor groove binding sites (boxed) were assigned from the observed cleavage patterns and the model described by Taylor, Schultz, and Dervan (Reference 25).

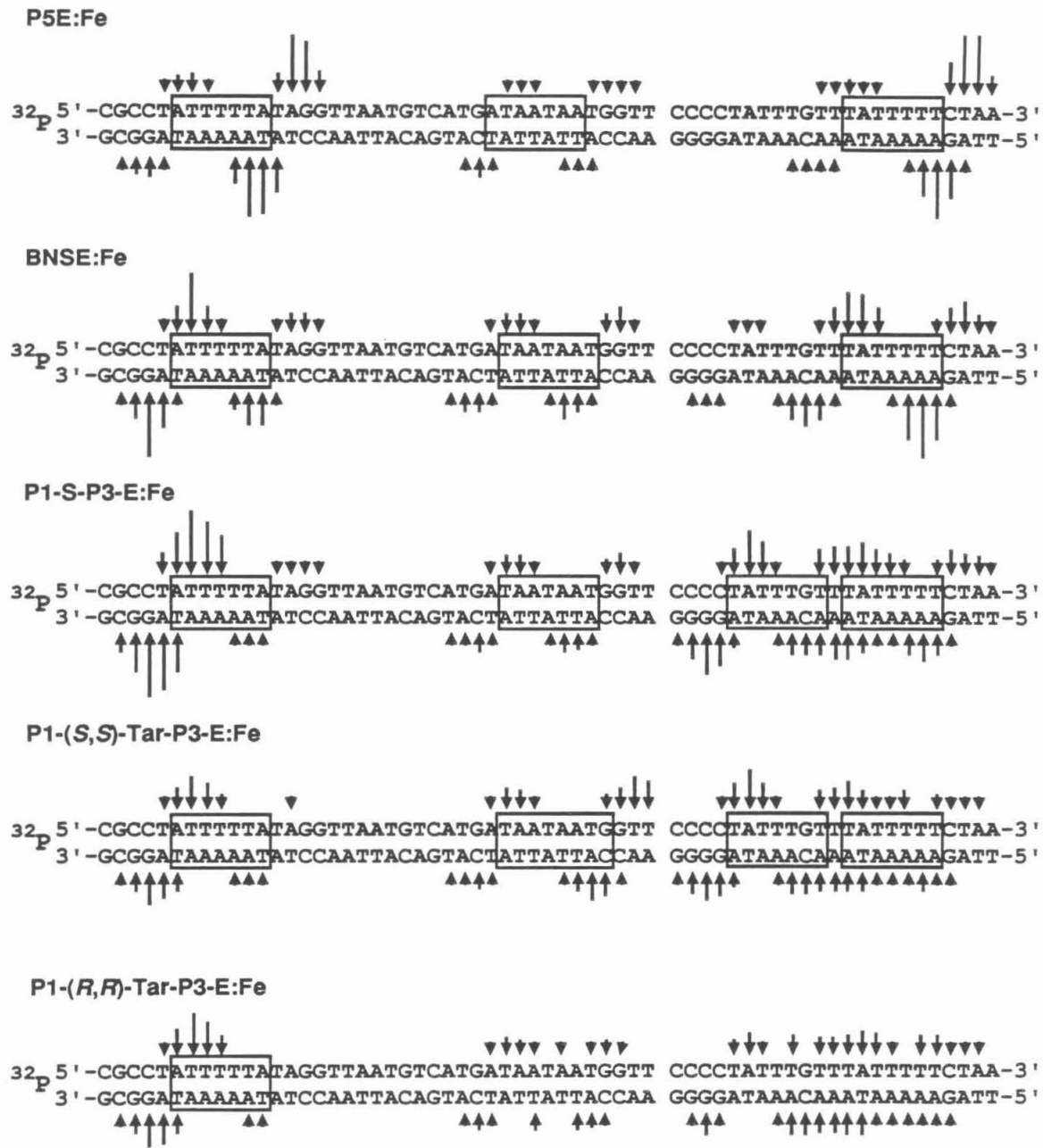


Figure 2.30. Histograms of DNA cleavage produced by P5E:Fe, BNSE:Fe, and P1-Linker-P3-EDTA:Fe compounds on the 517 bp DNA restriction fragment (Eco RI/Rsa I) from plasmid pBR322 DNA. Lengths of arrows correspond to the relative amounts of cleavage that result in removal of the indicated base. DNA minor groove binding sites (boxed) were assigned from the observed cleavage patterns and the model described by Taylor, Schultz, and Dervan (Reference 28).

affinity cleaving analysis. At Site B, **P5E:Fe** binds to the sequence 5'-ATAATAA-3', while **BNSE:Fe**, **BN-(S,S)-Tar-E:Fe**, **BN-(R,R)-Tar-E:Fe**, **BN-(RS,SR)-Tar-E:Fe**, **BN-2-(S)-Mal-E:Fe**, **BN-2-(R)-Mal-E:Fe**, **BN-2-DMAsp-E:Fe**, **BN-3-DMAsp-E:Fe**, and **P1-S-P3-E:Fe** bind to a sequence shifted by one base pair, 5'-TAATAAT-3'. **P1-(S,S)-Tar-P3-E:Fe** appears to bind to the eight base pair sequence 5'-TAATAATG-3' in this region. At Site C, all of the molecules that exhibit sequence-specific DNA binding/cleaving behavior bind to the seven base pair sequence 5'-TATTTTT-3'. This binding site lies within the nine base pair A:T sequence centered at pBR322 position 4237 and mapped by DNA double-strand affinity cleaving analysis. **P5E:Fe** produces very little cleavage at Site D, but **BNSE:Fe**, **P1-S-P3-E:Fe**, and the active DNA binding/cleaving chiral molecules all appear to bind to the seven base pair sequence 5'-ATTTGTT-3', which overlaps with the Site C binding sequence.

Densitometric analysis of the cleavage intensities produced by these molecules allowed values of binding orientation preferences and relative DNA binding/cleaving efficiencies to be calculated for these molecules at Sites A, B, C. These data are collected in the following tables. Estimated values of E_{rel} at Site D are also included. Because of overlap with Site C, orientation preference values were not calculated at Site D. It is predicted that these values are reproducible to $\pm 20\%$. Orientation preferences were calculated by dividing the total amount of cleavage observed on the lower side (towards the bottom of the autoradiograph) of a binding site by the total amount of cleavage observed on the higher side of that binding site. For **BNSE:Fe** and the chiral Bis(Netropsin)-EDTA:Fe compounds, orientation preferences ranged from 1:1 to 2.7:1. For the P1-Linker-P3-EDTA:Fe compounds, binding orientation preferences were pronounced at Site A, where they were approximately 10:1. At the other sites orientation preferences for these molecules ranged from 1.1:1 to 2.4:1. E_{rel} values were calculated by dividing the total amount of cleavage produced by a given compound at Sites A, B, C, and D by the total amount of cleavage produced by **P5E:Fe** at Site A, then correcting for differences in the

Orientation Preference

<u>Compound</u>	<u>Site A</u>	<u>Site B</u>	<u>Site C</u>
P5E:Fe	1:4.4	1.7:1	1:5.7
BNSE:Fe	1.7:1	1:2.0	1:1
BN-(S,S)-Tar-E:Fe	1.7:1	1:2.1	1.1:1
BN-(R,R)-Tar-E:Fe	1.2:1	1:1.7	1:1.1
BN-(RS,SR)-Tar-E:Fe	1.5:1	1:1.9	1:1
BN-2-(S)-Mal-E:Fe	2.6:1	1:2.7	1.9:1
BN-2-(R)-Mal-E:Fe	1.8:1	1:2.3	1:1
BN-2-DMAsp-E:Fe	1.6:1	1:1.6	1:1.2
BN-3-DMAsp-E:Fe	1.6:1	1:1.6	1:1
P1-S-P3-E:Fe	9.7:1	1:1.6	1:1.1
P1-(S,S)-Tar-P3-E:Fe	13.7:1	1:2.4	2.3:1
P1-(R,R)-Tar-P3-E:Fe	8.5:1	-----	-----

Relative DNA Binding/Cleaving Efficiency (E_{rel})

<u>Compound</u>	<u>Site A</u>	<u>Site B</u>	<u>Site C</u>	<u>Site D</u>
P5E:Fe	1.0	0.18	0.97	-----
BNSE:Fe	1.5	0.70	1.5	0.31
BN-(S,S)-Tar-E:Fe	0.04	0.03	0.03	0.01
BN-(R,R)-Tar-E:Fe	0.003	0.002	0.004	0.002
BN-(RS,SR)-Tar-E:Fe	0.02	0.01	0.01	0.006
BN-2-(S)-Mal-E:Fe	0.70	0.37	0.65	0.19
BN-2-(R)-Mal-E:Fe	0.30	0.14	0.29	0.16
BN-2-DMAsp-E:Fe	0.05	0.02	0.03	0.01
BN-3-DMAsp-E:Fe	0.11	0.04	0.07	0.02
P1-S-P3-E:Fe	1.7	0.56	1.09	1.6
P1-(S,S)-Tar-P3-E:Fe	0.04	0.04	0.02	0.04
P1-(R,R)-Tar-P3-E:Fe	0.03	-----	-----	-----

concentration of the compounds. At Site A, E_{rel} values range from 1.7 to 0.003 and decrease in the order BNSE:Fe, P1-S-P3-E:Fe > P5E:Fe > BN-2-(S)-Mal-E:Fe > BN-2-(R)-Mal-E:Fe > BN-3-DMAsp-E:Fe > BN-2-DMAsp-E:Fe, BN-(S,S)-Tar-E:Fe, P1-(S,S)-Tar-E:Fe > BN-(RS,SR)-Tar-E:Fe, P1-(R,R)-P3-E:Fe > BN-(R,R)-Tar-E:Fe > BN-(R,R)-TarAc-E:Fe, BN-(S,S)-TarAc-E:Fe, BN-(RS,SR)-TarAc-E:Fe, BN-(S)-AE:Fe, BN-(R)-AE:Fe. At Site B, E_{rel} values range from 0.70 to 0.002 and decrease in the order BNSE:Fe, P1-S-P3-E:Fe > BN-2-(S)-Mal-E:Fe > P5E:Fe, BN-2-(R)-Mal-E:Fe > BN-3-DMAsp-E:Fe, BN-(S,S)-Tar-E:Fe, P1-(S,S)-Tar-E:Fe > BN-2-DMAsp-E:Fe > BN-(RS,SR)-Tar-E:Fe > BN-(R,R)-Tar-E:Fe > BN-(R,R)-TarAc-E:Fe, BN-(S,S)-TarAc-E:Fe, BN-(RS,SR)-TarAc-E:Fe, BN-(S)-AE:Fe, BN-(R)-AE:Fe. At Site C, E_{rel} values range from 1.5 to 0.004 and decrease in the order BNSE:Fe > P1-S-P3-E:Fe, P5E:Fe > BN-2-(S)-Mal-E:Fe > BN-2-(R)-Mal-E:Fe > BN-3-DMAsp-E:Fe > BN-2-DMAsp-E:Fe, BN-(S,S)-Tar-E:Fe, P1-(S,S)-Tar-E:Fe > BN-(RS,SR)-Tar-E:Fe > BN-(R,R)-Tar-E:Fe > BN-(R,R)-TarAc-E:Fe, BN-(S,S)-TarAc-E:Fe, BN-(RS,SR)-TarAc-E:Fe, BN-(S)-AE:Fe, BN-(R)-AE:Fe. At Site D, E_{rel} values range from 1.6 to 0.002 and decrease in the order P1-S-P3-E:Fe > BNSE:Fe > BN-2-(S)-Mal-E:Fe > BN-2-(R)-Mal-E:Fe > P1-(S,S)-Tar-E:Fe > BN-3-DMAsp-E:Fe, BN-2-DMAsp-E:Fe, BN-(S,S)-Tar-E:Fe > BN-(RS,SR)-Tar-E:Fe > BN-(R,R)-Tar-E:Fe > BN-(R,R)-TarAc-E:Fe, BN-(S,S)-TarAc-E:Fe, BN-(RS,SR)-TarAc-E:Fe, BN-(S)-AE:Fe, BN-(R)-AE:Fe.

Discussion

Chiral dimers of Netropsin linked in tail-to-tail or head-to-tail fashion by chiral diacids or amino acids have been synthesized by extension of the general procedures described in Chapter One. However, the implementation of these procedures led to partial

racemization of **BN-(R,R)-Tar-E** and **BN-(S,S)-Tar-E**, and complete racemization of Bis(Netropsin)-Dimethylaminoaspartamide-EDTA compounds. Racemization of **BN-(R,R)-Tar-E** or **BN-(S,S)-Tar-E** might be avoided by hydrolysis of the penultimate EDTA triester intermediates under milder conditions. The step(s) at which racemization occurred during the preparation of Bis(Netropsin)-dimethylaminoaspartamide-EDTA compounds was (were) not determined. Racemization by these compounds may be related to the propensity of aspartyl residues in peptides to racemize.³⁰

Several patterns emerge from the DNA binding/cleaving properties of these molecules. First, Bis(Netropsin)-Succinamide-EDTA:Fe derivatives substituted with one hydroxyl substituent bind and cleave DNA more efficiently than derivatives substituted with one dimethylamino substituent, which bind and cleave DNA more efficiently than derivatives substituted with two hydroxyl substituents, which in turn bind and cleave DNA more efficiently than acetonide-substituted derivatives, which do not exhibit DNA binding/cleaving activity. Neither enantiomer of Bis(Netropsin)-Alanine-EDTA:Fe exhibits DNA binding/cleaving activity, while Bis(Netropsin)-Glycine-EDTA does bind and cleave DNA. Thus, progressively increasing the steric bulk of Bis(Netropsin)s by progressively increasing the size or number of substituents on their linkers leads to progressive decreases in their DNA binding/cleaving efficiency. Second, Bis(Netropsin)-Malicamide-EDTA:Fe compounds exhibit somewhat higher orientation preferences than either the Bis(Netropsin)-Tartaramide-EDTA:Fe compounds or Bis(Netropsin)-Dimethylaminoaspartamide-EDTA:Fe compounds. Thus, increasing the steric bulk of Bis(Netropsin)s by increasing the number or size of substituents on their linkers leads to a decrease in DNA binding orientation preference. Third, **BNSE:Fe** and **P1-S-P3-E:Fe** exhibit somewhat greater site selectivity than the Bis(Netropsin)-Malicamide-EDTA:Fe compounds, which exhibit greater site selectivity than the Bis(Netropsin)-Tartaramide-EDTA:Fe or P1-Tartaramide-P3-EDTA:Fe compounds. Thus, increasing the steric bulk of Bis(Netropsin)s or P1-Linker-

P3-EDTA:Fe compounds by increasing the number of hydroxyl substituents on their linkers leads to decreases in observed site selectivity.

To summarize, DNA binding/cleaving efficiency, DNA binding orientation preference, and DNA binding site selectivity are all inversely related to the steric bulk of these molecules. These inverse relationships are consistent with a model in which substituents on succinamide or glycine linkers clash with a narrow minor groove. Support for this model comes from crystal structures of d(CGCGAATTCGCG)₂ and its complex with Netropsin, which show that the minor groove of the DNA dodecamer is forced open by 0.5-2.0 Å upon binding of the antibiotic.^{31,32} Appending substituents of increasing steric bulk onto a Bis(Netropsin) framework would be expected to increase unfavorable steric interactions progressively, thereby decreasing the ability of the molecules to penetrate deeply within the minor groove and form hydrogen-bonds, dipolar interactions, and van der Waals contacts, which determine binding affinity, sequence specificity, and orientation preference.

The strong binding orientation preferences observed with P1-Linker-P3-EDTA:Fe compounds at Site A are consistent with the observed preference of oligo(N-methylpyrrolecarboxamide)s to bind with their N-termini at the 3' end of a run of Ts (Chapter One, Figure 1.24).²⁹

In terms of enantiospecificity, the data clearly indicate that for Bis(Netropsin)-Succinamide-EDTA or P1-Succinamide-P3-EDTA derivatives bearing hydroxyl substituents, molecules of (S)- or (S,S) configuration bind and cleave DNA more efficiently than their enantiomeric counterparts of (R)- or (R,R) configuration. The difference is the most pronounced for **BN-(S,S)-Tar-E** versus **BN-(R,R)-Tar-E**. Considering that some degree of racemization has probably occurred during the preparation of these two molecules, the observed level of binding enantiospecificity represents only a lower boundary to the extent to which the pure (S,S)- and (R,R)- enantiomers are discriminated upon binding in the minor groove of B DNA.

Crystal structures of malic and tartaric acid derivatives reveal that (*S*)- or (*S,S*)-enantiomers are twisted in a right-handed sense, while (*R*)- or (*R,R*)-enantiomers are twisted in a left-handed sense (Figure 2.31).³³⁻³⁶ NMR and VCD studies suggest that the solid-state conformations of malic and tartaric acid derivatives that give rise to their handedness are also the ground state conformations in nonpolar and aqueous solutions.^{37,38} In light of these results, and the findings that Netropsin and Distamycin A assume right-handed helical structures when bound in the minor groove of B DNA,^{31,32} it seems reasonable that Bis(Netropsin)s and P1-Linker-P3 compounds linked by (*S*)-malic acid or (*S,S*)-tartaric acid would better match the right-handed twist of B DNA than the left-handed twist of Bis(Netropsin)s or P1-Linker-P3 compounds linked by (*R*)-malic acid or (*R,R*)-tartaric acid. Overall, these results indicate that *similar helical screw sense recognition* is preferred to *opposite or complementary helical screw sense recognition* for the binding of small molecules in the minor groove of B DNA.³⁹ This principle has recently been formulated in different terms based on modelling studies of the interactions of various small molecules with the DNA minor groove.⁴⁰

Crystal structures of several protein:DNA complexes have shown that DNA binding sequence specificity is mediated by contacts formed by right-handed α -helices in the major groove of B DNA.⁴¹⁻⁴⁴ Similar interactions are predicted for the sequence-specific recognition of DNA by proteins of the "leucine zipper" family.^{45,46} Hence, it appears that similar helical screw sense recognition is a general motif for DNA:groove binding ligand interactions. This finding is seemingly at odds with the suggestion by Barton³ that intercalative binding by octahedral metal complexes is favored by what has been defined in this chapter as similar helical screw sense recognition, while surface or groove binding by these complexes is favored by opposite or complementary helical screw sense recognition.³ Realizing that it is the *groove bound* parts of intercalated tris(1,10-phenanthroline) metal complexes that determine binding enantiospecificity, the results for the major groove intercalating/groove binding complexes are in fact consistent with the principle of similar

Figure 2.31

CPK models of (R,R) - and (S,S) -tartaramide showing the inherent left-handed twist of the (R,R) -enantiomer and the inherent right-handed twist of the (S,S) -enantiomer. Top: Two views of (R,R) -tartaramide. Bottom: Two views of (S,S) -tartaramide.



helical screw sense recognition for groove bound DNA ligands. The structural details of DNA surface and/or groove binding modes for tris(1,10-phanthroline) metal complexes must be elucidated before Barton's suggestion that these interactions are favored by opposite or complementary helical screw sense recognition can be fully evaluated.

References

- ¹Dickerson, R.E.; *Sci. Amer.* **1983**, *249*, 94-111.
- ²Dickerson, R.E.; Drew, H.R.; Conner, B.N.; Wing, R.M.; Fratini, A.V.; Kopka, M.L. *Science* **1982**, *216*, 475-485.
- ³Barton, J.K. *Science* **1986**, *233*, 727-734.
- ⁴Kumar, C.V.; Barton, J.K.; Turro, N.J. *J. Am. Chem. Soc.* **1985**, *107*, 5518-5523.
- ⁵Barton, J.K.; Goldberg, J.M.; Kumar, C.V.; Turro, N.J. *J. Am. Chem. Soc.* **1986**, *108*, 2081-2088.
- ⁶Mei, H.-Y.; Barton, J.K. *Proc. Natl. Acad. Sci. USA* **1988**, *85*, 1339-1343.
- ⁷Barton, J.K.; Raphael, A.L. *Proc. Natl. Acad. Sci. USA* **1985**, *82*, 6460-6464.
- ⁸Kirshenbaum, M.R.; Tribolet, R.; Barton, J.K. *Nucleic Acids Res.* **1988**, *16*, 7943-7960.
- ⁹Martin, D.G.; Chidester, C.G.; DuChamp, D.J.; Mizesak, S.A. *J. Antibiot.* **1980**, *33*, 902-903.
- ¹⁰Reynolds, V.L.; Molineux, I.J.; Kaplan, D.J.; Swenson, D.H.; Hurley, L.H. *Biochemistry* **1985**, *24*, 6228-6237.
- ¹¹Reardon, D.B.; Bigger, C.A.H.; Strandberg, J.; Yagi, H.; Jerina, D.M.; Dipple, A. *Chem. Res. Toxicol.* **1989**, *2*, 12-14.
- ¹²Plumbridge, T.W.; Brown, J.R. *Biochim. Biophys. Acta* **1979**, *563*, 181-192.
- ¹³Arlandini, E.; Vigevani, A.; Arcamone, F. *Il Farmaco Ed. Sci.* **1977**, *32*, 315-323.
- ¹⁴Quigley, G.; Wang, A.; Ughetto, G.; van Boom, J.; Rich, A. *Proc. Natl. Acad. Sci. USA* **1980**, *77*, 7204-7208.
- ¹⁵Wang, A.H.-J.; Ughetto, G.; Quigley, G.J.; Rich, A. *J. Biomol. Struct. Dynam.* **1986**, *4*, 319-342.
- ¹⁶Takusagawa, F.; Dabrow, M.; Neidle, S.; Berman, H.M. *Nature* **1982**, *296*, 466-469.
- ¹⁷Myers, A.G.; Proteau, P.J.; Handel, T.M. *J. Am. Chem. Soc.* **1988**, *110*, 7212-7214.
- ¹⁸Ward, D.C.; Reich, E.; Goldberg, I.H. *Science* **1965**, *149*, 1259-1263.
- ¹⁹Lee, M.D.; Dunne, T.S.; Siegel, M.M.; Chang, C.C.; Morton, G.O.; Borders, D.B. *J. Am. Chem. Soc.* **1987**, *109*, 3464-3466.

²⁰Lee, M.D.; Dunne, T.S.; Chang, C.C.; Ellestad, G.A.; Siegel, M.M.; Morton, G.O.; McGahren, W.J.; Borders, D.B. *J. Am. Chem. Soc.* **1987**, *109*, 3466-3468.

²¹Golik, J.; Clardy, J.; Dubay, G.; Groenewold, G.; Kawaguchi, H.; Konishi, M.; Krishnan, B.; Ohkuma, H.; Saitoh, K.; Doyle, T.W. *J. Am. Chem. Soc.* **1987**, *109*, 3461-3462.

²²Stubbe, J.; Kozarich, J.W. *Chem. Rev.* **1987**, *87*, 1107-1136, and references therein.

²³Lee, J.S.; Waring, M.J. *Biochem. J.* **1978**, *173*, 129-144.

²⁴Fox, K.R.; Olsen, R.K.; Waring, M.J. *Br. J. Pharmac.* **1980**, *70*, 25-40.

²⁵Taylor, J.S.; Schultz, P.G.; Dervan, P.B. *Tetrahedron* **1984**, *40*, 457-465.

²⁶Musich, J.A.; Rapoport, H. *J. Am. Chem. Soc.* **1978**, *100*, 4865-4872.

²⁷Holy, A. *Coll. Czech. Chem. Commun.* **1979**, *44*, 593-612.

²⁸Bowman, R.E.; Stroud, H.H. *J. Chem. Soc.* **1950**, 1342-1345

²⁹Youngquist, R.S., Ph.D. Thesis, California Institute of Technology, Pasadena, California, 1988.

³⁰Racemization-get

³¹Kopka, M.L.; Yoon, C.; Goodsell, D.; Pjura, P.; Dickerson, R.E. *Proc. Natl. Acad. Sci. USA* **1985**, *82*, 1376-1380.

³²Kopka, M.L.; Yoon, C.; Goodsell, D.; Pjura, P.; Dickerson, R.E. *J. Mol. Biol.* **1985**, *183*, 553-563.

³³Parry, G.S. *Acta Crystallogr.* **1951**, *4*, 131-138.

³⁴Okaya, Y.; Stemple, N.R.; Kay, M.I. *Acta Crystallogr.* **1966**, *21*, 237-243.

³⁵van Bommel, A.J.; Bijvoet, J.M. *Acta Crystallogr.* **1958**, *11*, 61-70.

³⁶Van Loock, J.F.J.; Van Havere, W.; Lenstra, A.T.H. *Bull. Soc. Chim. Belg.* **1981**, *90*, 161-166.

³⁷Ascenso, J.; Gil, V.M.S. *Can. J. Chem.* **1980**, *58*, 1376-1379.

³⁸Su, C.N.; Keiderling, T.A. *J. Am. Chem. Soc.* **1980**, *102*, 511-512.

³⁹Griffin, J.H.; Dervan, P.B. *J. Am. Chem. Soc.* **1986**, *108*, 5008-5009.

⁴⁰Hawley, R.C.; Kiessling, L.L.; Schreiber, S.L. *Proc. Natl. Acad. Sci. USA* **1989**, *86*, 1105-1109.

⁴¹McClarin, J.A.; Frederick, B.C.; Wang, P.; Greene, H.; Boyer, J.; Grable, J.; Rosenberg, J. *Science* **1986**, 234, 1526-1541.

⁴²Aggarwal, A.K.; Rodgers, D.W.; Drottar, M.; Ptashne, M.; Harrison, S.C. *Science* **1988**, 242, 899-907.

⁴³Jordan, S.R.; Pabo, C.O. *Science* **1988**, 242, 893-899.

⁴⁴Otwinowski, Z.; Schevitz, R.W.; Zhang, R.-G.; Lawson, C.L.; Joachimiak, A.; Marmorstein, R.Q.; Luisi, B.F.; Sigler, P.B. *Nature* **1988**, 335, 321-329.

⁴⁵Landschulz, W.H.; Johnson, P.F.; McKnight, S.L. *Science* **1988**, 240, 1759-1764.

⁴⁶Landschulz, W.H.; Johnson, P.F.; McKnight, S.L. *Science* **1989**, 243, 1681-1688.

CHAPTER THREE: METAL-REGULATED DNA BINDING/CLEAVING MOLECULES

Introduction

Environmental signals such as temperature, the presence of specific organic molecules, or the presence of specific inorganic ions can exert remarkable effects on gene expression at the level of DNA transcription.¹ DNA transcription factor or repressor proteins can be the primary receptors of environmental signals, which induce changes in the sequence-specific DNA binding properties of the receptor proteins, leading to altered levels of transcription of specific genes.²⁻⁹ Three distinct forms of *metalloregulatory* protein:DNA interactions have been described.⁵⁻⁹ Neilands and coworkers have studied the mechanism by which siderophore-mediated iron assimilation in microbes is regulated. They identified, cloned, purified, and characterized the ferric uptake regulation (fur) protein. In the presence of manganous or ferrous ions, fur binds as a dimer within promoter regions for genes involved in iron uptake and represses transcription of these genes.⁶ The fur protein may be considered to be *positively metalloregulated* in that metals increase its ability to bind to DNA. Preliminary results from Hamer and coworkers indicate that a protein binding in control regions for yeast metallothionein genes may be *negatively metalloregulated* in that its DNA footprints are lost upon incubation with cupric ions.⁷ Walsh, Summers, and others have studied the molecular basis of mercuric ion resistance in prokaryotes.^{10,11} O'Halloran and Walsh identified, cloned, purified, and characterized the merR protein, which regulates transcription of the mer operon involved in mercuric ion detoxification.⁸ Through detailed studies of DNA binding, transcriptional repression, and transcriptional activation by merR, O'Halloran and coworkers have recently described the novel mode by which merR regulates DNA transcription.⁹ In the absence of mercuric ions, merR binds as a dimer within promoter -35 to -10 sequences and represses transcription by

blocking the binding of RNA polymerase. Upon binding a single mercuric ion, the merR dimer undergoes a conformational change that slightly decreases its intrinsic DNA binding affinity but allows it to bind synergistically with RNA polymerase and form an open transcription complex at the promoter. Metal ions also have effects on the DNA binding activities of some naturally occurring small molecules. The aureolic acid antibiotics (such as Chromomycin A3, Figure 2.2) require divalent cations in order to bind to DNA.^{12,13} The antitumor antibiotic Bleomycin (Figure 1.4) binds to DNA in the absence of metal ions, but metal ions such as Fe^{2+} are required for DNA cleavage by Bleomycin.¹⁴

In light of metalloregulatory DNA binding phenomena found in natural systems, and given our experience with DNA binding/cleaving molecules regulated by *intrinsic* structural and stereochemical features (see Chapters One and Two), we became interested in the regulation of synthetic DNA binding molecules by *extrinsic* factors. This chapter describes the design, synthesis, and characterization of metal-regulated DNA binding/cleaving molecules.

Part 1: Positive Metalloregulation in the Sequence-Specific Binding of a Synthetic Small Molecule to DNA.

Results

Design. Metalloregulated DNA binding involves multiple equilibria, some of which are illustrated in Figure 3.1. In order to design a metalloregulated DNA binding molecule, one must design a proper balance among these and other equilibria. To simplify this task, our approach was to combine DNA binding subunits of known sequence specificity with metal-binding subunits of known metallospecificity. The result was a series of homologous Bis(Netropsin)s linked in tail-to-tail fashion by tetra-, penta-, or hexaether tethers (Figure 3.2). The Netropsin subunits are analogs of the naturally occurring antibiotic Netropsin, which binds to sites of four contiguous A:T base pairs in the minor groove of B DNA. The

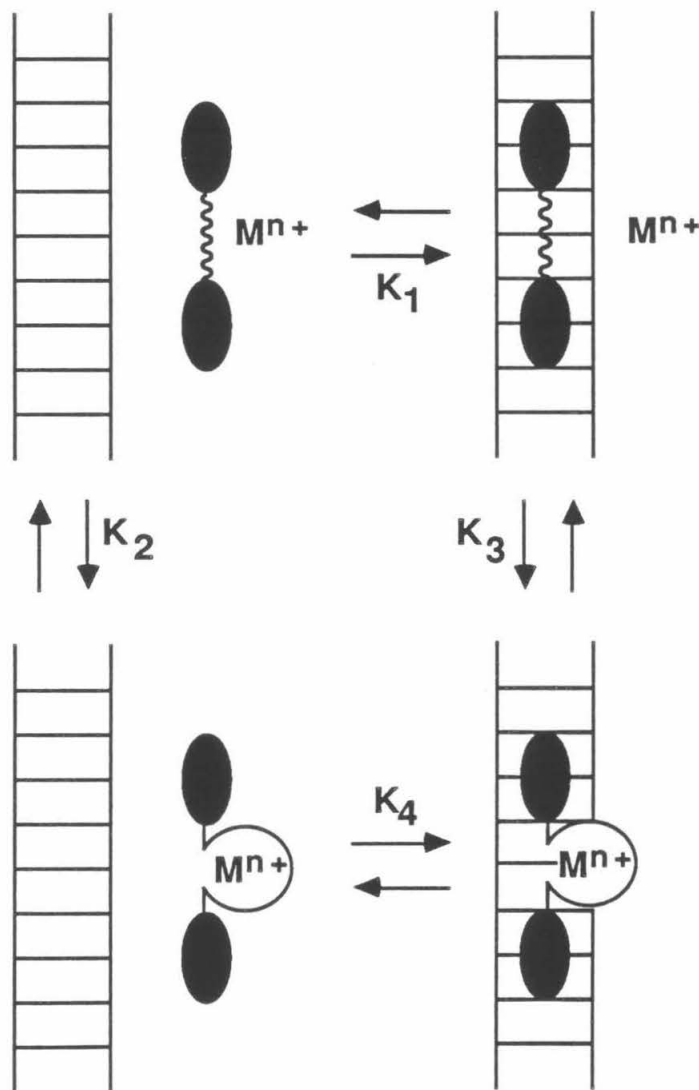


Figure 3.1. Some of the multiple equilibria associated with the metalloregulated binding of a molecule to DNA. K_1 : Binding of the molecule (connected black ovals) to DNA. K_2 : Binding of a metal ion (M^{n+}) to the molecule. K_3 : Binding of a metal ion to the molecule:DNA complex. K_4 : binding of the molecule:metal ion complex to DNA.

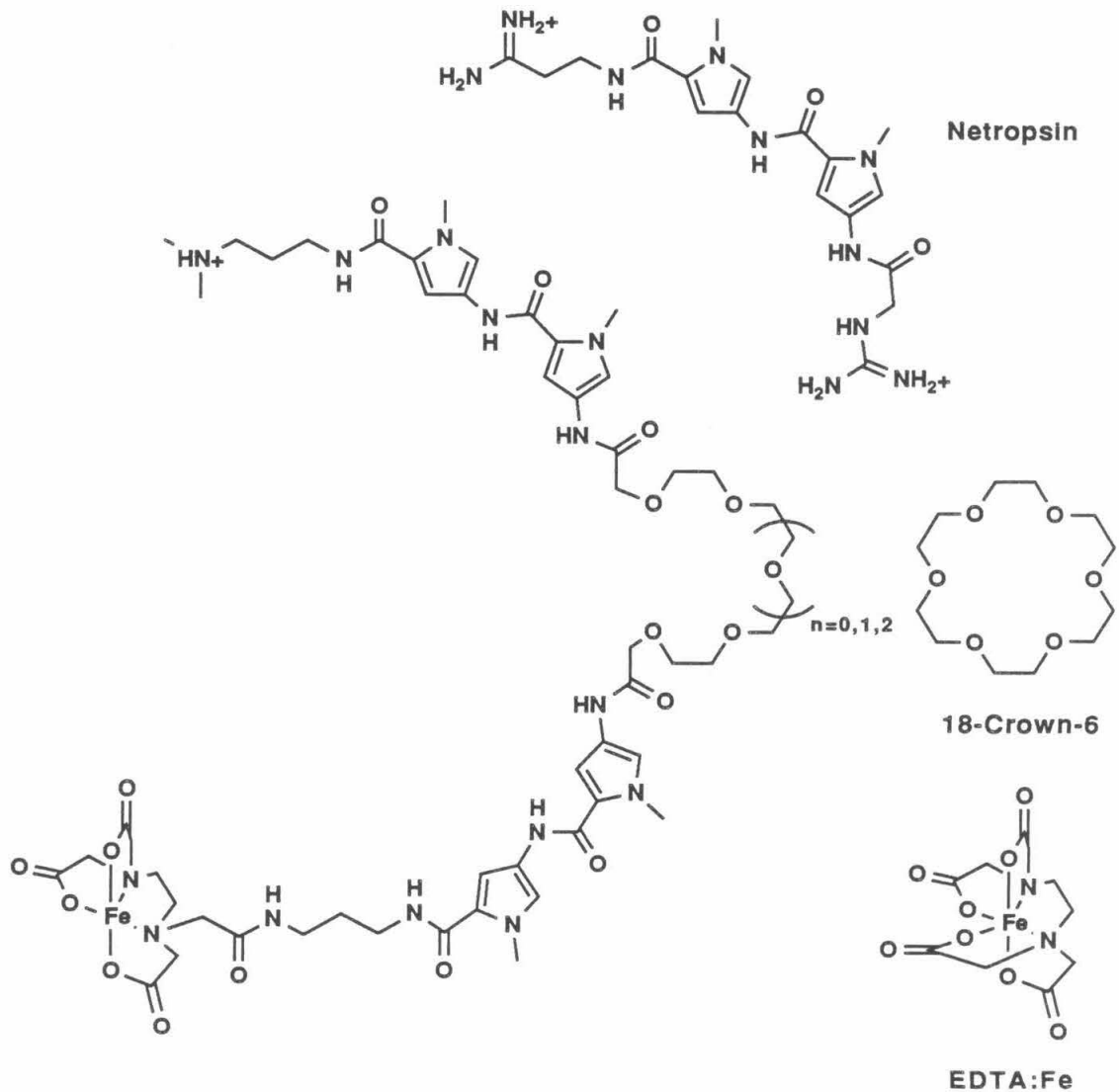


Figure 3.2. Design of metalloregulated DNA binding/cleaving small molecules containing Netropsin subunits, podand subunits, and EDTA:Fe subunits. $n = 0$, Bis(Netropsin)-3,6,9,12-Tetraoxatetradecanediamic-EDTA:Fe (**BNO4E:Fe**); $n = 1$, Bis(Netropsin)-3,6,9,12,15-Pentaoxaheptadecanediamic-EDTA:Fe (**BNO5E:Fe**); $n = 2$, Bis(Netropsin)-3,6,9,12,15,18-Hexaoxaecosanediamic-EDTA:Fe (**BNO6E:Fe**).

polyether tethers are multidentate acyclic neutral ligands for metal cations (podands),¹⁵ ring-opened forms of the crown ethers. The iron-chelating functionality EDTA was appended to one terminus of these molecules in order to determine their DNA binding properties by the technique of DNA affinity cleaving in the absence and presence of metal cations.¹⁶ We anticipated that there would be energetic benefits to filling the podands with specific metal cations, especially as part of a small molecule:metal cation:DNA ternary complex.

Synthesis. The synthesis of Bis(Netropsin)-EDTA compounds linked by polyether diacids is exemplified by the synthesis of **BNO5E** (**II-164**, Figure 3.3). This scheme is similar to the general procedure described in Chapter One for the synthesis of Bis(Netropsin) Diacid-EDTA compounds. The requisite linkers were prepared by condensation of the appropriate glycol with two equivalents of ethyl diazoacetate, followed by mono-hydrolysis. Thus, tetraethylene glycol afforded pentaether diacid, mono-ester **II-117**. **I-22** was reduced and coupled with one equivalent of **II-117** to produce an intermediate ester, which was hydrolyzed to afford Netropsin-3,6,9,12,15-pentaoxaheptadecanamic acid **II-121**. **IV-129** was reduced and coupled with **II-121** to afford Bis(Netropsin)-3,6,9,12,15-pentaoxaheptadecanediamide **II-126**. The terminal amino group of **II-126** was deprotected and coupled with the triethyl ester of EDTA. The EDTA ester groups were removed by hydrolysis to afford **BNO5E**.

DNA Affinity Cleaving. DNA affinity cleaving studies with the Bis(Netropsin) Polyether-EDTA compounds were carried out under conditions determined to be optimal for DNA binding/cleaving by oligo(*N*-methylpyrrolecarboxamide)-EDTA compounds.¹⁷ Figure 3.4 shows an autoradiograph of DNA double-strand cleavage patterns produced by these molecules on Sty I-linearized, 3'-³²P end-labeled pBR322 plasmid DNA. DNA cleavage products were separated by agarose gel electrophoresis and visualized by autoradiography. Bis(Netropsin) Polyether-EDTA:Fe compounds exhibit relatively weak DNA binding/cleaving, with DNA binding/cleaving efficiency (E_{rel}) decreasing in the

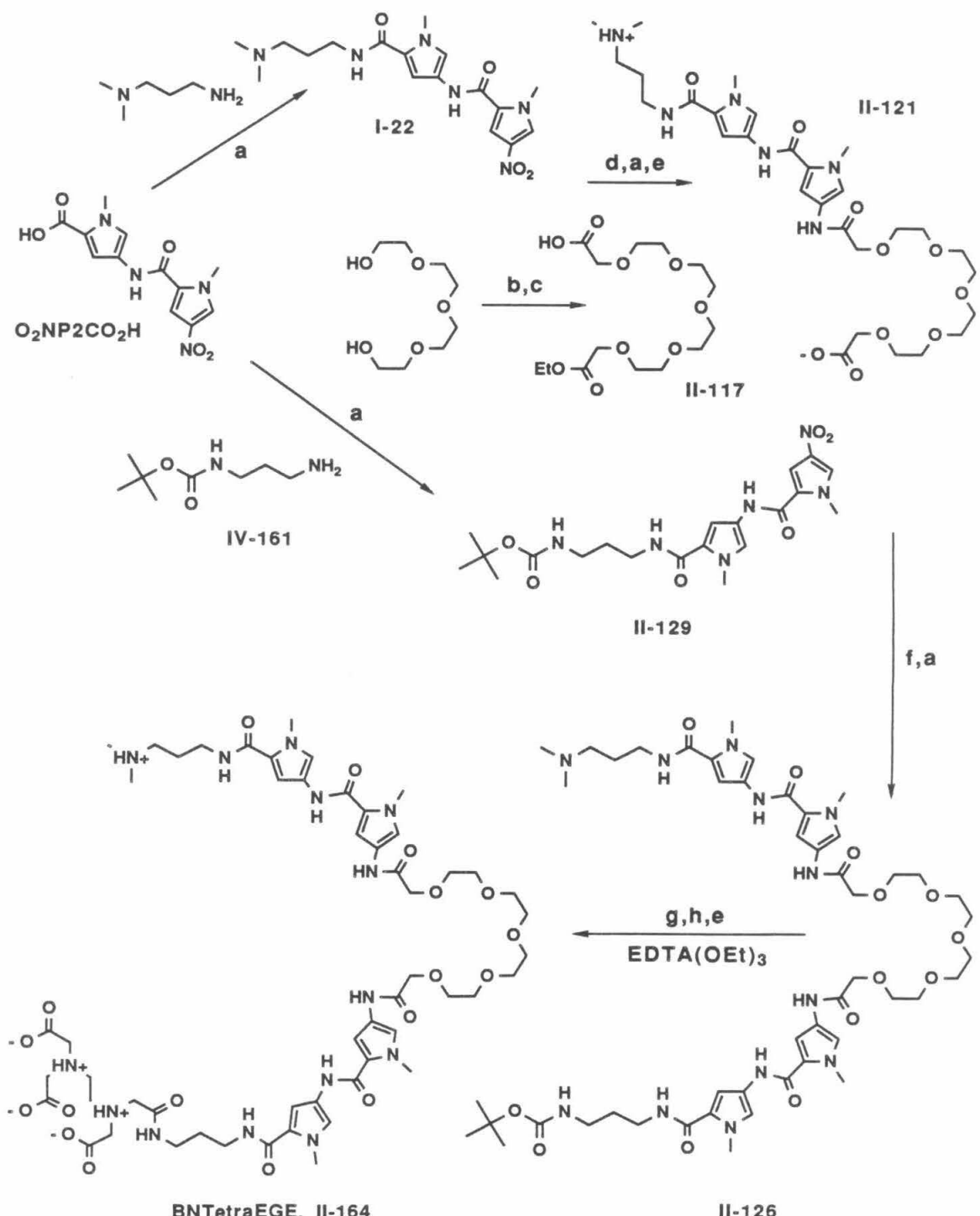
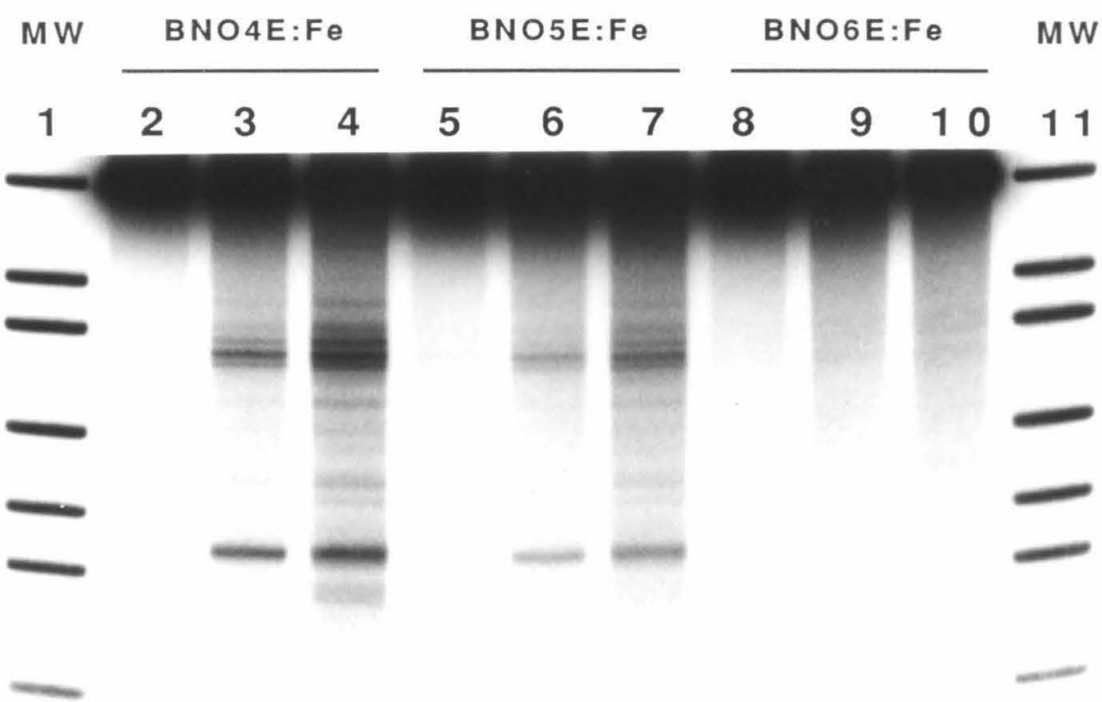


Figure 3.3. Scheme for the synthesis of BNO5E. Reaction conditions: **a**, DCC, HOBT, DMF; **b**, $\text{N}_2\text{CHCO}_2\text{Et}$ (2.5 equiv.), $\text{Rh}_2(\text{OAc})_4$ (0.01 equiv.), Et_2O ; **c**, LiOH (1.0 equiv.), MeOH, H_2O ; **d**, H_2 (1 atm), Pd/C, DMF; **e**, LiOH (excess), MeOH, H_2O ; **f**, H_2 (3 atm), Pd/C, DMF; **g**, TFA, CH_2Cl_2 ; **h**, EDTA(OEt)₃, CDI, DMF.

Figure 3.4

Autoradiograph of DNA double-strand cleavage patterns produced by Bis(Netropsin) Polyether-EDTA:Fe compounds on Sty I-linearized, 3'-³²P dATP end-labeled pBR322 plasmid DNA in the presence of dioxygen and dithiothreitol. Cleavage patterns were resolved by electrophoresis on a 1% agarose gel. Lanes 1 and 11, molecular weight markers consisting of pBR322 restriction fragments 4363, 3371, 2994, 2368, 1998, 1768, 1372, 995, and 666 bp in length; lanes 2-4, **BNO4E:Fe** at 5.0, 20, and 50 μ M concentrations; lanes 5-7, **BNO5E:Fe** at 5.0, 20, and 50 μ M concentrations; lanes 8-10, **BNO6E:Fe** at 5.0, 20, and 50 μ M concentrations.



order **BNO4E:Fe** > **BNO5E:Fe** > **BNO6E:Fe**. For comparison, 0.10 μ M Bis(Netropsin)-Succinamide-EDTA:Fe (**BNSE:Fe**, Chapters One and Two) produces cleavage comparable to that observed with 50 μ M **BNO4E:Fe**. Similar experiments carried out with **BNO4E:Fe** and **BNO6E:Fe** in the presence of 1 mM Li⁺, Na⁺, K⁺, Rb⁺, Cs⁺, Mg²⁺, Ca²⁺, Sr²⁺, Ba²⁺, NH₄⁺, Ni²⁺, Hg²⁺, Cd²⁺, Ag⁺ (Figure 3.5, Panels A and C), Tl⁺, Tl³⁺, Co²⁺, Cu²⁺, Zn²⁺, Fe²⁺, Fe³⁺, Pb²⁺, In³⁺, Au³⁺, Lu³⁺, Ho³⁺, Eu³⁺, Bi³⁺, La³⁺, Ce³⁺, or Ce⁴⁺ (not shown) indicate that the DNA binding properties of these molecules are not significantly affected by these cations at 1 mM concentration. Similar experiments performed with **BNO5E:Fe** in the presence of most of these cations also afforded no changes in DNA binding properties. However, addition of 1 mM strontium or, more effectively, barium cations produces strongly enhanced DNA binding/cleaving by **BNO5E:Fe** (Figure 3.5, Panel B).

That strontium or barium did not enhance DNA binding/cleaving by **BNO4E:Fe** or **BNO6E:Fe** suggests that these metals do not enhance DNA binding/cleaving by Netropsin derivatives in general. To determine the effects that various cations have on DNA affinity cleaving by a small molecule that does not have a polyether ionophore, an extensive series of control experiments was carried out with penta(*N*-methylpyrrolecarboxamide)-EDTA:Fe (**P5E:Fe**, Figure 1.6).¹⁷ The cations studied are indicated in Figure 3.6. Autoradiographs of DNA double-strand cleavage patterns produced by the Fe(II) or Fe(III) chelates of **P5E** in the presence of dioxygen and dithiothreitol (DTT) or ascorbic acid (ASC) reductants, and with cations at 0.1 or 1 mM concentrations, are shown in Figures 3.7-3.15. Cations have one or more of several different effects on DNA affinity cleaving by **P5E:Fe**. Some cations have little, if any, effect on affinity cleaving (\pm), while other cations lead to reduced (R), little (L), or no (N) cleavage by **P5E:Fe**. Some cations cause changes in the mobility of the DNA (M), or changes in the cleavage patterns produced by **P5E:Fe** (C). Some cations cause the DNA to precipitate (P), while a few cations promote complete degradation of the DNA under

Figure 3.5

Autoradiographs of DNA double-strand cleavage patterns produced by Bis(Netropsin) Polyether-EDTA:Fe compounds on Sty I-linearized, 3'-³²P dATP end-labeled pBR322 plasmid DNA in the presence of dioxygen and dithiothreitol, and in the absence and presence of added cations. Cleavage patterns were resolved on 1% agarose gels. Panel A, **BNO4E:Fe** at 5.0 μ M concentration. Panel B, **BNO5E:Fe** at 5.0 μ M concentration. Panel C, **BNO6E:Fe** at 5.0 μ M concentration. Lanes 1 and 12, molecular weight markers consisting of pBR322 restriction fragments 4363, 3371, 2994, 2368, 1998, 1768, 1372, 995, and 666 bp in length; lanes 2 and 13, DNA double-strand cleavage in the absence of added cations; lanes 3-11 and 14-19, DNA double-strand cleavage in the presence of 1 mM concentrations of LiOAc, NaOAc, KOAc, RbOAc, CsOAc, Mg(OAc)₂, Ca(OAc)₂, Sr(NO₃)₂, Ba(OAc)₂, NH₄OAc, Ni(OAc)₂, Hg(OAc)₂, Cd(OAc)₂, AgOAc, and Ba(OAc)₂, respectively.

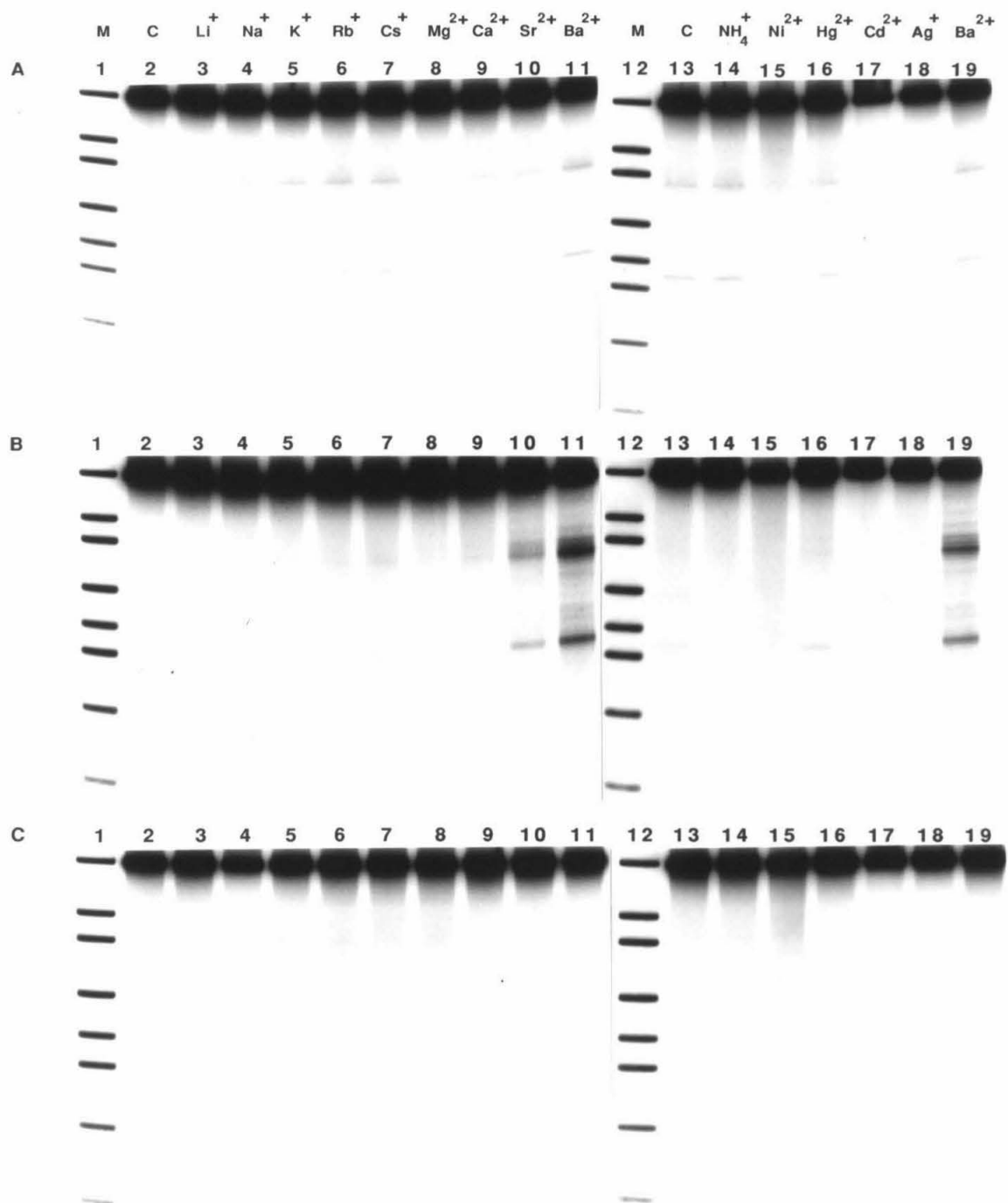
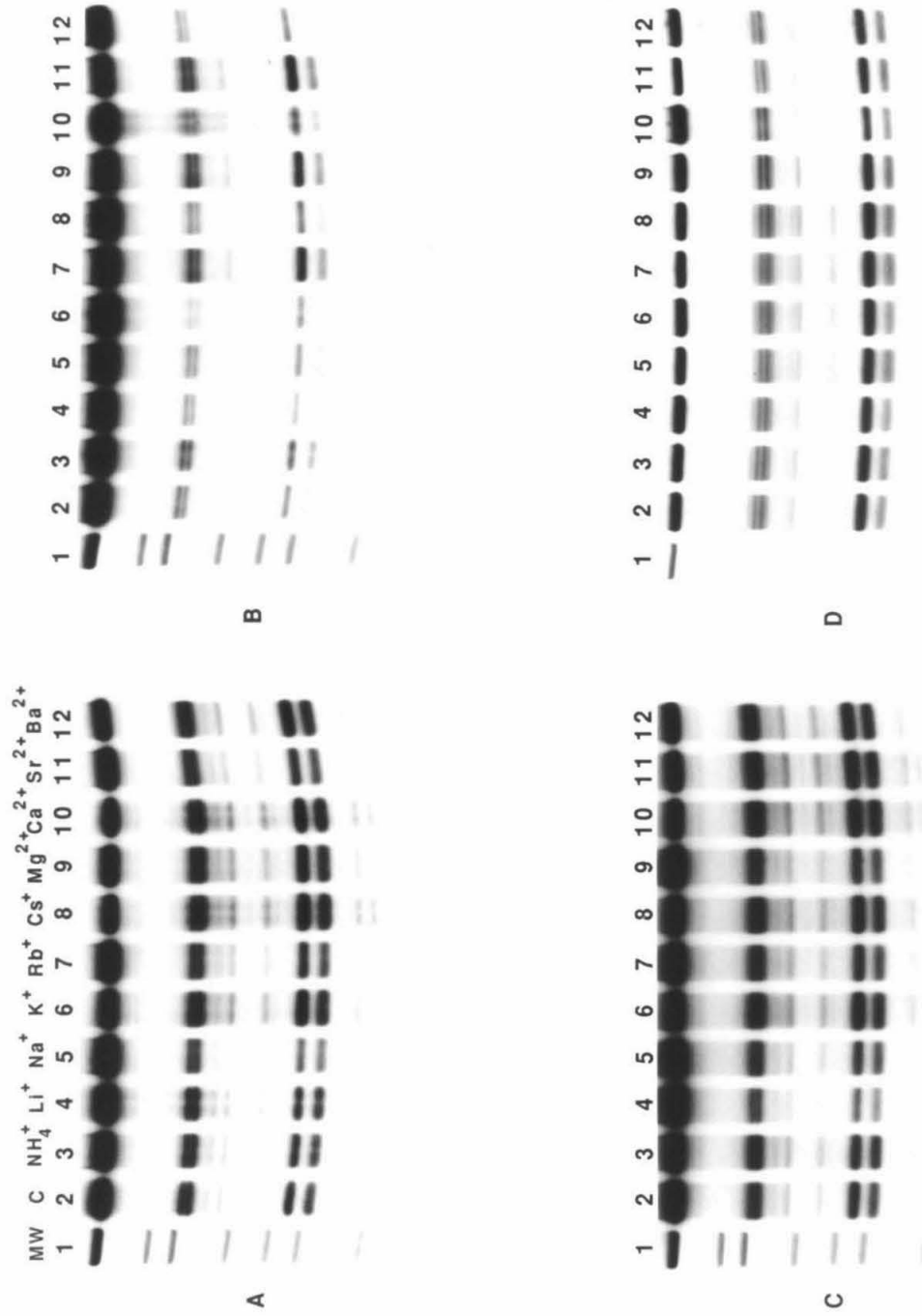


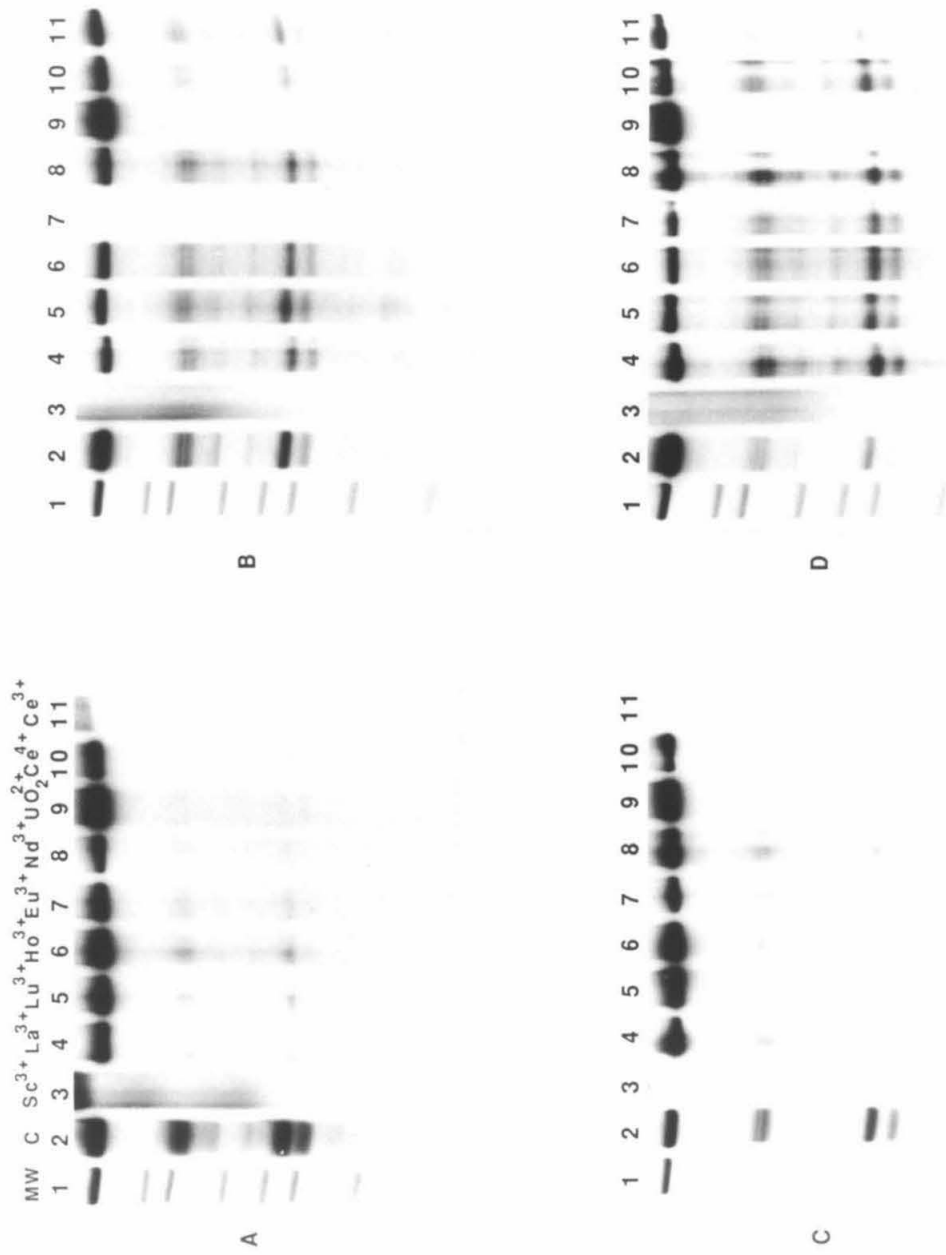
Figure 3.6

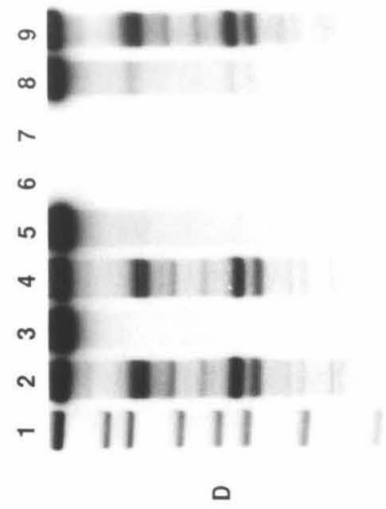
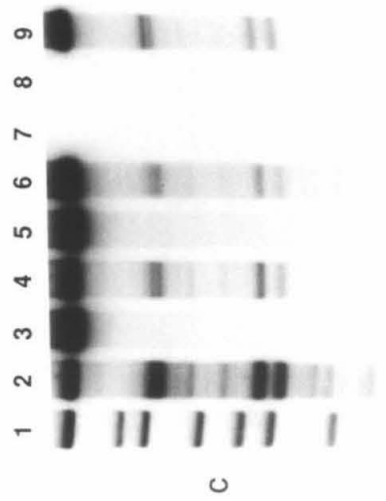
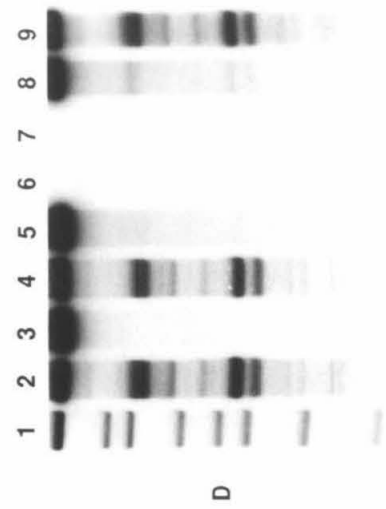
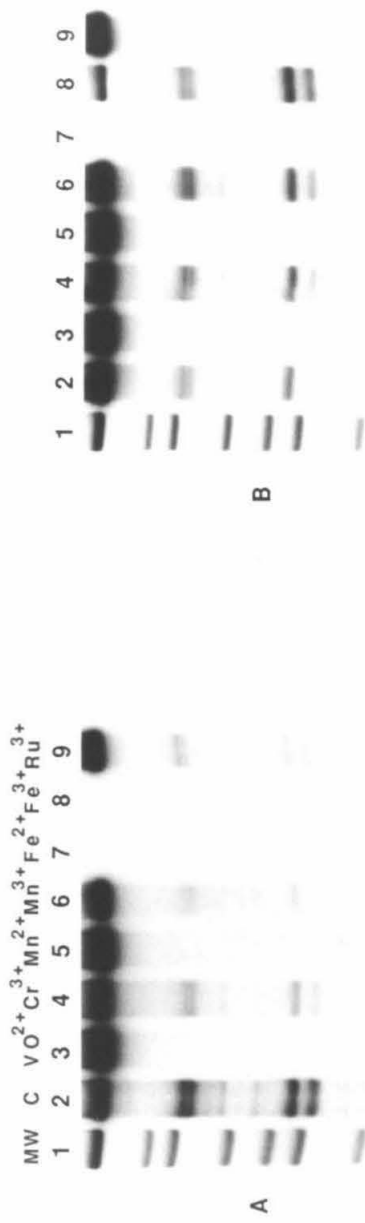
Periodic Table. Elements shown in bold type have been surveyed for their effects at 0.1 and 1.0 mM concentrations on DNA affinity cleaving by **P5E:Fe** at 0.75 μ M concentration.

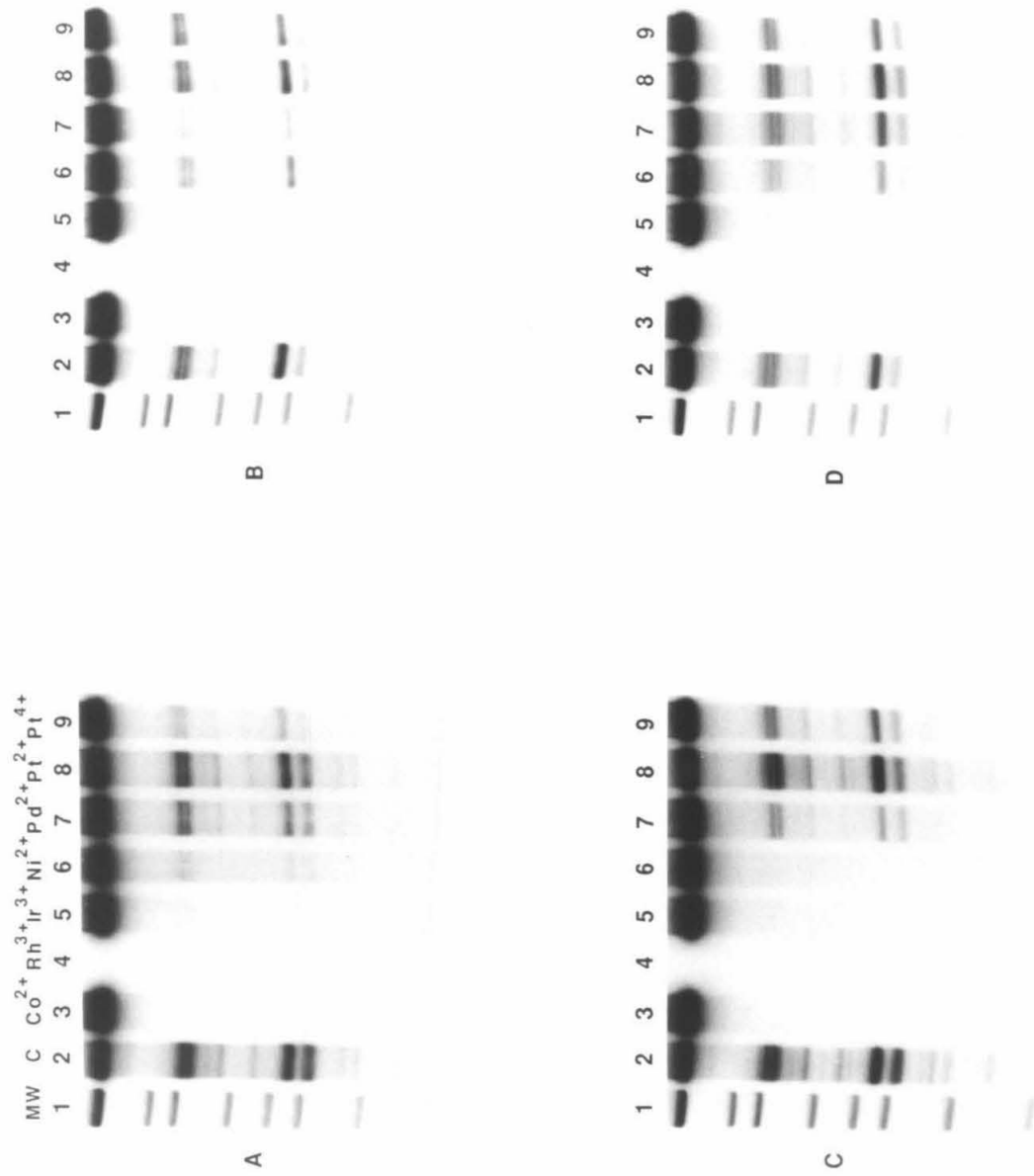
Figures 3.7-3.15

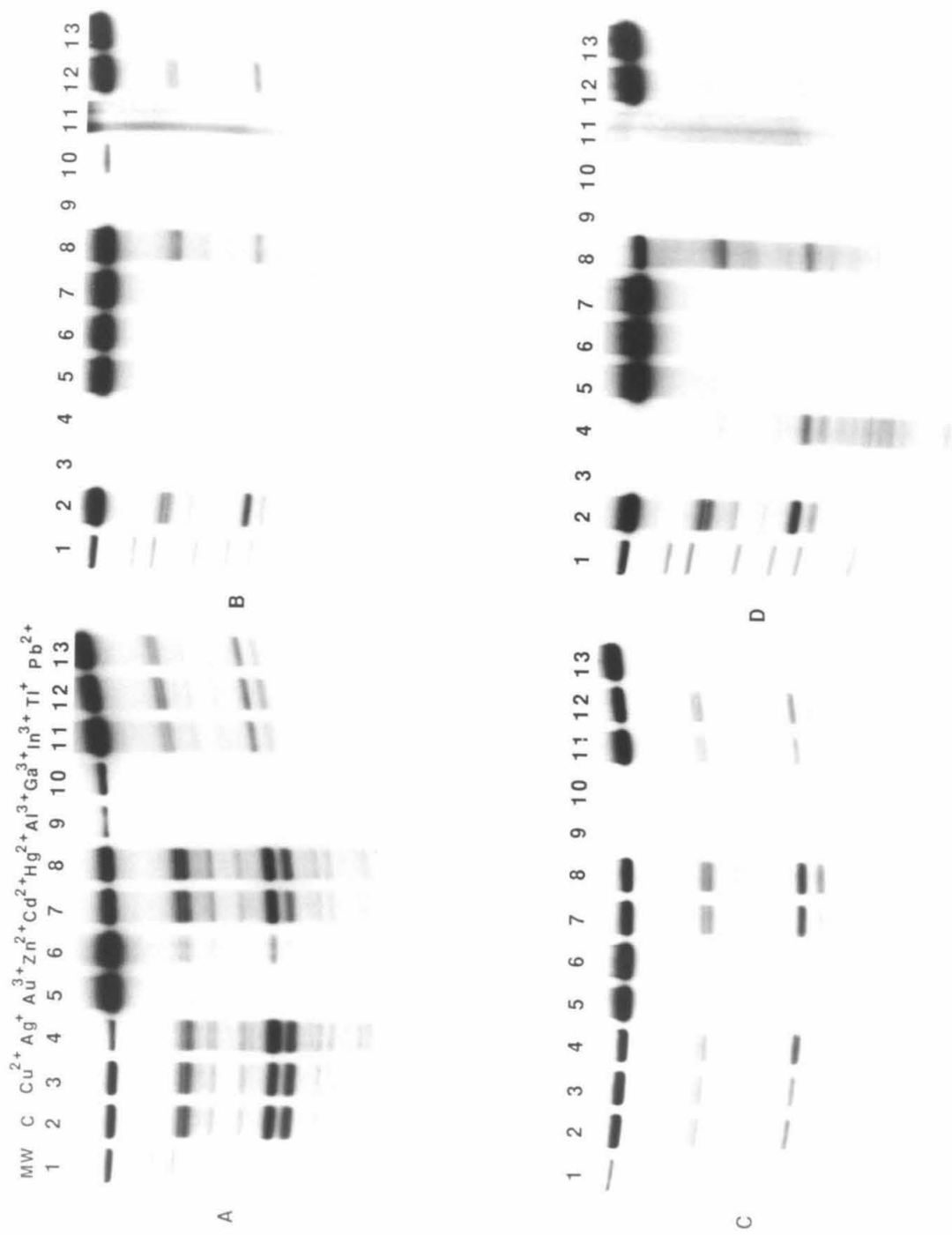
Autoradiographs of DNA double-strand cleavage patterns produced by **P5E:Fe(II)** or **P5E:Fe(III)** on Sty I-linearized, $3'$ - ^{32}P dATP end-labeled pBR322 plasmid DNA in the presence of dioxygen and dithiothreitol or ascorbic acid, and in the absence and presence of cations. Cleavage patterns were resolved on 1% agarose gels. **P5E:Fe** concentration was 0.75 μM . Figures 3.7-3.11 were with 1.0 mM added cations. Figures 3.12-3.15 were with 0.1 mM added cations. Panels A, cleavage by **P5E:Fe(II)** using dithiothreitol reductant. Panels B, cleavage by **P5E:Fe(II)** using ascorbic acid reductant. Panels C, cleavage by **P5E:Fe(III)** using dithiothreitol reductant. Panels D, cleavage by **P5E:Fe(III)** using ascorbic acid reductant. Lanes 1, molecular weight markers consisting of pBR322 restriction fragments 4363, 3371, 2994, 2368, 1998, 1768, 1372, 995, and 666 bp in length; lanes 2, cleavage by **P5E:Fe** in the absence of added cations. **Figure 3.7**, lanes 3-12, cleavage by **P5E:Fe** in the presence of 1 mM NH_4OAc , LiOAc , NaOAc , KOAc , CsOAc , $\text{Mg}(\text{OAc})_2$, $\text{Ca}(\text{OAc})_2$, $\text{Sr}(\text{NO}_3)_2$, and $\text{Ba}(\text{OAc})_2$, respectively. **Figure 3.8**, lanes 3-11, cleavage by **P5E:Fe** in the presence of 1 mM $\text{Sc}(\text{NO}_3)_3$, $\text{La}(\text{OAc})_3$, $\text{Lu}(\text{OAc})_3$, $\text{Ho}(\text{OAc})_3$, $\text{Eu}(\text{OAc})_3$, $\text{Nd}(\text{NO}_3)_3$, UO_2SO_4 , $(\text{NH}_4)_2\text{Ce}(\text{NO}_3)_6$, and $\text{Ce}(\text{NO}_3)_3$, respectively. **Figure 3.9**, panels A-C, lanes 3-9, cleavage by **P5E:Fe** in the presence of 1 mM $\text{VO}(\text{acac})_2$, CrCl_3 , MnSO_4 , $\text{Mn}(\text{OAc})_3$, $(\text{NH}_4)_2\text{Fe}(\text{SO}_4)_2$, $(\text{NH}_4)\text{Fe}(\text{SO}_4)_2$, and RuCl_3 , respectively. Panel D, cleavage by **P5E:Fe** in the presence of 1 mM $\text{VO}(\text{acac})_2$, CrCl_3 , MnSO_4 , $(\text{NH}_4)_2\text{Fe}(\text{SO}_4)_2$, $(\text{NH}_4)\text{Fe}(\text{SO}_4)_2$, RuCl_3 , and $\text{Mn}(\text{OAc})_3$, respectively. **Figure 3.10**, lanes 3-9, cleavage by **P5E:Fe** in the presence of 1 mM $\text{Co}(\text{OAc})_2$, $\text{Rh}(\text{NO}_3)_3$, IrCl_3 , $\text{Ni}(\text{OAc})_2$, K_2PdCl_4 , K_2PtCl_4 , and H_2PtCl_6 , respectively. **Figure 3.11**, lanes 3-13, cleavage by **P5E:Fe** in the presence of 1 mM $\text{Cu}(\text{OAc})_2$, AgNO_3 , AuCl_3 , $\text{Zn}(\text{OAc})_2$, $\text{Cd}(\text{OAc})_2$, $\text{Hg}(\text{OAc})_2$, $\text{Al}(\text{NO}_3)_3$, GaBr_3 , InCl_3 , Tl_2SO_4 , and $\text{Pb}(\text{OAc})_2$, respectively. **Figure 3.12**, lanes 3-11, cleavage by **P5E:Fe** in the presence of 0.1 mM $\text{Sc}(\text{NO}_3)_3$, $\text{La}(\text{OAc})_3$, $\text{Lu}(\text{OAc})_3$, $\text{Ho}(\text{OAc})_3$, $\text{Eu}(\text{OAc})_3$, $\text{Nd}(\text{NO}_3)_3$, UO_2SO_4 , $(\text{NH}_4)_2\text{Ce}(\text{NO}_3)_6$, and $\text{Ce}(\text{NO}_3)_3$, respectively. **Figure 3.13**, lanes 3-9, cleavage by **P5E:Fe** in the presence of 0.1 mM $\text{VO}(\text{acac})_2$, CrCl_3 , MnSO_4 , $\text{Mn}(\text{OAc})_3$, $(\text{NH}_4)_2\text{Fe}(\text{SO}_4)_2$, $(\text{NH}_4)\text{Fe}(\text{SO}_4)_2$, and RuCl_3 , respectively. **Figure 3.14**, lanes 3-9, cleavage by **P5E:Fe** in the presence of 0.1 mM $\text{Co}(\text{OAc})_2$, $\text{Rh}(\text{NO}_3)_3$, IrCl_3 , $\text{Ni}(\text{OAc})_2$, K_2PdCl_4 , K_2PtCl_4 , and H_2PtCl_6 , respectively. **Figure 3.15**, lanes 3-13, cleavage by **P5E:Fe** in the presence of 0.1 mM $\text{Cu}(\text{OAc})_2$, AgNO_3 , AuCl_3 , $\text{Zn}(\text{OAc})_2$, $\text{Cd}(\text{OAc})_2$, $\text{Hg}(\text{OAc})_2$, $\text{Al}(\text{NO}_3)_3$, GaBr_3 , InCl_3 , Tl_2SO_4 , and $\text{Pb}(\text{OAc})_2$, respectively.

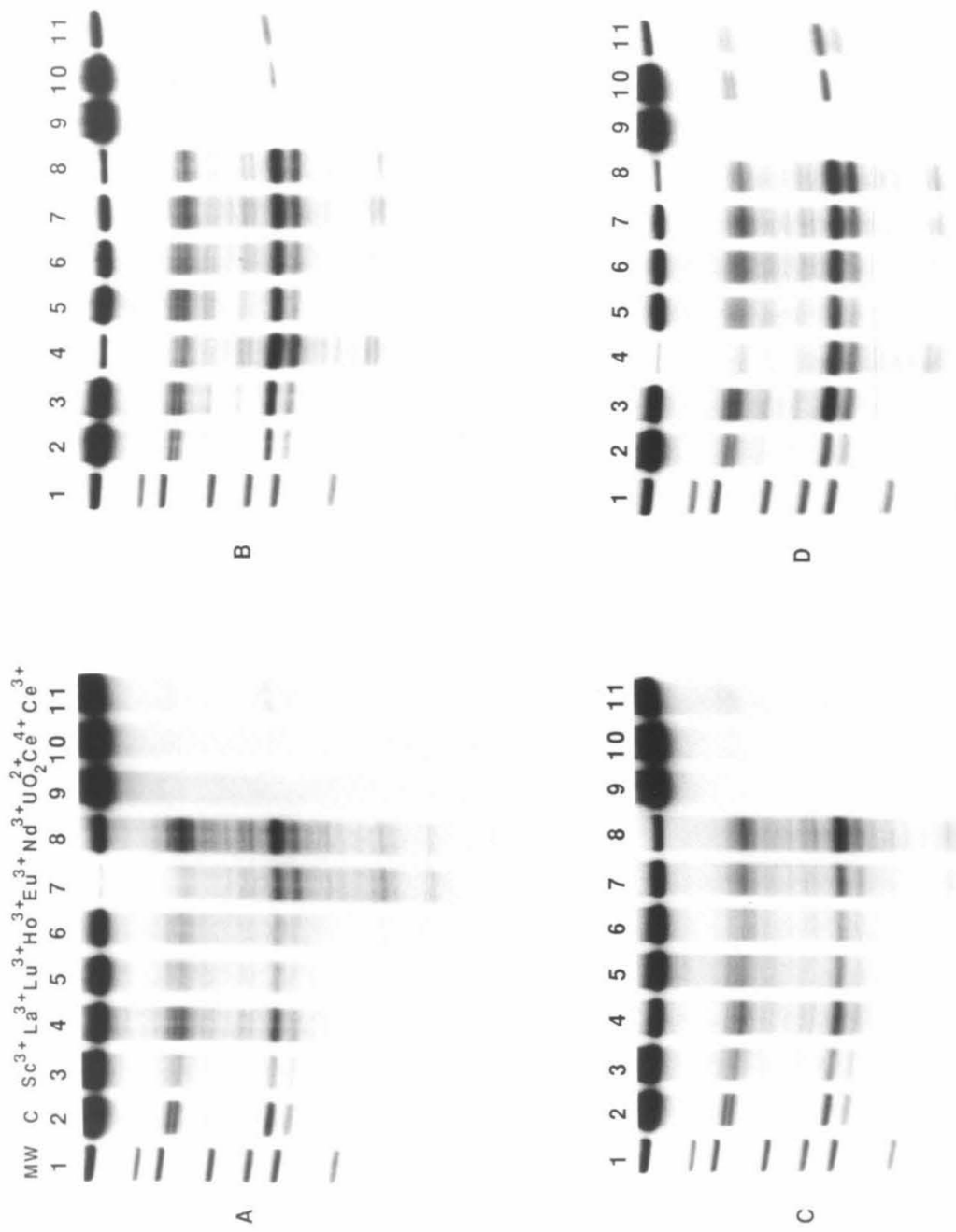


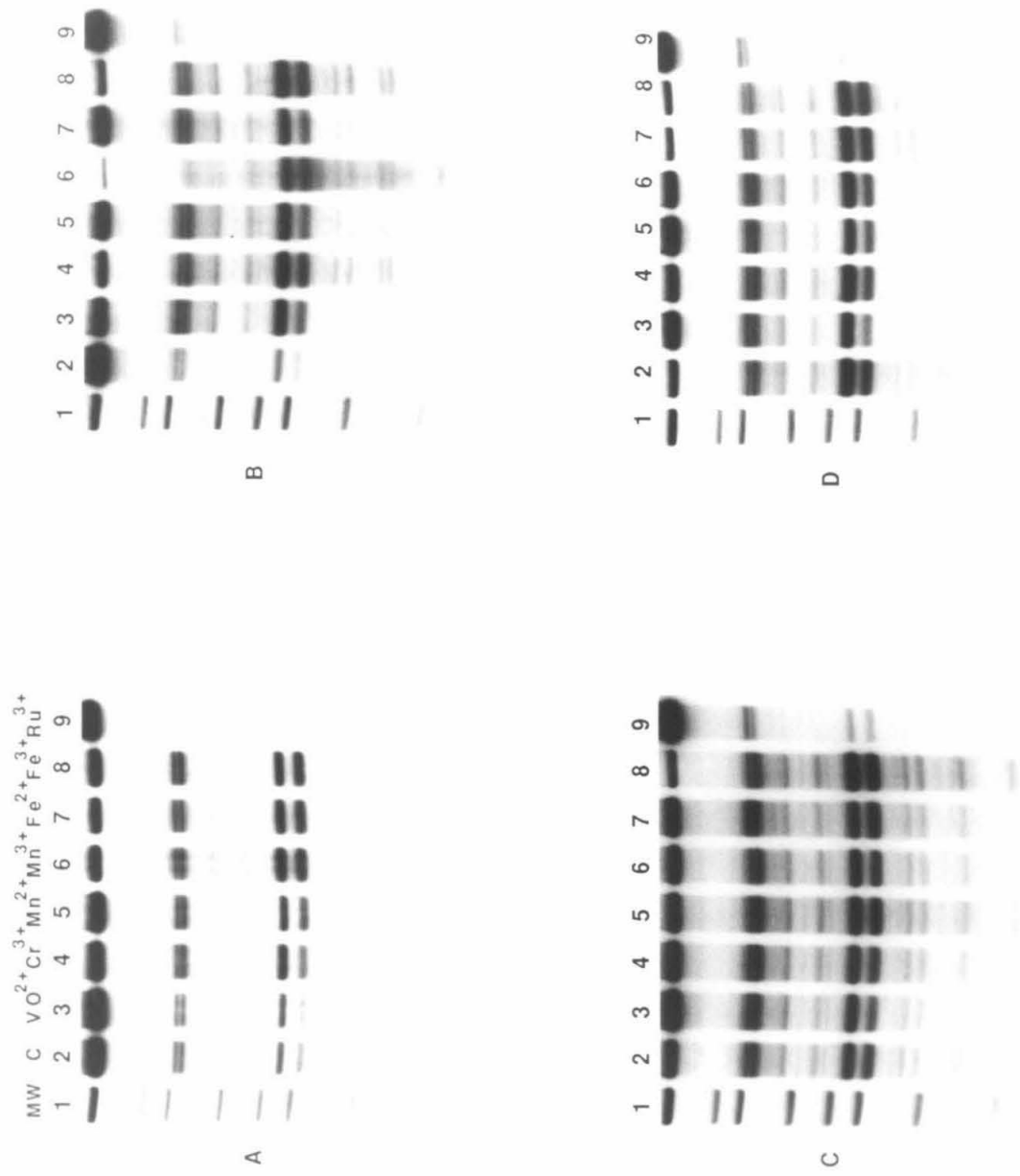


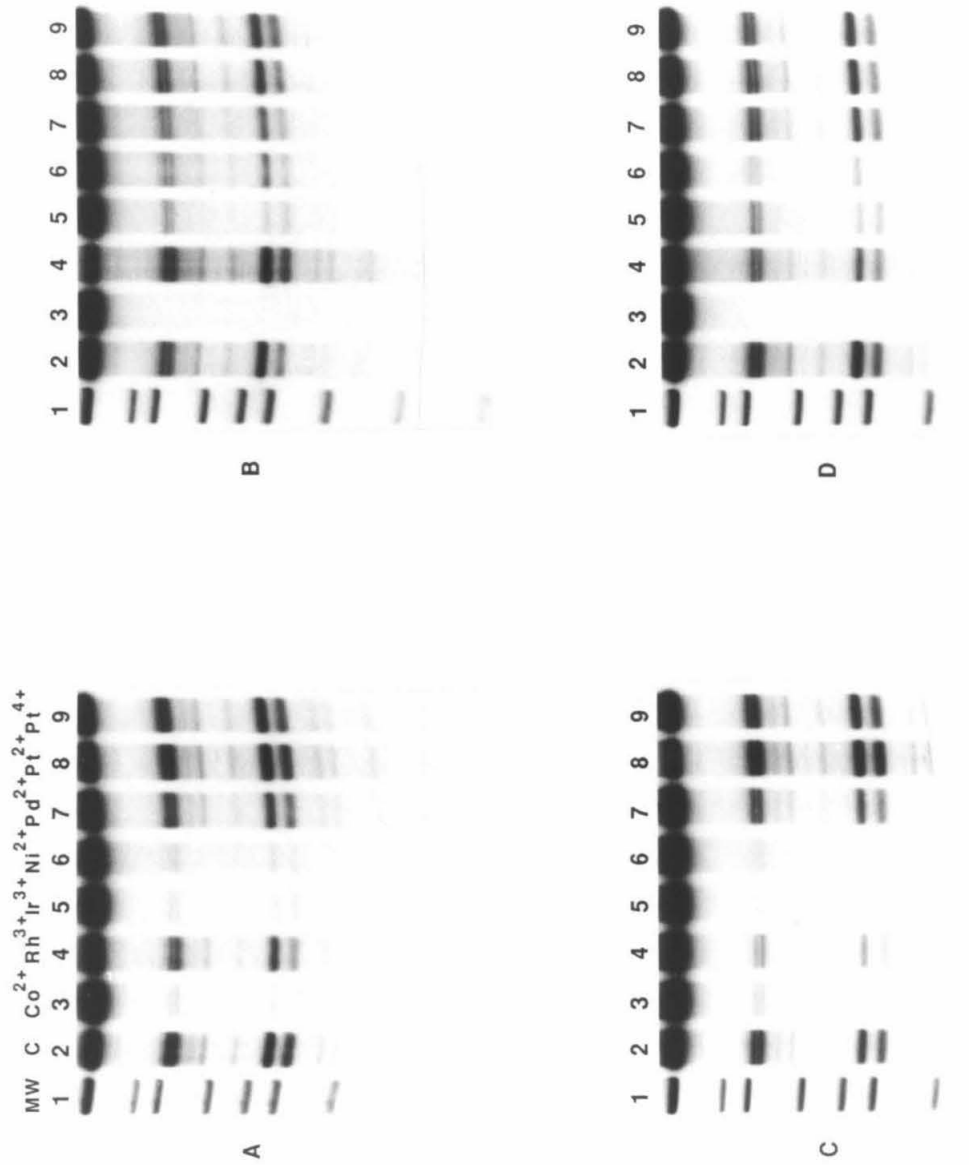


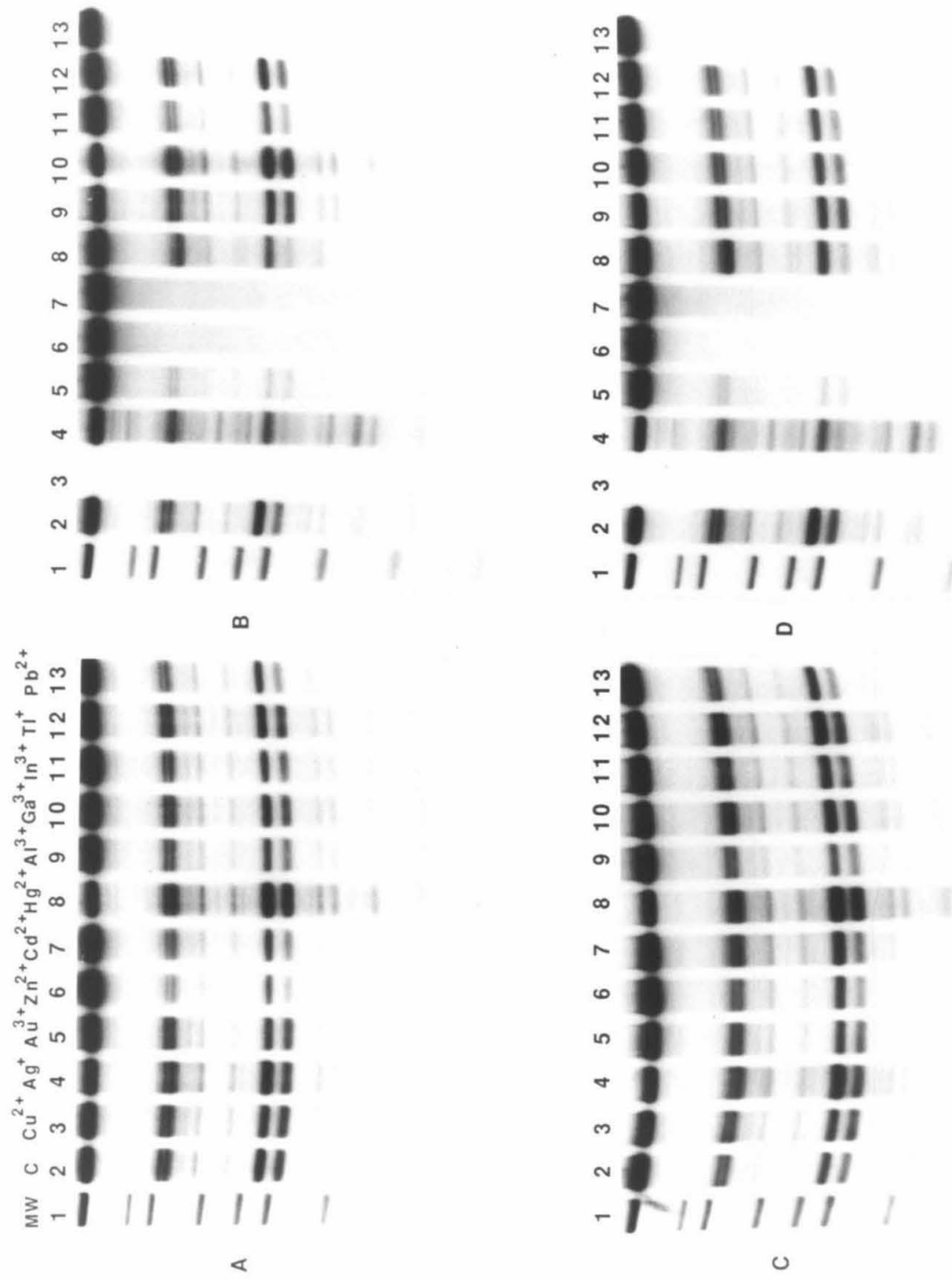












particular conditions (**D**). The effects observed for the individual cations under particular conditions of cation concentration, reductant employed, and initial **P5E:Fe** oxidation state are summarized in Tables 3.1 and 3.2. These data provide a basis against which to judge metalloregulatory effects. Most relevant to the results with **BNO5E:Fe**, the alkali and alkaline earth cations, including strontium and barium, have little or no effect on DNA affinity cleaving by **P5E:Fe** when present at 1 mM concentration. Additional experiments indicated that these metal ions have little effect even at 100 mM concentration. In contrast, 28 of 34 transition, post-transition, lanthanide, and actinide metals assayed produce effects (**N,L,P,D,M**) at 1 mM concentrations that would interfere with the study of DNA binding phenomena by DNA affinity cleaving in the presence of these cations at this concentration. Among these 34 cations, Cr^{3+} , Hg^{2+} , Tl^+ , Pd^{2+} , Pt^{2+} , and Pt^{4+} have little effect (\pm) or less serious effects (**R,C**) on affinity cleaving. DNA affinity cleaving studies could be carried out in the presence of these metals at 1 mM concentration. The majority of these cations (23 of 34) have at most minor effects on DNA affinity cleaving when present at 0.1 mM concentration. UO_2^{2+} , Ce^{3+} , Ce^{4+} , Cu^{2+} , Au^{3+} , Zn^{2+} , Cd^{2+} , Pb^{2+} , Co^{2+} , Ir^{3+} , Ni^{2+} , and Ru^{3+} can exert serious effects on DNA affinity cleaving even at 0.1 mM concentration. The ability of a given cation to influence DNA affinity cleaving will depend on the mode and strength of its interactions with EDTA, the DNA phosphate-sugar backbone, the DNA nucleotide bases, the reductant, and the DNA binding small molecule. The initial oxidation state of iron added to **P5E** has no significant effect on the ability of **P5E:Fe** to bind and cleave DNA in the presence of additional cations. This result is consistent with the known fast aerobic oxidation of EDTA:Fe(II) to EDTA:Fe(III),¹⁸ which should produce **P5E:Fe(III)** within seconds of mixing **P5E** and an Fe(II) salt. The affinity of a given cation for EDTA and its ability to inhibit DNA affinity cleaving are not strongly correlated. For example, Hg^{2+} and Pd^{2+} have little effect on DNA affinity cleaving at 1 mM concentration, yet they have greater affinity for EDTA than VO^{2+} or Zn^{2+} , which strongly inhibit DNA affinity cleaving at 1 mM concentration. The choice of

Table 3.1

Effects of metals at 1.0 mM concentration on DNA affinity cleaving by **P5E:Fe** at 0.75 μ M concentration using dithiothreitol or ascorbic acid reductants. Legend: \pm , cleavage at least 50% that observed in the absence of metal; **R**, cleavage reduced to 20-50% that observed in the absence of metal; **L**, little cleavage produced (less than 20% that observed in the absence of metal); **N**, no specific cleavage observed; **C**, cleavage pattern changed relative to that observed in the absence of metal; **D**, promotes DNA decomposition; **P**, precipitates DNA; **M**, causes altered mobility of DNA. ^aTaken from *Handbook of Chemistry and Physics*, 61st Ed.; Weast, R.C, Ed.; CRC Press: Boca Raton, Florida, 1980-1981. ^bTaken from *Stability Constants of Metal-Ion Complexes*; Sillen, A.G.; Martell, A.E., Eds.; Chemical Society, London: London, 1964, *Stability Constants of Metal-Ion Complexes*, Supplement #1; Sillen, A.G.; Martell, A.E., Eds.; Chemical Society, London: London, 1977. *Stability Constants of Metal-Ion Complexes-Part B, Organic Ligands*; Perrin, D.D., Ed.; Pergamon Press: Oxford, 1978. ^cTaken from Izatt, R.M.; Bradshaw, J.S.; Nielsen, S.A.; Lamb, J.D.; Christensen, J.J.; Sen, D. *Chem. Rev.* 1985, 85, 271-339.

Cation (1 mM)	Ionic Radius (Å) ^a	log K (EDTA) ^b	log K (18-C-6) ^c	Fe(II) DTT	Fe(II) Asc	Fe(III) DTT	Fe(III) Asc
NH ₄ ⁺	1.43		1.2	±	±	±	±
Li ⁺	0.68	2.8	0.0	±	±	±	±
Na ⁺	0.97	1.7	0.8	±	±	±	±
K ⁺	1.33	0.6	2.1	±	±	±	±
Rb ⁺	1.47	0.6	1.6	±	±	±	±
Cs ⁺	1.67	0.2	1.0	±	±	±	±
Mg ²⁺	0.66	8.7		±	±	±	±
Ca ²⁺	0.99	10.8	0.5	±	±	±	±
Sr ²⁺	1.12	8.6	2.8	±	±	±	±
Ba ²⁺	1.34	7.8	3.9	±	±	±	±
Sc ³⁺	0.73	23.1		M	M	M	M
La ³⁺	1.02	15.5		L/M	±/M	L/M	±/M
Lu ³⁺	0.85	19.5		L/M	±/M	L/M	±/M
Ho ³⁺	0.89	18		L/M	±/M	L/M	±/M
Eu ³⁺	0.95	17.4		L/M	D	L/M	±/M
Nd ³⁺	1.00	16.6		L/M	R/M	L/M	±/M
UO ₂ ²⁺				L	L	L	L
Ce ³⁺	1.03	16		P	R/M	P	±/M
Ce ⁴⁺	0.92	24		N	R/M	N	±/M
Cu ²⁺	0.72	18.8		±	D	±	D
Ag ⁺	1.26	7.3	1.6	±	D	±	±/D
Au ³⁺	0.85			N	L	N	L
Zn ²⁺	0.74	16.5		R	N	R	N
Cd ²⁺	0.97	16.5	0.5	±	N	±	N
Hg ²⁺	1.10	22	2.4	±	R/C	±	R/C
Al ³⁺	0.51	16		P	P	P	P
Ga ³⁺	0.62	20.3		P	P	P	P
In ³⁺	0.81	25.0		R	M	R	M
Tl ⁺	1.47	6	2.3	R	±	±	R
Pb ²⁺	1.20	17	4.3	R	N	L	N
Co ²⁺	0.72	16.3		N	N	N	N
Rh ³⁺	0.68			P	P	P	P
Ir ³⁺				L	L	L	L
Ni ²⁺	0.69	18.6		L	R	L	R
Pd ²⁺	0.80	18.5		R	R	R	±
Pt ²⁺	0.80			±	±	±	±
Pt ⁴⁺	0.65			R	±	R	±
VO ²⁺		18		N	N	N	N
Cr ³⁺	0.63	13		R	±	R	±
Mn ²⁺	0.80	14		N	L	N	L
Mn ³⁺	0.66	15-27		L	±	L	±
Fe ²⁺	0.74	14.3		P	P	P	P
Fe ³⁺	0.64	25.1		P	±	P	P
Ru ³⁺				L	R	R	L

Table 3.2

Effects of metals at 0.10 mM concentration on DNA affinity cleaving by **P5E:Fe** at 0.75 μ M concentration using dithiothreitol or ascorbic acid reductants. Legend: \pm , cleavage at least 50% that observed in the absence of metal; **R**, cleavage reduced to 20-50% that observed in the absence of metal; **L**, little cleavage produced (less than 20% that observed in the absence of metal); **N**, no specific cleavage observed; **C**, cleavage pattern changed relative to that observed in the absence of metal; **D**, completely decomposes DNA; **P**, precipitates DNA; **M**, causes altered mobility of DNA. ^aTaken from *Handbook of Chemistry and Physics*, 61st Ed.; Weast, R.C., Ed.; CRC Press: Boca Raton, Florida, 1980-1981. ^bTaken from *Stability Constants of Metal-Ion Complexes*; Sillen, A.G.; Martell, A.E., Eds.; Chemical Society, London: London, 1964, *Stability Constants of Metal-Ion Complexes*, Supplement #1; Sillen, A.G.; Martell, A.E., Eds.; Chemical Society, London: London, 1977. *Stability Constants of Metal-Ion Complexes-Part B, Organic Ligands*; Perrin, D.D., Ed.; Pergamon Press: Oxford, 1978. ^cTaken from Izatt, R.M.; Bradshaw, J.S.; Nielsen, S.A.; Lamb, J.D.; Christensen, J.J.; Sen, D. *Chem. Rev.* 1985, 85, 271-339.

Cation (1 mM)	Ionic Radius (\AA) ^a	$\log K$ (EDTA) ^b	$\log K$ (18-C-6) ^c	Fe(II) DTT	Fe(II) Asc	Fe(III) DTT	Fe(III) Asc
NH_4^+	1.43		1.2	\pm	\pm	\pm	\pm
Li^+	0.68	2.8	0.0	\pm	\pm	\pm	\pm
Na^+	0.97	1.7	0.8	\pm	\pm	\pm	\pm
K^+	1.33	0.6	2.1	\pm	\pm	\pm	\pm
Rb^+	1.47	0.6	1.6	\pm	\pm	\pm	\pm
Cs^+	1.67	0.2	1.0	\pm	\pm	\pm	\pm
Mg^{2+}	0.66	8.7		\pm	\pm	\pm	\pm
Ca^{2+}	0.99	10.8	0.5	\pm	\pm	\pm	\pm
Sr^{2+}	1.12	8.6	2.8	\pm	\pm	\pm	\pm
Ba^{2+}	1.34	7.8	3.9	\pm	\pm	\pm	\pm
Sc^{3+}	0.73	23.1		R	\pm	\pm	\pm
La^{3+}	1.02	15.5		R	\pm	\pm	\pm
Lu^{3+}	0.85	19.5		R	\pm	\pm	\pm
Ho^{3+}	0.89	18		R	\pm	R	\pm
Eu^{3+}	0.95	17.4		\pm	\pm	\pm	\pm
Nd^{3+}	1.00	16.6		\pm	\pm	\pm	\pm
UO_2^{2+}				N	N	N	N
Ce^{3+}	1.03	16		L	\pm	L	\pm
Ce^{4+}	0.92	24		L	\pm	L	\pm
Cu^{2+}	0.72	18.8		\pm	D	\pm	D
Ag^+	1.26	7.3	1.6	\pm	\pm/C	\pm	\pm/C
Au^{3+}	0.85			\pm	L	\pm	L
Zn^{2+}	0.74	16.5		R	N	\pm	N
Cd^{2+}	0.97	16.5	0.5	\pm	N	\pm	N
Hg^{2+}	1.10	22	2.4	\pm	\pm/C	\pm	\pm/C
Al^{3+}	0.51	16		\pm	\pm	\pm	\pm
Ga^{3+}	0.62	20.3		\pm	\pm	\pm	\pm
In^{3+}	0.81	25.0		\pm	\pm	\pm	\pm
Tl^+	1.47	6	2.3	\pm	\pm	\pm	\pm
Pb^{2+}	1.20	17	4.3	\pm	N	\pm	N
Co^{2+}	0.72	16.3		L	N	R	N
Rh^{3+}	0.68			\pm	\pm	R	\pm
Ir^{3+}				L	R	L	R
Ni^{2+}	0.69	18.6		L	R	L	R
Pd^{2+}	0.80	18.5		\pm	\pm	\pm	\pm
Pt^{2+}	0.80			\pm	\pm	\pm	\pm
Pt^{4+}	0.65			\pm	\pm	\pm	\pm
VO^{2+}		18		\pm	\pm	\pm	\pm
Cr^{3+}	0.63	13		\pm	\pm	\pm	\pm
Mn^{2+}	0.80	14		\pm	\pm	\pm	\pm
Mn^{3+}	0.66	15-27		\pm	\pm	\pm	\pm
Fe^{2+}	0.74	14.3		\pm	\pm	\pm	\pm
Fe^{3+}	0.64	25.1		\pm	\pm	\pm	\pm
Ru^{3+}				L	R	R	

reductant influences the effect a given metal cation has on DNA affinity cleaving. Strong cleavage inhibition by the lanthanide cations is observed in the presence of DTT reductant, but the use of ASC reductant results in reduced inhibition. Cleavage inhibition by Zn^{2+} , Pb^{2+} , and Cd^{2+} is alleviated when DTT reductant is employed in place of ASC. These results are consistent with the preference for "hard:hard" (lanthanide cation:ASC) and "soft:soft" (post-transition metal cation:DTT) complexation. Reductants (used in at least fivefold excess over metal cations) may sequester metal cations, making them unavailable to inhibit the cleavage reaction or promote a metalloregulatory phenomenon.

In the absence of added cations, Bis(Netropsin) Polyether-EDTA:Fe compounds produce the most notable DNA double-strand cleavage in two regions of pBR322. In the presence of strontium or barium cations, **BNO5E:Fe** produces DNA double-strand cleavage in the same regions, but with greater intensity. The observed cleavage bands were mapped to the pBR322 sequence by comparing the electrophoretic mobilities of the cleavage bands and the DNA bands in the molecular weight marker lanes. A histogram of DNA double-strand cleavage produced by **BNO5E:Fe** in the absence and presence of barium is shown in Figure 3.16. The cleavage band observed near position 3200 and the cluster of bands observed near the "ends" of the pBR322 map to A:T rich regions of the plasmid.

These regions of DNA cleavage were examined at nucleotide resolution. 517 base pair Eco RI/Rsa I restriction fragments from pBR322 were prepared with ^{32}P at either the 3'- or 5' Eco RI end. Cleavage of these fragments, which contain the cleavage loci clustered near pBR322 position 4300, was carried out under standard conditions in the absence and presence of cations. DNA cleavage products were separated by denaturing polyacrylamide gel electrophoresis and visualized by autoradiography. An autoradiograph of the cleavage patterns produced on the 5'- ^{32}P end-labeled 517 base pair restriction fragment by **BNO5E:Fe** in the absence of cations, in the presence of various cations at 1 mM concentration, and in the presence of a range of concentrations of barium (20 μM to

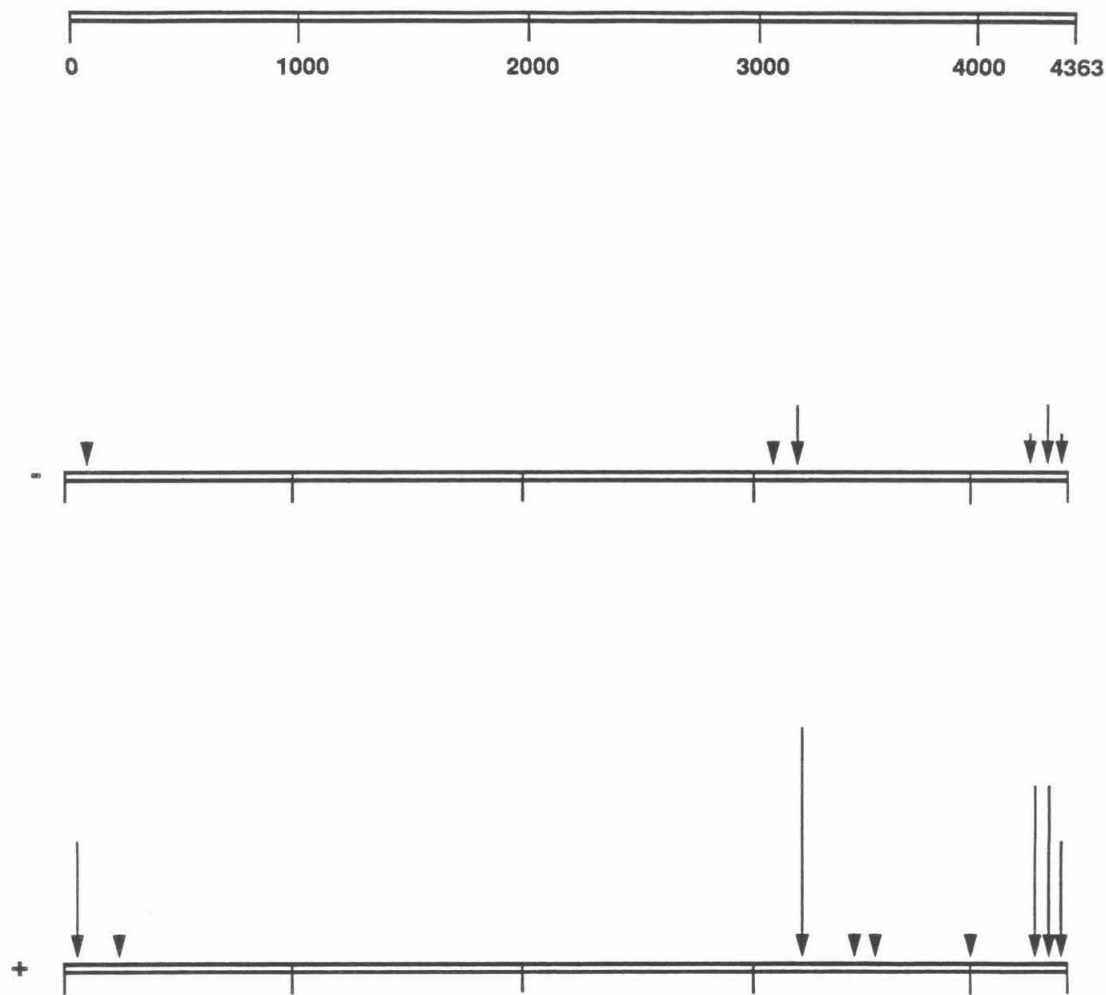


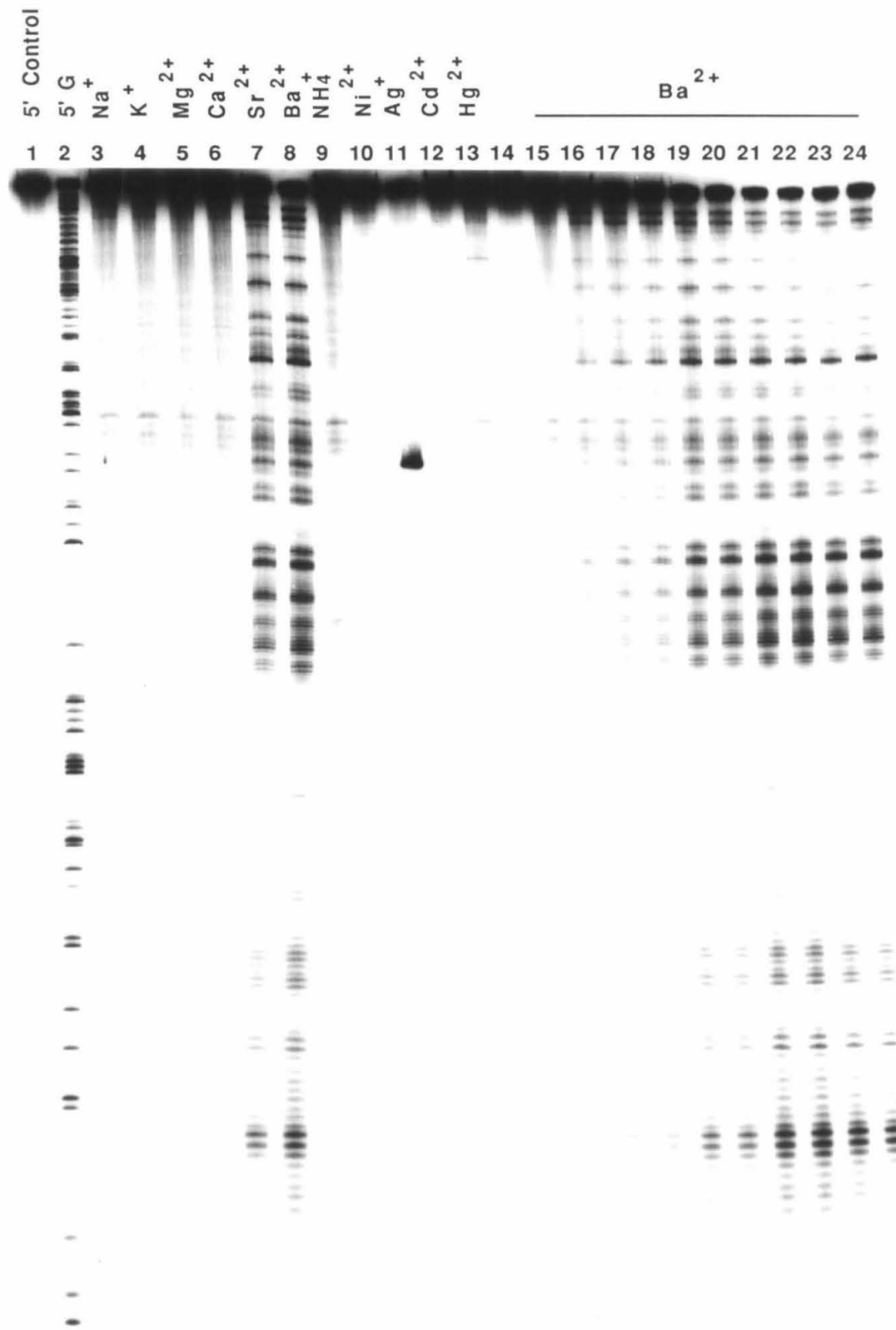
Figure 3.16. Histograms of DNA double-strand cleavage produced by BNO5E:Fe on Sty I-linearized pBR322 plasmid DNA in the absence and presence of barium cations. Lengths of arrows correspond to the relative amounts of cleavage, determined by optical densitometry, at the various cleavage loci. Positions of cleavage were determined by analyzing the measured electrophoretic mobilities of DNA cleavage fragments relative to a standard curve derived from the measured electrophoretic mobilities of marker fragments of known molecular weights. Top: Histogram of DNA double-strand cleavage by BNO5E:Fe at 5.0 μ M concentration in the absence of added barium cations. Bottom: Histogram of DNA double-strand cleavage by BNO5E:Fe at 5.0 μ M concentration in the presence of barium cations at 5.0 mM concentration.

100 mM) is shown in Figure 3.17. The positive metalloregulation of **BNO5E:Fe** by strontium and barium observed by DNA double-strand affinity cleaving analysis is also observed on this sequencing gel, which reports DNA single-strand breaks. Figure 3.18 shows a plot of relative cleavage produced by **BNO5E:Fe** (determined by densitometry of the lower part of the autoradiograph shown in Figure 3.17) versus the logarithm of the millimolar barium concentration reveals that one equivalent of barium enhances DNA cleavage by **BNO5E:Fe**, and that cleavage efficiency increases with barium concentration up to 10 mM. Barium concentrations greater than 10 mM decrease the cleavage efficiency of **BNO5E:Fe**. Half-maximal cleavage by 5.0 μ M **BNO5E:Fe** occurs with approximately 1 mM barium.

An autoradiograph of the cleavage patterns produced by the Bis(Netropsin) Polyether-EDTA:Fe compounds on the 517 base pair restriction fragments in the absence and presence of barium cations is shown in Figure 3.19. Most striking, the cleavage pattern produced by **BNO5E:Fe** in the presence of barium is not only *stronger* than, but also *different* from the pattern produced in the absence of barium. The DNA cleavage patterns produced on this autoradiograph by **BNO5E:Fe** in the absence and presence of barium were analyzed by densitometry and converted to histogram form (Figure 3.20). The equilibrium DNA minor groove binding sites for **BNO5E:Fe** and **BNO5E:Fe:Ba²⁺** (boxes in Figure 3.20) were assigned on the basis of the observed 3'-shifted, pseudo-*C*₂ symmetric DNA cleavage patterns,¹⁶ and were confirmed by **MPE:Fe** footprinting¹⁹⁻²³ of the redox-inactive complex **BNO5E:In(III)** in the absence and presence of barium. In the absence of added cations, **BNO4E:Fe**, **BNO5E:Fe**, and **BNO6E:Fe** produce weak cleavage flanking the eight base pair sequence 5'-ATTTTTAT-3' in the lower part of the autoradiograph, and within and flanking the sequence 5'-TATTGTTTATTCTAAATACATTCAAATA-3' in the upper middle part of the autoradiograph. In the presence of barium, **BNO5E:Fe** produces much stronger cleavage flanking two well-resolved binding sites in the lower part of the autoradiograph, 5'-

Figure 3.17

Autoradiograph of DNA cleavage patterns produced by **BNO5E:Fe** on a 5'-³²P end-labeled 517 bp restriction fragment (Eco RI/Rsa I) from pBR322 plasmid DNA, in the presence of dioxygen and dithiothreitol, and in the absence and presence of metal cations. Cleavage patterns were resolved by electrophoresis on a 1:20 cross-linked 8% polyacrylamide, 45% urea denaturing gel. Lane 1, uncleaved DNA; lane 2, Maxam-Gilbert chemical sequencing G reaction; lanes 3-13, **BNO5E:Fe** at 20 μ M concentration in the presence of 1 mM concentrations of NaOAc, KOAc, Mg(OAc)₂, Ca(OAc)₂, Sr(NO₃)₃, Ba(OAc)₂, NH₄OAc, AgOAc, Ni(OAc)₂, Cd(OAc)₂, and Hg(OAc)₂, respectively; lane 14, uncleaved DNA incubated with 1 mM Ba(OAc)₂ and dithiothreitol; lane 15, **BNO5E:Fe** at 20 μ M concentration in the absence of added cations; lanes 16-24, **BNO5E:Fe** at 20 μ M concentration in the presence of Ba(OAc)₂ at 0.02, 0.05, 0.10, 0.50, 1.0, 5.0, 10, 50, and 100 mM concentrations, respectively.



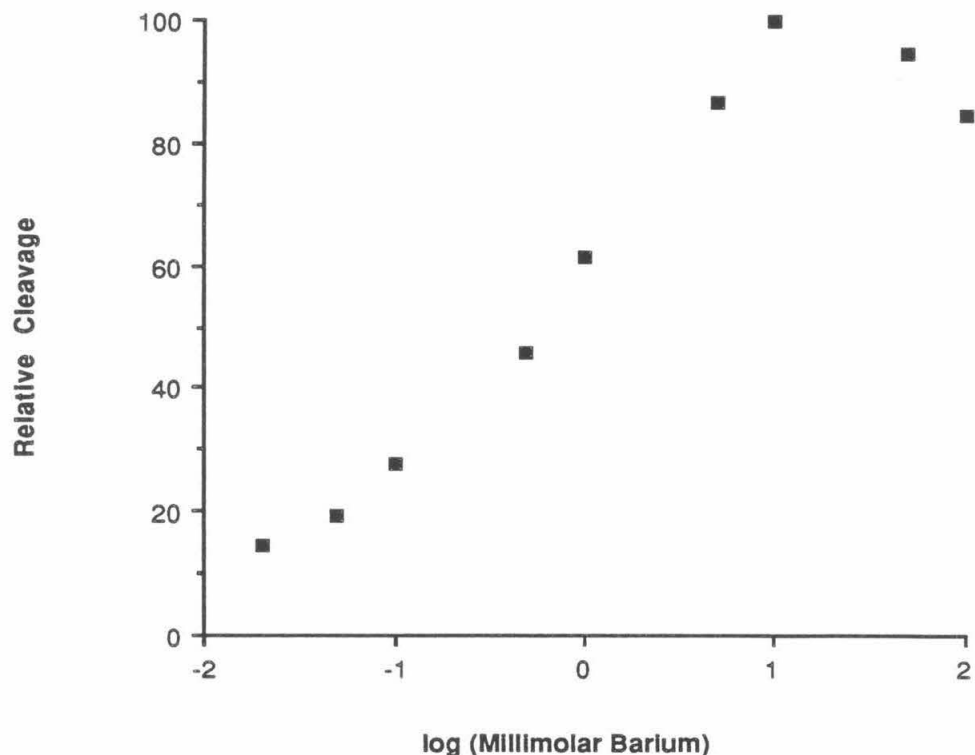
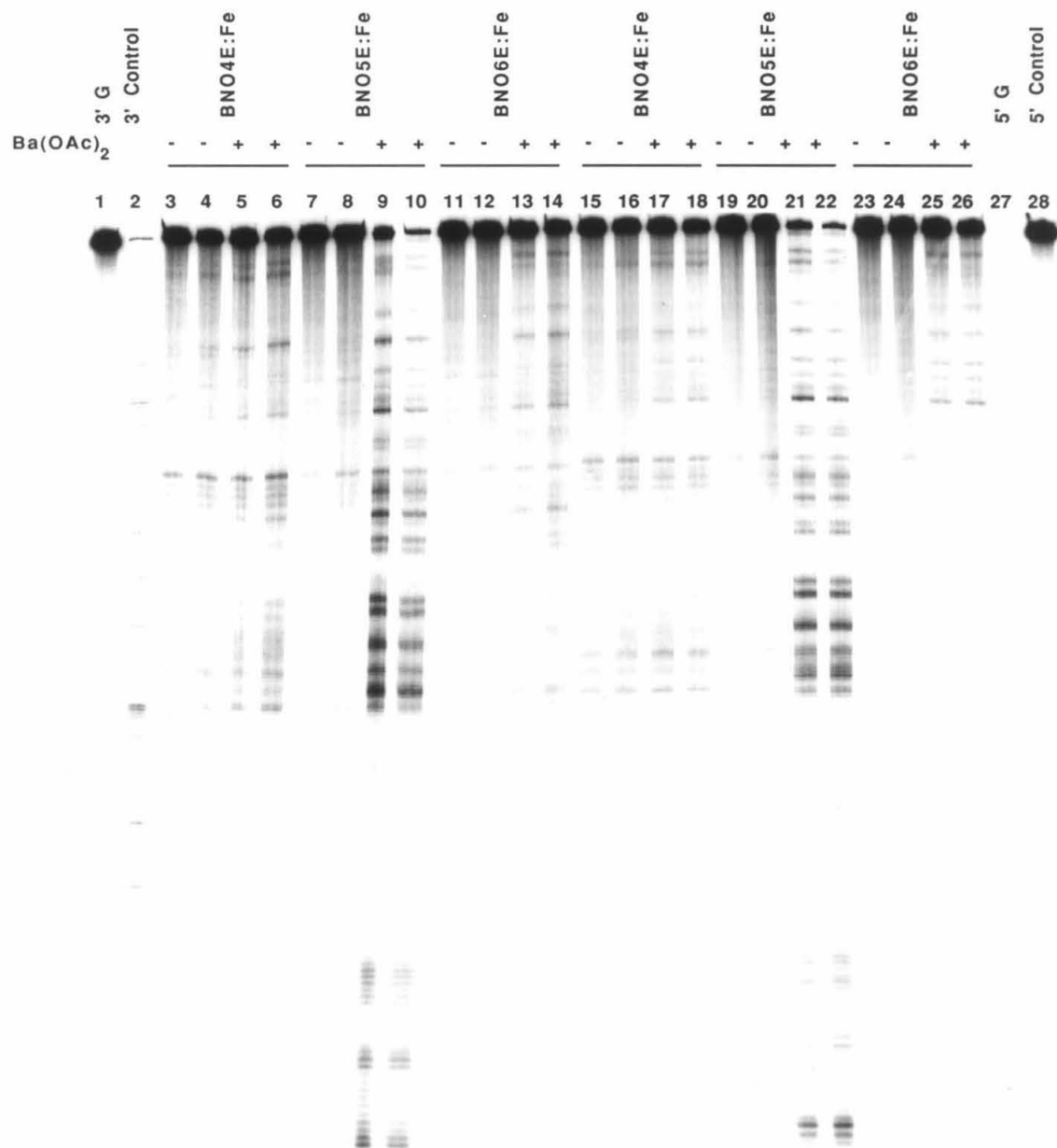


Figure 3.18. Plot of relative cleavage efficiency by BNO5E:Fe versus log(millimolar barium concentration). Cleavage was determined densitometrically at the lower cleavage site observed on the autoradiograph in Figure 3.17.

Figure 3.19

Autoradiograph of DNA cleavage patterns produced by Bis(Netropsin) Polyether-EDTA:Fe compounds on 3'- and 5'-³²P end-labeled 517 bp restriction fragments (Eco RI/Rsa I) from pBR322 plasmid DNA, in the presence of dioxygen and dithiothreitol, and in the absence and presence of added barium cations. Cleavage patterns were resolved by electrophoresis on a 1:20 cross-linked 8% polyacrylamide, 45% urea denaturing gel. Lanes 1-14 were with 3' end-labeled DNA. Lanes 15-28 were with 5' end-labeled DNA. Lanes 1 and 28, uncleaved DNA; lanes 2 and 27, Maxam-Gilbert chemical sequencing G reactions; lanes 3-6 and 15-18 contained **BNO4E:Fe**; lanes 7-10 and 19-22 contained **BNO5E:Fe**; lanes 11-14 and 23-26 contained **BNO6E:Fe**. Odd-numbered lanes 3-25 contained 10 μ M Bis(Netropsin) Polyether-EDTA:Fe compound. Even-numbered lanes 4-26 contained 20 μ M Bis(Netropsin) Polyether-EDTA:Fe compound. Lanes 3,4,7,8,11,12,15,16,19,20,23, and 24 contained no added cations. Lanes 5,6,9,10,13,14,17,18,21,22,25, and 26 contained 5.0 mM Ba(OAc)₂.



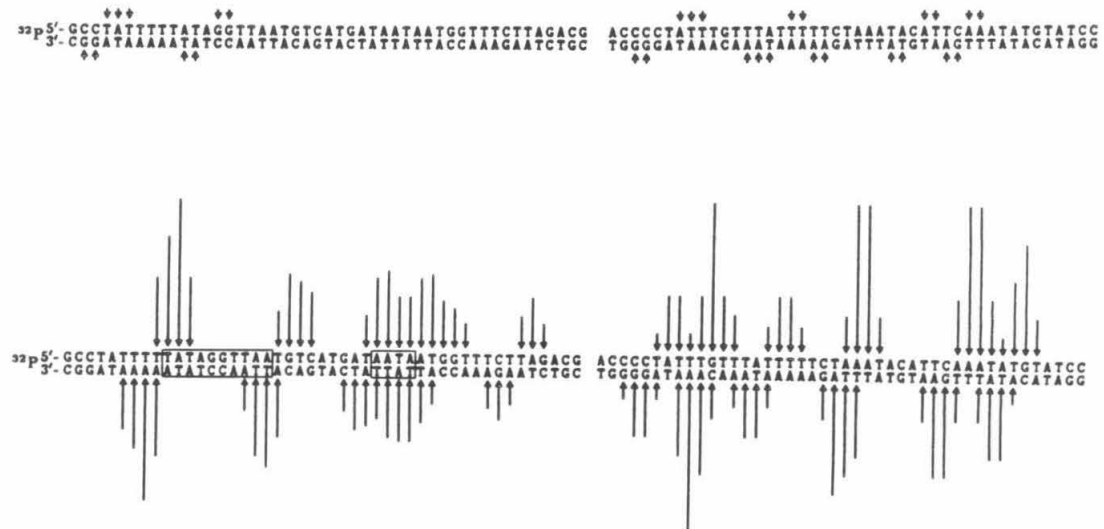


Figure 3.20. Histograms of DNA cleavage produced by **BNO5E:Fe** on the 517 bp DNA restriction fragment (Eco RI/Rsa I) from plasmid pBR322 DNA in the absence and presence of added barium cations. Lengths of arrows correspond to the relative amounts of cleavage, determined by optical densitometry, which result in removal of the indicated base. Sequence positions of cleavage were determined by comparing the electrophoretic mobilities of DNA cleavage fragments to bands in Maxam-Gilbert chemical sequencing lanes. DNA minor groove binding sites (boxed) were assigned from the observed cleavage patterns and the model described by Taylor, Schultz, and Dervan (Reference 16). Top: Histogram of DNA cleavage by **BNO5E:Fe** at 20 μ M concentration in the absence of added barium. Bottom: Histogram of DNA cleavage by **BNO5E:Fe** at 20 μ M concentration in the presence of barium at 5.0 mM concentration.

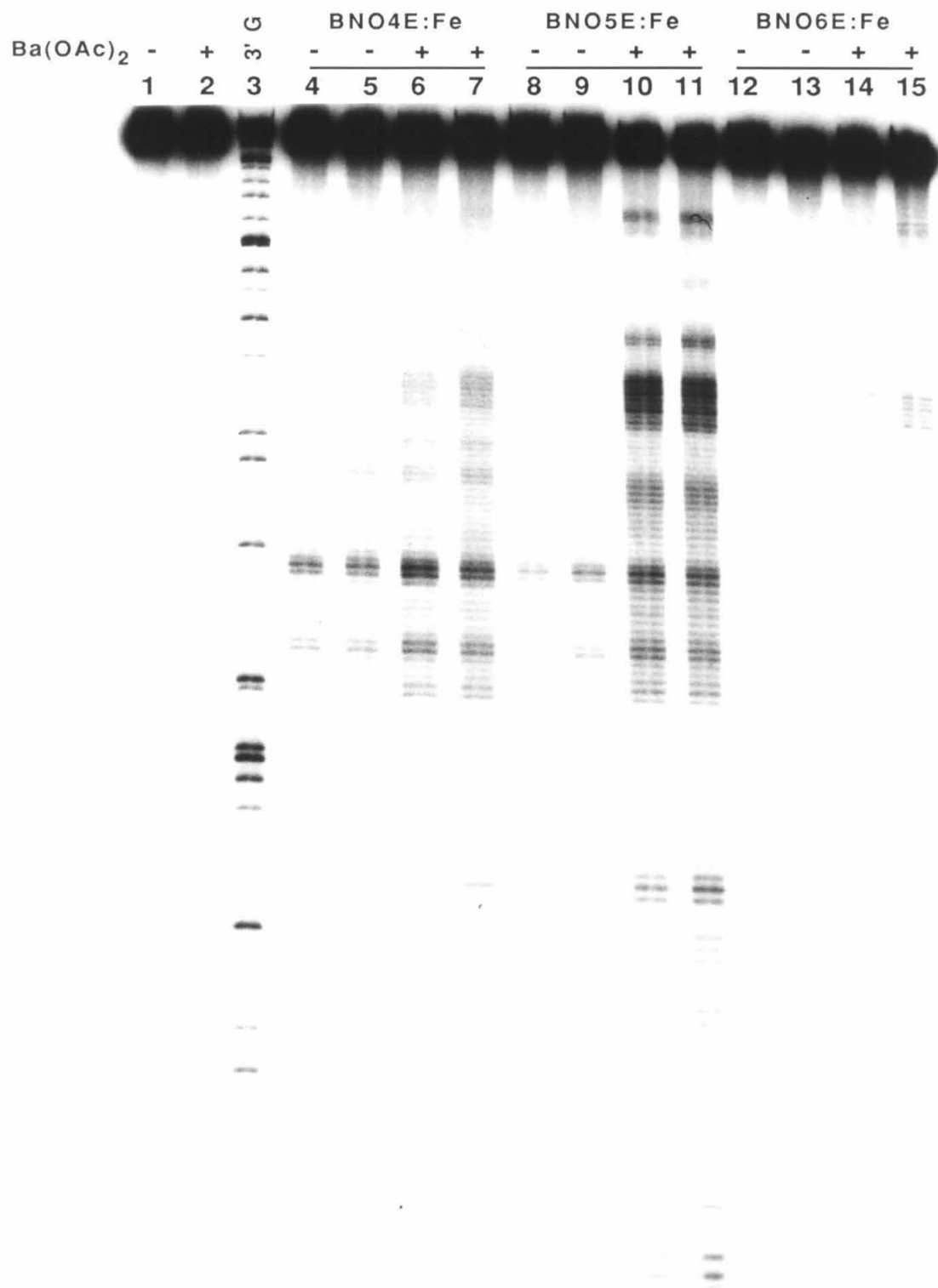
TATAGGTTAA-3', and 5'-AATA-3'. The cleavage pattern is more complex in the upper middle part of the autoradiograph, indicating the presence of multiple metalloregulated binding sites for **BNO5E:Fe:Ba²⁺** in this region. Several sites appear to consist of four contiguous A:T base pairs adjacent to a single G:C base pair.

To examine DNA cleavage produced by the Bis(Netropsin) Polyether-EDTA:Fe compounds at the cleavage locus near pBR322 position 3200, a 169 base pair Dde I restriction fragment was prepared with ³²P on one 3' end. This restriction fragment contains the longest contiguous stretch of A:T base pairs (15) found on pBR322. An autoradiograph of the cleavage patterns produced on this restriction fragment by **BNO4E:Fe**, **BNO5E:Fe**, and **BNO6E:Fe**, in the absence and presence of barium cations, is shown in Figure 3.21. The observed cleavage patterns were analyzed by densitometry. Histograms of DNA cleavage produced by **BNO5E:Fe** in the absence and presence of barium are shown in Figure 3.22. In the absence of added cations, **BNO5E:Fe** and the other Bis(Netropsin) Polyether-EDTA:Fe compounds produce weak DNA binding/cleaving within and flanking the stretch of 15 contiguous A:T base pairs. In the presence of barium, cleavage by **BNO5E:Fe** in this region is somewhat enhanced, but cleavage is more strongly enhanced within the sequence 5'-GTATATATGAGTAAAC-3'. The cleavage pattern observed in this region is consistent with multiple overlapping binding sites of four contiguous A:T base pairs adjacent to a G:C base pair.

The observation of binding sites containing only four A:T base pairs suggests that barium may induce **BNO5E:Fe** to bind in a monomeric mode in which only one of its Netropsin subunits intimately contacts DNA. In order to examine metalloregulated monomeric binding in greater detail, we designed and synthesized dimethylaminopropane-3,6,9,12,15-pentaoxaheptadecanediamide-Netropsin-EDTA (**O5NE, IV-159**) and the homolog dimethylaminopropane-3,6,9,12,15-pentaoxaheptadecanediamide-P5-EDTA (**O5P5E, IV-167**, Figure 3.23). To produce these molecules, **IV-129** (Figure 3.3) or the homologous Boc P5 Nitro compound, was reduced and coupled with dimethylamino-

Figure 3.21

Autoradiograph of DNA cleavage patterns produced by Bis(Netropsin) Polyether-EDTA:Fe compounds on a 3'-³²P-end-labeled 169 bp Dde I restriction fragment from plasmid pBR322 DNA, in the presence of dioxygen and dithiothreitol, and in the absence and presence of barium cations. Cleavage patterns were resolved by electrophoresis on a 1:20 cross-linked 8% polyacrylamide, 45% urea denaturing gel. Lane 1, uncleaved DNA; lane 2, uncleaved DNA incubated with 5.0 mM Ba(OAc)₂ and dithiothreitol; lane 3, Maxam-Gilbert chemical sequencing G reaction; lanes 4-7 contained **BNO4E:Fe**; lanes 8-11 contained **BNO5E:Fe**; lanes 12-15 contained **BNO6E:Fe**. Even-numbered lanes 4-14 contained 10 μ M Bis(Netropsin) Polyether-EDTA:Fe compound. Odd-numbered lanes 5-15 contained 20 μ M Bis(Netropsin) Polyether-EDTA:Fe compound. Lanes 4,5,8,9,12, and 13 contained no added cations. Lanes 6,7,10,11,14, and 15 contained 5.0 mM Ba(OAc)₂.



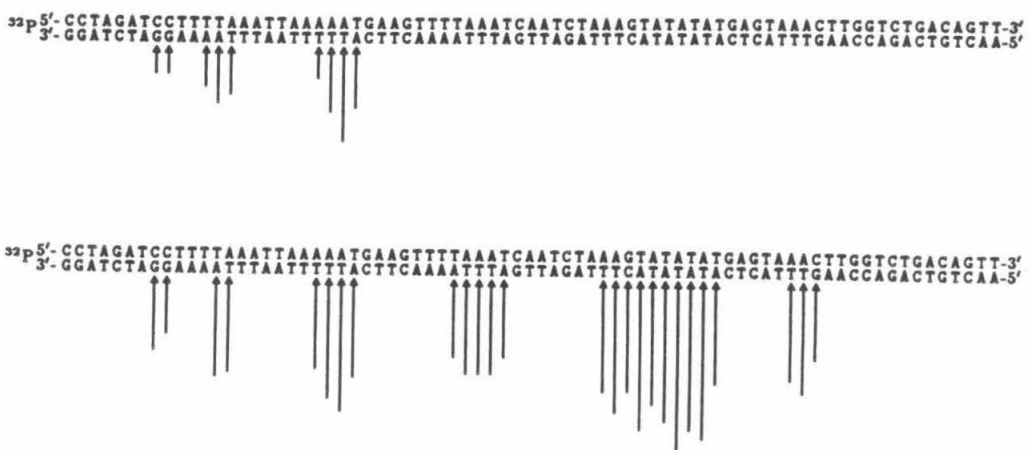


Figure 3.22. Histograms of DNA cleavage produced by BNO5E:Fe on the 169 bp Dde I DNA restriction fragment from plasmid pBR322 DNA in the absence and presence of added barium cations. Lengths of arrows correspond to the relative amounts of cleavage, determined by optical densitometry, which result in removal of the indicated base. Sequence positions of cleavage were determined by comparing the electrophoretic mobilities of DNA cleavage fragments to bands in Maxam-Gilbert chemical sequencing lanes. DNA minor groove binding sites (boxed) were assigned from the observed cleavage patterns and the model described by Taylor, Schultz, and Dervan (Reference 16). Top: Histogram of DNA cleavage by BNO5E:Fe at 20 μ M concentration in the absence of added barium. Bottom: Histogram of DNA cleavage by BNO5E:Fe at 20 μ M concentration in the presence of barium at 5.0 mM concentration.

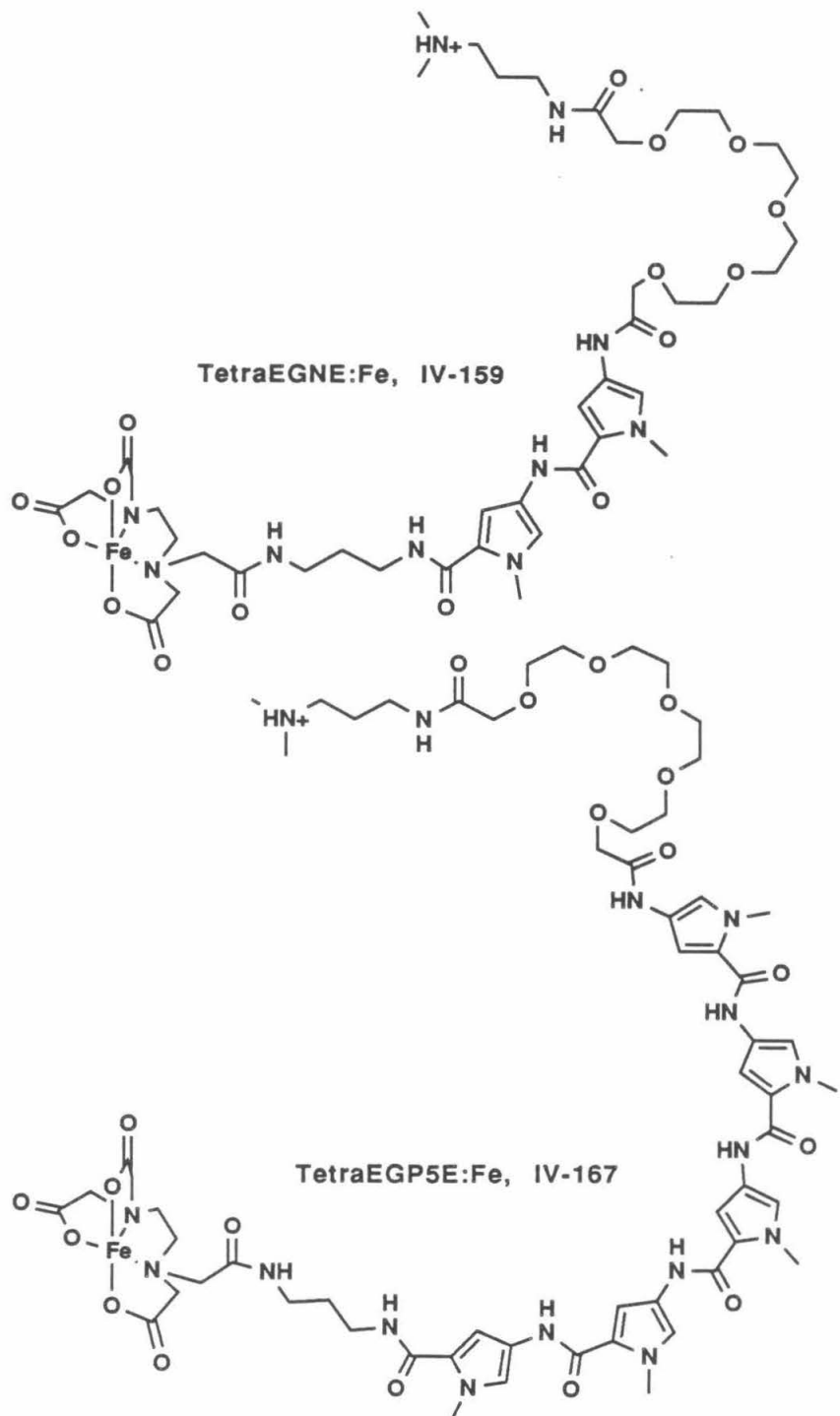


Figure 3.23. Top: Dimethylaminopropane-3,6,9,12,15-pentaoxaheptadecanediamide-Netropsin-EDTA:Fe (**O5NE:Fe**). Bottom: Dimethylaminopropane-3,6,9,12,15-pentaoxaheptadecanediamide-P5-EDTA:Fe (**O5P5E:Fe**).

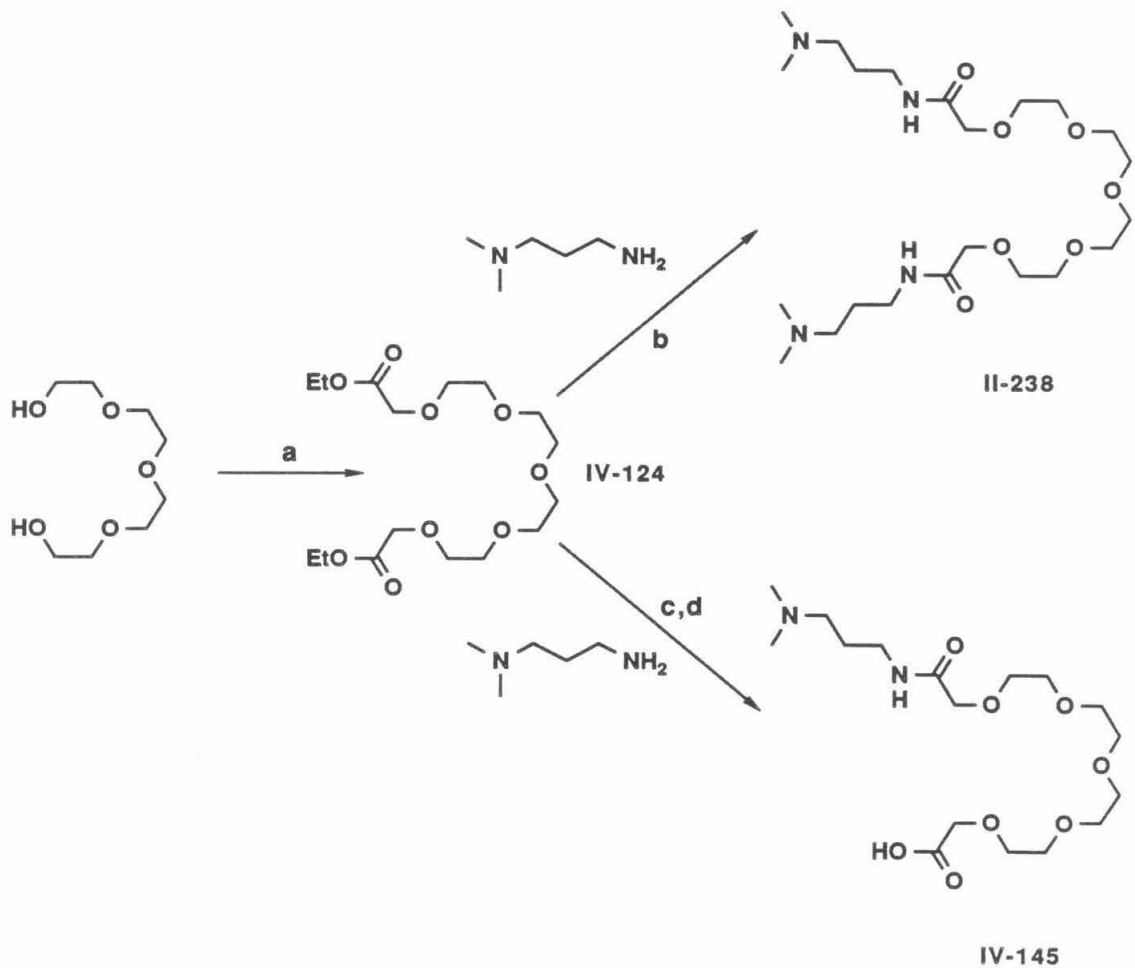


Figure 3.24. Scheme for the synthesis of Bis(Dimethylaminopropane)-3,6,9,12,15-Pentaoxaheptadecanediamide (Top Right), and (Dimethylaminopropane)-3,6,9,12,15-Pentaoxaheptadecanamic acid (Bottom Right). Reaction conditions: a, N₂CHCO₂Et (2.5 equiv.), Rh₂(OAc)₄ (0.01 equiv.), Et₂O; b, H₂N(CH₂)₃N(CH₃)₂ (excess), 60°C; c, H₂N(CH₂)₃N(CH₃)₂ (1.0 equiv.), 80°C; d, LiOH (2.0 equiv.), MeOH, H₂O.

propane-3,6,9,12,15-pentaoxaheptadecanamic acid (**IV-145**, Figure 3.24). The terminal amino groups of the resulting compounds were deprotected and coupled with the triethyl ester of EDTA. The EDTA ester groups were removed by hydrolysis to afford **O5NE** and **O5P5E**. **IV-145** was produced from **IV-124** (an intermediate in the synthesis of **BNO5E**) and dimethylaminopropylamine as depicted in Figure 3.24. Also depicted in Figure 3.24 is the synthesis of Bis(dimethylaminopropane)-3,6,9,12,15-pentaoxaheptadecandiamide **II-238**. **II-238** was prepared to determine whether such a molecule could act as a "barium binding finger," a small molecule analog of DNA binding proteins that interact with DNA through a "zinc finger" motif.²⁴

DNA binding properties of **O5NE:Fe** and **O5P5E:Fe** were determined by double-strand cleavage of Sty I-linearized, 3'-³²P end-labeled pBR322. **O5NE:Fe** does not produce specific DNA cleavage, even at 100 μM concentration in the absence or presence of 5 mM barium or strontium cations. **O5P5E:Fe** exhibits cleavage efficiency and specificity similar to **P5E:Fe**. However, neither the cleavage efficiency nor the cleavage specificity of **O5P5E:Fe** is affected by the addition of strontium or barium cations. Finally, **MPE:Fe** footprinting failed to detect significant DNA binding for **II-238** in the absence or the presence of barium cations.

Discussion

The synthesis of three Bis(Netropsin)-EDTA compounds linked in tail-to-tail fashion by homologous polyether diacids has been accomplished by direct extension of the method described in Chapter One for the preparation of Bis(Netropsin) Diacid-EDTA compounds.

Addition of strontium or barium cations converts **BNO5E:Fe** from a species that exhibits little DNA binding/cleaving activity to an efficient, sequence-specific DNA binding/cleaving agent. In light of experiments in which strontium and barium do not enhance DNA binding/cleaving by **BNO4E:Fe**, **BNO6E:Fe**, or **P5E:Fe**, the results

with **BNO5E:Fe** demonstrate *positive metalloregulation in the sequence-specific binding of a designed, synthetic molecule to DNA*. The effect is metal ion specific, occurring only with the heavier alkaline earth dications strontium and barium. Barium is more effective than strontium in activating **BNO5E:Fe**, a result that parallels the order of their binding affinities for 18-crown-6 in water (log K = 3.9 for Ba^{2+} , 2.8 for Sr^{2+}).²⁵ As strontium and barium are known to bind more strongly to 18-crown-6 in water than virtually any other cations (Tables 3.1 and 3.2),²⁵ the observed metallospecificity suggests that when complexed in the minor groove of B DNA, **BNO5E** forms an ionophore similar to 18-crown-6. Why certain cations such as mercury(II) or lead(II) have reasonable affinity for 18-crown-6 in water yet do not appear to activate **BNO5E:Fe** may be due to the propensity of these metals to disrupt DNA affinity cleaving. Alternatively, these "soft" metals may prefer to interact with "soft" donor sites on the heterocyclic DNA bases rather than with the "hard" oxygen donors on the linker or on the phosphate groups of the DNA backbone.²⁶

The metalloregulatory effect is also strongly dependent on the structure of the podand. **BNO4E** and **BNO6E**, having one fewer or one more ethylene glycol unit than **BNO5E**, respectively, do not exhibit significant metalloregulation. CPK models indicate that when the podands of these molecules are arranged in crown ether fashion around a metal cation, the crescent shape assumed by **BNO5E** is most complementary to the helical twist of B DNA.

The different DNA binding sequences exhibited by **BNO5E:Fe** in the absence versus the presence of strontium or barium are as striking as the increase in DNA binding affinity. While Netropsin and Netropsin-like molecules prefer homopolymeric A:T sequences, **BNO5E:Fe:M²⁺** ($\text{M}^{2+} = \text{Sr}^{2+}$ or Ba^{2+}) binds to the ten base pair site 5'-TATAGGTTAA-3' in preference to the adjacent ten base pair site 5'-TATTTTTATA-3' on the 517 base pair restriction fragment. On the 169 base pair restriction fragment, **BNO5E:Fe:M²⁺** prefers sites within the sequence 5'-GTATATATGAGTAAAC-3' to

sites within the longest contiguous stretch of A:T base pairs found on pBR322, 5'-TTTAAATTAAAAAT-3'. The results indicate that complexes of strontium or barium and the podand subunit of **BNO5E** prefer to interact with the minor groove of B DNA at sites containing G:C base pairs rather than A:T base pairs.^{27,28} We have previously proposed a model for the positively metalloregulated binding of **BNO5E:Fe** to the sequence 5'-TATAGTTAA-3' (Figure 3.25).^{29,30} Positive metalloregulation is proposed to arise from increases in favorable electrostatic and hydrogen-bonding interactions between **BNO5E:Fe:M²⁺** and the minor groove of B DNA relative to the weak interactions of **BNO5E:Fe** and DNA in the absence of barium or strontium. In this model, Netropsin subunits specific for (A:T)₄ flank a barium (or strontium) complex specific for 5'-GG-3'. The Netropsin subunits form a series of consecutive bifurcated hydrogen bonds between amide NHs and lone pair electrons from adenine N3 or thymine O2 atoms on the floor of the minor groove. This pattern of hydrogen-bonding is the same as that observed in the crystal structures of Netropsin and Distamycin A complexed to DNA dodecamer oligonucleotides.³¹⁻³³ The metal cation is heptacoordinated by the podand, contacting the two carboxamide oxygens from the tether's terminal glycolamide groups in addition to the five ether oxygens.³⁴ Such a complex may be capped on one or both sides by phosphate oxygen anions from the nearby DNA backbone, although capping would likely require significant changes in the local DNA conformation. Models indicate that lone pair electrons on the carboxamide oxygens anti to the metal may form specific hydrogen bonds to guanine NH₂ groups that protrude from the floor of the minor groove, consistent with the observed binding specificity for **BNO5E:Fe:M²⁺**. No direct evidence for these hydrogen bonds has been obtained, but they are reasonable in light of the fact that carboxamide oxygen atoms in proteins are often involved in hydrogen bonds with two different hydrogen atoms.³⁵ Steric effects/shape recognition may also contribute to the observed preference of **BNO5E:Fe:M²⁺** for sites containing G:C base pairs. The minor groove of B DNA is significantly wider in regions containing G:C base pairs than in regions containing only

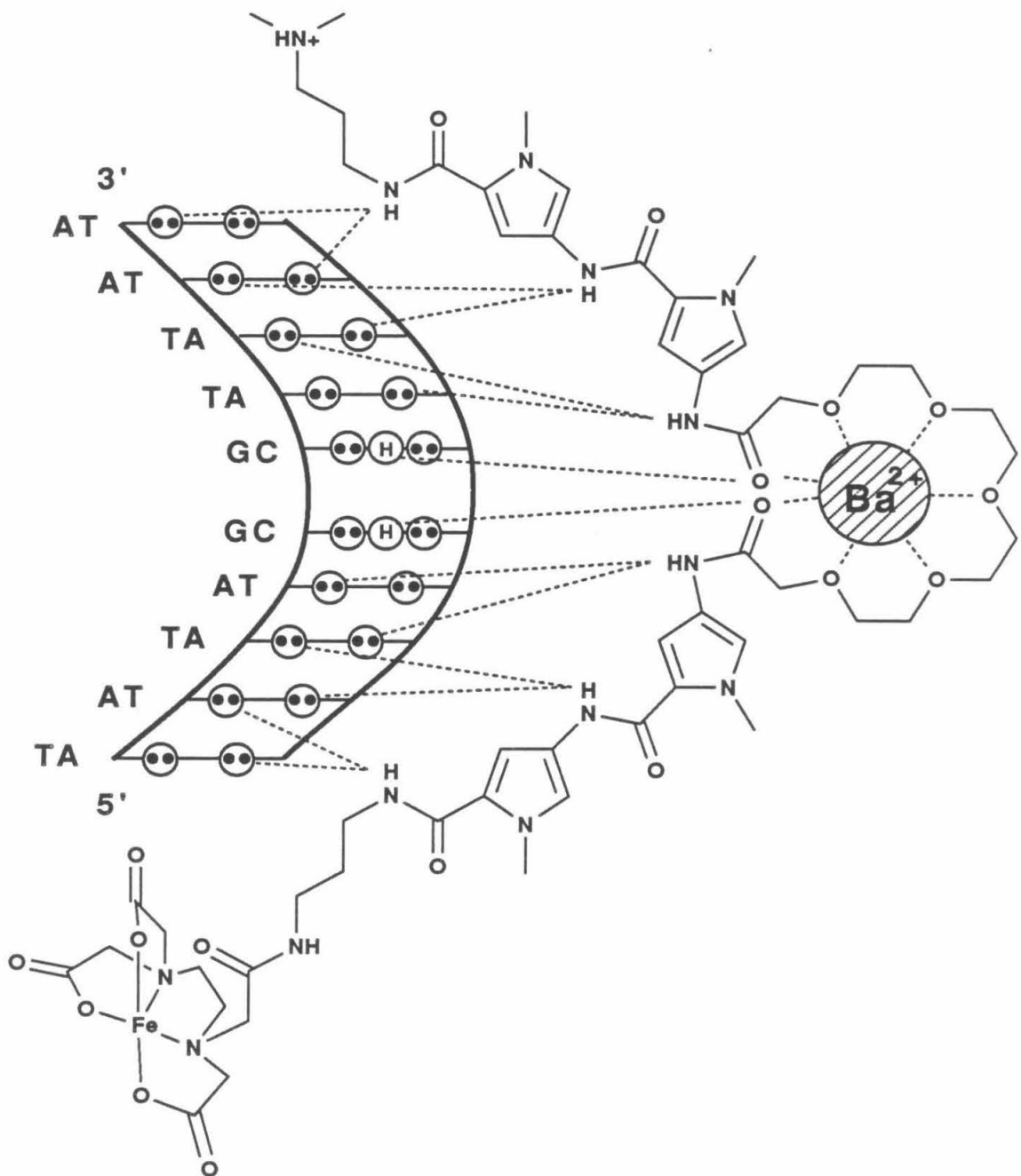


Figure 3.25. Proposed model for the metalloregulated minor groove binding of BNO5E:Fe to the ten base pair sequence 5'-TATAGGTTAA-3' in the presence of barium. Circles with two dots represent lone pairs of electrons on adenine N3, thymine O2, guanine N3, or cytosine O2 atoms at the edges of base pairs on the floor of the minor groove of the right-handed B DNA double helix. Circles with Hs represent guanine N2 amino groups that protrude from the floor of the minor groove.

A:T base pairs.^{33,36,37} The metal:podand subunit of **BNO5E:Fe:M²⁺** is likely to be more sterically encumbered than the flanking Netropsin subunits, especially if the strontium or barium cations (which prefer high coordination numbers) bear additional water ligands. It might be that bulky **BNO5E:Fe:M²⁺** may be most able to penetrate into the minor groove and form stabilizing electrostatic, dipolar, and van der Waals interactions at sites containing G:C base pairs adjacent to (A:T)₄ sequences.

The DNA affinity cleaving patterns at sequences other than 5'-TATAGGTTAA-3' indicate that metalloregulated monomeric binding to sites of four contiguous A:T base pairs adjacent to a G:C base pair constitutes the dominant DNA binding mode for **BNO5E:Fe** in the presence of strontium or barium. The negative results obtained for DNA binding by **O5NE:Fe** suggests that metalloregulated monomeric binding is more complex than one-half of the model presented in Figure 3.25 in which the upper Netropsin subunit has swung away from the DNA. However, the role of the "unbound" Netropsin subunit during metalloregulated monomeric binding is not known. The results with **O5P5E:Fe** suggest that the intrinsic binding affinity and specificity of this molecule are too great to be detectably altered by the binding of strontium or barium.

Part 2: Negative Metalloregulation in the Sequence-Specific Binding of Synthetic Molecules to DNA.

Results

Design. In light of the positive metalloregulation of **BNO5E:Fe** by strontium or barium cations, we undertook the design of similar molecules in which metallospecificity was altered by changing the nature of the donor atoms in the linkers. The result was a series of homologous Bis(Netropsin)s linked in tail-to-tail fashion by di-, tri-, tetra-, or pentaamine tethers (Figure 3.26). It was expected that the "softer" amino groups of these linkers would exhibit significant affinity for the "softer" transition and post-transition metals.³⁸

Synthesis. The synthesis of Bis(Netropsin) Polyamine-EDTA compounds is exemplified by the synthesis of Bis(Netropsin)-3,6,9-triaminoundecanediamide-EDTA (**BNN3E, IV-68**, Figure 3.27). This scheme is a direct extension of the general procedure described in Chapter One for the synthesis of Bis(Netropsin) Diacid-EDTA compounds, and required the development of a general method for the preparation of protected polyamino diacids. The requisite polyamine precursors, including diethylenetriamine shown in Figure 3.27, were commercially available. These were perteosylated and the terminal sulfonamide groups were *N*-alkylated with *t*-butylbromoacetate to afford *N*-tosyl protected polyamino dicarboxylic acid diester derivatives. The esters were removed under anhydrous acidic conditions. Tosyl groups were removed by reduction³⁹ to afford unprotected polyamino diacid compounds. The amino groups of these sticky materials were then protected with benzyloxycarbonyl (Z) groups. Starting from diethylenetriamine the result was 3,6,9-tri-(Z)-aminoundecanedioic acid **IV-25**. **I-22** was reduced and coupled with an excess of **IV-25** to afford Netropsin-3,6,9-tri-(Z)-aminoundecanamic acid **IV-39**. **IV-129** was reduced and coupled with **IV-39** to afford Boc Bis(Netropsin)-3,6,9-tri-(Z)-aminoundecanediamide **IV-44**. The terminal amino group of **IV-44** was deprotected and coupled with the triethyl ester of EDTA to produce Bis(Netropsin)-3,6,9-tri-(Z)-aminoun-

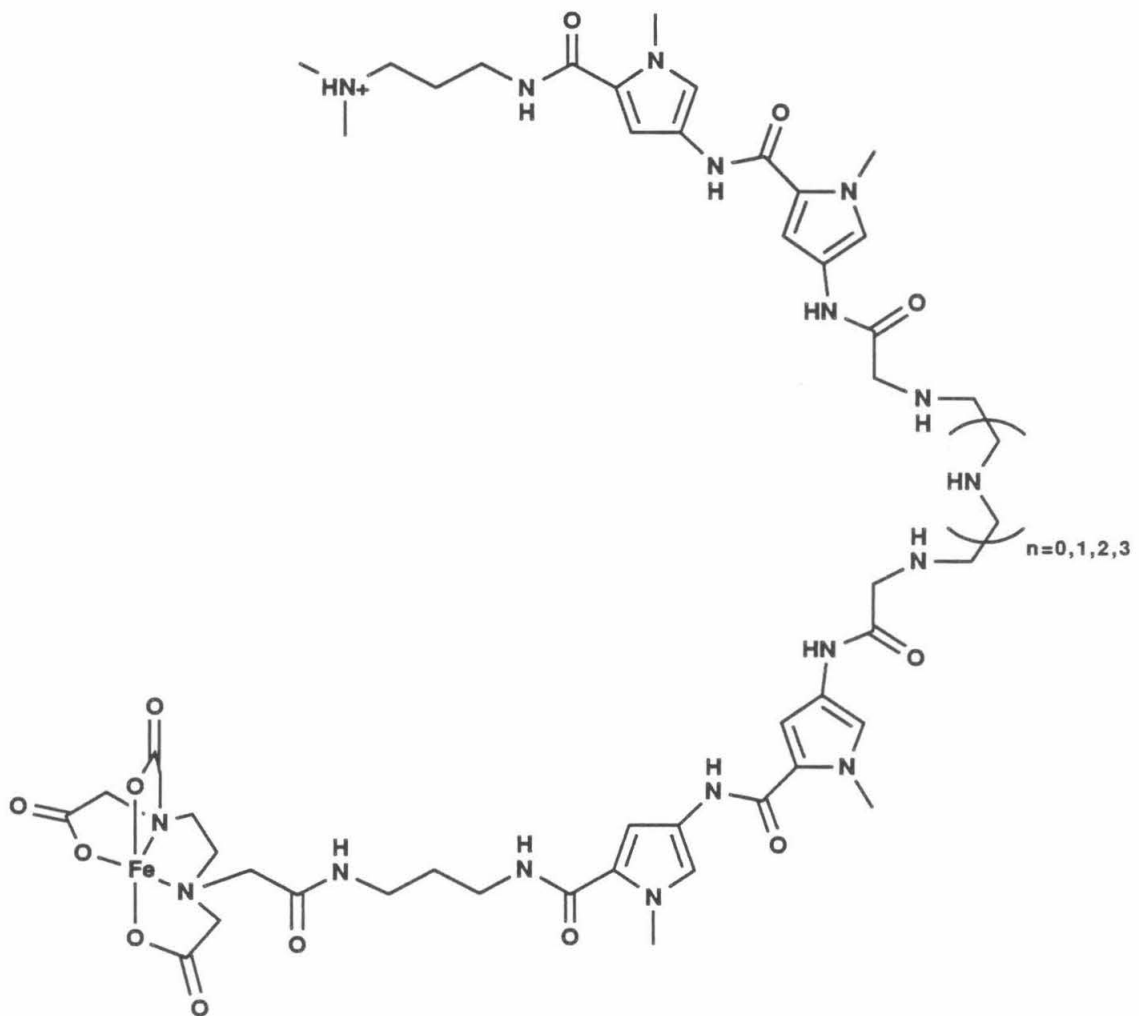


Figure 3.26. Bis(Netropsin) Polyamine-EDTA:Fe compounds. $n = 0$, Bis(Netropsin)-3,6-Diaminoctanediamide-EDTA:Fe (**BNN2E:Fe**); $n = 1$, Bis(Netropsin)-3,6,9-Triaminoundecanediamide-EDTA:Fe (**BNN3E:Fe**); $n = 2$, Bis(Netropsin)-3,6,9,12-Tetraaminotetradecanediamide-EDTA:Fe (**BNN4E:Fe**); $n = 3$, Bis(Netropsin)-3,6,9,12,15-Pentaaminohapedecanediamide-EDTA:Fe (**BNN5E:Fe**).

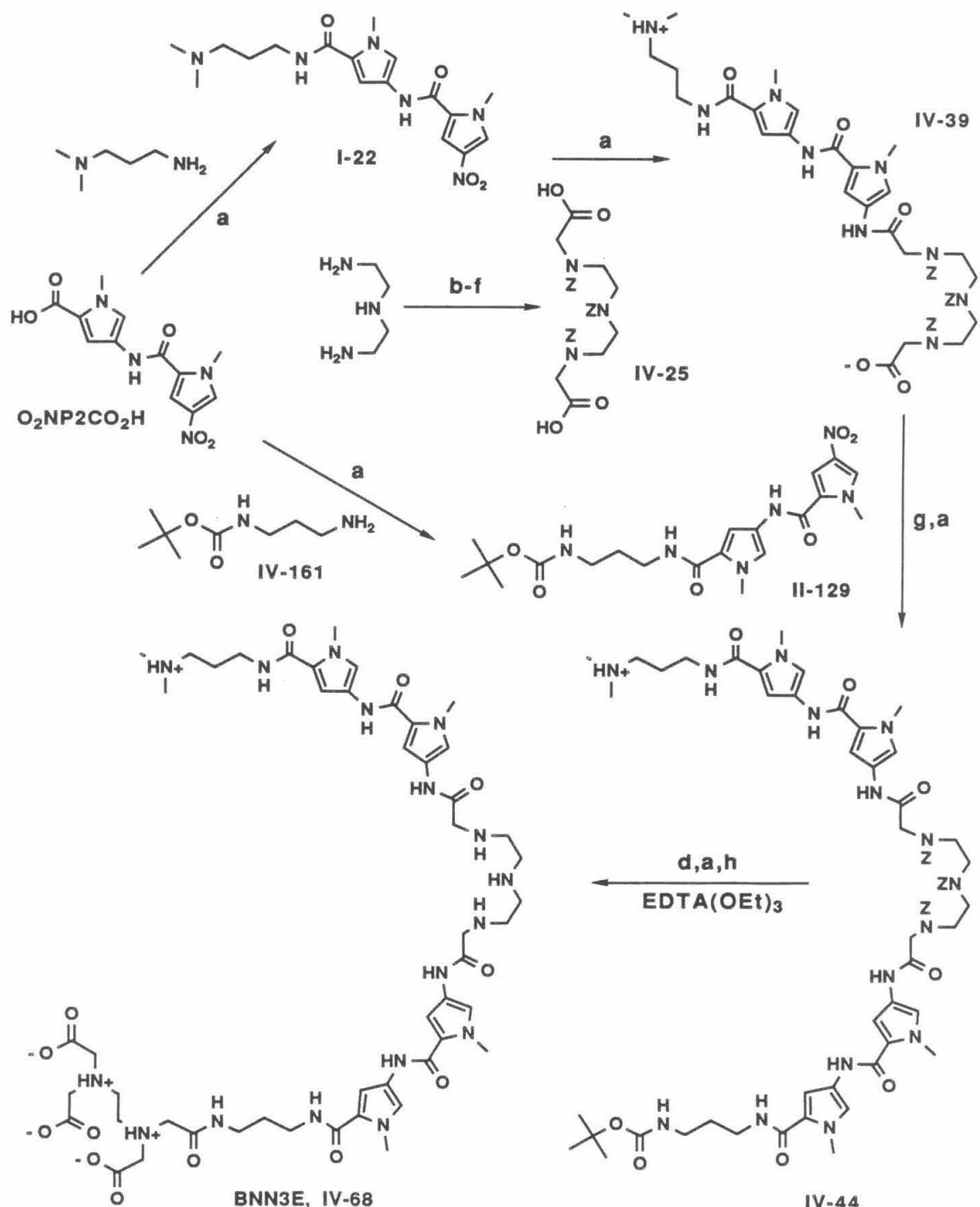


Figure 3.27. Scheme for the synthesis of BNN3E. Reaction conditions: **a**, DCC, HOBT, DMF; **b**, TsCl (1.33 equiv.), NaOH , CH_2Cl_2 , H_2O ; **c**, $\text{BrCH}_2\text{CO}_2\text{C}(\text{CH}_3)_3$, Cs_2CO_3 , DMF; **d**, TFA, CH_2Cl_2 ; **e**, Na/Hg , Na_2HPO_4 , MeOH ; **f**, $\text{C}_6\text{H}_5\text{CH}_2\text{OCOCl}$, NaHCO_3 , H_2O ; **g**, H_2 (3 atm), Pd/C , DMF; **h**, LiOH , MeOH , H_2O .

decanediamide-EDTA, triethyl ester. The Z groups of this material were removed under acidic conditions and EDTA ester groups were removed by hydrolysis under basic conditions to afford **BNN3E**.

DNA Affinity Cleaving. An autoradiograph of DNA double-strand cleavage patterns produced by the Bis(Netropsin) Polyamine-EDTA:Fe compounds on Sty I-linearized, 3'-³²P end-labeled pBR322 plasmid DNA is shown in Figure 3.28. Cleavage reactions were carried out at pH 7.9 under standard conditions determined to be optimal for DNA binding/cleaving by oligo(*N*-methylpyrrolecarboxamide)-EDTA:Fe compounds.¹⁷ DNA cleavage products were separated by agarose gel electrophoresis and visualized by autoradiography. In contrast to the Bis(Netropsin) Polyether-EDTA:Fe compounds described in Part 1 of this chapter, Bis(Netropsin) Polyamine-EDTA:Fe compounds bind and cleave DNA with high efficiency and specificity. **BNN2E:Fe**, **BNN3E:Fe**, **BNN4E:Fe**, and **BNN5E:Fe** bind and cleave DNA with similar efficiency but greater specificity than **P5E:Fe** (Chapter One). DNA binding/cleaving efficiency and specificity increase with the number of linker amino groups among this series of molecules.

Autoradiographs of DNA double-strand cleavage patterns produced by **P5E:Fe** and the Bis(Netropsin) Polyamine-EDTA:Fe compounds at a series of pH values between 5.4 and 9.0 are shown in Figure 3.29. These cleavage patterns were quantified by densitometry and the data displayed in graph format (Figure 3.30). The Bis(Netropsin) Polyamine-EDTA:Fe compounds produce maximal DNA double-strand cleavage near pH 6, while **P5E:Fe** produces maximal cleavage near pH 7.5.

The cleavage patterns produced by the Bis(Netropsin) Polyamine-EDTA:Fe compounds were mapped to pBR322 sequence positions by comparing their electrophoretic mobilities to those of DNA bands in molecular weight marker lanes. Cleavage position and intensity data are presented in histogram form in Figure 3.31. Bis(Netropsin) Polyamine-EDTA:Fe compounds produce cleavage in regions of pBR322 rich in A:T base pairs. The most intense cleavage locus observed near position 3250 maps to the longest contiguous

Figure 3.28

Autoradiograph of DNA double-strand cleavage patterns produced by Bis(Netropsin) Polyamine-EDTA:Fe compounds on Sty I-linearized, 3'-³²P end-labeled pBR322 plasmid DNA in the presence of dioxygen and dithiothreitol. Cleavage patterns were resolved by electrophoresis on a 1% agarose gel. Lanes 2, 4, 6, 8 contain DNA labeled at one end with α -³²P dATP, while lanes 3, 5, 7, 9 contain DNA labeled at the other end with α -³²P TTP. Lanes 1 and 10, molecular weight markers consisting of pBR322 restriction fragments 4363, 3371, 2994, 2368, 1998, 1768, 1372, 995, and 666 bp in length; lanes 2 and 3, **BNN2E:Fe** at 0.50 μ M concentration; lanes 4 and 5, **BNN3E:Fe** at 1.0 μ M concentration; lanes 6 and 7, **BNN4E:Fe** at 0.25 μ M concentration; lanes 8 and 9, **BNN5E:Fe** at 0.25 μ M concentration.

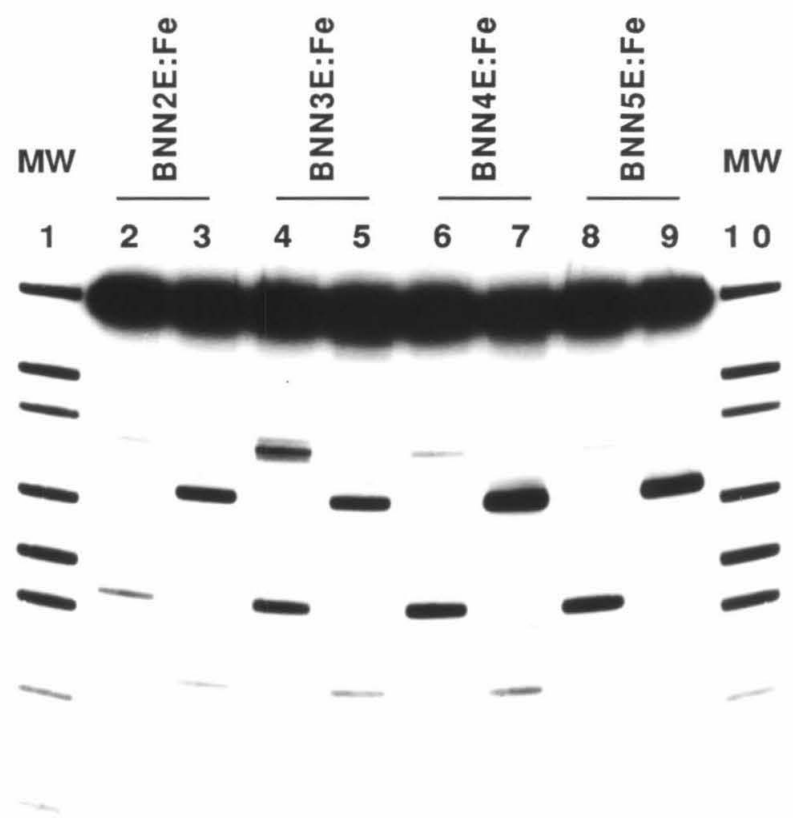
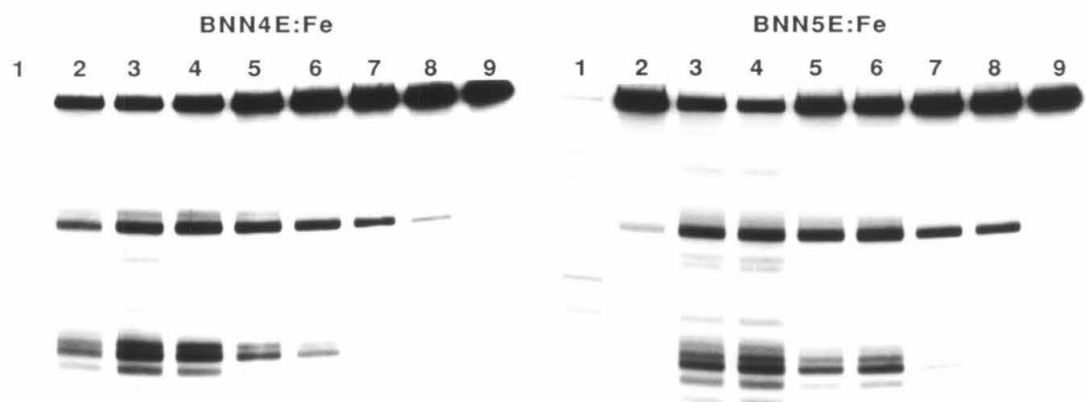
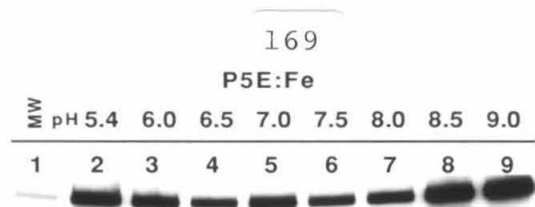


Figure 3.29

Autoradiographs of DNA double-strand cleavage patterns produced by **P5E:Fe** and Bis(Netropsin) Polyamine-EDTA:Fe compounds on Sty I-linearized, 3'-³²P TTP end-labeled pBR322 plasmid DNA in the presence of dioxygen and dithiothreitol, and at a series of pH values. Cleavage patterns were resolved by electrophoresis on 1% agarose gels. Top: 0.75 μ M **P5E:Fe**. Center Left: 1.0 μ M **BNN2E:F**. Center Right: 1.0 μ M **BNN3E:Fe**. Bottom Left: 0.50 μ M **BNN4E:Fe**. Bottom Right: 0.25 μ M **BNN5E:Fe**. Lanes 1, molecular weight markers consisting of pBR322 restriction fragments 4363, 3371, 2994, 2368, 1998, 1768, 1372, 995, and 666 bp in length; lanes 2-9, DNA double-strand cleavage reactions carried out at pH 5.4, 6.0, 6.5, 7.0, 7.5, 8.0, 8.5, and 9.0, respectively.



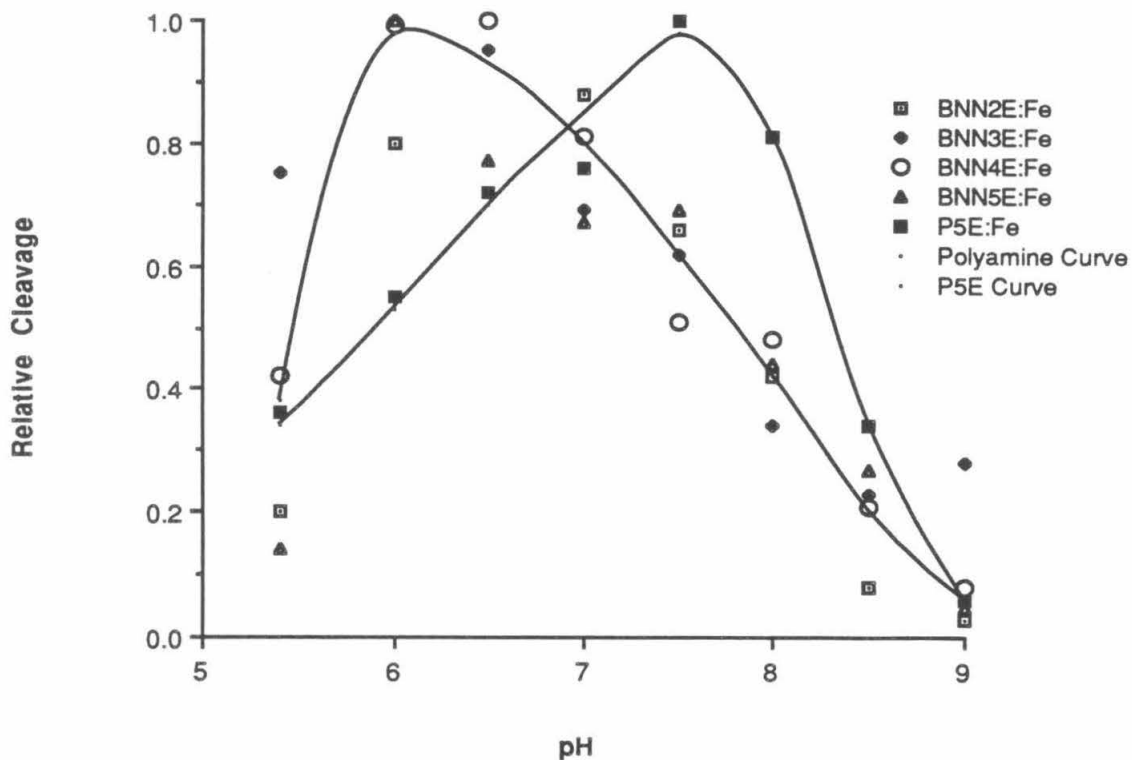


Figure 3.30. Graph of relative DNA double-strand cleavage by P5E:Fe and Bis(Netropsin) Polyamine-EDTA:Fe compounds in the presence of dioxygen and dithiothreitol as a function of reaction pH. Data were generated by optical densitometry of the autoradiographs shown in Figure 3.29 and others. Interpolated curves emphasize trends in the data and differences between the pH dependence of DNA cleavage by P5E:Fe and the Bis(Netropsin) Polyamine-EDTA:Fe compounds.

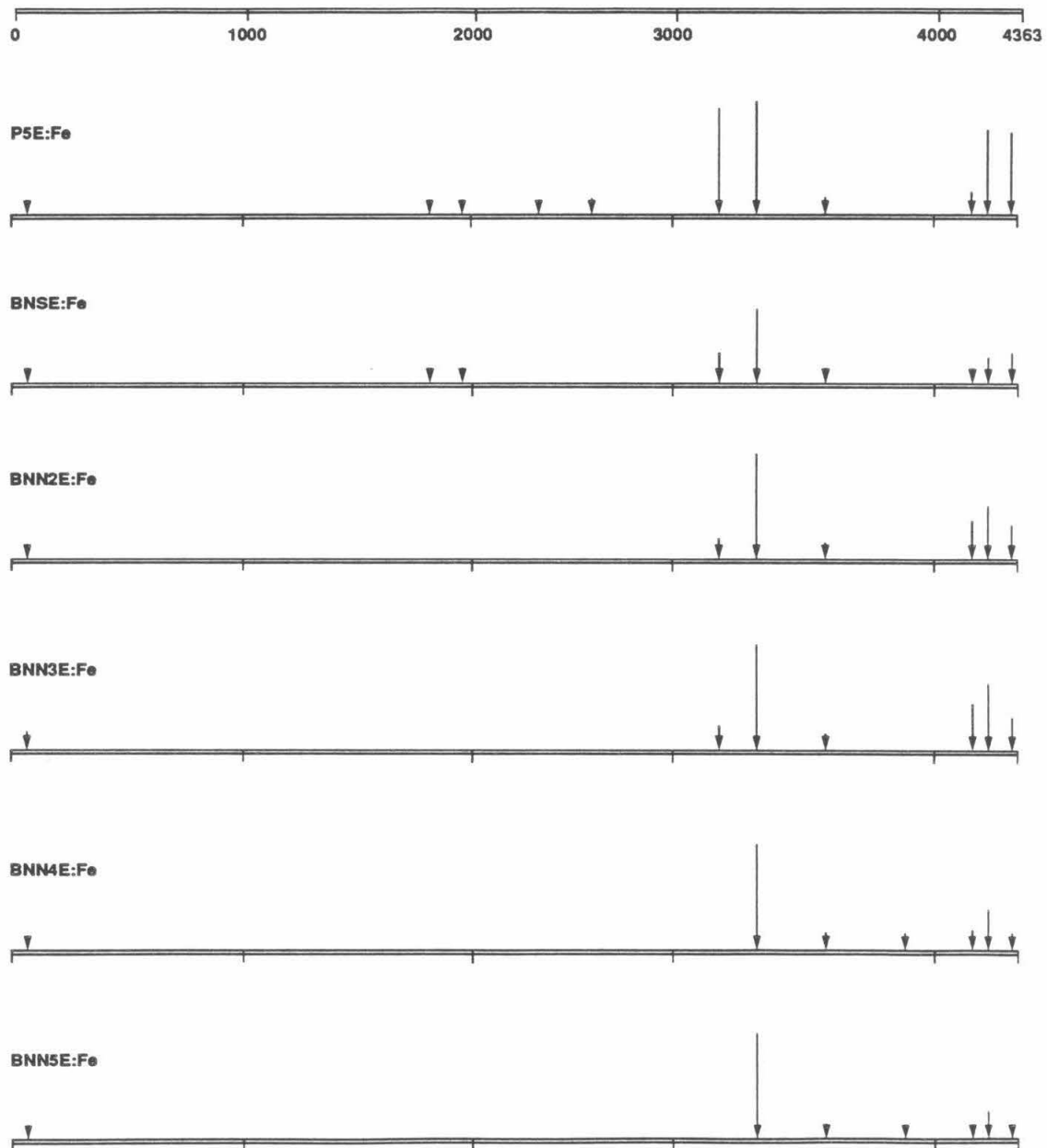


Figure 3.31. Histograms of DNA double-strand cleavage produced by P5E:Fe, BNSE:Fe, and Bis(Netropsin) Polyamine-EDTA:Fe compounds on Sty I-linearized pBR322 plasmid DNA. Lengths of arrows correspond to the relative amounts of cleavage, determined by optical densitometry, at the various cleavage loci. Positions of cleavage were determined by analyzing the measured electrophoretic mobilities of DNA cleavage fragments relative to a standard curve derived from the measured electrophoretic mobilities of marker fragments of known molecular weights.

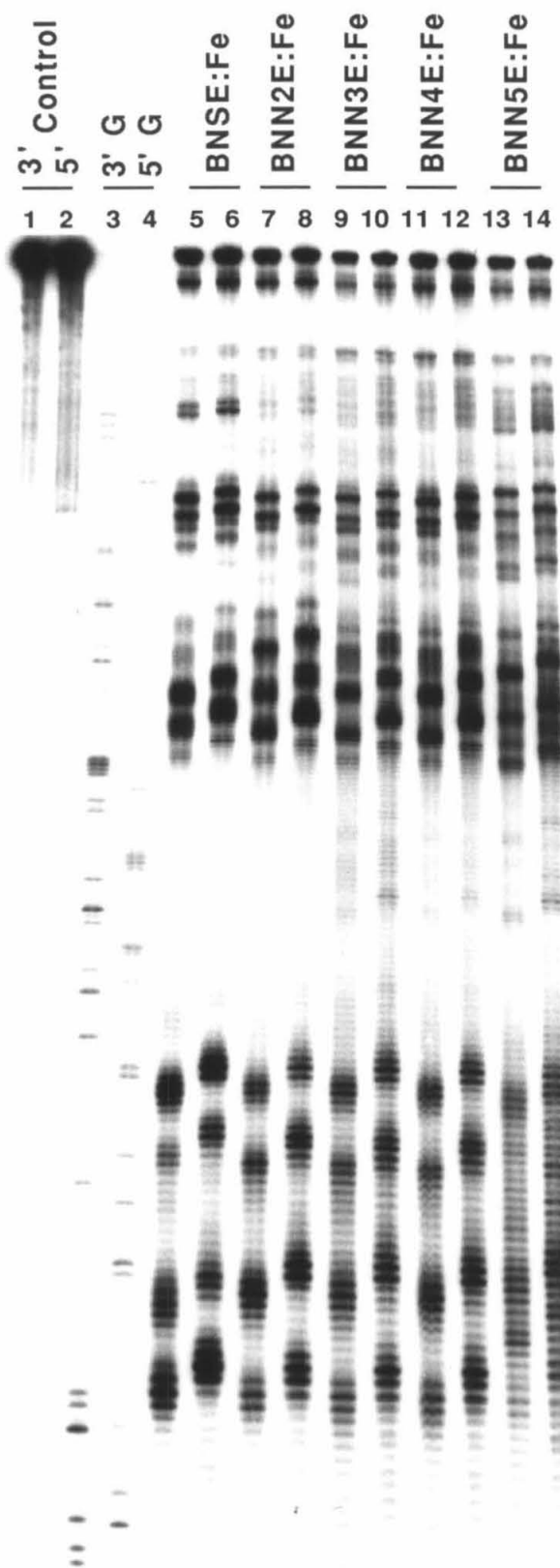
stretch of A:T base pairs (15) on pBR322, 5'-TTTTAAATTAAAAAT-3' (centered at position 3236). Other significant cleavage loci map to the nine base pair sequence 5'-TTTATTTT-3' (centered at position 4237), and the ten base pair sequence 5'-TATTTTATA-3' (centered at position 4325).

The DNA binding/cleaving loci produced by Bis(Netropsin) Polyamine:EDTA:Fe compounds and Bis(Netropsin)-Succinamide-EDTA:Fe (**BNSE:Fe**, Chapter One) were examined at nucleotide resolution. 517 base pair Eco RI/Rsa I restriction fragments from pBR322 were prepared with ^{32}P at either the 3'- or 5' Eco RI end. These fragments contain cleavage loci centered at or near pBR322 positions 4237 and 4325. DNA cleavage reactions were carried out under standard, optimal conditions at pH 6.0 for the Bis(Netropsin) Polyamine-EDTA:Fe compounds and pH 7.5 for **BNSE:Fe**. An autoradiograph of the DNA cleavage patterns produced by these compounds on these restriction fragments, resolved by denaturing polyacrylamide gel electrophoresis and visualized by autoradiography, is shown in Figure 3.32. **BNSE:Fe** and the Bis(Netropsin) Polyamine-EDTA:Fe compounds produce significant cleavage in four regions of the autoradiograph. In the bottom half of the autoradiograph, **BNSE:Fe**, **BNN2E:Fe**, **BNN3E:Fe**, and **BNN4E:Fe** produce cleavage flanking two sites, while **BNN5E:Fe** produces a delocalized pattern of cleavage flanking, within, and between these sites. In the top half of the autoradiograph, **BNSE:Fe** produces strong cleavage flanking two sites and weaker cleavage flanking several additional sites. The Bis(Netropsin) Polyamine-EDTA:Fe compounds produce more uniform cleavage at various sites in this region of the autoradiograph.

The DNA cleavage patterns observed on this autoradiograph were analyzed by densitometry and converted to histogram form (Figure 3.33). Equilibrium minor groove binding sites (boxes in Figure 3.33) were assigned on the basis of the observed 3'-shifted pseudo- C_2 symmetric cleavage patterns.¹⁶ In the lower part of the autoradiograph, **BNSE:Fe** binds to the seven base pair site 5'-ATTTTTA-3'. This site lies within the ten

Figure 3.32

Autoradiograph of DNA cleavage patterns produced by **BNSE:Fe** and Bis(Netropsin) Polyamine-EDTA:Fe compounds on 3'- and 5'-³²P end-labeled 517 bp restriction fragments (Eco RI/Rsa I) from pBR322 plasmid DNA, in the presence of dioxygen and dithiothreitol. Cleavage patterns were resolved on a 1:20 cross-linked 8% polyacrylamide, 45% urea denaturing gel. Odd-numbered lanes contain 3' end-labeled DNA. Even-numbered lanes contain 5' end-labeled DNA. Lanes 1 and 2, uncleaved DNA; lanes 3 and 4, Maxam-Gilbert chemical sequencing G reactions; lanes 5 and 6, **BNSE:Fe** at 0.25 μ M concentration; lanes 7 and 8, **BNN2E:Fe** at 1.0 μ M concentration; lanes 9 and 10, **BNN3E:Fe** at 2.5 μ M concentration; lanes 11 and 12, **BNN4E:Fe** at 1.0 μ M concentration; lanes 13 and 14, **BNN5E:Fe** at 0.50 μ M concentration.



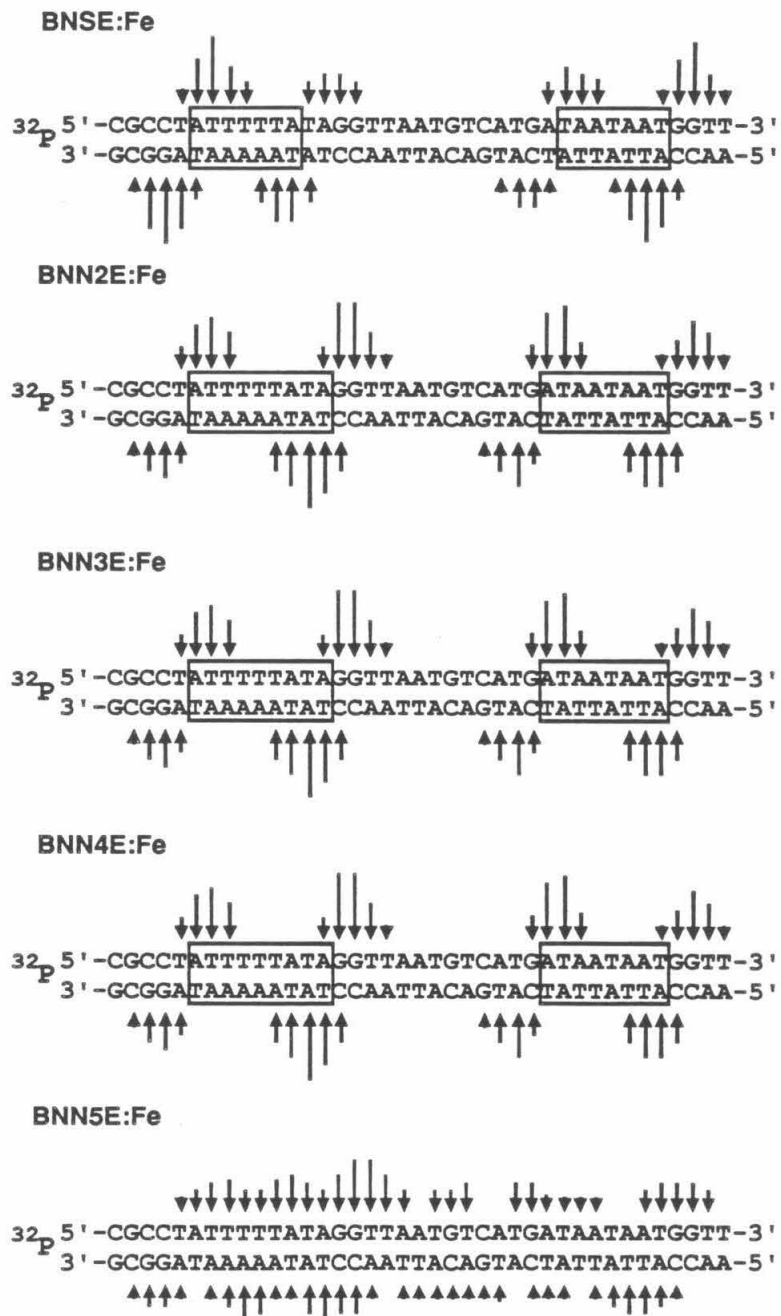


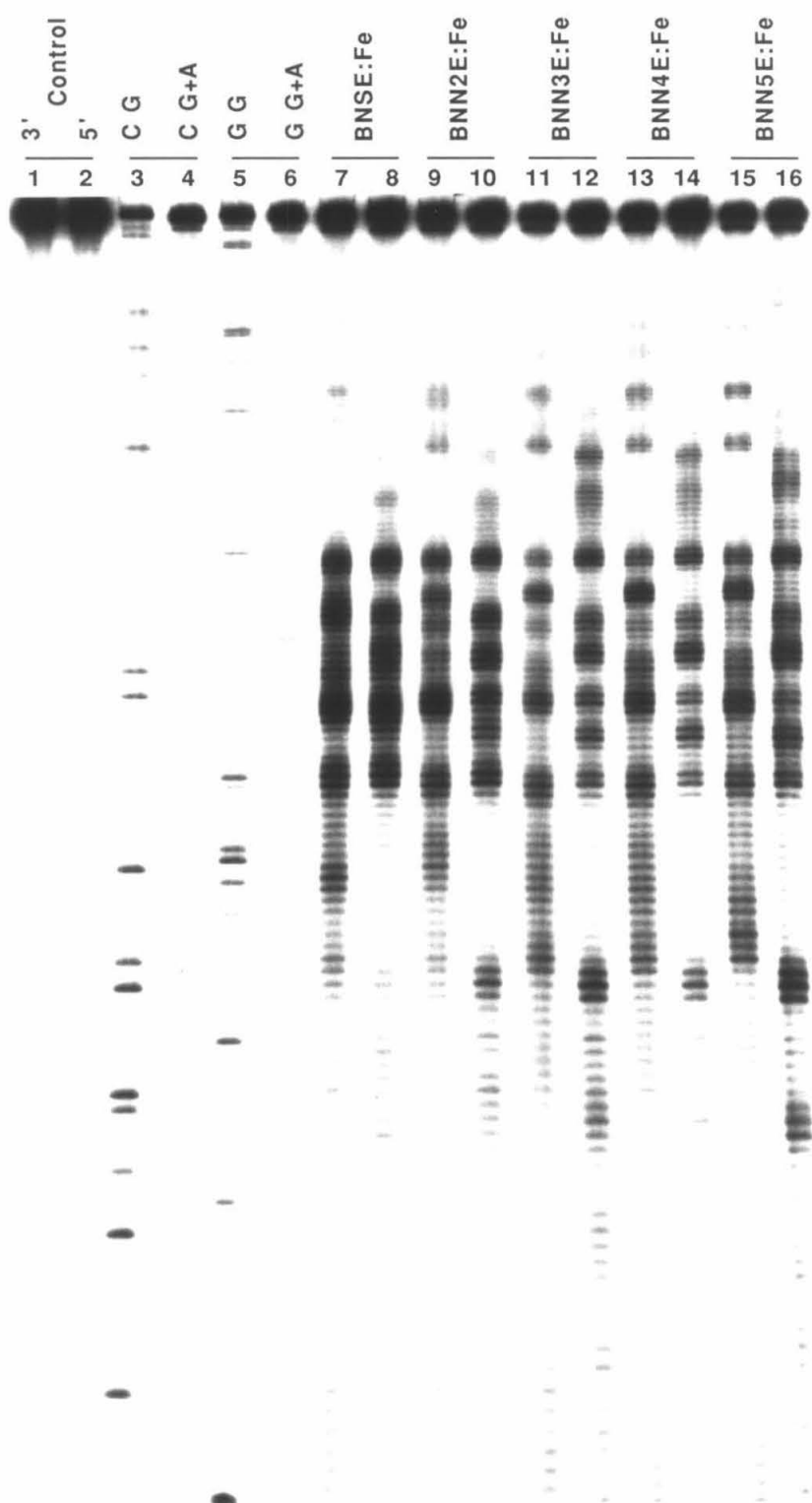
Figure 3.33. Histograms of DNA cleavage produced by BNSE:Fe and Bis(Netropsin) Polyamine-EDTA:Fe compounds on the 517 bp DNA restriction fragment (Eco RI/Rsa I) from plasmid pBR322 DNA. Lengths of arrows correspond to the relative amounts of cleavage, determined by optical densitometry, which result in removal of the indicated base. Sequence positions of cleavage were determined by comparing the electrophoretic mobilities of DNA cleavage fragments to bands in Maxam-Gilbert chemical sequencing lanes. DNA minor groove binding sites (boxed) were assigned from the observed cleavage patterns and the model described by Taylor, Schultz, and Dervan (Reference 16).

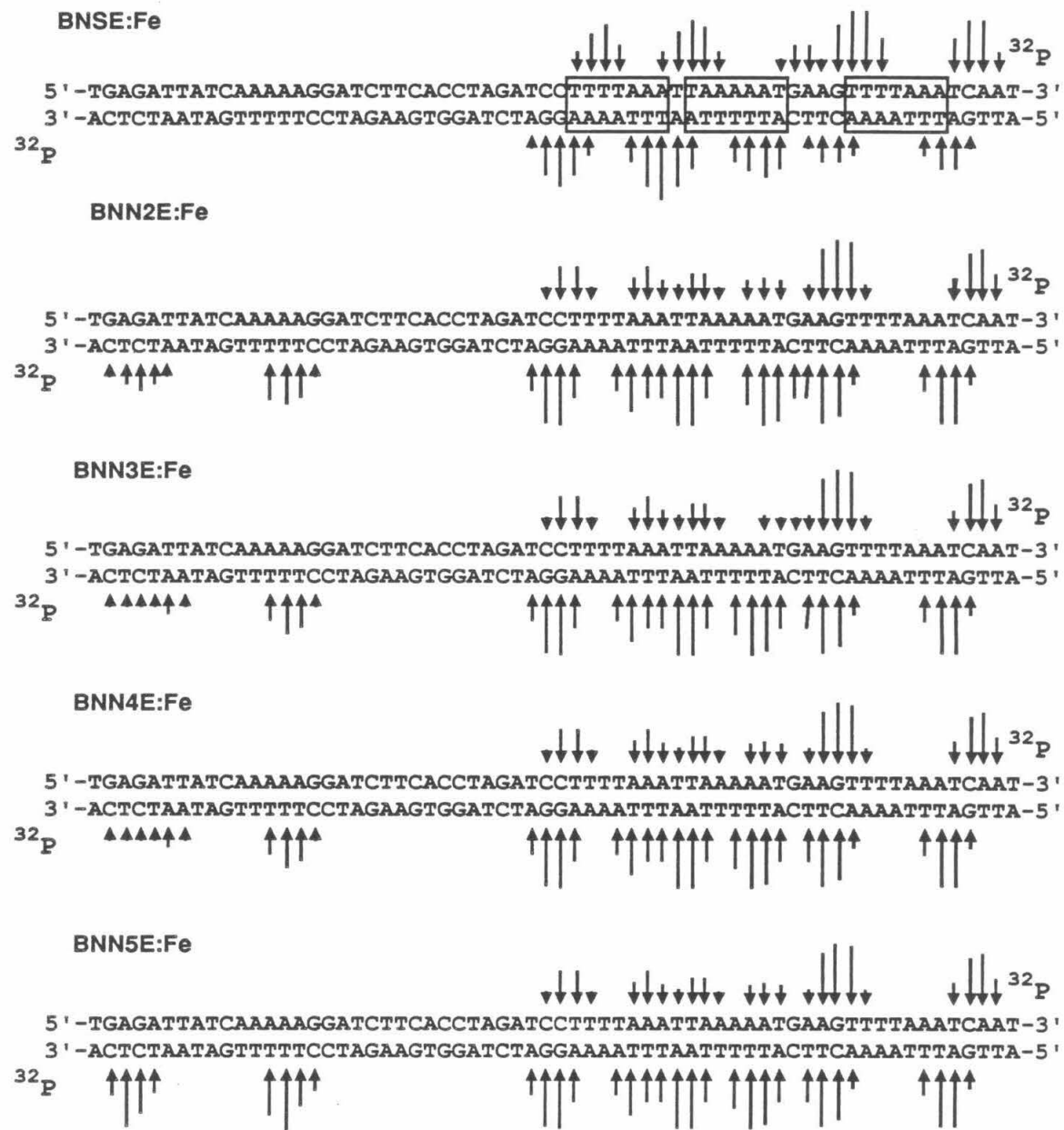
base pair A:T sequence centered at pBR322 position 4325 and mapped by double-strand affinity cleaving analysis. In the lower middle part of the autoradiograph, **BNSE:Fe** binds to the seven base pair site 5'-TAATAAT-3'. In the lower part of the autoradiograph, **BNN2E:Fe**, **BNN3E:Fe**, and **BNN4E:Fe** exhibit the nine base pair binding site 5'-ATTTTATA-3'. In the lower middle of the autoradiograph these molecules bind to the eight base pair binding site 5'-ATAATAAT-3'. **BNN5E:Fe** does not localize to any particular sequence in this part of the autoradiograph, but rather produces less specific cleavage throughout this A:T rich region. The major binding site for **BNSE:Fe** observed in the upper middle part of this autoradiograph has previously been assigned as the seven base pair sequence 5'-TATTTT-3' (Chapter One). The DNA cleavage patterns are not well-resolved in this region of the autoradiograph shown in Figure 3.32. However, by comparing the partially resolved cleavage patterns produced by **BNSE:Fe** and the Bis(Netropsin) Polyamine-EDTA:Fe compounds, the major DNA binding site for **BNN2E:Fe**, **BNN3E:Fe**, and **BNN4E:Fe** in this region appears to be the nine base pair sequence 5'-TTTATTTT-3'. **BNN5E:Fe** does not localize to a single major binding site in this region.

To examine the DNA locus at which these molecules produce the most intense double-strand cleavage, 169 base pair Dde I restriction fragments were prepared with ^{32}P at either 3' end. These restriction fragments span pBR322 positions 3158 to 3327, and were cleaved by **BNSE:Fe** and Bis(Netropsin) Polyamine-EDTA:Fe compounds under standard, optimal conditions at pH 6.0 for the Bis(Netropsin) Polyamine-EDTA:Fe compounds and pH 7.5 for **BNSE:Fe**. DNA cleavage products were separated by denaturing polyacrylamide gel electrophoresis and visualized by autoradiography. An autoradiograph of the cleavage patterns produced is shown in Figure 3.34. These molecules produce multiple cleavage envelopes in the upper middle part of the autoradiograph. The cleavage patterns were analyzed by densitometry and converted to histogram form (Figure 3.35). From the cleavage patterns, three closely spaced seven base

Figure 3.34

Autoradiograph of DNA cleavage patterns produced by **BNSE:Fe** and Bis(Netropsin) Polyamine-EDTA:Fe compounds on 3'-³²P end-labeled 169 bp Dde I restriction fragments from pBR322 plasmid DNA in the presence of dioxygen and dithiothreitol. Cleavage patterns were resolved on a 1:20 cross-linked 8% polyacrylamide, 45% urea denaturing gel. Lanes 1,3,4,7,9,11,13,15, DNA labeled at one 3' end with ³²P dCTP. Lanes 2,5,6,8,10,12,14,16, DNA labeled on the opposite strand at the 3' end with ³²P dGTP. Lanes 1 and 2, uncleaved DNA; lanes 3 and 5, Maxam-Gilbert chemical sequencing G reactions; lanes 4 and 6, Maxam-Gilbert chemical sequencing G+A reactions; lanes 7 and 8, **BNSE:Fe** at 0.25 μ M concentration; lanes 9 and 10, **BNN2E:Fe** at 1.0 μ M concentration; lanes 11 and 12, **BNN3E:Fe** at 2.5 μ M concentration; lanes 13 and 14, **BNN4E:Fe** at 1.0 μ M concentration; lanes 15 and 16, **BNN5E:Fe** at 0.50 μ M concentration.





pair binding sites for **BNSE:Fe** may be assigned, 5'-TTTTAAA-3', 5'-TTAAAAAA-3', and 5'-TTTAAAT-3'. Bis(Netropsin) Polyamine-EDTA:Fe compounds produce more complex patterns of cleavage in this A:T rich region, making confident assignment of specific binding sites difficult.

The DNA binding/cleaving properties of the Bis(Netropsin) Polyamine-EDTA:Fe compounds were not enhanced when cleavage reactions were carried out in the presence of various main group, transition, lanthanide, or actinide metal cations. However, it was found that the DNA binding/cleaving efficiencies of these molecules were reduced by preincubating them with K_2PdCl_4 prior to diluting them and adding them to a buffered solution of DNA substrate and carrier DNA for affinity cleaving reactions. This effect was not observed with **P5E:Fe**. Autoradiographs of DNA double-strand cleavage produced by **P5E:Fe** and Bis(Netropsin) Polyamine-EDTA:Fe compounds after preincubation in the absence of palladium, or in the presence of palladium at a range of concentrations, are shown in Figure 3.36. The cleavage patterns were quantified by densitometry and the data displayed in graph format (Figure 3.37). DNA cleavage by **BNN2E:Fe**, **BNN3E:Fe**, **BNN4E:Fe**, and **BNN5E:Fe** decreases upon preincubation with increasing concentrations of K_2PdCl_4 , but DNA cleavage by **P5E:Fe** is relatively unaffected upon preincubation with K_2PdCl_4 .

Discussion

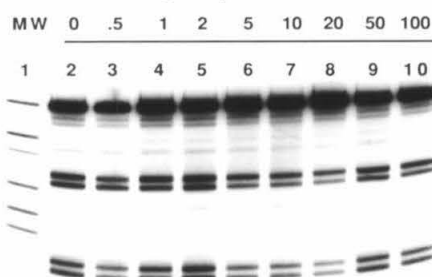
The general procedure developed in Chapter One for the preparation of Bis(Netropsin) Diacid-EDTA compounds has been successfully extended to the synthesis of Bis(Netropsin)-EDTA compounds linked by a series of homologous polyamino diacids. In addition, a general procedure for the synthesis of free and protected polyamino diacid derivatives has been developed.

The iron complexes of Bis(Netropsin) Polyamine-EDTA compounds produce strong and specific cleavage of B form DNA in regions rich in A:T base pairs. Polyamine

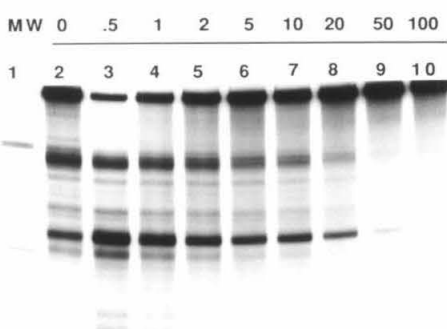
Figure 3.36

Autoradiographs of DNA double-strand cleavage patterns produced by **P5E:Fe(III)** and Bis(Netropsin) Polyamine-EDTA:Fe(III) compounds on Sty I-linearized, 3'-³²P end-labeled pBR322 plasmid DNA, in the presence of dioxygen and ascorbic acid, after preincubation in the absence and presence of palladium(II) cations. Cleavage patterns were resolved by electrophoresis on 1% agarose gels. Top: **P5E:Fe(III)** (0.50 μ M) with 3'-³²P TTP end-labeled DNA. Center Left: **BNN2E:Fe(III)** (5.0 μ M) with 3'-³²P dATP end-labeled DNA. Center Right: **BNN3E:Fe(III)** (1.0 μ M) with 3'-³²P dATP end-labeled DNA. Bottom Left: **BNN4E:Fe(III)** (0.25 μ M) with 3'-³²P TTP end-labeled DNA. Bottom Right: **BNN5E:Fe(III)** (0.25 μ M) with 3'-³²P TTP end-labeled DNA. Lanes 1, molecular weight markers; lanes 2, DNA double-strand cleavage in the absence of added cations; lanes 3-10, DNA double-strand cleavage after preincubation with 0.5, 1.0, 2.0, 5.0, 10, 20, 50, 100 equiv. K_2PdCl_4 , respectively.

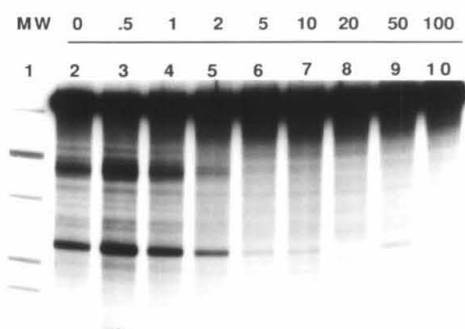
$[K_2PdCl_4] / [P5E:Fe]$



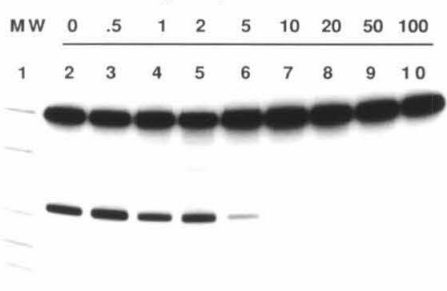
$[K_2PdCl_4] / [BNN2E:Fe]$



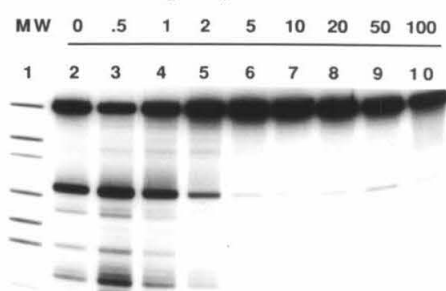
$[K_2PdCl_4] / [BNN3E:Fe]$



$[K_2PdCl_4] / [BNN4E:Fe]$



$[K_2PdCl_4] / [BNN5E:Fe]$



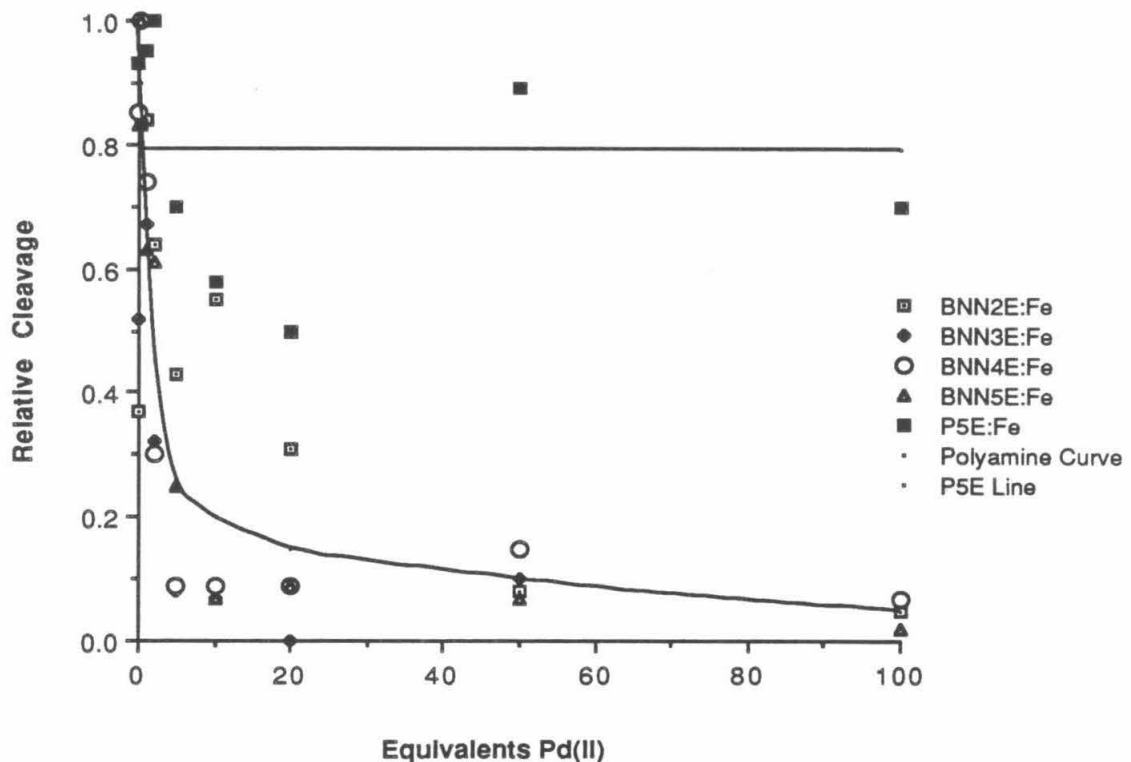


Figure 3.37. Graph of relative DNA double-strand cleavage by P5E:Fe(III) and Bis(Netropsin) Polyamine-EDTA:Fe(III) compounds in the presence of dioxygen and ascorbic acid as a function of equivalents palladium(II) added for pre-incubation. Data were generated by optical densitometric analysis of the autoradiographs shown in Figure 3.40. Interpolated curves emphasize trends in the data and differences between P5E:Fe(III) and the Bis(Netropsin) Polyamine-EDTA:Fe(III) compounds.

linkers should be partially protonated in the physiological pH range, increasing the positive charge on these molecules. In water, ethylenediamine, diethylenetriamine, triethylenetetraamine, and tetraethylenepentaamine all have at least one pK_a value in the range 6.5 to 9.0.⁴⁰ This feature would be expected to stabilize complexes of Bis(Netropsin) Polyamine-EDTA:Fe compounds with the DNA polyanion, and to increase with the number of amino groups in the linker. That Bis(Netropsin) Polyamine-EDTA:Fe compounds produce maximal DNA cleavage near pH 6 while **P5E:Fe** produces maximal cleavage near pH 7.5 supports the notion that linker protonation is important to the binding of these molecules to DNA.

It has been calculated that polyamines prefer to bind to B DNA in the minor groove at A:T rich regions, where they may form specific hydrogen bonds with adenine N3 and thymine O2 atoms, as well as interact favorably with a well of negative electrostatic potential.^{41,42} However, the conjugate spermidine:EDTA:Fe was found by Youngquist to produce nonspecific DNA cleavage.¹⁷ The high DNA binding specificity for A:T rich regions of DNA exhibited by Bis(Netropsin) Polyamine-EDTA:Fe compounds dictate that at a minimum, partially protonated polyamine linkers do not detract from the intrinsic DNA binding specificity of a Bis(Netropsin). At a maximum, partially protonated polyamine linkers may be sequence-specific recognition elements for A:T base pairs in the minor groove of B DNA. The high-resolution DNA affinity cleaving results with **BNN2E:Fe**, **BNN3E:Fe**, and **BNN4E:Fe** suggest that the linkers of these molecules can interact with the minor groove of B DNA at sites containing A:T base pairs in a number of ways which allow these Bis(Netropsin)s to occupy binding sites of eight or nine contiguous A:T base pairs. Limiting binding models for this behavior may be envisioned. When bound to sites of nine A:T base pairs, polyamine linkers may adopt an extended conformation, penetrate deeply within the minor groove, and form specific hydrogen bonds between amine/ammonium NHs and adenine N3 and/or thymine O2 atoms. When bound to an eight base pair A:T site, polyamine linkers may bow away from the floor of the minor groove

and interact with the phosphate backbone of the DNA. This brings the Netropsin subunits into closer juxtaposition where each binds to one of two adjacent sites of four contiguous A:T base pairs. **BNN5E:Fe** produces the most specific DNA double-strand cleavage among this series of molecules, yet also exhibits the least propensity to localize to specific binding sites within sequences of contiguous A:T base pairs. Perhaps the pentaamine linker of **BNN5E:Fe** is too long to allow this molecule to bind to sites of ten or fewer contiguous base pairs, and does not discriminate among different A:T sequences enough to allow **BNN5E:Fe** to localize to a major site within the tract of 15 contiguous A:T base pairs.

Preincubation with increasing concentrations of K_2PdCl_4 has little effect on the ability of **P5E:Fe(III)** to produce DNA cleavage. Thus, the finding that preincubation of Bis-(Netropsin) Polyamine-EDTA:Fe(III) compounds with increasing concentrations of K_2PdCl_4 progressively reduces their ability to produce DNA cleavage constitutes a *negative metalloc regulatory* phenomenon. The results are consistent with a model in which palladium(II) cations form kinetically inert complexes and/or aggregates with the polyamine linkers of Bis(Netropsin) Polyamine-EDTA:Fe compounds. These complexes/aggregates may have steric, electrostatic, and/or hydrogen-bonding properties that reduce their ability to interact with DNA.

Part 3: Design and Synthesis of Metalloregulated DNA Binding/Cleaving Proteins.

Results and Discussion

Design. Given our success in the design and synthesis of both positively and negatively metalloregulated, sequence-specific DNA binding small molecules, we undertook the design and synthesis of a metalloregulated DNA binding protein. Our approach was to incorporate a metal-binding subunit of known metallospecificity within the structure of a synthetically accessible protein of known DNA binding sequence specificity. The protein chosen for this study was the C-terminal 52 amino acid fragment (residues 139-190) of the Hin recombinase from *Salmonella*. (Figure 3.38). It has been shown that this segment of Hin recombinase may be prepared by solid-phase protein synthesis (SPPS), and that it binds to native Hin DNA half-sites for recombination.⁴³ Sequence similarities and algorithms for the prediction of protein secondary structures from amino acid sequences suggest that Hin(139-190) bears the conserved "α-helix-β-turn-α-helix" motif found in a variety of DNA binding proteins,^{44,45} as well as an additional N-terminal helix connected with the helix-turn-helix core by a turn or loop structure.^{46,47}

To introduce a metal-binding subunit within the Hin(139-190) sequence, a pentaether "ionoturn" was designed to be substituted for two residues of a β-turn. CPK models indicate that the ionoturn depicted in Figure 3.38 maintains the intramolecular hydrogen bond and directionality of incoming and outgoing peptide chains found in Type I or II β-turns.⁴⁸

Synthesis. Boc amino acid **IV-176** was required for introduction of the ionoturn by SPPS.⁴⁹ **IV-176** was prepared as outlined in Figure 3.38. Pentaethyleneglycol was condensed with one equivalent of ethyl diazoacetate to afford hydroxy ester **IV-150**. **IV-150** was converted to the azide derivative **IV-160**. The azido group of **IV-160** was

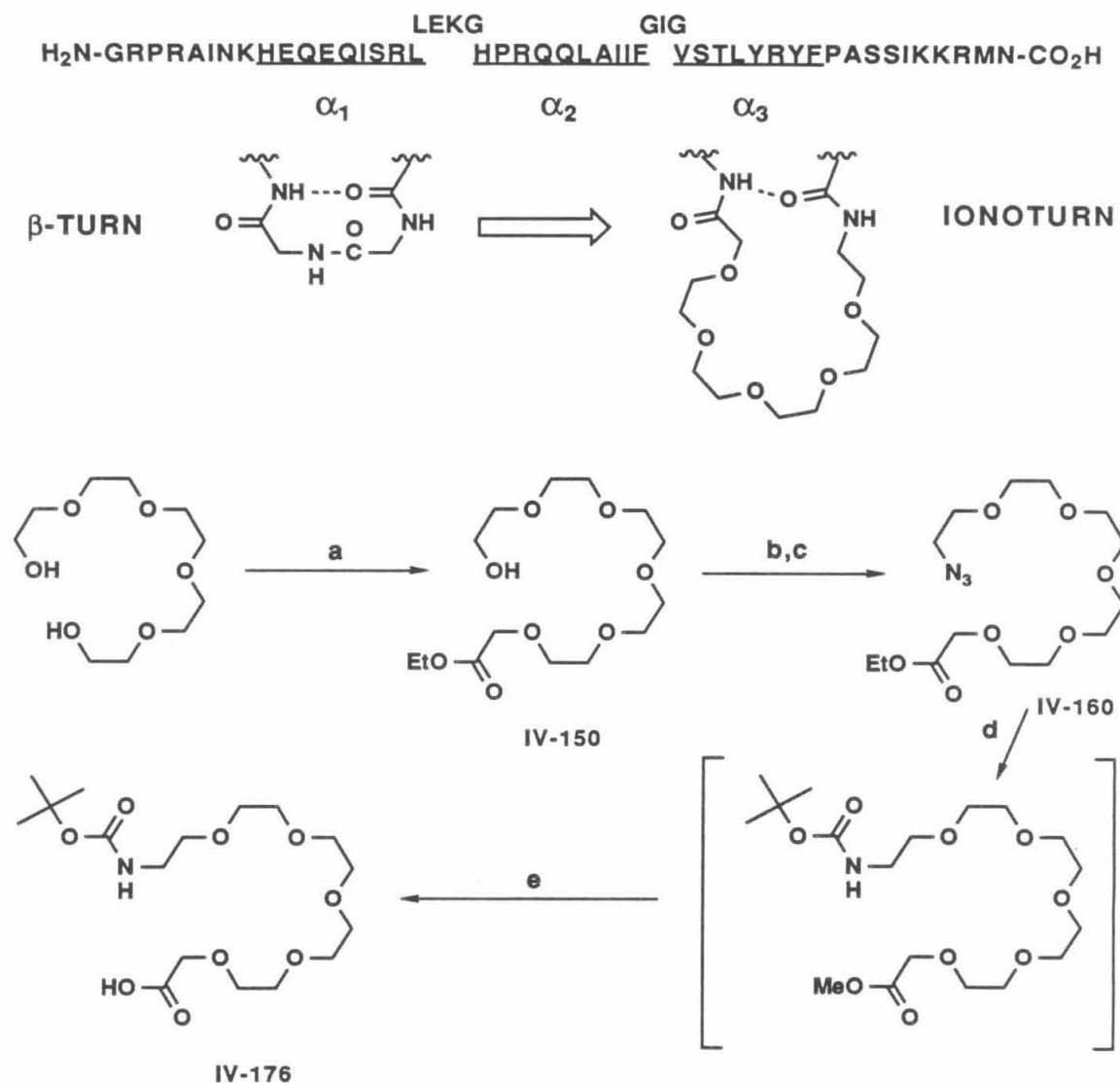


Figure 3.38. Design and synthesis of a peptide ionoturn. Top: Amino acid sequence for the carboxyl-terminal 52 amino acid residues (positions 139-190) of the Hin Recombinase from *Salmonella Typhimurium*. Underlined regions α_1 , α_2 , α_3 constitute predicted α -helical segments, while the raised sequences LEKG and GIG constitute predicted β -turn or loop segments. Center: Design of an amino acid that may form an ionophoric turn structure (ionoturn) which retains geometric and hydrogen-bonding features found in peptide β -turns. Bottom: Scheme for the synthesis of the protected ionophoric amino acid Boc 17-Amino-3,6,9,12,15-Pentaoxaheptadecanoic acid (IV-176, Lower Left). Reaction conditions: a, $\text{N}_2\text{CH}_2\text{CO}_2\text{Et}$ (1.0 equiv.), $\text{Rh}_2(\text{OAc})_4$ (0.01 equiv.), Et_2O ; b, TsCl , $\text{C}_5\text{H}_5\text{N}$; c, LiN_3 , DMF , 80°C ; d, H_2 (3 atm), PtO_2 , $[(\text{H}_3\text{C})_3\text{CO}_2\text{C}]_2\text{O}$, MeOH ; e, LiOH (1.5 equiv.), MeOH , H_2O .

reduced and protected *in situ* to afford a Boc amino acid ester, which was hydrolyzed to afford Boc 18-amino-3,6,9,12,15,17-pentaoxaheptadecanoic acid **IV-176**.

Five different Hin(139-190) ionomutant proteins were prepared in which the ionoturn was incorporated in place of five different dipeptide subunits in predicted turn or loop regions of the native protein (Figure 3.39). The proteins were synthesized by a combination of manual and automated SPPS procedures. By quantitative ninhydrin analysis,⁵⁰ **IV-176** was found to couple as efficiently as commercially available Boc α -amino acids.

In order to study the DNA binding properties of these Hin derivatives by DNA affinity cleaving, in the absence and presence of metal cations, EDTA was appended to the N-termini of the proteins at the end of SPPS. James Sluka had previously developed tribenzyl EDTA-Gaba (**BEG**) as a reagent for the introduction of EDTA into synthetic peptides. **BEG** was used to produce EDTA-Gabe-Hin(139-190), a synthetic, sequence-specific DNA binding/cleaving protein.^{46,47} We have more recently identified tricyclohexyl EDTA (**TriCyE**, Figure 3.40) as a reagent superior to **BEG**. **TriCyE** may be synthesized in large quantities in a single synthetic step. **TriCyE** is more stable than **BEG** and offers more flexibility than **BEG** with regard to the linker which joins the EDTA subunit to the peptide chain. **TriCyE** couples efficiently to resin-bound peptides and is cleanly deprotected by liquid HF under the normal conditions.⁵¹ Hin(139-190) ionomutant proteins were appended with Boc 4-aminobutanoic acid (Gaba) followed by **TriCyE**. The protected resin-bound proteins were deprotected using liquid HF, and purified by semi-preparative reverse-phase HPLC. Figure 3.41 shows HPLC chromatograms of one of the synthetic mutant proteins before and after purification. The presence of the ionoturn and EDTA subunits in each of the five proteins was ascertained by NMR spectroscopy. Figure 3.42 shows the 400 MHz ^1H NMR spectrum of one protein. In this spectrum of a protein of MW \sim 6000, the peak near 3.6 ppm diagnostic for the ionoturn and the three peaks near 4 ppm diagnostic for EDTA are clearly visible.

LEKG **GIG**
H₂N-GRPRAINKHEQEIQISRL HPRQQLAIE YSTLYRYFPASSIIKKRMN-CO₂H
 α_1 **α_2** **α_3**

Mutant 1 (IV-225): 99.75% / Step

--KG GIG
EDTA-Gaba-GRPRAINKHEQQISRL HPROQQLAIIF VSTLYRYFPASSIKKRMN

Mutant 2 (IV-235): 99.81% / Step

L--G GIG
EDTA-Gaba-GRPRAINKHEQEQISRL HPRQQLAIIF VSTLYRYFPASSIKKRMN

Mutant 3 (IV-243): 99.31% / Step

LE- GIG
EDTA-Gaba-GRPRAINKHEQEQISRL HPRQQLAIIF VSTLYRYFPASSIKKRMN

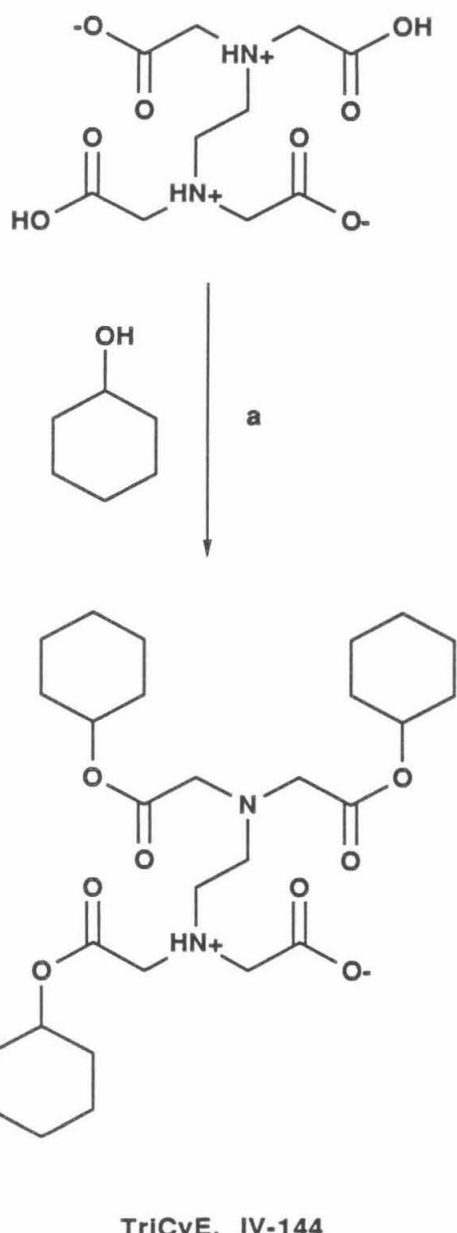
Mutant 4 (IV-208): 99.65% / Step

LEKG --G
EDTA-Gaba-GRPRAINKHEQE**QISRL** HPRQQLAI**IF** VSTLYRYFPASSIKKRMN

Mutant 5 (IV-216): 99.36% / Step

LEKG G--
EDTA-Gaba-GRPRAINKHEQEQLSRL HPRQQLAIIF VSTLYRYFPASSIKKRMN

Figure 3.39. Structures of ionomutant proteins prepared and average per step yields for the solid-phaseprotein syntheses. The double dash (--) indicates the two amino acid residues replaced by the ionophoric amino acid shown in Figure 3.38.



TrICyE, IV-144

Figure 3.40. Synthesis of EDTA, Tricyclohexyl ester (TriCyE). Reaction conditions: a, H_2SO_4 (cat.), 115°C .

Figure 3.41

Analytical reverse-phase HPLC chromatograms of ionomutant 1 protein. Top: Chromatogram of crude peptide mixture obtained after HF cleavage and deprotection. Bottom: Chromatogram of material after purification by reverse-phase HPLC.

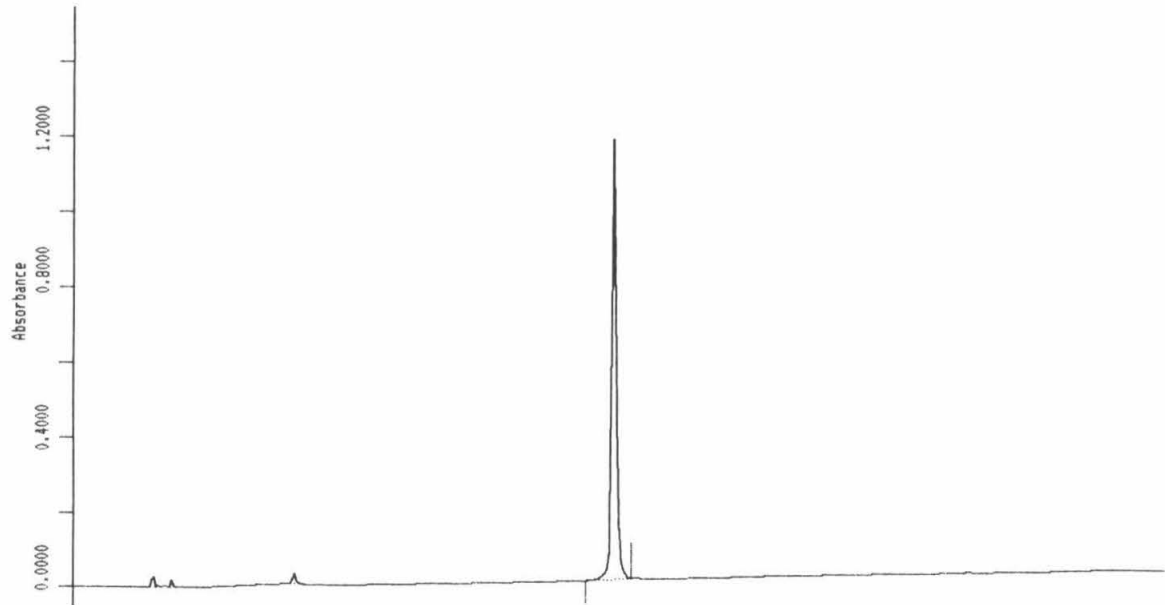
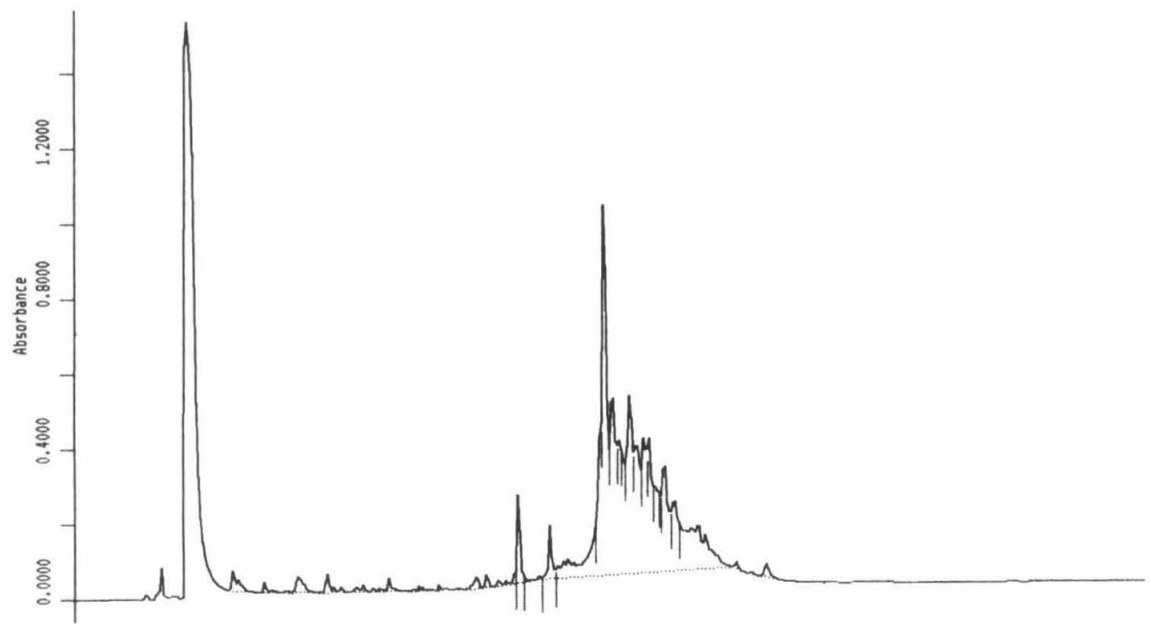
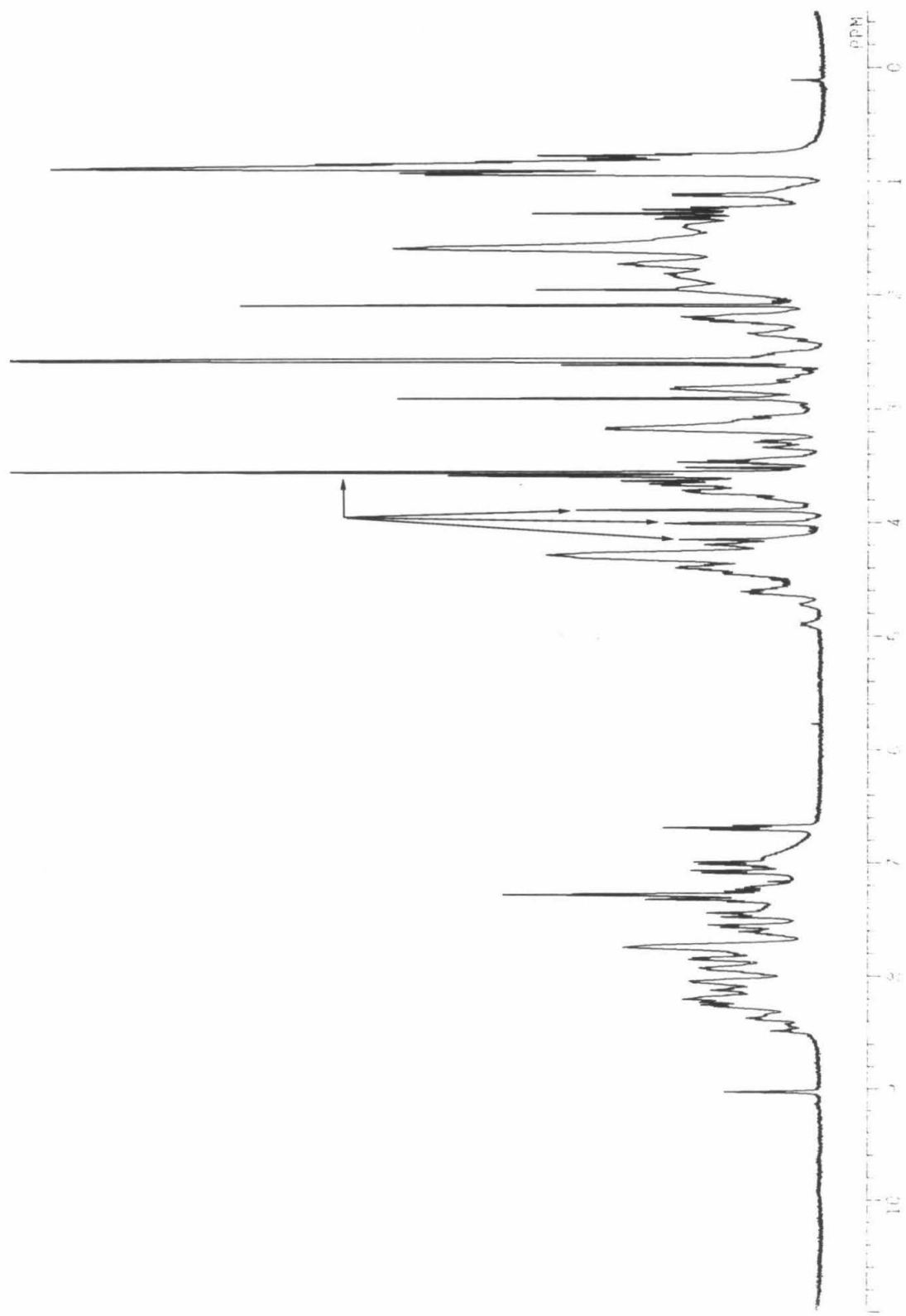


Figure 3.42

400 MHz ^1H NMR spectrum of ionomutant 5 protein. 1.81 mg of protein, purified by reverse-phase HPLC, was dissolved in 0.4 mL 10% TFA/Me₂SO-d₆ for the spectrum. The peak indicated at 3.6 ppm is diagnostic for the presence of the polyether ionophore. The peaks indicated near 4 ppm are diagnostic for the EDTA moiety.



DNA Affinity Cleaving. DNA binding/cleaving by Fe:EDTA-Gaba-Hin(139-190) ionomutant proteins, in the absence and presence of cations, was examined on Ava II-linearized, 3'-³²P end-labeled pMFB36 plasmid DNA.⁴³ DNA double-strand cleavage patterns were resolved by agarose gel electrophoresis and visualized by autoradiography. Under conditions where Fe:EDTA-Gaba-Hin(139-190) produces efficient and specific DNA double-strand cleavage, Fe:EDTA-Gaba-Hin(139-190) ionomutants produce little or no DNA cleavage in the absence or presence of various cations, including strontium or barium, at a range of concentrations. Thus, introduction of the ionoturn at any of five different locations disrupts the ability of the Hin derivatives to fold properly and/or to interact specifically with DNA. These effects are not visibly changed by the addition of metal cations.

Recently, the high-resolution crystal structures of three different helix-turn-helix protein:oligonucleotide complexes have been reported.⁵²⁻⁵⁵ These structures show that amino acid residues in the turn regions of these proteins (λ repressor, trp repressor, 434 repressor) play important roles in positioning the flanking helices for proper interaction with DNA and may make specific contacts with the DNA operator sequence. Perhaps the ionoturn does not allow for the proper juxtaposition of the flanking helical sequences to each other or to the DNA, does not reproduce specific DNA contacts involving the native turn residues, and/or provides unfavorable steric interactions with the DNA. The successful introduction of the artificial ionoturn within a synthetic protein sequence represents a practical advance in the design and synthesis of metalloregulated DNA binding proteins. Perhaps more sophisticated modelling based on protein:DNA crystal structures would provide insight into where and in what form ionophoric subunits should be introduced into protein sequences to render them metal-responsive. The discovery and development of **TriCyE** represents an advance in practical methodology for the synthesis of peptides or proteins bearing the metal-chelating functionality EDTA.

Part 4: Additional Studies.**Results and Discussion**

Design. Two additional Bis(Netropsin)-EDTA compounds tethered by designed linker/receptors were prepared. Bis(Netropsin)-6,9-dioxa-3,12-dithiatetradecanediamic-EDTA (**BN2S2OE**, **V-34**, Figure 3.43) has a linker with two sulfur atoms and two oxygen atoms. According to CPK models, the two sulfur atoms are favorably disposed to chelate a mercuric ion in its preferred linear coordination geometry. Bis(Netropsin)-dibenzylpiperazine-EDTA (**BNDBPE**, **III-239**, Figure 3.44) bears a linker which might fold up to form a hydrophobic binding cavity for organic guest molecules.

Synthesis. **BN2S2OE** and **BNDBPE** were synthesized by direct extension of the procedure described for the preparation of Bis(Netropsin) Polyether-EDTA compounds in Part 1 of this chapter (Figure 3.3). Schemes for the synthesis of the required mono ester linker synthons are shown in Figures 3.43 and 3.44. 6,9-Dioxa-3,12-dithiatetradecandioic acid, monoethyl ester **IV-188** was prepared from triethylene glycol. Triethylene glycol was converted to dibromide **IV-179**,⁵⁶ which was dialkylated with the cesium salt of ethyl thioglycolate to afford diester **IV-183**. **IV-183** was converted to **IV-188** by limited hydrolysis. Mono-ester **III-221** was prepared from ethyl p-tolylacetate. Ethyl p-tolylacetate was brominated to afford **III-200**. **III-200** was used to alkylate 0.5 equivalents of piperazine to afford diester **III-203**, which was converted to **III-221** by limited hydrolysis.

DNA Affinity Cleaving. The DNA binding/cleaving properties of these molecules, in the absence and presence of various possible activating agents, were determined by cleavage of ³²P end-labeled pBR322 restriction fragments. **BN2S2OE:Fe**, in the absence of added cations, produced double-strand cleavage with specificity similar to and efficiency somewhat greater than its analog with four oxygens in the linker, **BNO4E:Fe**, described in Part 1 of this chapter. When DNA cleavage by **BN2S2OE:Fe** was carried out in the

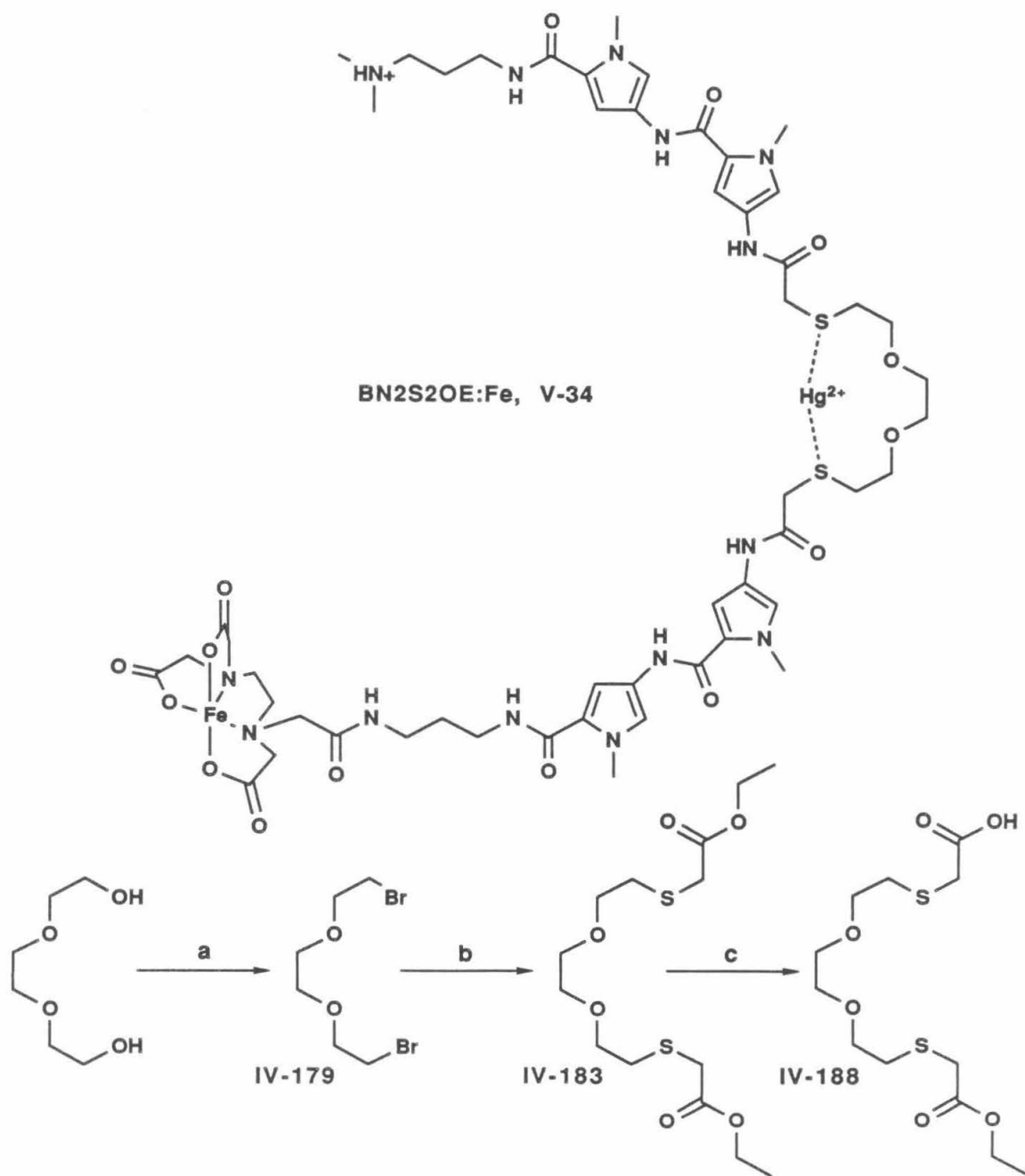


Figure 3.43. Top: Design of a mercury-regulated DNA binding/cleaving small molecule, Bis(Netropsin)-6,9-Dioxa-3,12-Dithiatetradecanediamic:Fe (BN2S2OE:Fe, V-34). Bottom: Scheme for the synthesis of the 6,9-dioxa-3,12-dithiatetradecanediamic acid, mono ethyl ester linker. Reaction conditions: **a**, PBr₃, C₅H₅N; **b**, HSCH₂CO₂Et (2.0 equiv.), Cs₂CO₃, DMF, 80°C; **c**, LiOH (1.0 equiv.), MeOH, H₂O.

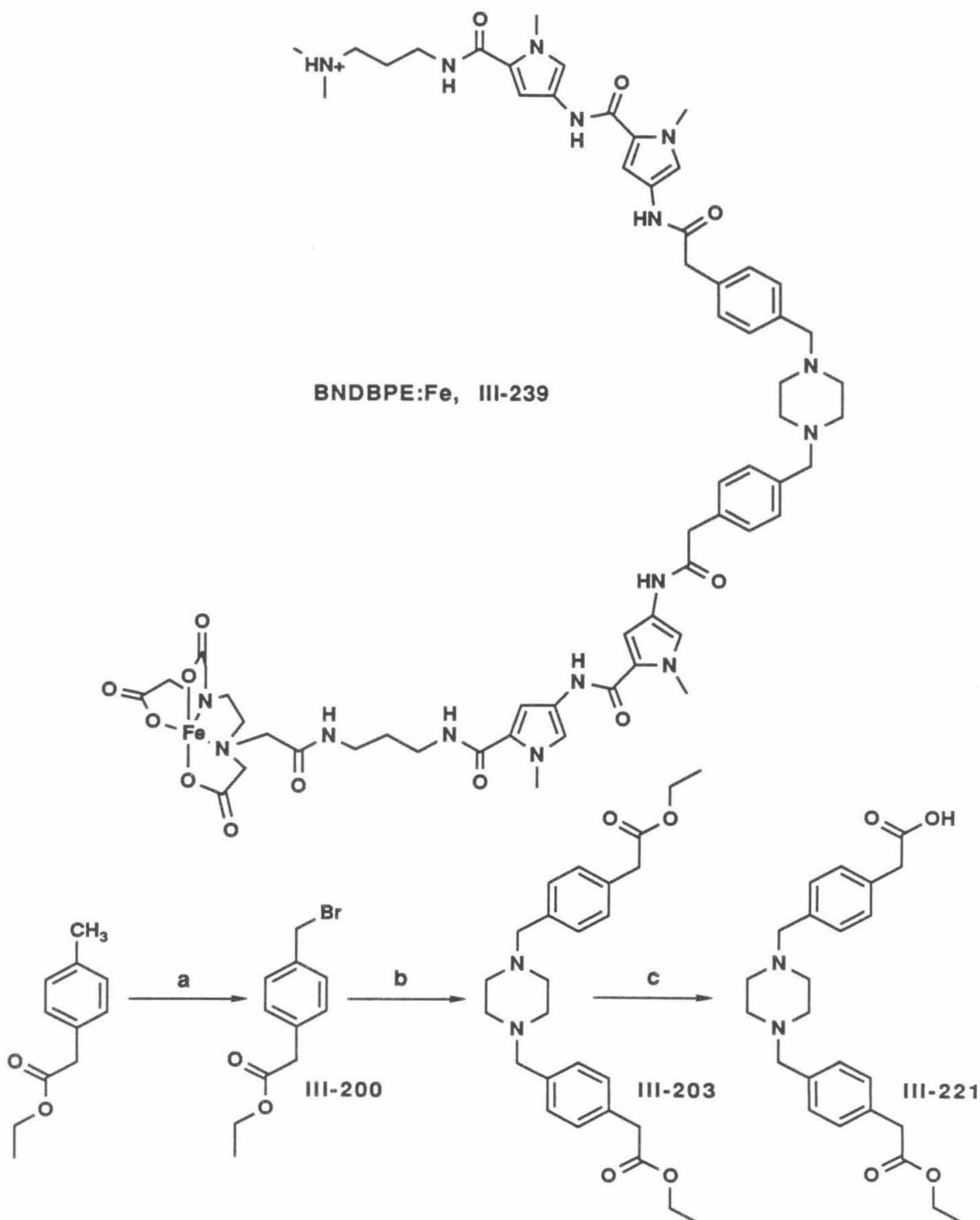


Figure 3.44. Top: Design of a DNA binding/cleaving small molecule with a hydrophobic cleft, Bis(Netropsin)-Dibenzylpiperazine-EDTA:Fe (BNDBPE:Fe, III-239). Bottom: Scheme for the synthesis of the substituted dibenzylpiperazine, mono ethyl ester linker. Reaction conditions: **a**, NBS, AIBN, CCl_4 , reflux; **b**, piperazine (0.5 equiv.), K_2CO_3 , DMF; **c**, LiOH (1 equiv.), MeOH, H_2O .

presence of mercuric ions and ascorbic acid reductant, enhancement of specific cleavage was observed. However, similar enhancement of cleavage was observed in control experiments as well. Bis(Netropsin)-Glycine-EDTA:Fe (**BNGE:Fe**, Chapter One) was used for the control experiments because it lacked an ionophoric linker, and because it bound and cleaved DNA with efficiency similar to **BN2S2OE:Fe**. As enhanced cleavage was observed when DNA affinity cleaving was carried out with **BNGE:Fe**, mercuric ions, and ascorbic acid relative to cleavage observed with **BNGE:Fe** and ascorbic acid alone, the results with **BN2S2OE:Fe** could not be interpreted in terms of positive metalloregulation. The basis for cleavage enhancement by these molecules in the presence of mercuric ions and ascorbic acid is not known. **BNDBPE:Fe** was found to produce specific cleavage in regions of DNA rich in A:T base pairs. However, neither the efficiency nor the specificity of DNA binding/cleaving by **BNDBPE:Fe** was altered by the addition of a variety of aliphatic or aromatic hydrocarbons, alcohols, or carboxylic acids.

References

- ¹Ronson, C.W.; Nixon, B.T.; Ausubel, F.M. *Cell* **1987**, *49*, 579-581.
- ²Wiederrecht, G.; Shuey, D.J.; Kibbe, W.A.; Parker, C.S. *Cell* **1987**, *48*, 507-515.
- ³Zhang, R.-G.; Joachimiak, A.; Lawson, C.L.; Schevitz, R.W.; Otwinowski, Z.; Sigler, P.B. *Nature* **1987**, *327*, 591-597.
- ⁴Guarente, L.; Mason, T. *Cell* **1983**, *32*, 1279-1286.
- ⁵O'Halloran, T.V. In *Metal Ions in Biological Systems*, Vol. 25; Sigel, H., Sigel, A., Eds.; Marcel Dekker, Inc.: New York, 1989.
- ⁶DeLorenzo, V.; Herrero, M.; Giovannini, F.; Neilands, J.B. *Eur. J. Biochemistry* **1988**, *173*, 537-546.
- ⁷Hamer, D.H. Lecture at UCLA Symposium "Metal Ion Homeostasis: Molecular Biology and Chemistry;" Frisco, CO, April, 1988.
- ⁸O'Halloran, T.; Walsh, C. *Science* **1986**, *235*, 211-214.
- ⁹O'Halloran, T.V.; Frantz, B.; Shin, M.K.; Ralston, D.M.; Wright, J.G. *Cell* **1989**, *56*, 119-129.
- ¹⁰Summers, A.O. *Ann. Rev. Microbiol.* **1986**, *40*, 607-634.
- ¹¹Walsh, C.T.; Distefano, M.D.; Moore, M.J.; Shewchuck, L.M.; Verdine, G.L. *FASEB J.* **1988**, *2*, 124-130.
- ¹²Ward, D.C.; Reich, E.; Goldberg, I.H. *Science* **1965**, *149*, 1259-1263.
- ¹³Van Dyke, M.W.; Dervan, P.B. *Biochemistry* **1983**, *22*, 2373-2377.
- ¹⁴Stubbe, J.; Kozarich, J.W. *Chem. Rev.* **1987**, *87*, 1107-1136, and references therein.
- ¹⁵Vogtle, F.; Weber, E. *Angew Chem., Int. Ed. Engl.* **1979**, *18*, 753-776.
- ¹⁶Taylor, J.S.; Schultz, P.G.; Dervan, P.B. *Tetrahedron* **1984**, *40*, 457-465.
- ¹⁷Youngquist, R.S., Ph.D. Thesis, California Institute of Technology, Pasadena, California, 1988.
- ¹⁸Kurimura, Y.; Ochiai, R.; Matsuura, N. *Bull. Chem. Soc. Japan* **1968**, *41*, 2234-2239.
- ¹⁹Hertzberg, R.P.; Dervan, P.B. *J. Am. Chem. Soc.* **1982**, *104*, 313-315.
- ²⁰Hertzberg, R.P.; Dervan, P.B. *Biochemistry* **1984**, *23*, 3934-3945.

²¹Van Dyke, M.W.; Hertzberg, R.P.; Dervan, P.B. *Proc. Natl. Acad. Sci. USA* **1982**, *79*, 5470-5474.

²²Van Dyke, M.W.; Dervan, P.B. *Biochemistry* **1983**, *22*, 2373-2377.

²³Van Dyke, M.W.; Dervan, P.B. *Nucleic Acids Res.* **1983**, *11*, 5555-5567.

²⁴Miller, J.; McLachlan, A.D.; Klug, A. *EMBO J.* **1985**, *4*, 1609-1614.

²⁵Izatt, R.M.; Bradshaw, J.S.; Nielsen, S.A.; Lamb, J.D.; Christensen, J.J.; Sen, D. *Chem. Rev.* **1985**, *85*, 271-339.

²⁶Saenger, W. *Principles of Nucleic Acid Structure*; Cantor, C., Ed.; Springer Verlag: New York; 1984; pp. 201-219.

²⁷Dervan, P.B.; Sluka, J.P. In *New Synthetic Methodology and Functionally Interesting Compounds*; Elsevier Scientific Publishing Co.: Amsterdam, 1986; pp. 307-322.

²⁸Wade, W.S.; Dervan, P.B. *J. Am. Chem. Soc.* **1987**, *109*, 1574-1575.

²⁹Griffin, J.H.; Dervan, P.B. *J. Am. Chem. Soc.* **1987**, *109*, 6840-6842.

³⁰Griffin, J.H.; Dervan, P.B. In *Metal Ion Homeostasis: Molecular Biology and Chemistry*; Alan R. Liss: New York; 1989; pp 21-30.

³¹Kopka, M.L.; Yoon, C.; Goodsell, D.; Pjura, P.; Dickerson, R.E. *Proc. Natl. Acad. Sci. USA* **1985**, *82*, 1376-1380.

³²Kopka, M.L.; Yoon, C.; Goodsell, D.; Pjura, P.; Dickerson, R.E. *J. Mol. Biol.* **1985**, *183*, 553-563.

³³Coll, M.; Frederick, C.; Wang, A.H.-J.; Rich, A. *Proc. Natl. Acad. Sci. USA* **1987**, *84*, 8385-8389.

³⁴Tummler, B.; Maass, G.; Vogtle, F.; Sieger, H.; Heimann, U.; Weber, E. *J. Am. Chem. Soc.* **1979**, *101*, 2588-2598.

³⁵Baker, E.N.; Hubbard, R.E. *Prog. Biophys. Mol. Biol.* **1984**, *44*, 97-179.

³⁶Dickerson, R.E.; Drew, H.R. *J. Molec. Biol.* **1981**, *149*, 761-786.

³⁷Nelson, H.C.M.; Finch, J.T.; Bonaventura, F.L.; Klug, A. *Nature*, **1987**, *330*, 221-226.

³⁸Lindoy, L.F. *Prog. Macroyclic Chem.* **1987**, *3*, 53-92.

³⁹Trost, B.M.; Arndt, H.C.; Stenge, P.E.; Verhoeven, T.R. *Tet. Lett.* **1976**, 3477-3478.

⁴⁰Perrin, D.D. *Dissociation Constants of Organic Bases in Aqueous Solution*; Butterworths: London; 1965, Supplement 1972.

⁴¹Gresh, N. *Biopolymers* **1985**, *24*, 1527-1542.

⁴²Zakrzewska, K.; Pullman, B. *Biopolymers* **1984**, *25*, 375-392.

⁴³Bruist, M.F.; Horvath, S.J.; Hood, L.E.; Steitz, T.A. *Science* **1987**, *235*, 777-780.

⁴⁴Struhl, K. *Trends Biochem. Sci.* **1989**, *14*, 137-140.

⁴⁵Pabo, C.O.; Sauer, R. *Ann. Rev. Biochem.* **1984**, *43*, 293-321.

⁴⁶Sluka, J.P., Ph.D. Thesis, California Institute of Technology, Pasadena, California, 1988.

⁴⁷Sluka, J.P.; Horvath, S.J.; Bruist, M.F.; Simon, M.I.; Dervan, P.B. *Science* **1987**, *238*, 1129-1132.

⁴⁸Schulz, G.E.; Schirmer, R.H. *Principles of Protein Structure*; Cantor, C. Ed.; Springer Verlag: New York; 1984; pp 74-75.

⁴⁹Kent, S.B.H. *Ann. Rev. Biochem.* **1988**, *57*, 957-989, and references therein.

⁵⁰Sarin, V.K.; Kent, S.B.H.; Tam, J.P.; Merrifield, R.B. *Anal. Biochem.* **1981**, *117*, 147-157.

⁵¹Tam, J.P. Wong, T.-W.; Riemen, M.W.; Tjoeng, F.S.; Merrifield, R.B. *Tet. Lett.* **1979**, 4033-4036.

⁵²Anderson, J.E.; Ptashne, M.; Harrison, S.C. *Nature* **1987**, *326*, 846-852.

⁵³Aggarwal, A.K.; Rodgers, D.W.; Drott, M.; Ptashne, M.; Harrison, S.C. *Science* **1988**, *242*, 899-907.

⁵⁴Jordan, S.R.; Pabo, C.O. *Science* **1988**, *242*, 893-899.

⁵⁵Otwinowski, Z.; Schevitz, R.W.; Zhang, R.-G.; Lawson, C.L.; Joachimiak, A.; Marmorstein, R.Q.; Luisi, B.F.; Sigler, P.B. *Nature* **1988**, *335*, 321-329.

⁵⁶Luttinghaus, A.; Cramer, F.; Prinzbach, H.; Henglein, F.M. *Liebigs Ann. Chem.* **1958**, *613*, 185-198.

CHAPTER FOUR: DNA CLEAVAGE MEDIATED BY [SalenMn(III)]⁺**Introduction**

Kochi and coworkers have reported that cationic complexes of manganese(III) and the tetradentate chelating ligand Salen (Salen = *N,N'*-ethylenebis(salicylideneaminato) or substituted derivatives of Salen are efficient catalysts for the synthesis of epoxides from olefins and the terminal oxidant iodosylbenzene.¹ They also reported that [SalenMn(III)]⁺ (MnS) catalyzes the oxidative activation of cyclohexane C-H bonds in the presence of iodosylbenzene. Based on these observations and results from relative reactivity and spectroscopic studies, Kochi et al. proposed that a radical-like [SalenMn(V)O]⁺ species is the active intermediate in olefin epoxidation/C-H activation reactions. We were prompted to examine the DNA binding/cleaving properties of MnS based on its positive charge, crescent shape, stability to air and water, and ability to mediate activation of aliphatic C-H bonds in the presence of terminal oxidants.

Results

Synthesis. MnS was prepared as the acetate salt from SalenH₂ and manganese(III) acetate (Figure 4.1). This route differed from the two-step procedure employed by Kochi et al., which afforded MnS as the hexafluorophosphate salt. [SalenMn(III)]OAc was obtained as an air-stable, water-soluble brown solid which exhibited the expected elemental analysis, mass spectrum, UV spectrum, IR spectrum, and magnetic susceptibility. Several additional Salen complexes of chromium(III), manganese(III), and iron(III) were prepared for this study (Figure 4.2). The chromium and iron complexes were prepared according to literature procedures.²⁻⁴ The substituted complex [(Et₂N)₂SalenMn(III)]OAc was prepared as violet crystals from manganese(III) acetate and (Et₂N)₂SalenH₂.

DNA Cleavage. The ability of Salen:metal complexes to promote DNA cleavage in the absence or presence of various additives was screened using Sty I-linearized, 3'-³²P end-

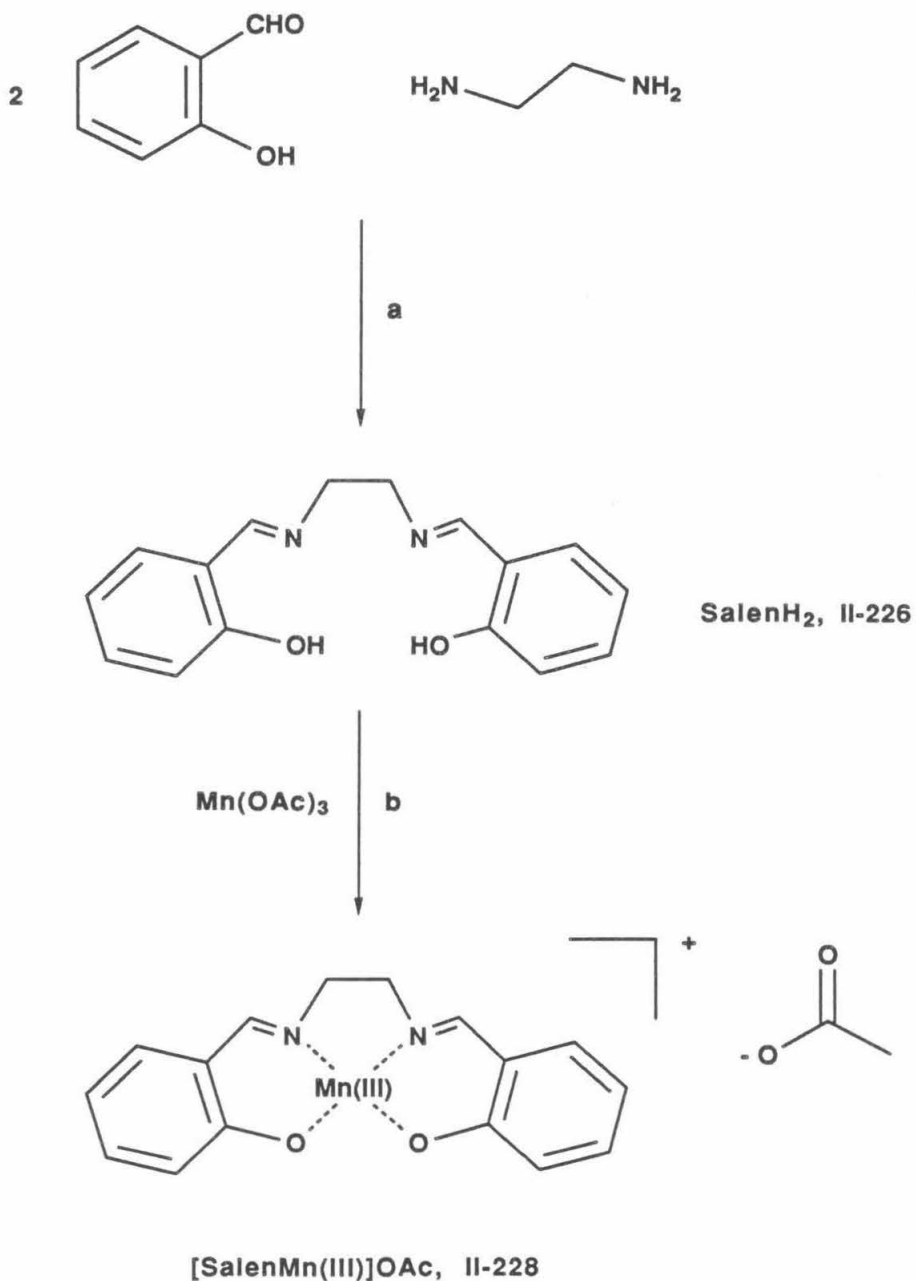


Figure 4.1. Scheme for the synthesis of *N,N'*-ethylenebis(salicylideneaminato)-manganese(III) acetate ($[\text{SalenMn(III)}]\text{OAc}$, MnS , II-228). Reaction conditions: **a**, EtOH, reflux; **b**, EtOH, CH_3CN .

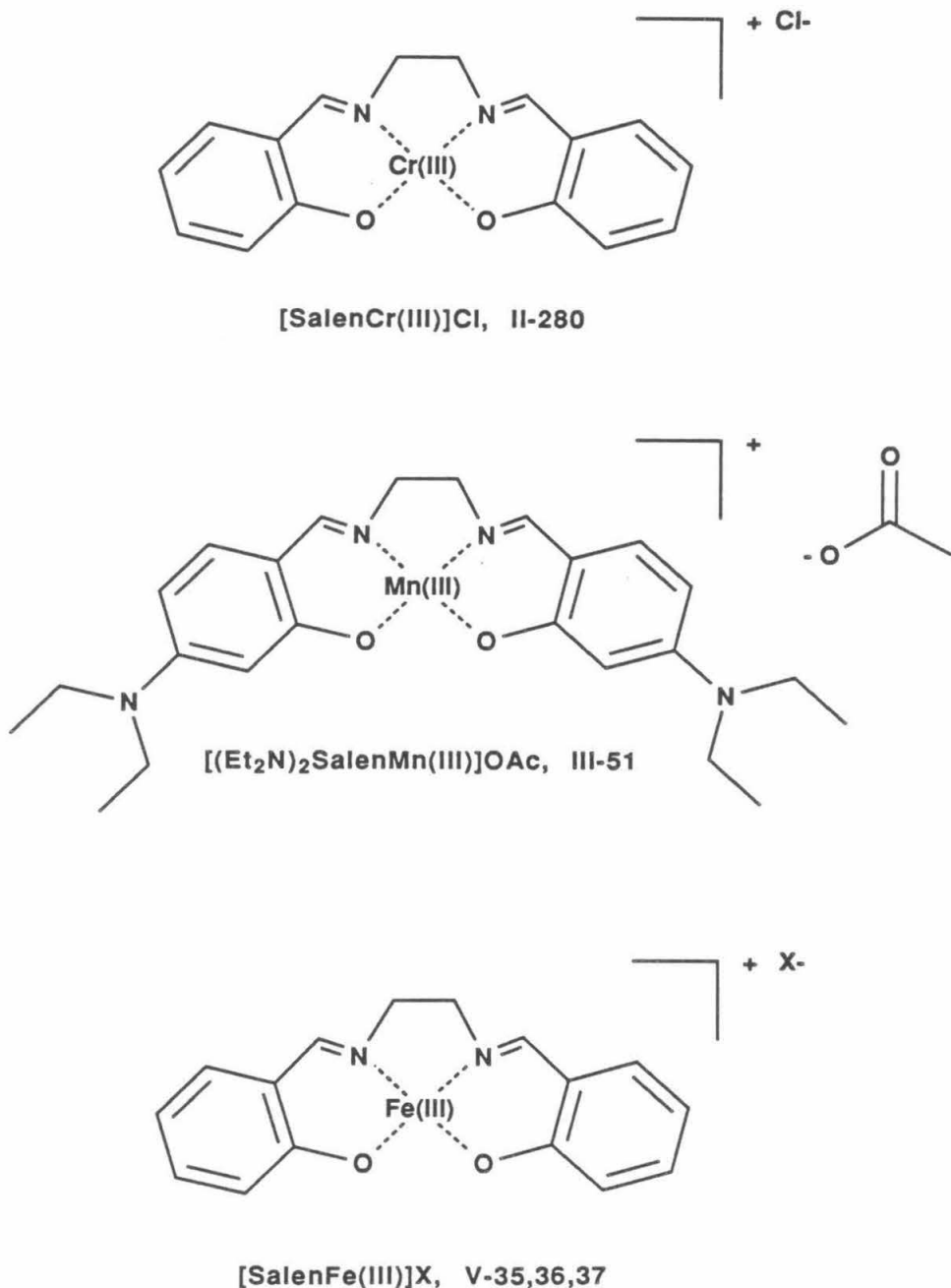


Figure 4.2. Additional Salen:Metal complexes tested for DNA binding/cleaving activity. Top: *N,N'*-ethylenebis(salicylideneaminato)chromium(III) chloride ([SalenCr(III)]Cl). Middle: *N,N'*-ethylenebis(4-*N,N'*-diethylaminosalicylideneaminato)manganese(III) acetate ([*(Et*₂N)₂SalenMn(III)]OAc). Bottom: *N,N'*-ethylenebis(salicylideneaminato)iron(III) derivatives (X = OAc, [SalenFe(III)]OAc; X = Cl, [SalenFe(III)]Cl, X = μ -O, [SalenFe(III)]₂O).

labeled pBR322 plasmid DNA. Salen:metal complexes were incubated under aerobic conditions in a buffered solution of DNA substrate and carrier DNA for 30 minutes at 37°C before additives were introduced. The reactions were then incubated for 2 hours at 37°C before DNA cleavage products were separated by agarose gel electrophoresis and visualized by autoradiography. No DNA cleavage was observed with $[\text{SalenCr(III)}]\text{Cl}$, $[\text{SalenFe(III)}]\text{X}$, or $[(\text{Et}_2\text{N})_2\text{SalenMn(III)}]\text{OAc}$ complexes (at 10 to 1000 μM concentrations) in the absence of additives or in the presence of millimolar dithiothreitol, ascorbic acid, hydrogen peroxide, ascorbic acid/hydrogen peroxide, t-butyl hydroperoxide, sodium hypochlorite, m-chloroperoxybenzoic acid, peracetic acid, magnesium monoperoxyphthalate, or iodosylbenzene. **MnS** also failed to produce DNA cleavage in the absence of additives or in the presence of dithiothreitol, ascorbic acid, t-butyl hydroperoxide, or sodium hypochlorite. However, it was found that **MnS** mediated strong and specific DNA double-strand cleavage in the presence of hydrogen peroxide, percarboxylic acids, or iodosylbenzene. Figure 4.3 shows an autoradiograph of DNA double-strand cleavage produced by **MnS** at a range of concentrations in the presence of 1 mM hydrogen peroxide. Under these conditions, **MnS** produces detectable cleavage at 5.0 μM , moderate cleavage at 10 μM , strong cleavage at 20 μM , and overdigestion at 50 μM .

Figure 4.4 shows an autoradiograph of the DNA double-strand cleavage patterns produced by **MnS** (20 μM) in the presence of hydrogen peroxide, magnesium monoperoxyphthalate, and iodosylbenzene at three concentrations. The use of these different terminal oxidants results in similar patterns of DNA cleavage. Magnesium monoperoxyphthalate is the superior terminal oxidant--it affords the most efficient cleavage (at 1 mM concentration) and is more soluble in water than either m-chloroperoxybenzoic acid or iodosylbenzene.

Figure 4.5 shows an autoradiograph of DNA cleavage produced by **MnS** (15 μM) in the presence of magnesium monoperoxyphthalate (2.0 mM) at a series of pH values between 5.4 and 9.0. These DNA cleavage patterns were quantified by densitometry and

Figure 4.3

Autoradiograph of DNA double-strand cleavage patterns produced by **MnS** on Sty I-linearized, 3'-³²P end-labeled pBR322 plasmid DNA in the presence of hydrogen peroxide. Cleavage patterns were resolved by electrophoresis on a 1% agarose gel. Lanes 2,4,6,8,10 contain DNA labeled at one end with ³²P dATP, while lanes 3,5,7,9,11 contain DNA labeled at the other end with ³²P TTP. Hydrogen peroxide concentration was 1.0 mM. Lane 1, molecular weight markers consisting of pBR322 restriction fragments 4363, 3371, 2994, 2368, 1998, 1768, 1372, 995, and 666 bp in length; lanes 2 and 3, uncleaved DNA; lanes 4 and 5, 6 and 7, 8 and 9, 10 and 11, **MnS** at 5.0, 10, 20, and 50 μ M concentrations, respectively.

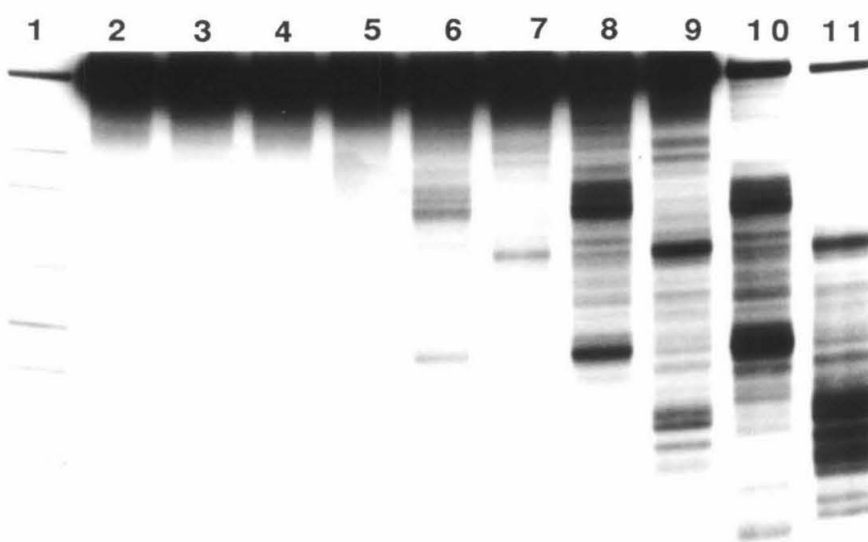


Figure 4.4

Autoradiograph of DNA double-strand cleavage patterns produced by **MnS** on Sty I-linearized, 3'-³²P TTP end-labeled pBR322 plasmid DNA in the presence of hydrogen peroxide (H₂O₂), magnesium monoperoxyphthalate (Mg(MPPA)₂), or iodosylbenzene (PhIO) oxidants. Cleavage patterns were resolved by electrophoresis on a 1% agarose gel. Lane 1, molecular weight markers consisting of pBR322 restriction fragments 4363, 3371, 2994, 2368, 1998, 1768, 1372, 995, and 666 bp in length; lanes 2-4, DNA cleavage by **MnS** (20 μ M) in the presence of H₂O₂ at 0.10, 1.0, and 10 mM concentrations; lanes 5-7, DNA cleavage by **MnS** (20 μ M) in the presence of Mg(MPPA)₂ at 0.10, 1.0, and 10 mM concentrations; lanes 8-10, DNA cleavage by **MnS** (20 μ M) in the presence of PhIO at 0.10, 1.0, and 10 mM concentrations.

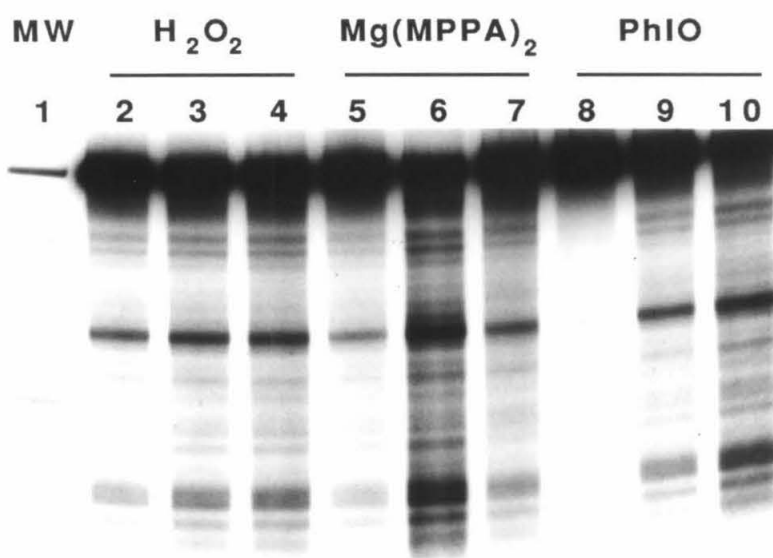
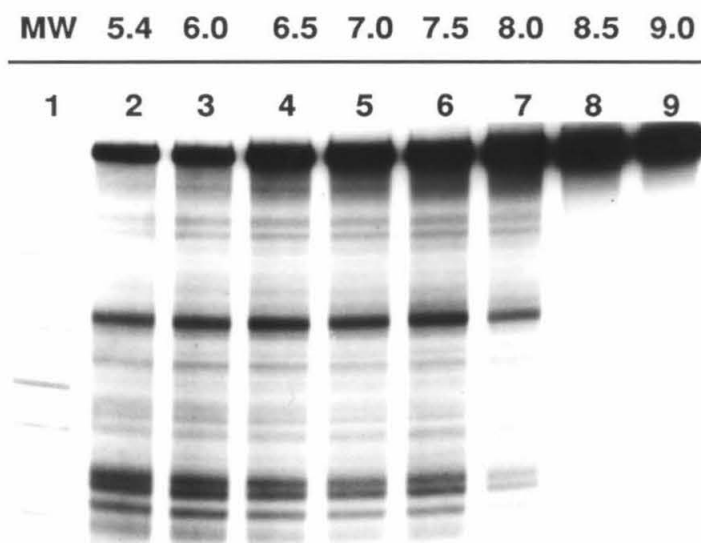


Figure 4.5

Autoradiographs of DNA double-strand cleavage patterns produced by **MnS** on Sty I-linearized, 3'-³²P TTP end-labeled pBR322 plasmid DNA in the presence of magnesium monoperoxyphthalate at a series of pH values. Cleavage patterns were resolved by electrophoresis on a 1% agarose gel. Lane 1, molecular weight markers consisting of pBR322 restriction fragments 4363, 3371, 2994, 2368, 1998, 1768, 1372, 995, and 666 bp in length; lanes 2-9, DNA double-strand cleavage by **MnS** (15 mM) and Mg(MPPA)₂ (2.0 mM) at pH 5.4, 6.0, 6.5, 7.0, 7.5, 8.0, 8.5, and 9.0, respectively.



the data displayed in graph form (Figure 4.6). **MnS**/magnesium monoperoxyphthalate produces efficient cleavage in the pH range 5.4 to 7.5, but cleavage efficiency decreases rapidly between pH 7.5 and 9.0, at which point little DNA cleavage is observed.

The specificity of DNA cleavage produced with **MnS** and several other DNA binding/cleaving small molecules was examined at low and high resolution. Figures 4.7 and 4.8 show autoradiographs of the DNA double-strand cleavage patterns produced by **MnS** (in the presence of hydrogen peroxide or magnesium monoperoxyphthalate), methidiumpropyl-EDTA:Fe (**MPE:Fe**, Figure 1.6, in the presence of dithiothreitol),⁵ Neocarzinostatin (**NCZS**, Figure 2.3, in the presence of mercaptoethanol),⁶ Bleomycin:Fe(II) (**Blm:Fe**, Figure 1.4),⁷ and Bis(Netropsin)-Succinamide-EDTA:Fe (**BNSE**, Figure 1.9, in the presence of dithiothreitol). **BNSE:Fe** produces the most specific DNA double-strand cleavage (fewest discrete cleavage bands) among this series of molecules. **MPE:Fe** produces the least specific cleavage, yet still affords darker regions of enhanced binding/cleaving and lighter regions of diminished binding/cleaving. The most striking observation to be made from these autoradiographs is that the most intense cleavage loci observed with **BNSE:Fe**, **MnS** and **NCZS** correlate with regions of diminished cleavage intensity observed with **MPE:Fe** and **Blm:Fe**. This can be seen more clearly in the densitometry traces collected in Figure 4.9, where the tallest "peaks" produced by **BNSE:Fe**, **MnS**, and **NCZS** align with deepest "valleys" observed with **MPE:Fe** and **Blm:Fe**. Based on the positions of these cleavage loci and lighter regions relative to the positions of DNA bands in the molecular weight marker lanes, the regions of alignment were mapped to the pBR322 sequence. The regions of alignment near pBR322 positions 3100, 3250, and 4000-4363 correspond to the most A:T rich segments of the plasmid.

DNA cleavage by small molecules in these regions was examined at nucleotide resolution using ³²P end-labeled restriction fragments from pBR322. 517 base pair Eco RI/Rsa I restriction fragments (spanning pBR322 positions 3848-2 and 4361-165,

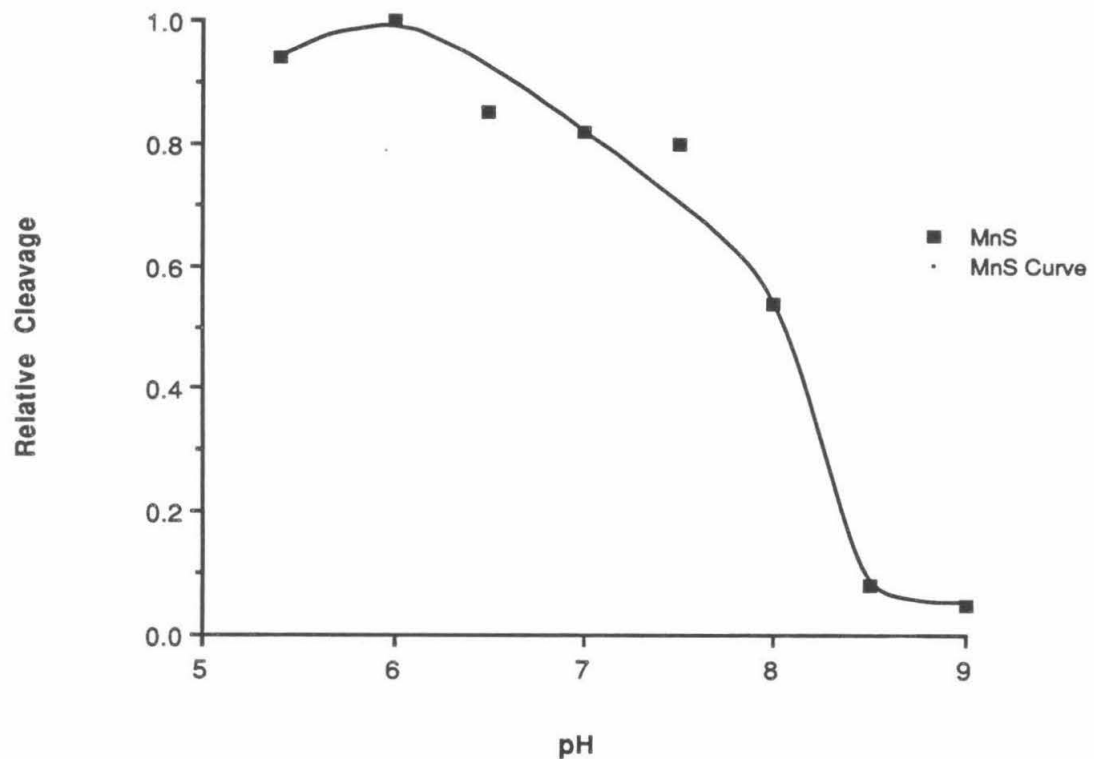


Figure 4.6. Graph of relative DNA double-strand cleavage by MnS in the presence of magnesium monoperoxyphthalate versus reaction pH. Data was generated by optical densitometry of the autoradiograph shown in Figure 4.5. The interpolated curve emphasizes trends in the data.

Figure 4.7

Autoradiograph of DNA double-strand cleavage patterns produced by **MnS**, **MPE:Fe**, **NCZS**, and **Blm:Fe(II)** on Sty I-linearized, 3'-³²P end-labeled pBR322 plasmid DNA. Cleavage patterns were resolved by electrophoresis on a 1% agarose gel. Lanes 2,4,6,8,10 contain DNA labeled at one end with ³²P dATP, while lanes 3,5,7,9,11 contain DNA labeled at the other end with ³²P TTP. Lane 1, molecular weight markers consisting of pBR322 restriction fragments 4363, 3371, 2994, 2368, 1998, 1768, 1372, 995, and 666 bp in length; lanes 2 and 3, uncleaved DNA; lanes 4 and 5, DNA cleavage by **MnS** (20 μ M) in the presence of hydrogen peroxide (1.0 mM); lanes 6 and 7, DNA cleavage by **MPE:Fe** (0.50 μ M) in the presence of dithiothreitol (5.0 mM) and dioxygen; lanes 8 and 9, DNA cleavage by **NCZS** (0.125 units) in the presence of mercaptoethanol (10 mM); lanes 10 and 11, DNA cleavage by **Blm:Fe(II)** (0.50 μ M) in the presence of dioxygen.

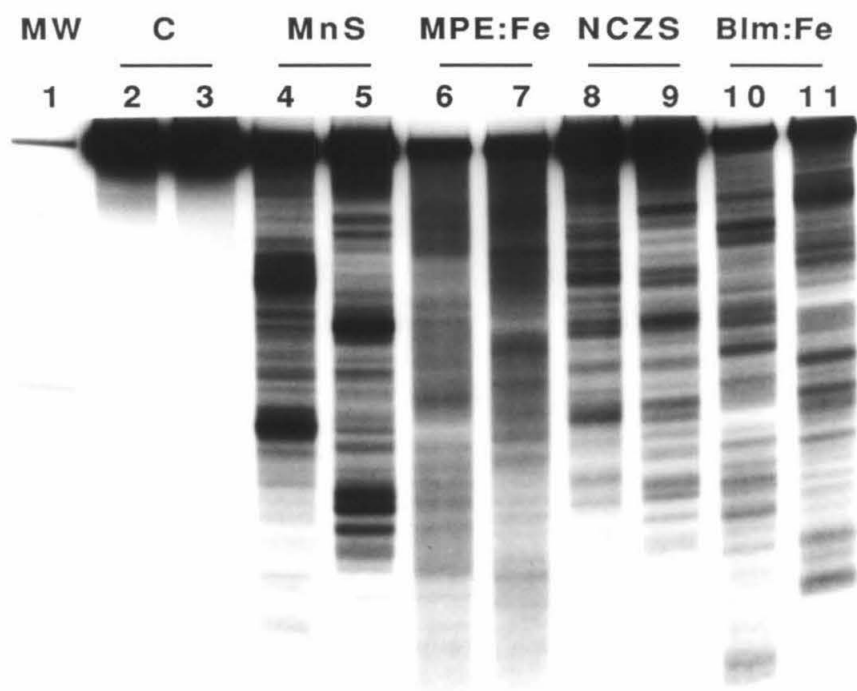


Figure 4.8

Autoradiograph of DNA double-strand cleavage patterns produced by **MnS** and **BNSE:Fe** on Sty I-linearized, 3'-³²P end-labeled pBR322 plasmid DNA. Cleavage patterns were resolved by electrophoresis on a 1% agarose gel. Lanes 2 and 4 contain DNA labeled at one end with ³²P dATP, while lanes 3 and 5 contain DNA labeled at the other end with ³²P TTP. Lane 1, molecular weight markers consisting of pBR322 restriction fragments 4363, 3371, 2994, 2368, 1998, 1768, 1372, 995, and 666 bp in length; lanes 2 and 3, DNA cleavage by **MnS** (10 μ M) in the presence of magnesium monoperoxyphthalate (1.0 mM); lanes 4 and 5, DNA cleavage by **BNSE:Fe** (0.05 μ M) in the presence of dithiothreitol (5.0 mM) and dioxygen.

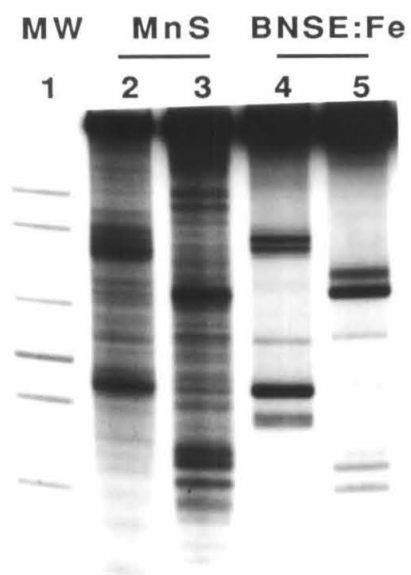
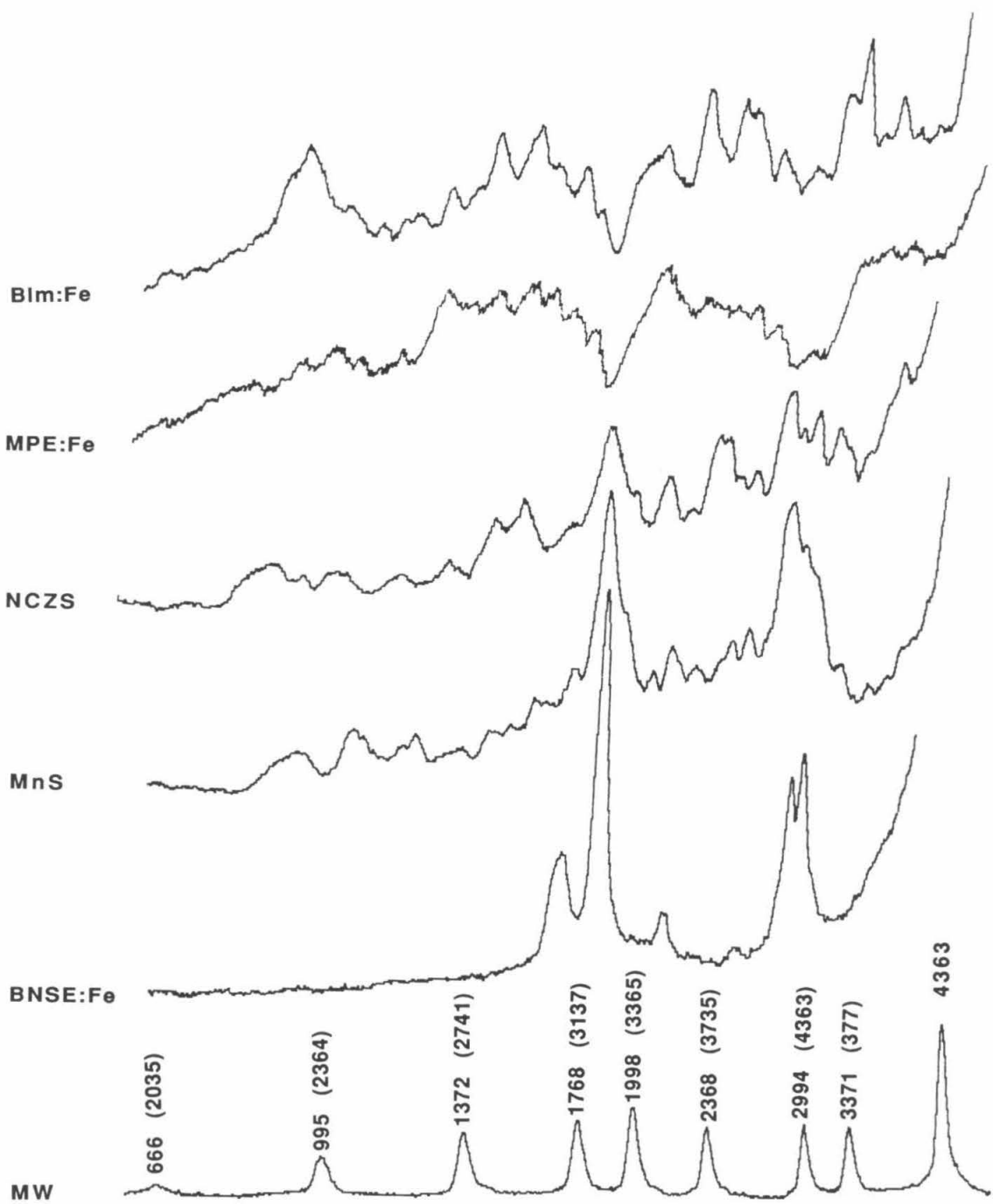
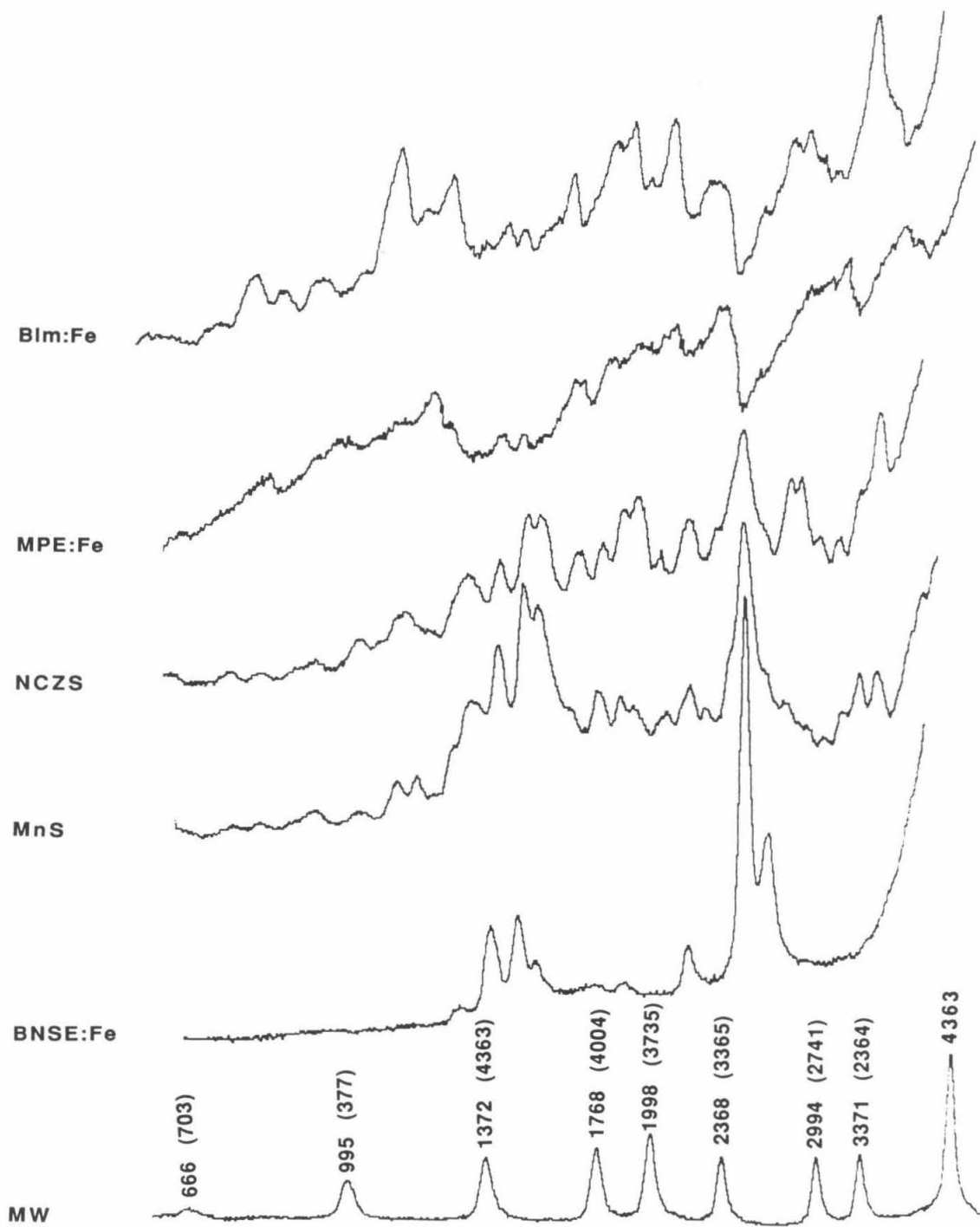


Figure 4.9

First Page: Optical densitometry of DNA double-strand cleavage produced by small molecules (**BIm:Fe**, **MPE:Fe**, **NCZS**, **MnS**, and **BNSE:Fe**, from top) on Sty I-linearized pBR322 plasmid DNA labeled at one 3' end with ^{32}P dATP. The autoradiographs shown in Figures 4.7 and 4.8 were used to generate the traces. At bottom is the densitometry trace of the molecular weight marker lane. Lengths of the double-stranded DNA fragments are indicated, as are the corresponding positions on pBR322 (in parentheses). Second Page: Optical densitometry of DNA double-strand cleavage produced by small molecules (**BIm:Fe**, **MPE:Fe**, **NCZS**, **MnS**, and **BNSE:Fe**, from top) on Sty I-linearized pBR322 plasmid DNA labeled at one 3' end with ^{32}P TTP. The autoradiographs shown in Figures 4.7 and 4.8 were used to generate the traces. At bottom is the densitometry trace of the molecular weight marker lane. Lengths of the double-stranded DNA fragments are indicated, as are the corresponding positions on pBR322 (in parentheses).

220





respectively) were prepared with ^{32}P at their the 3'- or 5' Eco RI ends. 169 base pair Dde I restriction fragments (spanning pBR322 positions 3159-3327) were prepared with ^{32}P at either 3' end. These restriction fragments were cleaved by Distamycin-EDTA:Fe (**DE:Fe**, Figure 1.6, in the presence of dithiothreitol),⁸ **MnS** (in the presence of magnesium monoperoxyphthalate), **NCZS** (in the presence of mercaptoethanol), **MPE:Fe** (in the presence of dithiothreitol), and **Blm:Fe**. DNA cleavage products were separated by denaturing polyacrylamide gel electrophoresis and visualized by autoradiography. Figures 4.10-4.12 show autoradiographs of the cleavage patterns produced by these molecules on the 517, 167, and 169 base pair DNA restriction fragments, respectively. On each of these autoradiographs, an inexact but notable correlation is observed between the positions of cleavage bands produced by **DE:Fe**, **MnS**, and **NCZS**, and positions at which cleavage by **MPE:Fe** and **Blm:Fe** is diminished. This is most clearly evident on the autoradiograph shown in Figure 4.12, where intense cleavage observed with **DE:Fe**, **MnS**, and **NCZS** in the upper middle region of the autoradiograph correlates with a region of noticeably diminished cleavage observed with **MPE:Fe** and **Blm:Fe**. This region encompasses the longest contiguous stretch of A:T base pairs (15) found on pBR322.

In order to assign DNA cleavage bands produced with **MnS** to particular DNA sequences, by comparing their electrophoretic mobilities to the electrophoretic mobilities of fragments produced by chemical sequencing reactions, the nature of the DNA end groups produced upon DNA cleavage with **MnS** must be determined, since they affect electrophoretic mobility. Maxam-Gilbert chemical sequencing reactions produce 3'- and 5'-phosphate terminal groups.⁹ **DE:Fe** and **MPE:Fe** produce 5'-phosphate termini and a mixture of 3'-phosphate and 3'-phosphoglycolate termini.^{5,10,11} Except for near the bottom of sequencing gels, DNA fragments with 3'-phosphoglycolate termini comigrate with corresponding DNA fragments with 3'-phosphate termini. **Blm:Fe** produces 5'-phosphate and 3'-phosphoglycolate termini under the aerobic conditions used for these studies.⁷ **NCZS** produces 3'-phosphate termini and a mixture of 5'-phosphate and

Figure 4.10

Autoradiograph of DNA cleavage patterns produced by small molecules (**DE:Fe**, **MnS**, **NCZS**, **MPE:Fe**, **Blm:Fe**) on 3'- and 5'-³²P end-labeled 517 bp restriction fragments (Eco RI/Rsa I) from pBR322 plasmid DNA. Cleavage patterns were resolved on a 1:20 cross-linked 8% polyacrylamide, 45% urea denaturing gel. Odd-numbered lanes, 3' end-labeled DNA. Even-numbered lanes, 5' end-labeled DNA. Lanes 1 and 2, uncleaved DNA; lanes 3 and 4, Maxam-Gilbert chemical sequencing G reactions; lanes 5 and 6, DNA cleavage by **DE:Fe** (10 μ M) in the presence of dithiothreitol (5.0 mM) and dioxygen; lanes 7 and 8, DNA cleavage by **MnS** (20 μ M) in the presence of magnesium monoperoxyphthalate (1.0 mM); lanes 9 and 10, DNA cleavage by **NCZS** (0.25 units) in the presence of mercaptoethanol (10 mM) and dioxygen; lanes 11 and 12, DNA cleavage by **MPE:Fe** (1.0 μ M) in the presence of dithiothreitol (5.0 mM) and dioxygen; lanes 13 and 14, DNA cleavage by **Blm:Fe(II)** (2.0 μ M) in the presence of dioxygen.

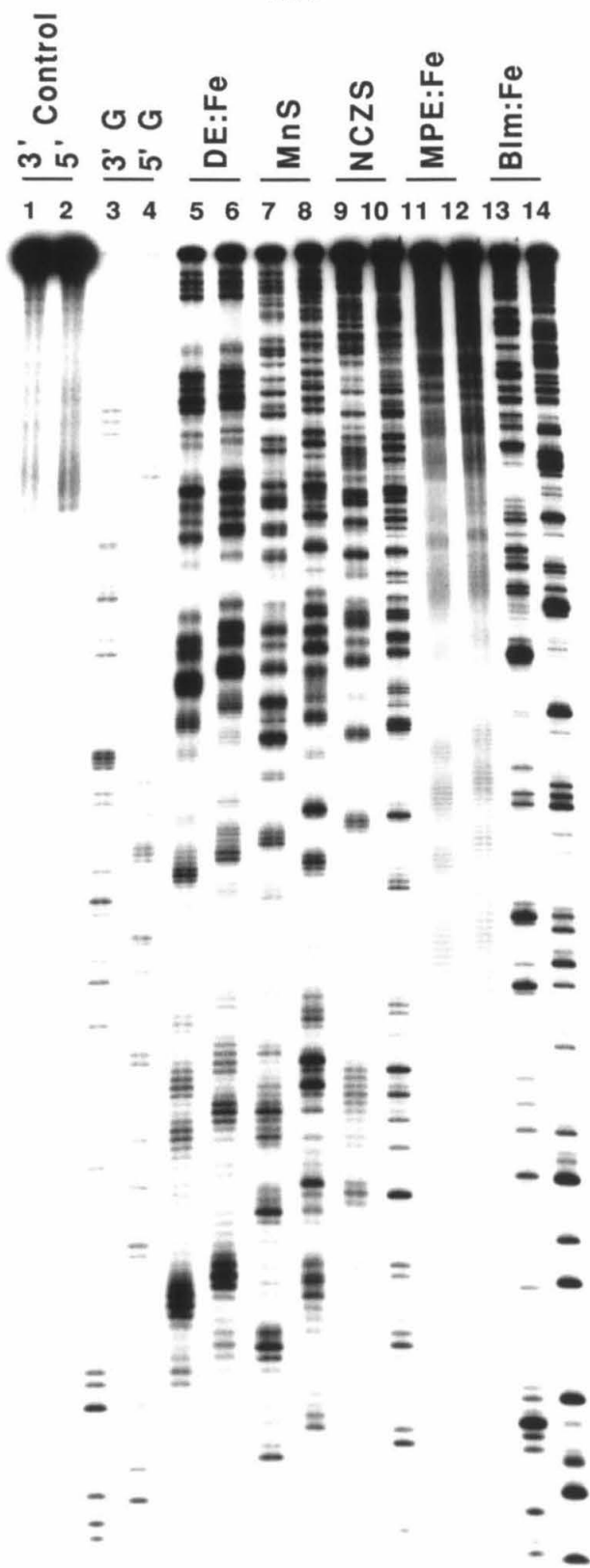


Figure 4.11

Autoradiograph of DNA cleavage patterns produced by small molecules (**DE:Fe**, **MnS**, **NCZS**, **MPE:Fe**, **Blm:Fe**) on 3'- and 5'-³²P end-labeled 167 bp restriction fragments (Eco RI/Rsa I) from pBR322 plasmid DNA. Cleavage patterns were resolved on a 1:20 cross-linked 8% polyacrylamide, 45% urea denaturing gel. Odd-numbered lanes, 3' end-labeled DNA. Even-numbered lanes, 5' end-labeled DNA. Lanes 1 and 2, uncleaved DNA; lanes 3 and 4, Maxam-Gilbert chemical sequencing G reactions; lanes 5 and 6, DNA cleavage by **DE:Fe** (10 μ M) in the presence of dithiothreitol (5.0 mM) and dioxygen; lanes 7 and 8, DNA cleavage by **MnS** (20 μ M) in the presence of magnesium monoperoxyphthalate (1.0 mM); lanes 9 and 10, DNA cleavage by **NCZS** (0.25 units) in the presence of mercaptoethanol (10 mM) and dioxygen; lanes 11 and 12, DNA cleavage by **MPE:Fe** (1.0 μ M) in the presence of dithiothreitol (5.0 mM) and dioxygen; lanes 13 and 14, DNA cleavage by **Blm:Fe(II)** (2.0 μ M) in the presence of dioxygen.

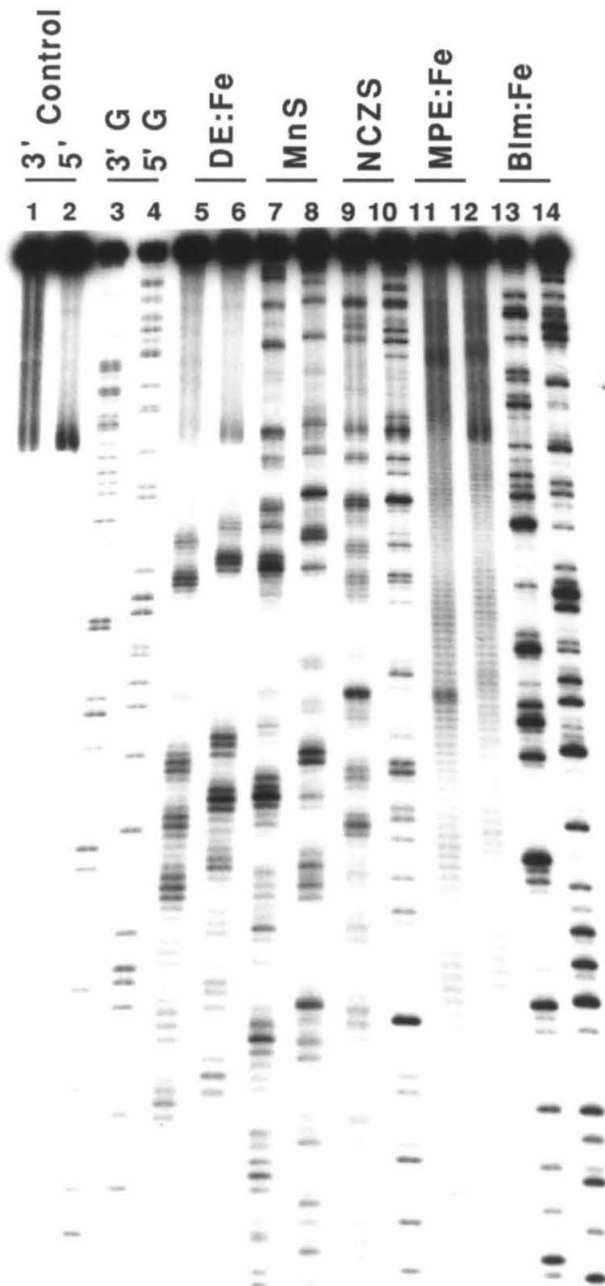
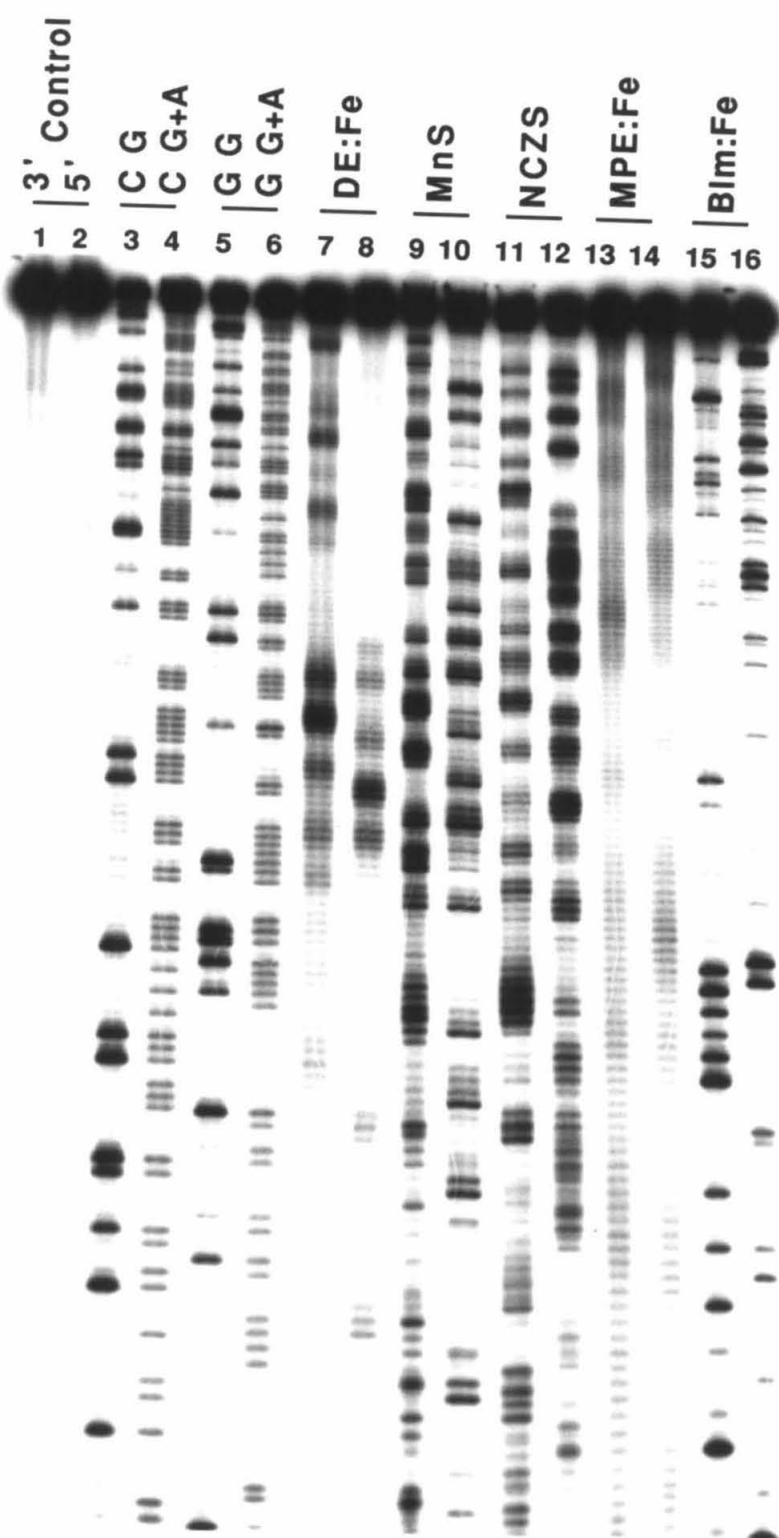


Figure 4.12

Autoradiograph of DNA cleavage patterns produced by small molecules (**DE:Fe**, **MnS**, **NCZS**, **MPE:Fe**, **Blm:Fe**) on 3'-³²P end-labeled 169 bp *Dde* I restriction fragments from pBR322 plasmid DNA. Cleavage patterns were resolved on a 1:20 cross-linked 8% polyacrylamide, 45% urea denaturing gel. Lanes 1,3,4,7,9,11,13,15, DNA labeled at one 3' end with ³²P dCTP. Lanes 2,5,6,8,10,12,14,16, DNA labeled on the opposite strand at the 3' end with ³²P dGTP. Lanes 1 and 2, uncleaved DNA; lanes 3 and 5, Maxam-Gilbert chemical sequencing G reactions; lanes 4 and 6, Maxam-Gilbert chemical sequencing G+A reactions; lanes 7 and 8, DNA cleavage by **DE:Fe** (10 μ M) in the presence of dithiothreitol (5.0 mM) and dioxygen; lanes 9 and 10, DNA cleavage by **MnS** (20 μ M) in the presence of magnesium monoperoxyphthalate (2.0 mM); lanes 11 and 12, DNA cleavage by **NCZS** (0.25 units) in the presence of mercaptoethanol (10 mM) and dioxygen; lanes 13 and 14, DNA cleavage by **MPE:Fe** (1.0 μ M) in the presence of dithiothreitol (5.0 mM) and dioxygen; lanes 15 and 16, DNA cleavage by **Blm:Fe(II)** (2.0 μ M) in the presence of dioxygen.



nucleoside 5'-aldehyde termini.⁶ DNA fragments bearing nucleoside 5'-aldehyde groups migrate more slowly than corresponding DNA fragments with 5'-phosphate termini, and may be converted to fragments with 5'-phosphate termini by base workup.

The DNA end products produced upon **MnS** cleavage were determined as part of an investigation into the mechanism(s) by which **MnS** mediates DNA cleavage. Figure 4.13 shows an autoradiograph of cleavage patterns produced by **MPE:Fe/dithiothreitol** and **MnS/magnesium monoperoxyphthalate** on the 5'-³²P end-labeled 167 base pair Eco RI/Rsa I restriction fragment. These cleavage reactions were carried out in the absence or presence of atmospheric dioxygen, and with or without post-treatment with base. Dioxygen is strictly required for DNA cleavage by **MPE:Fe/dithiothreitol**,^{5,10} but has no effect on DNA cleavage by **MnS/magnesium monoperoxyphthalate**. Base workup alters and enhances the DNA cleavage pattern produced with **MnS**. These results indicate that in the presence of terminal oxidants, **MnS** mediates the formation of direct DNA strand breaks and base-labile lesions via mechanisms not involving dioxygen.

The identities of DNA end products produced with **MnS** were determined by analyzing the electrophoretic mobilities of short DNA cleavage fragments on 20% denaturing polyacrylamide gels, and the way in which the mobilities of these fragments were affected by treatment with phosphatase enzymes. Figure 4.14 shows an autoradiograph of short DNA fragments produced by **MPE:Fe/dithiothreitol** and **MnS/magnesium monoperoxyphthalate**, with or without subsequent base treatment and/or digestion with T4 polynucleotide kinase (which converts 3'-phosphate groups to 3'-hydroxyl groups). The 5'-³²P end-labeled 167 base pair Eco RI/Rsa I restriction fragment from pBR322 was used for this study. Electrophoretic mobilities of radiolabeled cleavage fragments produced on this substrate depend on their length and the nature of their 3' termini. The doublets produced with **MPE:Fe** are due to faster-running fragments that terminate in 3'-phosphoglycolate groups and slower-running fragments that terminate in 3'-phosphate groups.^{5,10} The short DNA fragments produced by **MnS**, with or without base

Figure 4.13

Autoradiograph of DNA cleavage patterns produced with **MnS** and **MPE:Fe** on the 5'-³²P end-labeled 167 bp restriction fragment (Eco RI/Rsa I) from pBR322 plasmid DNA. Cleavage patterns were resolved on a 1:20 cross-linked 8% polyacrylamide, 45% urea denaturing gel. Base workup entailed heating the samples at 90°C for 30 minutes in 0.10 M NaOH solution. Lanes 1-4, uncleaved DNA incubated in the presence of dioxygen (lane 1), in the absence of dioxygen (lane 2), in the presence of dioxygen with subsequent base workup (lane 3) and in the absence of dioxygen with subsequent base workup (lane 4); lane 5, Maxam-Gilbert chemical sequencing G reaction; lanes 6-9, DNA cleavage by **MPE:Fe** (2.0 μ M) in the presence of dithiothreitol (5.0 mM) in the presence of dioxygen (lane 6), in the absence of dioxygen (lane 7), in the presence of dioxygen with subsequent base workup (lane 8), and in the absence of dioxygen with subsequent base workup (lane 9); lanes 10-13, DNA cleavage by **MnS** (50 μ M) in the presence of magnesium monoperoxyphthalate (2.0 mM) in the presence of dioxygen (lane 10), in the absence of dioxygen (lane 11), in the presence of dioxygen with subsequent base workup (lane 12), and in the absence of dioxygen with subsequent base workup (lane 13).

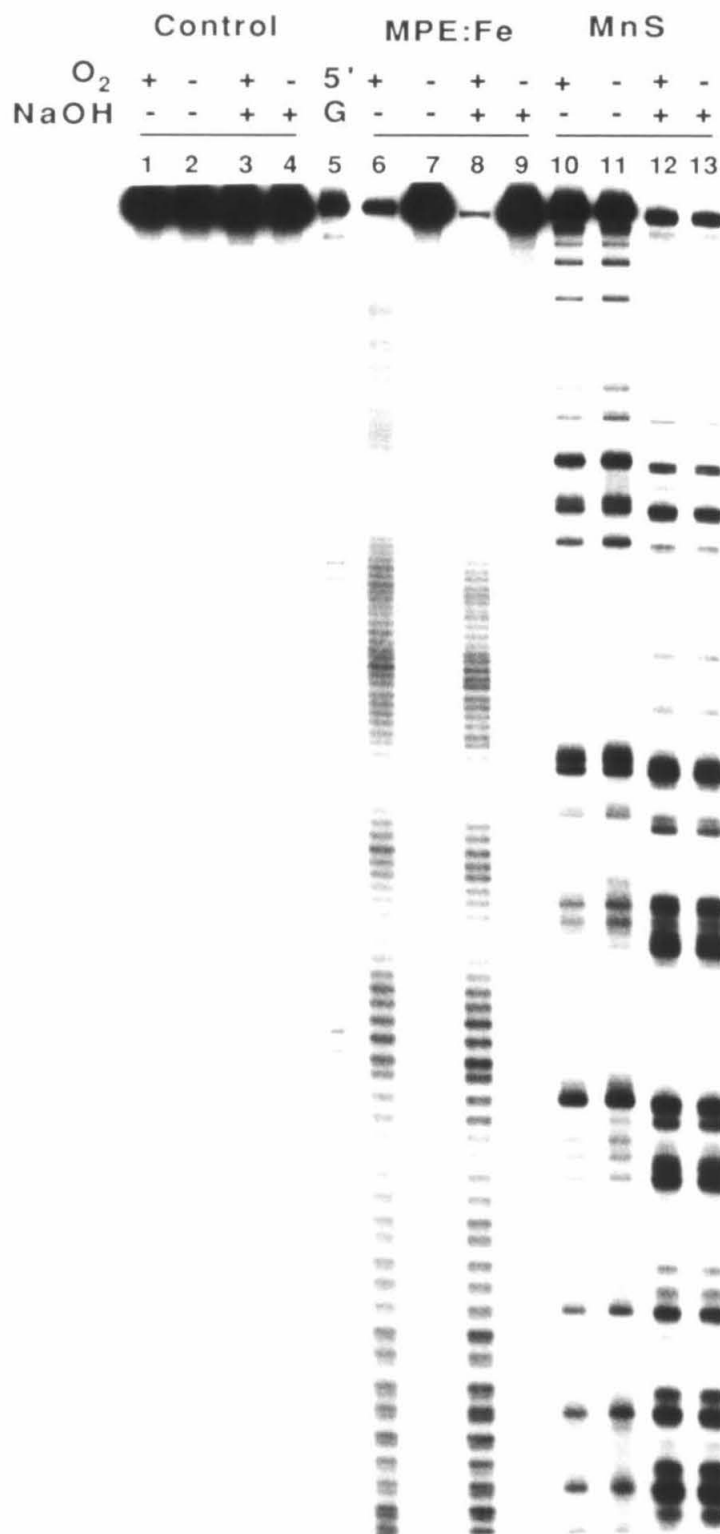
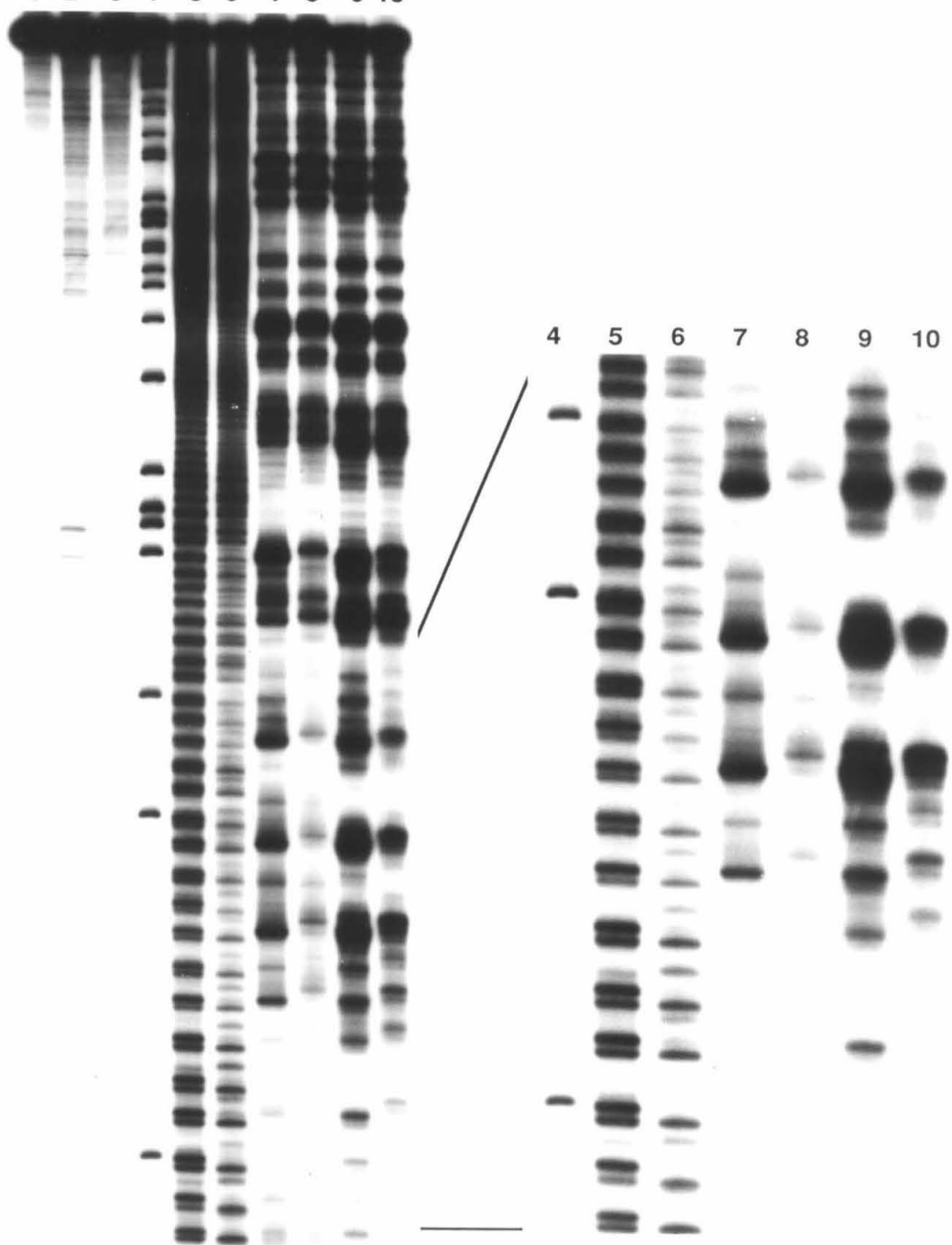


Figure 4.14

Analysis of DNA 3' end products produced with **MnS** on the 5'-³²P end-labeled 167 bp restriction fragment (Eco RI/Rsa I) from pBR322 plasmid DNA. Cleavage patterns were resolved by electrophoresis on a 1:20 cross-linked 20% polyacrylamide, 40% urea denaturing gel. Base workup entailed heating the samples at 90°C for 30 minutes in 0.10 M NaOH solution. Lane 1, uncleaved DNA; lane 2, uncleaved DNA with base workup; lane 3, uncleaved DNA with base workup and 3' dephosphorylation using T4 polynucleotide kinase; lane 4, Maxam-Gilbert chemical sequencing G reaction; lane 5, DNA cleavage by **MPE:Fe** at 2.0 μ M concentration in the presence of dithiothreitol (5.0 mM) and dioxygen; lane 6, DNA cleavage by **MPE:Fe** at 2.0 μ M concentration in the presence of dithiothreitol (5.0 mM) and dioxygen with subsequent 3' dephosphorylation using T4 polynucleotide kinase; lane 7, DNA cleavage by **MnS** at 50 μ M concentration in the presence of magnesium monoperoxyphthalate (2.0 mM); lane 8, DNA cleavage by **MnS** at 50 μ M concentration in the presence of magnesium monoperoxyphthalate (2.0 mM) with subsequent 3' dephosphorylation using T4 polynucleotide kinase; lane 9, DNA cleavage by **MnS** at 50 μ M concentration in the presence of magnesium monoperoxyphthalate (2.0 mM) with subsequent base workup; lane 10, DNA cleavage by **MnS** at 50 μ M concentration in the presence of magnesium monoperoxyphthalate (2.0 mM) with subsequent base workup and 3' dephosphorylation using T4 polynucleotide kinase.

	Control	MPE:Fe	MnS							
NaOH	-	+	+	5'	-	-	-	+	+	
Kinase	-	-	+	G	-	+	-	+	+	
	1	2	3	4	5	6	7	8	9	10

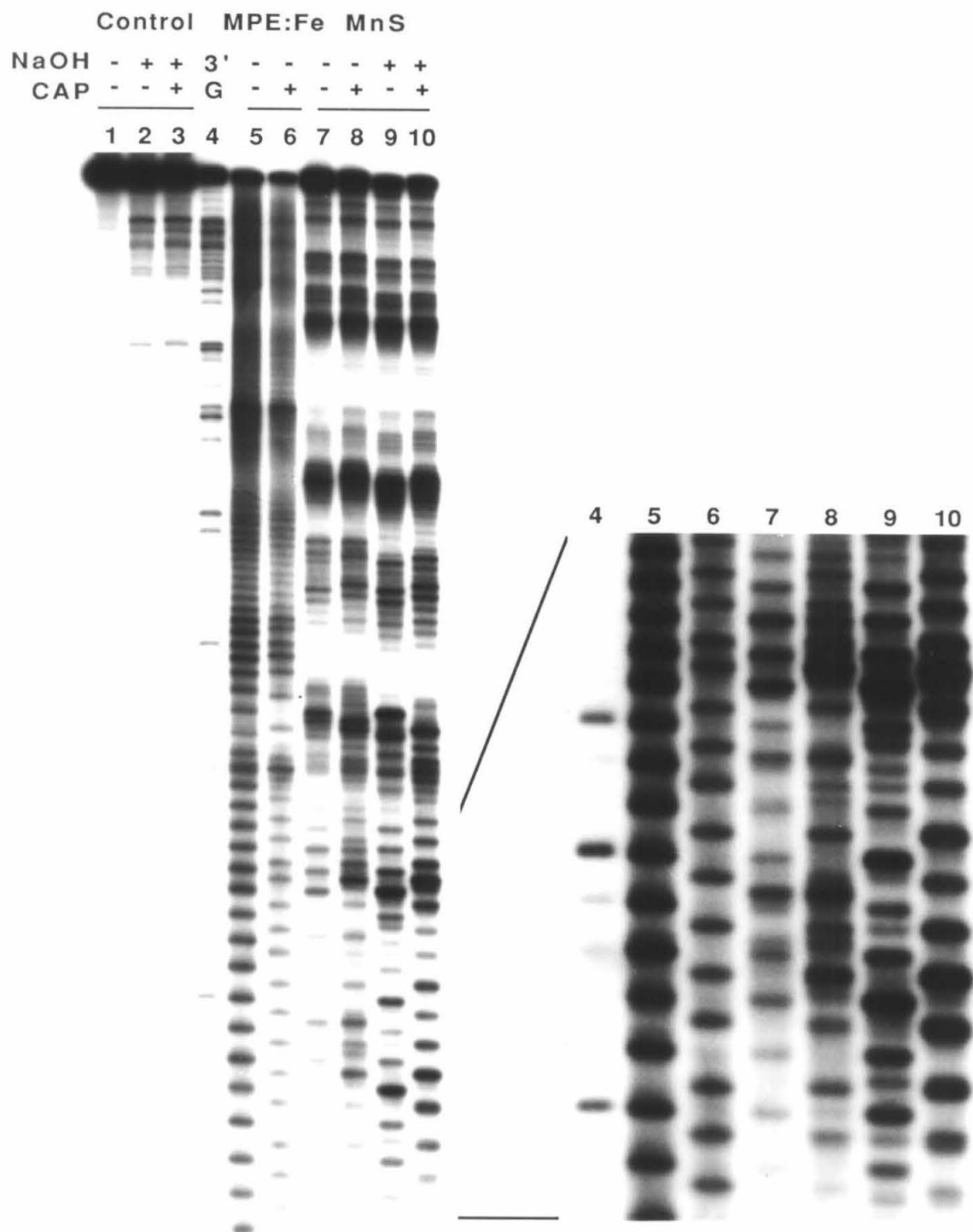


workup, comigrate with the **MPE:Fe** DNA fragments having 3'-phosphate groups. The electrophoretic mobilities of these fragments are reduced upon treatment with T4 polynucleotide kinase. Thus, **MnS** mediates the direct formation of DNA strand breaks having 3'-phosphate termini as well as latent lesions that afford DNA strand scission and 3'-phosphate termini upon base workup.

Figure 4.15 shows an autoradiograph of short DNA fragments produced by **MPE:Fe**/dithiothreitol and **MnS**/magnesium monoperoxyphthalate, with or without base workup and/or digestion with calf alkaline phosphatase (which converts 5'-phosphate groups to 5'-hydroxyl groups). The 3'-³²P end-labeled 167 base pair Eco RI/Rsa I restriction fragment from pBR322 was used for this study. Electrophoretic mobilities of radiolabeled fragments derived from this substrate depend on their lengths and the nature of their 5'-termini. Fragments produced by **MPE:Fe** or the Maxam-Gilbert chemical sequencing G reaction protocol terminate in 5'-phosphate groups.^{9,5,10} Without base workup, some of the short DNA fragments produced with **MnS** comigrate with fragments having 5'-phosphate groups, and some do not. The fragments bearing 5'-nonphosphate termini also do not comigrate with fragments having 5'-hydroxyl groups (prepared by phosphatase digestion of DNA cleavage fragments produced with **MPE:Fe**). Further, under conditions where phosphatase digestion quantitatively converts the 5'-phosphate groups of DNA fragments produced with **MPE:Fe** to 5'-hydroxyl groups, many of the DNA fragments produced with **MnS**, which comigrate with fragments having 5'-phosphate groups, are not quantitatively converted with phosphatase to fragments of reduced mobility. The extent of conversion varies from site to site--some fragments are wholly unaffected by phosphatase digestion, some fragments are partially converted to fragments of reduced mobility, while still others are completely converted to fragments of reduced mobility. Base workup of DNA cleaved by **MnS**/magnesium monoperoxyphthalate affords a cleavage pattern in which the great majority of fragments comigrate with fragments having 5'-phosphate groups. These fragments are cleanly

Figure 4.15

Analysis of DNA 5' end products produced with **MnS** on the 3'-³²P end-labeled 167 bp restriction fragment (Eco RI/Rsa I) from pBR322 plasmid DNA. Cleavage patterns were resolved by electrophoresis on a 1:20 cross-linked 20% polyacrylamide, 40% urea denaturing gel. Base workup entailed heating the samples at 90°C for 30 minutes in 0.10 M NaOH solution. Lane 1, uncleaved DNA; lane 2, uncleaved DNA with base workup; lane 3, uncleaved DNA with base workup and 5' dephosphorylation using calf alkaline phosphatase; lane 4, Maxam-Gilbert chemical sequencing G reaction; lane 5, DNA cleavage by **MPE:Fe** at 2.0 μ M concentration in the presence of dithiothreitol (5.0 mM) and dioxygen; lane 6, DNA cleavage by **MPE:Fe** at 2.0 μ M concentration in the presence of dithiothreitol (5.0 mM) and dioxygen with subsequent 5' dephosphorylation using calf alkaline phosphatase; lane 7, DNA cleavage by **MnS** at 50 μ M concentration in the presence of magnesium monoperoxyphthalate (2.0 mM); lane 8, DNA cleavage by **MnS** at 50 μ M concentration in the presence of magnesium monoperoxyphthalate (2.0 mM) with subsequent 5' dephosphorylation using calf alkaline phosphatase; lane 9, DNA cleavage by **MnS** at 50 μ M concentration in the presence of magnesium monoperoxyphthalate (2.0 mM) with subsequent base workup; lane 10, DNA cleavage by **MnS** at 50 μ M concentration in the presence of magnesium monoperoxyphthalate (2.0 mM) with subsequent base workup and 5' dephosphorylation using calf alkaline phosphatase.



converted by phosphatase to fragments of reduced mobility which comigrate with fragments having 5'-hydroxyl groups. Thus, **MnS** mediates the direct formation of DNA strand breaks having 5'-phosphate and 5'-nonphosphate, nonhydroxyl termini. The 5'-nonphosphate groups can be converted to 5'-phosphate groups by treatment with base, which also develops latent lesions into strand breaks having 5'-phosphate end groups. The most notable minor bands produced with **MnS** and base workup without phosphatase treatment comigrate with fragments having 5'-hydroxyl groups.

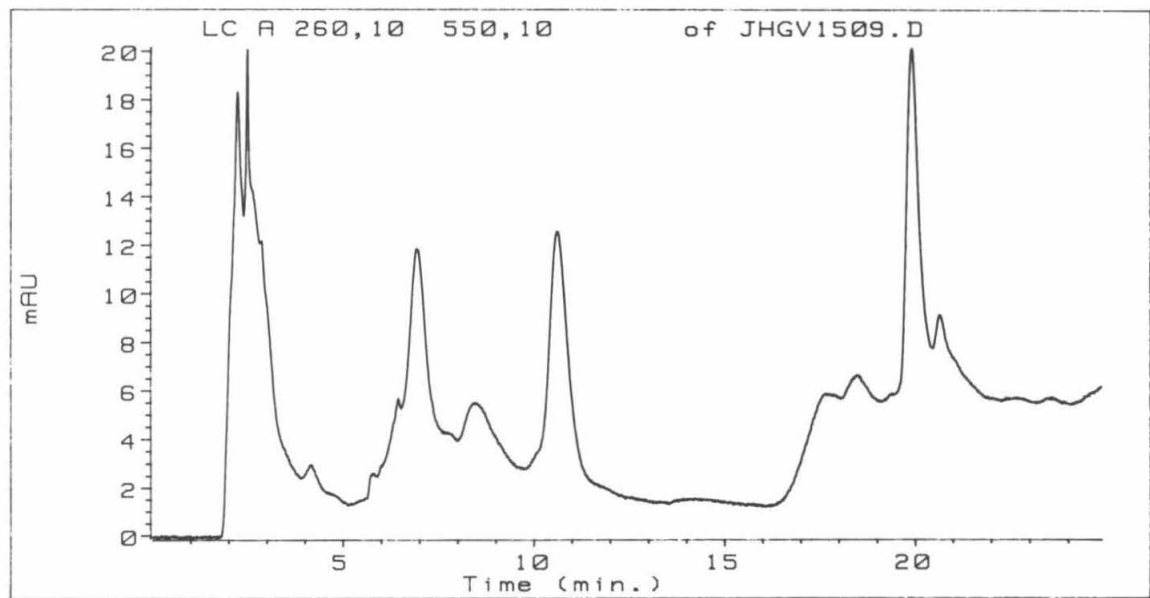
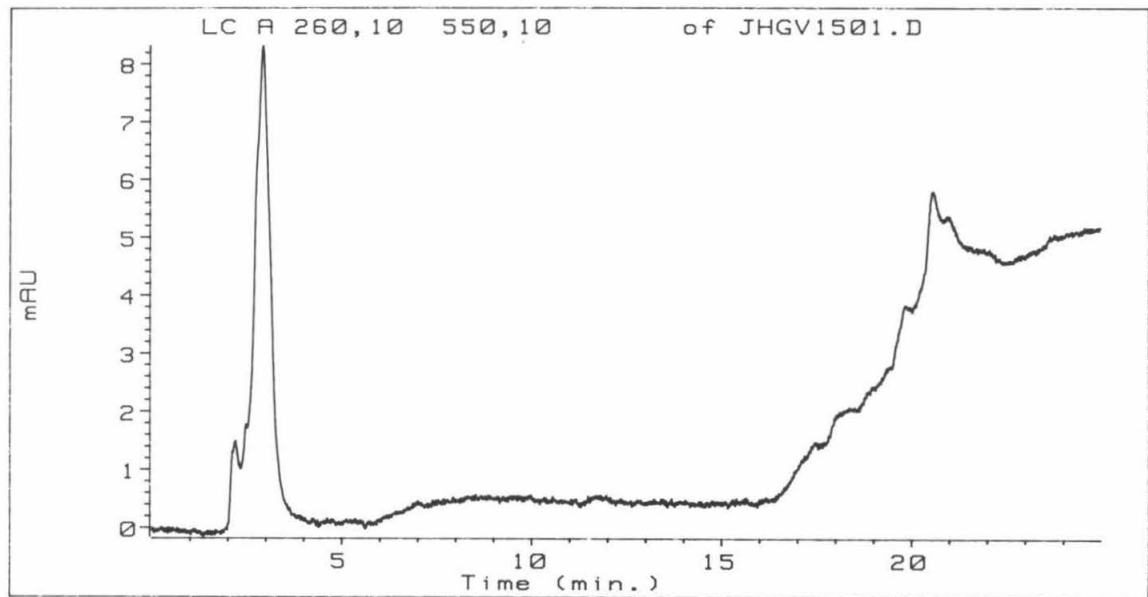
Figure 4.16 shows a reverse-phase HPLC chromatogram of the nucleotide base products formed upon cleavage of calf thymus DNA by **MnS**/hydrogen peroxide.^{5,10} The top chromatogram results from treatment of calf thymus DNA with no reagents or with hydrogen peroxide or **MnS** alone. The bottom chromatogram results from treatment of calf thymus DNA with **MnS** and hydrogen peroxide. The peaks observed with retention times near 7, 11, and 20 minutes correspond (by retention times and UV spectral analysis) to the free nucleotide bases cytosine, thymine, and adenine, respectively. The smaller, broader peak observed with a retention time near 9 minutes exhibits the mobility expected for guanine, though this peak was too small to afford a convincing diode-array UV spectrum. No peaks with longer retention times were observed.^{5,7,10} Thus, **MnS**-mediated DNA damage results in the release of each of the four DNA bases. This result and the results from the DNA end product analysis dictate that **MnS** mediates oxidation of DNA deoxyribose residues in the presence of terminal oxidants.

In results not shown, the electronic spectrum of **MnS** (20 μ M) was found to be unperturbed by the addition of calf thymus DNA (up to 1 mM in base pairs). This finding indicates that **MnS** interacts with DNA by groove or surface binding rather than by intercalation.¹²

Base treatment of DNA modified by **MnS** in the presence of terminal oxidants allows visualization of latent lesions in addition to those that lead to direct strand scission. Further, base workup affords DNA fragments with 3'- and 5'-phosphate termini, which

Figure 4.16

HPLC analysis of nucleotide base products released upon DNA cleavage by MnS.



may be compared directly to fragments produced by Maxam-Gilbert chemical sequencing reactions in order to assign nucleotide positions of DNA cleavage. Figures 4.17 and 4.18 show autoradiographs of DNA cleavage produced by **MnS**/magnesium monoperoxyphthalate with and without base workup on the 3'- and 5'-³²P end-labeled 167 and 517 base pair restriction fragments, and on the 3'-³²P end-labeled 169 base pair restriction fragments. Base treatment enhances and alters the cleavage patterns on each of these DNA substrates. Cleavage patterns observed after **MnS**-mediated cleavage and base workup were analyzed by densitometry and converted to histogram form (Figure 4.19). These histograms show that **MnS** mediates DNA cleavage at each of the four deoxynucleotides, with most DNA cleavage occurring in or near sequences of contiguous A:T base pairs. Further, **MnS** produces cleavage patterns with maxima shifted to the 3'-side on one DNA strand relative to the other. As **MnS** promotes DNA cleavage by deoxyribose oxidation, the observed 3'-shift is consistent with **MnS**-mediated cleavage occurring from the minor groove of right-handed DNA.⁸ The cleavage patterns produced with **MnS** are not uniform in shape--single bands are observed at some sites, while at other sites DNA cleavage extends symmetrically or unsymmetrically over several adjacent nucleotides. This result indicates that **MnS** mediates DNA cleavage via the intermediacy of a nonfreely diffusing reactive species.

Discussion

The ability of **MnS** to promote oxidative DNA cleavage in the presence of terminal oxidants is consistent with its ability to catalyze oxidative activation of cyclohexane C-H bonds in the presence of iodosylbenzene.¹ The effective oxidants (hydrogen peroxide, percarboxylic acids, and iodosylbenzene) are oxygen atom donors. The DNA binding/cleaving patterns observed with **MnS** are independent of the identity of the terminal oxidant. These results are consistent with the proposal of Kochi et al. that radical-like $[\text{SalenMn(V)O}]^+$ is the species directly responsible for C-H bond activation.¹ The

Figure 4.17

Autoradiographs of DNA cleavage patterns produced by **MnS** on 3'- and 5'-³²P end-labeled 167 bp (Left) and 517 bp (Right) restriction fragments (Eco RI/Rsa I) from pBR322 plasmid DNA in the presence of magnesium monoperoxyphthalate, and with and without base workup. Cleavage patterns were resolved on a 1:20 cross-linked 8% polyacrylamide, 45% urea denaturing gel. Base workup entailed heating the samples at 90°C for 30 minutes in 0.10 M NaOH solution. Odd-numbered lanes, 3' end-labeled DNA. Even-numbered lanes, 5' end-labeled DNA. Lanes 1-4, uncleaved DNA without base workup (lanes 1 and 2), and with base workup (lanes 3 and 4); lanes 5 and 6, Maxam-Gilbert chemical sequencing G reactions; lanes 7-10, DNA cleavage by **MnS** at 20 μ M concentration in the presence of $Mg(MPPA)_2$ (2.0 mM) without subsequent base workup (lanes 7 and 8), and with subsequent base workup (lanes 9 and 10).

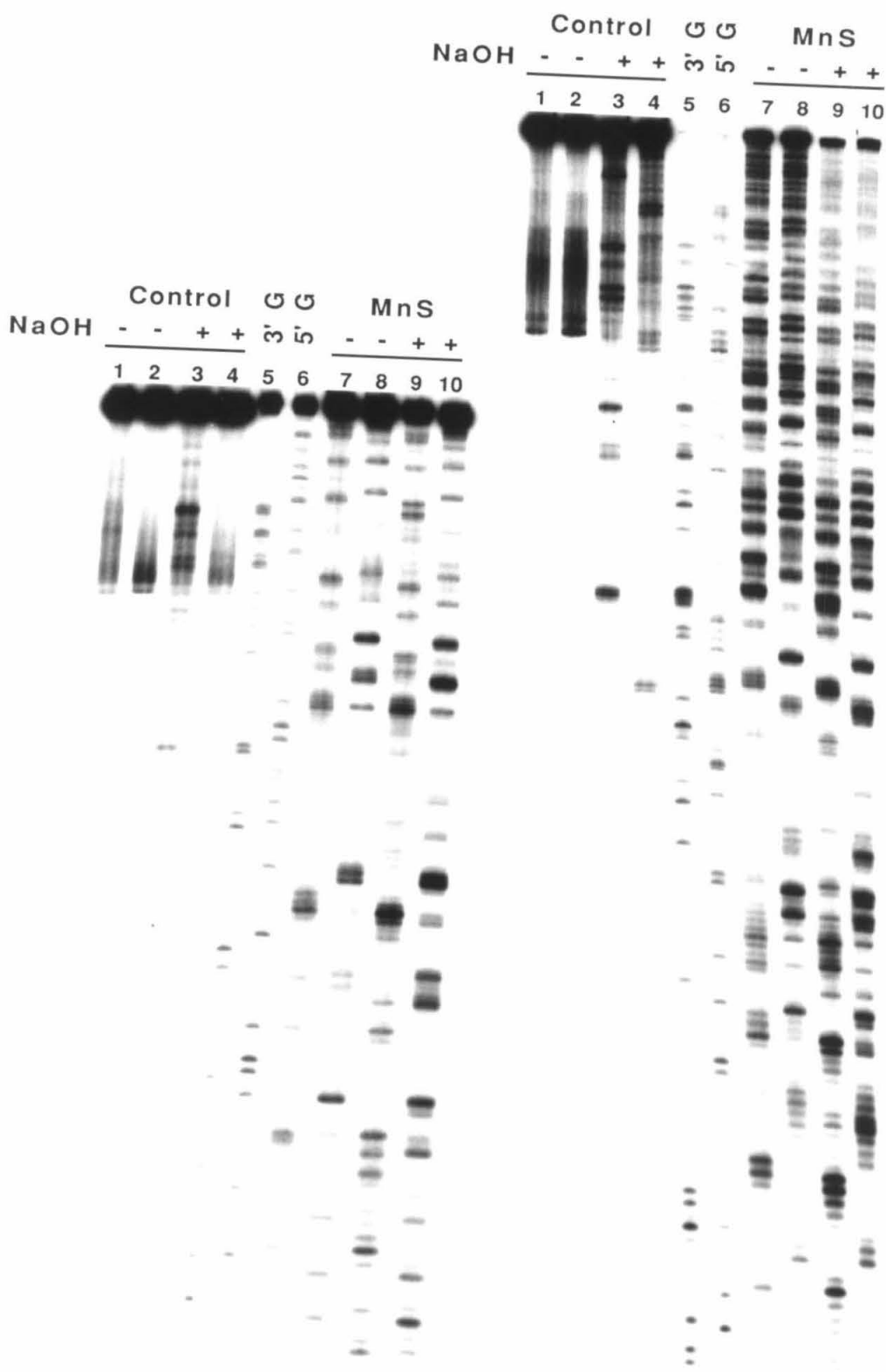


Figure 4.18

Autoradiograph of DNA cleavage patterns produced by **MnS** on 3'-³²P end-labeled 169 bp Dde I restriction fragments from pBR322 plasmid DNA in the presence of magnesium monoperoxyphthalate, and with and without base workup. Cleavage patterns were resolved on a 1:20 cross-linked 8% polyacrylamide, 45% urea denaturing gel. Base workup entailed heating the samples at 90°C for 30 minutes in 0.10 M NaOH solution. Lanes 1,3,5,6,9,11, DNA labeled at one 3' end with ³²P dCTP. Lanes 2,4,7,8,10,12, DNA labeled on the opposite strand at the 3' end with ³²P dGTP. Lanes 1-4, uncleaved DNA without base workup (lanes 1 and 2), and with base workup (lanes 3 and 4); lanes 5 and 7, Maxam-Gilbert chemical sequencing G reactions; lane 6 and 8, Maxam-Gilbert chemical sequencing G+A reactions; lanes 9-12, DNA cleaved by **MnS** at 20 μ M concentration in the presence of Mg(MPPA)₂ (2.0 mM) without subsequent base workup (lanes 9 and 10), and with subsequent base workup (lanes 11 and 12).

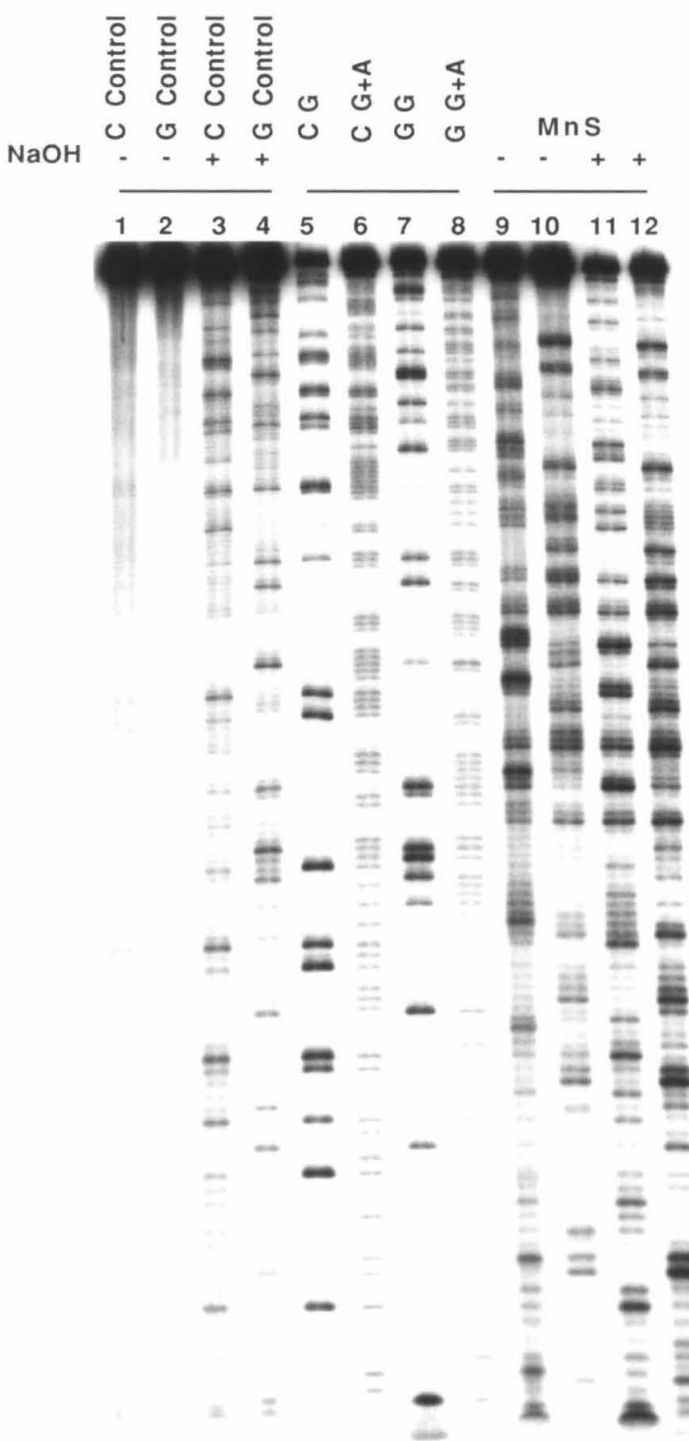
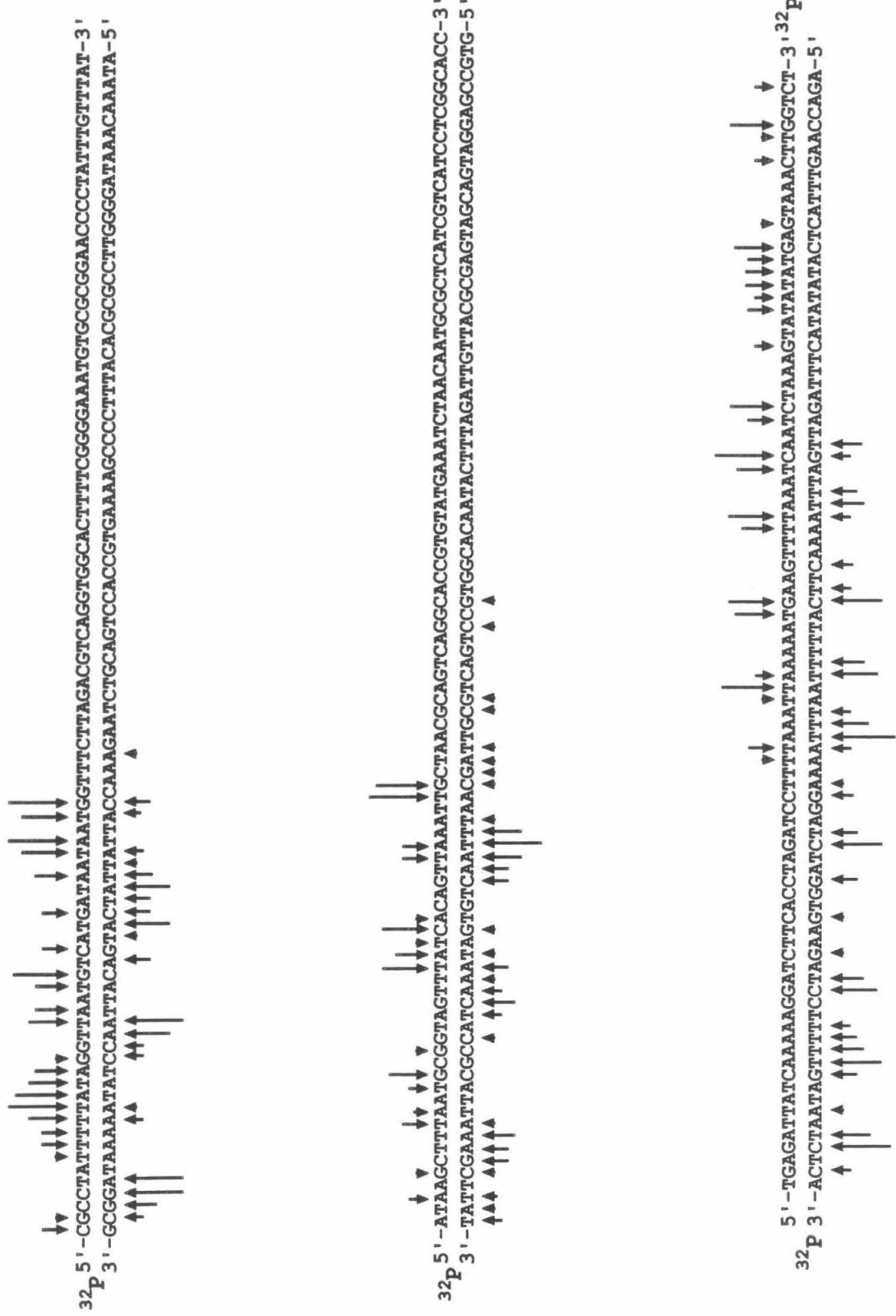


Figure 4.19

Histograms of DNA cleavage produced by **MnS** in the presence of magnesium monoperoxyphthalate on the 517, 167, and 169 base pair DNA restriction fragments from plasmid pBR322 DNA. Histograms were derived from densitometric analysis of the autoradiographs shown in Figures 4.17 and 4.18. Lengths of arrows correspond to the relative amounts of cleavage, determined by optical densitometry, which result in removal of the indicated base. Sequence positions of cleavage were determined by comparing the electrophoretic mobilities of DNA cleavage fragments to bands in Maxam-Gilbert chemical sequencing lanes. Top: Histogram of **MnS**-promoted cleavage on the 517 bp restriction fragment. Middle: Histogram of **MnS**-promoted cleavage on the 167 bp restriction fragment. Bottom: Histogram of **MnS**-promoted cleavage on the 169 bp restriction fragment.



inability of $[\text{SalenCr(III)}]^+$ to promote DNA cleavage in the presence of terminal oxidants parallels its inability to activate cyclohexane in the presence of iodosylbenzene.¹ This complex does catalyze olefin epoxidation,¹³ and Kochi and coworkers have identified, isolated, and determined the crystal structure of the active epoxidizing intermediate, $[\text{SalenCr(V)O}]^+$, which is water-stable.¹⁴ Based on its propensity to epoxidize electron-rich olefins and its inability to activate C-H bonds, Kochi et al. have proposed that this complex is more electrophilic than the amphiphilic $[\text{SalenMn(V)O}]^+$.¹ $[\text{SalenFe(III)}]^+$ complexes have been shown to mediate hydrocarbon activation in the presence of dioxygen and mercaptoethanol or ascorbic acid, but these reactions appear to be at least one order of magnitude less efficient than MnS-promoted C-H activation.¹⁵ The inability of the substituted complex $[(\text{Et}_2\text{N})_2\text{SalenMn(III)}]^+$ to promote direct DNA cleavage may arise from steric and/or electronic effects associated with the diethylamino substituents. Such bulky substituents might exclude $[(\text{Et}_2\text{N})_2\text{SalenMn(V)O}]^+$ from favorable DNA binding/cleaving sites. Alternatively, the presence of diethylamino groups may affect the electronic structure of $[(\text{Et}_2\text{N})_2\text{SalenMn(V)O}]^+$, making it unable to activate C-H bonds. This hypothesis can be tested by determining the ability of $[(\text{Et}_2\text{N})_2\text{SalenMn(III)}]\text{OAc}$ to catalyze olefin epoxidation and cyclohexane activation in the presence of iodosylbenzene.

DNA double-strand cleavage patterns produced with MnS are positively correlated with patterns produced by BNSE:Fe, a known minor groove binding/cleaving agent (Chapter One) and NCZS, which is believed to interact with DNA by both groove binding and intercalation.¹⁶ DNA double-strand cleavage patterns produced with MnS are negatively correlated with patterns produced by MPE:Fe, a known intercalating/cleaving agent,^{5,10} and Blm:Fe, which is believed to interact with DNA through both groove binding and intercalation.⁷ While more cases need to be examined, the correlations between DNA double-strand cleavage specificity and binding mode suggest that the DNA double-strand affinity cleaving assay may be a useful tool for discovering and

discriminating DNA minor groove binding/cleaving small molecules, DNA intercalating/cleaving small molecules, and DNA groove binding/intercalating/cleaving small molecules.

Based on the correlation between DNA binding/cleaving patterns produced by **BNSE:Fe** and **MnS**, the observation that the electronic spectrum of **MnS** is unchanged by the addition of excess DNA, and on the finding that **MnS** affords 3'-shifted cleavage patterns, it is proposed that **[SalenMn(III)]⁺**, and the corresponding oxo species **[SalenMn(V)O]⁺** directly responsible for DNA modification, are A:T specific DNA minor groove binding molecules. The considerable A:T binding/cleaving specificity observed with **MnS** is somewhat surprising in view of the small size of this complex and the fact that neither **MnS** nor the oxo complex has substituents which may form specific hydrogen bonds to adenine N3 or thymine O2 atoms on the floor of the minor groove. However, other crescent-shaped, hydrophobic, cationic molecules lacking hydrogen bond acceptor groups exhibit specificity for A:T rich regions of DNA.¹⁷ The A:T specificity of these molecules, as well as **MnS** and its oxo derivative, is likely based on DNA minor groove shape recognition. Hydrophobic (often aromatic) molecules can be partially or wholly sandwiched within the narrow minor groove found in A:T rich regions of DNA, where they engage in favorable van der Waals contacts and liberate ordered solvent molecules.^{18,19} Cationic ligands might also be drawn to the proposed well of negative electrostatic potential centered in the minor groove of A:T rich regions of B DNA.²⁰ The wider minor groove and the protruding guanine N2 amino groups found in regions of DNA containing G:C base pairs do not provide as favorable a receptor for the these DNA binding molecules. DNA minor groove shape recognition was first proposed to account for the DNA cleavage specificities of bis(1,10-phenanthroline)copper(II), DNase I, and DNase II.²¹

MnS-mediated DNA cleavage appears to be analogous to the metalloporphyrin-mediated DNA cleavage recently reported by Dabrowiak and coworkers.^{22,23} Dabrowiak

et al. found that iron(III), manganese(III), and cobalt(III) complexes of tetracationic *meso*-tetrakis(*N*-methyl-4-pyridiniumyl)porphine (Figure 4.20) produce oxidative cleavage of right-handed double helical DNA in the presence of iodosylbenzene, superoxide, or ascorbate. These +5 complexes produce similar, 3'-shifted, nonsymmetrical cleavage patterns at sites of three or more contiguous A:T base pairs. Based on the electrophoretic mobilities of short DNA cleavage fragments, it appears that 3'-phosphate, 5'-phosphate, and 5'-nonphosphate ends are produced in these reactions. The effects of base workup were not mentioned. Dabrowiak et al. proposed that the observed specificity may arise from the presence of favorable electrostatic interactions between the metalloporphyrins and the minor groove of B DNA at sites of contiguous A:T base pairs, and from unfavorable steric effects between the metalloporphyrins and the exocyclic N2 amino group of guanine at DNA sites containing G:C base pairs.

In light of the work of Kochi et al. and the results described in this chapter, several observations about the mechanism(s) by which **MnS** mediates DNA cleavage may be made. First, DNA cleavage stems from oxidative modification and breakdown of deoxyribose residues. Second, since the reactive intermediate is able to activate the C-H bonds of cyclohexane, it must be considered that this species is also able to activate any of the deoxyribose C-H bonds. Third, mechanisms involving dioxygen may be discounted, as **MnS**-promoted DNA cleavage proceeds with identical specificity and efficiency in the absence or presence of dioxygen. This rules out the accepted mechanism for DNA cleavage by **B1m:Fe** under aerobic conditions,⁷ and mitigates strongly against any mechanisms that proceed through alkyl peroxy radicals or alkyl hydroperoxide intermediates. Fourth, given that the DNA cleaving species is located in the DNA minor groove, C-H bonds within or on the edges of the minor groove (C-H_{1'}, C-H_{2'}, C-H_{4'}, C-H_{5'}) should be considered as the most likely candidates for activation. Fifth, the production of direct DNA strand breaks, base-labile lesions, and DNA fragments with

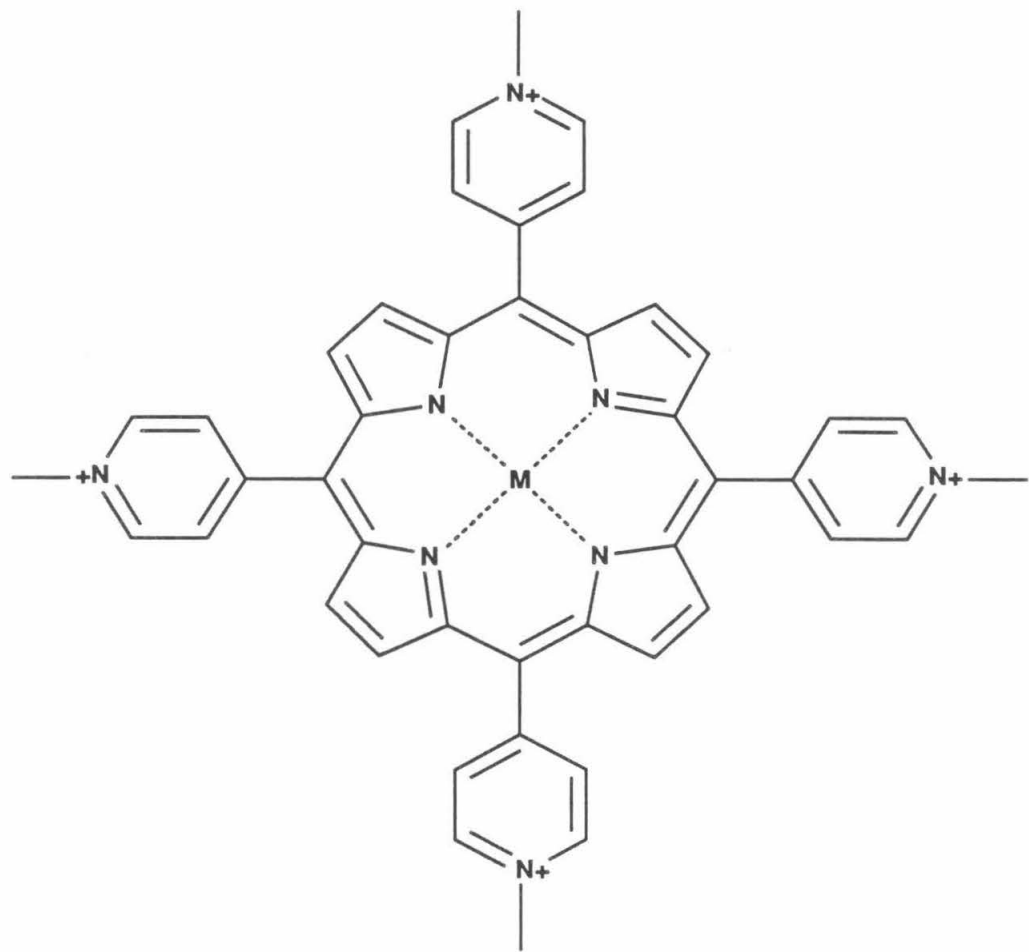


Figure 4.20.Cationic DNA binding/cleaving metalloporphyrins studied by Dabrowiak and coworkers. $M = \text{Fe(III)}, \text{Co(III)}, \text{Mn(III)}, \text{Zn(II)}, \text{Cu(II)}, \text{or Ni(II)}$.

heterogeneous 5'-end groups indicates that **MnS** promotes DNA cleavage via multiple, parallel pathways.

Figure 4.21 depicts four different pathways, each of which involves the catalytic activation of a deoxyribose C-H bond located within or on the edges of the DNA minor groove, by $[\text{SalenMn(V)O}]^+$ to afford hydroxylated products. Considering the work of Kochi et al., C-H activation is likely to involve initial hydrogen atom abstraction to form an alkyl radical and $[\text{SalenMn(IV)OH}]^+$, followed by radical oxidation to a carbenium ion (perhaps by electron transfer to the proximal $[\text{SalenMn(IV)OH}]^+$), and trapping of the carbenium ion by solvent water (or perhaps the coordinated hydroxyl of $[\text{SalenMn(III)OH}]^+$ produced upon electron transfer from the alkyl radical to $[\text{SalenMn(IV)OH}]^+$).

C-H_{1'} activation would produce a hemiortho ester which would decompose to an unstable 3'-dehydrolactone derivative with liberation of free base and a DNA fragment with a 5'-phosphate group. The dehydrolactone would undergo further decomposition under mild conditions (\leq room temperature at neutral pH) to liberate an unstable methylene dehydrolactone and a DNA fragment with a 3'-phosphate group. Activation of C-H_{1'} bonds has been shown to occur during DNA cleavage with bis(1,10-phenanthroline)copper(II).²⁴ It is likely that **NCZS** and the related antibiotics Esperamicin A₁ and Calicheamicin γ_1 ^I (Figure 2.4) activate C-H_{1'} bonds.^{6,25,26}

C-H_{2'} activation would afford a ribonucleotide residue within a DNA molecule. Ribonucleotides may be hydrolyzed under basic conditions to liberate DNA fragments having 5'-hydroxyl groups and 3'- or 2'-phosphate groups. Since **MnS** promotes the formation of small amounts of latent lesions which, after base workup, produce DNA fragments that comigrate with fragments having authentic 5'-hydroxyl groups, this pathway might be operative in some minor fashion. This pathway also provokes thought as to means by which the difficult task of formal DNA hydrolysis might be achieved via an oxidative reaction.²⁷

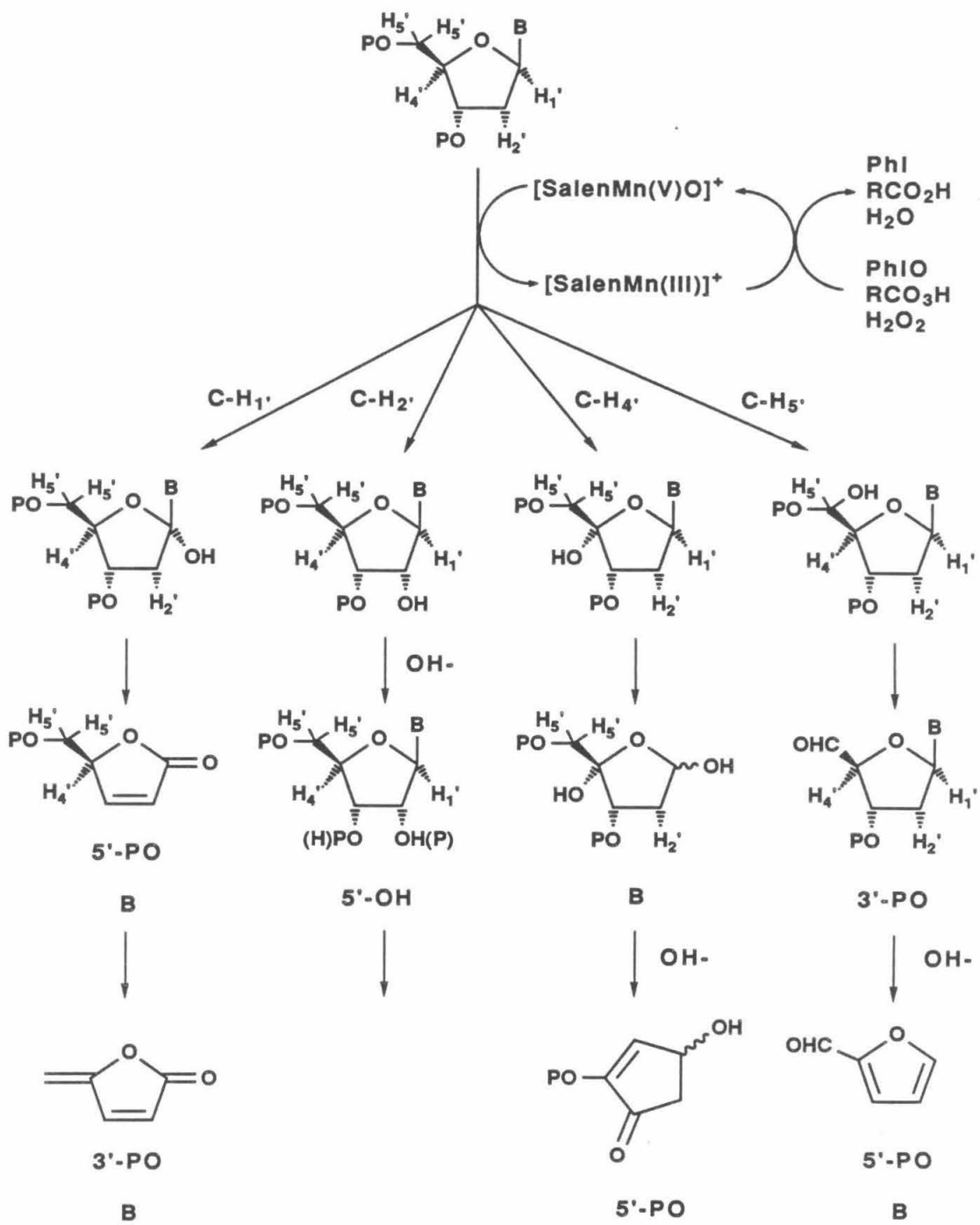


Figure 4.21. Plausible mechanisms for oxidative DNA cleavage by MnS in the presence of oxygen atom donors. Top Right: Catalytic formation of $[\text{SalenMn(V)O}]^+$ from $[\text{SalenMn(III)}]^+$ and oxygen atom donors. Upper Middle: Hydroxylation of DNA deoxyribose residues at positions $\text{C-H}_1'$ (Left), $\text{C-H}_2'$ (Center Left), $\text{C-H}_4'$ (Center Right), and $\text{C-H}_5'$ (Right). Lower Middle and Bottom: DNA cleavage products obtained from decomposition of hydroxylated deoxyribose residues with or without the aid of base.

C-H_{4'} activation would afford an unstable hemiacetal derivative which would decompose to liberate free base and produce a bis(hemiacetal). This species represents the base-labile lesion produced by **BIm:Fe** in the absence of sufficient dioxygen.²⁸ In the presence of base this species decomposes to a DNA fragment having a 5'-phosphate group and a DNA fragment having a 3'-nonphosphate group. Such a 3'-end group is not observed upon DNA cleavage with **MnS**.

C-H_{5'} activation would afford a hemiacetal phosphate ester which should decompose under ambient conditions to liberate a DNA fragment with a 3'-phosphate group and a DNA fragment with a nucleoside 5'-aldehyde group. These products are produced upon DNA cleavage with **NCZS** or the related antibiotics Esperamicin A₁ and Calicheamicin γ_1 .^{1,6,16,25,26} DNA fragments terminating in nucleoside 5'-aldehyde groups can be converted to corresponding fragments that terminate in 5'-phosphate groups by base workup, which would also liberate the DNA base and furfural.^{6,16}

These pathways do no account for the observed formation of latent lesions that are converted with base to DNA fragments having 3'- and 5'-phosphate end groups. This discrepancy indicates that an additional, unidentified mechanistic pathway is operative in this system. However, if hemiacetal phosphate ester lesions produced upon C-H_{5'} activation are marginally stable to the conditions under which sequencing gels are run (precipitation, heating at 100°C in 80% aqueous formamide buffer, pH 8.3, and electrophoresis at pH 8.3), the products observed upon **MnS**-mediated DNA cleavage could be accounted for by a combination of pathways involving C-H_{1'} and C-H_{5'} activation with perhaps a small contribution from activation at C-H_{2'}. Detection and quantification of the expected methylene dehydrolactone and furfural products derived from activation at C-H_{1'} and C-H_{5'}, respectively, would provide confirmation of these pathways.

While the results with $[(\text{Et}_2\text{N})_2\text{SalenMn(III)}]^+$ indicate that diethylamino substituents at these particular positions interfere with the DNA binding and/or DNA cleaving properties of its oxo derivative, a variety of substituents at several other positions

on the Salen nucleus may be examined for the effects that they have on DNA binding/cleaving properties relative to the parent MnS. Of particular interest would be Salen complexes substituted with additional DNA recognition elements.

References

- ¹Srinivasan, K.; Michaud, P.; Kochi, J.K. *J. Am. Chem. Soc.* **1986**, *108*, 2309-2320.
- ²Coggon, P.; McPhail, A.T.; Mabbs, F.E.; Richards, A.; Thornley, A.S. *J. Chem. Soc. (A)* **1970**, 3296-3303.
- ³Thielert, H.; Pfeiffer, P. *Chem. Ber.* **1938**, *71*, 1399-1403.
- ⁴LaMar, G.N.; Eaton, G.R.; Holm, R.H.; Walker, F.A. *J. Am. Chem. Soc.* **1973**, *95*, 63-75.
- ⁵Hertzberg, R.P., Ph.D. Thesis, California Institute of Technology, Pasadena, California, 1984.
- ⁶Povirk, L.F.; Houlgrave, C.W.; Han, Y.-H. *J. Biol. Chem.* **1988**, *263*, 19263-19266, and references therein.
- ⁷Stubbe, J.; Kozarich, J.W. *Chem. Rev.* **1987**, *87*, 1107-1136.
- ⁸Taylor, J.S.; Schultz, P.G.; Dervan, P.B. *Tetrahedron* **1984**, *40*, 457-465.
- ⁹Maxam, A.M.; Gilbert, W. *Methods Enzymol.* **1980**, *65*, 499-560.
- ¹⁰Hertzberg, R.P.; Dervan, P.B. *Biochemistry* **1984**, *23*, 3934-3945.
- ¹¹Schultz, P.G., Ph.D. Thesis, California Institute of Technology, Pasadena, California, 1984.
- ¹²Porumb, H. *Prog. Biophys. Mol. Biol.* **1978**, *34*, 175-195.
- ¹³Samsel, E.G.; Srinivasan, K.; Kochi, J.K. *J. Am. Chem. Soc.* **1985**, *107*, 7606-7617.
- ¹⁴Sidall, T.L.; Miyaura, N.; Huffman, J.C.; Kochi, J.K. *J. Chem. Soc. Chem. Comm.* **1983**, 1185-1186.
- ¹⁵Tabushi, I.; Nakajima, T., Seto, K. *Tet. Lett.* **1980**, 2565-2568.
- ¹⁶Dasgupta, D.; Goldberg, I.H. *Biochemistry* **1985**, *24*, 6913-6920.
- ¹⁷Zimmer, C.; Wahnert, U. *Prog. Biophys. Molec. Biol.* **1986**, *47*, 31-112.
- ¹⁸Kopka, M.L.; Yoon, C.; Goodsell, D.; Pjura, P.; Dickerson, R.E. *Proc. Natl. Acad. Sci. USA* **1985**, *82*, 1376-1380.
- ¹⁹Kopka, M.L.; Yoon, C.; Goodsell, D.; Pjura, P.; Dickerson, R.E. *J. Mol. Biol.* **1985**, *183*, 553-563.

²⁰Pullman, B.; Lavery, R.; Pullman, A. *Eur. J. Biochem.* **1982**, *124*, 229-238.

²¹Drew, H.R.; Travers, A.A. *Cell* **1984**, *37*, 491-502.

²²Ward, B.; Skorobogaty, A.; Dabrowiak, J.C. *Biochemistry* **1986**, *25*, 6875-6883.

²³Bromley, S.D.; Ward, B.W.; Dabrowiak, J.C. *Nucleic Acids Res.* **1986**, *14*, 9133-9148.

²⁴Sigman, D.S. *Acc. Chem. Res.* **1986**, *19*, 180-186.

²⁵Golik, J.; Clardy, J.; Dubay, G.; Groenewold, G.; Kawaguchi, H.; Konishi, M.; Krishnan, B.; Ohkuma, H.; Saitoh, K.; Doyle, T.W. *J. Am. Chem. Soc.* **1987**, *109*, 3461-3462.

²⁶Zein, N.; Sinha, A.M.; McGahren, W.J.; Ellestad, G.A. *Science* **1988**, *240*, 1198-1201.

²⁷Basile, L.A.; Raphael, A.L.; Barton, J.K. *J. Am. Chem. Soc.* **1987**, *109*, 7550-7551.

²⁸Sugiyama, H.; Xu, C.; Murugesan, N.; Hecht, S.M. *J. Am. Chem. Soc.* **1985**, *107*, 4104-4105.

CHAPTER FIVE: ADDITIONAL STUDIES

This Chapter summarizes progress on two additional projects. In the first project, analogs of Distamycin-EDTA having one or three *N*-isopropylpyrrolecarboxamide residues in place of *N*-methylpyrrolecarboxamide residues were designed and synthesized (Figure 5.1). It was felt that these derivatives might exhibit different DNA binding specificity than **DE** based on shape, preferring A:T rich regions where the minor groove could accommodate bulky *N*-isopropyl groups. The syntheses of **IDE** and **TriIDE** followed the procedure reported for the synthesis of **DE**.¹ The requisite *N*-isopropyl-4-nitropyrrrole-2-carboxylic acid synthon **II-86** was prepared in four steps from commercially available methyl 2,5-dihydro-2,5-dimethoxyfuran-2-carboxylic acid. This dihydrofuran was reduced to the corresponding tetrahydrofuran and then condensed with isopropylamine to afford *N*-isopropylpyrrole-2-carboxylic acid, methyl ester **II-84**.² **II-84** was nitrated and hydrolyzed to afford **II-86**. DNA affinity cleaving studies showed that DNA binding/cleaving efficiency decreased in the order **DE:Fe** > **IDE:Fe** > **TriIDE:Fe**. However, no significant differences in DNA binding/cleaving specificity were detected among this series of molecules. It may be that a minor groove wide enough to accommodate *N*-isopropyl groups does not form favorable van der Waals contacts with the pyrrolecarboxamide residues of the isopropyl **DE** derivatives.

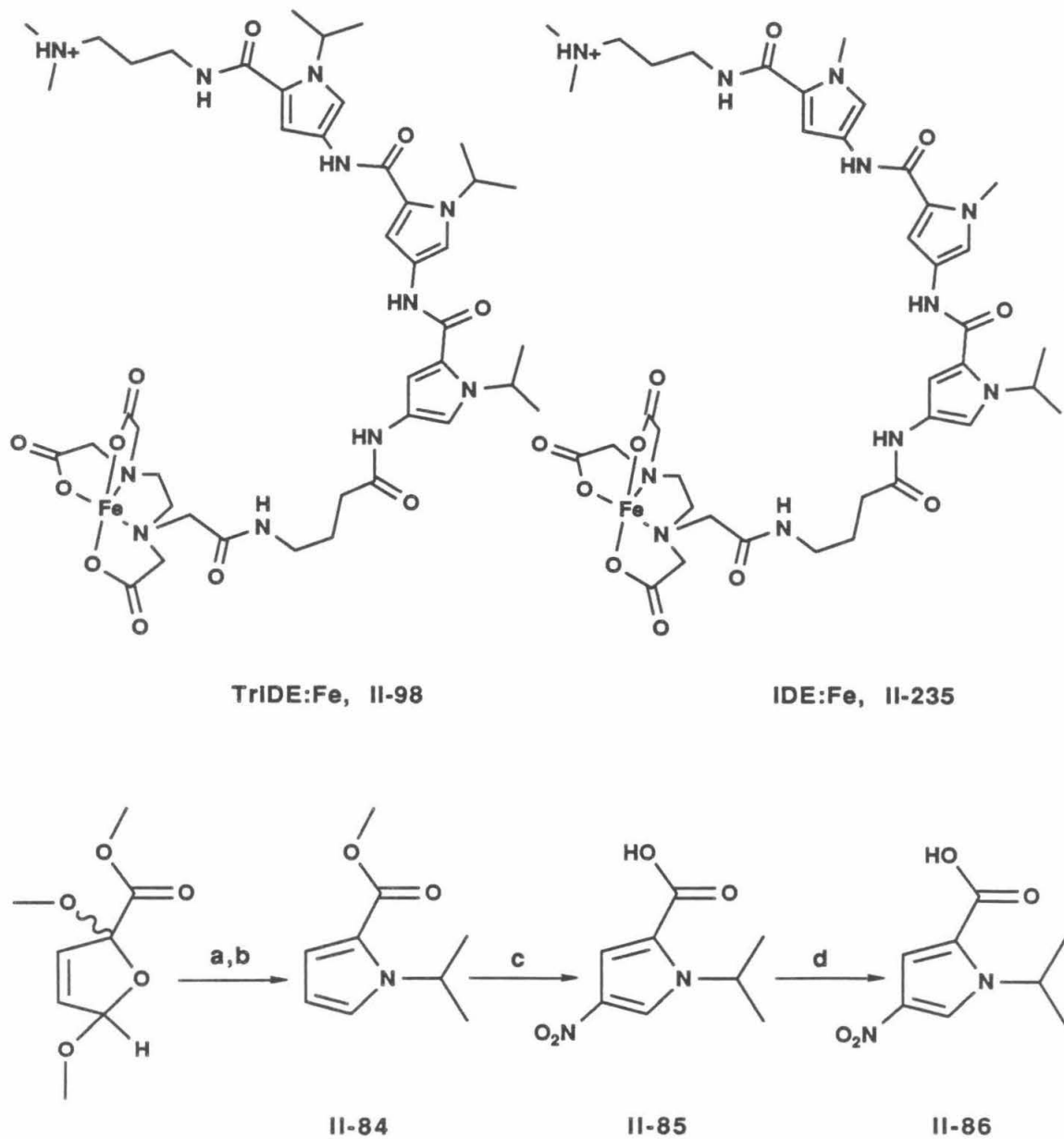


Figure 5.1. Top Left: *N,N',N''*-Triisopropyl-Distamycin-EDTA:Fe (TriIDE:Fe). Top Right: *N*-Isopropyl-Distamycin-EDTA:Fe (IDE:Fe). Bottom: Scheme for the synthesis of 4-Nitro-*N*-isopropylpyrrole-2-carboxylic acid. Reaction conditions: **a**, H_2 (3 atm), Rh/alumina, HOAc/ EtOH; **b**, $(\text{H}_3\text{C})_2\text{CHNH}_2$, HOAc, reflux; **c**, HNO_3 , Ac_2O ; **d**, NaOH, EtOH, H_2O , reflux.

To date, research in the Dervan laboratories has focused on the design and synthesis of sequence-specific DNA binding/cleaving molecules.³ The approach taken has been to combine sequence-specific DNA binding subunits with DNA cleaving subunits. This approach has provided a powerful method for studying DNA recognition (DNA affinity cleaving), and may have applications in DNA manipulation and medicinal therapy. As sophistication in the design of sequence-specific DNA binding molecules increases, it would be most interesting to combine DNA binding subunits with subunits that provide DNA-related phenomena other than DNA cleavage. Could chimeric molecules that induce DNA transcription, replication, or recombination be designed? With this question in mind, we have undertaken the design and synthesis of artificial activators of transcription using the chimeric subunit approach (Figure 5.2).

The DNA binding subunit chosen was a pyrimidine oligodeoxynucleotide, which can bind parallel to a complementary purine strand within a polypurine:polypyrimidine duplex and form a DNA triple helix.⁴ The transcription-activating subunit chosen was an acidic, amphipathic peptide designed by Giniger and Ptashne. This peptide was shown to activate transcription when appended to the N-terminal DNA binding domain of the yeast transcription factor Gal4.⁵ Two different pyrimidine oligonucleotide sequences, twenty nucleotides in length, were prepared with either 5'-thymidine-succinamic acid or 5'-phosphate termini. The oligonucleotide 5' terminal groups were designed such that they could be condensed with the Giniger/Ptashne peptide (which had been extended by one β -alanine residue at the N-terminus) to afford the nucleopeptide targets joined by stable amide or phosphoramidate linkages. Chu and Orgel have reported procedures for the coupling of amines to activated 5'-phosphate groups.⁶

Four pBR322-derived plasmids were prepared to test for nucleopeptide activation of *in vitro* run-off transcription. These plasmids (pJHG2-5, Figure 5.3) contained the Lac UV-5 promoter⁷ inserted at two different positions downstream from two different polypurine:polypyrimidine binding sequences for pyrimidine oligonucleotides. Lac UV-5

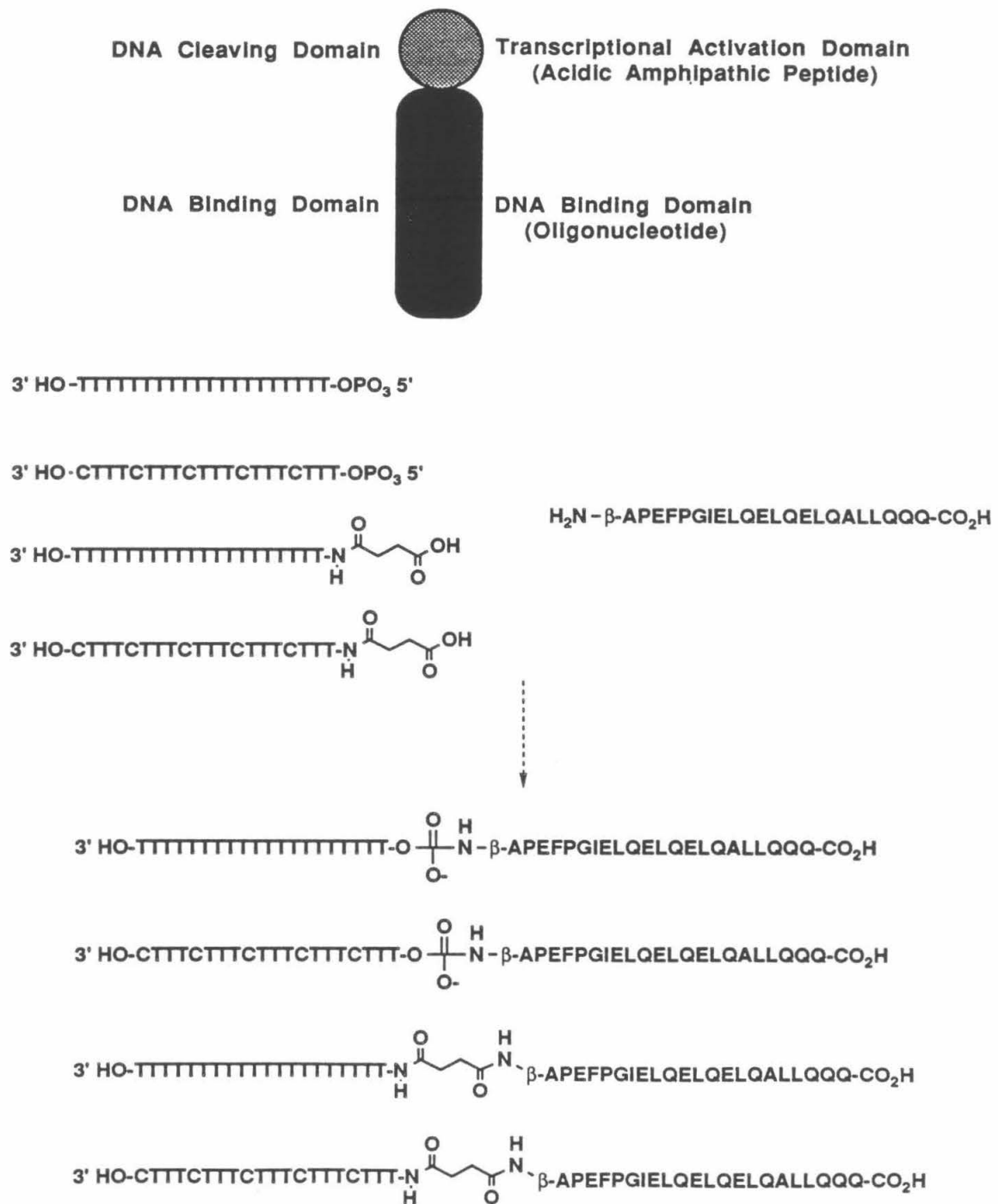
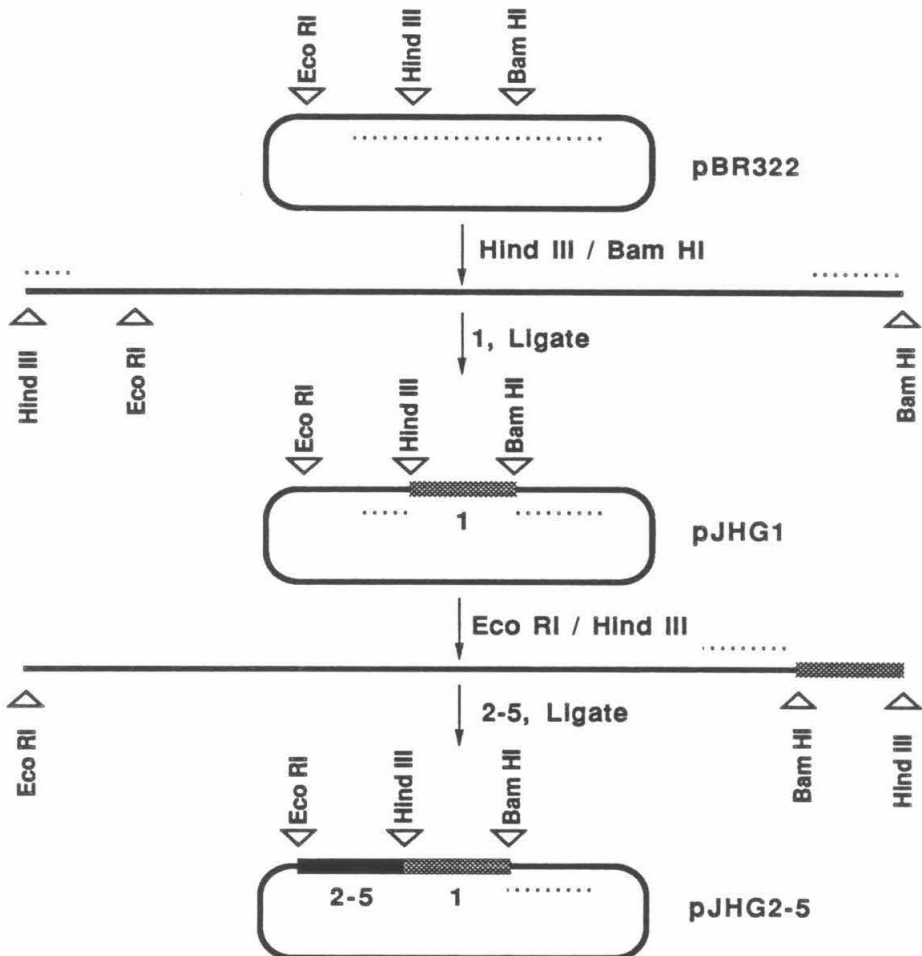


Figure 5.2. Top: Design of bifunctional DNA binding/cleaving and DNA binding/transcription activating agents through the chimeric subunit approach. Middle Left: Pyrimidine oligonucleotides for DNA recognition through DNA triple helix formation. Middle Right: Acidic amphipathic peptide for transcriptional activation. Bottom: Proposed nucleopeptides for bifunctional DNA binding/transcriptional activation.



- 1: 5' -AGCTTAGGCTTACACTTATGCTTCCGGCTCGTATGTTGTGT
ATCCGAAATGTGAAATACGAAGGCCGAGCATAAACACACCTAG
- 2: 5' -AATTCTCATGTTTTTTTTTTTTTTTTTA
GAGTACAAAAAAAAAAAAAAATTCTGA
- 3: 5' -AATTCTCATGCTTCTTTCTTCTTTCTTTA
GAGTACGAAAGAAAGAAAGAAATTCTGA
- 4: 5' -AATTCTCATGTTTTTTTTTTTTTTAACCCCAGGCA
GAGTACAAAAAAAAAAAAAAATTGGGGTCCGTTCTGA
- 5: 5' -AATTCTCATGCTTCTTTCTTCTTTCTTTAACCCCAGGCA
GAGTACGAAAGAAAGAAAGAAATTGGGGTCCGTTCTGA

Figure 5.3. Synthetic plasmids constructed for the study of transcriptional activation by the deoxypyrimidine oligonucleotides and nucleopeptides shown in Figure 5.2. The dotted line represents the gene encoding tetracycline resistance that is disrupted during plasmid construction. The striped bar represents the inserted oligonucleotide 1 that bears the Lac promoter sequence. The solid bar represents the inserted oligonucleotides 2-5, that bear the template activating sequences.

is an intrinsically weak promoter that deviates significantly from the canonical promoter -35 and -10 sequences.⁸ Transcription from the Lac UV-5 promoter normally requires activation by the binding of the catabolite gene activator protein (CAP) at upstream positions.⁹ In pJHG2-5, the polypurine:polypyrimidine sequences span positions -75 to -55 or -65 to -45 relative to the transcriptional start site. The polypurine:polypyrimidine tracts were inserted with the polypyrimidine sequence on the transcription template strand. With this orientation, pyrimidine oligonucleotides would bind with their 5'-termini towards the promoter sequence. Given that transcriptional activation in both prokaryotes and eukaryotes often depends upon acidic (negatively charged) regions of transcription factors, which bind upstream of promoter sequences and may physically contact RNA polymerases,^{10,11} polyanionic pyrimidine oligonucleotides may by themselves activate transcription when bound in appropriate juxtaposition to promoters.

To date, the Giniger/Ptashne peptide has not been coupled to the pyrimidine oligonucleotides, nor have experiments been run to determine whether pyrimidine oligonucleotides can by themselves activate run-off transcription¹² in *trans* via DNA triple helix formation. pJHG2-5 were designed such that digestion by Ban II, Dsa I, Sph I, and Sal I would afford templates for the generation of run-off transcripts from the Lac UV-5 promoter of 96, 153, 187, 247, and 276 nucleotides in length, respectively.

References

¹Taylor, J.S.; Schultz, P.G.; Dervan, P.B. *Tetrahedron* **1984**, *40*, 457-465.

²Elming, N.; Clauson-Kaas, N. *Acta Chem. Scand.* **1952**, *6*, 807-814.

³Dervan, P.B. *Science* **1986**, *232*, 464-471.

⁴Moser, H.E.; Dervan, P.B. *Science* **1987**, *238*, 645-650.

⁵Giniger, E.; Ptashne, M. *Nature* **1987**, *330*, 670-672.

⁶Chu, B.F.; Orgel, L.E. *Proc. Natl. Acad. Sci. USA* **1985**, *82*, 963-967.

⁷Dickson, R.C. Abelson, J.; Barnes, W.M.; Reznikoff, W.S. *Science* **1975**, *187*, 27-35.

⁸McClure, W.R. *Ann. Rev. Biochem.* **1985**, *54*, 171-204.

⁹de Crombrugghe, B.; Busby, S.; Buc, H. *Science* **1984**, *224*, 831-838.

¹⁰Hochschild, A.; Irwin, N.; Ptashne, M. *Cell* **1983**, *32*, 319-325.

¹¹Ptashne, M. *Nature* **1988**, *335*, 683-689.

¹²O'Halloran, T.V.; Frantz, B.; Shin, M.K.; Ralston, D.; Wright, J. *Cell* **1989**, *56*, 119-129.

CHAPTER SIX: EXPERIMENTAL SYNTHESIS

General. ^1H NMR spectra were recorded at 90 MHz on Varian EM-390 or JEOL FX-90Q instruments, or at 400 MHz on a JEOL JNM-GX400. Solvent for NMR was $\text{Me}_2\text{SO-d}_6$ unless otherwise noted. Chemical shifts are reported in parts per million downfield from Me_4Si . High-resolution fast atom bombardment mass spectra (FAB MS) were obtained from the Midwest Center for Mass Spectrometry at the University of Nebraska, Lincoln. IR spectra were recorded on a Shimadzu IR-435 instrument. UV spectra were recorded on Cary 219 Perkin-Elmer Lambda 4C spectrophotometers. Polarimetry was performed using a Jasco DIP-181 Digital Polarimeter.

Chromatography was carried out under positive air pressure using EM Science Kieselgel 60 (230-400 Mesh). Reagent-grade chemicals were used as received, except for *N,N*-dimethylformamide (DMF, Mallinckrodt), which was dried over 4 \AA molecular sieves, pyridine, which was distilled from barium oxide, *N*-bromosuccinimide (NBS) and *p*-toluenesulfonyl chloride (TsCl), which were recrystallized, and *N,N'*-carbonyldiimidazole (CDI), which was sublimed before use. Nonaqueous reactions were in general carried out under argon. Concentrations of Bis(Netropsin)-EDTA and P1-Linker-P3-EDTA compounds were determined by UV, using linear combinations of extinction coefficients measured for individual Netropsin, P1, or P3 subunits.¹

Penta-(*N*-methylpyrrolecarboxamide)-EDTA (P5E) was prepared by and obtained from R. Scott Youngquist.¹ ***N*-Methyl-4-[*N*-methyl-4-(*N*-methyl-4-pyrrole-2-carboxamide)-nitro-*pyrrole-2-carboxamide*]-*pyrrole-2-carboxylic acid* ($\text{O}_2\text{NP3CO}_2\text{H}$)²** and Distamycin-EDTA (DE)³ were prepared by and obtained from Linda C. Griffin. Methidiumpropyl-EDTA (MPE) was prepared by Robert P. Hertzberg.⁴

***N*-Methyl-4-(*N*-methyl-4-nitropyrrole-2-carboxamide)-pyrrole-2-carboxylic acid (O₂NP2CO₂H).**

2,5 Cold nitric acid (80 mL) was slowly added to cold acetic anhydride (Ac₂O, 300 mL) and this reagent kept chilled in an ice bath while aliquots were added dropwise over one hour with stirring to a slurry of *N*-methylpyrrole-2-carboxylic acid (Aldrich, 100 g, 800 mmol) in 500 mL Ac₂O, which was maintained below -20°C in a dry ice/ethanol bath. After addition was complete, the mixture was stirred for one hour at -20°C and then allowed to warm to 0°C over 1 hour (h). The mixture was poured into 1500 cc ice and allowed to stir at room temperature (RT) while the Ac₂O hydrolyzed. The brown solution was then chilled, first at 4°C, and then at -20°C, whereupon a beige solid was deposited. This material was filtered, washed with H₂O until the filtrate was colorless, and then dried in air. ¹H NMR showed this to be a 95:5 mixture of *N*-methyl-4-nitropyrrole-2-carboxylic acid and *N*-methyl-5-nitropyrrole-2-carboxylic acid. Recrystallization of the product from 600 mL 1:1 AcOH:H₂O afforded 57 g (335 mmol, 42%) of 99% ***N*-methyl-4-nitropyrrole-2-carboxylic acid.** ¹H NMR δ 8.20 (d, 1H), 7.25 (d, 1H), 3.93 (s, 3H). Some of this material (17.1 g, 100 mmol) was esterified by refluxing it in a solution of concentrated sulfuric acid (H₂SO₄, 17 mL) in methanol (MeOH, 170 mL) for 19 h. Upon cooling to RT, a mass of white crystals formed. The crystals were collected by filtration, washed with H₂O, saturated aqueous sodium bicarbonate solution (NaHCO₃), H₂O, and dried *in vacuo* to afford 16.2 g (88 mmol, 88%) of ***N*-methyl-4-nitropyrrole-2-carboxylic acid, methyl ester.** ¹H NMR (CDCl₃) δ 7.42 (d, 1H), 7.40 (d, 1H), 4.00 (s, 3H), 3.87 (s, 3H). The nitro ester (16.2 g, 88 mmol) was reduced at RT using 1 atmosphere (atm) hydrogen (H₂) pressure and 1.6 g 5% palladium on carbon (Pd/C) catalyst in 200 mL DMF solvent. When the reduction was complete, the catalyst was removed by filtering the mixture through celite. The filtrate was then treated with triethylamine Et₃N (20 mL, 200 mmol) and a DMF solution of ***N*-methyl-4-nitropyrrole-2-carboxylic acid chloride.** The acid chloride had been prepared by refluxing *N*-methyl-4-nitropyrrole-2-carboxylic acid (17 g, 100 mmol) in thionyl chloride

(SOCl₂, 55 mL) for 3 h, removing the SOCl₂ by distillation, and dissolving the crystalline residue in 30 mL DMF. The resulting mixture was allowed to stir overnight at RT before being treated with 400 mL ice water. The mixture was filtered and the solid washed with H₂O, cold MeOH, and dried *in vacuo* to afford 20 g (65 mmol, 74%) of **N-methyl-4-(N-methyl-4-nitropyrrole-2-carboxamide)-pyrrole-2-carboxylic acid, methyl ester**. ¹H NMR δ 10.2 (s, 1H), 8.16 (s, 1H), 7.58 (d, 1H), 7.45 (d, 1H), 6.89 (d, 1H), 3.96 (s, 3H), 3.85 (s, 3H), 3.75 (s, 3H). The ester (7.65 g, 25 mmol) was then hydrolyzed by refluxing it in 500 mL 1:1 EtOH:H₂O containing sodium hydroxide (NaOH, 8 g, 200 mmol) for 3 h. The solvent was removed and the residue slurried in 250 mL H₂O. The slurry was chilled in ice and acidified to pH 1 using 6 M hydrochloric acid (HCl). The mixture was filtered and the solid washed with dilute HCl, H₂O, anhydrous ether (Et₂O), dried in air and then *in vacuo* to afford 5.1 g (21 mmol, 84%) of **O₂NP₂CO₂H**. ¹H NMR δ 10.24 (s, 1H), 8.16 (s, 1H), 7.56 (s, 1H), 7.41 (s, 1H), 6.83 (d, 1H), 3.94 (s, 3H), 3.83 (s, 3H).

Nitro Netropsin Analog I-22. A solution of **O₂NP₂CO₂H** (1.46 g, 5.0 mmol), *N*-hydroxybenzotriazole hydrate (HOBT, Aldrich, 1.35 g, 10.0 mmol), and 3-dimethylaminopropylamine (Aldrich, 0.7 mL, 5.5 mmol) in 50 mL DMF was stirred under argon in an ice/water bath. Dicyclohexylcarbodiimide (DCC, Aldrich, 1.15 g, 5.5 mmol) in 5 mL DMF was added and the reaction mixture allowed to warm to RT and stir for 24 h. The mixture was filtered, the solvent distilled *in vacuo*, and the residue triturated with Et₂O. Chromatography on silica gel using 1% concentrated aqueous ammonia in MeOH (1% NH₄OH/MeOH) afforded 1.67 g (4.4 mmol, 88%) of **I-22**. ¹H NMR δ 10.23 (s, 1H), 8.13 (s, 1H), 8.07 (t, 1H), 7.53 (s, 1H), 7.17 (s, 1H), 6.77 (s, 1H), 3.90 (s, 3H), 3.77 (s, 3H), 3.2 (m, 2H); FAB MS, calcd. for C₁₇H₂₅N₆O₄ (M+H⁺): 377.1937. Found: 377.1925.

mono Boc 1,3-diaminopropane (IV-161). To a stirred solution of imidazole-*N*-carboxylic acid, *t*-butyl ester (IV-151)⁶ (16.8 g, 100 mmol) and sodium imidazole (1.0 g, 11 mmol) in 200 mL THF (distilled from sodium) was added 1,3-diaminopropane (Aldrich, 8.9 g, 120 mmol). The mixture was stirred overnight at RT, and the solvent removed at RT under reduced pressure. The product was purified by chromatography on silica gel using 2% NH₄OH/MeOH eluent followed by bulb-to-bulb distillation at 200°C using aspirator vacuum to afford 6.85 g (39.4 mmol, 39%) of **IV-161**. ¹H NMR (CDCl₃) δ 4.93 (br s, 1H), 3.18 (q, 2H), 2.72 (t, 2H), 1.66 (s, 2H), 1.58 (m, 2H), 1.42 (s, 9H).

Boc Nitro Netropsin Analog II-129. A solution of O₂NP₂CO₂H (4.5 g, 15.4 mmol), HOBT (4.1 g, 30 mmol), and **IV-161** (3.05 g, 17.5 mmol) in 50 mL DMF was stirred under argon in an ice/water bath. DCC (5.2 g, 25 mmol) was added and the reaction mixture allowed to warm to RT and stir for 24 h. The mixture was filtered, and the solvent distilled *in vacuo*. The residue was triturated with Et₂O, which removed most of the HOBT. Crystallization of the triturated solid from hot CHCl₃ afforded 5.91 g (13.2 mmol, 86%) of **II-129**. ¹H NMR δ 10.25 (s, 1H), 8.17 (s, 1H), 7.97 (t, 1H), 7.50 (s, 1H), 7.18 (s, 1H), 6.83 (s, 1H), 6.74 (t, 1H), 3.93 (s, 3H), 3.78 (s, 3H), 3.20 (m, 2H), 2.96 (m, 2H), 1.61 (m, 2H), 1.40 (s, 9H); FAB MS, calcd. for C₂₀H₂₉N₆O₆ (M+H⁺): 449.2149. Found: 449.2145.

Chapter One

Boc 4-Aminobutanoic acid (I-203). To a stirred, cooled solution of 4-aminobutanoic acid (Aldrich, 10.3 g, 100 mmol) in 400 mL 2:1:1 dioxane:H₂O:1 M NaOH was added di-*t*-butyldicarbonate (Aldrich, 24.0 g, 110 mmol) in 10 mL dioxane over 30 minutes (min). After addition was complete, the mixture was stirred for 30 min in the

cooling bath and then for 45 min at RT. Dioxane was removed at RT under reduced pressure. The aqueous solution was treated with 400 mL ethyl acetate (EtOAc), and then acidified to pH 2 using 2 M potassium hydrogen sulfate (KHSO₄) with cooling and vigorous stirring. The layers were separated and the aqueous phase extracted with 2 x 200 mL EtOAc. The combined extracts were washed with 200 mL H₂O, dried over sodium sulfate (Na₂SO₄), and concentrated to a thick oil, which solidified upon standing. Stirring the crushed solid with 100 mL hexane removed remaining *t*-butanol, affording 13.5 g (68 mmol, 68%) of **I-203**. ¹H NMR δ 6.81 (t, 1H), 2.92, (m, 2H), 2.19 (t, 2H), 1.59 (m, 2H), 1.37 (s, 9H).

Boc Netropsin Analog I-204. A solution of O₂NP2CO₂H (0.64 g, 2.2 mmol) and Et₃N (0.84 mL, 6.0 mmol) in 10 mL DMF was treated with 100 mg 5% Pd/C and hydrogenated at 1 atm and RT for 20 h. This mixture was added to a stirred solution of the imidazolide of **I-203** (prepared by stirring 0.41 g, 2.0 mmol **I-203** with 0.36 g, 2.2 mmol CDI in 5 mL DMF for 2 h). After stirring at RT for 16 h, the reaction mixture was filtered, the solvent distilled *in vacuo*, and the residue triturated with Et₂O. Chromatography on silica gel using 15% MeOH/methylene chloride (CH₂Cl₂) eluent afforded **I-204**. ¹H NMR δ 9.69 (br s, 2H), 7.20 (d, 1H), 7.08 (d, 1H), 6.79 (d, 1H), 6.76 (t, 1H), 6.70 (d, 1H), 3.85 (s, 3H), 3.83 (s, 3H), 2.92 (m, 2H), 2.22 (q, 2H), 1.67 (m, 2H), 1.39 (s, 9H); FAB MS, calcd. for C₂₁H₃₀N₅O₆ (M+H⁺): 447.2118. Found: 447.2140.

Boc Netropsin-Gaba (I-215). **I-22** (0.41 g, 1.1 mmol) was hydrogenated at 1 atm and RT for 20 h in 10 mL DMF using 35 mg 5% Pd/C. The mixture was then cooled in an ice/water bath and treated with HOBT (0.27 g, 2.0 mmol) and **I-203** (0.20 g, 1.1 mmol). DCC (0.23 g, 1.1 mmol) in 1 mL DMF was added. The cooling bath was removed and the mixture stirred at RT for 20 h. The mixture was filtered, the solvent distilled *in vacuo*, and

the residue triturated with Et₂O. Chromatography on silica gel using 1% NH₄OH/MeOH eluent afforded 0.45 g (0.85 mmol, 77%) of **I-215**. ¹H NMR δ 9.84 (s, 1H), 9.78 (s, 1H), 8.06 (t, 1H), 7.17 (d, 1H), 7.15 (d, 1H), 6.85 (d, 1H), 6.81 (d, 1H), 6.8 (br s, 1H), 3.83 (s, 3H), 3.80 (s, 3H), 3.19 (m, 2H), 2.95 (m, 2H), 2.23 (m, 4H), 2.15 (s, 6H), 1.67 (m, 2H), 1.62 (m, 2H), 1.39 (s, 9H); FAB MS, calcd. for C₂₆H₄₂N₇O₅ (M+H⁺): 532.3247. Found: 532.3236.

Boc Netropsin-Glycine (II-35), 85% from **I-22** and Boc glycine using the procedure for **I-215**. ¹H NMR δ 9.85 (s, 1H), 9.81 (s, 1H), 8.06 (t, 1H), 7.18 (d, 1H), 7.15 (d, 1H), 7.00 (t, 1H), 6.89 (d, 1H), 6.81 (s, 1H), 3.83 (s, 3H), 3.79 (s, 3H), 3.65 (d, 2H), 3.17 (m, 2H), 2.24 (t, 2H), 2.14 (s, 6H), 1.60 (m, 2H), 1.39 (s, 9H); FAB MS, calcd. for C₂₄H₃₈N₇O₅ (M+H⁺): 504.2934. Found: 504.2916.

Netropsin-Gaba (I-208). **I-215** (0.30 g, 0.56 mmol) was dissolved in 4 mL CH₂Cl₂, cooled in an ice water bath under argon, and treated with 1.5 mL trifluoroacetic acid (TFA). The mixture was removed from the cooling bath and stirred for 15 min. The product was precipitated with 15 mL Et₂O and the supernatant discarded. The residue was dissolved in 10 mL 10% NH₄OH/MeOH, and then concentrated. Chromatography on silica gel using 10% NH₄OH/MeOH eluent afforded 200 mg (0.46 mmol, 83%) of **I-208**. ¹H NMR δ 9.84 (s, 1H), 9.81 (s, 1H), 8.07 (t, 1H), 7.18 (d, 1H), 7.15 (d, 1H), 6.85 (d, 1H), 6.81 (d, 1H), 3.82 (s, 3H), 3.80 (s, 3H), 3.18 (m, 2H), 2.55 (t, 2H), 2.25 (t, 2H), 2.14 (s, 6H), 1.63 (m, 4H); FAB MS, calcd. for C₂₁H₃₄N₇O₃ (M+H⁺): 432.2723. Found: 432.2713.

Netropsin-Glycine (II-36), 83% from **II-35** using the procedure for **I-208**. ¹H NMR δ 9.84 (s, 2H), 8.06 (t, 1H), 7.19 (s, 1H), 7.18 (s, 1H), 6.93 (s, 1H), 6.81 (s, 1H), 3.83 (s, 3H), 3.79 (s, 3H), 3.22 (s, 2H), 3.18 (m, 2H), 2.23 (t, 2H), 2.13 (s, 6H),

1.60 (m, 2H); FAB MS, calcd. for $C_{19}H_{30}N_7O_3$ ($M+H^+$): 404.2410. Found: 404.2407.

Netropsin-2-Cyanoethanamide (I-255) was prepared from **I-22** and cyanoacetic acid in 79% yield using the procedure for **I-208**. 1H NMR δ 10.21 (s, 1H), 9.85 (s, 1H), 8.04 (t, 1H), 7.17 (d, 1H), 7.14 (d, 1H), 6.88 (d, 1H), 6.80 (d, 1H), 3.83 (s, 3H), 3.79 (s, 2H), 3.79 (s, 3H), 3.17 (m, 2H), 2.23 (t, 2H), 2.12 (s, 6H), 1.60 (m, 2H); FAB MS, calcd. for $C_{20}H_{28}N_7O_3$ ($M+H^+$): 414.2254. Found: 414.2239.

Netropsin- β -Alanine (I-257). **I-255** (350 mg, 0.85 mmol) was dissolved in 7 mL AcOH and treated with 70 mg platinum oxide (PtO_2). This mixture was hydrogenated at 3 atm and RT for 12 h, then filtered, concentrated, treated with 10 mL 10% $NH_4OH/MeOH$, and concentrated again. Chromatography on silica gel using 5% $NH_4OH/MeOH$ eluent afforded 230 mg (0.55 mmol, 65%) of **I-257**. 1H NMR δ 9.94 (s, 1H), 9.82 (s, 1H), 8.05 (t, 1H), 7.16 (d, 1H), 7.15 (d, 1H), 6.84 (d, 1H), 6.80 (d, 1H), 3.81 (s, 3H), 3.78 (s, 3H), 3.17 (m, 2H), 2.81 (t, 2H), 2.32 (t, 2H), 2.22 (t, 2H), 2.12 (s, 6H), 1.59 (m, 2H); FAB MS, calcd. for $C_{20}H_{32}N_7O_3$ ($M+H^+$): 418.2567. Found: 418.2590.

General Procedure for the Synthesis of Boc Bis(Netropsin) Amino Acid Compounds. A solution of Netropsin-Glycine, - β -Alanine, or -Gaba compound in DMF was treated with 2.0 equiv. of HOBT, 1.1 equivalents (equiv.) of **I-204**, and then 1.2 equiv. of DCC in 1 mL DMF. After stirring 24 h at RT, the mixture was filtered, the solvent distilled *in vacuo*, and the residue triturated with Et_2O . Chromatography on silica gel using 1% $NH_4OH/MeOH$ eluent afforded the Boc Bis(Netropsin) Amino acid compound.

Boc Bis(Netropsin)-Glycine (II-37), 68% from **II-36** and **I-204**. ^1H NMR δ 9.90 (s, 1H), 9.87 (s, 1H), 9.85 (s, 1H), 9.79 (s, 1H), 8.28 (t, 1H), 8.06 (t, 1H), 7.24 (s, 1H), 7.18 (s, 1H), 7.17 (d, 1H), 7.15 (s, 1H), 6.94 (s, 1H), 6.91 (s, 1H), 6.87 (s, 1H), 6.83 (br s, 1H), 6.81 (d, 1H), 3.90 (d, 2H), 3.83 (s, 6H), 3.79 (s, 6H), 3.18 (m, 2H), 2.94 (m, 2H), 2.24 (m, 4H), 2.13 (s, 6H), 1.66 (m, 2H), 1.60 (m, 2H), 1.38 (s, 9H); FAB MS, calcd. for $\text{C}_{40}\text{H}_{57}\text{N}_{12}\text{O}_8$ ($\text{M}+\text{H}^+$): 833.4421. Found: 833.4415.

Boc Bis(Netropsin)- β -Alanine (I-259), 64% from **I-257** and **I-204**. ^1H NMR δ 9.89 (s, 1H), 9.85 (s, 2H), 9.77 (s, 1H), 8.05 (m, 2H), 7.17 (m, 3H), 7.13 (d, 1H), 6.84 (m, 2H), 6.82 (s, 1H), 6.80 (d, 1H), 3.81 (s, 3H), 3.80 (s, 6H), 3.78 (s, 3H), 3.43 (m, 2H), 3.17 (m, 2H), 2.92 (m, 2H), 2.50 (t, 2H), 2.23 (t, 2H), 2.20 (t, 2H), 2.12 (s, 6H), 1.65 (m, 2H), 1.59 (m, 2H), 1.36 (s, 9H); FAB MS, calcd. for $\text{C}_{41}\text{H}_{59}\text{N}_{12}\text{O}_8$ ($\text{M}+\text{H}^+$): 847.4578. Found: 847.4584.

Boc Bis(Netropsin)-Gaba (I-218), 79% from **I-208** and **I-204**. ^1H NMR δ 9.85 (2s, 2H), 9.84 (s, 1H), 9.78 (s, 1H), 8.05 (m, 2H), 7.17 (s, 3H), 7.15 (s, 1H), 6.89 (s, 1H), 6.86 (s, 1H), 6.83 (t, 1H), 6.81 (s, 1H), 3.83 (s, 6H), 3.81 (s, 3H), 3.80 (s, 3H), 3.25 (m, 4H), 2.95 (m, 2H), 2.25 (m, 6H), 2.15 (s, 6H), 1.79 (m, 2H), 1.67 (m, 2H), 1.61 (m, 2H), 1.38 (s, 9H); FAB MS, calcd. for $\text{C}_{42}\text{H}_{61}\text{N}_{12}\text{O}_8$ ($\text{M}+\text{H}^+$): 861.4735. Found: 861.4706.

General Procedure for the Synthesis of Netropsin Alkanamic Acid Compounds. **I-22** (0.42 g, 1.1 mmol) was dissolved in 10 mL DMF and treated with 50 mg 5% Pd/C. This mixture was hydrogenated at 1 atm and RT for 16 h, then treated with HOBT (0.27 g, 2.0 mmol) and 5-10 mmol of malonic, succinic, or fumaric acid. The mixture was stirred under argon in an ice bath and treated with DCC (0.23 g, 1.1 mmol) in 1 mL DMF. The cooling bath was removed and the mixture stirred overnight at RT. The

mixture was filtered, the solvent distilled *in vacuo*, and the residue triturated with Et₂O. Chromatography on silica gel using 1-2% NH₄OH/MeOH eluent afforded the Netropsin Alkanamic acid compound.

Netropsin-Oxalamic acid (II-141). I-22 (0.38 g, 1.0 mmol) was dissolved in 10 mL DMF and treated with 75 mg 5% Pd/C. This mixture was hydrogenated at RT and 1 atm, cooled in an ice/water bath and then treated with Et₃N (0.42 mL, 3.0 mmol) followed by ethyloxalyl chloride (Aldrich, 0.168 mL, 1.5 mmol). After stirring 2 h at RT, the mixture was filtered, evaporated and the residue triturated with Et₂O. The crude ester was dissolved in 5 mL MeOH and treated with lithium hydroxide (LiOH, 144 mg, 6.0 mmol) in 2 mL H₂O, stirred at RT 30 min, and then concentrated. Chromatography of the residue on silica gel using 2% NH₄OH/MeOH eluent afforded 185 mg (0.44 mmol, 44%) of II-141. ¹H NMR δ 10.25 (s, 1H), 9.89 (s, 1H), 8.01 (br s, 1H), 7.26 (d, 1H), 7.24 (s, 1H), 7.17 (s, 1H), 7.15 (s, 1H), 3.82 (s, 3H), 3.79 (s, 3H), 3.23 (m, 2H), 3.01 (br s, 2H), 2.73 (s, 6H), 1.85 (m, 2H); FAB MS, calcd. for C₁₉H₂₆N₆O₅Li (M+Li⁺): 425.2125. Found: 425.2123.

Netropsin-Malonamic acid (I-115), 49% from I-22 and malonic acid. ¹H NMR δ 10.55 (s, 1H), 9.83 (s, 1H), 8.08 (t, 1H), 7.18 (d, 1H), 7.16 (d, 1H), 6.89 (s, 1H), 6.84 (s, 1H), 3.83 (s, 3H), 3.80 (s, 3H), 3.18 (m, 2H), 3.17 (s, 2H), 2.46 (t, 2H), 2.30 (s, 6H), 1.68 (m, 2H); FAB MS, calcd. for C₂₀H₂₉N₆O₅ (M+H⁺): 433.2199. Found: 433.2204.

Netropsin-Succinamic acid (II-78), 81% from I-22 and succinic acid. ¹H NMR δ 9.91 (s, 1H), 9.85 (s, 1H), 8.07 (t, 1H), 7.18 (d, 1H), 7.14 (d, 1H), 6.86 (d, 1H), 6.81 (d, 1H), 3.81 (s, 3H), 3.79 (s, 3H), 3.18 (m, 2H), 2.45 (s, 4H), 2.25 (t, 2H), 2.15 (s,

6H), 1.61 (m, 2H); FAB MS, calcd. for $C_{21}H_{31}N_6O_5$ ($M+H^+$): 447.2355. Found: 447.2339.

Netropsin-Fumaramic acid (II-79), 83% from **I-22** and fumaric acid. 1H NMR δ 10.38 (s, 1H), 9.92 (s, 1H), 8.06 (t, 1H), 7.28 (s, 1H), 7.18 (s, 1H), 6.94 (s, 1H), 6.84 (s, 2H), 6.69 (s, 1H), 3.83 (s, 3H), 3.80 (s, 3H), 3.2 (m, 2H), 2.50 (t, 2H), 2.38 (s, 6H), 1.7 (m, 2H); FAB MS, calcd. for $C_{21}H_{29}N_6O_5$ ($M+H^+$): 445.2199. Found: 445.2194.

General Procedure for the Synthesis of Boc Bis(Netropsin) Diacid Compounds. A solution of Netropsin-Alkanamic acid compound in 1 mL DMF was treated with 2.0 equiv. of HOBT and 1.1-1.5 equiv. of **II-129**, which had been hydrogenated using 5% Pd/C for 48-60 h at 3 atm and RT. This mixture was treated with 1.1 equiv. of DCC and stirred 24-48 h at RT. The mixture was filtered, the solvent distilled *in vacuo*, and the residue triturated with Et_2O . Chromatography on silica gel using 1% $NH_4OH/MeOH$ eluent afforded the Bis(Netropsin) Diacid compound.

Boc Bis(Netropsin)-Oxalamide (II-176), 29% from **II-141** and **II-129**. 1H NMR δ 10.91 (s, 2H), 9.99 (s, 1H), 9.98 (s, 1H), 8.08 (t, 1H), 7.98 (t, 1H), 7.34 (s, 2H), 7.19 (d, 2H), 7.12 (d, 2H), 6.86 (s, 1H), 6.82 (d, 1H), 6.81 (t, 1H), 3.86 (s, 6H), 3.80 (s, 6H), 3.17 (m, 4H), 2.95 (m, 2H), 2.26 (t, 2H), 2.15 (s, 6H), 1.60 (m, 4H), 1.38 (s, 9H); FAB MS, calcd. for $C_{39}H_{54}N_{12}O_8Li$ ($M+Li^+$): 825.4349. Found: 825.4344.

Boc Bis(Netropsin)-Malonamide (I-123), 57% from **I-115** and **II-129**. 1H NMR δ 10.07 (s, 2H), 9.86 (s, 1H), 9.85 (s, 1H), 8.06 (t, 1H), 7.96 (t, 1H), 7.18 (s, 4H), 6.89 (m, 2H), 6.84 (d, 1H), 6.82 (d, 1H), 6.78 (t, 1H), 3.84 (s, 6H), 3.80 (s, 6H), 3.34

(s, 2H), 3.17 (m, 4H), 2.96 (m, 2H), 2.26 (t, 2H), 2.15 (s, 6H), 1.6 (m, 4H), 1.38 (s, 9H); FAB MS, calcd. for C₄₀H₅₇N₁₂O₈ (M+H⁺): 833.4422. Found: 833.4400.

Boc Bis(Netropsin)-Succinamide (II-82), 50% from **II-78** and **II-129**. ¹H NMR δ 9.88 (s, 2H), 9.85 (s, 1H), 9.84 (s, 1H), 8.05 (t, 1H), 7.95 (t, 1H), 7.17 (s, 2H), 7.15 (s, 2H), 6.85 (s, 2H), 6.84 (s, 1H), 6.81 (s, 1H), 6.79 (t, 1H), 3.82 (s, 6H), 3.79 (s, 6H), 3.17 (m, 4H), 2.95 (m, 2H), 2.56 (s, 4H), 2.23 (t, 2H), 2.13 (s, 6H), 1.59 (m, 4H), 1.38 (s, 9H); FAB MS, calcd. for C₄₁H₅₉N₁₂O₈ (M+H⁺): 847.4578. Found: 847.4537.

Boc Bis(Netropsin)-Fumaramide (II-83), 70% from **II-79** and **II-129**. ¹H NMR δ 10.48 (s, 2H), 9.93 (s, 1H), 9.92 (s, 1H), 8.06 (t, 1H), 7.97 (t, 1H), 7.33 (s, 2H), 7.19 (d, 2H), 7.09 (s, 2H), 6.94 (s, 2H), 6.86 (s, 1H), 6.83 (d, 1H), 6.79 (t, 1H), 3.86 (s, 6H), 3.80 (s, 6H), 3.18 (m, 4H), 2.96 (m, 2H), 2.26 (t, 2H), 2.15 (s, 6H), 1.62 (m, 2H), 1.59 (m, 2H), 1.39 (s, 9H); FAB MS, calcd. for C₄₁H₅₇N₁₂O₈ (M+H⁺): 845.4421. Found: 845.4408.

General Procedure for the Synthesis of Bis(Netropsin) Compounds. A solution or slurry of Boc Bis(Netropsin) Diacid or Amino acid compound in CH₂Cl₂ (0.1 M) was stirred in an ice/water bath. One-half volume of TFA was added and the mixture removed from the cooling bath and stirred at RT for 15 min. The product was precipitated by adding 2-3 volumes of Et₂O, and the supernatant was discarded. The residue was dissolved in 10 mL 10% NH₄OH/MeOH, and concentrated. Chromatography on silica gel using 10% NH₄OH/MeOH eluent afforded the Bis(Netropsin) compound.

Bis(Netropsin)-Glycine (II-38), 71% from **II-37**. ¹H NMR δ 9.90 (s, 1H), 9.88 (s, 1H), 9.85 (s, 1H), 9.80 (s, 1H), 8.28 (t, 1H), 8.06 (t, 1H), 7.24 (s, 1H), 7.18 (2s,

2H), 7.17 (d, 1H), 7.15 (d, 1H), 6.94 (s, 1H), 6.91 (s, 1H), 6.87 (s, 1H), 6.81 (s, 1H), 3.90 (d, 2H), 3.83 (s, 6H), 3.81 (s, 3H), 3.79 (s, 3H), 3.18 (m, 2H), 2.54 (t, 2H), 2.26 (t, 2H), 2.23 (t, 2H), 2.13 (s, 6H), 1.61 (m, 4H); FAB MS, calcd. for C₃₅H₄₉N₁₂O₆ (M+H⁺): 733.3897. Found: 733.3888.

Bis(Netropsin)-β-Alanine (I-261), 80% from **I-259**. ¹H NMR δ 9.89 (s, 1H), 9.84 (s, 2H), 9.80 (s, 1H), 8.05 (m, 2H), 7.17 (m, 3H), 7.14 (d, 1H), 6.84 (m, 2H), 6.82 (s, 1H), 6.79 (d, 1H), 3.81 (s, 3H), 3.80 (s, 6H), 3.78 (s, 3H), 3.43 (m, 2H), 3.17 (m, 2H), 2.56 (t, 2H), 2.50 (t, 2H), 2.25 (t, 2H), 2.22 (t, 2H), 2.12 (s, 6H), 1.64 (m, 2H), 1.59 (m, 2H); FAB MS, calcd. for C₃₆H₅₁N₁₂O₆ (M+H⁺): 747.4054. Found 747.4044.

Bis(Netropsin)-Gaba (I-222), 74% from **I-218**. ¹H NMR δ 9.84 (s, 4H), 8.05 (m, 2H), 7.17 (s, 4H), 6.89 (s, 1H), 6.87 (s, 1H), 6.85 (s, 1H), 6.81 (s, 1H), 3.82 (s, 6H), 3.80 (s, 3H), 3.79 (s, 3H), 3.2 (m, 4H), 2.28 (m, 4H), 2.24 (t, 2H), 2.13 (s, 6H), 1.79 (m, 2H), 1.7 (br s, 2H), 1.62 (m, 2H). The findings that the resonance expected at δ 2.6 (H₂N-CH₂-) was not observed and that the methylene signal at δ 1.7 was so broad, were odd but reproducible; at first this was taken to mean that the terminal Gaba unit had been lost during the deprotection. However, subsequent transformation of this material to **I-228** revealed this unit again in the NMR. FAB MS, calcd. for C₃₇H₅₃N₁₂O₆ (M+H⁺): 761.4211. Found: 761.4224.

Bis(Netropsin)-Oxalamide (II-183), 91% from **II-176**. ¹H NMR δ 10.90 (br s, 2H), 10.02 (s, 1H), 9.99 (s, 1H), 8.12 (t, 1H), 8.08 (t, 1H), 7.34 (d, 2H), 7.19 (d, 2H), 7.12 (s, 2H), 6.88 (d, 1H), 6.82 (d, 1H), 3.86 (s, 6H), 3.80 (2s, 6H), 3.23 (m, 2H), 3.18 (m, 2H), 2.69 (t, 2H), 2.24 (t, 2H), 2.13 (s, 6H), 1.62 (m, 4H); FAB MS, calcd. for C₃₄H₄₆N₁₂O₆Li (M+Li⁺): 725.3824. Found: 725.3790.

Bis(Netropsin)-Malonamide (I-180), 75% from **I-123**. ^1H NMR δ 10.08 (s, 2H), 9.86 (s, 2H), 8.06 (m, 2H), 7.18 (s, 4H), 6.90 (s, 2H), 6.84 (s, 1H), 6.81 (s, 1H), 3.84 (s, 6H), 3.80 (s, 6H), 3.34 (s, 2H), 3.21 (m, 4H), 2.61 (t, 2H), 2.24 (t, 2H), 2.13 (s, 6H), 1.59 (m, 4H); FAB MS, calcd. for $\text{C}_{35}\text{H}_{49}\text{N}_{12}\text{O}_6$ ($\text{M}+\text{H}^+$): 733.3898. Found: 733.3865.

Bis(Netropsin)-Succinamide (II-87), 79% from **II-82**. ^1H NMR δ 9.88 (s, 2H), 9.83 (s, 2H), 8.04 (t, 2H), 7.17 (s, 2H), 7.15 (d, 2H), 6.86 (d, 2H), 6.83 (d, 1H), 6.81 (d, 1H), 3.82 (s, 6H), 3.79 (s, 6H), 3.19 (m, 4H), 2.58 (t, 2H), 2.56 (s, 4H), 2.23 (t, 2H), 2.13 (s, 6H), 1.60 (m, 2H), 1.55 (m, 2H); FAB MS, calcd. for $\text{C}_{36}\text{H}_{51}\text{N}_{12}\text{O}_6$ ($\text{M}+\text{H}^+$): 747.4054. Found: 747.4021.

Bis(Netropsin)-Fumaramide (II-91), 84% from **II-83**. ^1H NMR δ 10.49 (s, 2H), 9.92 (s, 2H), 8.06 (m, 2H), 7.32 (s, 2H), 7.17 (s, 2H), 7.08 (s, 2H), 6.93 (s, 2H), 6.87 (s, 1H), 6.81 (s, 1H), 3.85 (s, 6H), 3.79 (s, 6H), 3.16 (m, 4H), 2.66 (br s, 2H), 2.22 (t, 2H), 2.12 (s, 6H), 1.60 (m, 4H); FAB MS, calcd. for $\text{C}_{36}\text{H}_{49}\text{N}_{12}\text{O}_6$ ($\text{M}+\text{H}^+$): 745.3897. Found: 745.3901.

EDTA, Triethyl ester (EDTA(OEt)₃).⁷ EDTA (29.2 g, 100 mmol) was refluxed in a mixture of 500 mL absolute EtOH and 5 mL concentrated H_2SO_4 for 48 hours. The resulting solution was cooled to RT, treated with 200 mL saturated aqueous NaHCO_3 , and extracted with 3 X 250 mL CH_2Cl_2 . The combined organic extracts were washed with 2 X 150 mL saturated aqueous NaHCO_3 , and then 200 mL H_2O . The organic layer was dried over Na_2SO_4 , filtered, and concentrated to afford 31.3 g (77 mmole, 77%) of **EDTA, tetraethyl ester** as an oil, which solidified upon standing. ^1H NMR ($\text{CDCl}_3 + \text{D}_2\text{O}$) δ 4.10 (q, 8H), 3.60 (s, 8H), 2.85 (s, 4H), 1.25 (t, 12 H). The tetraester (12.1 g, 30 mmol) and cupric chloride (CuCl_2 , 5.1 g, 30 mmol) were dissolved in 500 mL H_2O . 1 M

NaOH (30 mL, 30 mmol) was added dropwise at a rate such that the pH of the solution remained below 5.0. After addition was complete, H₂S was bubbled through the solution for 15 min. The mixture was filtered to remove the brown CuS precipitate, and argon was bubbled through the filtrate with stirring for 30 min to remove dissolved H₂S. The solution was then concentrated. The residue was chromatographed on silica gel using 10% MeOH:CH₂Cl₂ eluent to afford 8.0 g (21.2 mmol, 71%) of **EDTA(OEt)₃** as a gum. ¹H NMR (90 MHz, Me₂SO-d₆) δ 4.06 (q, 6H), 3.50 (s, 6H), 3.43 (s, 2H); 2.73 (s, 4H), 1.17 (t, 9H).

General Procedure for the Synthesis of Bis(Netropsin)-EDTA, Triethyl Ester Compounds. A solution of **EDTA(OEt)₃** in DMF (0.25 M) was activated with 1.1 equiv. CDI and stirred for 2 h at RT under argon. The mixture was then added to 0.25-0.50 equiv. of Bis(Netropsin) compound (dissolved in 1 mL DMF). After stirring 24 h at RT under argon, the solvent was distilled *in vacuo*, and the residue triturated with Et₂O. Chromatography on silica gel using 1% NH₄OH/MeOH eluent afforded the Bis(Netropsin)-EDTA, Triethyl ester compound.

Bis(Netropsin)-Glycine-EDTA, Triethyl ester (II-39), 56% from II-38 and EDTA(OEt)₃. ¹H NMR δ 9.90 (s, 1H), 9.87 (s, 1H), 9.85 (s, 1H), 9.80 (s, 1H), 8.28 (t, 1H), 8.05 (t, 1H), 8.01 (t, 1H), 7.24 (s, 1H), 7.17 (s, 1H), 7.16 (s, 2H), 6.94 (s, 1H), 6.91 (s, 1H), 6.87 (s, 1H), 4.06 (m, 6H), 3.90 (d, 2H), 3.83 (s, 6H), 3.81 (s, 3H), 3.79 (s, 3H), 3.61-3.46 (series of singlets, 8H), 3.18 (m, 2H), 3.12 (m, 2H), 2.71 (m, 4H), 2.23 (m, 4H), 2.13 (s, 6H), 1.71 (m, 2H), 1.60 (m, 2H), 1.17 (m, 9H); FAB MS, calcd. for C₅₁H₇₅N₁₄O₁₃ (M+H⁺): 1091.5637. Found: 1091.5645.

Bis(Netropsin)-β-Alanine-EDTA, Triethyl ester (I-263), 67% from I-261 and EDTA(OEt)₃. ¹H NMR δ 9.90 (s, 1H), 9.87 (s, 1H), 9.85 (s, 1H), 9.80 (s, 1H), 8.06

(m, 2H), 8.00 (t, 1H), 7.18 (m, 3H), 7.15 (d, 1H), 6.86 (d, 1H), 6.84 (d, 1H), 6.83 (d, 1H), 6.80 (d, 1H), 4.07 (m, 6H), 3.82 (s, 3H), 3.81 (s, 6H), 3.79 (s, 3H), 3.60-3.46 (series of singlets, 8H), 3.31 (m, 2H), 3.16 (m, 4H), 3.12 (m, 2H), 2.71 (m, 4H), 2.50 (m, 2H), 2.23 (m, 4H), 2.13 (s, 6H), 1.70 (m, 2H), 1.60 (m, 2H), 1.17 (m, 9H); FAB MS, calcd. for $C_{52}H_{77}N_{14}O_{13}$ ($M+H^+$): 1105.5795. Found: 1105.5739.

Bis(Netropsin)-Gaba-EDTA, Triethyl ester (I-228), 54% from **I-222** and **EDTA(OEt)₃**. 1H NMR δ 9.86 (s, 1H), 9.85 (s, 1H), 9.84 (s, 1H), 9.81 (s, 1H), 8.06 (m, 2H), 8.02 (m, 1H), 7.17 (m, 3H), 7.15 (d, 1H), 6.89 (d, 1H), 6.86 (m, 2H), 6.81 (d, 1H), 4.07 (m, 6H), 3.82 (s, 6H), 3.80 (s, 3H), 3.79 (s, 3H), 3.61-3.46 (series of singlets, 8H), 3.19 (m, 6H), 2.71 (m, 4H), 2.26 (m, 6H), 2.14 (s, 6H), 1.79 (m, 2H), 1.71 (m, 2H), 1.61 (m, 2H), 1.17 (m, 9H); FAB MS, calcd. for $C_{53}H_{79}N_{14}O_{13}$ ($M+H^+$): 1119.5951. Found: 1119.5890.

Bis(Netropsin)-Oxalamide-EDTA, Triethyl ester (II-185), 85% from **II-183** and **EDTA(OEt)₃**. 1H NMR δ 10.91 (s, 2H), 9.99 (s, 1H), 9.98 (s, 1H), 8.09 (t, 1H), 8.03 (m, 2H), 7.34 (d, 2H), 7.19 (d, 2H), 7.12 (d, 2H), 6.86 (d, 1H), 6.83 (d, 1H), 4.07 (m, 6H), 3.86 (s, 6H), 3.80 (s, 6H), 3.61-3.46 (series of singlets, 8H), 3.18 (m, 6H), 2.72 (m, 4H), 2.33 (br s, 2H), 2.21 (br s, 6H), 1.63 (m, 4H), 1.17 (m, 9H); FAB MS, calcd. for $C_{50}H_{72}N_{14}O_{13}Li$ ($M+Li^+$): 1083.5564. Found: 1083.5543.

Bis(Netropsin)-Malonamide-EDTA, Triethyl ester (I-137), 99% from **I-180** and **EDTA(OEt)₃**. 1H NMR δ 10.06 (s, 2H), 9.86 (s, 1H), 9.84 (s, 1H), 8.04 (t, 1H), 8.03 (t, 1H), 7.97 (t, 1H), 7.18 (m, 4H), 6.90 (m, 2H), 6.85 (d, 1H), 6.82 (d, 1H), 4.07 (m, 6H), 3.84 (s, 6H), 3.80 (s, 6H), 3.61-3.47 (series of singlets, 8H), 3.34 (s, 2H), 3.19 (m, 6H), 2.72 (m, 4H), 2.30 (t, 2H), 2.18 (s, 6H), 1.62 (m, 4H), 1.19 (m, 9H); FAB MS, calcd. for $C_{51}H_{75}N_{14}O_{13}$ ($M+H^+$): 1091.5637. Found: 1091.5693.

Bis(Netropsin)-Succinamide-EDTA, Triethyl ester (I-51), 81% from II-87 and EDTA(OEt)₃. ¹H NMR δ 9.89 (s, 2H), 9.86 (s, 1H), 9.84 (s, 1H), 8.05 (m, 2H), 7.99 (m, 1H), 7.17 (s, 2H), 7.15 (s, 2H), 6.86 (s, 3H), 6.81 (s, 1H), 4.06 (m, 6H), 3.82 (s, 6H), 3.80 (s, 6H), 3.60-3.47 (series of singlets, 8H), 3.18 (m, 6H), 2.73 (m, 4H), 2.56 (br s, 4H), 2.24 (t, 2H), 2.14 (s, 6H), 1.60 (m, 4H), 1.18 (m, 9H); FAB MS, calcd. for C₅₂H₇₇N₁₄O₁₃ (M+H⁺): 1105.5795. Found: 1105.5795.

Bis(Netropsin)-Fumaramide-EDTA, Triethyl ester (III-245), 71% from II-91 and EDTA(OEt)₃. ¹H NMR δ 10.49 (s, 2H), 9.93 (m, 2H), 8.06 (m, 2H), 8.00 (t, 1H), 7.33 (s, 2H), 7.19 (s, 2H), 7.09 (s, 2H), 6.94 (s, 2H), 6.86 (d, 1H), 6.83 (d, 1H), 4.07 (m, 6H), 3.87 (s, 6H), 3.81 (s, 6H), 3.61-3.48 (series of singlets, 8H), 3.2 (m, 6H), 2.72 (m, 4H), 2.25 (t, 2H), 2.15 (s, 6H), 1.62 (m, 4H), 1.18 (m, 9H); FAB MS, calcd. for C₅₂H₇₅N₁₄O₁₃ (M+H⁺): 1103.5638. Found: 1103.5640.

General Procedure for the Synthesis of Bis(netropsin)-EDTA Compounds. A solution of Bis(Netropsin)-EDTA Triethyl ester in 2:1 MeOH/H₂O (0.5 M) was treated with 10 equiv. of LiOH and stirred overnight at RT. The mixture was concentrated and the residue chromatographed on silica gel using 1-2% NH₄OH/MeOH eluent to afford the Bis(Netropsin)-EDTA compound.

Bis(Netropsin)-Glycine-EDTA (BNGE, II-41), 72% from II-39. ¹H NMR (Me₂SO-d₆ + TFA) δ 9.92 (s, 1H), 9.90 (s, 1H), 9.89 (s, 1H), 9.84 (s, 1H), 8.44 (t, 1H), 8.30 (br s, 1H), 8.17 (br s, 1H), 7.25 (s, 1H), 7.18 (s, 3H), 6.97 (s, 1H), 6.94 (s, 2H), 6.90 (s, 1H), 4.08 (s, 2H), 3.93 (s, 4H), 3.85 (s, 6H), 3.83 (s, 6H), 3.78 (s, 4H), 3.33 (br s, 2H), 3.26 (m, 2H), 3.21 (m, 4H), 3.09 (m, 2H), 2.80 (d, 6H), 2.30 (t, 2H), 1.85 (m, 2H), 1.76 (m, 2H); FAB MS, calcd. for C₄₅H₆₃N₁₄O₁₃ (M+H⁺): 1007.4699. Found: 1007.4680; UV (H₂O) λ_{max} 298, 237 nm.

Bis(Netropsin)- β -Alanine-EDTA (BN- β -AE, I-265), 100% from I-263. ^1H NMR ($\text{Me}_2\text{SO-d}_6 + \text{TFA}$) δ 9.93 (s, 1H), 9.89 (s, 1H), 9.86 (s, 1H), 9.84 (s, 1H), 8.44 (t, 1H), 8.17 (t, 1H), 8.08 (br s, 1H), 7.19 (s, 2H), 7.18 (d, 1H), 7.16 (s, 1H), 6.93 (d, 1H), 6.89 (d, 1H), 6.87 (d, 1H), 6.86 (s, 1H), 4.08 (s, 2H), 3.92 (s, 2H), 3.84 (s, 3H), 3.83 (s, 3H), 3.82 (s, 3H), 3.77 (s, 3H), 3.47 (m, 2H), 3.31 (m, 2H), 3.2 (m, 6H), 3.09 (m, 2H), 2.80 (d, 6H), 2.54 (t, 2H), 2.29 (t, 2H), 1.86 (m, 2H), 1.75 (m, 2H); FAB MS, calcd. for $\text{C}_{46}\text{H}_{65}\text{N}_{14}\text{O}_{13} (\text{M}+\text{H}^+)$: 1021.4856. Found: 1021.4830; UV (H_2O) λ_{max} 300, 236 nm.

Bis(Netropsin)-Gaba-EDTA (BNGabaE, I-230), 79% from I-228. ^1H NMR ($\text{Me}_2\text{SO-d}_6 + \text{TFA}$) δ 9.89 (s, 1H), 9.86 (s, 2H), 9.84 (s, 1H), 8.45 (t, 1H), 8.18 (t, 1H), 8.07 (br s, 1H), 7.18 (s, 4H), 6.95 (s, 1H), 6.92 (s, 1H), 6.89 (s, 2H), 4.10 (s, 2H), 3.94 (s, 2H), 3.84 (s, 6H), 3.83 (s, 6H), 3.79 (s, 4H), 3.35 (m, 2H), 3.24 (m, 8H), 3.10 (m, 2H), 2.81 (d, 6H), 2.30 (m, 4H), 1.82 (m, 4H), 1.77 (m, 2H); FAB MS, calcd. for $\text{C}_{47}\text{H}_{67}\text{N}_{14}\text{O}_{13} (\text{M}+\text{H}^+)$: 1035.5054. Found: 1035.5036; UV (H_2O) λ_{max} 301, 235 nm.

Bis(Netropsin)-Oxalamide-EDTA (BNOE, II-187), 91% from II-185. ^1H NMR ($\text{Me}_2\text{SO-d}_6 + \text{TFA}$) δ 10.96 (s, 2H), 10.07 (s, 1H), 10.05 (s, 1H), 8.48 (t, 1H), 8.25 (br s, 1H), 8.10 (br s, 1H), 7.42 (d, 2H), 7.25 (m, 2H), 7.20 (s, 2H), 7.03 (d, 1H), 6.99 (d, 1H), 4.17 (s, 2H), 4.03 (s, 2H), 3.93 (s, 6H), 3.89 (s, 6H), 3.88 (s, 4H), 3.44 (m, 2H), 3.28 (m, 8H), 3.15 (m, 2H), 2.86 (d, 6H), 1.91 (m, 2H), 1.74 (m, 2H); FAB MS, calcd. for $\text{C}_{44}\text{H}_{60}\text{N}_{14}\text{O}_{13}\text{K} (\text{M}+\text{K}^+)$: 1031.4101. Found: 1031.3909; UV (H_2O) λ_{max} 310, 247 nm.

Bis(Netropsin)-Malonamide-EDTA (BNME, I-142), 90% from I-137. ^1H NMR ($\text{Me}_2\text{SO-d}_6 + \text{TFA}$) δ 10.08 (s, 2H), 9.87 (s, 1H), 9.86 (s, 1H), 8.37 (t, 1H), 8.15 (t,

1H), 8.01 (t, 1H), 7.19 (s, 2H), 7.17 (d, 1H), 7.16 (d, 1H), 6.93 (d, 1H), 6.90 (m, 3H), 4.07 (s, 2H), 3.91 (s, 2H), 3.84 (s, 6H), 3.82 (s, 3H), 3.80 (s, 3H), 3.74 (s, 4H), 3.35 (s, 2H), 3.30 (m, 2H), 3.24 (m, 8H), 3.07 (m, 2H), 2.79 (d, 6H), 1.84 (m, 2H), 1.66 (m, 2H); FAB MS, calcd. for C₄₅H₆₃N₁₄O₁₃ (M+H⁺): 1007.4699. Found: 1007.4660; UV (H₂O) λ_{max} 296, 241 nm.

Bis(Netropsin)-Succinamide-EDTA (BNSE, I-54), 87% from **I-51**. ¹H NMR (Me₂SO-d₆ + TFA) δ 9.90 (s, 2H), 9.87 (s, 1H), 9.85 (s, 1H), 8.40 (t, 1H), 8.16 (br s, 1H), 8.02 (br s, 1H), 7.16 (s, 4H), 6.96 (s, 1H), 6.91 (s, 1H), 6.89 (s, 2H), 4.11 (s, 2H), 3.95 (s, 2H), 3.84 (s, 6H), 3.83 (s, 3H), 3.82 (s, 3H), 3.81 (s, 4H), 3.37 (br s, 2H), 3.25 (m, 8H), 3.10 (br s, 2H), 2.81 (d, 6H), 2.59 (s, 4H), 1.86 (m, 2H), 1.68 (m, 2H); FAB MS, calcd. for C₄₆H₆₅N₁₄O₁₃ (M+H⁺): 1021.4856. Found: 1021.4781; UV (H₂O) λ_{max} 297, 237 nm.

Bis(Netropsin)-Fumaramide-EDTA (BNFE, III-250), 100% from **III-245**. ¹H NMR (Me₂SO-d₆ + TFA) δ 10.51 (s, 2H), 9.97 (s, 1H), 9.95 (s, 1H), 8.42 (t, 1H), 8.19 (br s, 1H), 8.05 (br s, 1H), 7.36 (s, 2H), 7.20 (m, 2H), 7.11 (s, 2H), 6.97 (s, 3H), 6.93 (d, 1H), 4.12 (s, 2H), 3.97 (s, 2H), 3.95 (s, 2H), 3.89 (s, 6H), 3.84 (s, 3H), 3.83 (s, 3H), 3.82 (s, 4H), 3.37 (m, 2H), 3.26 (m, 8H), 3.10 (m, 2H), 2.82 (d, 6H), 1.86 (m, 2H), 1.69 (m, 2H); FAB MS, calcd. for C₄₆H₆₃N₁₄O₁₃ (M+H⁺): 1019.4618. Found: 1019.4680; UV (H₂O) λ_{max} 301, 239 nm.

Chapter Two

(R,R)-2,2-Dimethyl-1,3-dioxolane-4,5-dicarboxylic acid, mono methyl ester ((R,R)-Tartaric acid acetonide, mono methyl ester, I-56), and (S,S)-2,2-dimethyl-1,3-dioxolane-4,5-dicarboxylic acid, mono methyl ester

((*S,S*)-Tartaric acid acetonide, mono methyl ester, **I-95**), were prepared from *d*- and *l*-tartaric acid (Aldrich), respectively, following the procedure of Musich and Rapoport.⁸

(*R,S*)-2,2-Dimethyl-1,3-dioxolane-4,5-dicarboxylic acid, mono methyl ester ((*RS,SR*)-Tartaric acid acetonide, mono methyl ester, **I-107**). The diester was synthesized via the procedure of Holy.⁹ Monohydrolysis using the conditions of Musich and Rapoport⁸ afforded, after acidic extraction, concentration, and distillation, a 1.5:1 ratio (NMR) of *threo:erythro* (*RS,SR*) monomethyl esters. ¹H NMR (CDCl₃) *threo* δ 4.80 (s, 2H), 3.80 (s, 3H), 1.54 (s, 6H); *erythro* (**I-107**) δ 4.87 (s, 2H), 3.73 (s, 3H), 1.64 (s, 3H), 1.43 (s, 3H). No attempt was made to separate the isomers at this point, since it was found that they could be separated following the next synthetic step.

(*S*)-*N,N*-Dimethylaspartic acid, β-Cyclohexyl ester (**I-84**). Boc L-Aspartic acid, β-cyclohexyl ester (Peninsula Laboratories, 3.15 g, 10.0 mmol) was stirred under argon at 0°C in 5 mL CH₂Cl₂. 4.0 mL TFA was added via syringe, and the mixture removed from the cooling bath and stirred at RT for 1 h. The product was precipitated by adding 10 mL Et₂O, and the supernatant decanted. The residue was dissolved in 10 mL 10% NH₄OH/MeOH, and concentrated at 30°C. Addition of 10 mL more solvent and concentration at 55°C gave a white solid, which was subjected to reductive alkylation.¹⁰ The solid was dissolved in 75 mL H₂O with heating. Formaldehyde (4.0 mL of a 37% aqueous solution, 50 mmol) was added. After cooling to RT, 25 mL additional H₂O, 4.0 mL additional formaldehyde solution, and 2.0 g 5% Pd/C were added. The mixture was hydrogenated at 3 atm and RT for 15 h, filtered, and the residue washed with 2 X 25 mL hot H₂O. Concentration of the filtrate *in vacuo* afforded a thick oil, which was treated with 5 mL H₂O and concentrated again. Treatment with 15 mL MeOH and concentration gave an oil that was chromatographed on silica gel using 0.5% NH₄OH/MeOH eluent to afford

1.33 g (5.7 mmol, 57% overall) of **I-84** as a white solid. ^1H NMR δ 4.68 (m, 1H), 3.59 (m, 1H), 2.72 (dd, 1H), 2.54 (dd, 1H), 2.40 (s, 6H), 1.9-1.6 (m, 4H), 1.5-1.2 (m, 6H).

(R)-N,N-Dimethylaspartic acid (I-136). D-Aspartic acid (Aldrich, 6.65 g, 50 mmol) was dissolved in 50 mL H_2O and treated with formaldehyde solution (12.1 mL, 150 mmol) and 5.0 g of 5% Pd/C. The mixture was hydrogenated at 3 atm and RT for 16 h, heated, filtered, and the residue washed with 25 mL hot H_2O . Cooling to RT and then 5°C afforded cubic crystals, which, upon recrystallization from $\text{H}_2\text{O}/\text{EtOH}/\text{acetone} (\text{Me}_2\text{CO})$, afforded 2.95 g (18 mmol, 37%) of **I-136** as white needles, mp 187-199°C (lit. mp 198°C). ^1H NMR (D_2O) δ 4.0 (m, 1H), 2.95-2.80 (m, 2H), 2.85 (s, 6H).

General Procedure for the Synthesis of Chiral Substituted Netropsin Alkanamic Acid Compounds followed that for the synthesis of unsubstituted Netropsin Alkanamic acid compounds (Chapter One). In the instances where a mono ester of a diacid was used, the ester product initially formed was hydrolyzed by stirring it with 2 equiv. LiOH in 2:1 MeOH: H_2O . Chromatography on silica gel using 1% $\text{NH}_4\text{OH}/\text{MeOH}$ eluent afforded the Bis(Netropsin) Alkanamic acid compound.

Netropsin-(R,R)-Tartaramic acid (I-108), 77% from **I-22** and *d*-tartaric acid (Aldrich). ^1H NMR ($\text{Me}_2\text{SO-d}_6 + \text{TFA}$) δ 9.84 (s, 1H), 9.54 (s, 1H), 8.14 (t, 1H), 7.22 (s, 1H), 7.14 (s, 2H), 6.57 (s, 1H), 4.35 (s, 2H), 3.85 (s, 3H), 3.84 (s, 3H), 3.19 (m, 4H), 2.81 (d, 6H), 1.87 (m, 2H); FAB MS, calcd. for $\text{C}_{21}\text{H}_{31}\text{N}_6\text{O}_7 (\text{M}+\text{H}^+)$: 479.2254. Found: 479.2234.

Netropsin-(S,S)-Tartaramic acid (I-149), 41% from **I-22** and *l*-tartaric acid (Aldrich). ^1H NMR δ 9.85 (s, 1H), 9.52 (s, 1H), 8.11 (t, 1H), 7.18 (s, 2H), 7.03 (s, 1H), 6.84 (s, 1H), 4.30 (s, 1H), 4.11 (s, 1H), 3.81 (s, 3H), 3.79 (s, 3H), 3.20 (m, 2H),

2.54 (t, 2H), 2.36 (s, 6H); FAB MS, calcd. for $C_{21}H_{31}N_6O_7$ ($M+H^+$): 479.2254. Found: 479.2241.

Netropsin-(RS,SR)-Tartaramic acid (I-121), 84% from **I-22** and *meso*-tartaric acid hydrate (Aldrich). 1H NMR δ 9.85 (s, 1H), 9.76 (s, 1H), 8.07 (t, 1H), 7.18 (s, 2H), 6.97 (s, 1H), 6.83 (s, 1H), 3.89 (s, 1H), 3.87 (s, 1H), 3.82 (s, 3H), 3.80 (s, 3H), 3.19 (m, 2H), 2.38 (t, 2H), 2.25 (s, 6H), 1.65 (m, 2H); FAB MS, calcd. for $C_{21}H_{31}N_6O_7$ ($M+H^+$): 479.2254. Found: 479.2227.

Netropsin-(R,R)-Tartaramic acid Acetonide, Methyl ester (I-61) was prepared in 92% yield from **I-22** and 1.0 equiv. **I-56**. 1H NMR δ 10.22 (s, 1H), 9.90 (s, 1H), 8.07 (t, 1H), 7.22 (s, 1H), 7.18 (s, 1H), 7.00 (s, 1H), 6.81 (s, 1H), 4.86 (d, 1H), 4.73 (d, 1H), 3.84 (s, 3H), 3.80 (s, 3H), 3.72 (s, 3H), 3.18 (m, 2H), 2.27 (t, 2H), 2.16 (s, 6H), 1.61 (m, 2H), 1.43 (s, 3H), 1.42 (s, 3H); FAB MS, calcd. for $C_{25}H_{37}N_6O_7$ ($M+H^+$): 533.2724. Found: 533.2716. Hydrolysis afforded **Netropsin-(R,R)-Tartaramic acid Acetonide (I-66)** in 90% yield. 1H NMR (two low-field NH resonances not recorded) δ 8.12 (t, 1H), 7.20 (s, 1H), 7.18 (s, 1H), 6.94 (s, 1H), 6.86 (s, 1H), 4.49 (d, 1H), 4.40 (d, 1H), 3.83 (s, 3H), 3.80 (s, 3H), 3.21 (m, 2H), 2.67 (t, 2H), 2.46 (s, 6H), 1.74 (m, 2H), 1.38 (s, 3H), 1.36 (s, 3H); FAB MS, calcd. for $C_{24}H_{35}N_6O_7$ ($M+H^+$): 519.2567. Found: 519.2578.

Netropsin-(S,S)-Tartaramic acid Acetonide, Methyl ester (I-96) was prepared in 59% yield from **I-22** and 1.0 equiv. **I-95**. NMR data matched that for **(I-61)**. Hydrolysis afforded **Netropsin-(S,S)-Tartaramic acid Acetonide (I-99)** in 90% yield. The 1H NMR spectrum matched that for **I-66**, but here a low-field resonance was recorded at δ 9.87. FAB MS, calcd. for $C_{24}H_{35}N_6O_7$ ($M+H^+$): 519.2567. Found: 519.2574.

Netropsin-(RS,SR)-Tartaramic acid Acetonide, Methyl ester was prepared as a mixture with the *d,l* compound from **I-22** and the mixture **I-107**. Separation of the diastereomers could be achieved following hydrolysis, affording **Netropsin-(RS,SR)-Tartaramic acid Acetonide (I-113)** was obtained in 8% overall yield from **I-22**. ^1H NMR δ 9.90 (s, 1H), 9.88 (s, 1H), 8.07 (t, 1H), 7.17 (s, 2H), 6.93 (s, 1H), 6.83 (s, 1H), 4.77 (d, 1H), 4.69 (d, 1H), 3.81 (s, 3H), 3.79 (s, 3H), 3.17 (m, 2H), 2.35 (t, 2H), 2.22 (s, 6H), 1.63 (m, 2H), 1.33 (s, 3H), 1.30 (s, 3H); FAB MS, calcd. for $\text{C}_{24}\text{H}_{35}\text{N}_6\text{O}_7$ ($\text{M}+\text{H}^+$): 519.2567. Found: 519.2575.

Netropsin-2-(S)-Malamic acid (I-181), 50% from **I-22** and L-malic acid (Aldrich). Only one regioisomer was isolated. ^1H NMR δ 9.85 (s, 1H), 9.80 (s, 1H), 8.07 (br s, 1H), 7.18 (m, 2H), 7.02 (d, 1H), 6.82 (d, 1H), 4.29 (dd, 1H), 3.82 (s, 3H), 3.79 (s, 3H), 3.18 (m, 2H), 2.58 (dd, 1H), 2.34 (dd, 1H), 2.30 (t, 2H), 2.18 (s, 6H), 1.62 (m, 2H); FAB MS, calcd. for $\text{C}_{21}\text{H}_{31}\text{N}_6\text{O}_6$ ($\text{M}+\text{H}^+$): 463.2305. Found: 463.2306.

Netropsin-2-(R)-Malamic acid (I-183), 63% from **I-22** and D-malic acid (Aldrich). Spectral data matched that for **I-181**. Along with **I-183** was obtained 100 mg (22%) of the regioisomeric 3-(R) compound. ^1H NMR δ 10.35 (s, 1H), 9.84 (s, 1H), 8.08 (t, 1H), 7.17 (m, 2H), 6.87 (d, 1H), 6.83 (d, 1H), 4.07 (m, 1H), 3.82 (s, 3H), 3.80 (s, 3H), 3.19 (m, 2H), 2.61 (dd, 1H), 2.43 (t, 2H), 2.38 (dd, 1H), 2.28 (s, 6H), 1.66 (m, 2H); FAB MS, calcd. for $\text{C}_{21}\text{H}_{31}\text{N}_6\text{O}_6$ ($\text{M}+\text{H}^+$): 463.2305. Found: 463.2306.

Netropsin-2-(S)-N,N-Dimethylaminoaspartamic acid, Cyclohexyl ester (I-85B) was prepared as a 1:1 mixture with the 3-(S) isomer **I-85A** in 65% combined yield from **I-22** and 1.0 equiv. **I-84**. The isomerization was puzzling, but the regioisomers were separable after hydrolysis to the free acids, **I-86A** and **I-86B**. ^1H NMR data for the least mobile isomer (**I-86B**) on silica gel using 1% $\text{NH}_4\text{OH}/\text{MeOH}$ eluent was similar to

that of **I-84**, indicating that this was the 2-(*S*) isomer. EI MS for the 2-(*R*) enantiomer **I-173** (see below) showed loss of -CH[N(CH₃)₂]COOH, -CH₂, and CO fragments not shown by **I-86A**, further supporting the structural assignment.

Netropsin-2-(*S*)-*N,N*-Dimethylaminoaspartamic acid (I-86B). ¹H NMR δ 10.57 (s, 1H), 9.84 (s, 1H), 8.06 (br s, 1H), 7.17 (d, 1H), 7.16 (d, 1H), 6.86 (d, 1H), 6.81 (d, 1H), 3.82 (s, 3H), 3.79 (s, 3H), 3.50 (m, 1H), 3.17 (m, 2H), 2.72 (dd, 1H), 2.53 (dd, 1H), 2.40 (s, 6H), 2.24 (t, 2H), 2.14 (s, 6H), 1.61 (m, 2H); FAB MS, calcd. for C₂₃H₃₆N₇O₅ (M+H⁺): 490.2778. Found: 490.2762.

Netropsin-3-(*S*)-*N,N*-Dimethylaminoaspartamic acid (I-86A). ¹H NMR δ 10.15 (s, 1H), 9.85 (s, 1H), 8.06 (t, 1H), 7.17 (s, 2H), 6.93 (s, 1H), 6.80 (s, 1H), 3.82 (s, 3H), 3.79 (s, 3H), 3.58 (m, 1H), 3.17 (m, 2H), 2.60 (dd, 1H), 2.39 (dd, 1H), 2.26 (t, 2H), 2.24 (s, 6H), 2.14 (s, 6H), 1.61 (m, 2H); FAB MS, calcd. for C₂₃H₃₆N₇O₅ (M+H⁺): 490.2778. Found: 490.2774.

Netropsin-2-(*R*)-*N,N*-Dimethylaminoaspartamic acid (I-173B) and Netropsin-3-(*R*)-*N,N*-Dimethylaminoaspartamic acid (I-173) were prepared as a 1:1 mixture from **I-22** and 5.0 equiv. **I-136**. Chromatography on silica gel using 1% NH₄OH/MeOH eluent separated the isomers, and each was obtained in 21% yield. **I-173B** ¹H NMR δ 10.30 (s, 1H), 9.84 (s, 1H), 8.06 (t, 1H), 7.17 (d, 1H), 7.16 (d, 1H), 6.86 (d, 1H), 6.81 (d, 1H), 3.82 (s, 3H), 3.79 (s, 3H), 3.62 (m, 1H), 3.18 (m, 2H), 2.76 (dd, 1H), 2.56 (dd, 1H), 2.44 (s, 6H), 2.25 (t, 2H), 2.14 (s, 6H), 1.61 (m, 2H); FAB MS, calcd. for C₂₃H₃₆N₇O₅ (M+H⁺): 490.2778. Found: 490.2789; EI MS, *m/z* 442, 428, 388 (-C₄H₇NO₂), 374 (-C₅H₉NO₂), 346 (-C₆H₉NO₃). **I-173A** ¹H NMR δ 9.90 (s, 1H), 9.86 (s, 1H), 8.07 (t, 1H), 7.18 (s, 1H), 6.95 (d, 1H), 6.81 (m, 2H), 3.82 (s, 3H), 3.80 (s, 3H), 3.62 (m, 1H), 3.19 (m, 2H), 2.65 (dd, 1H), 2.44 (dd, 1H), 2.28

(t, 2H), 2.24 (s, 6H), 2.17 (s, 6H), 1.62 (m, 2H); FAB MS, calcd. for $C_{23}H_{36}N_7O_5$ ($M+H^+$): 490.2778. Found: 490.2776. EI MS, m/z 442, 428, 346 ($-C_6H_9NO_3$).

General Procedure for the Synthesis of Chiral Boc Bis(Netropsin) Compounds followed that for the synthesis of unsubstituted Boc Bis(Netropsin) compounds (Chapter One).

Boc Bis(Netropsin)-(R,R)-Tartaramide (I-119), 29% from **I-108** and **II-129**. 1H NMR δ 9.87 (s, 2H), 9.63 (s, 2H), 8.07 (t, 1H), 7.96 (t, 1H), 7.24 (s, 2H), 7.18 (m, 2H), 7.07 (s, 2H), 6.85 (d, 1H), 6.83 (d, 1H), 6.78 (t, 1H), 5.79 (br s, 1H), 5.77 (br s, 1H), 4.45 (s, 1H), 4.44 (s, 1H), 3.84 (s, 6H), 3.80 (s, 6H), 3.18 (m, 4H), 2.96 (m, 2H), 2.31 (t, 2H), 2.20 (s, 6H), 1.63 (m, 2H), 1.57 (m, 2H), 1.38 (s, 9H); FAB MS, calcd. for $C_{41}H_{59}N_{12}O_{10}$ ($M+H^+$): 879.4476. Found: 879.4491.

Boc Bis(Netropsin)-(S,S)-Tartaramide (I-165), 84% from **I-149** and **II-129**. NMR data matched that for **I-119**. FAB MS, calcd. for $C_{41}H_{59}N_{12}O_{10}$ ($M+H^+$): 879.4476. Found: 879.4457.

Boc Bis(Netropsin)-(RS,SR)-Tartaramide (I-126), 35% from **II-121** and **II-129**. 1H NMR δ 9.85 (s, 1H), 9.84 (s, 1H), 9.54 (s, 2H), 8.04 (t, 1H), 7.94 (t, 1H), 7.20 (s, 2H), 7.17 (s, 2H), 7.05 (s, 2H), 6.84 (s, 1H), 6.81 (d, 1H), 6.78 (t, 1H), 6.00 (br s, 1H), 5.99 (br s, 1H), 4.34 (s, 1H), 4.33 (s, 1H), 3.82 (s, 6H), 3.79 (s, 6H), 3.17 (m, 4H), 2.95 (m, 2H), 2.25 (t, 2H), 2.14 (s, 6H), 1.60 (m, 4H), 1.38 (s, 9H); FAB MS, calcd. for $C_{41}H_{59}N_{12}O_{10}$ ($M+H^+$): 879.4476. Found: 879.4436.

Boc Bis(Netropsin)-(R,R)-Tartaramide Acetonide (I-67), 59% from **I-66** and **II-129**. 1H NMR δ 10.20 (s, 2H), 9.90 (s, 1H), 9.89 (s, 1H), 8.06 (t, 1H), 7.96 (t,

1H), 7.24 (s, 2H), 7.17 (s, 2H), 7.00 (m, 2H), 6.84 (d, 1H), 6.81 (d, 1H), 6.78 (t, 1H), 4.77 (s, 2H), 3.84 (s, 6H), 3.80 (s, 6H), 3.17 (m, 4H), 2.95 (m, 2H), 2.26 (t, 2H), 2.15 (s, 6H), 1.6 (m, 4H), 1.49 (s, 6H), 1.38 (s, 9H); FAB MS, calcd. for $C_{44}H_{63}N_{12}O_{10}$ ($M+H^+$): 919.4790. Found: 919.4791.

Boc Bis(Netropsin)-(S,S)-Tartaramide Acetonide (I-101), 57% from **I-99** and **II-129**. NMR data matched that of **I-67**. FAB MS, calcd. for $C_{44}H_{63}N_{12}O_{10}$ ($M+H^+$): 919.4790. Found: 919.4753.

Boc Bis(Netropsin)-(RS,SR)-Tartaramide Acetonide (I-114), from **I-113** and **II-129**. 1H NMR δ 9.84 (2s, 2H), 9.69 (s, 2H), 8.04 (t, 1H), 7.93 (t, 1H), 7.15 (s, 2H), 7.12 (m, 2H), 6.94 (m, 2H), 6.83 (s, 1H), 6.80 (s, 1H), 6.75 (t, 1H), 4.91 (s, 2H), 3.80 (s, 6H), 3.79 (s, 6H), 3.17 (m, 4H), 2.95 (m, 2H), 2.27 (t, 2H), 2.16 (s, 6H), 1.65 (s, 3H), 1.60 (m, 4H), 1.43 (s, 3H), 1.38 (s, 9H); FAB MS, calcd. for $C_{44}H_{63}N_{12}O_{10}$ ($M+H^+$): 919.4790. Found: 919.4749.

Boc Bis(Netropsin)-2-(S)-Malicamide (I-221), 58% from **I-181** and **II-129**. NMR data matched that of **I-223**. FAB MS, calcd. for $C_{41}H_{59}N_{12}O_9$ ($M+H^+$): 863.4528. Found: 863.4520.

Boc Bis(Netropsin)-2-(R)-Malicamide (I-223), 52% from **I-183** and **II-129**. 1H NMR δ 9.90 (s, 1H), 9.86 (s, 2H), 9.80 (s, 1H), 8.06 (t, 1H), 7.95 (t, 1H), 7.19 (m, 2H), 7.18 (s, 2H), 7.05 (d, 1H), 6.88 (d, 1H), 6.85 (s, 1H), 6.82 (d, 1H), 6.79 (t, 1H), 5.90 (s, 1H), 5.88 (s, 1H), 4.48 (m, 1H), 3.84 (s, 3H), 3.83 (s, 3H), 3.80 (s, 6H), 3.18 (m, 4H), 2.96 (m, 2H), 2.70 (dd, 1H), 2.53 (dd, 1H), 2.25 (t, 2H), 2.15 (s, 6H), 1.61 (m, 4H), 1.38 (s, 9H); FAB MS, calcd. for $C_{41}H_{59}N_{12}O_9$ ($M+H^+$): 863.4528. Found: 863.4508.

Boc Bis(Netropsin)-2-(S)-N,N-Dimethylaminoaspartamide (I-89), 63% from **I-86B** and **II-129**. ^1H NMR δ 9.94 (s, 1H), 9.89 (s, 1H), 9.86 (s, 1H), 9.85 (s, 1H), 8.06 (t, 1H), 7.96 (t, 1H), 7.19 (s, 1H), 7.17 (s, 2H), 7.15 (s, 1H), 6.93 (s, 1H), 6.84 (s, 2H), 6.81 (s, 1H), 6.79 (t, 1H), 3.82 (s, 6H), 3.79 (s, 6H), 3.77 (m, 1H), 3.17 (m, 4H), 2.95 (m, 2H), 2.70 (dd, 1H), 2.55 (dd, 1H), 2.27 (s, 6H), 2.23 (t, 2H), 2.13 (s, 6H), 1.60 (m, 4H), 1.38 (s, 9H); FAB MS, calcd. for $\text{C}_{43}\text{H}_{64}\text{N}_{13}\text{O}_8$ ($\text{M}+\text{H}^+$): 890.5001. Found: 890.4952.

Boc Bis(Netropsin)-2-(R)-N,N-Dimethylaminoaspartamide (I-180), 59% from **I-173B** and **II-129**. NMR data matched that for **I-89**. FAB MS, calcd. for $\text{C}_{43}\text{H}_{64}\text{N}_{13}\text{O}_8$ ($\text{M}+\text{H}^+$): 890.5001. Found: 890.4996.

Boc Bis(Netropsin)-3-(S)-N,N-Dimethylaminoaspartamide (I-87), 51% from **I-86A** and **II-129**. ^1H NMR δ 9.94 (s, 1H), 9.89 (s, 1H), 9.85 (s, 2H), 8.06 (t, 1H), 7.95 (t, 1H), 7.18 (d, 1H), 7.17 (m, 2H), 7.15 (d, 1H), 6.93 (d, 1H), 6.84 (s, 2H), 6.80 (s, 1H), 6.78 (t, 1H), 3.82 (s, 3H), 3.81 (s, 3H), 3.79 (s, 6H), 3.77 (m, 1H), 3.18 (m, 4H), 2.95 (m, 2H), 2.71 (dd, 1H), 2.53 (dd, 1H), 2.27 (s, 6H), 2.24 (t, 2H), 2.13 (s, 6H), 1.60 (m, 4H), 1.38 (s, 9H); FAB MS, calcd. for $\text{C}_{43}\text{H}_{64}\text{N}_{13}\text{O}_8$ ($\text{M}+\text{H}^+$): 890.5001. Found: 890.5020.

General Procedure for the Synthesis of Chiral Bis(Netropsin) Compounds followed that for the synthesis of unsubstituted Bis(Netropsin) compounds (Chapter One).

Bis(Netropsin)-(R,R)-Tartaramide (I-129), 76% from **I-119**. ^1H NMR δ 9.86 (s, 2H), 9.64 (s, 2H), 8.06 (m, 2H), 7.23 (m, 2H), 7.18 (m, 2H), 7.08 (s, 2H), 6.86 (s, 1H), 6.82 (d, 1H), 5.79 (br s, 2H), 4.45 (br s, 2H), 3.84 (s, 6H), 3.80 (s, 6H), 3.2 (m,

4H), 2.62 (t, 2H), 2.24 (t, 2H), 2.14 (s, 6H), 1.6 (m, 4H); FAB MS, calcd. for $C_{36}H_{51}N_{12}O_8$ ($M+H^+$): 779.3953. Found: 779.3952.

Bis(Netropsin)-(S,S)-Tartaramide (I-166), 60% from **I-165**. NMR data matched that for **I-129**; FAB MS, calcd. for $C_{36}H_{51}N_{12}O_8$ ($M+H^+$): 779.3953. Found: 779.3920.

Bis(Netropsin)-(RS,SR)-Tartaramide (I-127), 54% from **I-126**. 1H NMR δ 9.84 (s, 2H), 9.55 (s, 2H), 8.05 (m, 2H), 7.19 (m, 2H), 7.17 (m, 2H), 7.05 (s, 2H), 6.84 (s, 1H), 6.81 (d, 1H), 6.03 (br s, 2H), 4.34 (br s, 2H), 3.83 (s, 6H), 3.79 (s, 6H), 3.2 (m, 4H), 2.61 (t, 2H), 2.23 (t, 2H), 2.13 (s, 6H), 1.60 (m, 4H); FAB MS, calcd. for $C_{36}H_{51}N_{12}O_8$ ($M+H^+$): 779.3953. Found: 779.3898.

Bis(Netropsin)-(R,R)-Tartaramide Acetonide (I-77), 80% from **I-67**. 1H NMR δ 10.19 (s, 2H), 9.89 (s, 2H), 8.06 (m, 2H), 7.24 (s, 2H), 7.17 (s, 2H), 7.01 (s, 2H), 6.84 (s, 1H), 6.81 (s, 1H), 4.77 (s, 2H), 3.85 (s, 6H), 3.80 (s, 6H), 3.2 (m, 4H), 2.60 (t, 2H), 2.24 (t, 2H), 2.14 (s, 6H), 1.59 (m, 4H), 1.49 (s, 6H).

Bis(Netropsin)-(S,S)-Tartaramide Acetonide (I-104), 83% from **I-101**. Spectral data matched that for **I-77**. FAB MS, m/z 819 ($M+H^+$).

Bis(Netropsin)-(RS,SR)-Tartaramide Acetonide (I-120), 33% from **I-113**. 1H NMR δ 9.84 (s, 2H), 9.70 (s, 2H), 8.05 (m, 2H), 7.15 (m, 2H), 7.12 (s, 2H), 6.94 (s, 2H), 6.87 (s, 1H), 6.80 (d, 1H), 4.91 (s, 2H), 3.80 (s, 6H), 3.79 (s, 6H), 3.2 (m, 4H), 2.68 (t, 2H), 2.24 (t, 2H), 2.14 (s, 6H), 1.65 (s, 3H), 1.62 (m, 4H), 1.43 (s, 3H).

Bis(Netropsin)-2-(S)-Malicamide (I-225), 63% from **I-221**. NMR data matched that for **I-227**; FAB MS, calcd. for $C_{36}H_{51}N_{12}O_7$ ($M+H^+$): 763.4004. Found: 763.3993.

Bis(Netropsin)-2-(R)-Malicamide (I-227), 41% from **I-223**. 1H NMR δ 9.92 (s, 1H), 9.87 (s, 2H), 9.81 (s, 1H), 8.07 (m, 2H), 7.19 (m, 4H), 7.05 (d, 1H), 6.88 (d, 1H), 6.84 (d, 1H), 6.82 (d, 1H), 5.95 (br s, 1H), 4.48 (m, 1H), 3.83 (2s, 6H), 3.80 (s, 6H), 3.2 (m, 4H), 2.70 (dd, 1H), 2.59 (t, 1H), 2.52 (dd, 1H), 2.24 (t, 2H), 2.13 (s, 6H), 1.61 (m, 4H); FAB MS, calcd. for $C_{36}H_{51}N_{12}O_7$ ($M+H^+$): 763.4004. Found: 763.4029.

Bis(Netropsin)-2-(S)-N,N-Dimethylaminoaspartamide (I-92), 80% from **I-89**. 1H NMR δ 9.94 (s, 1H), 9.89 (s, 1H), 9.85 (m, 2H), 8.06 (m, 2H), 7.18 (d, 1H), 7.17 (m, 2H), 7.15 (d, 1H), 6.93 (d, 1H), 6.89 (d, 1H), 6.83 (s, 1H), 6.81 (d, 1H), 3.82 (s, 6H), 3.79 (s, 6H), 3.77 (m, 1H), 3.2 (m, 4H), 2.71 (dd, 1H), 2.56 (dd, 1H), 2.27 (s, 6H), 2.23 (t, 2H), 2.13 (s, 6H), 1.60 (m, 2H), 1.55 (m, 2H); FAB MS, calcd. for $C_{38}H_{56}N_{13}O_6$ ($M+H^+$): 790.4477. Found: 790.4447.

Bis(Netropsin)-2-(R)-N,N-Dimethylaminoaspartamide (I-226), 68% from **I-180**. NMR data matched that for **I-92**; FAB MS, calcd. for $C_{38}H_{56}N_{13}O_6$ ($M+H^+$): 790.4477. Found: 790.4448.

Bis(Netropsin)-3-(S)-N,N-Dimethylaminoaspartamide (I-91), 70% from **I-87**. 1H NMR δ 9.93 (s, 1H), 9.88 (s, 1H), 9.84 (2s, 2H), 8.05 (m, 2H), 7.18 (d, 1H), 7.17 (s, 2H), 7.14 (s, 1H), 6.93 (d, 1H), 6.85 (d, 1H), 6.83 (d, 1H), 6.81 (d, 1H), 3.82 (2s, 6H), 3.79 (s, 6H), 3.77 (m, 1H), 3.2 (m, 4H), 2.72 (dd, 1H), 2.58 (m, 3H), 2.27 (s,

6H), 2.24 (t, 2H), 2.14 (s, 6H), 1.61 (m, 2H), 1.55 (m, 2H); FAB MS, calcd. for C₃₈H₅₆N₁₃O₆ (M+H⁺): 790.4477. Found: 790.4454.

General Procedure for the Synthesis of Chiral Bis(Netropsin)-EDTA Triethyl Ester Compounds followed that for the synthesis of unsubstituted Bis(Netropsin)-EDTA Triester compounds (Chapter One).

Bis(Netropsin)-(R,R)-Tartaramide-EDTA, Triethyl ester (I-138), 78% from I-129 and EDTA(OEt)₃. ¹H NMR δ 9.86 (s, 1H), 9.85 (s, 1H), 9.62 (s, 2H), 8.05 (t, 1H), 7.97 (t, 1H), 7.23 (m, 2H), 7.17 (m, 2H), 7.07 (m, 2H), 6.85 (d, 1H), 6.82 (d, 1H), 5.76 (d, 2H), 4.45 (d, 2H), 4.06 (m, 6H), 3.84 (s, 6H), 3.80 (s, 6H), 3.61-3.47 (series of singlets, 8H), 3.17 (m, 6H), 2.72 (m, 4H), 2.28 (t, 2H), 2.17 (s, 6H), 1.61 (m, 4H), 1.17 (m, 9H); FAB MS, calcd. for C₅₂H₇₇N₁₄O₁₅ (M+H⁺): 1137.5691. Found: 1137.5666; IR (KBr) 3300, 2940, 1720, 1640, 1580, 1530, 1460, 1440, 1400, 1260, 1200, 1120 cm⁻¹; [α]_D²³ + 60° (c=0.58, MeOH).

Bis(Netropsin)-(S,S)-Tartaramide-EDTA, Triethyl ester (I-170), 61% from I-166 and EDTA(OEt)₃. NMR data matched that of I-138. [α]_D²³ -51° (c=0.61, MeOH); FAB MS, calcd. for C₅₂H₇₇N₁₄O₁₅ (M+H⁺): 1137.5691. Found: 1137.5671.

Bis(Netropsin)-(RS,SR)-Tartaramide-EDTA, Triethyl ester (I-139), 83% from I-127 and EDTA(OEt)₃. ¹H NMR δ 9.84 (s, 1H), 9.83 (s, 1H), 9.52 (m, 2H), 8.02 (m, 2H), 7.96 (t, 1H), 7.19 (m, 2H), 7.17 (s, 2H), 7.04 (s, 2H), 6.85 (d, 1H), 6.81 (d, 1H), 5.98 (d, 2H), 4.33 (d, 2H), 4.07 (m, 6H), 3.82 (s, 6H), 3.79 (s, 6H), 3.61-3.47 (series of singlets, 8H), 3.17 (m, 6H), 2.73 (m, 4H), 2.27 (t, 2H), 2.16 (s, 6H), 1.61 (m, 4H), 1.17 (m, 9H); FAB MS, calcd. for C₅₂H₇₇N₁₄O₁₅ (M+H⁺): 1137.5691. Found: 1137.5732.

Bis(Netropsin)-(R,R)-Tartaramide Acetonide-EDTA, Triethyl ester (I-78), 87% from **I-77** and **EDTA(OEt)₃**. ¹H NMR δ 10.19 (s, 2H), 9.90 (s, 1H), 9.89 (s, 1H), 8.05 (m, 2H), 7.98 (t, 1H), 7.24 (s, 2H), 7.18 (s, 2H), 7.00 (s, 2H), 6.85 (d, 1H), 6.82 (d, 1H), 4.77 (s, 2H), 4.06 (m, 6H), 3.84 (s, 6H), 3.80 (m, 6H), 3.61-3.47 (series of singlets, 8H), 3.17 (m, 6H), 2.72 (m, 4H), 2.33 (t, 2H), 2.21 (s, 6H), 1.63 (m, 4H), 1.48 (s, 6H), 1.17 (m, 9H); FAB MS, calcd. for C₅₅H₈₁N₁₄O₁₅ (M+H⁺): 1177.6006. Found: 1177.6047.

Bis(Netropsin)-(S,S)-Tartaramide Acetonide-EDTA, Triethyl ester (I-105), 87% from **I-104** and **EDTA(OEt)₃**. NMR data matched that for **I-78**; FAB MS, calcd. for C₅₅H₈₁N₁₄O₁₅ (M+H⁺): 1177.6006. Found: 1177.5997.

Bis(Netropsin)-(RS,SR)-Tartaramide Acetonide-EDTA, Triethyl ester (I-141), 39% from **I-120** and **EDTA(OEt)₃**. ¹H NMR δ 9.85 (s, 1H), 9.84 (s, 1H), 9.69 (s, 2H), 8.0 (m, 3H), 7.15 (s, 2H), 7.12 (s, 2H), 6.94 (s, 2H), 6.84 (s, 1H), 6.82 (s, 1H), 4.91 (s, 2H), 4.06 (m, 6H), 3.79 (2s, 12H), 3.64-3.47 (series of singlets, 8H), 3.19 (m, 6H), 2.33 (t, 2H), 2.21 (s, 6H), 1.64 (s, 3H), 1.6 (m, 4H), 1.42 (s, 3H), 1.18 (m, 9H).

Bis(Netropsin)-2-(S)-Malicamide-EDTA, Triethyl ester (I-232), 78% from **I-225** and **EDTA(OEt)₃**. ¹H NMR δ 9.94 (s, 1H), 9.87 (s, 1H), 9.86 (s, 1H), 9.84 (s, 1H), 8.05 (m, 2H), 7.99 (t, 1H), 7.19 (m, 4H), 7.05 (d, 1H), 6.88 (s, 1H), 6.85 (d, 1H), 6.82 (d, 1H), 6.01 (br s, 1H), 4.48 (m, 1H), 4.06 (m, 6H), 3.84 (s, 3H), 3.83 (s, 3H), 3.80 (2s, 6H), 3.61-3.47 (series of singlets, 8H), 3.17 (m, 6H), 2.70 (m, 5H), 2.61 (dd, 1H), 2.24 (t, 2H), 2.14 (s, 6H), 1.61 (m, 4H), 1.17 (m, 9H); FAB MS, calcd. for C₅₂H₇₇N₁₄O₁₄ (M+H⁺): 1121.5744. Found: 1121.5699.

Bis(Netropsin)-2-(R)-Malcamide-EDTA, Triethyl ester (I-233), 52% from I-227 and EDTA(OEt)₃. NMR data matched that for I-232; FAB MS, calcd. for C₅₂H₇₇N₁₄O₁₄ (M+H⁺): 1121.5744. Found: 1121.5760.

Bis(Netropsin)-2-(S)-N,N-Dimethylaminoaspartamide-EDTA, Triethyl ester (I-94), 28% from I-92 and EDTA(OEt)₃. NMR data matched that of I-229.

Bis(Netropsin)-2-(R)-N,N-Dimethylaminoaspartamide-EDTA, Triethyl ester (I-229), 45% from I-226 and EDTA(OEt)₃. ¹H NMR δ 9.93 (s, 1H), 9.88 (s, 1H), 9.86 (s, 1H), 9.84 (s, 1H), 8.05 (m, 2H), 7.98 (t, 1H), 7.18 (m, 3H), 7.14 (d, 1H), 6.94 (s, 1H), 6.85 (m, 2H), 6.81 (d, 1H), 4.06 (m, 6H), 3.83 (s, 3H), 3.82 (s, 3H), 3.80 (2s, 6H), 3.78 (m, 1H), 3.61-3.47 (series of singlets, 8H), 3.18 (m, 6H), 2.72 (m, 5H), 2.50 (m, 1H), 2.27 (s, 6H), 2.24 (t, 2H), 2.14 (s, 6H), 1.61 (m, 4H), 1.19 (m, 9H); FAB MS, calcd. for C₅₄H₈₂N₁₅O₁₃ (M+H⁺): 1148.6217. Found: 1148.6162.

Bis(Netropsin)-3-(S)-N,N-Dimethylaminoaspartamide-EDTA, Triethyl ester (I-93), 69% from I-91 and EDTA(OEt)₃. ¹H NMR δ 9.94 (s, 1H), 9.89 (s, 1H), 9.86 (s, 2H), 8.04 (m, 2H), 7.99 (t, 1H), 7.17 (s, 3H), 7.15 (s, 1H), 6.93 (s, 1H), 6.84 (s, 2H), 6.80 (s, 1H), 4.06 (m, 6H), 3.81 (s, 6H), 3.79 (s, 6H), 3.76 (m, 1H), 3.61-3.47 (series of singlets, 8H), 3.19 (m, 6H), 2.72 (m, 5H), 2.53 (dd, 1H), 2.26 (s, 6H), 2.24 (t, 2H), 2.13 (s, 6H), 1.60 (m, 4H), 1.17 (m, 9H); FAB MS, calcd. for C₅₄H₈₂N₁₅O₁₃ (M+H⁺): 1148.6217. Found: 1148.6171.

General Procedure for the Synthesis of Chiral Bis(Netropsin)-EDTA Compounds followed that for the synthesis of unsubstituted Bis(Netropsin)-EDTA compounds (Chapter One).

Bis(Netropsin)-(R,R)-Tartaramide-EDTA (BN-(R,R)-Tar-E, I-143), 77% from **I-138**. ^1H NMR ($\text{Me}_2\text{SO-d}_6$ + TFA) δ 9.88 (s, 1H), 9.87 (s, 1H), 9.63 (s, 2H), 8.37 (t, 1H), 8.14 (t, 1H), 8.01 (t, 1H), 7.23 (s, 2H), 7.16 (s, 2H), 7.08 (s, 2H), 6.94 (s, 1H), 6.90 (s, 1H), 4.45 (s, 2H), 4.07 (s, 2H), 3.92 (s, 2H), 3.84 (s, 6H), 3.82 (s, 3H), 3.80 (s, 3H), 3.74 (s, 4H), 3.30 (m, 2H), 3.2 (m, 8H), 3.08 (m, 2H), 2.79 (d, 6H), 1.84 (m, 2H), 1.66 (m, 2H); FAB MS, calcd. for $\text{C}_{46}\text{H}_{64}\text{N}_{14}\text{O}_{15}\text{K}$ ($\text{M}+\text{K}^+$): 1091.4313. Found: 1091.4150; IR (KBr) 3300, 2880, 1640, 1590, 1530, 1460, 1440, 1400, 1330, 1260, 1200 cm^{-1} ; UV (H_2O) λ_{max} 299, 238 nm; $[\alpha]_D^{24} +8.0^\circ$ ($c=0.323$, 10% $\text{NH}_4\text{OH/EtOH}$).

Bis(Netropsin)-(S,S)-Tartaramide-EDTA (BN-(S,S)-Tar-E, I-171), 68% from **I-170**. Spectral data matched that for **I-143**; FAB MS, calcd. for $\text{C}_{46}\text{H}_{64}\text{N}_{14}\text{O}_{15}\text{K}$ ($\text{M}+\text{K}^+$): 1091.4313. Found: 1091.4200; $[\alpha]_D^{24} -17.9^\circ$ ($c=0.330$, 10% $\text{NH}_4\text{OH/EtOH}$).

Bis(Netropsin)-(RS,SR)-Tartaramide-EDTA (BN-(RS,SR)-Tar-E, I-144), 92% from **I-139**. ^1H NMR ($\text{Me}_2\text{SO-d}_6$ + TFA) δ 9.86 (s, 1H), 9.85 (s, 1H), 9.54 (s, 1H), 9.53 (s, 1H), 8.37 (t, 1H), 8.14 (t, 1H), 8.00 (t, 1H), 7.20 (m, 2H), 7.16 (m, 2H), 7.06 (m, 2H), 6.94 (d, 1H), 6.90 (d, 1H), 4.35 (s, 2H), 4.08 (s, 2H), 3.93 (s, 2H), 3.83 (s, 6H), 3.82 (s, 3H), 3.80 (s, 3H), 3.76 (s, 4H), 3.31 (m, 2H), 3.2 (m, 8H), 3.07 (m, 2H), 2.79 (d, 6H), 1.84 (m, 2H), 1.66 (m, 2H); FAB MS, calcd. for $\text{C}_{46}\text{H}_{64}\text{N}_{14}\text{O}_{15}\text{K}$ ($\text{M}+\text{K}^+$): 1091.4313. Found: 1091.4182; UV (H_2O) λ_{max} 298, 235 nm.

Bis(Netropsin)-(R,R)-Tartaramide Acetonide-EDTA (BN-(R,R)-TarAc-E, I-102), 63% from **I-78**. ^1H NMR ($\text{Me}_2\text{SO-d}_6$ + TFA) δ 10.20 (s, 2H), 9.92 (s, 2H), 8.39 (br s, 1H), 8.17 (br s, 1H), 8.02 (br s, 1H), 7.25 (s, 2H), 7.18 (s, 2H), 7.03 (s, 2H), 6.95 (s, 1H), 6.91 (s, 1H), 4.79 (s, 2H), 4.09 (s, 2H), 3.94 (s, 2H), 3.86 (s, 6H), 3.83

(s, 3H), 3.81 (s, 3H), 3.78 (s, 4H), 3.34 (br s, 2H), 3.2 (m, 8H), 3.09 (br s, 2H), 2.80 (d, 6H), 1.86 (m, 2H), 1.66 (m, 2H), 1.50 (s, 6H); FAB MS, calcd. for C₄₉H₆₈N₁₄O₁₅K (M+K⁺): 1131.4626. Found: 1131.4636; UV (H₂O) λ_{max} 298, 237 nm; $[\alpha]_D^{24}$ -19.7° (c=0.360, 10% NH₄OH/EtOH).

Bis(Netropsin)-(S,S)-Tartaramide Acetonide-EDTA (BN-(S,S)-TarAc-E, I-106), 88% from **I-105**. Spectral data matched that of **I-102**; FAB MS, calcd. for C₄₉H₆₈N₁₄O₁₅K (M+K⁺): 1131.4626. Found: 1131.4520; $[\alpha]_D^{24}$ +15.6° (c=0.379, 10% NH₄OH/EtOH).

Bis(Netropsin)-(RS,SR)-Tartaramide Acetonide-EDTA (BN-(RS,SR)-TarAc-E, I-147), 80% from **I-141**. ¹H NMR (Me₂SO-d₆ + TFA) δ 9.91 (s, 1H), 9.87 (s, 1H), 9.85 (s, 1H), 9.74 (s, 1H), 8.37 (t, 1H), 8.16 (t, 1H), 8.00 (t, 1H), 7.26 (s, 2H), 7.17 (m, 2H), 7.00 (s, 2H), 6.94 (s, 1H), 6.93 (s, 1H), 4.92 (s, 2H), 4.06 (s, 2H), 3.8 (m, 14H), 3.73 (d, 4H), 3.2 (m, 12H), 2.79 (d, 6H), 1.83 (m, 2H), 1.64 (s, 3H), 1.6 (m, 2H), 1.42 (s, 3H); FAB MS, calcd. for C₄₉H₆₉N₁₄O₁₅ (M+H⁺): 1093.5067. Found: 1093.5050; UV (H₂O) λ_{max} 297, 237 nm.

Bis(Netropsin)-2-(S)-Malicamide-EDTA (BN-2(S)-Mal-E, I-234), 18% from **I-232**. ¹H NMR (Me₂SO-d₆ + TFA) δ 9.92 (s, 1H), 9.90 (s, 1H), 9.88 (s, 1H), 9.82 (s, 1H), 8.40 (t, 1H), 8.17 (t, 1H), 8.03 (br s, 1H), 7.21 (d, 1H), 7.20 (d, 1H), 7.18 (d, 1H), 7.17 (d, 1H), 7.08 (d, 1H), 6.96 (d, 1H), 6.91 (s, 2H), 4.50 (m, 1H), 4.10 (s, 2H), 3.95 (s, 2H), 3.85 (s, 3H), 3.84 (s, 3H), 3.83 (s, 3H), 3.81 (s, 3H), 3.79 (s, 4H), 3.34 (br s, 2H), 3.22 (m, 8H), 3.09 (m, 2H), 2.80 (d, 6H), 2.70 (m, 1H), 2.5 (m, 1H), 1.85 (m, 2H), 1.68 (m, 2H); FAB MS, calcd. for C₄₆H₆₄N₁₄O₁₄K (M+K⁺): 1075.4362. Found: 1075.4357. UV (H₂O) λ_{max} 299, 239 nm; $[\alpha]_D^{24}$ -14.8° (c=0.290, 10% NH₄OH/EtOH).

Bis(Netropsin)-2-(*R*)-Malicamide-EDTA (BN-2(*R*)-Mal-E, I-235), 71% from I-233. Spectral data matched that of I-234. FAB MS, calcd. for C₄₆H₆₅N₁₄O₁₄ (M+H⁺): 1037.4805. Found: 1037.4750; [α]_D²⁴ -11.4° (c=0.298, 10% NH₄OH/EtOH).

Bis(Netropsin)-2-(*S*)-*N,N*-Dimethylaminoaspartamide-EDTA (BN-2-(*S*)-DMAsp-E, I-109), 100% from I-94. ¹H NMR (Me₂SO-d₆ + TFA) δ 10.75 (s, 1H), 10.26 (s, 1H), 9.92 (s, 1H), 9.88 (s, 1H), 8.39 (br s, 1H), 8.15 (br s, 1H), 8.02 (br s, 1H), 7.26 (s, 1H), 7.18 (s, 1H), 7.16 (s, 2H), 6.96 (s, 1H), 6.94 (s, 1H), 6.91 (s, 1H), 6.85 (s, 1H), 4.38 (m, 1H), 4.09 (s, 2H), 3.95 (s, 2H), 3.87 (s, 3H), 3.83 (s, 3H), 3.82 (s, 3H), 3.81 (s, 3H), 3.79 (s, 4H), 3.35 (br s, 2H), 3.2 (m, 8H), 3.10 (br s, 4H), 2.89 (br s, 6H), 2.80 (d, 6H), 1.85 (m, 2H), 1.68 (m, 2H); FAB MS, calcd. for C₄₈H₆₉N₁₅O₁₃K (M+K⁺): 1102.4836. Found: 1102.4820; UV (H₂O) λ_{max} 298, 236 nm; [α]_D²⁴ -1.0° (c=0.202, 10% NH₄OH/EtOH).

Bis(Netropsin)-2-(*R*)-*N,N*-Dimethylaminoaspartamide-EDTA (BN-2-(*R*)-DMAsp-E, I-231), 71% from I-229. Spectral data matched that of I-109; FAB MS, calcd. for C₄₈H₇₀N₁₅O₁₃ (M+H⁺): 1064.5278. Found: 1064.5251; [α]_D²⁴ -0.9° (c=0.216, 10% NH₄OH/EtOH).

Bis(Netropsin)-3-(*S*)-*N,N*-Dimethylaminoaspartamide-EDTA (BN-3-(*S*)-DMAsp-E, I-103), 63% from I-93. ¹H NMR (Me₂SO-d₆ + TFA) δ 10.76 (s, 1H), 10.27 (s, 1H), 9.94 (s, 1H), 9.87 (s, 1H), 8.40 (t, 1H), 8.18 (br s, 1H), 8.02 (br s, 1H), 7.27 (s, 1H), 7.18 (m, 2H), 7.15 (s, 1H), 6.97 (s, 1H), 6.96 (s, 1H), 6.91 (s, 1H), 6.85 (s, 1H), 4.40 (m, 1H), 4.11 (s, 2H), 3.96 (s, 2H), 3.87 (s, 3H), 3.86 (s, 4H), 3.84 (s, 3H), 3.83 (s, 3H), 3.81 (s, 3H), 3.37 (br s, 2H), 3.2 (br s, 8H), 3.11 (m, 4H), 2.89 (br s, 6H), 2.81 (d, 6H), 1.86 (m, 2H), 1.68 (m, 2H); FAB MS, calcd. for C₄₈H₆₉N₁₅O₁₃K

(M+K⁺): 1102.4836. Found: 1102.4750; UV (H₂O) λ_{max} 298, 235 nm; $[\alpha]_D^{24}$ 0.0^o (c=0.217, 10% NH₄OH/EtOH).

Bis(Netropsin)-(S)-Alanine-EDTA (BN-(S)-AE) and Bis(Netropsin)-(R)-Alanine (BN-(R)-AE) were synthesized from Boc L- and D-alanine (Peninsula Laboratories), respectively, following the general procedures for the synthesis of Bis(Netropsin) Amino acid compounds (Chapter One).

Boc Netropsin-(S)-Alanine (II-184), 84% from **I-22** and Boc L-alanine. ¹H NMR δ 9.87 (s, 1H), 9.83 (s, 1H), 8.07 (t, 1H), 7.18 (s, 1H), 7.15 (s, 1H), 6.99 (d, 1H), 6.90 (s, 1H), 6.82 (s, 1H), 4.07 (m, 1H), 3.83 (s, 3H), 3.79 (s, 3H), 3.18 (m, 2H), 2.29 (t, 2H), 2.17 (s, 6H), 1.62 (m, 2H), 1.38 (s, 9H), 1.22 (d, 3H).

Boc Netropsin-(R)-Alanine (II-188), 79% from **I-22** and Boc D-alanine. NMR data matched that for **II-184**.

Netropsin-(S)-Alanine (II-186), 100% from **II-184**. ¹H NMR δ 10.35 (br s, 1H), 9.92 (s, 1H), 8.12 (t, 1H), 7.21 (d, 1H), 7.18 (d, 1H), 6.91 (d, 1H), 6.86 (d, 1H), 3.90 (m, 1H), 3.85 (s, 3H), 3.80 (s, 3H), 3.20 (m, 2H), 2.63 (t, 2H), 2.44 (s, 6H), 1.71 (m, 2H), 1.38 (d, 3H).

Netropsin-(R)-Alanine (II-189), 98% from **II-188**. NMR data matched that for **II-186**.

Boc Bis(Netropsin)-(S)-Alanine (II-193), 67% from **II-184** and **I-204**. ¹H NMR δ 9.87 (s, 2H), 9.85 (s, 1H), 9.79 (s, 1H), 8.07 (m, 1H), 7.18 (m, 4H), 7.03 (s, 1H), 6.91 (s, 1H), 6.86 (s, 1H), 6.80 (s, 1H), 4.49 (m, 1H), 3.83 (s, 6H), 3.79 (s, 6H),

3.18 (m, 2H), 2.94 (m, 2H), 2.24 (m, 4H), 2.14 (s, 6H), 1.66 (m, 2H), 1.60 (m, 2H), 1.37 (s, 9H), 1.36 (d, 3H).

Boc Bis(Netropsin)-(R)-Alanine (II-194), 75% from II-189 and I-204. NMR data matched that for II-193.

Bis(Netropsin)-(S)-Alanine (II-195), 59% from II-193. ^1H NMR δ 9.90 (s, 1H), 9.88 (s, 1H), 9.87 (s, 1H), 9.83 (s, 1H), 8.11 (d, 1H), 8.07 (t, 1H), 7.20 (s, 1H), 7.18 (s, 1H), 7.17 (s, 2H), 7.04 (s, 1H), 6.91 (s, 1H), 6.87 (s, 1H), 6.81 (s, 1H), 4.49 (q, 1H), 3.83 (s, 6H), 3.79 (s, 6H), 3.18 (m, 2H), 2.55 (t, 2H), 2.23 (m, 4H), 2.13 (s, 6H), 1.62 (m, 4H), 1.36 (d, 3H).

Bis(Netropsin)-(R)-Alanine (II-196), 64% from II-194. NMR data matched that for II-195.

Bis(Netropsin)-(S)-Alanine, Triethyl ester (II-197), 53% from II-193 and EDTA(OEt)₃. ^1H NMR δ 9.89 (s, 1H), 9.88 (s, 1H), 9.86 (s, 1H), 9.82 (s, 1H), 8.09 (m, 2H), 8.01 (t, 1H), 7.20 (s, 1H), 7.18 (s, 1H), 7.16 (s, 2H), 7.03 (s, 1H), 6.91 (s, 1H), 6.86 (s, 1H), 6.81 (s, 1H), 4.49 (s, 1H), 4.06 (m, 6H), 3.83 (s, 6H), 3.79 (s, 6H), 3.60-3.46 (series of singlets, 8H), 3.16 (m, 4H), 2.70 (m, 4H), 2.30 (m, 2H), 2.23 (m, 2H), 2.18 (s, 6H), 1.71 (m, 2H), 1.62 (m, 2H), 1.36 (d, 3H), 1.17 (m, 9H); FAB MS, calcd. for C₅₂H₇₆N₁₄O₁₃K (M+K⁺): 1143.5353. Found: 1143.5324.

Bis(Netropsin)-(R)-Alanine, Triethyl ester (II-199), 65% from II-196 and EDTA(OEt)₃. NMR data matched that for II-197; FAB MS, calcd. for C₅₂H₇₆N₁₄O₁₃K (M+K⁺): 1143.5353. Found:

Bis(Netropsin)-(S)-Alanine-EDTA (BN-(S)-AE, II-198), 58% from **II-197**. ^1H NMR ($\text{Me}_2\text{SO-d}_6 + \text{TFA}$) δ 9.98 (s, 1H), 9.96 (s, 2H), 9.91 (s, 1H), 8.50 (t, 1H), 8.24 (t, 1H), 8.18 (t, 1H), 7.27 (d, 1H), 7.24 (s, 1H), 7.12 (d, 1H), 7.00 (d, 2H), 6.95 (d, 1H), 4.57 (m, 1H), 4.15 (s, 2H), 3.99 (s, 2H), 3.90 (s, 6H), 3.88 (s, 3H), 3.87 (s, 3H), 3.84 (s, 4H), 3.39 (m, 2H), 3.34-3.21 (m, 6H), 3.14 (m, 2H), 2.86 (d, 6H), 2.36 (t, 2H), 1.91 (m, 2H), 1.82 (m, 2H), 1.44 (d, 3H); FAB MS, calcd. for $\text{C}_{46}\text{H}_{64}\text{N}_{14}\text{O}_{13}\text{K}$ ($\text{M}+\text{K}^+$): 1059.4414. Found: 1059.4393; UV (H_2O) λ_{max} 296, 236 nm; $[\alpha]_D^{24} +73.2^\circ$ ($c=0.313$, 10% $\text{NH}_4\text{OH}/\text{EtOH}$).

Bis(Netropsin)-(R)-Alanine-EDTA (BN-(R)-AE, II-200), 92% from **II-199**. Spectral data matched that for **II-198**. FAB MS, calcd. for: $\text{C}_{46}\text{H}_{64}\text{N}_{14}\text{O}_{13}\text{K}$ ($\text{M}+\text{K}^+$): 1059.4414. Found: 1059.4414; UV (H_2O) λ_{max} 296, 236 nm; $[\alpha]_D^{24} +72.3^\circ$ ($c=0.292$, 10% $\text{NH}_4\text{OH}/\text{EtOH}$).

Nitro P1 Analog I-200 was prepared in 84% yield from *N*-methyl-4-nitropyrrrole-2-carboxylic acid and 3-dimethylaminopropylamine following the procedure for **I-22**, except that solvent for chromatography was 0.5% $\text{NH}_4\text{OH}/\text{MeOH}$. ^1H NMR δ 8.4 (br s, 1H), 8.05 (d, 1H), 7.33 (s, 1H), 3.87 (s, 3H), 3.2 (m, 2H), 2.22 (t, 2H), 2.12 (s, 6H), 1.61 (m, 2H); FAB MS, calcd. for $\text{C}_{11}\text{H}_{19}\text{N}_4\text{O}_3$ ($\text{M}+\text{H}^+$): 255.1457. Found: 255.1456.

Boc Nitro P3 Analog I-209 was prepared in 50% yield from $\text{O}_2\text{NP}_3\text{CO}_2\text{H}$ and **IV-161** following the procedure for **II-129**. ^1H NMR δ 10.30 (s, 1H), 9.96 (s, 1H), 8.19 (s, 1H), 7.98 (t 1H), 7.60 (s, 1H), 7.28 (s, 1H), 7.20 (s, 1H), 7.04 (s, 1H), 6.86 (s, 1H), 6.80 (t, 1H), 3.97 (s, 3H), 3.86 (s, 3H), 3.80 (s, 3H), 3.17 (m, 2H), 2.96 (m, 2H), 1.58 (m, 2H), 1.38 (s, 9H); FAB MS, calcd. for $\text{C}_{26}\text{H}_{55}\text{N}_8\text{O}_7$ ($\text{M}+\text{H}^+$): 571.2629. Found: 571.2574.

P1-Succinamic acid (I-254) was prepared in 73% yield from **I-200** and succinic acid following the procedure for Netropsin Alkanamic acid compounds (Chapter One). ^1H NMR δ 9.86 (s, 1H), 8.03 (br s, 1H), 7.06 (s, 1H), 6.62 (s, 1H), 3.75 (s, 3 H), 3.2 (br s, 2H), 2.43 (s, 4H), 2.25 (t, 2H), 2.14 (s, 6H), 1.59 (m, 2H), FAB MS, calcd. for $\text{C}_{15}\text{H}_{25}\text{N}_4\text{O}_4$ ($\text{M}+\text{H}^+$): 325.1876. Found: 325.1869.

P1-(S,S)-Tartaramic acid (I-206) was prepared in 73% yield from **I-200** and *l*-tartaric acid (Aldrich) following the procedure for Netropsin Alkanamic acid compounds (Chapter One). ^1H NMR δ 9.53 (s, 1H), 8.19 (t, 1H), 7.20 (s, 1H), 6.89 (s, 1H), 4.34 (s, 1H), 4.13 (s, 1H), 3.79 (s, 3H), 3.22 (m, 2H), 2.75 (t, 2H), 2.51 (s, 6H), 1.81 (m, 2H); FAB MS, calcd. for $\text{C}_{15}\text{H}_{25}\text{N}_4\text{O}_6$ ($\text{M}+\text{H}^+$): 357.1774. Found: 357.1770.

P1-(R,R)-Tartaramic acid (I-205) was prepared in 84% yield from **I-200** and *d*-tartaric acid (Aldrich) following the procedure for Netropsin Alkanamic acid compounds (Chapter One). NMR data matched that for **I-206**; FAB MS, calcd. for $\text{C}_{15}\text{H}_{25}\text{N}_4\text{O}_6$ ($\text{M}+\text{H}^+$): 357.1774. Found: 357.1771.

Boc P1-Succinamide-P3 (I-256) was prepared in 61% yield from **I-254** and **II-129** following the procedure for Boc Bis(Netropsin) Diacid compounds (Chapter One). ^1H NMR δ 9.89 (s, 1H), 9.88 (s, 1H), 9.87 (s, 1H), 9.81 (s, 1H), 8.05 (t, 1H), 7.96 (t, 1H), 7.23 (d, 1H), 7.17 (d, 1H), 7.14 (d, 1H), 7.07 (d, 1H), 7.02 (d, 1H), 6.87 (d, 1H), 6.85 (d, 1H), 6.79 (t, 1H), 6.61 (d, 1H), 3.83 (s, 3H), 3.82 (s, 3H), 3.79 (s, 3H), 3.75 (s, 3H), 3.16 (m, 4H), 2.94 (m, 2H), 2.54 (s, 4H), 2.22 (t, 2H), 2.12 (s, 6H), 1.58 (m, 4H), 1.37 (s, 9H); FAB MS, calcd. for $\text{C}_{41}\text{H}_{59}\text{N}_{12}\text{O}_8$ ($\text{M}+\text{H}^+$): 847.4579. Found: 847.4571.

Boc P1-(S,S)-Tartaramide-P3 (I-219) was prepared in 50% yield from **I-206** and **II-129** following the procedure for Boc Bis(Netropsin) Diacid compounds (Chapter One). ^1H NMR δ 9.93 (s, 1H), 9.90 (s, 1H), 9.64 (s, 1H), 9.59 (s, 1H), 8.08 (t, 1H), 7.97 (t, 1H), 7.24 (m, 2H), 7.19 (m, 2H), 7.09 (s, 1H), 7.05 (s, 1H), 6.87 (s, 1H), 6.84 (s, 1H), 6.79 (t, 1H), 5.79 (br s, 1H), 5.78 (br s, 1H), 4.43 (s, 2H), 3.85 (s, 6H), 3.80 (s, 3H), 3.79 (s, 3H), 3.18 (m, 4H), 2.96 (m, 2H), 2.27 (t, 2H), 2.16 (s, 6H), 1.60 (m, 4H), 1.39 (s, 9H); FAB MS, calcd. for $\text{C}_{41}\text{H}_{59}\text{N}_{12}\text{O}_{10}$ ($\text{M}+\text{H}^+$): 879.4477. Found: 879.4451.

Boc P1-(R,R)-Tartaramide-P3 (I-216) was prepared in 40% yield from **I-205** and **II-129** following the procedure for Boc Bis(Netropsin) compounds (Chapter One). NMR data matched that for **I-219**; FAB MS, calcd. for $\text{C}_{41}\text{H}_{59}\text{N}_{12}\text{O}_{10}$ ($\text{M}+\text{H}^+$): 879.4477. Found: 879.4468.

P1-Succinamide-P3 (I-260) was prepared in 71% yield from **I-256** following the procedure for Bis(Netropsin) compounds (Chapter One). ^1H NMR δ 9.88 (s, 1H), 9.87 (s, 2H), 9.81 (s, 1H), 8.05 (m, 2H), 7.22 (s, 1H), 7.17 (s, 1H), 7.14 (d, 1H), 7.07 (d, 1H), 7.03 (d, 1H), 6.86 (d, 1H), 6.85 (s, 1H), 6.61 (d, 1H), 3.83 (s, 3H), 3.82 (s, 3H), 3.79 (s, 3H), 3.75 (s, 3H), 3.21 (m, 2H), 3.16 (m, 2H), 2.59 (t, 2H), 2.54 (s, 4H), 2.21 (t, 2H), 2.11 (s, 6H), 1.57 (m, 4H); FAB MS, calcd. for $\text{C}_{36}\text{H}_{51}\text{N}_{12}\text{O}_6$ ($\text{M}+\text{H}^+$): 747.4055. Found: 747.4074.

P1-(S,S)-Tartaramide-P3 (I-224) was prepared in 65% yield from **I-219** following the procedure for Bis(Netropsin) compounds (Chapter One). ^1H NMR δ 9.92 (s, 1H), 9.89 (s, 1H), 9.65 (s, 1H), 9.60 (s, 1H), 8.08 (m, 2H), 7.24 (s, 2H), 7.19 (s, 1H), 7.18 (s, 1H), 7.09 (s, 1H), 7.05 (s, 1H), 6.88 (s, 1H), 6.84 (s, 1H), 5.8 (br s, 2H), 4.44 (s, 2H), 3.85 (s, 6H), 3.81 (s, 3H), 3.79 (s, 3H), 3.2 (m, 4H), 2.65 (t, 2H), 2.24 (t, 2H),

2.14 (s, 6H), 1.61 (m, 4H); FAB MS, calcd. for $C_{36}H_{51}N_{12}O_8$ ($M+H^+$): 779.3953. Found: 779.3940.

P1-(R,R)-Tartaramide-P3 (I-220) was prepared in 77% yield from **I-216** following the procedure for Bis(Netropsin) compounds. NMR data matched that for **I-224**; FAB MS, calcd. for $C_{36}H_{51}N_{12}O_8$ ($M+H^+$): 779.3953. Found: 779.3928.

P1-Succinamide-P3-EDTA, Triethyl ester (I-262) was prepared in 81% yield from **I-260** and **EDTA(OEt)₃** following the procedure for Bis(Netropsin)-EDTA Triester compounds (Chapter One); 1H NMR δ 9.88 (s, 2H), 9.87 (s, 1H), 9.81 (s, 1H), 8.04 (t, 1H), 8.02 (t, 1H), 7.98 (t, 1H), 7.22 (d, 1H), 7.17 (d, 1H), 7.14 (d, 1H), 7.07 (d, 1H), 7.02 (d, 1H), 6.86 (d, 1H), 6.85 (d, 1H), 6.61 (d, 1H), 4.06 (m, 6H), 3.83 (s, 3H), 3.82 (s, 3H), 3.79 (s, 3H), 3.75 (s, 3H), 3.60-3.46 (series of singlets, 8 H), 3.15 (m, 6H), 2.71 (m, 4H), 2.54 (s, 4H), 2.22 (t, 2H), 2.11 (s, 6H), 1.58 (m, 4H), 1.16 (m, 9H); FAB MS, calcd. for $C_{52}H_{77}N_{14}O_{13}$ ($M+H^+$): 1105.5795. Found: 1105.5752.

P1-(S,S)-Tartaramide-P3-EDTA, Triethyl ester (I-238) was prepared in 50% yield from **I-224** and **EDTA(OEt)₃** following the procedure for Bis(Netropsin)-EDTA Triester compounds (Chapter One). 1H NMR δ 9.94 (s, 1H), 9.92 (s, 1H), 9.67 (s, 1H), 9.62 (s, 1H), 8.06 (m, 2H), 8.00 (t, 1H), 7.25 (s, 2H), 7.19 (s, 2H), 7.10 (s, 1H), 7.05 (s, 1H), 6.87 (s, 1H), 6.84 (s, 1H), 5.84 (br s, 2H), 4.45 (s, 1H), 4.43 (s, 1H), 4.06 (m, 6H), 3.85 (s, 6H), 3.80 (s, 3H), 3.79 (s, 3H), 3.61-3.48 (series of singlets, 8H), 3.17 (m, 6H), 2.72 (m, 4H), 2.24 (t, 2H), 2.14 (s, 6H), 1.61 (m, 4H), 1.17 (m, 9H); FAB MS, calcd. for $C_{52}H_{76}N_{14}O_{15}Li$ ($M+Li^+$): 1143.5777. Found: 1143.5742.

P1-(R,R)-Tartaramide-P3-EDTA, Triethyl ester (I-236) was prepared in 52% yield from **I-220** and **EDTA(OEt)₃** following the procedure for Bis(Netropsin)-EDTA

Triester compounds (Chapter One). NMR data matched that for **I-238**; FAB MS, calcd. for C₅₂H₇₇N₁₄O₁₅ (M+H⁺): 1137.5693. Found: 1137.5662.

P1-Succinamide-P3-EDTA (P1-S-P3-E, I-264) was prepared in 85% yield from **I-262** using the procedure for Bis(Netropsin)-EDTA compounds (Chapter One). ¹H NMR (Me₂SO-d₆ + TFA) δ 9.90 (s, 3H), 9.86 (s, 1H), 8.40 (t, 1H), 8.15 (t, 1H), 8.02 (t, 1H), 7.23 (s, 1H), 7.17 (s, 1H), 7.16 (s, 1H), 7.11 (d, 1H), 7.07 (s, 1H), 6.92 (s, 1H), 6.89 (d, 1H), 6.73 (d, 1H), 4.08 (s, 2H), 3.94 (s, 2H), 3.86 (s, 3H), 3.84 (s, 3H), 3.82 (s, 3H), 3.80 (s, 3H), 3.76 (s, 4H), 3.32 (m, 2H), 3.25-3.18 (m, 8H), 3.07 (m, 2H), 2.79 (d, 6H), 2.57 (s, 4H), 1.84 (m, 2H), 1.68 (m, 2H); FAB MS, calcd. for C₄₆H₆₅N₁₄O₁₃M+H⁺): 1021.4856. Found: 1021.4820; UV (H₂O) λ_{max} 296, 237 nm.

P1-(S,S)-Tartaramide-P3-EDTA (P1-(S,S)-Tar-P3-E, I-239) was prepared in 74% yield from **I-238** using the procedure for Bis(Netropsin)-EDTA compounds (Chapter One). ¹H NMR (Me₂SO-d₆ + TFA) δ 9.91 (s, 1H), 9.88 (s, 1H), 9.64 (s, 1H), 9.60 (s, 1H), 8.39 (t, 1H), 8.14 (br s, 1H), 8.00 (br s, 1H), 7.23 (d, 1H), 7.21 (s, 1H), 7.18 (d, 1H), 7.15 (s, 1H), 7.10 (s, 1H), 7.07 (s, 1H), 6.94 (d, 1H), 6.92 (s, 1H), 4.44 (s, 2H), 4.09 (s, 2H), 3.94 (s, 2H), 3.84 (s, 6H), 3.80 (s, 6H), 3.36 (br s, 2H), 3.22 (m, 8H), 3.06 (m, 2H), 2.78 (d, 6H), 1.83 (m, 2H), 1.66 (m, 2H); FAB MS, calcd. for C₄₆H₆₄N₁₄O₁₅K (M+K⁺): 1091.4313. Found: 1091.4242. UV (H₂O) λ_{max} 296, 237 nm; [α]_D²⁴ -31.1° (c=0.305, 10% NH₄OH/EtOH).

P1-(R,R)-Tartaramide-P3-EDTA (P1-(R,R)-Tar-P3-E, I-237) was prepared in 63% yield from **I-236** using the procedure for Bis(Netropsin)-EDTA compounds (Chapter One). Spectral data matched that for **I-239**; FAB MS, calcd. for C₄₆H₆₅N₁₄O₁₅ (M+H⁺): 1053.4754. Found: 1053.4710; [α]_D²⁴ +32.9° (c=0.347, 10% NH₄OH/EtOH).

Chapter Three

3,6,9,12,15-Pentaoxaheptadecanedioic acid, Diethyl ester (II-115). Ethyl diazoacetate (Aldrich, 1.95 mL, 25 mmol) was added over 8 h via syringe pump to a mixture of tetraethylene glycol (Aldrich, 1.94 g, 10 mmol) and dirhodium tetraacetate ($\text{Rh}_2(\text{OAc})_4$, Aldrich, 50 mg) in 20 mL Et_2O . The resulting mixture was allowed to stir overnight at RT, and then concentrated. The residue was chromatographed on silica gel using EtOAc eluent to afford **II-115** (2.34 g, 6.4 mmol, 64%) as an oil. ^1H NMR δ 4.17 (q, 4H), 4.14 (s, 4H), 3.71 (s, 8H), 3.67 (s, 8H), 1.30 (t, 6H). A larger scale reaction (**IV-124**) was carried out with 100 mmol of tetraethylene glycol, 250 mmol of ethyl diazoacetate, and 200 mg of $\text{Rh}_2(\text{OAc})_4$ in 100 mL Et_2O . The product was purified by bulb-to-bulb distillation. Initial distillation at 150-200°C (0.5 mm Hg) removed diethyl maleate and diethyl fumarate impurities. Distillation at 200-250°C afforded the diester (29.6 g, 81 mmol, 81%).

3,6,9,12-Tetraoxatetradecanedioic acid, Diethyl ester (II-155) was synthesized in 76% yield from triethylene glycol (Aldrich) and ethyl diazoacetate using the procedure for **II-115**. ^1H NMR δ 4.10 (q, 4H), 4.03 (s, 4H), 3.61 (s, 8H), 3.53 (s, 4H), 1.17 (t, 6H).

3,6,9,12,15,18-Hexaoxaeicosanedioic acid, Diethyl ester (II-114) was synthesized in 66% yield from pentaethylene glycol (Aldrich) and ethyl diazoacetate using the procedure for **II-115**. ^1H NMR δ 4.17 (q, 4H), 4.13 (s, 4H), 3.72 (s, 8H), 3.67 (s, 12H), 1.30 (t, 6H).

3,6,9,12,15-Pentaoxaheptadecanedioic acid, mono Ethyl ester (II-117). **II-115** (2.36 g, 6.4 mmol) was dissolved in 8 mL 1:1 $\text{H}_2\text{O:EtOH}$ and treated dropwise with a

solution of LiOH (0.17 g, 7.0 mmol). The reaction mixture was stirred 2 h at RT, then concentrated. Unreacted diester was extracted from the solid residue with 2 X 30 mL Et₂O. The remaining residue was dissolved in 1 mL H₂O, acidified using concentrated HCl, concentrated, and flash chromatographed on a short column of silica gel using 50% EtOH/EtOAc eluent to afford **II-117** (0.62 g, 1.87 mmol, 29%) as a sticky solid. ¹H NMR δ 7.85 (br s, 1H), 4.12 (q, 2H), 4.10 (s, 4H), 3.67, 3.70 (2s, 16H), 1.2 (t, 3H).

3,6,9,12-Tetraoxatetradecanedioic acid, mono Ethyl ester (II-156), 45% from **II-155** using the procedure for **II-117**. ¹H NMR δ 9.13 (br s, 1H), 4.07 (q, 2H), 4.00 (s, 2H), 3.97 (s, 2H), 3.58 (s, 8H), 3.52 (s, 4H), 1.12 (t, 3H).

3,6,9,12,15,18-Hexaoxaeicosanedioic acid, mono Ethyl ester (II-123), 28% from **II-122** using the procedure for **II-117**. ¹H NMR δ 4.12 (q, 2H), 4.10 (s, 2H), 4.00 (br s, 2H), 3.62 (s, 8H), 3.60 (s, 12H), 1.26 (t, 3H).

Netropsin-3,6,9,12,15-Pentaoxaheptadecanamic acid, Ethyl ester (II-118). **I-22** (0.41 g, 1.1 mmol) was hydrogenated at RT and 1 atm using 75 mg 5% Pd/C in 10 mL DMF. This mixture was filtered through a glass frit and added to a solution of activated **II-117**, prepared by stirring **II-117** (0.34 g, 1.0 mmol) with HOBT (0.27 g, 2.0 mmol) and DCC (0.41 g, 2.0 mmol) in 2 mL DMF for 1 h at RT. The resulting mixture was stirred overnight at RT, filtered, the solvent distilled *in vacuo*, and the residue triturated with Et₂O. Chromatography using 1-3%NH₄OH/MeOH eluent afforded **II-118** (0.46 g, 0.69 mmol, 69%). ¹H NMR δ 9.87 (s, 1H), 9.62 (s, 1H), 8.07 (t, 1H), 7.18 (s, 2H), 6.98 (d, 1H), 6.81 (d, 1H), 4.11 (q, 2H), 4.10 (s, 2H), 4.03 (s, 2H), 3.83 (s, 3H), 3.79 (s, 3H), 3.63-3.50 (m, 16H), 3.18 (m, 2H), 2.24 (t, 2H), 2.14 (s, 6H), 1.60 (m, 2H), 1.19 (t, 3H); FAB MS, calcd. for C₃₂H₅₁N₆O₁₀ (M+H⁺): 667.3667. Found: 667.3642.

Netropsin-3,6,9,12-Tetraoxatetradecanamic acid, Ethyl ester (II-157), 80% from **II-156** and **I-22** using the procedure for **II-118**. ^1H NMR δ 9.87 (s, 1H), 9.62 (s, 1H), 8.07 (t, 1H), 7.18 (s, 2H), 6.98 (d, 1H), 6.82 (d, 1H), 4.11 (q, 2H), 4.10 (s, 2H), 4.03 (s, 2H), 3.83 (s, 3H), 3.79 (s, 3H), 3.63-3.51 (m, 12H), 3.18 (m, 2H), 2.30 (t, 2H), 2.18 (s, 6H), 1.62 (m, 2H), 1.18 (t, 3H); FAB MS, calcd. for $\text{C}_{29}\text{H}_{47}\text{N}_6\text{O}_9$ ($\text{M}+\text{H}^+$): 623.3404. Found: 623.3410.

Netropsin-3,6,9,12,15,18-Hexaoxaecicosanamic acid, Ethyl ester (II-124), 60% from **II-123** and **I-22** using the procedure for **II-118**. ^1H NMR δ 9.87 (s, 1H), 9.61 (s, 1H), 8.07 (t, 1H), 7.18 (s, 2H), 6.98 (d, 1H), 6.81 (d, 1H), 4.10 (q, 2H), 4.10 (s, 2H), 4.03 (s, 2H), 3.83 (s, 3H), 3.79 (s, 3H), 3.64-3.49 (m, 20H), 3.18 (m, 2H), 2.25 (t, 2H), 2.14 (s, 6H), 1.60 (m, 2H), 1.19 (t, 3H); FAB MS, calcd. for $\text{C}_{33}\text{H}_{55}\text{N}_6\text{O}_{11}$ ($\text{M}+\text{H}^+$): 711.3929. Found: 711.3932.

Netropsin-3,6,9,12,15-Pentaoxaheptadecanamic acid (II-121). **II-118** (0.44 g, 0.66 mmol) was dissolved in 6 mL 1:1 EtOH:H₂O. LiOH (18 mg, 0.75 mmol) was added and the mixture stirred 5 min at RT. The mixture was acidified to pH 2, and then lyophilized. Chromatography of the residue using 3% NH₄OH/MeOH eluent afforded **II-121** (0.30 g, 0.47 mmole, 71%). ^1H NMR δ 9.89 (s, 1H), 9.63 (s, 1H), 7.20 (s, 2H), 6.97 (s, 1H), 6.80 (s, 1H), 4.03 (s, 2H), 3.85 (s, 2H), 3.83 (s, 3H), 3.79 (s, 3H), 3.63-3.50 (m, 16H), 3.19 (m, 2H), 2.43 (t, 2H), 2.27 (s, 6H), 1.67 (m, 2H); FAB MS, calcd. for $\text{C}_{29}\text{H}_{47}\text{N}_6\text{O}_{10}$ ($\text{M}+\text{H}^+$): 639.3354. Found: 639.3331.

Netropsin-3,6,9,12-Tetraoxatetradecanamic acid (II-159), 90% from **II-157** using the procedure for **II-121**. ^1H NMR δ 9.92 (s, 1H), 9.62 (s, 1H), 8.14 (t, 1H), 7.21 (m, 2H), 6.97 (d, 1H), 6.83 (d, 1H), 4.03 (s, 2H), 3.84 (s, 2H), 3.82 (s, 3H), 3.79

(s, 3H), 3.61 (m, 4H), 3.55 (m, 8H), 3.20 (m, 2H), 2.50 (t, 2H), 2.32 (s, 6H), 1.69 (m, 2H); FAB MS, calcd. for $C_{27}H_{43}N_6O_9$ ($M+H^+$): 595.3092. Found: 595.3088.

Netropsin-3,6,9,12,15,18-Hexaoxaecosanamic acid (II-125), 89% from **II-124** using the procedure for **II-121**. 1H NMR δ 9.91 (s, 1H), 9.67 (s, 1H), 8.12 (t, 1H), 7.20 (s, 2H), 6.98 (d, 1H), 6.82 (d, 1H), 4.03 (s, 2H), 3.82 (s, 5H), 3.79 (s, 3H), 3.63-3.48 (m, 20H), 3.19 (m, 2H), 2.42 (t, 2H), 2.26 (s, 6H), 1.66 (m, 2H); FAB MS, calcd. for $C_{31}H_{51}N_6O_{11}$ ($M+H^+$): 683.3616. Found: 683.3606.

General Procedure for the Synthesis of Boc Bis(Netropsin) Polyether Compounds followed that for the synthesis of Boc Bis(Netropsin) Diacid compounds (Chapter One).

Boc Bis(Netropsin)-3,6,9,12-Tetraoxatetradecanediamide (II-161), 37% from **II-159** and **II-129**. 1H NMR δ 9.87 (s, 2H), 9.62 (s, 2H), 8.07 (t, 1H), 7.96 (t, 1H), 7.17 (s, 4H), 6.97 (s, 2H), 6.84 (s, 1H), 6.83 (s, 1H), 6.79 (t, 1H), 4.02 (s, 4H), 3.82 (s, 6H), 3.79 (s, 6H), 3.62 (d, 8H), 3.59 (s, 4H), 3.16 (m, 4H), 2.94 (m, 2H), 2.37 (br s, 2H), 2.24 (s, 6H), 1.62 (m, 2H), 1.56 (m, 2H), 1.37 (s, 9H); FAB MS, calcd. for $C_{47}H_{71}N_{12}O_{13}$ ($M+H^+$): 995.5310. Found: 995.5364.

Boc Bis(Netropsin)-3,6,9,12,15-Pentaoxaheptadecanediamide (II-126), 68% from **II-121** and **II-129**. 1H NMR δ 9.87 (s, 1H), 9.86 (s, 1H), 9.61 (s, 2H), 8.06 (t, 1H), 7.96 (t, 1H), 7.17 (s, 4H), 6.97 (s, 2H), 6.84 (s, 1H), 6.81 (s, 1H), 6.80 (t, 1H), 4.02 (s, 4H), 3.82 (s, 6H), 3.79 (s, 6H), 3.60 (m, 8H), 3.54 (m, 8H), 3.17 (m, 4H), 2.95 (m, 2H), 2.24 (t, 2H), 2.13 (s, 6H), 1.60 (m, 2H), 1.58 (m, 2H), 1.38 (s, 9H); FAB MS, calcd. for $C_{49}H_{75}N_{12}O_{13}$ ($M+H^+$): 1039.5577. Found: 1039.5607.

Boc Bis(Netropsin)-3,6,9,12,15,18-Hexaoxaeicosanediamide (II-131), 54% from II-125 and II-129. ^1H NMR δ 9.87 (s, 1H), 9.86 (s, 1H), 9.60 (s, 2H), 8.06 (t, 1H), 7.96 (t, 1H), 7.18 (s, 2H), 7.17 (s, 2H), 6.97 (2s, 2H), 6.84 (d, 1H), 6.81 (d, 1H), 6.79 (t, 1H), 4.02 (s, 4H), 3.82 (s, 6H), 3.80 (s, 6H), 3.61 (m, 8H), 3.54 (m, 8H), 3.50 (s, 4H), 3.17 (m, 4H), 2.95 (m, 2H), 2.26 (t, 2H), 2.15 (s, 6H), 1.61 (m, 4H), 1.38 (s, 9H); FAB MS, calcd. for $\text{C}_{51}\text{H}_{79}\text{N}_{12}\text{O}_{14}$ ($\text{M}+\text{H}^+$): 1083.5839. Found: 1083.5852.

General Procedure for the Synthesis of Bis(Netropsin) Polyether Compounds followed that for the synthesis of Bis(Netropsin) compounds (Chapter One).

Bis(Netropsin)-3,6,9,12-Tetraoxatetradecanediamide (II-162), 94% from II-162. ^1H NMR δ 9.87 (s, 1H), 9.63 (s, 1H), 8.07 (m, 2H), 7.17 (s, 4H), 6.97 (s, 2H), 6.85 (s, 1H), 6.81 (s, 1H), 4.03 (s, 4H), 3.82 (s, 6H), 3.79 (s, 6H), 3.62 (m, 8H), 3.59 (s, 4H), 3.22 (m, 2H), 3.17 (m, 2H), 2.61 (t, 2H), 2.23 (t, 2H), 2.13 (s, 6H), 1.59 (m, 4H); FAB MS, calcd. for $\text{C}_{42}\text{H}_{63}\text{N}_{12}\text{O}_{10}$ ($\text{M}+\text{H}$): 895.4790. Found: 895.4751.

Bis(Netropsin)-3,6,9,12,15-Pentaoxaheptadecanediamide (II-127), 93% from II-126. ^1H NMR δ 9.86 (s, 2H), 9.62 (s, 1H), 9.61 (s, 1H), 8.12 (t, 1H), 8.06 (t, 1H), 7.17 (s, 4H), 6.97 (s, 2H), 6.86 (s, 1H), 6.81 (s, 1H), 4.02 (s, 4H), 3.82 (s, 6H), 3.79 (s, 6H), 3.60 (m, 8H), 3.54 (s, 8H), 3.23 (m, 2H), 3.17 (m, 2H), 2.65 (t, 2H), 2.23 (t, 2H), 2.13 (t, 2H), 1.61 (m, 2H), 1.60 (m, 2H); FAB MS, calcd. for $\text{C}_{44}\text{H}_{67}\text{N}_{12}\text{O}_{11}$ ($\text{M}+\text{H}^+$): 939.5052. Found: 939.5024.

Bis(Netropsin)-3,6,9,12,15,18-Hexaoxaeicosanediamide (II-132), 69% from II-131. ^1H NMR δ 9.86 (s, 2H), 9.60 (s, 2H), 8.06 (t, 2H), 7.17 (s, 4H), 6.97 (s, 2H), 6.83 (s, 1H), 6.81 (s, 1H), 4.02 (s, 4H), 3.82 (s, 6H), 3.79 (s, 6H), 3.61 (m, 8H), 3.53

(m, 8H), 3.50 (s, 4H), 3.21 (m, 2H), 3.17 (m, 2H), 2.58 (t, 2H), 2.23 (t, 2H), 2.13 (s, 6H), 1.60 (m, 2H), 1.55 (m, 2H); FAB MS, calcd. for $C_{46}H_{71}N_{12}O_{12}$ ($M+H^+$): 983.5314. Found: 983.5355.

General Procedure for the Synthesis of Bis(Netropsin) Polyether-EDTA Triethyl Ester Compounds followed that for the synthesis of Bis(Netropsin)-EDTA, Triethyl ester compounds (Chapter One).

Bis(Netropsin)-3,6,9,12-Tetraoxatetradecanediamide-EDTA, Triethyl ester (II-163), 46% from **II-162** and **EDTA(OEt)₃**. 1H NMR δ 9.88 (s, 1H), 9.87 (s, 1H), 9.63 (s, 2H), 8.05 (m, 2H), 7.99 (t, 1H), 7.17 (s, 4H), 6.97 (s, 2H), 6.85 (d, 1H), 4.05 (m, 6H), 4.02 (s, 4H), 3.82 (s, 6H), 3.79 (s, 6H), 3.62-3.47 (m, 20H), 3.18 (m, 6H), 2.73 (m, 4H), 2.23 (t, 2H), 2.13 (s, 6H), 1.60 (m, 4H), 1.17 (m, 9H); FAB MS, calcd. for $C_{58}H_{88}N_{14}O_{17}$ ($M+Li^+$): 1259.6614. Found: 1259.6650.

Bis(Netropsin)-3,6,9,12,15-Pentaoxaheptadecanediamide-EDTA, Triethyl ester (II-135), 79% from **II-127** and **EDTA(OEt)₃**. 1H NMR δ 9.88 (s, 1H), 9.86 (s, 1H), 9.61 (s, 2H), 8.04 (m, 2H), 7.99 (t, 1H), 7.18 (2s, 4H), 6.97 (s, 2H), 6.85 (d, 1H), 6.81 (d, 1H), 4.06 (m, 6H), 4.02 (s, 4H), 3.82 (s, 6H), 3.79 (2s, 6H), 3.63-3.47 (m, 24H), 3.17 (m, 6H), 2.72 (m, 4H), 2.23 (t, 2H), 2.13 (s, 6H), 1.60 (m, 4H), 1.17 (m, 9H); FAB MS, calcd. for $C_{60}H_{92}N_{14}O_{18}Li$ ($M+Li^+$): 1303.6876. Found: 1303.6892.

Bis(Netropsin)-3,6,9,12,15,18-Hexaoxaeicosanediamide-EDTA, Triethyl ester (II-140), 75% from **II-132** and **EDTA(OEt)₃**. 1H NMR δ 9.88 (s, 1H), 9.86 (s, 1H), 9.61 (s, 2H), 8.05 (m, 2H), 7.99 (t, 1H), 7.17 (s, 4H), 6.97 (s, 2H), 6.85 (d,

1H), 6.81 (d, 1H), 4.05 (m, 6H), 4.02 (s, 4H), 3.82 (s, 6H), 3.79 (s, 6H), 3.63-3.47 (m, 28H), 3.18 (m, 6H), 2.72 (m, 4H), 2.23 (t, 2H), 2.13 (s, 6H), 1.60 (m, 4H), 1.17 (m, 9H); FAB MS, calcd. for $C_{62}H_{96}N_{14}O_{19}Li$ ($M+H^+$): 1347.7136. Found: 1347.7068.

General Procedure for the Synthesis of Bis(Netropsin) Polyether-EDTA Compounds followed that for the synthesis of Bis(Netropsin)-EDTA compounds (Chapter One).

Bis(Netropsin)-3,6,9,12-Tetraoxatetradecanediamide-EDTA (BNO4E, II-164), 98% from **II-163**. 1H NMR (Me_2SO-d_6 + TFA) δ 9.95 (s, 1H), 9.93 (s, 1H), 9.67 (s, 2H), 8.48 (t, 1H), 8.23 (br s, 1H), 8.07 (br s, 1H), 7.22 (m, 4H), 7.07 (d, 2H), 7.00 (d, 1H), 6.97 (d, 1H), 4.17 (s, 2H), 4.09 (s, 4H), 4.03 (s, 2H), 4.02 (s, 2H), 3.92 (s, 2H), 3.89 (s, 6H), 3.87 (s, 3H), 3.86 (s, 3H), 3.69 (m, 8H), 3.66 (s, 4H), 3.48 (m, 2H), 3.38 (m, 2H), 3.27 (m, 6H), 3.14 (m, 2H), 2.85 (d, 6H), 1.91 (m, 2H), 1.73 (m, 2H); FAB MS, calcd. for $C_{52}H_{77}N_{14}O_{17}$ ($M+H^+$): 1169.5591. Found: 1169.5581; UV (H_2O) λ_{max} 299, 235 nm.

Bis(Netropsin)-3,6,9,12,15-Pentaoxaheptadecanediamide-EDTA (BNO5E, II-136), 100% from **II-135**. 1H NMR (Me_2SO-d_6 + TFA) δ 9.97 (s, 1H), 9.95 (s, 1H), 9.70 (s, 2H), 8.46 (t, 1H), 8.24 (t, 1H), 8.10 (t, 1H), 7.24 (m, 4H), 7.07 (m, 2H), 7.01 (d, 1H), 6.96 (d, 1H), 4.15 (s, 2H), 4.10 (s, 4H), 4.00 (s, 2H), 3.99 (s, 2H), 3.90 (s, 6H), 3.89 (s, 3H), 3.87 (s, 3H), 3.84 (s, 2H), 3.68 (m, 8H), 3.62 (s, 8H), 3.39 (m, 2H), 3.3 (m, 8H), 3.14 (m, 2H), 2.86 (d, 6H), 1.91 (m, 2H), 1.73 (m, 2H); FAB MS, calcd. for $C_{54}H_{81}N_{14}O_{18}$ ($M+H^+$): 1213.5853. Found: 1213.5806; UV (H_2O) λ_{max} 299, 235 nm.

Bis(Netropsin)-3,6,9,12,15,18-Hexaoxaecosanediamide-EDTA (BNO6E, II-143), 89% from **II-140**. ^1H NMR (Me₂SO-d₆ + TFA) δ 9.97 (s, 1H), 9.95 (s, 1H), 9.69 (s, 2H), 8.47 (t, 1H), 8.24 (br s, 1H), 8.09 (br s, 1H), 7.25 (s, 4H), 7.07 (s, 2H), 7.01 (s, 1H), 6.97 (s, 1H), 4.16 (s, 2H), 4.10 (s, 4H), 4.00 (s, 2H), 3.99 (s, 2H), 3.90 (s, 6H), 3.88 (s, 3H), 3.87 (s, 3H), 3.85 (s, 2H), 3.68 (m, 8H), 3.61 (m, 8H), 3.57 (s, 4H), 3.41 (m, 2H), 3.31 (m, 8H), 3.15 (m, 2H), 2.86 (d, 6H), 1.91 (m, 2H), 1.73 (m, 2H); FAB MS, calcd. for C₅₆H₈₅N₁₄O₁₉ (M+H⁺): 1257.6115. Found: 1257.6085; UV (H₂O) λ_{max} 299, 236 nm.

Bis(Dimethylaminopropane)-3,6,9,12,15-Pentaoxaheptadecanediamide (II-238). **IV-124** (0.41 g, 1.0 mmol) was treated with 3-dimethylaminopropylamine (1.3 mL, 10 mmol) and heated overnight at 60°C. The mixture was then evaporated *in vacuo*, treated with 5 mL DMF, and evaporated again. Chromatography on silica gel using 5% NH₄OH/MeOH eluent afforded 0.40 g (0.77 mmol, 77%) of **II-238** as an oil. ^1H NMR δ 7.40 (br s, 2H), 3.80 (s, 4H), 3.50 (s, 16H), 3.20 (q, 4H), 2.20 (t, 4H), 2.07 (s, 12 H), 1.52 (quintet, 4H).

Dimethylaminopropane-3,6,9,12,15-Pentaoxaheptadecanamic acid (IV-145). **IV-124** (1.83 g, 5.0 mmol) was treated with 3-dimethylaminopropylamine (0.63 mL, 5.0 mmol). The mixture was stirred at 80°C until tlc indicated complete loss of amine starting material. The mixture was diluted with 10 mL 1:1 MeOH:H₂O, and treated with LiOH (0.24 g, 10 mmol). After stirring overnight at RT, the solvent was removed under reduced pressure and the residue chromatographed on silica gel using 2% NH₄OH/MeOH eluent to afford 1.57 g, 3.6 mmol, 72% of **IV-145** as an oil. ^1H NMR δ 7.84 (t, 1H), 3.85 (s, 2H), 3.71 (s, 2H), 3.53 (m, 16H), 3.12 (m, 2H), 2.33 (t, 2H), 2.20 (s, 6H), 1.59 (m, 2H).

Dimethylaminopropane-3,6,9,12,15-Pentaoxaheptadecanediamide-

Netropsin (IV-149). **II-129** (225 mg, 0.50 mmol) was hydrogenated at RT and 3 atm using 75 mg 5% Pd/C in 8 mL DMF. The mixture was filtered through a glass frit and added to a solution of activated **IV-145**, prepared by stirring **IV-145** (240 mg, 0.60 mmol) with HOBT (210 mg, 1.5 mmol) and DCC (150 mg, 0.7 mmol) in 3 mL DMF for 1 h at RT. After stirring overnight, the mixture was filtered, the solvent distilled *in vacuo*, and the residue chromatographed on silica gel using 1% NH₄OH/MeOH eluent to afford **Boc Dimethylaminopropane-3,6,9,12,15-Pentaoxaheptadecanediamide-Netropsin (IV-147)** as an oil that was not characterized. This material was dissolved in 1.5 mL CH₂Cl₂ and treated with 2 mL TFA. After stirring 15 min at RT, the reaction mixture was concentrated. The residue was treated with 10 mL 5% NH₄OH/MeOH and concentrated again. Chromatography on silica gel using 10% NH₄OH/MeOH eluent afforded **IV-149** (42 mg, 12% from **II-129**) as a gum. ¹H NMR δ 9.86 (s, 1H), 9.61 (s, 1H), 8.05 (t, 1H), 7.78 (t, 1H), 7.18 (2s, 2H), 6.98 (s, 1H), 6.83 (s, 1H), 4.03 (s, 2H), 3.84 (s, 2H), 3.83 (s, 3H), 3.79 (s, 3H), 3.62 (m, 4H), 3.54 (m, 12H), 3.22 (m, 2H), 3.12 (m, 2H), 2.57 (m, 2H), 2.18 (m, 2H), 2.09 (s, 6H), 1.53 (m, 4H).

Nitro Boc Penta(*N*-methylpyrrolecarboxamide)-3-Aminopropane (IV-152) was prepared from **Penta(*N*-methylpyrrolecarboxamide) Nitro Acid¹** and **IV-161** following the procedure for **II-129**. ¹H NMR δ 10.29 (s, 1H), 9.99 (s, 1H), 9.95 (s, 1H), 9.89 (s, 1H), 8.20 (d, 1H), 7.96 (t, 1H), 7.60 (d, 1H), 7.28 (d, 1H), 7.26 (d, 1H), 7.25 (d, 1H), 7.18 (d, 1H), 7.07 (d, 1H), 7.06 (m, 2H), 6.86 (d, 1H), 6.79 (t, 1H), 3.97 (s, 3H), 3.88 (s, 3H), 3.87 (s, 3H), 3.85 (s, 3H), 3.80 (s, 3H), 3.17 (m, 2H), 2.97 (m, 2H), 1.58 (m, 2H), 1.38 (s, 9H).

Dimethylaminopropane-3,6,9,12,15-Pentaoxaheptadecanediamide-Penta(*N*-methylpyrrolecarboxamide) (IV-163) was prepared as a solid in 14% overall yield

from **IV-152** and **IV-145** following the procedure for **IV-149**. ^1H NMR δ 9.96 (s, 2H), 9.94 (s, 1H), 9.90 (s, 1H), 9.63 (s, 1H), 8.07 (t, 1H), 7.78 (t, 1H), 7.25 (s, 3H), 7.19 (s, 2H), 7.07 (s, 2H), 7.06 (s, 1H), 7.01 (s, 1H), 6.85 (s, 1H), 4.04 (s, 2H), 3.86 (s, 6H), 3.84 (s, 9H), 3.80 (s, 2H), 3.62 (m, 4H), 3.55 (s, 12H), 3.22 (m, 2H), 3.11 (m, 2H), 2.59 (t, 2H), 2.18 (t, 2H), 2.09 (s, 6H), 1.53 (m, 4H).

Dimethylaminopropane-3,6,9,12,15-Pentaoxaheptadecanediamide-

Netropsin-EDTA, Triethyl ester (IV-157). EDTA(OEt)_3 (188 mg, 0.50 mmole) was activated by stirring with HOBT (135 mg, 1.0 mmole) and DCC (130 mg, 0.60 mmole) in 1 mL DMF under argon. This mixture was added to a solution of **IV-149** (140 mg, 0.20 mmole) in 1 mL DMF, and the reaction stirred overnight at RT. The mixture was filtered, the solvent distilled *in vacuo*, and the residue chromatographed on silica gel using 1% $\text{NH}_4\text{OH}/\text{MeOH}$ eluent to afford **IV-157** (166 mg, 0.16 mmole, 80%) as a gum. ^1H NMR δ 9.87 (s, 1H), 9.59 (s, 1H), 8.02 (t, 1H), 7.98 (t, 1H), 7.76 (t, 1H), 7.18 (s, 1H), 6.97 (d, 1H), 6.84 (d, 1H), 4.05 (m, 8H), 3.84 (s, 3H), 3.79 (s, 3H), 3.64-3.47 (m, 24H), 3.13 (m, 6H), 2.72 (m, 4H), 2.18 (t, 2H), 2.09 (s, 6H), 1.60 (m, 2H), 1.53 (m, 2H), 1.17 (m, 9H).

Dimethylaminopropane-3,6,9,12,15-Pentaoxaheptadecanediamide-Penta(*N*-methylpyrrolecarboxamide)-EDTA, Triethyl ester (IV-166) was prepared as a solid in 70% yield from **IV-163** and EDTA(OEt)_3 following the procedure for **IV-157**. ^1H NMR δ 9.95 (s, 2H), 9.93 (s, 1H), 9.90 (s, 1H), 9.62 (s, 1H), 8.03 (t, 1H), 7.99 (t, 1H), 7.78 (t, 1H), 7.24 (s, 3H), 7.19 (2s, 2H), 7.07 (m, 3H), 7.01 (d, 1H), 6.87 (d, 1H), 4.07 (m, 8H), 3.86 (s, 6H), 3.84 (s, 9H), 3.80 (s, 2H), 3.62 (m, 4H), 3.56-3.52 (m, 18H), 3.47 (s, 2H), 3.20 (m, 6H), 2.72 (m, 4H), 2.18 (t, 2H), 2.09 (s, 6H), 1.60 (m, 2H), 1.53 (m, 2H), 1.17 (m, 9H).

Dimethylaminopropane-3,6,9,12,15-Pentaoxaheptadecanediamide-

Netropsin-EDTA (O5NE, IV-159) was prepared as a solid in 100% yield from **II-157** following the general procedure for the synthesis of Bis(Netropsin)-EDTA compounds (Chapter One). ^1H NMR ($\text{Me}_2\text{SO-d}_6 + \text{TFA}$) δ 9.94 (s, 1H), 9.69 (s, 1H), 8.45 (t, 1H), 8.08 (t, 1H), 7.96 (t, 1H), 7.27 (s, 1H), 7.23 (s, 1H), 7.15 (s, 1H), 6.90 (s, 1H), 4.14 (s, 2H), 4.11 (s, 2H), 3.99 (s, 2H), 3.96 (s, 2H), 3.91 (s, 3H), 3.87 (s, 3H), 3.82 (s, 4H), 3.70 (m, 4H), 3.64 (br s, 8H), 3.61 (s, 4H), 3.38 (br s, 2H), 3.25 (m, 8H), 3.09 (m, 2H), 2.83 (d, 6H), 1.85 (m, 2H), 1.73 (m, 2H); UV (H_2O) λ_{max} 296, 235 nm; FAB MS, calcd. for $\text{C}_{42}\text{H}_{68}\text{N}_{10}\text{O}_{16}\text{K}$ ($\text{M}+\text{K}^+$): 1007.4452. Found: 1007.4374.

Dimethylaminopropane-3,6,9,12,15-Pentaoxaheptadecanediamide-Penta(*N*-methylpyrrolecarboxamide)-EDTA (O5P5E, IV-167) was prepared as a solid in 78% yield from **IV-166** following the general procedure for the synthesis of Bis(Netropsin)-EDTA compounds (Chapter One). ^1H NMR ($\text{Me}_2\text{SO-d}_6 + \text{TFA}$) δ 10.02 (s, 3H), 9.97 (s, 1H), 9.70 (s, 1H), 8.46 (t, 1H), 8.09 (br s, 1H), 7.96 (t, 1H), 7.31 (s, 3H), 7.26 (s, 1H), 7.24 (s, 1H), 7.18 (s, 1H), 7.16 (s, 2H), 7.09 (s, 1H), 6.99 (s, 1H), 4.16 (s, 2H), 4.12 (s, 2H), 4.01 (s, 2H), 3.96 (s, 2H), 3.94 (s, 6H), 3.88 (s, 9H), 3.85 (s, 4H), 3.70 (m, 4H), 3.64 (s, 8H), 3.61 (s, 4H), 3.41 (m, 2H), 3.25 (m, 8H), 3.08 (m, 2H), 2.83 (d, 6H), 1.85 (m, 2H), 1.74 (m, 2H); UV (H_2O) λ_{max} 306, 240 nm; FAB MS, calcd. for $\text{C}_{60}\text{H}_{87}\text{N}_{16}\text{O}_{19}$ ($\text{M}+\text{H}^+$): 1335.6458. Found: 1335.6369.

General Procedure for the Synthesis of Poly-(Z)-Aminodicarboxylic Acid Linker Compounds. Commercially available ethylenediamine, diethylenetriamine, triethylenetetraamine, or tetraethylpentammine (Aldrich, 20 mmol) was treated with $n+1$ molar equiv. of 1 M NaOH (where n =the number of amine groups in the starting material).

The solution was stirred at RT and treated with $n+1$ molar equiv. TsCl as a slurry in 100 mL CH_2Cl_2 . The resulting mixture was then stirred overnight at RT, filtered, and the white solid washed with H_2O . The wet product was then placed in a flask and digested with 2 X 100 mL boiling Et_2O , and then dried in air to afford the **Poly(p-toluenesulfonamide)** compound. A 0.3 M solution of this material in DMF was treated with 0.6(n) molar equiv. Cs_2CO_3 and the resulting mixture stirred 10 min at RT. 2.2 Molar equiv. *t*-butyl bromoacetate (Aldrich) were added dropwise in 10 mL DMF over 30 min.¹¹ The resulting mixture was stirred overnight at RT, filtered through a fine frit, and the solvent distilled *in vacuo*. The residue was dissolved in 200 mL CH_2Cl_2 , extracted with 3 X 50 mL H_2O , dried over Na_2SO_4 , filtered, and concentrated. The solid was redissolved in 100 mL CH_2Cl_2 , heated to boiling, treated with 100 mL EtOH, and the CH_2Cl_2 distilled off at 55°C. Upon cooling to RT, a white solid mass was deposited which was filtered, washed with EtOH, and dried in air to afford the **Poly(p-toluenesulfonamide)Di-*t*-butyl acetate** compound. This was deprotected in a two-step *in situ* procedure. In the first step, a 1 M solution of the diester in CH_2Cl_2 was treated with 2 volumes TFA and the resulting solution stirred 1 h at RT. The mixture was concentrated (first under reduced pressure and then *in vacuo*), treated with one volume of CHCl_3 , concentrated again, treated with one volume of MeOH, and concentrated again. The resulting crude **Poly(p-Toluenesulfonamide)Diacetic acid** compound was then dissolved in 250 mL MeOH (dried by distillation from $\text{Mg}(\text{OEt})_2$) and treated with 5(n) molar equiv. Na_2HPO_4 followed by 5(n) molar equiv. 6% Na/Hg amalgam.¹² The slurry was then refluxed for 24 h, filtered through paper while still hot, and the residue washed with 2 X 10 mL MeOH. The filtrate was slurried in MeOH and chromatographed on silica gel using MeOH followed by 20% $\text{NH}_4\text{OH}/\text{MeOH}$ eluents to afford the α,ω -**Polyaminodicarboxylic acid**. A 0.3 M solution of the sticky amino acid in H_2O was treated with 2.5(n) molar equiv. NaHCO_3 and then, with vigorous stirring, 1.2(n) molar equiv. benzyloxycarbonyl chloride (BzCl, Aldrich) were added portionwise over 30 min.

The resulting mixture was stirred overnight at RT, diluted with additional H₂O, and extracted with 2 X 40 mL Et₂O. The aqueous layer was then treated with 60 mL EtOAc, cooled in an ice bath, and, with vigorous stirring, acidified to pH 1 using concentrated H₂SO₄. The mixture was poured into a separatory funnel, the layers separated, and the aqueous layer extracted with 50 mL additonal EtOAc. The organic extracts were combined, washed with 2 X 50 mL H₂O, dried over Na₂SO₄, filtered, and concentrated to afford the **Poly-(Z)-aminodicarboxylic acid**.

Diethylenetri(p-Toluenesulfonamide) (IV-17), 83% from diethylenetriamine and TsCl. ¹H NMR δ 7.65 (m, 6H), 7.54 (d, 2H), 7.40 (m, 6H), 3.01 (t, 4H), 2.80 (t, 4H), 2.39 (s, 6H), 2.38 (s, 3H).

Triethylenetetra(p-Toluenesulfonamide) (IV-16), 83% from triethylenetetraamine and TsCl. ¹H NMR δ 7.70 (t, 2H), 7.66 (d, 4H), 7.61 (d, 4H), 7.39 (t, 8H), 3.11 (s, 4H), 3.06 (t, 4H), 2.82 (q, 4H), 2.40 (s, 6H), 2.37 (s, 6H).

Tetraethylenepenta(p-Toluenesulfonamide) (III-299), 68% from tetraethylenepentaamine and TsCl. ¹H NMR δ 7.66 (m, 12H), 7.38 (m, 10H), 3.14 (s, 8H), 3.09 (t, 4H), 2.84 (q, 4H), 2.42 (s, 3H), 2.39 (s, 6H), 2.37 (s, 6H).

Diethylenetri(p-Toluenesulfonamide)-Di-*t*-Butyl Acetate (IV-22), 79% from IV-17 and *t*-butyl bromoacetate. ¹H NMR δ 7.66 (t, 6H), 7.44 (d, 2H), 7.39 (d, 4H), 3.97 (s, 4H), 3.25 (m, 8H), 2.41 (s, 3H), 2.39 (s, 6H), 1.30 (s, 18H).

Triethylenetetra(p-Toluenesulfonamide)-Di-*t*-Butyl Acetate (IV-21), 73% from IV-16 and *t*-butyl bromoacetate. ¹H NMR δ 7.67 (d, 8H), 7.44 (d, 4H), 7.38 (d, 4H),

3.97 (s, 4H), 3.29 (m, 4H), 3.23 (m, 4H), 3.19 (s, 4H), 2.41 (s, 6H), 2.38 (s, 6H), 1.28 (s, 18H).

Teraethylenepenta(p-Toluenesulfonamide)-Di-*t*-Butyl Acetate (III-300), 35% from **III-299** and *t*-butyl bromoacetate. ^1H NMR δ 7.67 (m, 10H), 7.43 (m, 6H), 7.37 (m, 4H), 3.97 (s, 4H), 3.23 (m, 16H), 2.41 (s, 3H), 2.40 (s, 6H), 2.37 (s, 6H), 1.26 (s, 18H).

3,6,9-Triaminoundecanedicarboxylic acid (IV-23), 46% overall from **IV-22**. ^1H NMR ($\text{Me}_2\text{SO-d}_6$ + TFA) δ 3.97 (s, 4H), 3.33 (br s, 8H).

3,6,9,12-Tetraaminotetradecanedicarboxylic acid (IV-26), 27% overall from **IV-21**. ^1H NMR ($\text{Me}_2\text{SO-d}_6$ + TFA) δ 3.98 (s, 4H), 3.33 (br s, 12H).

3,6,9,12,15-Pentaaminoheptadecanedicarboxylic acid (IV-29), 77% overall from **III-300**. ^1H NMR ($\text{Me}_2\text{SO-d}_6$ + TFA) δ 3.97 (s, 4H), 3.33 (br s, 16H).

3,6-Di-(Z)-Aminooctanedicarboxylic acid (N2 Synthon, III-296), 82% from commercially available ethylene diamine-*N,N'*-diacetic acid (Aldrich) and benzyloxycarbonyl chloride. ^1H NMR δ 7.3 (s, 10H), 5.10 (br s, 4H), 4.00 (s, 2H), 3.90 (s, 2H), 3.45 (s, 4H).

3,6,9-Tri-(Z)-Aminoundecanedicarboxylic acid (N3 Synthon, IV-25), 74 % from **IV-23** and benzyloxycarbonyl chloride. ^1H NMR δ 7.30 (s, 15H), 5.02 (s, 6H), 3.87 (br s, 4H), 3.32 (s, 8H).

3,6,9,12-Tetra-(Z)-Aminotetradecanedicarboxylic acid (N4 Synthon, IV-33), 62% from **IV-26** and benzyloxycarbonyl chloride. ^1H NMR δ 7.28 (s, 20H), 5.02 (br s, 8H), 3.89 (br s, 4H), 3.32 (s, 12H).

3,6,9,12,15-Penta-(Z)-Aminoheptadecanedicarboxylic acid (N5 Synthon, IV-34), 29% from **IV-29** and benzyloxycarbonyl chloride. ^1H NMR δ 7.28 (s, 25H), 5.00 (br s, 10H), 3.88 (br s, 4H), 3.35 (br s, 16H).

General Procedure for the Synthesis of Netropsin Poly-(Z)-Amino Alkanamic Acid Compounds followed that for the synthesis of Netropsin Alkanamic acid compounds (Chapter One).

Netropsin-3,6-Di-(Z)-Aminooctanamic acid (IV-24), 71% from **I-22** and **III-296**. ^1H NMR δ 9.95 (2s, 2H), 9.87 (s, 1H), 8.09 (t, 1H), 7.30 (m, 10H), 7.18 (s, 1H), 7.14 (d, 1H), 6.92 (d, 1H), 6.83 (s, 1H), 5.03 (m, 4H), 4.01 (m, 2H), 3.90 (m, 2H), 3.83,3.82 (2s, 3H), 3.79 (s, 3H), 3.45 (br s, 4H), 3.19 (m, 2H), 2.42 (t, 2H), 2.26 (s, 6H), 1.66 (m, 2H).

Netropsin-3,6,9-Tri-(Z)-Aminoundecanamic acid (IV-39), 69% from **I-22** and **IV-25**. ^1H NMR δ 10.01 (br s, 1H), 9.89, 9.86 (2s, 1H), 8.09 (m, 1H), 7.29 (m, 15H), 7.19 (s, 1H), 7.14 (d, 1H), 6.94 (m, 1H), 6.84 (s, 1H), 5.02 (m, 6H), 4.01 (m, 2H), 3.90 (m, 2H), 3.83 (2s, 3H), 3.79 (s, 3H), 3.40 (br s, 8H), 3.19 (m, 2H), 2.44 (br s, 2H), 2.28 (d, 6H), 1.66 (m, 2H).

Netropsin-3,6,9,12-Tetra-(Z)-Aminotetradecanamic acid (IV-42), 40% from **I-22** and **IV-33**. ^1H NMR δ 10.11 (br s, 1H), 8.85 (m, 1H), 8.14 (m, 1H), 7.27 (br s, 20H), 7.06 (m, 3H), 6.80 (m, 1H), 5.00 (m, 8H), 4.01 (m, 2H), 3.83 (2s, 3H), 3.79 (s,

3H), 3.76 (m, 2H), 3.36 (m, 12H), 3.20 (m, 2H), 2.58 (d, 2H), 2.37 (m, 6H), 1.72 (m, 2H).

Netropsin-3,6,9,12,15-Penta-(Z)-Aminoheptadecanamic acid (IV-43), 37% from I-22 and IV-34. ^1H NMR δ 10.03 (br s, 1H), 9.86 (d, 1H), 8.10 (m, 1H), 7.28 (m, 25H), 7.12 (s, 1H), 6.98 (m, 2H), 6.82 (br s, 1H), 5.02 (m, 10H), 3.98 (m, 2H), 3.89 (m, 2H), 3.81 (2s, 3H), 3.79 (s, 3H), 3.33 (br s, 16H), 3.19 (m, 2H), 2.50 (m, 2H), 2.32 (br s, 6H), 1.68 (m, 2H).

General Procedure for the Synthesis of Boc Bis(Netropsin) Poly-(Z)-Amino Compounds followed that for the synthesis of Boc Bis(Netropsin) compounds (Chapter One).

Boc Bis(Netropsin)-3,6-Di-(Z)-Aminoctadecanediamide (IV-41), 67% from II-129 and IV-24. ^1H NMR δ 9.95 (m, 2H), 9.84 (s, 2H), 8.05 (t, 1H), 7.96 (t, 1H), 7.25 (m, 10H), 7.17 (s, 2H), 7.15 (d, 2H), 6.91 (s, 2H), 6.84 (s, 1H), 6.82 (s, 1H), 6.78 (t, 1H), 5.05 (m, 4H), 4.04 (m, 4H), 3.83 (s, 3H), 3.82 (s, 3H), 3.80 (s, 6H), 3.52 (br s, 4H), 3.17 (m, 4H), 2.95 (m, 2H), 2.30 (t, 2H), 2.18 (s, 6H), 1.62 (m, 2H), 1.57 (m, 2H), 1.38 (s, 9H).

Boc Bis(Netropsin)-3,6,9-Tri-(Z)-Aminoundecanediamide (IV-44), 66% from II-129 and IV-39. ^1H NMR δ 9.91 (s, 1H), 9.97 (s, 1H), 9.87 (s, 2H), 8.11 (t, 1H), 7.97 (t, 1H), 7.28 (m, 15H), 7.17 (s, 3H), 7.16 (s, 1H), 6.91 (br s, 2H), 6.86 (d, 1H), 6.84 (s, 1H), 6.80 (t, 1H), 5.01 (m, 6H), 3.99 (m, 4H), 3.83 (s, 3H), 3.82 (s, 3H), 3.80 (s, 6H), 3.79 (s, 3H), 3.38 (m, 8H), 3.20 (m, 2H), 3.15 (m, 2H), 2.94 (m, 2H), 2.58 (br s, 2H), 2.40 (s, 6H), 1.70 (m, 2H), 1.56 (m, 2H), 1.38 (s, 9H).

Boc Bis(Netropsin)-3,6,9,12-Tetra-(Z)-Aminotetradecanediamide (IV-46), 100% from **II-129** and **IV-42**. ^1H NMR δ 9.97 (s, 1H), 9.94 (s, 1H), 9.86 (s, 2H), 8.07 (t, 1H), 7.97 (t, 1H), 7.26 (m, 20H), 7.17 (s, 3H), 7.16 (s, 1H), 6.90 (s, 2H), 6.84 (s, 1H), 6.81 (s, 1H), 6.81 (t, 1H), 5.00 (m, 8H), 3.97 (m, 4H), 3.83 (s, 3H), 3.81 (s, 3H), 3.79 (s, 6H), 3.37 (m, 12H), 3.17 (m, 4H), 2.94 (m, 2H), 2.26 (t, 2H), 2.15 (s, 6H), 1.61 (m, 4H), 1.38 (s, 9H).

Boc Bis(Netropsin)-3,6,9,12,15-Penta-(Z)-Aminoheptadecanediamide (IV-47), 64% from **II-129** and **IV-43**. ^1H NMR δ 9.97 (s, 1H), 9.94 (s, 1H), 9.85 (s, 2H), 8.06 (t, 1H), 7.96 (t, 1H), 7.26 (m, 25H), 7.17 (s, 3H), 7.16 (s, 1H), 6.90 (s, 2H), 6.84 (s, 1H), 6.81 (s, 1H), 6.80 (t, 1H), 5.01 (m, 10H), 3.96 (m, 4H), 3.83 (s, 3H), 3.81 (s, 3H), 3.79 (s, 6H), 3.28 (br s, 16H), 3.17 (m, 4H), 2.94 (m, 2H), 2.24 (t, 2H), 2.14 (s, 6H), 1.60 (m, 4H), 1.37 (s, 9H).

General Procedure for the Synthesis of Bis(Netropsin) Poly-(Z)-Amino Compounds followed that for the synthesis of Bis(Netropsin) compounds (Chapter One).

Bis(Netropsin)-3,6-Di-(Z)-Aminoctadecanediamide (IV-45), 67% from **IV-41**. ^1H NMR δ 9.99 (d, 1H), 9.96 (s, 1H), 9.86 (s, 2H), 8.08 (m, 2H), 7.30 (m, 10H), 7.18 (s, 2H), 7.17 (s, 1H), 7.15 (s, 1H), 6.92 (s, 1H), 6.91 (s, 1H), 6.84 (s, 1H), 6.81 (s, 1H), 5.09, 5.03, 5.02, 5.00 (4s, 4H), 4.08, 4.05, 4.03, 4.01 (4s, 4H), 3.83 (s, 3H), 3.82 (s, 3H), 3.79 (s, 6H), 3.51 (br s, 4H), 3.22 (m, 2H), 3.18 (m, 2H), 2.59 (t, 2H), 2.23 (t, 2H), 2.13 (s, 6H), 1.58 (m, 4H).

Bis(Netropsin)-3,6,9-Tri-(Z)-Aminoundecanediamide (IV-48), 53% from **IV-44**. ^1H NMR δ 9.98 (br s, 1H), 9.96 (br s, 1H), 9.86 (s, 2H), 8.07 (m, 2H), 7.27 (m,

15H), 7.17 (s, 3H), 7.16 (s, 1H), 6.91 (br s, 2H), 6.83 (s, 1H), 6.81 (s, 1H), 5.01 (m, 6H), 3.98 (m, 4H), 3.83 (s, 3H), 3.81 (s, 3H), 3.79 (s, 6H), 3.37 (m, 8H), 3.22 (m, 2H), 3.18 (m, 2H), 2.59 (t, 2H), 2.27 (t, 2H), 2.13 (s, 6H), 1.58 (m, 4H).

Bis(Netropsin)-3,6,9,12-Tetra-(Z)-Aminotetradecanediamide (IV-49), 77% from IV-46. ^1H NMR δ 9.98 (s, 1H), 9.95 (s, 1H), 9.86 (s, 2H), 8.08 (m, 2H), 7.27 (m, 20H), 7.18 (s, 3H), 7.16 (s, 1H), 6.91 (s, 2H), 6.84 (s, 1H), 6.81 (s, 1H), 5.01 (m, 8H), 3.98 (m, 4H), 3.83 (s, 3H), 3.81 (s, 3H), 3.79 (s, 6H), 3.36 (br s, 12H), 3.22 (m, 2H), 3.18 (m, 2H), 2.61 (t, 2H), 2.23 (t, 2H), 2.13 (s, 6H), 1.58 (m, 4H).

Bis(Netropsin)-3,6,9,12,15-Penta-(Z)-Aminoheptadecanediamide (IV-50), 52% from IV-47. ^1H NMR δ 9.97 (s, 1H), 9.94 (s, 1H), 9.86 (s, 2H), 8.08 (m, 2H), 7.26 (m, 25H), 7.17 (s, 4H), 6.90 (s, 2H), 6.85 (s, 1H), 6.81 (s, 1H), 5.01 (m, 10H), 3.99 (m, 4H), 3.83 (s, 3H), 3.81 (s, 3H), 3.79 (s, 6H), 3.33 (br s, 16H), 3.22 (m, 2H), 3.18 (m, 2H), 2.63 (t, 2H), 2.23 (t, 2H), 2.13 (s, 6H), 1.60 (m, 4H).

General Procedure for the Synthesis of Bis(Netropsin) Poly-(Z)-Amino-EDTA, Triethyl Ester Compounds followed that for the synthesis of Bis(Netropsin) Polyether-EDTA, Triethyl ester compounds (Chapter Three).

Bis(Netropsin)-3,6-Di-(Z)-Aminoctadecanediamide-EDTA, Triethyl ester (IV-56), 74% from IV-45 and $\text{EDTA}(\text{OEt})_3$. ^1H NMR δ 9.96 (m, 2H), 9.85 (m, 2H), 8.07 (m, 2H), 7.99 (t, 1H), 7.30 (m, 10H), 7.18 (m, 4H), 6.91 (s, 1H), 6.90 (s, 1H), 6.85 (s, 1H), 6.81 (s, 1H), 5.09, 5.03, 5.02, 5.00 (4s, 4H), 4.05 (m, 10H), 3.83 (s, 3H), 3.82 (s, 3H), 3.79 (s, 6H), 3.60-3.47 (series of singlets, 8H), 3.34 (br s, 4H), 3.18 (m, 6H), 2.72 (m, 4H), 2.28 (t, 2H), 2.17 (s, 6H), 1.61 (m, 4H), 1.17 (m, 9H); FAB MS, calcd. for $\text{C}_{70}\text{H}_{95}\text{N}_{16}\text{O}_{17}$ ($\text{M}+\text{H}^+$): 1431.7061. Found: 1431.7039.

Bis(Netropsin)-3,6,9-Tri-(Z)-Aminoundecanediamide-EDTA, Triethyl ester (IV-57), 87% from **IV-48** and **EDTA(OEt)₃**. ¹H NMR δ 9.95 (m, 2H), 9.86 (s, 1H), 9.85 (s, 1H), 8.06 (t, 2H), 8.03 (t, 1H), 7.99 (t, 1H), 7.25 (m, 15H), 7.18 (s, 2H), 7.16 (s, 2H), 6.91 (s, 2H), 6.85 (s, 1H), 6.81 (s, 1H), 5.01 (m, 6H), 4.06 (m, 6H), 3.98 (m, 4H), 3.83 (s, 3H), 3.81 (s, 3H), 3.79 (s, 6H), 3.60-3.47 (series of singlets, 8H), 3.33 (br s, 8H), 3.17 (m, 6H), 2.72 (m, 4H), 2.27 (t, 2H), 2.16 (s, 6H), 1.61 (m, 4H), 1.18 (m, 9H); FAB MS, calcd. for $C_{80}H_{105}N_{17}O_{19}Li$ ($M+Li^+$): 1614.7934. Found: 1614.7893.

Bis(Netropsin)-3,6,9,12-Tetra-(Z)-Aminotetradecanediamide-EDTA, Triethyl ester (IV-58), 63% from **IV-49** and **EDTA(OEt)₃**. ¹H NMR δ 9.97 (s, 1H), 9.94 (s, 1H), 9.87 (s, 1H), 9.85 (s, 1H), 8.05 (m, 2H), 7.99 (t, 1H), 7.26 (m, 20H), 7.17 (s, 2H), 7.16 (s, 2H), 6.90 (s, 2H), 6.84 (s, 1H), 6.81 (s, 1H), 5.01 (m, 8H), 4.06 (m, 6H), 3.99 (m, 4H), 3.83 (s, 3H), 3.81 (s, 3H), 3.79 (s, 6H), 3.60-3.47 (series of singlets, 8H), 3.34 (br s, 12H), 3.17 (m, 6H), 2.72 (m, 4H), 2.26 (t, 2H), 2.15 (s, 6H), 1.61 (m, 4H), 1.16 (m, 9H); FAB MS, calcd. for $C_{90}H_{117}N_{18}O_{21}$ ($M+H^+$): 1785.8641. Found: 1785.8649.

Bis(Netropsin)-3,6,9,12,15-Penta-(Z)-Aminoheptadecanediamide-EDTA, Triethyl ester (IV-59), 30% from **IV-50** and **EDTA(OEt)₃**. ¹H NMR δ 9.97 (s, 1H), 9.94 (s, 1H), 9.87 (s, 1H), 9.86 (s, 1H), 8.07 (m, 2H), 8.00 (t, 1H), 7.26 (m, 25H), 7.18 (s, 2H), 7.16 (s, 2H), 6.90 (s, 2H), 6.84 (d, 1H), 6.81 (d, 1H), 5.01 (m, 10H), 4.06 (m, 6H), 3.99 (m, 4H), 3.82 (s, 3H), 3.81 (s, 3H), 3.79 (s, 6H), 3.60-3.47 (series of singlets, 8H), 3.34 (br s, 16H), 3.17 (m, 6H), 2.71 (m, 4H), 2.27 (br s, 2H), 2.16 (s, 6H), 1.61 (m, 4H), 1.16 (m, 9H); FAB MS, calcd. for $C_{100}H_{128}N_{19}O_{23}$ ($M+H^+$): 1963.9461. Found: 1963.9399.

General Procedure for the Synthesis of Bis(Netropsin) Polyamine-EDTA Compounds. A small sample (2-10 mg) of Bis(Netropsin) Poly-(Z)-Amino-EDTA, Triethyl ester compound was treated with 1 mL 30% HBr/HOAc (Mallinckrodt). After standing at RT for 10 min, the mixture was frozen and lyophilized. The residue was dissolved in 0.5 mL MeOH and treated with 50 molar equiv. 1 M LiOH. After stirring for 3 h at RT, the mixture was neutralized with HOAc, frozen, and lyophilized to afford the Bis(Netropsin) Polyamine-EDTA compound admixed with LiOAc.

Bis(Netropsin)-3,6-Diaminoctadecanediamide-EDTA (BNN2E, IV-69). ^1H NMR ($\text{Me}_2\text{SO-d}_6$ + TFA) δ 10.10 (s, 2H), 10.02 (s, 1H), 10.01 (s, 1H), 8.33 (br s, 1H), 8.24 (br s, 1H), 8.10 (br s, 1H), 7.34-7.24 (m, 4H), 7.07-6.96 (m, 4H), 4.14 (s, 4H), 4.07 (s, 2H), 4.00 (s, 2H), 3.95-3.85 (m, 16H), 3.48 (s, 4H), 3.40 (s, 4H), 3.29 (m, 6H), 3.14 (m, 2H), 2.85 (d, 6H), 1.8 (m, 4H); UV (H_2O) λ_{max} 295, 237 nm.

Bis(Netropsin)-3,6,9-Triaminoundecanediamide-EDTA (BNN3E, IV-68). ^1H NMR ($\text{Me}_2\text{SO-d}_6$ + TFA) δ 10.62 (s, 2H), 10.06 (s, 1H), 9.99 (s, 1H), 8.33 (br s, 1H), 8.25 (br s, 1H), 8.10 (br s, 1H), 7.34-7.23 (m, 4H), 7.07-6.96 (m, 4H), 4.17 (s, 4H), 4.09 (s, 2H), 4.04 (s, 2H), 3.93-3.86 (m, 16H), 3.48-3.40 (m, 12H), 3.27 (m, 6H), 3.13 (m, 2H), 2.83 (d, 6H), 1.8 (m, 4H); UV (H_2O) λ_{max} 297, 238 nm.

Bis(Netropsin)-3,6,9,12-Tetraaminotetradecanediamide-EDTA (IV-67). ^1H NMR ($\text{Me}_2\text{SO-d}_6$ + TFA) δ 10.63 (s, 2H), 10.06 (s, 1H), 9.98 (s, 1H), 8.30 (br s, 1H), 8.24 (br s, 1H), 8.09 (br s, 1H), 7.36-7.22 (m, 4H), 7.08-6.96 (m, 4H), 4.18 (s, 4H), 4.09 (s, 2H), 4.05 (s, 2H), 3.94-3.80 (m, 16H), 3.46 (br s, 8H), 3.42 (br s, 8H), 3.28 (m, 6H), 3.14 (m, 2H), 2.83 (br s, 6H), 1.8 (m, 4H); UV (H_2O) λ_{max} 296, 238 nm.

Bis(Netropsin)-3,6,9,12,15-Pentaaminoheptadecanediamide-EDTA (IV-66).

¹H NMR (Me₂SO-d₆ + TFA) δ 10.56 (s, 2H), 9.94 (s, 1H), 9.92 (s, 1H), 9.4 (br s, 1H), 8.42 (br s, 1H), 8.16 (br s, 1H), 8.02 (br s, 1H), 7.23 (s, 2H), 7.17 (s, 1H), 7.16 (s, 1H), 6.98 (d, 1H), 6.93 (s, 1H), 6.89 (2s, 2H), 4.09 (s, 2H), 4.03 (s, 2H), 3.87-3.79 (series of singlets, 16H), 3.40 (br s, 20H), 3.27 (m, 6H), 3.07 (m, 2H), 2.77 (d, 6H), 1.84 (m, 2H), 1.66 (m, 2H); UV (H₂O) λ_{max} 297, 238 nm.

Synthesis of Boc 18-Amino-3,6,9,12,15-Pentaoxaoctadecanoic Acid (IV-176). Pentaethylene glycol (11.9 g, 50 mmol) was dissolved in 250 mL Et₂O, and treated with Rh₂(OAc)₄ (200 mg). This mixture was stirred at RT and treated with ethyl diazoacetate (5.3 mL, 50 mmol) via syringe pump over 8 h. After stirring overnight at RT, the mixture was concentrated and chromatographed on silica gel using EtOAc followed by 20% EtOH/EtOAc eluents afforded 7.6 g (23.5 mmol, 47%) of **18-Hydroxy-3,6,9,12,15-pentaoxaoctadecanoic acid, ethyl ester (IV-150)** as an oil. ¹H NMR δ 4.55 (t, 1H), 4.11 (q, 2H), 4.11 (s, 2H), 3.60-3.40 (m, 20H), 1.20 (t, 3H). The alcohol (7.4 g, 23 mmol) was dissolved in 10 mL pyridine and treated at RT with a solution of TsCl in 60 mL pyridine. After stirring 2 h at RT, the reaction was quenched by the addition of 70 mL ice. The mixture was poured into 400 mL H₂O and extracted with 250 mL Et₂O followed by 250 mL EtOAc. The organic extracts were combined, dried over Na₂SO₄, filtered, and concentrated. Drying *in vacuo* removed remaining pyridine, leaving 8.12 g (17 mmol, 75%) of **18-(p-Toluenesulfonato)-3,6,9,12,15-pentaoxaoctadecanoic acid, ethyl ester (IV-158)** as a thick oil. ¹H NMR δ 7.79 (d, 2H), 7.48 (d, 2H), 4.12 (s, 2H), 4.11 (q, 2H), 3.60-3.48 (m, 18H), 2.42 (s, 3H), 1.19 (t, 3H). The tosylate (8.0 g, 16.7 mmol) was dissolved in 20 mL DMF and treated with a solution of LiN₃ (4.17 g, 85 mmol) in 80 mL DMF. The resulting mixture was placed in an 80°C heating bath for 30 min. The solvent was distilled *in vacuo*, and the residue subjected to chromatography on silica gel using EtOAc eluent to afford 5.42 g

(15.5 mmol, 90%) of **18-Azido-3,6,9,12,15-pentaoxaoctadecanoic acid, ethyl ester (IV-160)** as an oil. ^1H NMR δ 4.12 (q, 2H), 4.11 (s, 2H), 3.60 (m, 4H), 3.57-3.52 (m, 14H), 3.39 (t, 2H), 1.20 (t, 3H). This material was then subjected to an *in situ* reduction/protection/hydrolysis sequence. The azide (3.5 g, 10 mmol) was dissolved in 100 mL MeOH and treated with di-*t*-butyldicarbonate (4.4 g, 20 mmol) and PtO₂ (1.0 g). The mixture was hydrogenated at RT and 3 atm for 3 h, filtered, concentrated, and dried *in vacuo* to afford the intermediate **Boc 18-amino-3,6,9,12,15-pentaoxaoctadecanoic acid, ethyl ester**. This material was dissolved in 20 mL MeOH and treated with LiOH (0.36 g, 15 mmol) in 10 mL H₂O. After stirring 3.5 h at RT, the mixture was concentrated and chromatographed on silica gel using 1:5 3% NH₄OH/MeOH:CH₂Cl₂ followed by 1:1 3% NH₄OH/MeOH:CH₂Cl₂ eluents to afford 1.12 g (2.8 mmol, 28%) of **Boc 18-amino-3,6,9,12,15-pentaoxaoctadecanoic acid (IV-176)** as an oil. ^1H NMR δ 6.77 (t, 1H), 3.72 (s 2H), 3.52 (s, 14H), 3.50 (s, 2H), 3.37 (t, 2H), 3.06 (m, 2H), 1.37 (s, 9H); FAB MS, calcd. for C₁₇H₃₃NO₉ (M⁺): 395. . Found: .

Synthesis of EDTA, Tricyclohexyl Ester (TriCyE, IV-144). EDTA (20 g, 68 mmol) was slurried in 150 mL cyclohexanol and treated with 4 mL concentrated H₂SO₄. The resulting mixture was heated at 110°C for 10 h. The mixture was then cooled to RT, poured into 500 mL 10% NaHCO₃ solution, and extracted with 2 X 200 mL Et₂O. The combined organic extracts were concentrated on a rotary evaporator, first using a water aspirator to remove Et₂O and then using a vacuum pump and heat (50°C) to remove cyclohexanol. The remaining oil was placed on the vacuum line for several days before being purified by chromatography on silica gel using CH₂Cl₂ followed by 5% MeOH/CH₂Cl₂, 10% MeOH/CH₂Cl₂, and 50% MeOH/CH₂Cl₂ eluents to afford separation of **TriCyE** (9.2 g, 17 mmol, 25%) from cyclohexanol and EDTA, tetracyclohexyl ester. Depending on the preparation, **TriCyE** may be obtained as a brittle solid or as a thick gum. ^1H NMR δ 4.68 (m, 3H), 3.50 (s, 4H), 3.49 (s, 2H), 3.37 (s,

2H), 2.71 (s, 4H), 1.76 (m, 6H), 1.65 (m, 6H), 1.49-1.1 (m, 18 H); FAB MS, calcd. for C₂₈H₄₆N₂O₈ (M⁺): 538.3254. Found: 538.3240.

Synthesis of Ionomutant Proteins was carried out on an Applied Biosystems Model 430A Protein Synthesizer. The Boc chemistry programs for automated synthesis were developed and provided by Dr. S.B.H. Kent and coworkers at Caltech.¹³ Boc amino acid derivatives were obtained from Peninsula Laboratories. The protecting groups employed were: Arg, tosyl; Lys, chloro-Z; Ser, benzyl; Tyr, bromo-Z; Thr, benzyl; His, 2,4-dinitrophenyl; Glu, benzyl. Asparagine-derivatized phenylacetamidomethyl (Asn-PAM) resin (Applied Biosystems, 0.670 mmol/g) was used for the syntheses. Quantitative ninhydrin analysis¹⁴ was performed after each coupling step in the synthesis to determine stepwise coupling yields. Automated synthesis was carried out on 0.5 mmol scale for the addition of residues Met 189 through Val 173. At this point ~40% of the peptide/resin was removed (for synthesis of mutants 4 and 5) and the remaining peptide/resin homologated through His 160. Synthesis of the individual ionomutants was then carried out on a 0.1 mmol scale. The synthetic ionophoric amino acid **IV-176**, two succeeding residues, Boc-Gaba (**I-203**), and **TriCyE** were added by manual solid phase protein synthesis as described by Sluka.⁵

Coupling of **IV-176** was carried out for 2 h in DMF using 2.0 equiv. **IV-176**, 4.0 equiv. HOBT, and 2.0 equiv. DCC. Yields for these couplings to mutants 1-5 were 99.70%, 99.83%, 99.65%, 99.77%, and 99.83%, respectively. **I-203** was double-coupled using symmetric anhydride (SA) followed by preformed symmetric anhydride (PSA) protocols. Yields for these couplings to mutants 1-5 were 99.86%, 99.75%, 99.16%, 99.79%, and 99.44%, respectively. **TriCyE** was coupled to the free amino terminus of Gaba-Hin (139-190) mutants using the HOBT active ester protocol described for the coupling of **IV-176**. Yields for these couplings to mutants 1-5 were 99.36%, 98.55%, 99.33%, 99.80%, and 98.43%, respectively.

The protected, support-bound ionomutant protein derivatives (~120 mg peptide/resin) were deprotected and cleaved from the resin by the following protocol:⁵

- 1) 65% TFA/CH₂Cl₂, 1 min
- 2) 65% TFA/CH₂Cl₂, 15 min
- 3) CH₂Cl₂ flow wash, 5X
- 4) 10% DIPEA/CH₂Cl₂, 1 min
- 5) CH₂Cl₂ flow wash, 5X
- 6) 10% DIPEA/CH₂Cl₂, 1 min
- 7) CH₂Cl₂ flow wash, 10X
- 8) 5 mL 20% mercaptoethanol, 10% DIPEA in DMF, 30 min, 2X
- 9) DMF flow wash, 5X
- 10) CH₂Cl₂ flow wash, 10X
- 11) Vacuum dry
- 12) 0.5 mL p-thiocresol, 0.5 mL p-cresol, 10 mL HF, 0°C, 1 h.

The crude peptide was precipitated with 20 mL Et₂O and washed with 3 X 20 mL Et₂O. The peptide was then dissolved using 3 X 10 mL H₂O. 100 µL of this solution was passed through a 0.45 µ filter and analyzed by reverse-phase HPLC (Vydac C4 column, 210 X 4 mm, 0.7 mL/min, 37°C, 60 min 0-100% linear gradient of 0.1% TFA/3:2 CH₃CN:H₂O in 0.1% TFA/H₂O). The remainder of crude peptide was frozen and lyophilized. The solid was transferred to a 50 mL polypropylene centrifuge tube, treated with 5 mL 20% mercaptoethanol in 4 M guanidinium chloride, 50 mM Tris·HCl, pH 8.5 buffer, and heated 1 h at 50°C to remove residual His 2,4-dinitrophenyl protecting groups. This solution was then passed through a 0.45 µ filter and purified by reverse-phase HPLC (Vydac C4 column, 210 X 25 mm, 3.0 mL/min, 37°C, 240 min 0-100% linear gradient of 0.1% TFA/3:2 CH₃CN:H₂O in 0.1% TFA/H₂O started after initial large peak eluted). Aliquots from 1.5 mL fractions were analyzed by HPLC to locate the desired material.

These fractions were combined, frozen, lyophilized. The proteins were stored in solid form at -20°C prior to use.

Bis(Netropsin)-6,9-Dioxa-3,12-Dithiatetradecanediamide-EDTA (BN2S2OE, V-34) was synthesized following the general procedures for the synthesis of Bis(Netropsin) Polyether-EDTA compounds.

Synthesis of 6,9-Dioxa-3,12-Dithiatetradecanedicarboxylic acid, mono Methyl ester. Redistilled triethylene glycol (66 g, 0.44 mol) was treated with pyridine (13.3 g, 0.17 mol) and stirred vigorously in an ice/water bath. To this solution was added phosphorous tribromide (PBr₃, MCB, 100 g, 0.37 mol), dropwise, over 2 h. After addition was complete, the reaction mixture was allowed to warm slowly to RT and to stir overnight. The thick mixture was poured into 400 mL H₂O and then extracted with Et₂O (300 mL). The organic extract was washed with 2 X 300 mL H₂O (at this point the aqueous wash was pH 6). The organic extract was dried over Na₂SO₄, filtered, and evaporated to afford 76.2 g of oil. The product was distilled twice at 0.3-0.4 mm Hg to afford 62 g (225 mmol, 51%) of **1,8-Dibromo-3,6-dioxaoctane (IV-179)**¹⁵ as an oil. ¹H NMR δ 3.83 (t, 4H), 3.69 (s, 4H), 3.49 (t, 4H). The dibromide (5.5 g, 20 mmol) was combined with ethyl thioglycolate (Aldrich, 4.4 mL, 40 mmol) in 5 mL DMF. This solution was then added dropwise over 30 min to a hot (80°C) mixture of Cs₂CO₃ (13 g, 40 mmol) in 10 mL DMF. The reaction was allowed to stir overnight at 80°C. After cooling to RT, the mixture was filtered, the solvent distilled *in vacuo*, and the residue chromatographed on silica gel using EtOAc eluent to afford 5.2 g (14.7 mmol, 73%) of **6,9-Dioxa-3,12-dithiatetradecanedioic acid, diethyl ester (IV-183)** as an oil. ¹H NMR δ 4.19 (q, 4H), 3.70 (t, 4H), 3.63 (s, 4H), 3.30 (s, 4H), 2.84 (t, 4H), 1.29 (t, 6H). The diester was converted to **6,9-Dioxa-3,12-dithiatetradecanedioic acid, mono methyl ester (IV-188)** as described for 3,6,9,12,15-Pentaoxaheptadecanedioic

acid, mono ethyl ester (**II-117**), except that MeOH reaction solvent was used, affording transesterification to the methyl ester. ^1H NMR δ 4.08 (br s, 1H), 3.81 (s, 3H), 3.75 (m, 4H), 3.70 (s, 4H), 3.39 (s, 2H), 3.33 (s, 2H), 2.91 (s, 2H), 2.84 (s, 2H).

Netropsin-6,9-Dioxa-3,12-Dithiatetradecanamic acid, mono Methyl ester (V-29**)**, 74% from **I-22** and **IV-188**. ^1H NMR δ 9.98 (s, 1H), 9.87 (s, 1H), 8.07 (t, 1H), 7.18 (s, 1H), 7.17 (s, 1H), 6.88 (d, 1H), 6.81 (d, 1H), 3.83 (s, 3H), 3.79 (s, 3H), 3.63 (s, 3H), 3.57 (m, 4H), 3.50 (s, 4H), 3.39 (s, 2H), 3.26 (s, 2H), 3.17 (m, 2H), 2.78 (t, 2H), 2.73 (t, 2H), 2.24 (t, 2H), 2.13 (s, 6H), 1.60 (m, 2H).

Netropsin-6,9-Dioxa-3,12-Dithiatetradecanamic acid (V-30**)**, 90% from **V-29**. ^1H NMR δ 10.10 (s, 1H), 9.90 (s, 1H), 8.11 (t, 1H), 7.20 (d, 1H), 7.16 (d, 1H), 6.92 (d, 1H), 6.82 (d, 1H), 3.83 (s, 3H), 3.79 (s, 3H), 3.57 (m, 4H), 3.49 (s, 4H), 3.27 (s, 2H), 3.18 (s, 2H), 3.18 (m, 2H), 2.77 (t, 2H), 2.69 (t, 2H), 2.42 (t, 2H), 2.26 (s, 6H), 1.66 (m, 2H).

Boc Bis(Netropsin)-6,9-Dioxa-3,12-Dithiatetradecanediamide (V-31**)**, 75% from **V-30** and **II-129**. ^1H NMR δ 9.99 (s, 2H), 9.87 (s, 2H), 8.07 (t, 1H), 7.97 (t, 1H), 7.18 (s, 4H), 6.88 (s, 2H), 6.84 (s, 1H), 6.81 (s, 1H), 6.81 (t, 1H), 3.83 (s, 6H), 3.79 (s, 6H), 3.58 (m, 4H), 3.51 (s, 4H), 3.26 (s, 4H), 3.17 (m, 4H), 2.95 (m, 2H), 2.78 (t, 2H), 2.73 (t, 2H), 2.24 (t, 2H), 2.13 (s, 6H), 1.60 (m, 4H), 1.38 (s, 9H).

Bis(Netropsin)-6,9-Dioxa-3,12-Dithiatetradecanediamide (V-32**)**, 64% from **V-31**. ^1H NMR δ 9.99 (2s, 2H), 9.87 (s, 2H), 8.07 (m, 2H), 7.17 (s, 4H), 6.88 (2s, 2H), 6.82 (d, 1H), 6.81 (d, 1H), 3.82 (s, 6H), 3.79 (s, 6H), 3.58 (t, 4H), 3.51 (s, 4H), 3.26 (s, 4H), 3.20 (m, 4H), 2.78 (t, 4H), 2.58 (t, 2H), 2.23 (t, 2H), 2.12 (s, 6H), 1.60 (m, 2H), 1.55 (m, 2H).

Bis(Netropsin)-6,9-Dioxa-3,12-Dithiatetradecanediamide-EDTA, Triethyl ester (V-33), 80% from **V-32** and **EDTA(OEt)₃**. ¹H NMR δ 9.99 (s, 2H), 9.88 (s, 1H), 9.87 (s, 1H), 8.07 (t, 1H), 8.04 (t, 1H), 8.00 (t, 1H), 7.18 (s, 4H), 6.88 (2s, 2H), 6.85 (d, 1H), 6.81 (d, 1H), 4.05 (m, 6H), 3.82 (s, 6H), 3.79 (s, 6H), 3.60-3.46 (m, 16H), 3.26 (s, 4H), 3.18 (m, 6H), 2.78 (t, 4H), 2.72 (m, 4H), 2.24 (t, 2H), 2.14 (s, 6H), 1.60 (m, 4H), 1.16 (t, 9H). FAB MS, calcd. for $C_{58}H_{89}N_{14}O_{15}S_2$ ($M+H^+$): 1285.6073. Found: 1285.6088.

Bis(Netropsin)-6,9-Dioxa-3,12-Dithiatetradecanediamide-EDTA (BN2S2OE, V-34), 77% from **V-33**. ¹H NMR (Me_2SO-d_6 + TFA) δ 10.07 (s, 2H), 9.97 (s, 1H), 9.95 (s, 1H), 9.47 (br s, 1H), 8.47 (t, 1H), 8.24 (t, 1H), 8.10 (t, 1H), 7.24 (s, 4H), 7.00 (s, 1H), 6.97 (s, 3H), 4.15 (s, 2H), 4.00 (s, 2H), 3.90 (s, 6H), 3.88 (s, 3H), 3.87 (s, 3H), 3.84 (s, 4H), 3.66 (t, 4H), 3.59 (s, 4H), 3.40 (m, 2H), 3.37 (s, 4H), 3.29 (m, 8H), 3.14 (m, 2H), 2.86 (m, 10H), 1.91 (m 2H), 1.73 (m, 2H); FAB MS, calcd. for $C_{52}H_{76}N_{14}O_{15}S_2K$ ($M+K^+$): 1239.4802. Found: 1239.4739; UV (H_2O) λ_{max} 300, 239 nm.

Bis(Netropsin)-Dibenzylpiperazine-EDTA (BNDBPE, III-239) was synthesized following the general procedures for the synthesis of Bis(Netropsin) Polyether-EDTA compounds.

Synthesis of *N,N'*-Dibenzylpiperazinedicarboxylic acid, mono Ethyl ester. Ethyl p-tolylacetate (Aldrich, 10 g, 56 mmol) was slurried with NBS (MCB, 10.8 g, 61 mmol) in 50 mL CCl_4 , and brought to a gentle reflux. Azobis(isobutyrylnitrile) (AIBN, Kodak, 80 mg, 0.5 mmol) was added and the mixture refluxed for 2 h before being cooled to RT and then in the refrigerator. The mixture was filtered, concentrated, and the resulting oil chromatographed on silica gel using 10% Et_2O /Hexane eluent to afford 7.3 g (28 mmol,

50%) of **Ethyl p-(bromomethylene)phenylacetate (III-200)** as an oil. ^1H NMR δ 7.35 (d, 2H), 7.26 (d, 2H), 4.48 (s, 2H), 4.15 (q, 2H), 3.60 (s, 2H), 1.25 (t, 3H). The bromide (2.57 g, 10.0 mmol) was dissolved in 10 mL DMF and added to a mixture of piperazine (Aldrich, 0.43 g, 5.0 mmol) and powdered potassium carbonate (K_2CO_3 , 2.07 g, 15.0 mmol) in 10 mL DMF. The resulting mixture was stirred at RT for 24 h. The mixture was filtered and the residue was extracted with 25 mL CHCl_3 . The CHCl_3 extract was filtered through a medium frit and evaporated to afford 1.3 g (3.0 mmol, 30%) of crystalline ***N,N'*-Dibenzylpiperazinedicarboxylic acid, diethyl ester (III-203)**. ^1H NMR δ 7.25 (q, 8H), 4.14 (q, 4H), 3.57 (s, 4H), 3.46 (s, 4H), 2.44 (br s, 8H), 1.13 (t, 6H). The diester (1.2 g, 2.7 mmol) was dissolved in 2:1 $\text{THF:H}_2\text{O}$ and treated, dropwise over 20 min, with a solution of LiOH (65 mg, 2.7 mmol) in 2 mL H_2O . The resulting mixture was stirred 8 h at RT. The mixture was then evaporated and the residue dissolved in 8 mL TFA and transferred to 2 50 mL centrifuge tubes. 20 mL Et_2O was added to each centrifuge tube, and the resulting heterogeneous mixtures were allowed to stand 1 h at RT. The tubes were then spun and the supernatants drawn off. The solids were washed with 2 X 10 mL Et_2O before being chromatographed on silica gel using 1% $\text{NH}_4\text{OH}/\text{MeOH}$ eluent to afford 0.58 g (1.40 mmol, 52%) of ***N,N'*-Dibenzylpiperazinedicarboxylic acid, mono Ethyl Ester (III-221)** as a solid. ^1H NMR δ 7.18 (m, 8H), 4.06 (q, 2H), 4.47 (s, 2H) 3.61, 3.47, 3.41, 3.41 (4s, 8H), 2.35 (br s, 8H), 1.17 (t, 3H).

Netropsin-Dibenzylpiperazinecarboxylic acid, Ethyl ester (III-223) was prepared from **I-22** and **III-221**. Without characterization, it was hydrolyzed to afford **III-224**.

Netropsin-Dibenzylpiperazinecarboxylic acid (III-224), 25% from **I-22**. ^1H NMR δ 10.04 (s, 1H), 9.83 (s, 1H), 8.06 (t, 1H), 7.26-7.14 (m, 10H), 6.87 (s, 1H),

6.79 (s, 1H), 3.80 (s, 3H), 3.79 (s, 3H), 3.52 (s, 2H), 3.49 (s, 2H), 3.41 (s, 4H), 3.16 (m, 2H), 2.35 (br s, 8H), 2.27 (t, 2H), 2.15 (s, 6H), 1.61 (m, 2H).

Boc Bis(Netropsin)-Dibenzylpiperazine (III-226), 92% from III-224 and II-129. ^1H NMR δ 10.04 (s, 2H), 9.85 (s, 1H), 9.84 (s, 1H), 8.06 (s, 1H), 7.96 (s, 1H), 7.22 (m, 8H), 7.17 (s, 2H), 7.14 (s, 2H), 6.86 (s, 2H), 6.83 (s, 1H), 6.80 (s, 1H), 6.80 (t, 1H), 3.80 (s, 6H), 3.79 (s, 6H), 3.52 (s, 4H), 3.40 (s, 4H), 3.16 (m, 4H), 2.94 (m, 2H), 2.34 (br s, 8H), 2.26 (t, 2H), 2.15 (s, 6H), 1.61 (m, 4H), 1.38 (s, 9H).

Bis(Netropsin)-Dibenzylpiperazine (III-228), 92% from III-226. ^1H NMR δ 10.06 (s, 2H), 9.85 (s, 2H), 8.07 (t, 3H), 7.22 (m, 8H), 7.17 (s, 2H), 7.15 (2s, 2H), 6.86 (s, 2H), 6.82 (s, 1H), 6.80 (s, 1H), 3.80 (s, 6H), 3.79 (s, 6H), 3.52 (s, 4H), 3.40 (s, 4H), 3.21 (m, 2H), 3.17 (m, 2H), 2.58 (t, 2H), 2.34 (br s, 8H), 2.23 (t, 2H), 2.12 (s, 6H), 1.60 (m, 2H), 1.55 (m, 2H).

Bis(Netropsin)-Dibenzylpiperazine-EDTA, Triethyl ester (III-238), 95% from III-228 and EDTA(OEt)₃. ^1H NMR δ 10.04 (s, 2H), 9.85 (s, 1H), 9.84 (s, 1H), 8.06 (t, 1H), 8.03 (t, 1H), 7.99 (t, 1H), 7.23 (m, 8H), 7.17 (s, 2H), 7.14 (s, 2H), 6.86 (d, 2H), 6.83 (d, 1H), 6.80 (d, 1H), 4.05 (m, 6H), 3.80 (s, 6H), 3.79 (2s, 6H), 3.59-3.51 (series of singlets, 8H), 3.40 (s, 4H), 3.33 (s, 4H), 3.17 (m, 6H), 2.72 (m, 4H), 2.34 (br s, 8H), 2.25 (t, 2H), 2.14 (s, 6H), 1.60 (m, 4H), 1.17 (m, 9H); FAB MS, calcd. for C₇₀H₉₆N₁₅O₁₃K (M+K⁺): 1407. . Found: .

Bis(Netropsin)-Dibenzylpiperazine-EDTA (BNDBPE, III-239), 100% from III-238. ^1H NMR (Me₂SO-d₆ + TFA) δ 10.24 (s, 2H), 9.95 (s, 1H), 9.94 (s, 1H), 8.47 (t, 1H), 8.24 (t, 1H), 8.10 (t, 1H), 7.49 (m, 8H), 7.23 (2s, 4H), 7.00 (d, 1H), 6.96 (d, 1H), 6.95 (d, 2H), 4.41 (br s, 4H), 4.14 (s, 2H), 3.99 (s, 2H), 3.88 (s, 9H), 3.87 (s,

3H), 3.82 (s, 4H), 3.68 (s, 4H), 3.40 (br s, 8H), 3.38 (m, 2H), 3.28 (m, 8H), 3.15 (m, 2H), 2.86 (d, 6H), 1.91 (m, 2H), 1.73 (m, 2H); FAB MS, calcd. for $C_{65}H_{84}N_{16}O_{13}K$ ($M+K^+$): . Found: ; UV (H_2O) λ_{max} 300, 246(s), 220(s).

Chapter Four

Synthesis of *N,N'*-EthyleneBis(Salicylideneaminato)Manganese(III) Acetate ([SalenMn(III)]OAc, MnS, II-228). Salicylaldehyde (Aldrich, 2.44 g, 20 mmol) was dissolved in 10 mL EtOH and treated with a solution of ethylenediamine (0.60 g, 10 mmol) in 5 mL EtOH. The resulting solution was refluxed for 1.5 h, cooled to RT, and filtered. The yellow crystals obtained were washed with EtOH and dried to afford 2.42 g (9.03 mmol, 90%) of *N,N'*-Ethylenebis(salicylideneamine) (SalenH₂, II-226). SalenH₂ (1.0 g, 3.7 mmol) was slurried in 30 mL 2:1 EtOH:acetonitrile (CH₃CN) and stirred at RT. A deep red-black slurry of Mn(OAc)₃·2H₂O (Aldrich, 1.0 g, 3.7 mmol) in 20 mL EtOH was then added in 1 mL aliquots over 1 h. After addition was complete, the reaction was stirred 2 h at RT, depositing a fine yellow-brown precipitate. The mixture was filtered and the solid washed with 2 X 2 mL EtOH, then dried *in vacuo* to afford 0.88 g (2.1 mmol, 57%) of brown, light [SalenMn(III)]OAc. The compound was soluble in EtOH and H₂O, slightly soluble in CH₃CN, and insoluble in acetone (Me₂CO). Magnetic susceptibilities were determined by NMR at 90 MHz in D₂O using t-butanol external standard.¹⁶ IR (cm⁻¹, Nujol) 1630 (s), 1595 (s), 1540 (s), 1460 (s), 1440 (s), 1380 (s), 1325 (s), 1290 (s), 1200 (m), 1140 (m), 1120 (s), 1080 (m), 1020 (m), 960 (m), 900 (s), 790 (s), 760 (s), 640 (m), 620 (s), 590 (s); UV-Vis (EtOH) λ_{max} (ϵ , M⁻¹cm⁻¹) 405 (9200), 350 (12600), 315 (22900), 287 (33400), 237 (73700), 225 (64200) nm; μ_{eff} 4.89; Analysis, calcd. for C₁₈H₁₇N₂O₄Mn: C 56.85%, H 4.50%, N 7.37%. Found: C 56.52%, H 4.57%, N 7.30%; FAB MS, calcd. for C₁₆H₁₄N₂O₂Mn ([SalenMn(III)]⁺): 321.0436. Found: 321.0448.

Synthesis of *N,N'*-EthyleneBis(Salicylideneaminato)Chromium(III) Chloride ([SalenCr(III)]Cl, II-280).¹⁷ A solution of CrCl₃·6H₂O (0.27 g, 1.0 mmol) in 10 mL H₂O was reduced with 100 g 0.65% Zn/Hg amalgam. The resulting solution of Cr(II) was then cannulated into a solution of I-226 (0.27 g, 1.0 mmol) in 10 mL (CH₃)₂CO. The brown mixture was then exposed to air and stirred for 30 min. The mixture was concentrated to 8 mL at 40°C, then cooled in an ice/water bath. The red-brown solid was filtered off, washed with 1 mL H₂O followed by 2 X 1 mL (CH₃)₂CO, and dried to afford 65 mg (0.17 mmol, 17%) of [SalenCr(III)]Cl·2H₂O. The compound was soluble in EtOH and H₂O, but insoluble in CH₃CN and (CH₃)₂CO. IR (cm⁻¹, Nujol) 1630 (s), 1600 (s), 1555 (m), 1540 (m), 1465 (s), 1450 (s), 1395 (m), 1380 (m), 1340 (m), 1290 (s), 1190 (m), 1150 (m), 1130 (m), 900 (m), 860 (s); UV-Vis (H₂O) λ_{max} (ϵ , M⁻¹cm⁻¹) 392 (5000), 325 (4100), 270 (21250), 235 (34100), 218 (38000); μ_{eff} 3.59; Analysis, calcd. for C₁₆H₁₄ClN₂O₂Mn·2H₂O: C 49.4%, H 4.6%, N 7.2%. Found: C 49.42%, H 4.76%, N 7.11%; FAB MS, calcd. for C₁₆H₁₄N₂O₂Cr ([SalenCr(III)]⁺): 318.0460. Found: 318.0472.

Synthesis of *N,N'*-EthyleneBis(4-*N''*,*N''* - Diethylaminosalicylideneaminato)Manganese(III) Acetate ([(*Et*₂N)₂SalenMn(III)]OAc, II-228). 4-Diethylaminosalicylaldehyde (Aldrich, 3.86 g, 20 mmol) was dissolved in 10 mL EtOH and treated with a solution of ethylenediamine (0.60 g, 10 mmol) in 5 mL EtOH. The resulting solution was refluxed for 1 h, cooled to RT, and filtered. The yellow-orange crystals obtained were washed with EtOH and dried to afford 3.44 g (8.4 mmol, 84%) of *N,N'*-EthyleneBis(4-*N''*,*N''*-Diethylaminosalicylideneamine) ((*Et*₂N)₂SalenH₂, III-33). This material (0.41 g, 1.0 mmol) was slurried in 5 mL EtOH and stirred at RT. A deep red-black slurry of Mn(OAc)₃·2H₂O (0.27 g, 1.0 mmol) in 5 mL EtOH was then added dropwise via cannula over 30 min. After addition was complete, the reaction was stirred 30 min at RT, depositing some violet microcrystals. 100

mL Et₂O was added, the mixture filtered, and the violet microcrystals dried to afford 0.44 g (0.65 mmol, 65%) of [(Et₂N)₂SalenMn(III)]OAc. UV-Vis (CH₃CN) λ_{max} (ϵ , M⁻¹cm⁻¹) 555 (4500), 535 (5000), 412 (39000), 325 (45500), 227 (50000) nm; μ_{eff} 5.08; Analysis, calcd. for C₂₆H₃₅N₄O₄Mn: C 59.76%, H 6.75%, N 10.72%. Found: C 58.95%, H 6.66%, N 10.60%; FAB MS, calcd. for C₂₄H₃₂N₄O₂Mn [(Et₂N)₂SalenMn(III)]⁺): 463.1904. Found: 463.1914.

N,N'-EthyleneBis(Salicylideneaminato)Iron(III) Chloride ([SalenFe(III)]Cl V-35), **Bis- μ -(N,N'-EthyleneBis(Salicylideneaminato)Iron(III)) Oxide** ([SalenFe(III)]₂O, V-36), and **N,N'-EthyleneBis(Salicylideneaminato)-Iron(III) Acetate** ([SalenFe(III)]OAc, V-37) were prepared according to the literature procedures.¹⁸⁻²⁰

Iodosylbenzene (PhIO) was prepared according to the literature procedure.²¹

Analysis of Base Products Released Upon DNA Cleavage by MnS.⁴ 180 μ L of solution containing MnS and calf thymus DNA in pH 7.0 sodium phosphate buffer was incubated 30 min at 37°C. DNA cleavage was initiated by the addition of 20 μ L hydrogen peroxide solution. Final concentrations in 200 μ L total volume were: MnS, 1 mM; calf thymus DNA, 1 mM bp; phosphate, 20 mM; H₂O₂, 10 mM. DNA cleavage was allowed to proceed 2 h at 37°C before the reaction was precipitated from NaOAc/EtOH. The supernatant was transferred to a clean tube and concentrated to dryness on the Speed Vac. The residue was dissolved in 30 μ L H₂O. 10 μ L of this solution was analyzed by reverse-phase HPLC (Hewlett-Packard 1090 HPLC system with diode array detection, Beckman Ultrasphere-ODS C₁₈ column, 25 X 4.6 mm) using a 0-100% gradient of 1:1 MeOH:10 mM pH 5.5 KH₂PO₄ buffer in 10 mM pH 5.5 KH₂PO₄ buffer over 18 minutes. HPLC analysis of control experiments carried out in the absence of MnS or H₂O₂, in the absence

of **MnS**, and in the absence of H_2O_2 were also performed. The identities of base peaks were established based on their HPLC retention times and UV spectra relative to authentic base samples.

Chapter Five

Synthesis of *N*-Isopropyl-4-Nitropyrrole-2-Carboxylic Acid (II-86).²² A solution of 2,5-dimethoxy-2,5-dihydrofuran-2-carboxylic acid, methyl ester (Aldrich, 7.94 g, 42 mmol) in 100 mL MeOH was treated with 4.0 g rhodium on alumina (Rh/Al₂O₃, Aldrich) and 0.5 mL HOAC. The mixture was hydrogenated at RT and 3 atm for 2 h, then filtered, and concentrated to afford 7.60 g (40 mmol, 95%) of **2,5-Dimethoxytetrahydrofuran-2-carboxylic acid, methyl ester (II-40)** as an oil. ¹H NMR δ 5.17 (m, 1H), 3.80 (s, 3H), 3.43, 3.37, 3.33, 3.28 (4s, 6H), 2.15 (m, 4H). This material (3.8 g, 20 mmol) was combined with isopropylamine (Aldrich, 3.40 mL, 40 mmol) and 7 mL AcOH. The mixture was refluxed for 16 h, poured into 75 mL H₂O, and extracted with 3 X 75 mL Et₂O. The organic extracts were combined, washed with 50 mL H₂O, 50 mL saturated aqueous NaHCO₃, and 50 mL H₂O before being dried over Na₂SO₄, filtered, and concentrated (at RT and 150 mm Hg to avoid loss of the product). Chromatography of the residue on silica gel using 1:10 to 1:2 Et₂O:pentane eluent afforded 1.5 g (9.0 mmol, 45%) of ***N*-Isopropylpyrrole-2-carboxylic acid, methyl ester (II-84)** as an oil. ¹H NMR δ 7.32 (m, 1H), 6.84 (dd, 1H), 6.13 (m, 1H), 5.33 (septet, 1H), 3.72 (s, 3H), 1.36 (d, 6H). The pyrrole was dissolved in 8 mL Ac₂O and cooled to -50°C. To this was added a cold solution of 2 mL HNO₃ in 8 mL Ac₂O dropwise over 1 h. The reaction mixture was maintained below -40°C during the course of addition, and then allowed to warm to -10°C over 5 h. The reaction was quenched by the addition of 50 g ice and stirred at RT. This mixture was extracted with 3 X 75 mL Et₂O. The organic extracts were combined, washed with 50 mL H₂O, 3 X 50 mL saturated aqueous NaHCO₃, dried

over Na_2SO_4 , and concentrated. Chromatography on silica gel using 1:5 Et_2O :pentane afforded 0.50 g (2.4 mmol, 26%) of ***N*-Isopropyl-4-nitropyrrole-2-carboxylic acid, methyl ester (II-85)** as an oil. ^1H NMR (CDCl_3) δ 7.77 (d, 1H), 7.39 (d, 1H), 5.44 (septet, 1H), 3.83 (s, 3H), 1.44 (d, 6H). The ester (0.39 g, 1.8 mmol) was dissolved in 4 mL EtOH and treated with NaOH (0.2 g, 5.0 mmol) in 4 mL H_2O . The resulting solution was refluxed for 10 min, then cooled to RT and concentrated. The residue was redissolved in 2 mL H_2O , cooled in an ice/water bath, and acidified with 2 mL 3 M HCl. The mixture was filtered, the white solid was washed with H_2O and hexane and then dried in air to afford 0.32 g (1.62 mmol, 94%) of **4-Nitro-*N*-Isopropylpyrrole-2-Carboxylic Acid (II-86)**. ^1H NMR δ 8.36 (d, 1H), 7.28 (d, 1H), 5.42 (septet, 1H), 1.43 (d, 6H).

N,N',N''-TriisopropylDistamycin-EDTA (TriIDE, II-98) and ***N-IsopropylDistamycin-EDTA (IDE, II-235)*** were prepared from **II-85**, **II-86**, and ***N*-methylpyrrole-carboxylic acid** derivatives following the general procedures for the synthesis of Netropsin and Distamycin analogs (Chapter One and References 2 and 3).

Nitro *N,N'-Diisopropyl-P2-Carboxylic acid, Methyl ester (II-88)*, 90% from **II-85** and **II-86**. ^1H NMR δ 10.33 (s, 1H), 8.35 (s, 1H), 7.61 (s, 1H), 7.47 (s, 1H), 6.91 (s, 1H), 5.47 (septet, 1H), 5.35 (septet, 1H), 3.74 (s, 3H), 1.44 (d, 6H), 1.38 (d, 6H).

Nitro *N,N',N''-Triisopropyl-P3-Carboxylic acid, Methyl ester (II-90)*, 82% from **II-88** and **II-86**. ^1H NMR δ 10.36 (s, 1H), 10.03 (s, 1H), 8.35 (d, 1H), 7.64 (s, 1H), 7.49 (d, 1H), 7.44 (s, 1H), 6.97 (s, 1H), 6.92 (d, 1H), 5.48 (m, 2H), 5.35 (septet, 1H), 3.74 (s, 3H), 1.45 (d, 6H), 1.38 (d, 6H), 1.36 (d, 6H).

Nitro *N,N',N''*-Triisopropyl-P3-Carboxylic acid (II-92), 95% from II-90. ^1H NMR δ 10.36 (s, 1H), 10.01 (s, 1H), 8.35 (s, 1H), 7.60 (s, 1H), 7.49 (s, 1H), 7.43 (s, 1H), 6.96 (s, 1H), 6.85 (s, 1H), 5.48 (m, 2H), 5.41 (septet, 1H), 1.45 (d, 6H), 1.36 (d, 12H).

Nitro *N,N',N''*-TriisopropylDistamycin Analog (II-93), 73% from II-92 and 3-dimethylaminopropylamine. ^1H NMR δ 10.35 (s, 1H), 9.97 (s, 1H), 8.35 (d, 1H), 8.09 (t, 1H), 7.49 (d, 1H), 7.43 (d, 1H), 7.37 (d, 1H), 6.94 (d, 1H), 6.75 (d, 1H), 5.48 (m, 3H), 3.19 (m, 2H), 2.26 (t, 2H), 2.15 (s, 6H), 1.61 (m, 2H), 1.45 (d, 6H), 1.37 (d, 6H), 1.32 (d, 6H).

***N,N',N''*-TriisopropylDistamycin-EDTA, Triethyl ester (II-96), 34% from II-93 and Gaba-EDTA(OEt)₃.³** ^1H NMR δ 9.94 (s, 1H), 9.92 (s, 1H), 9.83 (s, 1H), 8.09 (t, 1H), 8.01 (t, 1H), 7.41 (d, 1H), 7.37 (d, 1H), 7.34 (d, 1H), 6.94 (d, 1H), 6.77 (d, 1H), 6.75 (d, 1H), 5.47 (m, 3H), 4.06 (m, 6H), 3.61-3.46 (series of singlets, 8H), 3.17 (m, 2H), 3.13 (m, 2H), 2.71 (m, 4H), 2.23 (m, 4H), 2.14 (s, 6H), 1.71 (m, 2H), 1.61 (m, 2H), 1.34 (m, 18H), 1.17 (m, 9H).

***N,N',N''*-TriisopropylDistamycin-EDTA (TriIDE, II-98), 100% from II-96.** ^1H NMR (Me₂SO-d₆ + TFA) δ 9.94 (s, 2H), 9.93 (s, 1H), 9.37 (br s, 1H), 8.42 (t, 1H), 8.16 (t, 1H), 7.38 (d, 1H), 7.34 (s, 2H), 6.98 (d, 1H), 6.90 (d, 1H), 6.77 (d, 1H), 5.46 (m, 3H), 4.06 (s, 2H), 3.91 (s, 2H), 3.75 (s, 4H), 3.30 (m, 2H), 3.24 (m, 2H), 3.16 (m, 4H), 3.07 (m, 2H), 2.78 (d, 6H), 2.27 (t, 2H), 1.84 (m, 2H), 1.73 (m, 2H), 1.35 (m, 18H); UV (H₂O) λ_{max} 302, 238 nm.

Nitro *N*-IsopropylDistamycin Analog (II-192), 76% from I-22 and II-86. ^1H NMR δ 10.35 (s, 1H), 9.94 (s, 1H), 8.35 (s, 1H), 8.08 (t, 1H), 7.51 (s, 1H) 7.28 (s,

1H), 7.19 (s, 1H), 7.04 (s, 1H), 6.83 (s, 1H), 5.47 (septet, 1H), 3.86 (s, 3H), 3.80 (s, 3H), 3.18 (m, 2H), 2.25 (t, 2H), 2.14 (s, 6H), 1.61 (m, 2H), 1.45 (d, 6H).

N-IsopropylDistamycin-EDTA, Triethyl ester (II-234), 51% from II-192 and Gaba-EDTA(OEt)₃.³ ¹H NMR δ 9.93 (s, 1H), 9.89 (s, 1H), 9.83 (s, 1H), 8.07 (t, 1H), 8.01 (t, 1H), 7.34 (s, 1H) 7.24 (s, 1H), 7.19 (s, 1H), 7.04 (s, 1H), 6.83 (s, 1H), 6.78 (s, 1H), 5.45 (septet, 1H), 4.06 (m, 6H), 3.84 (s, 3H), 3.80 (s, 3H), 3.61-3.46 (series of singlets, 8H), 3.17 (m, 2H), 3.13 (m, 2H), 2.71 (m, 4H), 2.24 (m, 4H), 2.14 (s, 6H), 1.71 (m, 2H), 1.61 (m, 2H), 1.34 (d, 6H), 1.17 (m, 9H).

N-IsopropylDistamycin-EDTA (IDE, II-235), 92% from II-234. ¹H NMR (Me₂SO-d₆ + TFA) δ 10.01 (s, 1H), 9.98 (s, 1H), 9.94 (s, 1H), 9.62 (br s, 1H), 8.52 (t, 1H), 8.24 (t, 1H), 7.41 (d, 1H) 7.30 (d, 1H), 7.25 (d, 1H), 7.15 (d, 1H), 7.02 (d, 1H), 6.87 (d, 1H), 5.53 (septet, 1H), 4.14 (s, 2H), 3.99 (s, 2H), 3.92 (s, 3H), 3.89 (s, 3H), 3.84 (s, 4H), 3.38 (m, 2H), 3.32 (m, 2H), 3.25 (m, 4H), 3.15 (m, 2H), 2.86 (d, 6H), 2.36 (t, 2H), 1.92 (m, 2H), 1.82 (m, 2H), 1.42 (d, 6H); UV (H₂O) λ_{max} 303, 236 nm.

Thymidine-5'-Succinamic Acid, Methyl ester (IV-169). Mono methyl succinate (Aldrich, 132 mg, 1.0 mmol) was dissolved in 1 mL DMF and treated with HOBT (270 mg, 2.0 mmol) and DCC (230 mg, 1.1 mmol). The resulting mixture was stirred 30 min at RT and then added to a solution of 5'-aminothymidine²³ (241 mg, 1.0 mmol) in 4 mL DMF. The coupling reaction was stirred overnight at RT, filtered, and the solvent distilled *in vacuo*. The residue was chromatographed on silica gel using 0-5% MeOH/CH₂Cl₂ eluent to afford 0.17 g (9.48 mmol, 48%) of IV-169 as a solid. ¹H NMR δ 11.26 (s, 1H), 8.04 (t, 1H), 7.45 (s, 1H), 6.10 (t, 1H), 5.24 (d, 1H), 4.10 (br s, 1H), 3.69 (br s, 1H), 3.53 (s, 3H), 3.3 (m, 2H), 2.48 (m, 2H), 2.36 (m, 2H), 2.04 (m, 2H), 1.77 (s, 3H).

Thymidine-5'-Succinamic Acid, Methyl ester Phosphoramidite (IV-180).

IV-169 (107 mg, 0.30 mmol) was dissolved in 5 mL 1:1 CH₂Cl₂:DMF and treated with *N,N*-diisopropylethylamine (3.0 equiv. at a time) and 2-cyanoethyl-*N,N*-diisopropylchlorophosphoramidite (Aldrich, 1.5 equiv. at a time). The reaction was stirred at RT and reagents were added until tlc (10% MeOH/CH₂Cl₂ eluent) indicated complete loss of **IV-169** starting material. The mixture was diluted with 25 mL EtOAc, washed with 2 X 20 mL 10% NaHCO₃ solution, 2 X 20 mL saturated NaCl solution, dried over Na₂SO₄, filtered, and concentrated *in vacuo*. The residue was chromatographed on a 15 X 2 cm column of silica gel using 1% Et₃N in CH₂Cl₂ followed by 1% Et₃N in 1:50 MeOH:CH₂Cl₂ eluents to afford homogeneous phosphoramidite which produced a foam upon concentration from CH₂Cl₂ *in vacuo*. This material was dissolved in dry CH₃CN (0.1 M) and placed on the Beckman System 1 Plus DNA synthesizer for the preparation of oligonucleotides shown in Figure 5.2.

DNA MANIPULATIONS²⁴

General. Distilled, deionized water was used for all aqueous reactions and dilutions. Enzymes were purchased from either Boehringer-Mannheim or New England Biolabs and were stored and used under conditions of temperature, buffer, etc. recommended by the manufacturer. Deoxynucleoside triphosphates were purchased from Pharmacia as 100 mM solutions. 5'-[α -³²P]dNTPs (3000 Ci/mmol) and 5'-[γ -³²P]ATP (>5000 Ci/mmol) were obtained from Amersham. DNA reactions were in general carried out in 1.5 mL polypropylene tubes obtained from West Coast Scientific. Calf thymus DNA was purchased from Sigma, sonicated, and then extracted with 3 X 0.2 volumes (vol.) water-saturated phenol, 0.2 vol. 24:1 CHCl₃:isoamyl alcohol, and 0.2 vol. CHCl₃. After extensive dialysis against H₂O, the DNA was passed through a 0.45 μ Centrex filter (Schleicher and Schuell) and assayed for concentration by UV (assuming ϵ_{260} 11,800

$\text{Lmol}^{-1}\text{bp}^{-1}\text{cm}^{-1}$. DNA was precipitated from either 1:3 0.3 M NaOAc (pH 5.2):EtOH or 1:2 2.5 M NH_4OAc :EtOH. DNA pellets were dried in a Savant Speed Vac. Agarose gel electrophoresis was carried out using 40 mM Tris acetate, 5 mM NaOAc, 1 mM EDTA, pH 7.9 buffer. Tenfold concentrated (10X) loading buffer for agarose gels was 25% (w/v) ficoll solution that contained 0.2% (w/v) bromophenol blue (BPB) and xylene cyanol (XC) tracking dyes. Polyacrylamide gel electrophoresis was carried out using 100 mM Tris borate, 1 mM EDTA, pH 8.3 buffer. Loading buffer for denaturing polyacrylamide gels was 80% formamide in 100 mM Tris borate, 1 mM EDTA, pH 8.3 buffer. Specific radioactivity was measured with a Beckman LS 3801 scintillation counter. Gels were dried (after transferring them to Whatman 3 MM paper) on a Bio-Rad Model 483 slab drier at 80°C. Autoradiography was carried out without intensifier screens, using Kodak X-Omat film. In most cases the photographic emulsion on the side of the film away from the gel was removed with bleach in order to obtain sharper images and higher contrast. Optical densitometry was performed using an LKB Bromma Ultroncan XL Laser Densitometer operating at 633 nm. Relative peak area for each cleavage band or locus was equated to the relative cleavage efficiency at that site.

Preparation of ^{32}P End-Labeled DNA Restriction Fragments.

Procedure for the Preparation of Sty I-Linearized, 3'- ^{32}P End-Labeled pBR322 Plasmid DNA. 30 μg pBR322 plasmid DNA was precipitated from NaOAc/EtOH, washed with 70% EtOH, and dried. The pellet was dissolved in 155 μL H_2O , treated with 20 μL 10X high salt restriction enzyme buffer (Boehringer-Mannheim), 20 μL 0.7% (v/v) mercaptoethanol, and 5 μL Sty I (50 u). The digest was incubated 2 h at 37°C, then extracted with 200 μL water-saturated phenol, 3 X 900 μL Et_2O , precipitated from NaOAc/EtOH, washed with 70% EtOH, and dried. The pellet was dissolved in 10 μL 10X Hae III buffer (10X = 60 mM Tris-HCl, 500 mM NaCl, 60 mM MgCl_2 , pH 7.4),

32 μ L H₂O, 10 μ L 10 mg/mL DTT, 10 μ L 10 mM dGTP, and 10 μ L 10 mM dCTP. The solution was divided into two 36 μ L portions. One portion was treated with 10 μ L 5'-[α -³²P] dATP and 4 μ L Klenow enzyme (20 u), while the other portion was treated with 10 μ L 5'-[α -³²P] TTP and 4 μ L Klenow enzyme. The 3' end-labeling reactions were incubated 15 min at RT before 1 μ L of each 10 mM dNTP was added to the reactions and the mixtures incubated an additional 5 min at RT. The end-labeled DNA was precipitated from NH₄OAc/EtOH, washed with 70% EtOH, and dried. The pellets were dissolved in 2.5% ficoll loading buffer, heated 5 min at 65°C to insure resuspension, loaded onto a 20 cm long X 4 mm thick 1% agarose gel, and electrophoresed at 120-160 V until the BPB tracking dye was near the bottom of the gel. The bands of linearized, end-labeled plasmid DNA were visualized by autoradiography and excised from the gel. The DNA was eluted from the gel slices at 100 V using Schleicher and Schuell Elutrap and agarose gel buffer. The eluents were reduced in volume to 300 μ L by extraction with anhydrous 1-butanol. The DNA was recovered by precipitation from NH₄OAc/EtOH, precipitation from NaOAc/EtOH, washing with 70% EtOH, and drying. The pellets were resuspended at 20,000 cpm/ μ L in H₂O and stored frozen at -20°C before use.

Molecular weight standards were prepared by digesting four separate mixtures of 100,000 cpm dATP-labeled plasmid mixed with 100,000 cpm TTP-labeled plasmid with Bam HI, Eco RI, Pvu I, and Xmn I. Each digest (100 μ L final volume) contained end-labeled DNA (200,000 cpm), the appropriate restriction enzyme buffer, 1 μ g λ -phage DNA (Boehringer-Mannheim), 5 mM mercaptoethanol, and 1 μ L restriction enzyme. The digests were incubated 2 h at 37°C, precipitated from NaOAc/EtOH, washed with 70% EtOH, and dried. The pellets were resuspended at 1000 cpm/ μ L in 2.5% ficoll loading buffer. These solutions and uncleaved DNA were then combined and diluted with 2.5% ficoll loading buffer to produce a molecular weight marker cocktail in which 20 μ L (the volume loaded onto gels) contained 500 cpm of each radioactive fragment.

Procedure for the Preparation of 3'- and 5'-³²P End-Labeled 517 and 167 Base Pair Eco RI/Rsa I DNA Restriction Fragments. 30 μ g pBR322 plasmid DNA was precipitated from NaOAc/EtOH, washed with 70% EtOH, and dried. The pellet was redissolved in 20 μ L 10X Eco RI restriction enzyme buffer (Boehringer-Mannheim), 20 μ L 10 mg/mL DTT, and 55 μ L H₂O. Eco RI (5 μ L, 50 u) were added and the digest incubated 2 h at 37°C before being extracted, precipitated, washed and dried as described for the Sty I digestion of pBR322. The pellet was dissolved in 42 μ L H₂O and divided into two 21 μ L protions. One portion was treated with 10 μ L 10X phosphatase buffer (10X = 500 mM Tris-HCl, 1 mM EDTA, pH 8.0), 66 μ L H₂O, and 3 μ L calf alkaline phosphatase (66 u). The digest was incubated 1 h at 37°C before being extracted, precipitated, washed, and dried as described for the Sty I digestion of pBR322. This pellet was dissolved in 28 μ L H₂O, 5 μ L 10X kinase buffer (10X = 700 mM Tris-HCl, 100 mM MgCl₂, 1 mM spermidine, 1 mM EDTA, pH 7.6), and 5 μ L 10 mg/mL DTT. This solution was treated with 10 μ L 5'-[α -³²P]ATP and 2 μ L T4 Polynucleotide Kinase (20 u). The 5' end-labeling was allowed to proceed 45 min at 37°C. The second 21 μ L portion of Eco RI-linearized pBR322 was treated with 5 μ L 10X Hae III buffer, 5 μ L 10 mM TTP, 5 μ L 10 mg/mL DTT, 10 μ L 5'-[α -³²P]dATP, and 4 μ L Klenow enzyme (20 u). The 3' end-labeling was allowed to proceed 15 min at RT before 1 μ L of each 10 mM dNTP was added and the mixture incubated an additional 5 min at RT. The end-labeling reactions were precipitated from NH₄OAc/EtOH, washed with 70% EtOH, and dried. The pellets were dissolved in 33 μ L H₂O, 5 μ L low salt restriction enzyme buffer (Boehringer-Mannheim), 5 μ L 10 mg/mL DTT, and treated with 7 μ L Rsa I (70 u). The digests were incubated 3 h at 37°C, treated with 5 μ L 25% ficoll loading buffer, loaded onto a 15 cm long X 2 mm thick 1:20 cross-linked 5% polyacrylamide gel and electrophoresed at 240 V until the BPB tracking dye was near the bottom of the gel. The four bands of end-labeled DNA were visualized by autoradiography, excised from the gel, crushed, transferred to 1.5 mL polypropylene tubes, treated with 1 mL elution buffer (500 mM NH₄OAc, 10 mM

MgCl_2 , 1 mM EDTA, 0.25% sodium dodecyl sulfate) and shaken overnight at 37°C. The end-labeled DNA restriction fragments were recovered by passing the eluents through a 0.45 μ Centrex filter, extracting with 500 μL water-saturated phenol, reducing the volume of the eluents to 300 μL by extraction with anhydrous 1-butanol, precipitating from $\text{NH}_4\text{OAc}/\text{EtOH}$, precipitating from NaOAc/EtOH , washing with 70% EtOH, and drying. The pellets were resuspended at 20,000 cpm in H_2O and the DNA stored frozen at -20°C before use.

Procedure for the Preparation of 3'- ^{32}P End-Labeled 169 Base Pair Dde I pBR322 DNA Restriction Fragments. Two 30 μg portions of pBR322 plasmid DNA were precipitated from NaOAc/EtOH , washed, and dried. The pellets were dissolved in 82 μL H_2O , 10 μL high salt restriction enzyme buffer (Boehringer-Mannheim), and treated with 8 μL Dde I (48 u). The digests were incubated 3 h at 37°C, then treated with 10 μL 25% ficoll loading buffer, loaded onto a 20 cm long X 2 mm thick 1:20 cross-linked 5% polyacrylamide gel and electrophoresed at 240 V and 4°C until the BPB tracking dye reached the bottom of the gel. DNA restriction fragment bands were visualized by staining with 50 μL 10 mg/mL Ethidium Bromide. The desired 166 bp fragment (second-fastest running band) was carefully separated from the fastest-running 162 bp fragment. The 166 bp fragment was recovered from the gel slices as described in the preparation of 3'- and 5'- ^{32}P end-labeled 167 and 517 bp restriction fragments. The two pellets obtained after precipitation, washing, and drying were each dissolved in 5 μL 10X Hae III buffer, 11 μL H_2O , 5 μL 10 mg/mL DTT, 5 μL 100 mM dATP, and 5 μL 10 mM TTP. One solution was treated with 5 μL 10 mM dCTP, 10 μL 5'-[α - ^{32}P]dGTP, and 4 μL Klenow enzyme (20 u). The other solution was treated with 5 μL 10 mM dGTP, 10 μL 5'-[α - ^{32}P]dCTP, and 4 μL Klenow enzyme (20 u). The 3' end-labeling reactions were incubated 15 min at RT, treated with 1 μL of each 10 mM dNTP, and incubated 5 additional min at RT. The reactions were precipitated from $\text{NH}_4\text{OAc}/\text{EtOH}$, washed with 70% EtOH, and dried. The

pellets were dissolved in 2.5% ficoll loading buffer, loaded onto a 20 cm long X 2 mm thick 1:20 cross-linked 10% polyacrylamide gel and electrophoresed at 4°C and 240 V until the XC tracking dye had migrated 15 cm. The bands were visualized by staining with Ethidium Bromide, and were then excised and recovered from the gel slices as described in the preparation of 3'- and 5'-³²P end-labeled 167 and 517 bp DNA restriction fragments. The pellets obtained after precipitation, washing, and drying were dissolved at 20,000 cpm/μL and stored frozen at -20°C before use.

Procedure for Maxam-Gilbert Chemical Sequencing G Reactions.²⁵ 5 μL ³²P end-labeled DNA restriction fragment was treated with 1.5 μL 1 mM bp calf thymus DNA and 200 μL start buffer containing 50 mM sodium cacodylate, pH 8.0, 10 mM MgCl₂, and 1 mM EDTA. The solution was cooled in an ice/water bath and treated with 1 μL dimethylsulfate. The mixture was vortexed and placed in a RT water bath for 0-8 min (depending on the length of the DNA restriction fragment). The reaction was quenched by adding 50 μL stop buffer (containing 19 μL 4 M NaOAc (pH 5.2), 3.6 μL mercaptoethanol, 2.4 μL 2 mg/mL tRNA (Sigma), and 25 μL H₂O) and 750 μL EtOH. The DNA was precipitated, washed with 70% EtOH, and dried. The pellet was dissolved in 100 μL 10% (v/v) piperidine and heated 30 min at 90°C. The mixture was then frozen, lyophilized, treated with 10 μL H₂O, frozen, lyophilized, treated with 10 μL H₂O, frozen, and lyophilized again. The pellet was resuspended at 5,000 cpm/μL in 80% formamide loading buffer and stored at -20°C before use.

Procedure for Maxam-Gilbert Chemical Sequencing G+A Reactions.²⁵ 5 μL ³²P end-labeled DNA restriction fragment was treated with 5 μL H₂O and 25 μL formic acid. The reaction was incubated 4 min at RT, treated with 2.4 μL 2 mg/mL tRNA, precipitated from NaOAc/EtOH, washed with 70% EtOH, and dried. The pellet was

treated with piperidine, lyophilized, resuspended, and stored as described for the Maxam-Gilbert G reaction.

General Procedure for DNA Cleavage Reactions with Bis(Netropsin)-EDTA:Fe Compounds (Figures 1.15, 1.16, 1.19-1.21, 2.15-2.18, 2.23-2.26, 3.4, 3.28, 3.32, 3.34, 4.8). 3 μ L Bis(Netropsin)-EDTA:Fe compound solution (prepared by mixing equal volumes of 1mM Bis(Netropsin)-EDTA compound and 1 mM $(\text{NH}_4)_2\text{Fe}(\text{SO}_4)_2 \cdot 6\text{H}_2\text{O}$ or $(\text{NH}_4)\text{Fe}(\text{SO}_4)_2 \cdot 12\text{H}_2\text{O}$ and diluting) was added to 9 μ L of a solution containing ^{32}P end-labeled DNA restriction fragment (10,000-30,000 cpm), calf thymus DNA, and sodium acetate in Tris acetate buffer (pH values are given in figure legends). After equilibrating 1 h at 37°C, DNA cleavage was initiated by the addition of 3 μ L dithiothreitol solution. Final concentrations in 15 μ L total volume were: Bis(Netropsin)-EDTA:Fe compound, as given in the figure legends; calf thymus DNA, 100 μ M bp; NaOAc, 5 mM; Tris, 40 mM; DTT, 5 mM. DNA cleavage was allowed to proceed 2 h at 37°C before DNA cleavage products were separated by gel electrophoresis. For studies of DNA double strand cleavage, cleavage reactions were treated with 3 μ L 25% ficoll loading buffer, loaded onto a 20 cm long X 4 mm thick 1% agarose gel, and electrophoresed at 120-160 V until the BPB tracking dye reached the bottom of the gel. The gel was then dried and autoradiographed. For high-resolution DNA cleavage studies, cleavage reactions were terminated by freezing and lyophilization or by precipitation from NaOAc/EtOH, washing with 70% EtOH, and drying. The resulting pellets were resuspended in 5 μ L 80% formamide loading buffer, heat-denatured 2 min at 100°C, loaded onto a 40 cm long X 0.25-0.6 mm thick 1:20 cross-linked 8% polyacrylamide, 45% urea gel and electrophoresed at 1200-2000 V until the BPB tracking dye reached the bottom of the gel. The gel was then dried and autoradiographed.

General Procedure for DNA Cleavage Reactions with Bis(Netropsin) Polyether-EDTA:Fe Compounds in the Presence of Metal Ions (Figures 3.5, 3.17, 3.19, 3.21).¹ 3 μ L Bis(Netropsin) Polyether-EDTA:Fe compound solution (prepared by mixing equal volumes of 1 mM Bis(Netropsin) Polyether-EDTA compound and 1 mM $(\text{NH}_4)_2\text{Fe}(\text{SO}_4)_2 \cdot 6\text{H}_2\text{O}$ or $(\text{NH}_4)\text{Fe}(\text{SO}_4)_2 \cdot 12\text{H}_2\text{O}$ and diluting) was added to 6 μ L of a solution containing ^{32}P end-labeled DNA restriction fragment (10,000-30,000 cpm) and calf thymus DNA in Tris acetate buffer (pH values are given in the figure legends). 3 μ L metal cation solution was added and the mixture equilibrated 1 h at 37°C. DNA cleavage was initiated by the addition of 3 μ L dithiothreitol solution. Final concentrations in 15 μ L total volume were: Bis(Netropsin) Polyether-EDTA:Fe compound, as given in the figure legends; metal cation, as given in the figure legends; calf thymus DNA, 100 μ M bp; Tris, 40 mM; DTT, 5 mM. DNA cleavage was allowed to proceed 2 h at 37°C before the reactions were precipitated from NaOAc/EtOH, washed with 70% EtOH, dried, and the DNA cleavage products separated by gel electrophoresis. For studies of DNA double strand cleavage, the pellets were dissolved in 15 μ L 2.5% ficoll loading buffer, electrophoresed, and visualized as described for Bis(Netropsin)-EDTA:Fe compounds. For high-resolution DNA cleavage studies, the pellets were resuspended, heat-denatured, electrophoresed, and visualized as described for Bis(Netropsin)-EDTA:Fe compounds.

General Procedure for Control Studies of DNA Cleavage by P5E:Fe in the Presence of Metal Cations (Figures 3.7-3.15). 3 μ L 3.75 μ M P5E:Fe (prepared by mixing equal volumes of 1 mM P5E and $(\text{NH}_4)_2\text{Fe}(\text{SO}_4)_2 \cdot 6\text{H}_2\text{O}$ or $(\text{NH}_4)\text{Fe}(\text{SO}_4)_2 \cdot 12\text{H}_2\text{O}$ and diluting) was added to 6 μ L of a solution containing ^{32}P end-labeled DNA restriction fragment (10,000-30,000 cpm) and calf thymus DNA in Tris acetate buffer (pH 7.9). 3 μ L 5.0 or 0.5 mM metal cation solution was added and this mixture equilibrated 1 h at 37°C. DNA cleavage was initiated by the addition of 3 μ L

dithiothreitol solution. Final concentrations in 15 μ L total volume were: **P5E:Fe**, 0.75 μ M; metal cation, 1.0 or 0.1 mM; calf thymus DNA, 100 μ M bp; Tris, 40 mM; DTT or Asc, 5 mM. DNA cleavage was allowed to proceed 2 h at 37°C before DNA cleavage products were separated by agarose gel electrophoresis and visualized as described for Bis(Netropsin)-EDTA:Fe compounds.

General Procedure for DNA Cleavage Reactions with Bis(Netropsin) Polyamine-EDTA:Fe Compounds at Different pH Values (Figure 3.29). 10.5 μ L of a solution containing 32 P end-labeled DNA restriction fragment (10,000-30,000 cpm), calf thymus DNA, and Bis(Netropsin) Polyamine-EDTA:Fe compound solution (prepared by mixing equal volumes of 1 mM Bis(Netropsin) Polyamine-EDTA compound and 1 mM $(\text{NH}_4)\text{Fe}(\text{SO}_4)_2 \cdot 12\text{H}_2\text{O}$, diluting, and combining with the other ingredients) was treated with 1.5 μ L 10X Tris acetate buffer (10X = 400 mM Tris at pH values given in the figure legend). This mixture was equilibrated 1 h at 37°C. DNA cleavage was initiated by the addition of 3 μ L dithiothreitol solution. Final concentrations in 15 μ L total volume were: Bis(Netropsin) Polyamine-EDTA:Fe compound, as given in the figure legend; calf thymus DNA, 100 μ M bp; Tris, 40 mM; DTT, 5 mM. DNA cleavage was allowed to proceed 2 h at 37°C before DNA cleavage products were separated by agarose gel electrophoresis and visualized as described for Bis(Netropsin)-EDTA:Fe compounds.

General Procedure for DNA Cleavage Reactions with Bis(Netropsin) Polyamine-EDTA:Fe Compounds After Pre-Equilibration with Pd(II) Cations (Figure 3.36). 3 μ L 1 mM Bis(Netropsin) Polyamine-EDTA:Fe compound (prepared by mixing equal volumes of 2 mM Bis(Netropsin) Polyamine-EDTA compound and 2 mM $(\text{NH}_4)\text{Fe}(\text{SO}_4)_2 \cdot 12\text{H}_2\text{O}$) was treated with 3 μ L K_2PdCl_4 solution and the mixture incubated 1 h at RT or 37°C. The mixture was then diluted and 3 μ L was added to 9 μ L of a solution containing 32 P end-labeled DNA restriction fragment (10,000-30,000

cpm) and calf thymus DNA in Tris acetate buffer (pH values are given in the figure legend). This mixture was equilibrated 1 h at 37°C. DNA cleavage was initiated by the addition of 3 μ L ascorbic acid solution. Final concentrations in 15 μ L total volume were: Bis(Netropsin) Polyamine-EDTA:Fe compound, as given in the figure legend; K₂PdCl₄, as given in the figure legend; calf thymus DNA, 100 μ M bp; Tris, 40 mM; Asc, 5 mM. DNA cleavage was allowed to proceed 2 h at 37°C before DNA cleavage products were separated by agarose gel electrophoresis and visualized as described for Bis(Netropsin)-EDTA:Fe compounds.

Procedure for DNA Cleavage Reactions with [SalenMn(III)]OAc at Different Concentrations (Figure 4.3). 3 μ L [SalenMn(III)]OAc solution was added to 9 μ L of a solution containing ³²P end-labeled DNA restriction fragment (10,000-30,000 cpm) and calf thymus DNA in Tris acetate buffer (pH 7.9). This mixture was equilibrated 30 min at 37°C. DNA cleavage was initiated by the addition of 3 μ L hydrogen peroxide solution. Final concentrations in 15 μ L total volume were: [SalenMn(III)]OAc, as given in the figure legend; calf thymus DNA, 100 μ M bp; Tris, 40 mM; H₂O₂, 1 mM. DNA cleavage was allowed to proceed 2 h at 37°C before DNA cleavage products were separated by agarose gel electrophoresis and visualized as described for Bis(Netropsin)-EDTA:Fe compounds.

Procedure for DNA Cleavage Reactions with [SalenMn(III)]OAc Using Different Oxidants (Figure 4.4). 3 μ L 100 μ M [SalenMn(III)]OAc was added to 9 μ L of a solution containing ³²P end-labeled DNA restriction fragment (10,000-30,000 cpm) and calf thymus DNA in Tris acetate buffer (pH 7.9). This mixture was equilibrated 30 min at 37°C. DNA cleavage was initiated by the addition of 3 μ L oxidant (hydrogen peroxide, magnesium monoperoxyphthalic acid, or iodosylbenzene) solution. Final concentrations in 15 μ L total volume were: [SalenMn(III)]OAc, 20 μ M; calf thymus

DNA, 100 μ M bp; Tris, 40 mM; oxidant, 0.1, 1.0, or 10 mM. DNA cleavage was allowed to proceed 2 h at 37°C before DNA cleavage products were separated by agarose gel electrophoresis and visualized as described for Bis(Netropsin)-EDTA:Fe compounds.

Procedure for DNA Cleavage Reactions with [SalenMn(III)]OAc at Different pH Values (Figure 4.5). 10.5 μ L of a solution containing [SalenMn(III)]OAc, 32 P end-labeled DNA restriction fragment (10,000-30,000 cpm), and calf thymus DNA was treated with 1.5 μ L 10X Tris acetate buffer (pH values are given in the figure legend). This mixture was equilibrated 30 min at 37°C. DNA cleavage was initiated by the addition of 3 μ L magnesium monoperoxyphthalic acid solution. Final concentrations in 15 μ L total volume were: [SalenMn(III)]OAc, 15 μ M; calf thymus DNA, 100 μ M bp; Tris, 40 mM; Mg(MPPA)₂, 2 mM. DNA cleavage was allowed to proceed 2 h at 37°C before DNA cleavage products were separated by agarose gel electrophoresis and visualized as described for Bis(Netropsin)-EDTA:Fe compounds.

Procedure for DNA Cleavage Reactions with [SalenMn(III)]OAc, DE:Fe, NCZS, MPE:Fe, and Blm:Fe (Figures 4.7, 4.8, 4.10-4.12). [SalenMn(III)]OAc. 3 μ L 100 μ M [SalenMn(III)]OAc was added to 9 μ L of a solution containing 32 P end-labeled DNA restriction fragment (10,000-30,000 cpm) and calf thymus DNA in Tris acetate buffer (pH 7.5). This mixture was equilibrated 30 min at 37°C. DNA cleavage was initiated by the addition of 3 μ L hydrogen peroxide or magnesium monoperoxyphthalic acid solution. Final concentrations in 15 μ L total volume were: [SalenMn(III)]OAc, 20 μ M; calf thymus DNA, 100 μ M bp; Tris, 40 mM; oxidant, 1 mM. DNA cleavage was allowed to proceed 2 h at 37°C. DE:Fe. 3 μ L 50 μ M DE:Fe (prepared by mixing equal volumes of 1 mM DE and 1 mM (NH₄)Fe(SO₄)₂·12H₂O and diluting) was added to 9 μ L of a solution containing 32 P end-labeled DNA restriction fragment (10,000-30,000 cpm) and calf thymus DNA in Tris

acetate buffer (pH 7.5). This mixture was equilibrated 30 min at 37°C. DNA cleavage was initiated by the addition of 3 μ L dithiothreitol solution. Final concentrations in 15 μ L total volume were: **DE:Fe**, 10 μ M; calf thymus DNA, 100 μ M bp; Tris, 40 mM; DTT, 5 mM. DNA cleavage was allowed to proceed 2 h at 37°C. **NCZS**. 3 μ L **NCZS Holocomplex** solution (obtained from Bristol Labs) was added to 12 μ L of a solution containing 32 P end-labeled DNA restriction fragment (10,000-30,000 cpm), calf thymus DNA, and mercaptoethanol in Tris acetate buffer (pH 7.5). Final concentrations in 15 μ L total volume were: **NCZS**, as given in the figure legends; calf thymus DNA, 100 μ M bp; Tris, 40 mM; HSCH₂CH₂OH, 10 mM. The DNA cleavage reaction was allowed to proceed 2 h at 37°C. **MPE:Fe**. 3 μ L **MPE:Fe** solution (prepared by mixing equal volumes of 1 mM **MPE** and 1 mM (NH₄)₂Fe(SO₄)₂·12H₂O and diluting) was added to 9 μ L of a solution containing 32 P end-labeled DNA restriction fragment (10,000-30,000 cpm) and calf thymus DNA in Tris acetate buffer (pH 7.5). This mixture was equilibrated 30 min at 37°C. DNA cleavage was initiated by the addition of 3 μ L dithiothreitol solution. Final concentrations in 15 μ L total volume were: **MPE:Fe**, as given in the figure legends; calf thymus DNA, 100 μ M bp; Tris, 40 mM; DTT, 5 mM. DNA cleavage was allowed to proceed 30 min at RT. **Blm:Fe**. 3 μ L **Blm:Fe(II)** solution (prepared by mixing equal volumes of 1 mM **Blm** and 1 mM (NH₄)₂Fe(SO₄)₂·6H₂O and diluting) was added to 12 μ L of a solution containing 32 P end-labeled DNA restriction fragment (10,000-30,000 cpm) and calf thymus DNA in Tris acetate buffer (pH 7.5). Final concentrations in 15 μ L total volume were: **Blm:Fe**, as given in the figure legends; calf thymus DNA, 100 μ M bp; Tris, 40 mM. DNA cleavage was allowed to proceed 30 min at 37°C. DNA cleavage products were separated by agarose gel electrophoresis and visualized as described for Bis(Netropsin)-EDTA:Fe compounds.

Procedure for DNA Cleavage Reactions with [SalenMn(III)]OAc and MPE:Fe in the Absence and Presence of Dioxygen and With and Without Base Workup (Figures 4.13, 4.17, 4.18). For studies of cleavage in the absence and presence of dioxygen (Figure 4.12), reactions were run in duplicate with one reaction of each pair being carried out under ambient dioxygen concentration and the other reaction being degassed several times on a vacuum line prior to the initiation of DNA cleavage. DNA cleavage was carried out under an atmosphere of argon. **[SalenMn(III)]OAc.** 6 μ L [SalenMn(III)]OAc solution was added to 18 μ L of a solution containing 32 P end-labeled DNA restriction fragment (100,000 cpm) and calf thymus DNA in Tris acetate buffer (pH 7.0). This mixture was equilibrated 30 min 37°C. DNA cleavage was initiated by the addition of 6 μ L magnesium monoperoxyphthalic acid solution. Final concentrations in 30 μ L total volume were: **[SalenMn(III)]OAc**, as given in the figure legends; calf thymus DNA, 100 μ M bp; Tris, 40 mM; Mg(MPPA)₂, 2 mM. DNA cleavage was allowed to proceed 30 min at RT before the reaction was divided into two equal portions, precipitated from NaOAc/EtOH, washed with 70% EtOH, and dried. One pellet was dissolved in 50 μ L 0.1 M NaOH, heated 30 min at 90°C, neutralized by the addition of 4 μ L 10% HOAc solution, precipitated from NaOAc/EtOH, washed with 70% EtOH, and dried. **MPE:Fe.** 6 μ L MPE:Fe solution (prepared by mixing equal volumes of 1 mM MPE and 1 mM (NH₄)Fe(SO₄)₂·12H₂O and diluting) was added to 18 μ L of a solution containing 32 P end-labeled DNA restriction fragment (100,000 cpm) and calf thymus DNA in Tris acetate buffer (pH 7.5). This mixture was equilibrated 30 min at 37°C. DNA cleavage was initiated by the addition of 6 μ L dithiothreitol solution. Final concentrations in 30 μ L total volume were: **MPE:Fe**, 2.0 μ M; calf thymus DNA, 100 μ M bp; Tris, 40 mM; DTT, 5 mM. DNA cleavage was allowed to proceed 30 min at RT before the reaction was divided into two equal portions, precipitated from NaOAc/EtOH, washed with 70% EtOH, and dried. One pellet was dissolved in 50 μ L 0.1 M NaOH, heated 30 min at 90°C, neutralized by the addition of 4 μ L 10% HOAc solution, precipitated from NaOAc/EtOH,

washed with 70% EtOH, and dried. The pellets were resuspended, heat denatured, electrophoresed, and visualized as described for Bis(Netropsin)-EDTA compounds.

Procedure for Molecular Analysis of 3' End-Terminal Lesions Produced upon DNA Cleavage with [SalenMn(III)]OAc (Figure 4.13).⁴ 12 μ L 250 μ M [SalenMn(III)]OAc was added to 36 μ L of a solution containing 32 P end-labeled DNA restriction fragment (200,000 cpm) and calf thymus DNA in Tris acetate buffer (pH 7.0). This mixture was equilibrated 30 min at 37°C. DNA cleavage was initiated by the addition of 12 μ L magnesium monoperoxyphthalic acid solution. Final concentrations in 60 μ L total volume were: [SalenMn(III)]OAc, 50 μ M; calf thymus DNA, 100 μ M bp; Tris, 40 mM; Mg(MPPA)₂, 2 mM. DNA cleavage was allowed to proceed 2 h at 37°C before the reaction was divided into four 15 μ L aliquots, which were precipitated from NaOAc/EtOH, washed with 70% EtOH, and dried. Two pellets were dissolved in 50 μ L 0.1 M NaOH, heated 30 min at 90°C, neutralized by the addition of 4 μ L 10% HOAc solution, precipitated from NaOAc/EtOH, washed with 70% EtOH, and dried. One of these pellets and one pellet that had not been worked up with base were dissolved in 43 μ L H₂O, and treated with 5 μ L 10X kinase buffer, heated 5 min at 90°C, cooled to RT, and treated with 2 μ L (20 u) T4 Polynucleotide Kinase. The digest was incubated 1 h at 37°C, extracted with 50 μ L water-saturated phenol, extracted with 3 X 50 μ L Et₂O, precipitated from NaOAc/EtOH, washed with 70% EtOH, and dried. As controls, DNA incubated in the absence of cleaving agent was treated with base and subsequently with kinase as well. These reactions were carried out as described for cleavage/base workup/kinase digestion with [SalenMn(III)]OAc, except that the metal complex and oxidant were not included. DNA cleavage by MPE:Fe with and without subsequent kinase digestion was analyzed. 6 μ L 10 μ M MPE:Fe (prepared by mixing equal volumes of 1 mM MPE and 1 mM (NH₄)Fe(SO₄)₂·12H₂O and diluting) was added to 18 μ L of a solution containing 32 P end-labeled DNA restriction fragment (100,000 cpm) and calf thymus DNA in Tris acetate

buffer (pH 7.9). This mixture was equilibrated 30 min at 37°C. DNA cleavage was initiated by the addition of 6 µL dithiothreitol solution. Final concentrations in 30 µL total volume were: **MPE:Fe**, 2.0 µM; calf thymus DNA, 100 µM bp; Tris, 40 mM; DTT, 5 mM. DNA cleavage was allowed to proceed 30 min at RT before the reaction was divided into two equal portions, which were precipitated from NaOAc/EtOH, washed with 70% EtOH, and dried. One pellet was then digested with kinase and worked up as described for DNA cleaved by **[SalenMn(III)]OAc**. Each final pellet was resuspended at 10,000 cpm/µL in 80% formamide loading buffer, and heat-denatured 2 min at 100°C. 4 µL of each sample was loaded onto a 40 cm long X 0.4 mm thick 1:20 cross-linked 20% polyacrylamide, 45% urea gel and electrophoresed at 1800 V until the BPB tracking dye reached the bottom of the gel. The gel was then autoradiographed at -78°C without drying.

Procedure for Molecular Analysis of 5' End-Terminal Lesions Produced upon DNA Cleavage with **[SalenMn(III)]OAc (Figure 4.14).⁴** 12 µL 250 µM **[SalenMn(III)]OAc** was added to 36 µL of a solution containing ³²P end-labeled DNA restriction fragment (200,000 cpm) and calf thymus DNA in Tris acetate buffer (pH 7.0). This mixture was equilibrated 30 min at 37°C. DNA cleavage was initiated by the addition of 12 µL magnesium monoperoxyphthalic acid solution. Final concentrations in 60 µL total volume were: **[SalenMn(III)]OAc**, 50 µM; calf thymus DNA, 100 µM bp; Tris, 40 mM; Mg(MPPA)₂, 2 mM. DNA cleavage was allowed to proceed 2 h at 37°C before the reactions were divided into four 15 µL aliquots, which were precipitated from NaOAc/EtOH, washed with 70% EtOH, and dried. Two pellets were dissolved in 50 µL 0.1 M NaOH, heated 30 min at 90°C, neutralized by the addition of 4 µL 10% HOAc solution, precipitated from NaOAc/EtOH, washed with 70% EtOH, and dried. One of these pellets and one pellet that had not been worked up with base were dissolved in 80 µL H₂O, treated with 10 µL 10X phosphatase buffer (10X = 400 mM Tris-HCl, 5 mM NaOAc, pH 7.8), heated 5 min at 90°C, cooled to RT, and treated with 10 µL (10 u) Calf Alkaline

Phosphatase. The digest was incubated 1 h at 37°C, extracted with 50 μ L water-saturated phenol, extracted with 3 X 50 μ L Et₂O, precipitated from NaOAc/EtOH, washed with 70% EtOH, and dried. As controls, DNA incubated in the absence of a cleaving agent was treated with base and subsequently with CAP as well. These reactions were carried out as described for cleavage/base workup/CAP digestion with [SalenMn(III)]OAc, except that the metal complex and oxidant were not included. DNA cleavage by MPE:Fe with and without subsequent CAP digestion was also analyzed. 6 μ L 10 μ M MPE:Fe (prepared by mixing equal volumes of 1 mM MPE and 1 mM (NH₄)Fe(SO₄)₂·12H₂O and diluting) was added to 18 μ L of a solution containing ³²P end-labeled DNA restriction fragment (100,000 cpm) and calf thymus DNA in Tris acetate buffer (pH 7.9). This mixture was equilibrated 30 min at 37°C. DNA cleavage was initiated by the addition of 6 μ L dithiothreitol solution. Final concentrations in 30 μ L total volume were: MPE:Fe, 2.0 μ M; calf thymus DNA, 100 μ M bp; Tris, 40 mM; DTT, 5 mM. DNA cleavage was allowed to proceed 30 min at RT before the reactions were divided into two equal portions, which were precipitated from NaOAc/EtOH, washed with 70% EtOH, and dried. One pellet was then digested with CAP and worked up as described for DNA cleaved by [SalenMn(III)]OAc. The final pellets were resuspended, heat denatured, and electrophoresed as described for DNA cleaved by [SalenMn(III)]OAc.

Procedure for the Preparation of pBR322 Plasmid DNA. L-Broth. 10 g Bactotryptone (Difco), 5 g yeast extract (Difco), 10 g NaCl, and 50 mg thymine (Sigma) were dissolved in 700 mL H₂O and the pH was adjusted to 7.5 using 1 M NaOH. This solution was diluted to 1 L and autoclaved for 20 min. After cooling to below 60°C, the broth could be supplemented with 0.1% (v/v) of 50 mg/mL ampicillin (Amp, Sigma) or 15 mg/mL tetracycline·HCl (Tet, Sigma). L-Plates. 980 mL L-broth was poured into a flask containing 15 g Bacto-Agar (Difco). The mixture was autoclaved for 20 min, swirled gently to mix, and poured into sterile petri plates until they were 2/3 full. Adding Amp

and/or Tet to the L-broth/Agar mixture, once it had cooled below 60°C afforded Amp, Tet, or Amp/Tet plates. Plates were cooled to RT and then baked at 37°C until dry.

Escherichia Coli strain HB101 harboring plasmid pBR322 was selected on Amp/Tet plates. One colony was transferred by sterile wire into 5 mL Amp supplemented L-broth in a sterile 30 mL culture tube and swirled overnight at 37°C. 50 µL of this culture was transferred to 5 mL fresh L-broth and the culture grown again. Four mL of this stationary-phase culture was used to inoculate a large-scale growth medium in a 2 L flask. The large-scale growth medium was prepared by dissolving 2 g casamino acids (Difco), 25 mL 40X Vogel-Bonner salts (40X = 4 g MgSO₄·7H₂O, 40 g citric acid, 200 g K₂HPO₄, 70 g NaNH₄HPO₄·4H₂O in 355 mL H₂O), and 50 mL 1mg/mL thymine in 900 mL H₂O, autoclaving for 30 min, cooling to RT, then treating with 20 mL autoclaved 20% (w/v) glucose, 1 mL sterile filtered 50 mg/mL Amp, and 1 mL sterile filtered 1 mg/mL thiamine·HCl (Sigma). The large-scale culture was swirled at 37°C and 175 rpm until an OD₅₉₀ (relative to uninoculated broth) of 0.9 had been reached. The culture was then amplified by adding 2 mL 100 mg/mL chloramphenicol (chloromycetin sodium succinate, LymphoMed) solution and swirling overnight at 37°C.

The cells were then cooled 20 min on ice and pelleted by centrifugation at 4°C and 5000 rpm for 20 min. The pellets were resuspended in 25% (w/v) sucrose, 50 mM Tris·HCl, pH 8 buffer, transferred to polycarbonate 70Ti tubes, and treated with 1.6 mL 5 mg/mL lysozyme (Sigma). The mixture was incubated 5 min on ice with occasional stirring, then treated with 5 mL 0.5 M Na₂EDTA, pH 8 and incubated 5 additional min on ice with occasional stirring. The lysis was treated with 10% (w/v) Triton X-100 in 50 mM Tris·HCl, 60 mM EDTA, pH 8 buffer to almost fill the tube, which was then shaken vigorously for 1 min to clear the lysate. After centrifugation at 4°C and 30,000 rpm for 30 min, the supernatant was poured off (avoiding removal of viscous, yet clear material near the cell debris) into a 50 mL polypropylene centrifuge tube. The supernatant was treated with 350 µL DNase-free RNase (prepared by boiling 20 mg Ribonuclease A (Sigma) in

10 mL 10 mM Tris-HCl, 15 mM NaCl, pH 7.5 buffer for 15 min and then allowing the solution to cool slowly to RT) and incubated 20 min at 37°C. 10 mL 30% (w/v) PEG 8000, 1.5 M NaCl was added, and the tube mixed by inverting 10 times. The mixture was incubated 4 h on ice to precipitate DNA. The DNA was pelleted by centrifugation at 4°C and 6000 rpm for 20 min. The pellet was resuspended in 5 mL 100 mM Tris-HCl, 10 mM EDTA, pH 8 buffer with the aid of a sterile glass rod. This mixture was added to a solution of 29.76 g CsCl and 1.6 mL 10 mg/mL Ethidium Bromide in 10 mM Tris-HCl, 1mM EDTA, pH 8 buffer to give a total weight of 62 g ($\rho=1.55$). The solution was loaded into a 40 mL VTi 50 quickseal ultracentrifuge tube, balanced to ± 0.01 g against another tube, heat-sealed, and centrifuged at 17°C and 42,000 rpm for 20 h. The plasmid DNA (lower band) was visualized with the aid of a hand-held UV lamp and withdrawn using a 5 mL disposable syringe. This solution was loaded into a 5 mL quickseal ultracentrifuge tube, balanced to ± 0.01 g against another tube, heat-sealed, and centrifuged at 17°C and 55,000 rpm for 17 h. The band of plasmid DNA was withdrawn as before. Ethidium Bromide was removed by extraction with 10 X 1 vol. isoamyl alcohol (saturated with 10 mM Tris-HCl, 1 mM EDTA, pH 8 buffer. The DNA solution was then dialyzed extensively against 10 mM Tris-HCl, 1 mM EDTA, pH 8 buffer). The concentration of plasmid was determined by UV, assuming ϵ_{260} 11,800 Lmol⁻¹bp⁻¹cm⁻¹. The DNA was stored frozen at -80°C.

Preparation of Plasmids pJHG1-5.²⁶

Oligonucleotide Synthesis. Oligonucleotide synthesis was carried out on a Beckman System 1 Plus DNA synthesizer using solid-phase phosphite triester chemistry and commercially available nucleoside 3'- β -cyanoethyl-*N,N*-diisopropyl phosphoramidites or the thymidine-5'-succinamic acid derivative described in the experimental section. Oligonucleotides were deprotected and cleaved from the controlled pore glass support by treating the support containing the protected oligonucleotide with 1.5 mL concentrated

aqueous ammonia per μ mol oligonucleotide and heating at 55°C for 24 h in screw-cap plastic vials. The mixture was then decanted into a larger vial and the ammonia removed using a stream of argon. The remaining solution was frozen, lyophilized, resuspended in 200 μ L 80% formamide loading buffer and electrophoresed at 550-750 V on a 40 cm long X 2 mm thick 1:20 cross-linked 20% polyacrylamide, 45% urea denaturing gel until the BPB tracking dye was near the bottom of the gel. The oligonucleotide band was visualized by UV, cut out, crushed, and the DNA eluted at 37°C using 3 mL 0.1 M NaCl, 1 mM EDTA elution buffer per μ mol of oligonucleotide. The mixtures were filtered through 0.45 μ Centrex filters, and the filtrates dialyzed for several days against H₂O at 4°C with ~6 solvent changes. Oligonucleotide concentrations were determined by UV, using ϵ_{260} values calculated based on the sequences of the oligonucleotides.

For oligonucleotides bearing a thymidine-5'-succinamic acid terminus (Figure 5.2), the carboxylic acid group was protected as the methyl ester during synthesis. These oligonucleotides were deprotected at 55°C for 24 h using 0.1 N NaOH in place of concentrated aqueous ammonia. The mixtures were neutralized with HOAc and passed through 4 cm³ columns of G10-120 Sephadex (2 columns per μ mol oligonucleotide). The columns were washed with 2 X 200 mL H₂O. The combined filtrates were frozen, lyophilized, resuspended, purified by electrophoresis, visualized, excised, eluted, and dialyzed as described for unsubstituted oligonucleotides.

5'-Phosphorylation of oligonucleotides for transcriptional activation (Figure 5.2) was done on the DNA synthesizer, using a chemical phosphorylating reagent (Glen Research Corporation). 5'-Phosphorylation of oligonucleotides for plasmid construction (Figure 5.3) was done enzymatically. 500 pmol of oligonucleotide was treated with 20 μ L 10X kinase buffer, 20 μ L 100 mM DTT, 5 μ L 100 mM ATP (Pharmacia), and H₂O to afford 190 μ L total volume. 10 μ L T4 Polynucleotide Kinase (100 u) was added and the mixture incubated 2 h at 37°C. 2.5 μ L additional 100 mM ATP and 5 μ L additional kinase were then added and the mixture incubated 2 additional h at 37°C. The mixture was

extracted with 200 μ L water-saturated phenol, 200 μ L 1:1 water-saturated phenol:CHCl₃, 200 μ L CHCl₃, precipitated from NaOAc/isopropanol, washed with 70% EtOH, and dried. Phosphorylated oligonucleotide pellets were dissolved in 100 μ L 10 mM Tris-HCl, 100 mM NaCl, 1 mM EDTA, pH 8 buffer and combined with their complementary phosphorylated oligonucleotides. The resulting 200 μ L solutions were heated 5 min at 90°C and then cooled slowly to RT overnight in order to effect hybridization. Solutions of hybridized double-stranded oligonucleotides were stored frozen at -20°C before use.

pJHG1. 30 μ g plasmid pBR322 was digested with Bam HI followed by Hind III to produce a vector for insertion of synthetic double-stranded oligonucleotide **1** (Figure 5.3). The vector was stored frozen at -20°C in 100 μ L 10 mM Tris-HCl, 100 mM NaCl, 1 mM EDTA, pH 8 buffer before use. 50 μ L of this solution (containing 15 μ g DNA) was treated with 100 μ L (250 pmol) duplex **1**, 30 μ L 10X T4 DNA Ligase buffer (10X = 500 mM Tris-HCl, 100 mM MgCl₂, pH 7.8), 30 μ L 200 mM DTT, 3 μ L 100 mM ATP, 67 μ L H₂O, and 20 μ L T4 DNA Ligase (8000 u). The resulting solution was incubated 2 h at 16°C, treated with 10 μ L additional ligase and 3 μ L additional 100 mM ATP, and incubated 24 h at 16°C. The ligation mixture was extracted with 2 X 200 μ L water-saturated phenol, 200 μ L CHCl₃, precipitated from NaOAc/EtOH, washed with 70% EtOH, and dried. The pellet was redissolved in 100 μ L 10 mM Tris-HCl, 100 mM NaCl, 1 mM EDTA, pH 8 buffer. 15 μ L of this solution was digested with Hinc II and the products analyzed by 1% agarose minigel versus Hinc II-digested vector which had not been ligated. This indicated that DNA species of higher MW had been produced in the ligation reaction. The ligation mixture was then used to transform *E.Coli* strain HB101 cells. Transformation competent cells were prepared by growing a 100 mL culture of HB101 in L-broth until an OD₅₉₀ of 0.2 had been reached, chilling the culture on ice, pelleting the cells by centrifugation at 4°C and 8000 rpm for 5 min, resuspending the pellets with 8 mL 0.1 M CaCl₂, chilling the suspension 20 min on ice, pelleting the cells as

before, resuspending the pellet in 1 mL 0.1 M CaCl₂ and incubating the cells on ice overnight. 100 μ L of competent cells was treated with 9 μ L 10 mM Tris-HCl, 10 mM CaCl₂, 10 mM MgCl₂, pH 8 buffer, and 5 μ L of the ligation mixture. A parallel control transformation was also performed in which 5 μ L 10 mM Tris-HCl, 100 mM NaCl, 1 mM EDTA, pH 8 buffer was substituted for the 5 μ L of ligation mixture. The transformations were carried out in sterile 15 mL culture tubes, and were incubated 15 min on ice, 5 min at 37°C, and then 5 min at RT. 2 mL L-broth was added and the mixtures swirled 2 h at 30°C. 100 μ L aliquots of undiluted cultures and cultures diluted by 1:10, 1:100, and 1:1000 with L-broth were then spread onto L-plates and Amp plates and the cultures grown at 37°C. The control transformation cells showed strong growth on L-plates but no growth on Amp plates. The cells transformed with the pBR322 vector/Oligonucleotide **1** ligation mixture showed strong growth on L plates and reduced but significant growth on Amp plates. 50 Amp-resistant colonies were re-selected for growth on Amp plates and Tet plates. Removal of the smaller Bam HI/Hind III fragment from pBR322 disrupts the gene for Tet resistance. Four Amp-resistant, Tet-sensitive colonies were then transferred to liquid culture and subjected to large-scale growth and purification as described for pBR322. Maxam-Gilbert chemical sequencing (G and G+A reactions) of 3'- and 5'-³²P end-labeled Eco RI/Sal I restriction fragments (prepared as described for 3'- and 5'-³²P end-labeled 167 and 517 bp Eco RI/Rsa I restriction fragments) from each of the four plasmid preparations confirmed the expected **pJHG1** sequences.

pJHG2-5 were prepared following the procedures described for the preparation of **pJHG1**. The vector was obtained by sequential Hind III/Eco RI digest of four 30 μ g portions of **pJHG1**. 5'-phosphorylated duplex oligonucleotides **2-5** (Figure 5.3) were ligated into the vector. The ligation mixtures were transformed into competent HB101 cells, the transformation mixtures plated out, and colonies selected for Amp-resistance and Tet-sensitivity. Ten colonies from each transformation were grown in 5 mL L-broth overnight cultures for mini-plasmid prep analysis²⁴ in order to determine whether the Amp-

resistant, Tet-sensitive cells harbored the desired **pJHG2-5**, **pJHG1**, or **pJHG2-5** derivatives with more than one duplex inserted. Antibiotic resistance criteria could not distinguish among these possibilities. For each mini-plasmid prep, cells from 1.5 mL overnight culture were pelleted by centrifugation for 1 min at RT in a microcentrifuge. The pellet was treated with 100 μ L 50 mM glucose, 10 mM EDTA, 25 mM Tris base and vortexed 30 seconds at setting 7. After sitting 5 min at RT, 200 μ L 0.4 M NaOH, 2% (w/v) sodium dodecyl sulfate was added and the mixture vortexed 5 seconds at setting 3. After sitting 5 min on ice, 150 μ L 3 M NaOAc (pH 5.2) was added, the mixture was inverted 20 times to mix, and then cooled 5 min on ice. After centrifugation for 5 min at RT, the supernatant was transferred to a clean tube and extracted with 450 μ L 1:1 water-saturated phenol:CHCl₃. This supernatant was transferred to a clean tube and extracted with 200 μ L CHCl₃. 675 μ L isopropanol was added and the mixture cooled 15 min at -78°C. Nucleic acids were pelleted by centrifugation at 4°C for 10 min. The pellet was washed with 100 μ L 70% EtOH and dried. To degrade RNAs, the pellet was dissolved in 50 μ L 10 mM Tris-HCl, 1 mM EDTA, pH 8 buffer, treated with 3 μ L 2 mg/mL DNase-free RNase, and incubated 30 min at 37°C. 20 μ L of this solution was digested with Cla I and analyzed by 1% agarose minigel against undigested DNA to test for the insertion of oligonucleotides **2-5** (substitution of **2-5** for the smaller Hind III/Eco RI fragment of **pJHG1** affords a plasmid without the Cla I site). For each set of preps, the desired plasmid **pJHG2-5**, as well as **pJHG1** and dimeric **pJHG2-5** plasmids were observed by Cla I restriction/minigel analysis. Colonies harboring the desired plasmids were then transferred to liquid culture, grown on large scale, and isolated as described for pBR322. Maxam-Gilbert chemical sequencing (G and G+A reactions) of 3'- and 5'-³²P end-labeled Eco RI/Sal I restriction fragments confirmed the expected **pJHG2-5** sequences.

References

¹Youngquist, R.S., Ph.D. Thesis, California Institute of Technology, Pasadena, California, 1988.

²Bialer, M.; Yagen, B.; Mechoulam, R. *Tetrahedron* **1978**, *34*, 2389-2391.

³Taylor, J.S.; Schultz, P.G.; Dervan, P.B. *Tetrahedron* **1984**, *40*, 457-465.

⁴Hertzberg, R.P., Ph.D. Thesis, California Institute of Technology, Pasadena, California, 1984.

⁵Sluka, J.P., Ph.D. Thesis, California Institute of Technology, Pasadena, California, 1988.

⁶Klee, W.; Brenner, M. *Helv. Chim. Acta* **1961**, *44*, 2151-2153.

⁷Hay, R.; Nolan, K. *J. Chem. Soc., Dalton Trans.* **1975**, 1348-1351.

⁸Musich, J.A.; Rapoport, H. *J. Am. Chem. Soc.* **1978**, *100*, 4865-4872.

⁹Holy, A. *Coll. Czech. Chem. Commun.* **1979**, *44*, 593-612.

¹⁰Bowman, R.E.; Stroud, H.H. *J. Chem. Soc.* **1950**, 1342-1345

¹¹Vriesema, B.K., Ph.D. Thesis, University of Groningen, Groningen, The Netherlands, 1986.

¹²Trost, B.M.; Arndt, H.C.; Stuge, P.E.; Verhoeven, T.R. *Tet. Lett.* **1976**, 3477-3478.

¹³Kent, S.B.H. *Ann. Rev. Biochem.* **1988**, *57*, 957-989, and references therein.

¹⁴Sarin, V.K.; Kent, S.B.H.; Tam, J.P.; Merrifield, R.B. *Anal. Biochem.* **1981**, *117*, 147-157.

¹⁵Luttinghaus, A.; Cramer, F.; Prinzbach, H.; Henglein, F.M. *Liebigs Ann. Chem.* **1958**, *613*, 185-198.

¹⁶Evans, D.F. *J. Chem. Soc.* **1959**, 2003-2005.

¹⁷Coggon, P.; McPhail, A.T.; Mabbs, F.E.; Richards, A.; Thornley, A.S. *J. Chem. Soc. (A)* **1970**, 3296-3303.

¹⁸Pfeiffer, P.; Breith, E. Lubbe, E.; Tsumaki, T. *Justus Liebigs Ann. Chem.* **1933**, *503*, 84-130.

¹⁹Thielert, H.; Pfeiffer, P. *Chem. Ber.* **1938**, *71*, 1399-1403.

²⁰LaMar, G.N.; Eaton, G.R.; Holm, R.H.; Walker, F.A. *J. Am. Chem. Soc.* **1973**, *95*, 63-75.

²¹Lucas, H.J.; Kennedy, E.R. *Org. Syn. Coll. Vol. 3*, 482-485.

²²Elming, N.; Clauson-Kaas, N. *Acta Chem. Scand.* **1952**, *6*, 807-814.

²³Gibbs, D.E.; Orgel, L.E. *J. Carbohydrates, Nucleosides, Nucleotides* **1976**, *13*, 315-334.

²⁴Maniatis, T.; Fritsch, E.F.; Sambrook, J. *Molecular Cloning: A Laboratory Manual*. Cold Spring Harbor Laboratory: Cold Spring Harbor, New York; 1982.

²⁵Maxam, A.M.; Gilbert, W. *Methods Enzymol.* 1980, *65*, 499-560.

²⁶Mendel, D., Ph.D. Thesis, California Institute of Technology, Pasadena, California, 1989.